HR Wallingford

HYDRAULIC DESIGN OF STRAIGHT COMPOUND CHANNELS

VOLUME 1

by

P Ackers, Hydraulics Consultant

Contents of Volume 1

Report SR 281
OCTOBER 1991

Address: Hydraulics Research Ltd, Wallingford, Oxfordshire OX10 8BA, United Kingdom.
Telephone: 0491 35381 International + 44 491 35381 Telex: 848552 HRSWAL G.
Facsimile: 0491 32233 International + 44 491 32233 Registered in England No. 1622174

HYDRAULIC DESIGN OF TWO-STAGE CHANNELS : HR REPORT SR 281, DEC 1991

CORRIGENDA : to 22 Feb 1991, Volume 1

p9, line 2; should refer to plate 2

p20, last line levels should read levees

p47, para 2.4.8,	13;	0.43	should read	0.3
	16;	0.85		0.5
		0.94		0.9
	18;	0.61		0.52

p53; the two sentences at the foot of this page should be at the head of p55.

p64, para 3.4.20, 16;	3.18	should read	3.11
p64, para 3.4.21, 14;	3.12		3.13

p110, para 5.5.4; The information in the last sentence is based on a misunderstanding of earlier information, since amended by a personal communication from Dr Myers.

p112, 113, paras 5.5.9 to 5.5.10; The actual geometry of the R Main cross-section 14 differs from that used here, which was based on published information corrected since the report was written. The reach is now known to be of irregular gradient with non-uniform flow, so the hydraulic gradients used in the analysis are not valid. The information on the R Maine in the text, figs 5, 9 and 5.10 and in table 5.3 should be disregarded. This reach of river is no longer considered suitable for this type of analysis.

This report describes the development of new and improved design procedures for two-stage (compound) flood channels. This work was carried out by Peter Ackers as consultant to HR Wallingford, with funding made available by the Regional Water Authorites in 1988, prior to their demise when their responsibilities in this context passed to the National Rivers Authority. These funds were provided for the better dissemination of research results on this subject into engineering practice.

The report is in two volumes. The first begins with a Summary and Design Method which effectively provides a Manual for the hydraulic design of two-stage channels. The detailed review supporting these new procedures follows, continuing into volume 2, which also contains several Appendices.

The hydraulic engineer will find the essential information in the first section, Summary and Design Method, but will probably wish to refer to some of the details given in the main body of the report and in the Appendices to extend his understanding of the complex behaviour of two-stage flood channels.

Appendix 7 provides a design example of the computation procedures, including tables indicating how observed stage-discharge data might be used to extend the stage-discharge function. These tables will also provide a cross-check for any computer programme developed to solve the recommended hydraulic equations and logic procedures.

It is stressed that the equations given in this Manual are for the hydraulic design of straight parallel two-stage conveyances, although information will be found extending the application to small angles of skew (not exceeding 10°). Information given on meandering channels in Chapter 8 of the main text (see volume 2) shows that they behave quite differently. Improvements in the hydraulic calculations for meandered and irregular channels must await further work.

HYDRAULIC DESIGN OF STRAIGHT COMPOUND CHANNELS

SUMMARY AND DESIGN METHOD

CONTENTS

DETAILED DEVELOPMENT OF DESIGN METHOD

CONTENTS

PART 1

CONTENTS (CONT'd)

CONTENTS (CONT'd)

CONTENTS (CONT'd)

SUMMARY AND DESIGN METHOD

1. WHY COMPOUND CHANNELS NEED SPECIAL TREATMENT

1.1 The term "compound channel" covers channel cross-sections having berms or flood plains that come into action at high flows but which are normally dry. The mechanics of flow in such two-stage channels presents the drainage engineer with a problem. How is he to assess the stage discharge relationship for a situation where the flow may have radically differing depths and roughnesses over different parts of the cross-section? Is it acceptable to treat the channel as if its overall hydraulic mean depth (defined as cross-sectional area over wetted perimeter) adequately describes its cross-section? How should the effect of variations of roughness over the various flow zones be incorporated into a resistance equation? Are the usual resistance equations such as Manning able to cover complex sections, bearing in mind that their derivations were based on simple cross section shapes? These questions have to be resolved if the water levels to be expected during floods are to be assessed with reasonable accuracy and assurance.

1.2 The usual approach to design found in hydraulic text books is outlined in the following quotation: "..it is necessary to split the section into subsections.... Manning's formula may be applied to each in turn, and the discharges can be summed. The division of the section into sub-sections is a little arbitrary. Since the shear stress across the arbitrary divisions will be small compared with the bed shear stress, it may be ignored." (Chadwick and Morfett, 1986). *Note: all references appear in Volume 2, section 12.*

1.3 This "text book" procedure begs several questions, not least of which is the assumption that the simple addition of the calculated flows through the separated flow zones will give the correct answer. This is not so even in the most basic case of a straight channel, and the discrepancy is too great to ignore. The interference between the slower moving berm flows and the main channel flow increases head losses significantly, so that the discharge calculated by these methods will significantly over-estimate the true channel capacity, in extreme cases by as much as the bank-full discharge. However, the basic method is attractively simple. What is required, therefore, is an assessment of the corrections needed to allow for the inter-zone interference.

1.4 The different velocities in the deep channel and over the berms generates strong shear and turbulence at the junction between the zones, and this influences the flow for a considerable distance either side of the bank line. This turbulence is the mechanism for extra head loss, and it must depend on the transverse gradient of velocity which characterises the shear layer. Modern turbulence theory is capable of handling such situations and can provide very general solutions. However, the present stage of development does not yet encourage its use in normal engineering design, partly because of complexity but mainly because of uncertainty accuracy as a general prediction method, and so the method proposed here uses empirical adjustment factors. These are straight-forward to apply and represent the available data well.

1.5 Figure 1 illustrates a compound channel cross section with horizontal berms and defines terminology. Figure 2 shows the variation of the usual hydraulic properties of a real compound channel; the cross-section area A, the wetted perimeter P and the hydraulic mean depth R = A/P, treating the section as one unit. *(Note: nomerclature will be found in volume 2, section 13)*. The case illustrated is a natural channel, the River Severn at Montford Bridge (Knight et al., 1989). The Montford Bridge section has flood plains of unequal width with appreciable crossfall so that there is no discontinuity in P, nor therefore in R, but even so the overall hydraulic mean depth halves as the flow expands to cover the flood plains. The basic form typically researched has horizontal berms and so shows discontinuities in P and hence in R at bank full stage.

1.6 There have been many flow gaugings at Montford Bridge and, treating the flow section as a unit, these observations may be interpreted within the conventional frameworks of resistance functions. Figure 3 shows how the calculated value of Manning's n varies with stage when based on 'whole section' analysis. As flow spreads to cover the flood plain the n value drops by a third, despite the knowledge that in reality the roughness of the flood plains is not less than that of the main channel. This spurious reduction in resistance arises because of the form of the Manning equation:

$$n = R^{2/3} S^{1/2} / V \qquad \ldots 1$$

Thus as R calculated for the whole section falls by a factor of 2 as the flood plains are covered, this is reflected in a reduction in the calculated n value, even though in no sense is there a reduction in the actual roughness of the flow boundaries. It is a spurious effect of treating such a complex section as a unit. This not only demonstrates the inadvisability of treating compound sections as a unit, it also demonstrates the confusion that arises if Manning's n is used as an all embracing coefficient covering not only the physical roughness of the boundary but all other influences on head loss as well as corrections for irrational methods of computation. It is firmly recommended therefore, that for the purposes of hydraulic design, Manning's n should be used only as a roughness coefficient related to the physical roughness of the channel. Other influences on channel resistance should be expressed separately, through appropriate adjustment factors.

2. INTERACTION EFFECTS

2.1 The influence of various flow and geometric features on the degree of interaction between the main channel and the flood plain is exemplified by the ratio of the actual discharge (or conveyance) to the nominal discharge (or conveyance), the latter being derived as the sum of the flows estimated separately for the main channel and flood plain zones, from a knowledge of their geometry and roughness by using a standard resistance formula, e.g. Manning. This ratio, the discharge adjustment factor DISADF, thus allows for the interaction effects, and so to obtain a realistic estimate of the actual discharge (or conveyance) at any stage, the basic calculation given by the sum of the nominal zonal values has to be multiplied by DISADF. The main features that affect this interaction and hence loss of discharge capacity when flow is above bank are:

- relative depth of flood plain flow to main channel flow
- roughness of flood plain compared with roughness of main channel
- ratio of flood plain width to main channel width
- number of flood plains
- side slope of main channel
- aspect ratio of main channel

In small scale smooth compound channels, the Reynolds Numbers on the flood plains and in the main channel would have to be added to this list, but in almost all practical circumstances viscous effects are not important enough to require consideration of Reynolds Numbers.

2.2 The depth of flow on the flood plains relative to that in the main channel is a major factor. As soon as the flood plains become inundated, the flow in the main channel suffers from the interference of the slower flood plain flow. With similar roughnesses in the main channel and on the flood plains, this influence increases to a maximum at a relative depth, H_*, of the order of perhaps 0.1 to 0.3. (H_* = depth on flood plains/depth of flow in main channel). The maximum reduction in flow (referred to as the discharge deficit) due to this interaction may be anywhere in the range 10 - 20% depending on other factors (DISADF approx 0.8 to 0.9). As the relative depth increases further, the loss of capacity due to interaction diminishes again because there is likely to be less difference between main channel and flood plain velocities, but in practice the interference effect does not become negligible unless the berms are relatively narrow or the relative flow depth becomes considerable. The ratio of flood plain width to main channel width is an important factor, wide flood plains tending to show worse interaction effects than narrow ones.

2.3 The difference between the average velocities on the flood plain and in the main channel influences the degree of interference. Thus one would expect extra flood plain roughness to exacerbate the effect and the unlikely combination of relatively smooth berms with a somewhat rougher deep section to diminish it. Bank slope is also a significant factor as with vertical banks i.e. a rectangular main channel, there is closest proximity of the fast channel flow to the slower flood plain flow. Gentle side slopes to the main channel on the other hand provide a transition zone that might limit the interaction effects.

2.4 The likely influence of the interaction between main channel and flood plain flows clearly depends on how comparable the hydraulic conditions in these zones might be: if velocities and depths are very similar, then we can expect interaction effects to be small; if they are very dissimilar, then major effects are to be expected. The degree to which the different zones exhibit flow similarity is a rather new concept, the section's "coherence", and this may be defined theoretically. The closer the coherence is to unity, the more likely is the hydraulics of the section to approach that of a non-compound channel. Coherence is defined within the main text, see section 2.4 therein, and explained more fully in Appendix 3. In effect, it is the ratio of the flow calculated for the whole section (with zonal friction factors weighted according to the respective wetted perimeters) to the sum of the separately calculated zonal flows (before any allowance for interference).

2.5 This parameter varies with flow depth in a given channel, and the function for the Montford Bridge natural river section is shown in fig 4. Channel coherence brings together in one parameter most of the factors expected to influence the hydraulics of compound channels, and thus provides an important clue to the interaction effect.

3. THE RESEARCH BACKGROUND FOR THIS PUBLICATION

3.1 The Flood Channel Facility (FCF) at Wallingford was jointly funded by the Science and Engineering Research Council and Hydraulics Research Ltd, at whose premises the equipment was built. The program of investigation was organised as a series of individual but closely co-ordinated projects by University groups, and has been instrumental in providing an unique set of large scale data, which are both accurate and comprehensive. The facilities themselves have been fully described elsewhere (see Knight and Sellin, 1987). This SERC-FCF is illustrated in Plates 1 to 4. Other information on the performance of compound channels was also assembled and utilised where possible to extend the coverage of the prediction procedures to a wider range of geometries. However, several of the other sources of laboratory research data contained uncertainties or inaccuracies, and many dealt with geometries far removed from those of practical interest. These other data sets were generally of less value than had been hoped, though some proved very useful in confirming the methods to be described and further developing them to cover a wider range of circumstances. Particularly important in that respect are the collections of field observations that were used to validate the recommended procedures.

3.2 The basis of analysis of all the experimental data was through a comparison of the measured discharge with the nominal total discharge, as calculated from zones separated by vertical divisions. Alternative parameters were considered to establish their relevance and significance, and those recommended here were found to best represent the interference effect. The most relevant parameters to represent changing depths on the flood plain are:

- relative depth, $(H-h)/H = H_*$
- channel coherence, COH

(H is the total flow depth; h is the depth of the main channel). The discrepancy between the basic calculation (i.e. the sum of the separately computed flows in main channel and on flood plain before allowance for interaction) and the measured flow was treated in several different ways, of which the following proved most useful:

- adjustment factor, measured discharge/basic calculation, DISADF
- discharge deficit as proportion of bank full flow, DISDEFBF
- discharge deficit normalised by the calculated velocity difference and the product of total flow depth and main channel depth, $Q_{*2} = (Q_{CALC} - Q_{MEAS} / (V_C - V_F) \; H \; h$

3.3 The degree of interference between the channel flow and main channel flow shows different trends as the flow depth varies. Figure 5 shows the observed stage-discharge results for a particular geometry, with B/b = 4.20. This figure shows the discharge adjustment factor, DISADF, i.e. the factor by which the sum of the calculated zonal flows has to be multiplied to agree with the observed discharge, plotted against relative depth. The flow passes through three distinct regions of behaviour, each of which requires a different function to represent the trends:

- *Region 1* is at relatively shallow depths where the interference effects progressively increase with depth, up to relative depth 0.2, when the "loss" of capacity is over 10 percent.

- *Region 2* covers depth ratios from 0.2 to 0.4 for this particular geometry, with the interference effect diminishing towards a discharge loss of about 4 percent.

- *Region 3* occurs with further increase in depth, which causes an increase in the interference effect again.

- Also shown on Figure 5 is the theoretical coherence for that sample geometry, COH, and it will be seen that DISADF always lies between COH and unity. The implication of this is that the channel conveyance always exceeds the "single channel" computation but is less than the sum of the zonal computations. Had these particular experiments been continued to greater depths, they would most probably have followed the COH function, ie a single channel computation becomes appropriate at considerable depths of flood berm inundation. This forms *Region 4*. Note that Region 4 does not imply that there is no interaction between the main channel and the flood plains: the main channel discharge continues to be affected by the presence of flood plains.

3.4 The depth limitations between the regions shown in the sample plot of Figure 5 are not general; they depend on various parameters, and differ considerably with rougher flood plains: nor can it be assumed that if $(H-h)/h > 0.5$, the interference effects are entirely negligible. What is clear, however, is that different flow regions exist, and consequently different design formulae are required for each zone, as well as the means for establishing which region a particular design case will lie within. Predicting the stage discharge curve is therefore a rather complicated procedure, though easily handled by means of a modest computer program.

3.5 A detailed exposition of the analysis of the different groups of test results is given in the main report, see Chapter 3. This summary provides the overall picture and provides the design method deduced from those analyses. Empirical formulae were obtained for each region of flow, and progressively developed into general functions covering all the geometries tested. These were then compared with other data in the research literature, to further develop the method to cover main channel width/depth ratios other than the single value of 10 covered in the research in the FCF. This necessitated the introduction of an allowance in the predictive equations for width/depth ratio, the aspect ratio factor ARF. This refers particularly to region 1, there being no evidence that aspect ratio influences the predicted flows in other regions. When the width to depth ratio for the main channel is ten, ARF = 1, but more typically ARF = $2b/10h$, where b is the semi bed width. When the main channel width/depth ratio exceeds 20, it may be considered to be wide, with ARF = 2 for all greater aspect ratios.

3.6 Detailed information was also obtained on velocity distributions, and this provided a basis for assessing the discharges within the main channel and over flood plain zones separately. Figure 6 shows the discharge deficits, ie the differences between nominal calculated discharges and those actually occurring, normalised by bank full flow, and this is typical of the information about the separate influences of flow interaction on the two zones. This shows that the bulk of the discharge deficit compared with the basic calculated value arises because of interference effects in the main channel: the flood plains contribute a relatively small discharge addition.

3.7 In certain of the tests at Wallingford the flood plains were roughened by surface piercing rods (see Plate 3). Preliminary tests were made to determine the basic friction formula for this form of roughness under non-compound conditions. The basic friction law developed adds the drag of the rods to the friction arising from the smooth cement mortar finish of the solid channel surface, allowing also for the blockage effect of the rods. The rod roughness provided much higher friction factors on the flood plain than in the unroughened main channel. Thus the series of tests with added flood pain roughness provided a radically different case from those with main channel and flood plains of equal roughness. The methods proposed here cover the extremes of roughness ratio satisfactorily, so are expected to cover any intermediate roughness condition.

3.8 To illustrate the effect of extra rough flood plains, results for comparable tests are plotted in Figure 7 as discharge adjustment factor against relative depth. The four regions for test 02 are indicated but, bearing in mind that region 1 is the zone of increasing interference with depth, there is no evidence that the tests with very rough flood plains ever entered region 2. The results show progressively increasing interference effects up to the maximum depths covered, reaching the very severe condition approaching 40% loss of channel capacity (in excess of bank full discharge in fact) when the depth on the flood plains equals the depth of the main channel. Incidentally, if the flood plains are much rougher than the main channel, the section coherence does not approach unity as the depth increases. For the FCF tests with rough flood plains it remained around 0.4.

4. HOW TO ASSESS STAGE/DISCHARGE

4.1 The calculation for any depth in the range of stages of interest begins with the "standard" hydraulic computations for the main channel and flood plains separately, using the preferred resistance equation with appropriate roughness coefficients based on the known surface conditions. No preference for any particular basic resistance law is implied in what follows. In many field situations the Manning equation would be considered most appropriate, though in artificial channels the Colebrook-White equation may be preferred. The first step is to divide the channel section into its component parts, with vertical divisions between main channel and flood plains, and to work out their separate parameters: area, wetted perimeter, and hydraulic mean depth. Only the solid perimeter is included: the vertical interface is not included in the wetted perimeter. The hydraulic gradient has also to be known, of course. These "standard" calculations provide the basic discharge for the given depth, the sum of main channel and flood plain flows. This has to be adjusted for interference effects, to obtain the true predicted flow, utilising the equations summarised below.

4.2 Because there are four possible regions of flow, in effect four sets of computatations are required, to assess the discharge as if it were in each flow region in turn. There is a logical procedure then for selecting which region is in fact applicable at each of the depths considered. The methodology is thus rather complex, though readily programmed for computer solution. Because of this unavoidable complexity, and to avoid imposing on all the users of the new methods the need to develop software, in due course it is hoped that a PC disc will be issued which enables the user to go directly to a solution. Until such general user-friendly software is developed, the hydraulic engineer is provided with the appropriate equations, for which he/she may prepare an appropriate program for solution. Something like 500 - 600 program instructions are required for a comprehensive applications package. The various parameters used in the solution are defined on first appearance, but they are also listed in Chapter 13 of the main text.

Region 1.

4.3 This is the region of relatively shallow depths where interference effects increase progressively with depth. This is best represented by Q_{*2}, the discharge deficit normalised by the velocity differential and the product of flow depth and main channel depth. The relevant equations are:

$$Q_{*2F} = -1.0\ H_* f_C/f_F \qquad \ldots\ 2$$

$$Q_{*2C} = -1.240 + 0.395\ B/w_C + G\ H_* \qquad \ldots\ 3$$

where:

$$\text{Flood plain discharge deficit} = Q_{*2F}(V_C-V_F)\ Hh\ (ARF) \qquad \ldots\ 4$$

and:

$$\text{Main channel discharge deficit} = Q_{*2}(V_C-V_F)\ Hh\ (ARF) \qquad \ldots\ 5$$

$$\text{For } s_C \geqslant 1.0: \quad G = 10.42 + 0.17\ f_F/f_C \qquad \ldots\ 6$$

$$\text{For } s_C < 1.0: \quad G = 10.42 + 0.17\ s_C f_F/f_C + 0.34\ (1-s_C) \qquad \ldots\ 7$$

There is a narrow range of conditions for which Q_{*2C} as calculated above might be negative, implying that interaction effects would increase discharge. This is not ever likely in practice of course, and so to retain some minimum interaction effect, with shallow flood plain depths or with partial inundation of sloping flood plains, it is suggested that a minimum value of Q_{*2C} might be, say 0.5, and Q_{*F} should then be set to zero. This will have the effect of generating a step, not exceeding 5% of bank-full flow in the stage discharge function at bank-full elevation.

In the above:

H_* = (H-h)/H
f_C = friction factor calculated for main channel, $8gR_CS/V_C^2$
f_F = friction factor calculated for flood plains, $8gR_FS/V_F^2$
B = semi-width of section including flood plain(s) at elevation of flood plain(s); or water surface width if partally inundated
w_C = semi top width of main channel at elevation of flood plain(s)
s_C = side slope of main channel

Then:

$$\text{DISDEF} = (Q_{*2C} + N_F\, Q_{*2F})(V_C - V_F)Hh \times \text{ARF} \qquad \ldots \; 8$$

$$Q_{R1} = Q_{basic} - \text{DISDEF} \qquad \ldots \; 9$$

where:

N_F = number of flood plains(1 or 2)
V_C = calculated basic velocity in main channel
V_F = calculated basic velocity on flood plains
Q_{basic} = the sum of the zonal basic discharge calculations
Q_{R1} = required flow prediction for region 1
ARF = aspect ratio factor, typically 2b/10h

Region 2.

4.4 This is the zone of greater depth where the interference effect diminishes again. The most general function in this region expresses the requisite discharge adjustment in terms of the channel coherence, COH, and the relative depth H_*. It expresses the observation, in Figure 5 for example, that the graph of DISADF in Region 2 runs parallel to but below the graph of COH. It follows that the adjustment to discharge is given by the coherence calculated for a greater relative depth that the actual value. This is an empirical observation, not a theoretical deduction. Hence:

$$\text{DISADF}_2\,(H_*\,,\ \text{channel geometry and roughness})$$
$$= \text{COH}([H_*+\text{shift}],\ \text{channel geometry and roughness}) \qquad \ldots \; 10$$

where for $s_C \geqslant 1.0$, $\quad$ shift = $0.05 + 0.05\, N_F$ $\qquad \ldots$ 11

for $s_C < 1.0$, $\quad$ shift = $-0.01 + 0.05\, N_F + 0.6\, s_C$ $\qquad \ldots$ 12

The basic definition of COH may be expressed in terms of the geometric ratios of the compound channel: let $A_*=N_F\, A_F\, /A_C$; $P_*=N_F P_F/P_C$; $f_*=f_F/f_C$.

Then:

$$\text{COH} = \frac{(1 + A_*)\sqrt{[(1 + A_*)/(1 + f_*P_*)]}}{1 + A_*\,\sqrt{(A_*\,/f_*\,P_*)}} \qquad \ldots \; 13$$

So to work out DISADF in region 2, the values of A_*, P_* and f_* inserted in the above relate not to the actual relative depth, H_*, but to the "shifted" value, H_* + shift. Note that the corresponding "shifted" depth, H', used to calculate COH is given by:

$$H' = Hh/(h - \text{shift } H) \qquad \dots \quad 14$$

Then:

$$Q_{R2} = Q_{basic} \times DISADF_2 \qquad \dots \quad 15$$

Region 3.

4.5 This is a relatively narrow region of flow, best represented by DISADF as a function of COH, calculated in this case for the actual relative depth.

$$DISADF_3 = 1.567 - 0.667\ COH \qquad \dots \quad 16$$

$$Q_{R3} = Q_{basic} \times DISADF_3 \qquad \dots \quad 17$$

Region 4.

4.6 This is the region where the coherence of the cross-section is such that it may be treated as a single section, with perimeter weighting of friction factors, when calculating overall flow. This does not, however, mean that the separate zonal flows so calculated provide accurate assessments of the flows in those zones. For total flow computation however:

$$DISADF_4 = COH \qquad \dots \quad 18$$

$$Q_{R4} = Q_{basic} \times DISADF_4 \qquad \dots \quad 19$$

Choice of region.

4.7 The logic behind the selection of the appropriate predictive equation is dependent upon the calculation of discharge for all regions in turn, referred to above as Q_{R1}, Q_{R2}, Q_{R3} and Q_{R4} respectively. The choice of the appropriate region and hence appropriate total discharge proceeds as follows:

If $Q_{R1} \geq Q_{R2}$ then $Q = Q_{R1}$ ... 20

If $Q_{R1} < Q_{R2}$ and $Q_{R2} \leq Q_{R3}$ then $Q = Q_{R2}$ ... 21

If $Q_{R1} < Q_{R2}$ and $Q_{R3} < Q_{R2}$ then $Q = Q_{R3}$ ... 22
unless $Q_{R4} > Q_{R3}$ when $Q = Q_{R4}$

5. TOLERANCES

5.1 The performance of this set of predictive equations was first checked by reference back to the experimental data obtained from the FCF by the various research teams working on different aspects of the research. The percentage discrepancies between the individual results and the predicted discharges for the observed depths, geometries etc were assessed, and analysed statistically, to obtain mean errors and the standard error of estimate. Table 3.2 of the detailed text summarises these results, with statistics for groups of experiments as well as for the total set, including those with roughened flood plains. Broadly speaking, over the whole data set there was no residual mean error, and the standard error of the estimate (the variability) was under 1%. As a set of predictive equations they represent the actual flows to high accuracy, but of course the tolerance in any application in practice involves other tolerances as well as any errors in the predictive functions themselves. These include:

- discrepancies arising because of interpolations between, and extrapolations beyond, the conditions tested
- knowledge of, and variability in, the geometry of the section
- the simplification of the actual geometry to suit the method
- the basic friction law used in the calculations
- the accuracy of the friction coefficients used
- the hydraulic gradient and the assumption of steady uniform conditions

The computational accuracy may well be within 2 or 3 percent, as demonstrated by some of the better quality field data examined in Chapter 5, but there are probably larger tolerances in discharge from other uncertainties.

6. ANCILLARY MATTERS

Skew channels

6.1 The stage/discharge functions obtained for flood plains aligned with the deep channel outlined above were compared with results for channels skewed by up to 9° from the valley floor (see Plate 3). There was a limited set of information for this condition in the SERC-FCF (Elliott and Sellin, 1990), but as might be expected they indicated rather greater interference effects. See Section 4 of the main report. The predictive functions for straight channels may be applied to angles of skew (Φ) up to 10° provided this extra interference is allowed for. The necessary adjustment is obtained through:

$$DISDEF_{SKEW} = DISDEF_{ALIGNED} \times (1.03 + 0.074\Phi) \quad \ldots \quad 23$$

where Φ is in degrees. This will be conservative, i.e. an under-estimation of conveyance, if the flood plains are much rougher than the main channel, when it appears that a modest skewness has little additional effect.

Separating the main channel and flood plain discharges

6.2 Within Region 1, the predictive method provides these discharges, in that

$$Q_{R1C} = Q_{Cbasic} - Q_{*2C} (V_C - V_F) Hh \ ARF \quad \ldots \quad 24$$

and

$$Q_{R1F} = Q_{Fbasic} - Q_{*2F} (V_C - V_F) Hh \ ARF \quad \ldots \quad 25$$

where Q_{R1F} is the discharge for each flood plain. Knowing these separate discharges, the mean velocities in these zones can be calculated of course.

6.3. The computations of total discharge for the other flow regions is obtained by an overall adjustment for interference effects to the total basic flow: the separate adjustments for main channel and flood plain are not assessed in this procedure. However, in terms of the accuracy required for engineering purposes, the addition to the flood plain flow is much smaller than the reduction in the main channel flow, and so in Regions 2, 3 and 4 it would be reasonable to ignore the adjustment to the flood plain discharge, allocating it all to the main channel. Hence:

$$Q_{R2,3,4C} = Q_{Cbasic} - DISDEF \quad \ldots \quad 26$$

where DISDEF is the predicted overall discharge deficit, and

$$Q_{R2,3,4F} = Q_{Fbasic} \quad \ldots \quad 27$$

An alternative procedure is suggested in Chapter 3 where calculations are proceeding through increasing depths to establish the stage discharge function. In that case, there is evidence that the discharge adjustment for the main channel, $DISADF_C$, does not change much beyond the limit of Region 1, at least up to relative depth, H_*, = 0.50. Hence for higher flows in Regions 2, 3 and 4, the value of $DISADF_C$ at the limit of Region 1 could be retained.

Converting river cross-sections to basic trapezoidal compound geometry

6.4 When available, the data handling routines on the PC software disc will include an option for doing this on screen, either for a single section or for the average of several sections defining a reach of river. The essential elements of the process are as follows: they are illustrated in Figure 7.1 in Volume 2 and an example is given in Appendix 6.

- average the river bank elevations for the two sides (unless there is a flood plain on only one side)
- define the bank lines, which form the vertical divisions between main channel and flood plains
- choose a realistic bank slope, say by averaging the surveyed slope over the upper two thirds of the bank height: this gives s_C
- work out an average bed level that gives the same cross-sectional area below bank level: this defines h
- identify the back of each flood plain and so obtain the total width across the valley floor (2B)
- the various predictive functions can be applied even if the flood plains are not horizontal, as the calculation of Q_{Fbasic} can be carried out for any given flood plain profile and flow depth.

Extension of existing stage discharge information to greater depths

6.5 The methods of computation given above can be applied in the reverse direction, in that for any known point on the stage discharge curve, the predictive procedures can be applied for a range of assumed flood plain roughness coefficients, in order to select the one which most closely represents the observed discharge. To do this satisfactorily, it will first be necessary to have a reliable value for the main channel roughness coefficient. This is best obtained by analysing the upper range of within bank flows, checking whether there is any apparent trend in coefficient values with depth that might continue to the above bank condition. The functions are too complex to apply directly in the reverse direction with flood plain roughness unknown, though clearly a computer program can be written to do just that by iteration. Information on typical roughness coefficients will be found in Appendix 5, with discussion in Section 7.4 of Volume 2.

6.6. Thus the existing stage discharge information can be used to obtain realistic roughness coefficients, separated from any extra head loss due to interference and so providing a more reliable basis of extending the stage discharge curve than has existed heretofore. It is explained in Chapter 7 how gross errors may have occurred in the traditional approach to assessing field data for two stage flow: frequently the flood plain roughness has been adjusted to match observed discharges, whereas in fact it is the main channel flow that suffers from reduction due to interference effects. An example of extending the stage discharge function is given in Appendix 6, Volume 2.

Incorporating these new methods into 1-D computational models

6.7 1-D computational models require geometric information at the many cross-sections used to define the hydraulic system, as well as a method of assessing hydraulic resistance. Some models may use the cross-section data to define a unitary channel: this is not recommended because by so doing the roughness coefficient is also required to take account of spurious changes due to the geometric anomalies introduced by flow over the flood plains, as well as real changes in roughness with stage as the flood plains are inundated, and the extra resistance due to interference effects. However, if the model requires the sections to be treated as units, not divided into main channel and flood plain zones, the predictive method given above could be used as a roughness/cross-section pre-processor, to deduce overall equivalent resistance coefficients and/or conveyances as functions of flow depth.

6.8 Other models will use cross-section information in its more rational form, with separate data for flood plain and main channel. In this case also it would seem appropriate to use the predictive methods given here in the form of a pre-processor to provide the conveyance/depth function at each section in the model. Conveyance, K, is usually defined by:

$$K = Q/\sqrt{S} \qquad \ldots\ 28$$

where S is the hydraulic gradient, and can calculated using the predictive equations over the required range of depths.

Boundary shear stress

6.9 Some information on boundary shear stress is given in Section 7.2 of Volume 2. In effect, the higher velocities in the main channel spill over on to the flood plain and so give increased shear stress close to the channel bank. On the other hand, the interfacial shear stress tends to limit the main channel flow and so reduces the boundary stress compared to that which would arise in the absence of interference effects. Local increases on the flood plain can be as much as by a factor of 5 relative to the value that would be calculated from the local flow depth and channel gradient.

6.10 The average shear stress on the main channel bed is approximated by reducing the basic value, $\tau_o = \rho gHS$ or ρgR_CS by the factor $DISADF_C^2$, on the basis that with a square law resistance function such as the Manning equation for rough surfaces, the boundary shear will be proportional to velocity squared. Experimental data suggests that the mean bed shear stress will be somewhat above that based on hydraulic mean depth R_C, but closer to that than to the depth based value.

Sediment transport

6.11 Later phases of the research programme in the FCF at Wallingford envisage studies of the transport of both bed material and suspended sediment. In theory, the main channel's transport capacity for bed material must be reduced by the interference from flood plain flows compared with the transport capacity if there were no interference. This follows from the fact that the channel discharge, velocity and boundary shear stress are all reduced when flow is overbank, compared with the values that would otherwise occur at that depth. Some sample calculations of total bed material transport given in Chapter 8 of Volume 2 show that the reduction might typically be by a factor of 2 or 3. Another significant feature is that when the total transport of bed material is expressed as a transport concentration, this is appreciably less with overbank flow than when the channel was running within banks. Clearly, any consideration of channel regime (including the simulation of overbank flows in morphological models) must take account of the interference effect. These are tentative findings as they are based on the transfer of sediment transport functions for simple channels to compound channels: further research is needed to confirm or amend this assumption.

6.12. Suspended solid transport may spread through the full flow depth, and certainly the finest material in suspension, the wash load, will be found in the near-surface layers. The interfacial shear not only transports momentum across the bank line, from main channel to flood plain, it also transports sediment due to lateral turbulent diffusion. So sediment kept in suspension within the deep water channel can diffuse sideways into the slower moving flows on the flood plains, where it might settle out. Although the lateral diffusion process has been studied in the SERC-FCF using dye tracers, comparable research using sediment is in a future programme, so no quantitative information is available for use now. However, the process of lateral diffusion and settlement will be recognised as that which generates the levels of major lowland rivers.

7. ACKNOWLEDGEMENTS

This analysis of compound channels would not have been possible without the support of funding from several Water Authorities, whose river duties have now been taken over by the National Rivers Authority. It has depended on support from staff of HR Wallingford, as well as detailed liaison with the SERC Project Co-ordinator, Dr D W Knight, of the University of Birmingham. The careful and detailed work of the UK research groups involved deserves special mention. Without their research and the availability of their high calibre results, the work described here could not have proceeded to a successful conclusion. The co-operation of many other research groups and individuals is also acknowledged (see Chapter 5 and the acknowledgements (Chapter 11) of the main report).

Figures

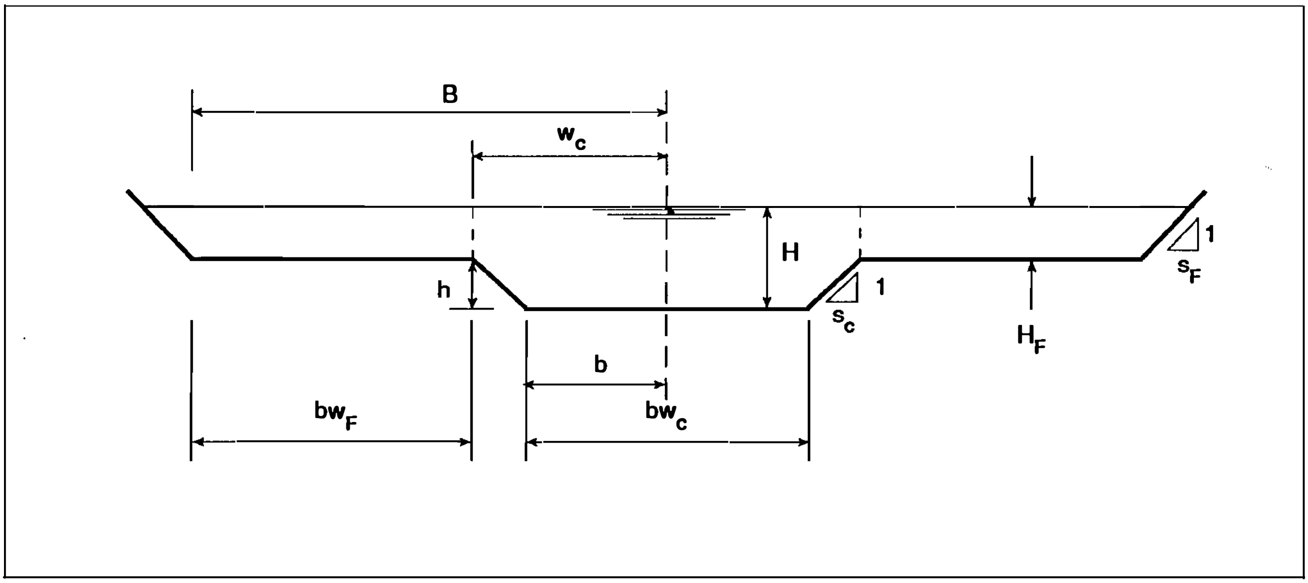

Fig 1 Compound channel cross-section: geometry and terminology

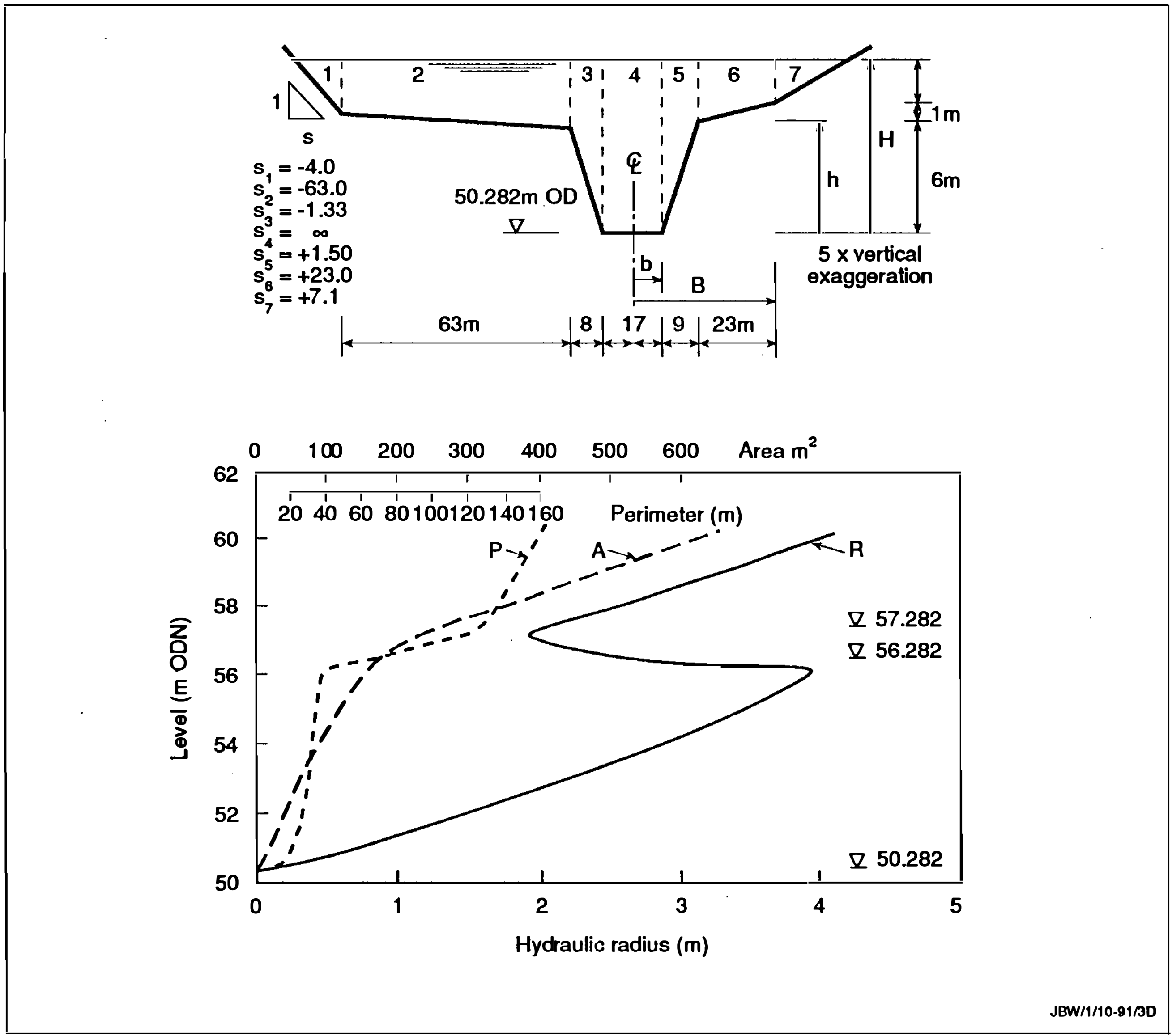

Fig 2 Channel at Montford Bridge on River Severn; (i) cross-section (ii) hydraulic parameters; cross-sectional area, A, wetted perimeter, P, hydraulics mean depth, R. (Knight et al, 1989)

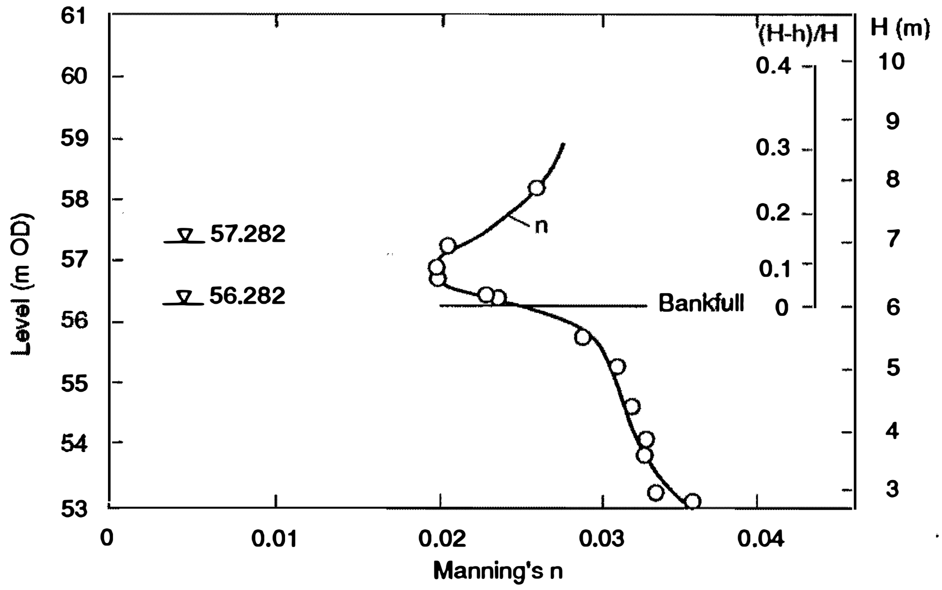

Fig 3 River Severn at Montford Bridge: variation of Manning's n with stage when considered as single section; based on field measurements (Knight et al, 1989)

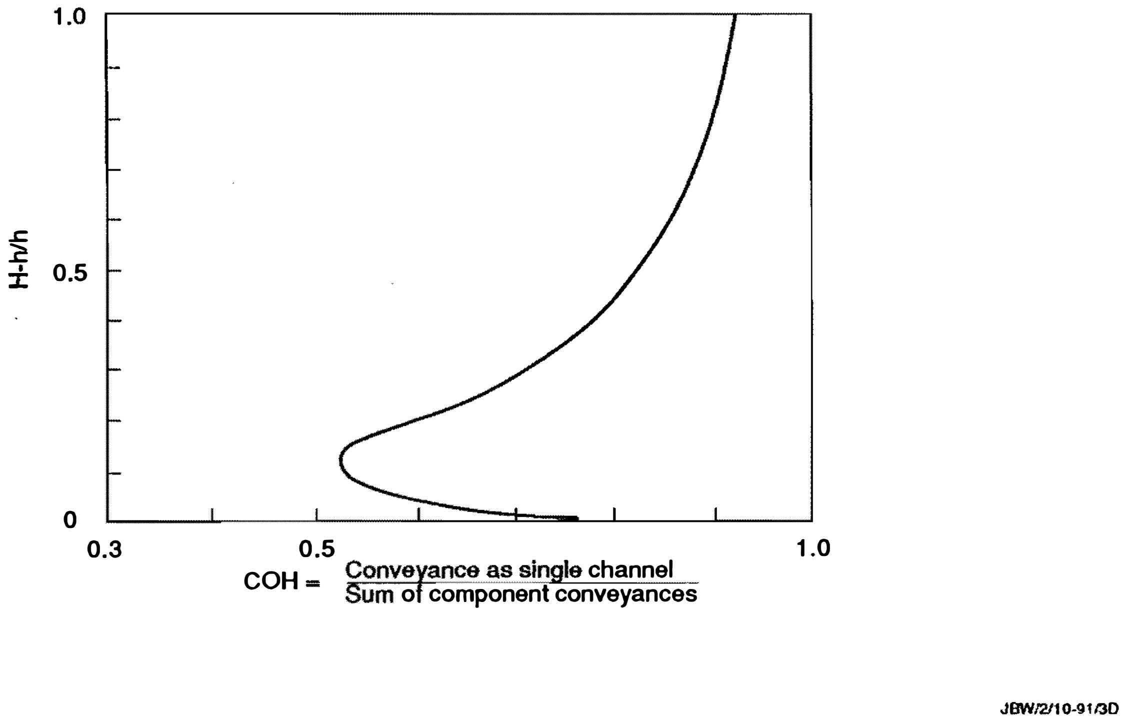

Fig 4 River Severn at Montford Bridge: variation of channel coherence - COH, with relative depth

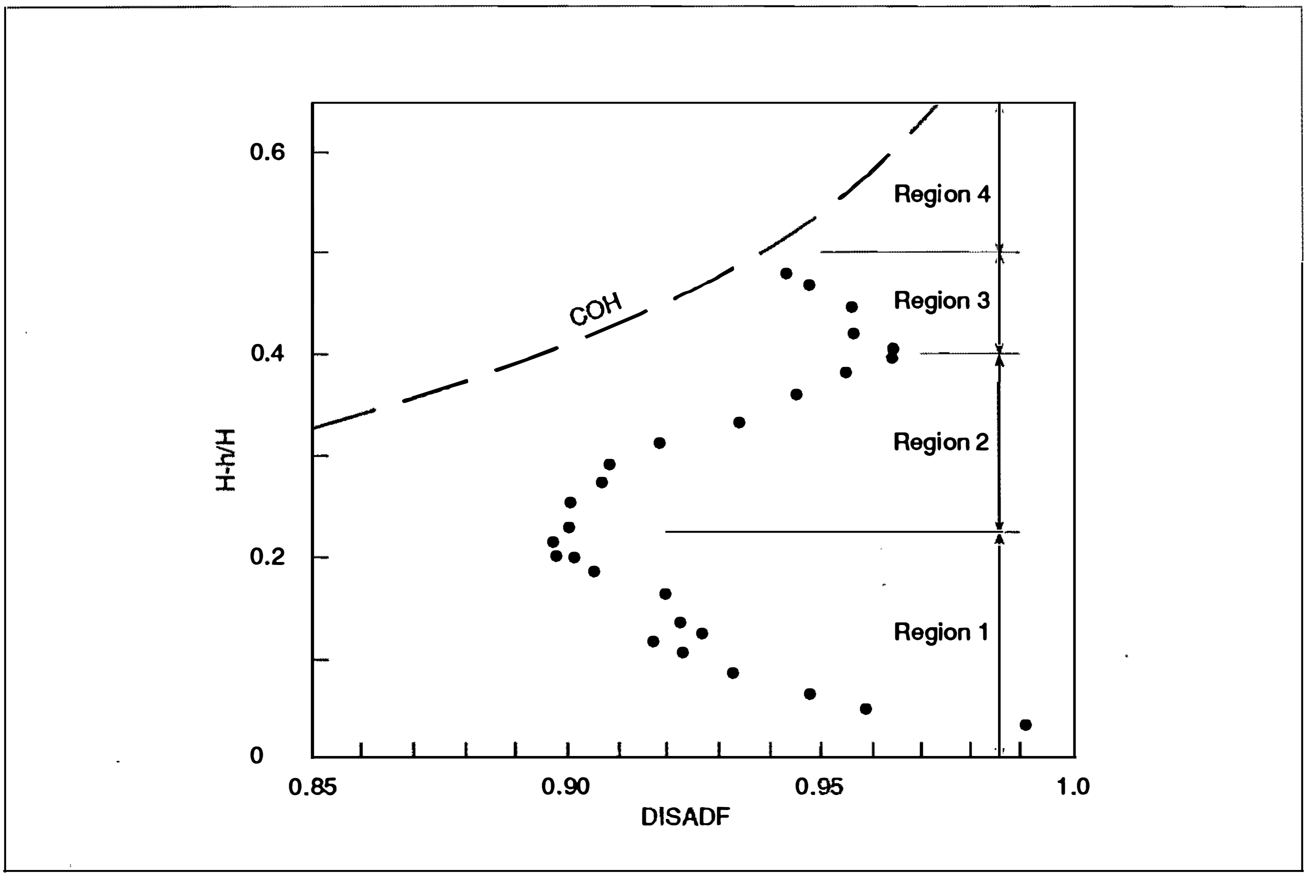

Fig 5 Sample test results from SERC-FCF: plot of DISADF (ratio of measured discharge to sum of zonal calculated discharges); also coherence - COH, to same scales; test 02, averages of 3

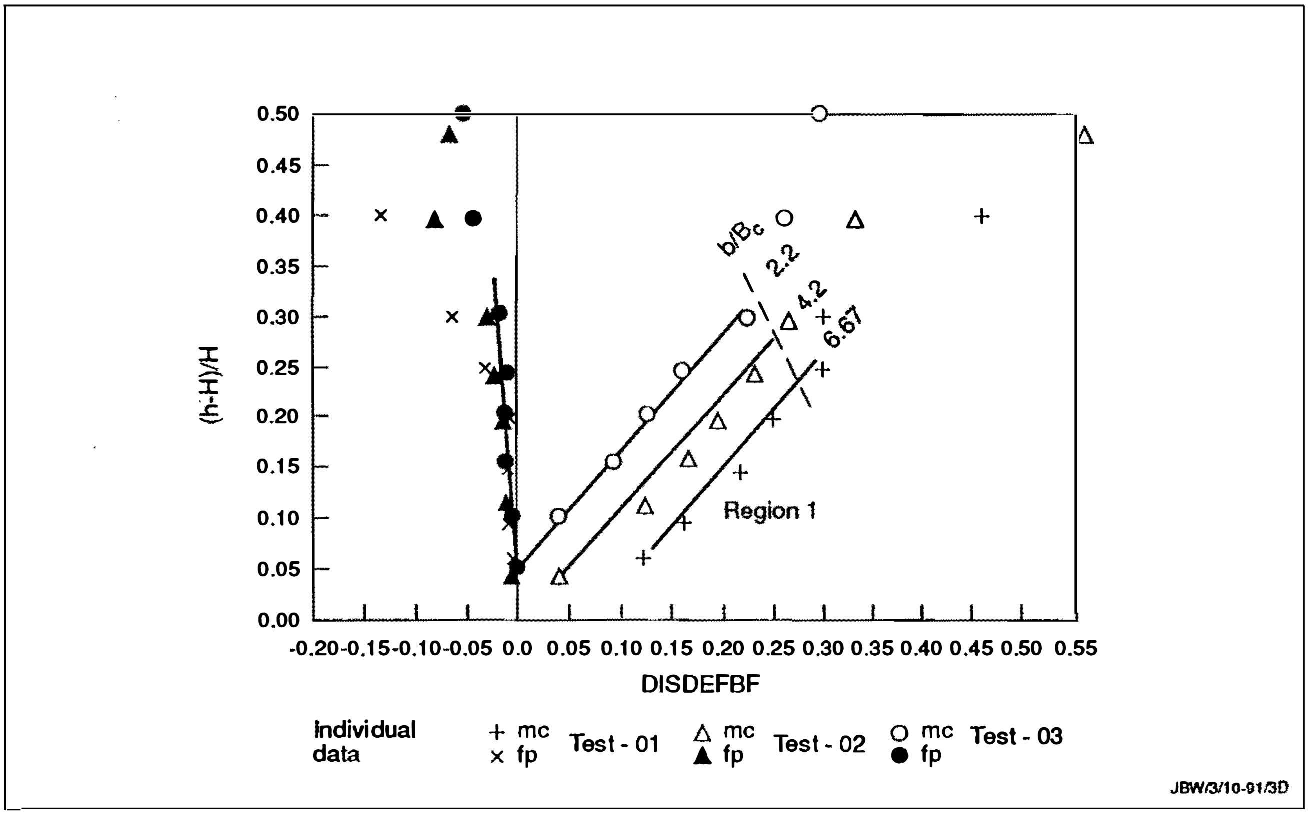

Fig 6 SERC-FCF results for three widths of flood plain: discharge deficits for flood plains (-ve) and main channel (+ve) as proportions of bank full flow. (Lines drawn apply only to region 1)

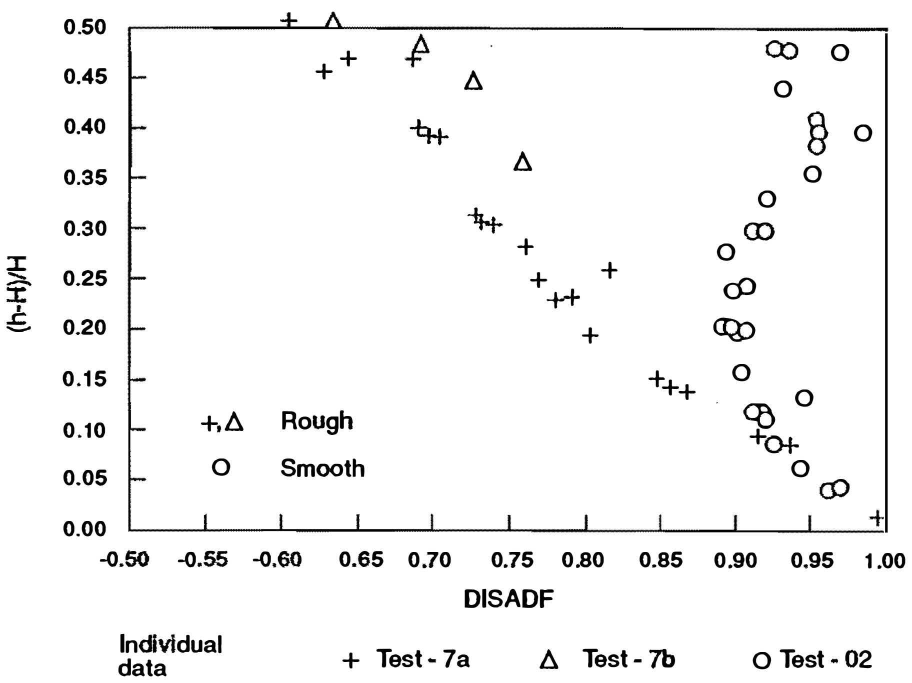

JBW/4/10-91/3D

Fig 7 SERC-FCF results: comparison of roughened flood plains and smooth flood plains in terms of discharge adjustment factor, DISADF

Plates

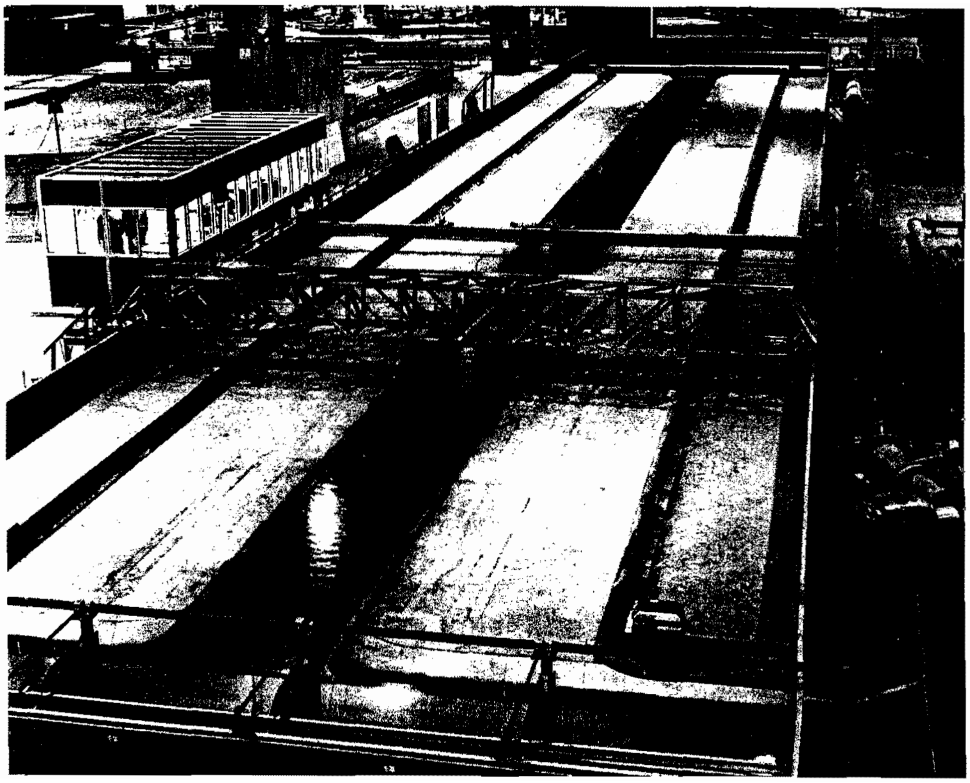

Plate 1 General view of SERC-FCF at HR Wallingford. Straight channel with flood-plain width restricted by movable wall, seen from downstream

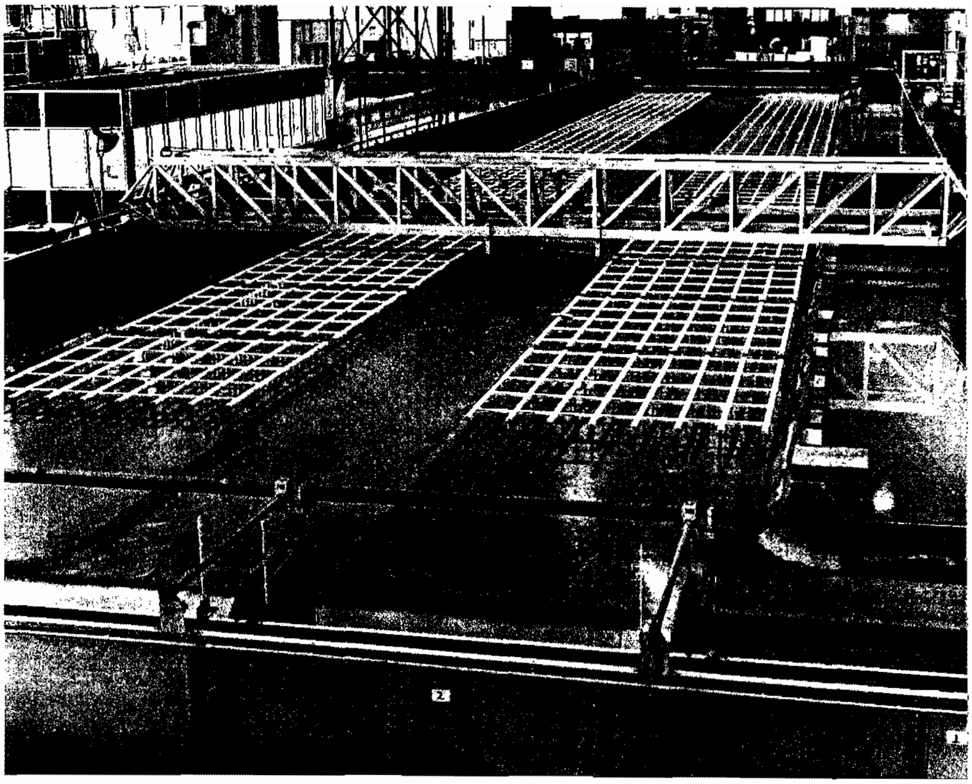

Plate 2 Flood-plains roughened by pattern of vertical rods supported from timber frame

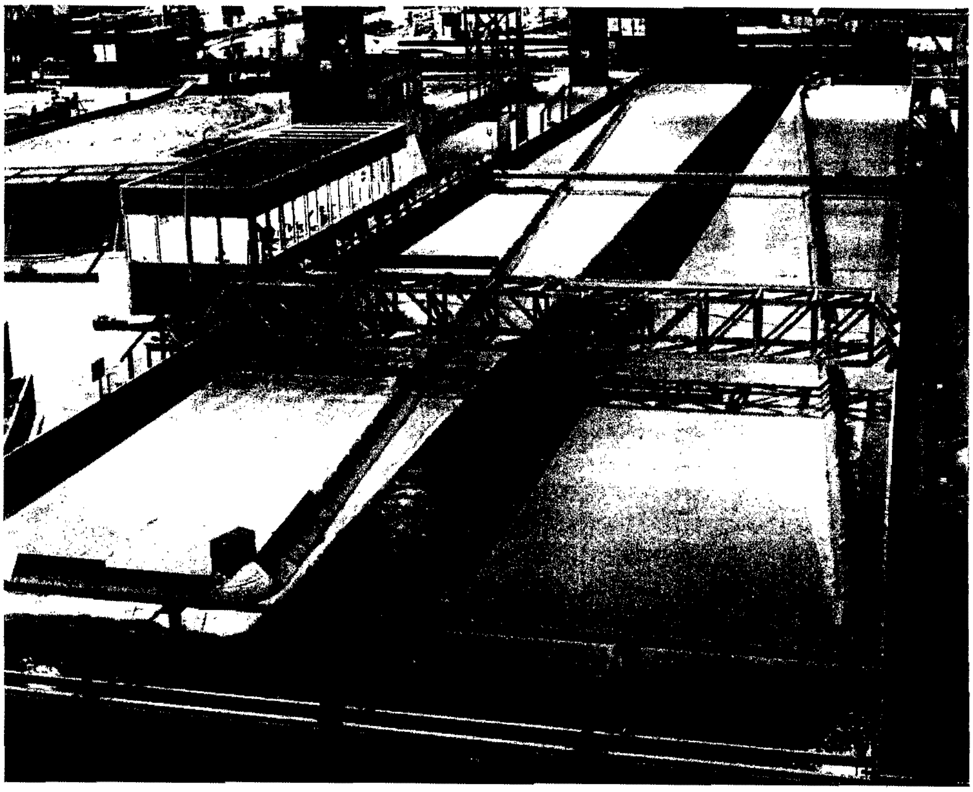

Plate 3 Layout of flume for skew channel experiments. Note that the flood-plain limits form the angle of skew

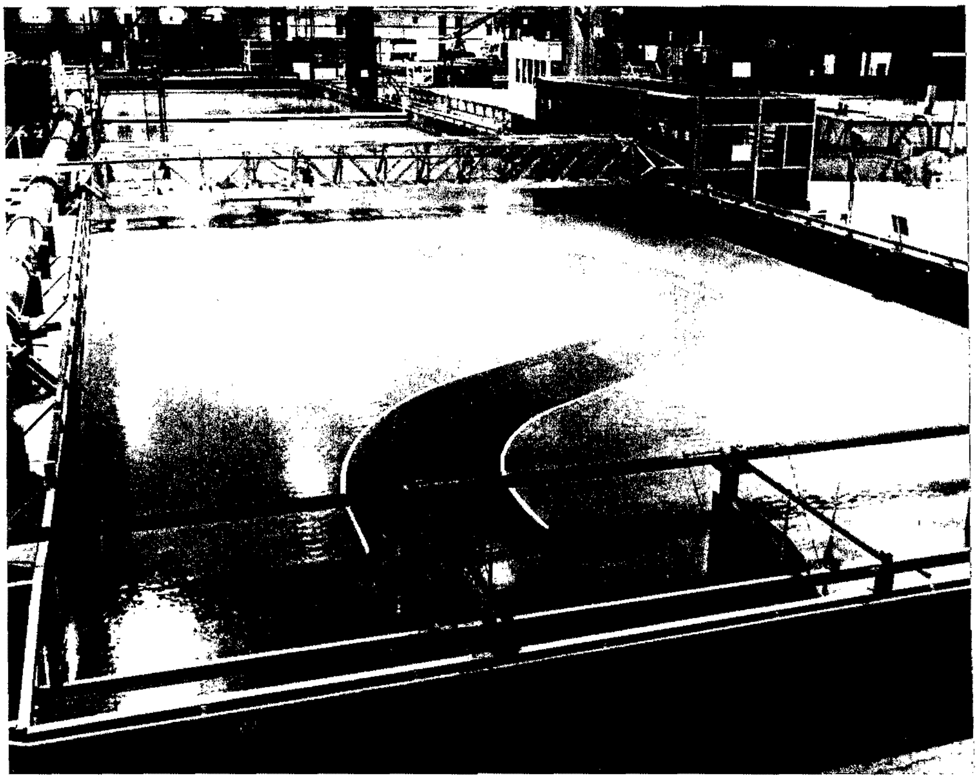

Plate 4 Experiment in progress with meandered channel: 60° cross-over channel

PART I

DETAILED DEVELOPMENT OF DESIGN METHOD

1. INTRODUCTION

1.1 The importance of compound channels and over-bank flows.

1.1.1 The term "compound channel" covers channel cross-sections having berms or flood plains that come into action at high flows but which are normally dry. The basic form of compound cross-section is a central deep channel with symmetrical side berms (or flood plains) which themselves have a horizontal bed. Man-made drainage channels may come close to that idealised form, but in hydraulic engineering practice compound channels will not in general have such a simple cross section: they may be asymmetric, have a less regular deep channel section, unequal berm widths with cross-falls etc. Clearly natural rivers differ considerably from the idealised cross-section, and also have the added complexity of plan irregularity: although relatively straight reaches may occur, natural rivers contain many changes of direction often with irregular meanders, with flood plains of variable width. Compound channels thus take many forms, some basically simple but many being of considerable complexity.

1.1.2 The more complex forms of compound channel are also favoured in terms of environmental management. Schemes including such man-made channels are closer to naturally occuring systems, and they are increasingly favoured over simple artificial drainage channels. Their berms will provide suitable habitats for water-side vegetation and the wild-life it will support and shelter (Hydraulics Research, 1988). Also, the deep channel within a compound section is more likely to be self-maintaining from the sediment point of view than a single wider channel with the same flood capacity.

1.1.3 The mechanics of flow in such two-stage channels presents the drainage engineer with a problem. How is he to assess the stage discharge relationship for a situation where the flow may have radically differing depths and roughnesses over different parts of the cross-section? Is it acceptable to treat the channel as if its overall hydraulic mean depth (defined as cross-sectional area over wetted perimeter) adequately describes its cross-section? How should the effect of variations of roughness over the various flow zones be incorporated into a resistance equation? Are the usual resistance equations such as Manning able to cover complex sections, bearing in mind that their derivations were based on simple cross section shapes? These questions have to be resolved if the water levels to be expected during floods are to be assessed with reasonable accuracy and assurance.

1.1.4 The problem of representing the flow resistance of complex, yet commonplace, channels applies equally to computational river models. In the interests of economy, one dimensional, lumped cross-section models have traditionally been used, with their inherent simplifications of the flow, for conditions which may include not only compound channel cross-sections but also exchanges of flow between the deep main river channel and the flood-plain. If even the basic case of a straight prismatic compound channel is not well understood, it is unlikely that numerical models with their many other simplifications of the geometry and flow will be able to simulate accurately the hydraulics of real river systems.

1.1.5 Natural rivers overflow their banks during periods of high discharge, causing potential damage to life and property. Those responsible for flood protection expend a considerable proportion of their budgets on schemes to limit the frequency, extent and impact of floods, by the provision of flood embankments, channel improvements and warning systems. They therefore require reliable methods for predicting river levels, and an essential element of that is a reliable method for assessing the capacity of the drainage system. In all probability the system includes compound channels for which conventional methods of hydraulic assessment are inadequate. The main object of this publication is to up-date those conventional methods to incorporate the results of recent research.

1.2 Scope of treatment

Straight channels.

1.2.1 Although most natural channels are curvilinear over the bulk of their lengths, reasonably straight sections do occur, and are the preferred reaches for hydrologic measurement. In those situations, a reliable method for extrapolating beyond the observed range of discharge, based on sound physical principles of hydraulic performance, is required to cover extreme events with appreciable flood plain flow. Straight drainage channels of compound section are also used as river improvements, and in urban situations where berms may have considerable amenity value. As well as providing the basic configuration on which much research has been conducted, straight channels are thus of very real importance. An understanding of their hydraulics is a necessary foundation for understanding the more complex cases.

Skew channels.

1.2.2 The term "skew channel" refers to the situation where the deep channel and the valley floor are not aligned with each other. This means that as one flood plain contracts and the other expands, flow is forced across the deep channel, a process which one would anticipate introduces radically different flow patterns in the main channel. This is a common situation for natural rivers during floods: there is interchange of flow between river and flood plain, and the skew channel provides a basic case for describing the effects on overall resistance and river stage of this flow exchange process.

Meandering and curvature.

1.2.3 A channel crossing the valley floor at an angle must do so over a limited length, related to the angle of skew and combined width of the flood plains. It follows that in natural rivers skewnesss is closely associated with curvature and meandering. The hydraulics of the skewed channel is thus a pointer to the hydraulics of meandered channels, where there is a sequence of flow exchanges from right flood plain to left and vice versa. This process, together with the influence on resistance of the intervening bends, provides a logical progression to the true complexity of many river systems.

1.2.4 This report follows this progression from straight compound channels, through skew channels to meandering and irregular rivers, though concentrating on straight channels. Supplementary information on rivers of complex plan form will follow as a result of later work. Particular use is made of research carried out with support from SERC (the Science and Engineering Research Council), HR, Wallingford, DOE (Department of the Environment), MAFF (Ministry of Agriculture, Fisheries and Food) and several of the water authorites (now replaced in terms of responsibility for rivers by the National River Authority). It sets out to explain why and in what way the design procedures applicable to simple channels require modification for these other, yet commonplace, situations. This leads to recommended design methods that may be used for the range of situations facing the drainage engineer: how to calculate the stage-discharge curve for a given compound cross-section, roughness and channel gradient; how to design a channel with berms for a specified duty; the modification to those procedures where the channel is gently skewed; methods for natural rivers of greater cross-section complexity; suggestions for the incorporation of similar hydraulics into one dimensional models; the broad effects on the flow and boundary stresses in the main channel and on the flood plain; and some preliminary views on sediment transport under compound channel conditions.

1.3 Approach to design

1.3.1 The usual method found in hydraulic text books is outlined in the following quotations: "The cross-section of a channel may be composed of several distinct subsections with each subsection different in roughness from the others. For example, an alluvial channel subject to seasonal floods generally consists of a main channel and two side channels. The side channels are usually found to be rougher than the main channel; so the mean velocity in the main channels is greater than the mean velocities in the side channels. In such a case, the Manning formula may be applied separately to each subsection in determining the mean velocity of the subsection. Then, the discharges in the subsections can be computed. The total discharge is, therefore, equal to the sum of these discharges." (Ven Te Chow, 1959). "..it is necessary to split the section into subsections... Manning's formula may be applied to each in turn, and the discharges can be summed. The division of the section into sub-sections is a little arbitrary. Since the shear stress across the arbitrary divisions will be small compared with the bed shear stress, it may be ignored." (Chadwick and Morfett, 1986).

1.3.2 The above seemingly simple procedure begs several questions, not least of which is the unsupported assumption that the simple addition of the calculated flows through the arbitrarily separated flow zones will give the correct answer. It will be apparent in what follows that this is not so even in the basic case of a straight channel, and that the discrepancy is too great to ignore. The interference between the slower moving berm flows and the main channel flow increases head losses significantly, so that the discharge calculated by these "text book" methods will be an over-estimate of the true channel capacity, in extreme cases by as much as the bank-full discharge. However, once a decision is made about the division lines between the zones, the basic method is attractively simple. What is required, therefore, at least as a first step, is an assessment of the corrections needed to allow for the inter-zone interference. The establishment of empirical adjustment factors forms the basis of chapter 3, and this concept is extended to skewed channels in chapter 4.

1.3.3 The potentially different velocities in the deep channel and over the berms generate strong shear and turbulence at the junction between the zones, and this influences the flow for a considerable distance either side of the bank line. This extra turbulence is the mechanism for extra head loss and it must depend on the transverse gradient of velocity which characterises the shear layer. Modern turbulence theory is capable of handling such situations and has the considerable advantage of having complete generality. Empirical adjustment factors are restricted to the range of cross sections tested, and these tend to be "classic" compound sections with a trapezoidal deep channel and horizontal berms. Methods based on turbulence theory can deal with any shape of cross section, so deserve careful assessment. These methods are reviewed in chapter 6.

1.3.4 Given an improved method of handling the hydraulics of compound channels, the conventional algorithms of one-dimensional models may be updated. The extra computational effort to do this will be minimal provided simple directly solvable expressions can be found for the various factors influencing the correction required to the basic compound section calculation. As far as possible, therefore, algebraic formulations will be provided giving a direct solution to the problem of computing the stage/discharge function in compound channels.

1.3.5 This report thus provides a reasonably comprehensive treatment of compound channels, including basic theory and a review of research as well as the recommended design methods that have resulted from that work. The hydraulic engineer need not follow through the whole publication each time he wishes to design a compound channel. The Summary Report contains the basic methodology for assessing the stage-discharge function for a "standard" compound channel consisting of a trapezoidal channel with berms, and also explains how a typical river section with flood plains can be dealt with, even if its section is not the ideal compound trapezium. The detailed support for the recommended method will be found in Chapter 3. An example manual solution of the design equations will be found in Appendix 6, though in due course it is anticipated that computer soft-ware will be developed to simplify application.

2. FLOW RESISTANCE IN CHANNELS OF COMPLEX CROSS SECTION

2.1 Resumé of resistance for simple open channels

Available formulae:

2.1.1 The most commonly applied formula for open channels is the Manning equation:

$$V = (1/n)\, R^{2/3}\sqrt{S} \qquad \ldots\ 2.1$$

where

V = average velocity of flow through the cross-section
n = Manning's roughness coefficient
R = hydraulic radius (hydraulic mean depth) given by cross section area, A, / wetted perimeter, P.

(Nomenclature is defined on first appearance and is listed in full in Section 13)

Although generally ascribed to Manning, in fact this equation was not one of those recommended in the usually quoted paper (Manning, 1891). It is, nevertheless, of almost universal popularity for typical open channels. It should be used with some care, however, because it is by no means a universal resistance function: it is unsuitable for extremely rough conduits, such as corrugated culverts and unlined rock tunnels or for the smoother range of man-made structures, such as good quality concrete spillways and drainage channels.

2.1.2 The limitations of the Manning equation for simple (non-compound) channels are best explained by reference to the comprehensive framework for flow resistance provided by turbulence theory. It would not be appropriate to go into great detail here, but in essence turbulence theory provides a description of the velocity distribution and its dependence on the roughness of the boundary and on fluid properties, including viscosity. The velocity distribution functions for smooth and rough boundaries usually quoted are those derived by Prandtl (1933), although more recent theories have also been propounded giving somewhat more complex expressions:

$$u / v_* = (1/K) \ln (z/z_0) \qquad \text{... 2.2}$$

where

u = the local mean stream velocity a distance z from the boundary
v_* = the shear velocity defined as (τ/ρ)
τ = the shear stress at the boundary
ρ = the density of the fluid
K = a turbulence constant (the von Karman constant)
z_0 = a constant of integration representing a boundary displacement

For smooth boundaries:

$$z_0 = \beta \nu / v_* \qquad \text{... 2.3}$$

where

ν = fluid viscosity
β = a constant

For rough boundaries:

$$z_0 = \alpha k_S \qquad \text{... 2.4}$$

where αk_S = a linear measure of the textural roughness of the boundary

Thus for smooth and rough boundaries respectively the velocity distribution is given by similar functions:

Smooth:

$$u/v_* = A \ln (v_* z/\nu) + B \qquad \text{... 2.5}$$

Rough:

$$u/v_* = A \ln (z / k_S) + B' \qquad \ldots 2.6$$

with $A = 1/K = 2.5$, $B = 5.5$ and $B' = 8.5$ (according to Nikuradse's results, 1933).

2.1.3. These quite fundamental functions for the local velocity distribution may be integrated over the cross-section of flow to give resistance equations. Although that procedure might in theory cover a range of cross-section shapes, only two are relevant here: a circular section and an open channel wide enough to ignore the influence of its banks. It is usual too to abandon Naperian logs (ln) in favour of common logs (base 10, log), and also to modify the coefficient values on the basis of classical experiments on pipe friction by Nikuradse, thus obtaining:

Circular pipes:

Smooth:

$$1/\sqrt{f} = 2.0 \log (Re\sqrt{f}/2.51) \qquad \ldots 2.7$$

Rough:

$$1/\sqrt{f} = 2.0 \log (3.71\ D/k_S) = 2.0 \log (14.8\ R/k_S) \qquad \ldots 2.8$$

where

f = friction factor, given by $2gDS/V^2$
Re = Reynolds number defined as VD/ν
D = pipe diameter
S = friction gradient (the slope of the energy gradient)

Note that R for a circular cross-section = $D/4$.

Wide open channels:

Smooth:

$$1/\sqrt{f} = 2.0 \log (Re\sqrt{f}/3.02) \quad \ldots\ 2.9$$

Rough:

$$1/\sqrt{f} = 2.0 \log (12.3\ R/k_s) \quad \ldots\ 2.10$$

Comparing the pipe functions with the wide open channel functions, both the smooth and rough expressions are affected in exactly the same way by the cross section shape.

2.1.4 Many surfaces of practical interest have a degree of roughness that renders them transitional between smooth and rough: this is so for many lined channels but is much less likely to be the case for natural channels and flood plains which will be hydraulically rough. The most frequently used resistance equation for surfaces that may lie anywhere in the range smooth to rough is that due to Colebrook and White, (Colebrook 1939) often shown in graphical form and referred to as "the Moody diagram" (see for example Chadwick and Morfett, 1985) This very general equation is available as design charts (Hydraulics Research, 1990) and tables (Hydraulics Research, 1990) and takes the form <u>for pipes</u>:

$$V/\sqrt{(2gDS)} = -2 \log [(k_s/3.7D) + 2.51\nu/D\sqrt{(2gDS)}] \quad \ldots\ 2.11$$

For sections not too far removed from circular, this may be generalised by replacing the pipe diameter, D, by the hydraulic mean depth, R,(D = 4R), to give:

$$V/\sqrt{(8gRS)} = -2 \log [(k_s/14.8R) + 0.628\nu/R\sqrt{(2gRS)}] \quad \ldots\ 2.12$$

However, for wide open channels the "correct" version is:

$$V/\sqrt{(8gRS)} = -2 \log [(k_s/12.3R) + 0.755\nu/R\sqrt{(8gRS)}] \quad \ldots\ 2.13$$

2.1.5 The first term of the above is the rough turbulent equation for wide open channels:

$$V/\sqrt{(8gRS)} = 2 \log [12.3R/k_s] \quad \ldots\ 2.14$$

Note that flow depends on relative roughness, k_S/R, but not on the viscosity of the fluid in this region of flow. Also that resistance follows a square law: S is proportional to (velocity) for constant relative roughness. Also, it may be shown that power law resistance formulae are in good agreement with the more academic logarithmic relation over certain ranges of relative roughness, for example the Manning equation with $R^{2/3}$ is a good fit in the range $7 < R/k_S < 130$ with $n \approx k_S^{1/6}/26$ (k_S in mm.).

2.1.6 At this point, no preference need be expressed for one equation over all others in terms of representing the basic resistance to flow in a simple channel. The straight conversion of the Colebrook-White transition equation by replacing D by 4R is not accurate for wide channels, but then there are such uncertainties in the roughness value k_S that they probably swamp the difference between the factors 14.8 and 12.3. In what follows, however, reference to the Colebrook-White equation will be to the wide channel version. This very general formula is preferable to the Manning equation for relatively smooth lined channels, for which there will also be reliable information on the values of k_S to use (see appendix 6). Provided a good estimate of k_S is available, it is also applicable to rough channels. However, the hydraulic engineer has traditionally used the Manning equation for such channels (not inappropriately, of course) so that because of its popularity and the availability of values of the roughness coefficient n for many cases, the Manning equation could hardly be discarded. Although inappropriate for the analysis of laboratory experiments on smooth channels, it is far from being superseded in engineering design.

2.2 Compound cross-sections

2.2.1 Figure 2.1 illustrates a conventional compound channel cross section and serves also to define some of the terminology used in the manual:

h = depth of main channel below the berms (flood plains)

H = depth of flow in main channel

$H_F = H - h$ = depth of flow over berms (flood plains)

b = half bed width of main channel

B = half total channel width at flood plain level, i.e. $2B$ = top width of channel plus width of berm(s) or flood plain(s).

s_C = main channel side slope, horizontal/vertical

s_F = flood plain side slope
bw_C = bed width of main channel
bw_F = base width of each flood plain

2.2.2 Figures 2.2 and 2.3 show the variation of the conventional hydraulic properties of compound channels, the cross-section area A, the wetted perimeter P and the hydraulic mean depth R = A/P, treating the section as one unit. Two cases are illustrated, a natural channel (R Severn, at Montford Bridge: Knight et al., 1989) and an artificial section (the experimental channel at Wallingford, with B/b = 4.2). The latter shown in Figure 2.3 has horizontal flood plains and so shows radical discontinuities at the bank full level in P and R, arising from the sudden increase in water surface width when flow exceeds bank full. The Montford Bridge section (Fig 2.2) has flood plains of unequal width with appreciable crossfall so that there is no discontinuity in P or therefore in R, but even so the overall hydraulic mean depth halves as the flow expands to cover the flood plains.

2.2.3 There have been many flow gaugings at Montford Bridge and, treating the flow section as a unit, these observations may be interpreted within the conventional frameworks of resistance functions. Figure 2.4(i) shows how the calculated value of Manning's n varies with stage (Knight et al. 1989). As flow spreads to cover the flood plain the n value drops by a third, despite the knowledge that in reality the roughness of the flood plains is not less than that of the main channel. This spurious reduction in resistance arises because of the form of the Manning equation:

$$n = R^{2/3}S^{1/2}/ V \qquad \text{... 2.15}$$

Thus as R calculated for the whole section falls by a factor of 2 as the flood plains are covered, this is reflected in a reduction in the calculated n value, even though in no sense is there a reduction in the actual roughness of the flow boundaries. It is a spurious effect of treating such a complex section as a unit.

2.2.4 The variation of the friction factor, f = 8gRS/V, with Reynolds Number, Re = 4VR/v is shown in figure 2.4(ii) (Knight et al, 1989) and a looped function emerges. It is most unlikely that any design method could result from such a presentation and there are two reasons for this:

- as the flood plains become inundated, the reduction of R with increase of stage provides a somewhat artificial reduction in the calculated friction factor, not related to the flow resistance, which actually increases

- expressing the Reynolds number as $4Q/P\nu$, the rapid increase of P as the flood plains become covered over-rides any increase in discharge

These combine to produce a looped function that has no physical meaning, so that quite apart from rejecting Reynolds number as a suitable parameter for large scale rough turbulent flows, it is obvious that treating the flow section as a unit creates problems because R is not monotonic with stage. It would seem, therefore, that any rational basis of design must treat the flood plains (berms) separately, in order to avoid the problems posed by treating the cross-section as a unit.

2.2.5 The above findings are confirmed by laboratory tests. Figure 2.5 shows sample results from the Wallingford channel expressed as the variation of Manning's n with flow depth (Myers and Brennan, 1990). Here the channel and flood plains have equal roughness, being moulded in smooth cement mortar. Again the radical reduction in apparent n value causing a discontinuity at bank full flow is a spurious result of the sudden change in the hydraulic mean depth. This not only demonstrates the inadvisability of treating compound sections as a unit, it also demonstrates the confusion that would arise if an overall value of Manning's n were to be used as an all embracing coefficient covering not only the physical roughness of the boundary but all other influences on resistance and corrections for irrational methods of computation. It is firmly recommended therefore, that for the purposes of design, Manning's n should be used only as a roughness coefficient related to the physical roughness of the channel. Other influences on channel resistance will be expressed separately, through appropriate adjustment factors.

2.2.6 Figure 2.6 shows these results in the form of friction factor plotted against Reynolds Number, Re, treating the Wallingford compound channel as a unit. Rather than a looped function as for the River Severn observations, the horizontal flood plains produce a discontinuity and overlap in Re, coupled with the artificial reduction in friction factor when the banks are inundated. Not only would such a discontinuous function be a problematic basis of design, it also has little physical significance: any real dependence of resistance on Reynolds number is masked by the discontinuity in R when used in this way to describe the flow cross- section.

2.2.7 When conducting field measurements of rivers using the velocity area method, in essence the mean velocity in each vertical is established and then the resulting discharge intensities, q = average velocity x depth, are integrated across the channel width. This same procedure is applied when flow is above bank, of course, when the discharge intensity in the main channel depends largely on its depth, gradient and boundary roughness and that over the flood plains depends on their flow depths, hydraulic gradients and roughnesses. It is not surprising, therefore, that a similar approach to calculation should be expected to provide at least first order accuracy of estimation when assessing the upper range of the stage-discharge curve, knowing the cross section geometry, gradient and the roughnesses of the different elements of the cross-section. The section would typically be divided vertically into zones with different depths and/or roughnesses, a resistance equation such as Manning would be applied to each zone separately and the component discharges would be summed to give the total discharge for the given stage. If that procedure were accurate, there would be little need for a new design method: the purpose here is to demonstrate its shortcomings and hence to improve upon it.

2.2.8 When applied to a basic compound channel with a central deep channel and side berms, the basic method reduces to three component calculations: the main channel and the two flood plains. By analogy with the velocity area method of flow measurement, vertical divisions between main channel and flood plains would be the natural choice, and these division lines would be left out of the computation of wetted perimeter for the component parts, of course. There has been considerable discussion, however, over the choice of the zone boundaries, on the premise that if it were possible to define a surface of zero shear stress, this would be more logical than the assumption of a vertical plane of separation. On this basis, sloping planes of separation at the bank line have been considered. However, the basic premise that an adequate knowledge of the location of a zero shear surface would solve the problem is faulty. This would only be so if the extra turbulence generated by the interference between the shallow slower flood plain flows and the deeper faster main channel flow did not also influence the flow patterns and hence the boundary shears in those zones. Even if surfaces of zero shear could be defined for all cases on the basis of research, a design method would also require full information on how the interference affected the estimation of flow in the separate flow zones. Because of their underlying logic and simplicity, only vertical divisions between the deep channel and flood plains are considered. Methods of correcting the basic flow resistance calculations either side of these divisions - or after combination - for the effect of interference between them will be derived and explained.

2.3. Allowing for the effects of interaction

2.3.1 Quantification of the effects of the interference between main channel and flood plain has been attempted by several authors using a range of methods. The main methods in the literature are:

1. Adjusting the division line between the deep and shallow zones of flow, perhaps coupled with including those sections in the wetted perimeter of one or more zones

2. Using Manning's n as a lumped resistance coefficient and seeking empirical functions with the ratio of flood plain depth to main channel depth, and any other relevant flow parameters

3. Assessing the apparent shear force on the assumed interface by reference to empirical information and so allowing for this in the computations for each zone

4. Using experimental research to assess adjustment factors for the separate flow zones

5. Similarly, but applying the correction factors to the total flow

6. Turbulence models predicting the lateral spread of the interacting shear layer and hence the lateral velocity profile.

2.3.2 None of the methods based on alternative division lines between the main channel and the flood plains removes the need for further adjustment factors and so they do not provide the sought after solution. This was demonstrated by Nalluri and Judy (1985), see Figure 2.7(a), and independently by Prinos and Townsend (1984) see Figures 2.7(b) and (c). Consequently, vertical divisions are used in all that follows, as it is more basic than the alternatives that have been tested with little success. Using the Manning equation as a lumped resistance parameter rather than solely as a measure of true roughness is theoretically unsound. Figure 2.4(i) showed how unreal such a procedure is for a real river, and Figure 2.5 shows a typical set of data from the Wallingford facility analysed in terms of Manning's n. The considerable reduction of n when the flow inundates the flood plain is spurious, as there is no actual reduction in the boundary roughness. Thus methods 1 and 2 listed above are considered inappropriate for design.

2.3.3 Method 3 above is based on the consideration of the force equilibrium on the compound channel, for example as sketched in Figure 2.8. For steady uniform flow, the weight component per unit length down slope is balanced by the the boundary shear stress integrated over the entire wetted perimeter.

$$\rho g \, A_T S = \tau_{AV} \, (bw_C + 2bw_F + 2H) \qquad \ldots \; 2.16$$

where subscripts AV, T, C and F denote average, the total section, the deep channel and the flood plain respectively. In effect this defines the average shear stress, which must vary considerably around the perimeter. Inserting the vertical division between the flow on flood plains and main channel, the equilibrium for the separate zones can be expressed as:

Main channel:

$$\rho g \, A_C S = \tau_{AVC} \, (bw_C + h) + SF_I \qquad \ldots \; 2.17$$

Flood plains:

$$\rho g \, A_F S = \tau_{AVF} \, (bw_F + H - h) - SF_I \qquad \ldots \; 2.18$$

where

SF_I = the shear force at the interface, assumed to assist flood plain flow and resist main channel flow

and

$$SF_I = \tau_{AVI}\ (H - h) \qquad \ldots\ 2.19$$

2.3.4 Correlations of depth-averaged apparent shear stresses on the interface have been carried out by Myers (1978), Wormleaton et al (1982), Knight et al (1983), Baird and Ervine (1984) and others for a range of channel and flood plain geometries, bed slopes and boundary roughnesses. The method is to measure all the components in the force balance equation with the exception of the interface shear, which can then be deduced from equs 2.17 and 2.18. Wormleaton et al offered the empirical relationship:

$$\tau_{AVI} = 13.84\ (\delta V)^{0.882}\ (bw_C/bw_F)^{0.727} \qquad \ldots\ 2.20$$

where δV is the difference in mean velocity between the channel and flood plain. Baird and Ervine's function was based on experiments on sixteen different cross-sections, with smooth boundaries:

$$\frac{\tau_{AVI}}{\rho g(H-h)S} = (H/(H-h)-\phi)^{1.5}\sqrt{(bw_C/h)}\ [0.5 + 0.3\ \ln(bw_F/h] \qquad \ldots\ 2.21$$

where ϕ is the relative flow depth at which velocities either side of the division between main channel and flood plain are close enough for $\tau\phi_{AVI}$ to be negligible.

2.3.5 The ratio of shear forces at the solid boundary to the streamwise weight component was suggested by Radojkovic (1976) as an index of the degree of interaction between the main channel and flood plain sub-sections. The coefficients are given by:

$$\Phi_C = \tau_{AVC}\ P_C/\rho g A_C\ S = \tau_{AVC}/[\tau_{AVC} + \tau_{AVI}(H-h)/P_C] \qquad \ldots\ 2.22$$

$$\Phi_F = \tau_{AVF}\ P_F/\rho g A_F\ S = \tau_{AVF}/[\tau_{AVF} - \tau_{AVI}(H-h)/P_F] \qquad \ldots\ 2.23$$

This formulation can be developed to give the total discharge, if one knew what the discharges in the separate zones would be in the absence of interface shear, Q_C' and Q_F':

$$Q_T = Q_C + Q_F = Q_C' \sqrt{\Phi_C} + Q_F' \sqrt{\Phi_F} \qquad \text{... 2.24}$$

Unfortunately the matter is not so straight forward, as Q_C' and Q_F' cannot be calculated from an unmodified resistance equation: interaction affects the shear at the solid surfaces as well as providing shear at the division line.

2.3.6 The problem with approach number 3 is thus that it is only a partial solution to the design problem. Firstly, a knowledge of the interfacial shear stress is by itself insufficient: we also need to have a method of assessing how the shear stresses at the solid boundaries are influenced by the flow interference. Figure 2.9 sketches how these boundary shears might be affected, and it is known from measurements made that they depart significantly over an appreciable width from the values that would be calculated from a basic friction law for the separate sections. It seems that the interaction changes the pattern of secondary currents in such a way that these external boundary stress changes are no less significant than the internal interfacial shear stress. Knowledge of the latter without the former is of no avail in terms of design.

2.3.7 If empirical information is to provide a design method, then it makes sense to include adjustment factors that cover both the effects mentioned above: the change in solid boundary shear stress from a normally calculated mean value due to interaction and the shear at the assumed vertical interface. Thus, with Q_C'' and Q_F'' the calculated components of discharge using a standard resistance formula for the two zones, with their individual geometries, roughnesses and gradients, then the total flow is given by:

$$Q_T = F_C Q_C'' + F_F Q_F'' \qquad \text{... 2.25}$$

where F_C and F_F are the respective adjustment factors, to be determined on the basis of experiment. This is the basis of method 4 listed above.

2.3.8 Appendix 1 lists the independent variables that control the flow in a straight compound channel: all the geometric properties of the section, density and viscosity of fluid, gravity and slope, and the roughnesses of the main channel and flood plain. If the flow is rough turbulent then the fluid viscosity does not influence the problem, and the dimensional analysis of Appendix 1 shows that:

$$F_{C,F} = \text{function}_{C,F} \left[H/(H-h);\ k_{SC}/H;\ k_{SF}/(H-h)\ ;\ b_C'/H;\ b_F'/(H-h)\ ;\ s_C;\ s_F \right] \qquad \ldots\ 2.26$$

where b_C' and b_F' are mean widths rather than bed widths. For smooth channels, the Reynolds numbers of the zones would replace the relative roughnesses in the above statement; transitional flow conditions would require both for completeness.

2.3.9 Clearly an impossibly wide range of experiments would be needed to cover all ranges of the many relevant parameters in any one research programme. However, there are some 40 or so references in the literature to experiments on compound channels. If all were available for further analysis there may well be a wide enough body of information, though mostly on small laboratory channels (Hollinrake, 1987, 1988, 1989). In attempting to develop empirical methods, simplifications were sought by individual authors, for example by assuming that the primary effect of some of these variables is adequately taken care of within the computations of Q_C'' and Q_F''. Different authors have therefore used a range of sub-sets and simplifications of the above, although, as Appendix 1 makes clear, any departure from the complete form of dimensionless statement makes the remainder questionable: it is a matter for careful experimental and field calibration to ensure that what remains is in practice sufficient. One such sub-set would be:

$$F_{C,F} = \text{function}_{C,F} \left[H/(H-h);\ f_C/f_F;\ b_C'/b_F';\ S_C \right] \qquad \ldots\ 2.27$$

The simplifications in this are:

- the ratio of friction factors, f, suffices as a measure of the interaction, the influence of Reynolds Number (if any) and relative roughness being taken care of by the sub-section flow calculations

- the influence of the slope of the bank forming the edge of the flood plain is too remote to affect the overall hydraulics
- the primary geometric effects are the relative depths and widths

2.3.10 To evaluate F_C and F_F from experiments requires that the flows in the flood plains and main channel are measured separately, through careful velocity traverses for example. Although this has been done in some test series, notably those carried out on the Wallingford flood channel facility, most experimenters have knowledge of the total flow only. This leads on to method 5 listed in 2.3.1, the introduction and assessment of an overall correction factor:

$$Q_T = F_T(Q_C'' + Q_F'') \qquad \ldots\ 2.28$$

where

$$F_T = \text{function}_T\ [\ H/(H-h);\ k_{SC}/H;\ k_{SF}/(H-h);\ b_C'/H;\ b_F'/(H-h);\ s_C;\ s_F\ ] \qquad \ldots\ 2.29$$

A typical simplified sub-set of the above is similarly:

$$F_T = \text{function}_T\ [\ H/(H-h);\ f_C/f_F;\ b_C'/b_F';\ s_C\ ] \qquad \ldots\ 2.30$$

Again, if there is a viscous influence on flow, as with smooth and transitional channels, then the two Reynolds Numbers would be required in addition. Whether such restricted functions suffice is a matter to be tested, of course.

2.3.11 Reasoning from the case where both the main channel and the flood plain are very wide, Appendix 1 postulated that the basic form of overall discharge adjustment might preferably be considered as a deduction from rather than as a multiplying factor for the sum of the flows calculated for the zones separately:

$$Q_T = Q_C + Q_F + \delta Q_C + \delta Q_F \qquad \ldots\ 2.31$$

This method appears to have been first proposed in 1971 (Zheleznyakov, 1985). Zheleznyakov also suggested that Q_C was much greater than Q_F, the former being subtractive and the latter additive. He also anticipated one of the suggestions in Appendix 1 that the correction term should be normalised, i.e. expressed in non-dimensional form, by the bank full discharge Q_{BF}. We might examine the following functional relationship for straight compound channels, alongside the other methods suggested in Appendix 1 for normalising the discharge defect:

$$\delta Q_T/Q_{BF} = \text{function} \; [\; H/(H-h);\; f_F/f_C;\; s_C;\; b_C'/b_F';\; (s_F)\;] \qquad \ldots\; 2.32$$

with the last term, the slope at the outside of the flood plains, being significant only when the flood plains are narrow.

2.3.12 Method 5 thus provides a feasible empirical approach to compound channel design. What remains is to establish the requisite correction terms for a wide range of conditions. The Wallingford experiments provide the initial data set to be used, but it will be essential to bring in other sets of experimental data, both to cover a wider range of geometries and roughness combinations and to provide independent confirmation of any empirical deductions.

2.3.13 Method 6, turbulence modelling, has been described by Elsawy et al (1983), Keller and Rodi (1984), Radojkovic and Djordjevic (1985), Samuels (1989), Knight, Shiono and Pirt (1989) and others. Whereas other methods are essentially one-dimensional, ie they seek an overall representation of the mean flow in the section, turbulence theory is essentially three dimensional: it seeks a solution of the Navier-Stokes equation for steady uniform flow in an open channel of general shape where there is both bed generated shear and lateral shear. The solution of the full Navier-Stokes equation is feasible, and becoming more accessible as the availability of powerful computers increases, but it cannot yet be regarded as an economical tool normally available to hydraulic engineers. It is for this reason that the more practical developments have in essence reduced the method to a two-dimensional approach, by using the depth integrated form of the basic turbulence equation. This allows for the effect of lateral variation in discharge intensity though not for secondary current effects, a significant limitation, although more recently methods have appeared in the literature that seek to account too for the effect of secondary currents, in effect by lumping these two influences together in an overall parameter.

2.3.14 The solution proposed by Knight et al (1989) uses the depth integrated equation together with the depth averaged eddy viscosity, to obtain analytical solutions for constant transverse depth and for linear depth variation. These solutions are functions of the assumed eddy viscosity, the friction factor for the flow zone, its depth and cross slope, as well as the channel gradient. This method was tested against the stage-discharge data for the River Severn at Montford Bridge (see Fig 2.2 (i) for its cross-sectional parameters), in effect being calibrated for that situation until it achieved a close degree of agreement in terms of stage-discharge. One of the inputs to the model is a set of values for the friction factors in the seven flow zones: so also are values of the eddy viscosity. Calibration of the model consisted of assessing and adjusting these individual values, the friction factors being functions of the local depth but the eddy viscosities, though varying from zone to zone, being constant with flow depth.

2.3.15 Figure 2.10 illustrates the level of agreement finally achieved in terms of depth mean velocity distribution across the width, for three discharges that were observed in detail in the field (Knight et al, 1989) The model represents the main features of the flow distribution well: maximum velocity in the main channel and the discharge distribution across its width and typical flood plain velocities. Its deficiency is mainly close to the upper edge of the bank between main channel and flood plain, where the model indicates a more pronounced dip in the discharge intensity than was observed. Although promising, this approach must still be regarded as a research area. Indeed, until there is good information on the values of the turbulent eddy viscosity to use in different zones of flow, and their dependence on all the geometric and flow parameters, unfortunately it does not yet provide a general design method.

2.3.16 Keller and Rodi (1988) use a k - ϵ turbulence model, again in a vertically integrated form, and used a series of experiments on compound channels of four different shapes, including cases where channel and flood plain roughnesses differed, to calibrate and validate the model. These procedures give a great deal of detailed information, such as the distributions of shear stress and velocity across the width, and so testing them against experimental results is not just a comparison of the stage discharge curves. Figure 2.11 shows samples of their results for velocity and shear distributions across the channel width, with experimental velocities for comparison. The Keller and Rodi model has some problems with vertical and steeply inclined banks, but is nevertheless promising. Undoubtedly an improved understanding of the fluid mechanics is the way forward, and turbulence modelling is the natural line of development. Whether it is yet able to provide a general method of design for compound channels is doubtful, the criterion being the achievement of an accuracy of prediction within one or two percent without individual calibration in respect of the values of eddy viscosity to use.

2.3.17 The scope of turbulence modelling as a design procedure is considered further in Chapter 6. The vertically-integrated two-dimensional theory is given in Appendix 4.

2.4 Features influencing the degree of interaction

2.4.1 Equation 2.28 provides a framework for considering what might already be known about the influence of various flow and geometric features on the degree of interaction between the main channel and the flood plain, exemplified by their influence on the factor F_T by which the total flow calculated without regard to interaction has to be multiplied to provide a realistic estimate. The relevant features are contained in the functional statement of equation 29, generalised to include the viscous effects for smooth and transitional surfaces, which then becomes:

$$F_T = \text{function}\ [\ H/(H-h);\ k_{SC}/H;\ k_{SF}/(H-h);\ Re_C;\ Re_F;\ b_C'/H;\ b_F'/(H-h);\ s_C;\ s_F\ ] \qquad \ldots\ 2.32$$

These features are thus:

- relative depth of flood plain flow to main channel flow
- relative roughness of main channel
- relative roughness of flood plain
- main channel Reynolds Number
- flood plain Reynolds Number
- aspect ratio of main channel
- aspect ratio of flood plain

- side slope of main channel
- side slope of flood plain

2.4.2 Before considering in detail the large scale experiments conducted on the Flood Channel Facility at Wallingford, some broad indications from previously published work will provide a measure of the problem faced by the designers of even straight simply-bermed channels. No researcher has covered all the above possible influences: each worker has been restricted to various degrees by the scale of apparatus available, and time scale and funding for his activities. All have therefore had to compromise on the implications of the dimensionless statement of equation 2.32 by covering a limited number of variables. The problem here is that it can not be assumed that the results of the empirical analysis of, say, varying the widths of the flood plains in smooth channels will apply without modification to rough channels. We might hope it would, but this needs to be demonstrated. Thus there are many sources of information but in terms of the empirical functions derived therein, they are unlikely to apply to compound channels in general.

2.4.3 It is generally agreed that relative depth is a major factor. As soon as the flood plains become inundated, the flow in the main channel suffers from the interference of the slower flood plain flow. Most researchers found this influence to be at a maximum at a relative depth, H_*, of the order of perhaps 0.1 to 0.3 and then to diminish progressively as the depth of flow on the flood plain increased. The maximum reduction in flow due to this interaction may be anywhere in the range 10 - 50% depending on the source of information and cross-section geometry. As the relative depth increases, then interaction diminishes because there is likely to be less difference between main channel and flood plain velocities, but in practice it does not become negligible unless the berms are relatively narrow. This is another major factor: the ratio of flood plain width to main channel width, wide flood plains tending to show worse interaction effects than narrow ones.

2.4.4 The difference between the average velocities on the flood plain and in the main channel is often used as a parameter for the degree of interference. Thus one would expect extra flood plain roughness to exacerbate the effect and the unlikely combination of relatively smooth berms with a somewhat rougher deep section to diminish it. How the overall roughness of the system affects the issue is not clear, partly because few experimenters have covered both smooth and rough surfaces in otherwise twin sets of tests. Reynolds number is not expected to have any influence in rivers and streams because they will operate in the rough turbulent range of flow. However, Reynolds Number is a factor in laboratory scale tests because the generally smooth laboratory channels do suffer from viscous effects. Bank slope must be a significant factor as with vertical banks i.e. a rectangular deep channel, there is closest proximity of the fast channel flow to the slower flood plain flow. Gentle side slopes to the main channel on the other hand would provide a transition zone that might limit the interaction effects. Any skewness between the axis of the main channel and valley floor would be expected to have a major effect on the interaction process, because the flow exchange forced by tapering flood plain on one side and expanding flood plain on the other would radically influence the exchange of momentum. That more complex condition is covered later in Chapter 4: here only straight channels with aligned flood plains are considered.

2.4.5 The likely influence of the interaction between main channel and flood plain flows depends on how comparable the hydraulic conditions in these zones might be: if velocities and depths are very similar, then we can expect interaction effects to be small; if they are very dissimilar, then major effects are to be expected. The degree to which the different zones exhibit flow similarity will be referred to as their *"coherence"*: the greater their coherence the more likely is the hydraulics of the section to approach simple channel (negligible interaction) conditions.

2.4.6 <u>Channel conveyance</u> is a useful parameter in considering how the concept of coherence might be defined. Conveyance, K_V, was defined by Ven Te Chow (1959) as:

$$K_V = Q/\sqrt{S} \qquad \ldots 2.33$$

but it is preferable to redefine it to be consistent with dimensional analysis, as:

$$K_D = Q/\sqrt{(8gS)} = A\sqrt{(A/fP)} \qquad \ldots 2.34$$

Thus the conveyance of a simple channel can be represented by the cross-section area, wetted perimeter and friction factor. For a compound section, the theoretical conveyance *before allowing for any interaction effects* is given by the sum of the conveyances of the main channel and flood plains:

$$K_D = A_C\sqrt{(A_C/f_C P_C)} + 2\ A_F\sqrt{(A_F/f_F P_F)} \qquad \text{... 2.35}$$

for the situation of two symmetrical flood plains.

2.4.7 This leads to a parameter for the coherence of the channel section, namely the ratio of the theoretical conveyance calculated by treating it as a single unit to that calculated by summing the conveyances of the separate zones. This concept is developed in Appendix 3 and in its most general form, the section coherence is defined as:

$$\mathrm{COH} = \frac{\sum_{i=1}^{i=n} A_i \sqrt{[\sum_{i=1}^{i=n} A_i / \sum_{i=1}^{i=n} (f_i P_i)]}}{\sum_{i=1}^{i=n} [A_i \sqrt{(A_i/f_i P_i)}]} \qquad \text{... 2.36}$$

This parameter varies with flow depth in a given channel, of course, and three cases are illustrated in Figure 2.12: the Wallingford channel illustrated in Figure 2.3; the same but with flood plains reduced to 0.25m wide; and the Montford Bridge natural river section shown in Figure 2.2a. For the smooth Wallingford channel, the appropriate friction factor was used (varying with depth) and for the Montford Bridge section a constant value of Manning's n was applied for this illustration, with depths related to the lower edge of the flood plains.

2.4.8 The artificial channel with horizontal flood plain and flood plain/main channel width ratio 3 shows a particularly low COH value of about 0.43 when the flood plains are first inundated, increasing to 0.95 when the flood plain flow depth equals the depth of main channel. With narrow flood plains, width ratio 0.3, COH is less sensitive to depth and closer to unity, lying between 0.85 and 0.94. The natural river section has wide flood plains with some cross fall (note that Figure 2.2a has considerable vertical exaggeration) with minimum COH value (0.61), not just above bank full but when the full width of flood plain is inundated. Above this the trend is very similar to the wide laboratory channel, whilst below the trend is towards unity because its sloping flood plains avoid the disconuity in COH at bank full. (For these calculations the main channel zones 3,4 and 5 of Figure 2.2a were taken together, as were the remaining flood plain areas)

2.4.9 Whether this definition of channel coherence provides a co-ordinating parameter in the analysis of experimental results remains to be seen. Its potential benefit is that it brings together in one parameter most of the factors expected to influence the hydraulics of compound channels. A corollary is that the closer to unity COH approaches, the more likely it is that the channel can be treated as a single unit, using the overall geometry.

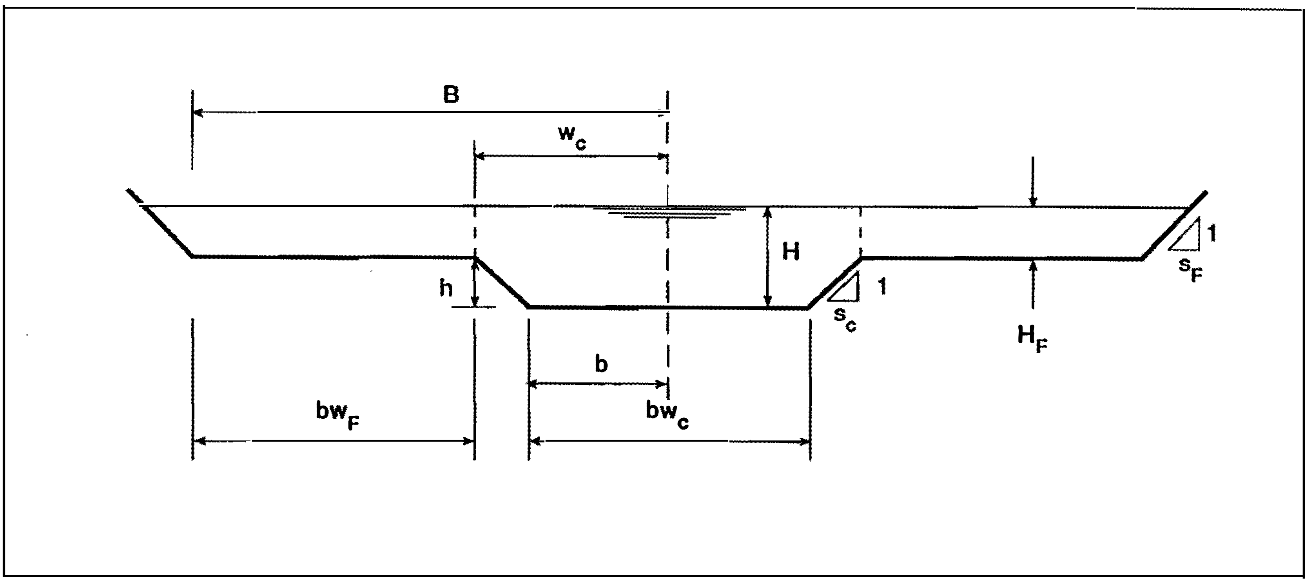

Fig 2.1 Compound channel cross-section: definitions and terminology

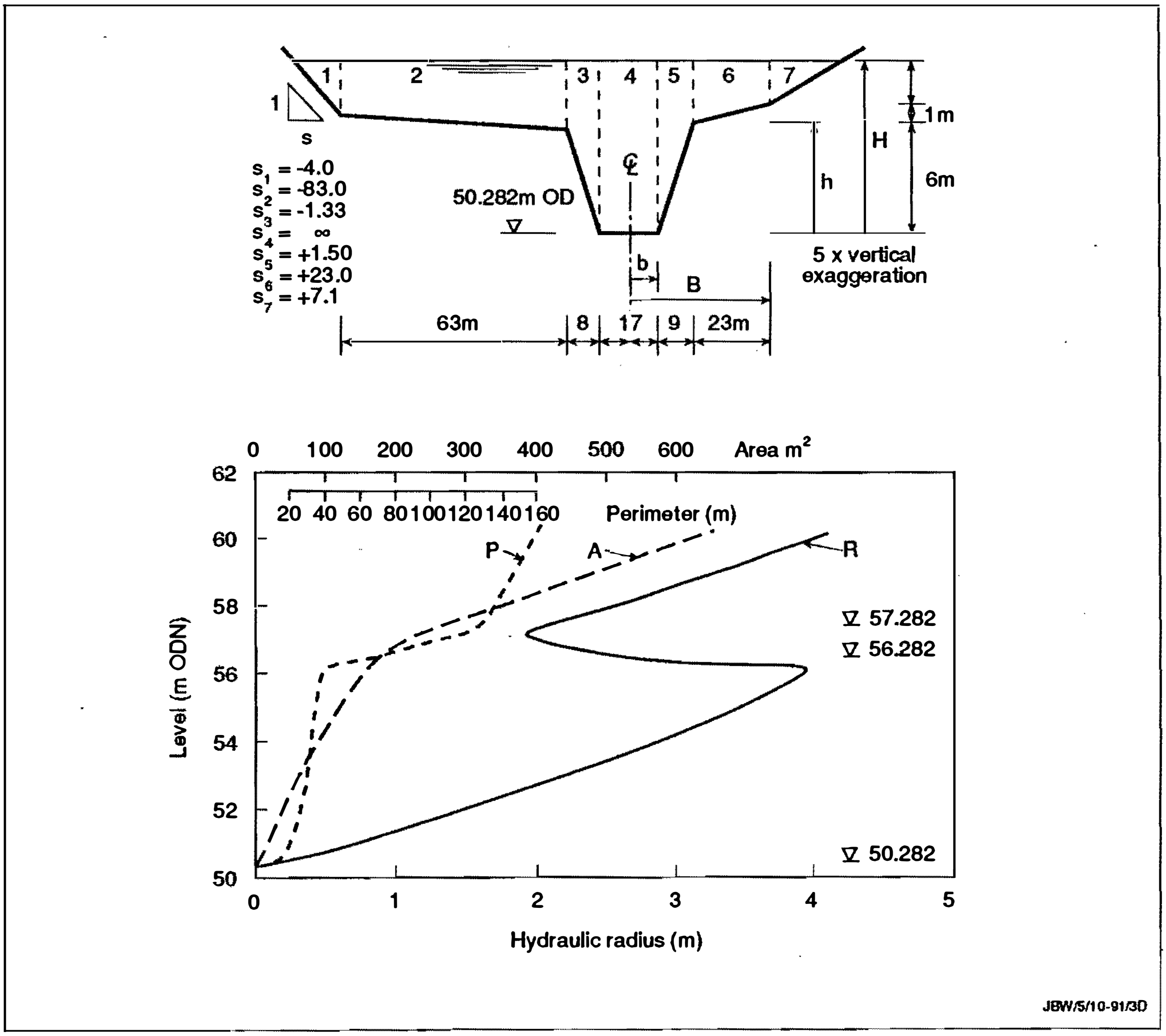

Fig 2.2 Channel at Montford Bridge, River Severn; (i) cross-section (ii) hydraulic parameters; cross-sectional area, A, wetted perimeter, P, hydraulics mean depth, R. (Knight et al, 1989)

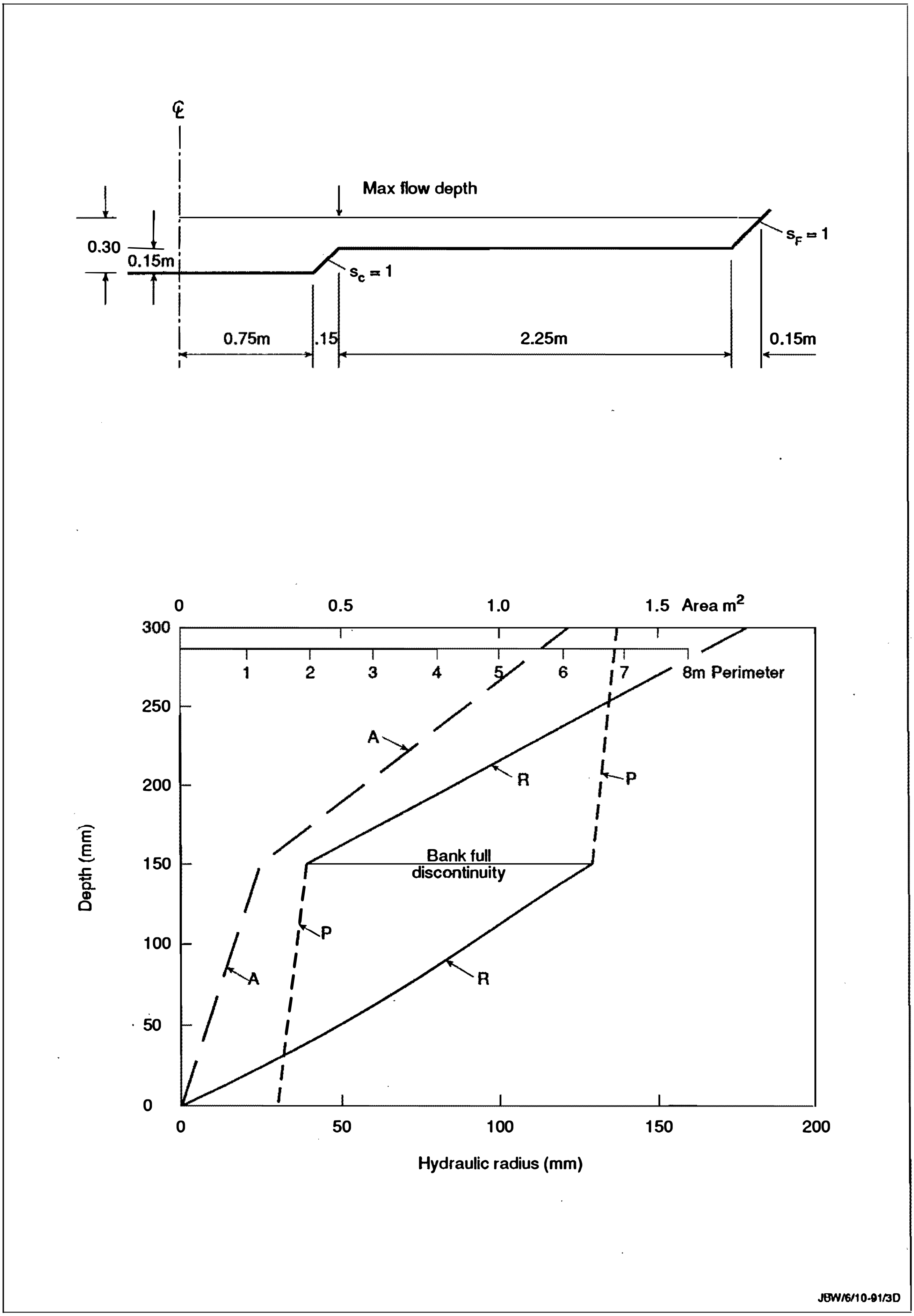

Fig 2.3 Flood Channel Facility at Wallingford: (i) cross-section (ii) hydraulic parameters; cross-sectional area - A, wetted perimeter - P, hydraulic mean depth - R

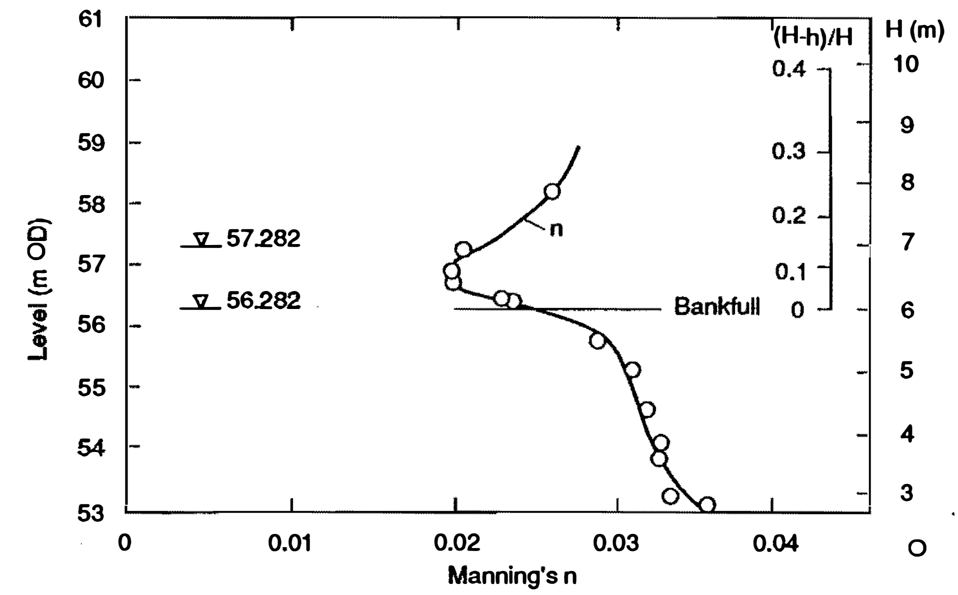

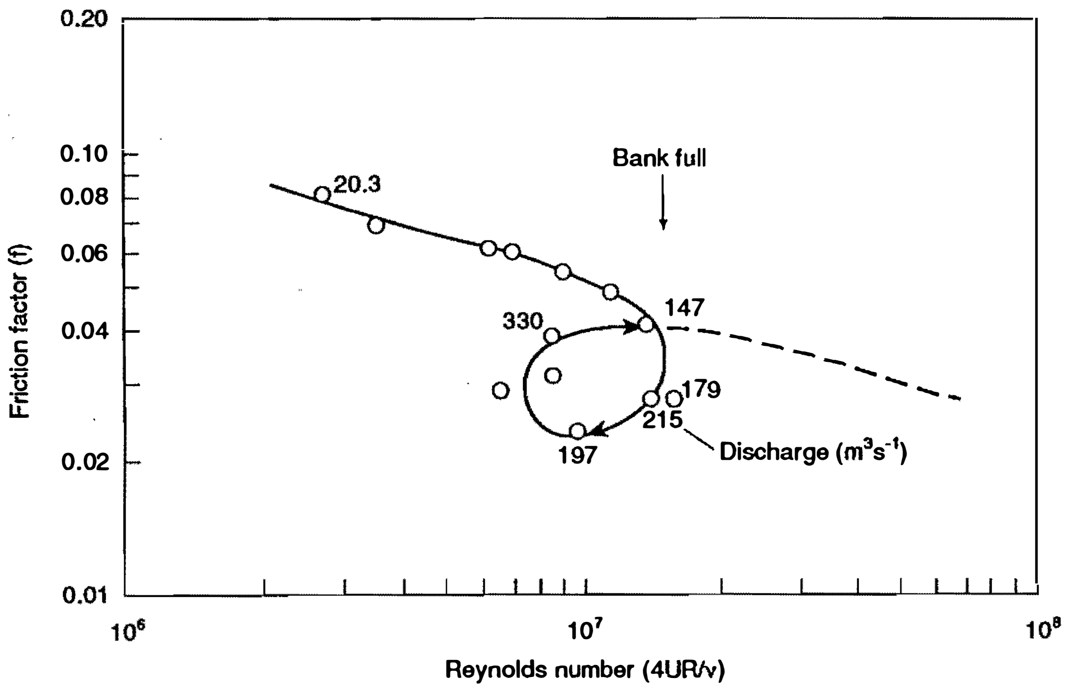

Fig 2.4 River Severn at Montford Bridge: (i) variation of apparent value of Manning's n with stage (ii) variation of friction factor - f, with Reynolds Number - Re. (Knight et al, 1989)

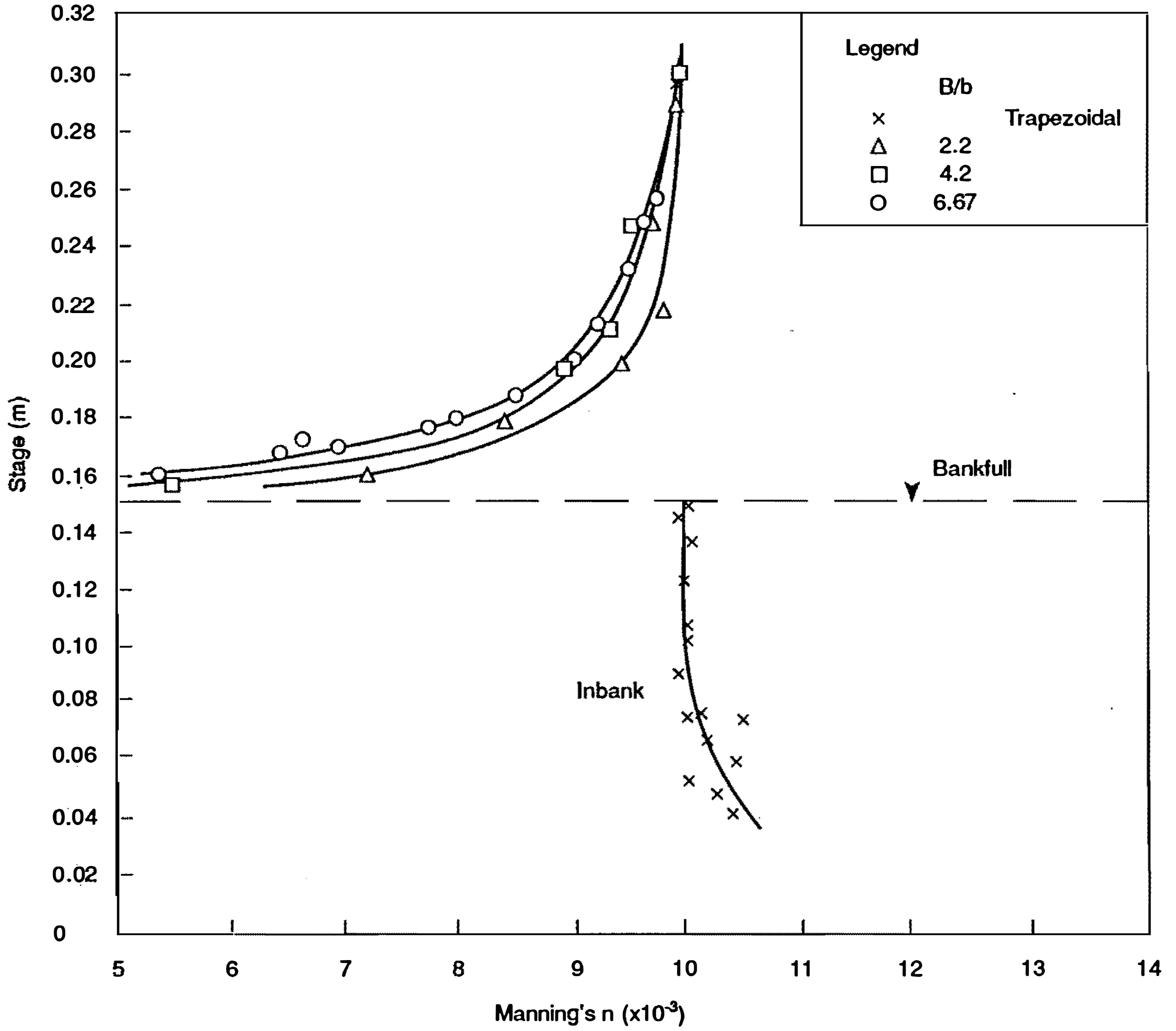

Fig 2.5 Flood Channel Facility at Wallingford: variation of apparent value of Manning's n with stage. (Myers and Brennan, 1990)

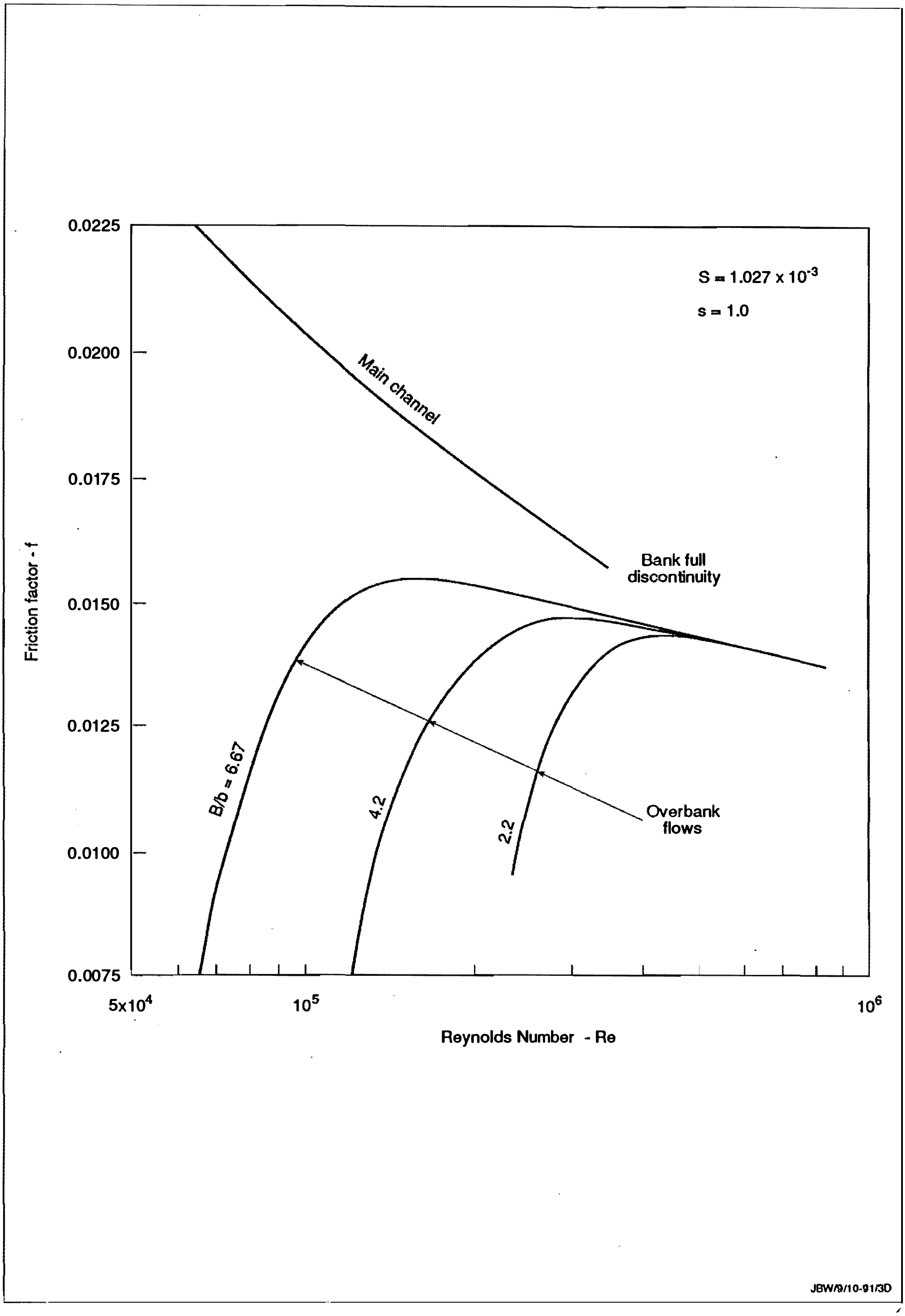

Fig 2.6 Flood Channel Facility at Wallingford: variation of friction factor - f with Reynolds Number - Re.

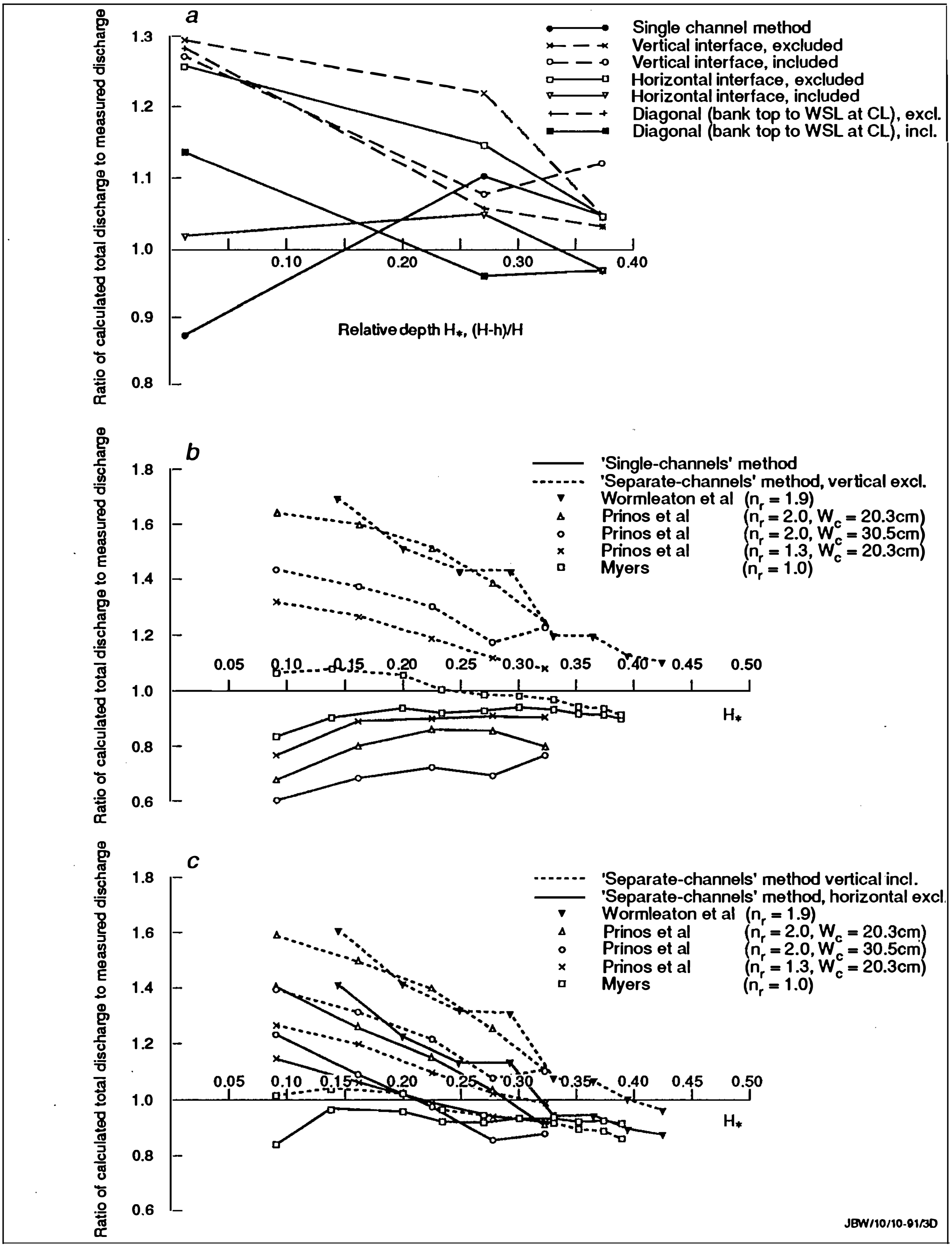

Fig 2.7 Various treatments of division between zones in calculation of total flow from basic zonal flows, in comparison with measured discharge.
(a) Nalluri and Judy (1985) data for assymetric channel, b = 0.195m, B = 0.695m, h = 0.15m, seven division methods.
(b) Results reported by Prinos and Townsend (1984), full line single channel with common average velocity, broken line vertical interface not included in wetted perimeter.
(c) Ditto, broken line vertical interface included in wetted perimeter, full line horizontal interface not included.

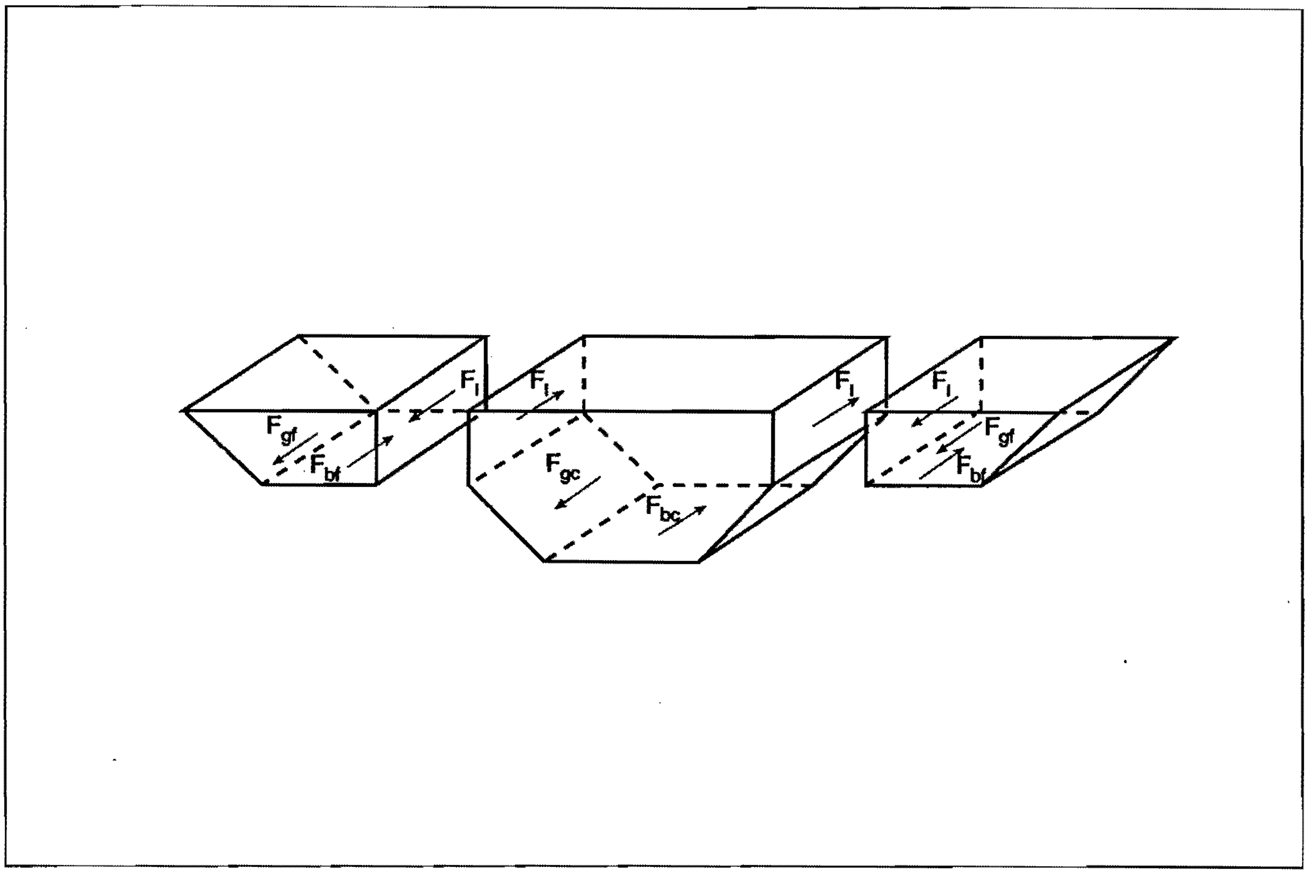

Fig 2.8 Balance of forces in elements of a vertical sided compound channel. (Wormleaton and Merret, 1990)

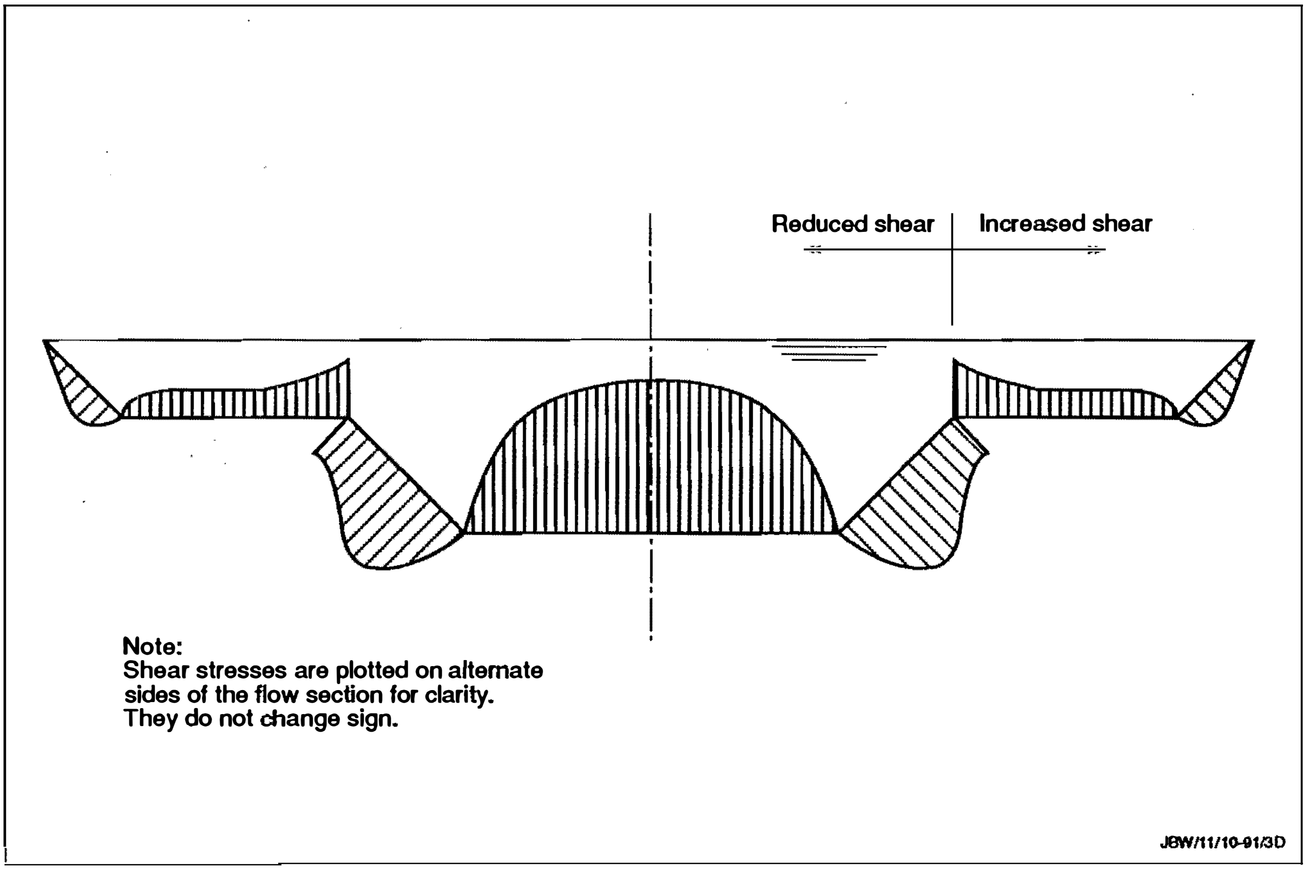

Fig 2.9 Sketch of boundary shear stress distribution in compound channel

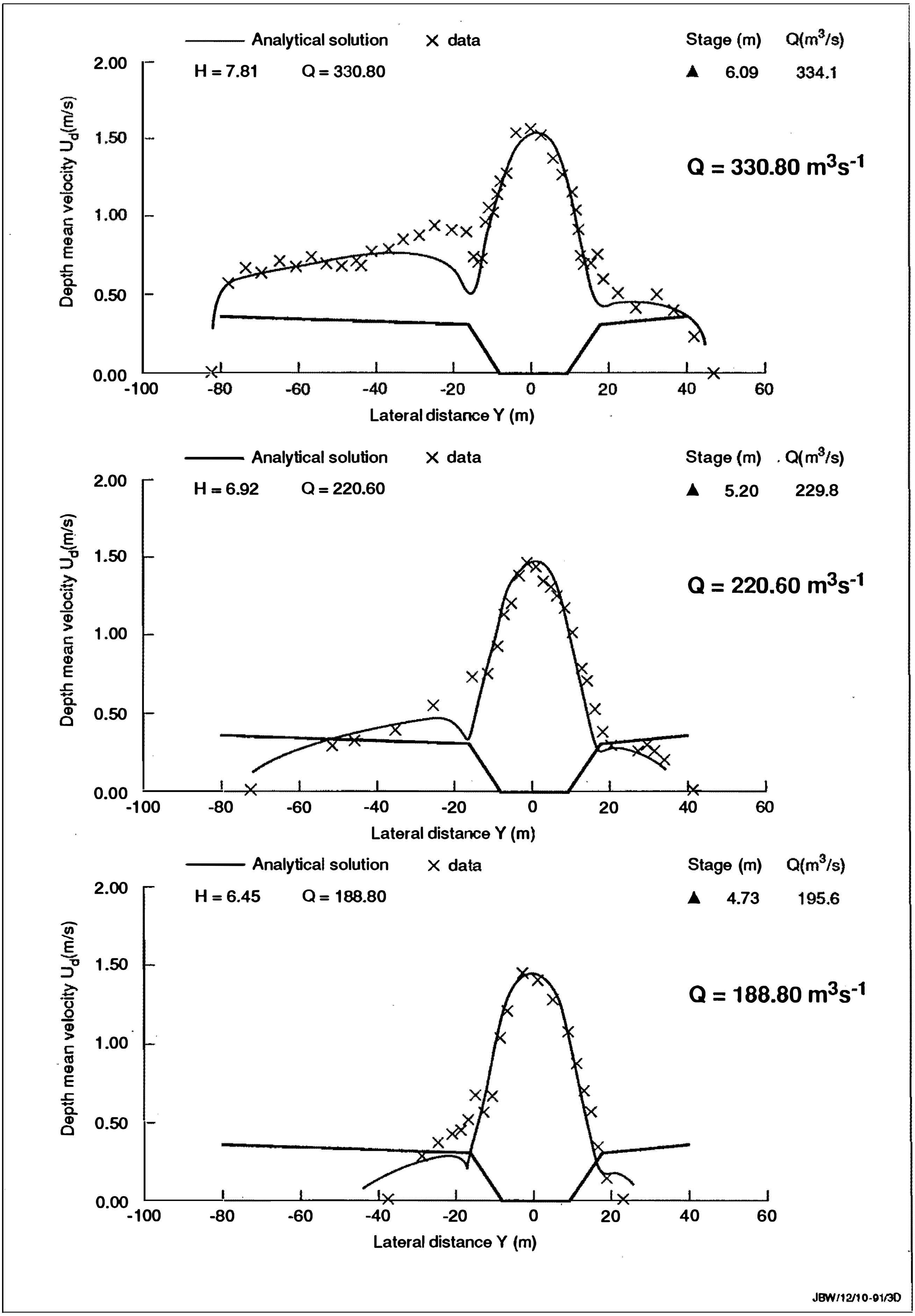

Fig 2.10 Depth mean velocities deduced from Knight et al model compared with field data from Montford Bridge

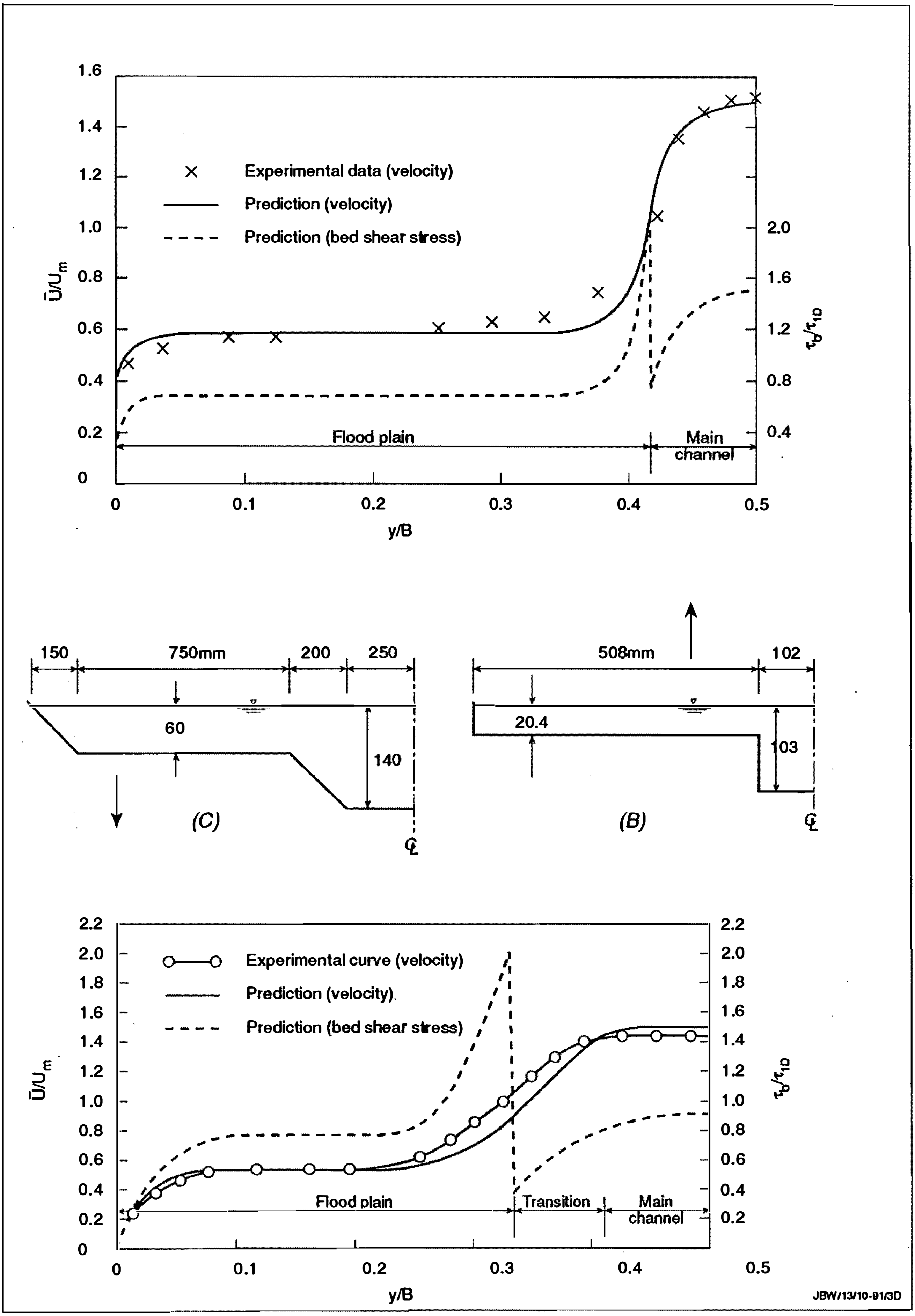

Fig 2.11 Velocity and shear stress predictions compared with laboratory measurements, by Keller and Rodi K-ε model

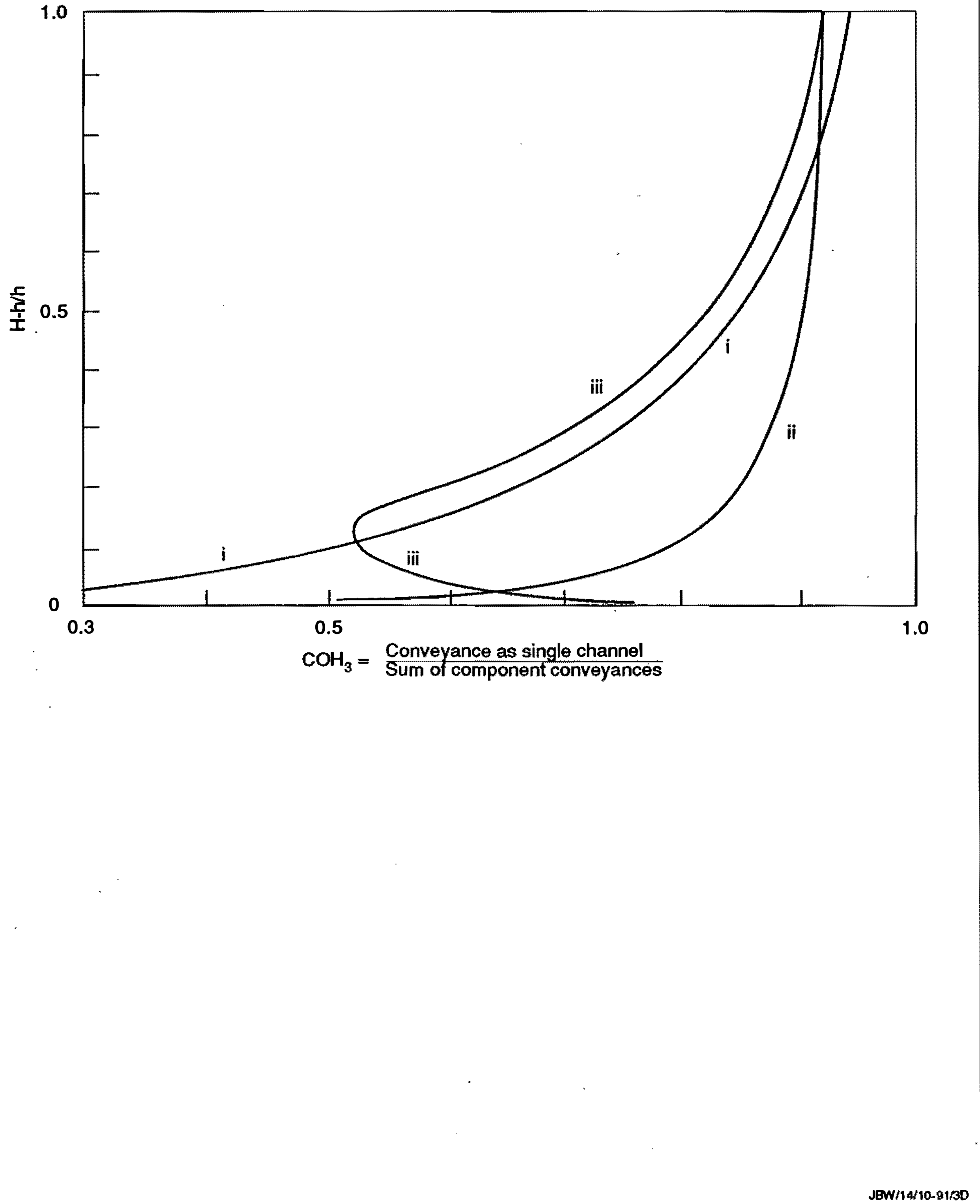

Fig 2.12 Channel coherence - COH_3, as function of ratio of flood plain flow depth to main channel depth: (i) wide horizontal flood plains; (ii) narrow horizontal flood plains; (iii) natural river channel with sloping flood plains.

3. HYDRAULIC DESIGN BASED ON EXPERIMENTAL ADJUSTMENT FACTORS

3.1 Research at Wallingford

3.1.1 With the exception of some large-scale tests several years ago in an outdoor facility in America (US WES, 1956) most of the work to date on compound channels had taken place in various laboratory channels in universities, between 6 and 15 m in length and between 0.6 and 1.2 m wide. These were often too small for a realistic flood plain width to be simulated, and at a scale which gave shallow flood plain flows and low Reynolds numbers so that fully turbulent flow may not always have been achieved. For this reason, it was decided to concentrate newly available special UK resources in a large central facility. The SERC Flood Channel Facility (SERC-FCF) was jointly funded by the Science and Engineering Research Council and Hydraulics Research Ltd, (HR, Wallingford) at whose premises the equipment was built. The research program was organised as a series of individual but closely co-ordinated projects, largely but not exclusively funded by SERC. The research carried out at this national centre for flood channel research has been instrumental in providing an unique set of large scale data, which are both accurate and comprehensive.

3.1.2 The facility at Wallingford provided a channel 56m long with total width 10m, with discharge up to $1.08m^3/s$. The layout of the flume is shown in Figure 3.1 and Plate 1. It was fully instrumented for measurement of water levels (hence hydraulic gradient), discharge (by standard orifice meters), velocity traverses using miniature propeller meters, boundary shear stress (by Preston tube), three dimensional flow patterns and turbulence measurements, using laser anemometry. Many of the measurements involved computer control of the instruments themselves, as well as sophisticated data logging.

3.1.3 It would not have been practicable within the funds available to make the slope of the facility adjustable. Hence all experiments were with fixed channel gradient of nominally 1 in 1000. The channel depth in the first series of experiments on straight channels was kept at 0.15m and maximimum flow depth was 0.30m, expected to cover the main region of adverse interaction between the flow zones. The bed width of the deep channel was 1.5m in all these tests, but flood plain widths, and channel and flood plain bank slopes, were varied. Table 3.1 shows the various geometries used in the Series A tests on straight channels. Most of the research was with channel and flood plains formed of smooth cement mortar, but some tests were also made with the flood plains roughened by rods through the full depth of flow (see Plate 2). Later series of tests concerned skew and meandering channels (see Plates 3 and 4), and also dispersion.

3.1.4 Preliminary tests were conducted to establish the appropriate resistance function for the cement mortar surfaces, and also for the rod-roughened flood plains. The former included tests at depths above the normal bank full condition of 0.15m depth, having extended the banks upwards to give a simple trapezoidal cross-section 0.3m deep. The results of these calibrations are reported in Appendix 2.

3.2 Other sources of experimental data

3.2.1 Other sources of information were also utilised in extending the data base of stage/discharge information for compound channels. This additional data came from the following publications in the research literature:

Asano, Hashimoto and Fujita, 1985
Ervine and Jasem, 1991
Kiely, 1991
Knight, Demetriou and Hamed, 1984
Knight and Demetriou, 1983
Myers, 1978, 1984, 1985
Prinos and Townsend, 1983, 1984
US WES, U S Waterways Experiment Station, 1956
Wormleaton, Allen and Hadjipanos, 1982

References are given in Chapter 12, Volume 2.

3.2.2 These tests in hydraulics laboratories covered a wide range of conditions, both in terms of geometry and roughness ratio between main channel and flood plain. The range of main channel width/depth ratios was from 1.3 to 30; overall width ratio B/b up to 30; gradients from 0.22 to 1.8/1000; and flood plain roughnesses up to three times the main channel value, in terms of Manning's n. However, much of this research was carried out in University hydraulics laboratories, and so was of relatively small scale. In order to avoid severe Reynold's number effects e.g. possibly laminar flow, as well as measurement difficulties, depths had to be kept relatively high compared with widths. There is thus a dominance of work at channel aspect ratios of the order of two, far removed from the usual range of practical compound channels, and certainly far different from rivers with flood plains. The exception to this is the research by Asano and colleagues, who used a range of channel aspect ratios based on an analysis of rivers in Japan. This is the only work at aspect ratios greater than than ten, as used in the FCF at Wallingford. The Japanese rivers show a dominant aspect ratio between 20 and 30; and a dominant B/b ratio of 3 to 5. These values may be representative of many alluvial rivers of modest size in the UK too.

3.2.3 The largest scale studies other than those in the FCF were the limited series of tests at Vicksburg, at the US Waterways Experiment Station. These were conducted in an out-of-doors 9m wide flume, and included tests with flood plains roughened by the addition of sheets of expanded metal.

3.2.4 The criterion for choosing data for analysis was largely the availability of a set of stage-discharge results, though the information given was not always as comprehensive as required for reliable analysis. Typical gaps in published information are accurate resistance functions for both the main channel and flood plains, without which interpretation of the stage-discharge data in the context of determining corrections to basic zonal computation procedure is very problematical. This is especially so where artificial roughness is used on the flood plains. Another typical gap in information is the water temperature. Much of the research was with smooth surfaced cross-sections, so water temperature is required to estimate the fluid viscosity, which is relevant in smooth - and fairly smooth - turbulent flow conditions. The published papers are dominated by the use of the Manning formula, whether for smooth or rough conditions. This resistance formula is most appropriate for rough turbulent conditions, though it can represent smooth conditions in an open channel system at a given gradient reasonably well, with the coefficient n then taking on some of the role of Reynolds number and hydraulic gradient (see Appendix 2). However, with the forms of artificial roughness typically used, it can not be assumed that quoted values of Manning's n are accurate over a range of depths.

3.2.5 There have been many research projects on compound channels, so not all data from past research could be included in the analyses. In one or two cases, the research was at too small scale or at geometries too far removed from practical conditions to be considered worth following up anyway. In other cases there was a lack of basic information that could not be resolved through correspondence with the research group. The aim of the analysis of stage/ discharge data from other sources was essentially to validate the predictive formulae obtained from the FCF research, by applying those results to quite different geometries and roughness conditions. This work is fully described in Chapter 5, where it is used to validate, and in certain respects further calibrate, the methods of predicting stage discharge developed in this Chapter.

3.3 Recommended basic method

3.3.1 Hydraulic design methods previously described in the extensive literature on compound channels were reviewed earlier, and it was concluded that for engineering purposes the most appropriate method would be to make separate calculations for the main channel and flood plain and to adjust the sum of these zonal calculations for interference effects to provide the overall discharge at the chosen flow depth. The adjustments required are in essence empirical coefficients derived from experimental work, especially the definitive results from the FCF at Wallingford. By carrying out the analysis within a non-dimensional framework, general adjustment factors were anticipated that could be transferred to other sizes of channel, and other roughnesses, including of course field scale systems.

3.3.2 The dimensional analysis given in Appendix 1 indicated an appropriate line of attack, deducing the main parameters upon which the interaction effect was expected to depend. These were reviewed earlier and, for a smooth channel and flood plain as in most of the tests at Wallingford, reduce to:

$(H-h)/H$:	relative depth of flood plain flow to main channel flow
b_C'/H:	width/depth ratio of main channel
$b_F'/(H-h)$:	width/depth ratio of flood plain flow

s_C: side slope of main channel
s_F: side slope of flood plain
Re_C: main channel Reynolds Number
Re_F: flood plain Reynolds Number

The nomenclature is illustrated in Figure 2.1 and is defined in section 13 of Volume 2. Note that width/depth ratio is also referred to as 'aspect ratio'.

3.3.3 The experimental constraints meant that with a fixed channel slope and single value of main channel depth, the two Reynolds Numbers depend directly on flow depth and hence on (H-h)/H. Reynolds number could not be varied independently but in any event the main viscous influence would be accounted for in the computation of basic zonal flows. The width/depth ratio (also referred to as the aspect ratio) of the main channel was not adjusted (except as a secondary consequence of changing the main channel side slopes), and this was a significant constraint. In most tests the flood plain side slope was fixed at 1 in 1, though this was not an important factor. Thus the experiments on smooth channels are fully covered by a reduced set of dimensionless *independent* variables: relative depth, ratio of flood plain width to main channel width, and channel side slope. The experiments with roughened flood plains bring in an additional parameter, accommodated as a ratio of main channel and flood plain friction factors.

3.3.4 The influence on the flow of the interaction between main channel and flood plain flows depends on how comparable the hydraulic conditions in these zones are: if velocities and depths are very similar, then we can expect interaction effects to be small; if they are very dissimilar, then major effects are to be expected. The degree to which the different zones exhibit flow similarity is referred to as their "coherence": the greater their coherence (unity being the maximum value) the more likely is the hydraulics of the section to approach simple channel (negligible interaction) conditions. The development of this concept is explained in Appendix 2.3. Several different formulations were considered, although all incorporated the basic definition:

3.3.6 If the Manning equation applies, and perimeter weighting of the friction factor is applied, then the coherence equation becomes:

"Coherence is the ratio of the conveyance calculated as a single cross-section to that calculated by summing the conveyances of the separate flow zones"

These calculated values come from a standard friction formula before making any allowance for interference effects.

3.3.4 The treatment as a single section requires some assumption about the overall resistance, and for this purpose the perimeter weighted friction factor is used, deduced from the separate (and calculable) values for main channel and flood plains.

$$COH = \frac{\sum_{i=1}^{i=n} A_i \sqrt{\left[\sum_{i=1}^{i=n} A_i / \sum_{i=1}^{i=n} (f_i P_i)\right]}}{\sum_{i=1}^{i=n} \left[A_i \sqrt{(A_i / f_i P_i)}\right]} \qquad \ldots 3.1$$

In the above i identifies each of the flow zones, and in the basic case of a trapezoidal channel with two flood plains n = 3. Note that this is the form denoted COH_3 in Appendix 3.

3.3.5 For a conventional compound cross-section geometry, the coherence of the section may be expressed in terms of the geometric ratios: let $A_* = N_F A_F / A_C$; $P_* = N_F P_F / P_C$; $H_* = (H-h)/H$; and $f_* = f_F / f_C$, where N_F is the number of flood plains. Then

$$COH = \frac{(1 + A_*)\sqrt{[(1 + A_*)/(1 + f_* P_*)]}}{1 + A_* \sqrt{(A_* / f_* P_*)}} \qquad \ldots 3.2$$

In this form it is obvious that as A_* becomes large (deep flow on flood plain) then COH approaches unity, for equal roughness of main channel and flood plain (when f_* approaches unity as the depth increases). Also when A_* is very small (flood plains just inundated) COH approaches $1/(1 + f_* P_*)$. As A_* and P_* depend on H_*, then for a given geometry COH also depends on H_*.

$$COH_2 = \frac{(1 + A_*)^{3/2}/\sqrt{(1 + P_*^{4/3}n_*^2/A_*^{1/3})}}{1 + A_*^{5/3}/n_*P_*^{2/3}} \quad \text{... 3.3}$$

3.3.7 As will emerge later, the most general formula for channel coherence (equation 3.1) provides a useful co-ordinating parameter in the analysis of the experimental results. Its benefit is that it brings together in one parameter most of the factors expected to influence the hydraulics of compound channels, and so can take the place of relative depth as an indicator of how like a single channel the performance might prove. A corollary is that the closer to unity COH approaches, the more likely it is that the channel can be treated as a single unit, using the overall geometry. As f_* is included in the general definition of COH (see equ 3.2), dissimilar roughnesses are within its scope. COH is thus an independent variable calculated from the known geometry and basic resistance function that may take the place of other independent variables (relative depth, side slope etc.).

3.3.8 The dimensional analysis of Appendix 1 envisages several alternative dependent variables that could provide the adjustment needed to the zonal calculation of discharge. These alternatives were tested, to see which provided the most appropriate explanation of the test results and which would therefore provide a good basis of design. Of course in the design situation, the zonal calculations would be based on the engineer's favoured resistance function with resistance coefficient appropriate to the known surface texture. The zonal calculations of discharge for the research results at any given flow depth are well specified as a result of the series of tests to establish the resistance functions for the smooth and rough conditions. The relevant smooth equation was as follows:

$$1/\sqrt{f} = 2.02 \log (Re\sqrt{f}) - 1.38 \quad \text{... 3.4}$$

and the calculation for rod roughness is explained in Appendix 2.

3.3.9 Fuller details of the analyses of experimental results will be found elsewhere (Technical Report Number 4, Oct 1990, unpublished information). In what follows, the main thrust of the analysis is described but only the successful lines of attack in what was a complex sequence of testing of alternatives will be detailed.

3.4. Analysis of experimental results

General

3.4.1 Table 3.1 lists the tests carried out on straight aligned channels at Wallingford. It shows their geometries and the number of stage/discharge results available in each series, with flow above bank height. These experiments were designed so that they could be grouped in various ways to demonstrate the effect of relevant parameters in turn. Thus series 1, 2, 3 and 5 cover a range of different flood plain widths, with main channel bank slope of 1:1. This bank slope also applied to the flood plain edge with the exception of series 1, at maximum flood plain width, when in any case its influence would be minimal. Tests 2, 8 and 10 kept flood plain width constant but covered main channel bank slopes of 0, 1 and 2 (horizontal/vertical). The flood plain was edged at a slope of 1 in all these cases. Tests 2 and 6 provide a comparison between the symmetric case of twin flood plains and the asymmetric case of a single flood plain. Tests 2 and 7, 8 and 9, 10 and 11 are pairs with the odd numbers having rod roughened flood plains to compare with the even numbered smooth cases.

3.4.2 The basis of analysis was through a comparison of the total discharge calculated from zones separated by vertical divisions with the measured discharge at that depth of flow. Alternative parameters were considered to establish their relevance and significance. Flow depth was represented in three alternative ways:

- relative depth, $(H-h)/H = H_*$
- ratio of flood plain flow depth to depth of main channel, $(H-h)/h$
- channel coherence, COH, as defined in para 3.3.5 and equ 3.2.

The second of these parameters for depth of flood plain inundation was soon abandoned as the first, defined as relative depth H_*, gave clearer, more linear functions.

3.4.3 The discrepancy between the basic calculation and the measured flow was parameterised in five ways:

- adjustment factor, measured discharge/basic calculation, DISADF
- proportionate discharge deficit, $(Q_{CALC} - Q_{MEAS})/Q_{CALC}$, DISDEFP
- discharge deficit as proportion of bank full flow, DISDEFBF
- discharge deficit normalised by the calculated velocity difference and the product of flood plain flow depth and main channel depth,
  $Q_{*1} = (Q_{CALC} - Q_{MEAS})/(V_C - V_F)(H-h)h$
- the same apart from using the product of total flow depth and main channel depth, $Q_{*2} = (Q_{CALC} - Q_{MEAS})/(V_C - V_F)\ H\ h$

The philosophy behind these parameters was developed in Appendix 1: Q_{*1} and Q_{*2} incorporate the main channel depth, h, on the basis that width of the zone of influence would be related to channel depth rather than channel width if the system was effectively wide (2b/h and 2B/H very large). h is coupled with (H-h) or H to yield a plausible cross-sectional area of influence, to couple with the velocity difference between main channel and flood plain as an indicator of the scale of influence - and, of course, providing the requisite dimensions. Q_{*1} and Q_{*2} are both very similar non-dimensional expressions for the discharge deficit due to interference effects (hence the * subscript) but Q_{*2} was found more useful: Q_{*1} has been discarded therefore from what follows.

Regions of flow

3.4.4 It is well established, mainly but not only from the FCF results, that the magnitude of the interference between the channel flow and main channel flow shows different trends as the flow depth varies. As an example, Figure 3.2 shows the stage-discharge results for geometry 2, with B/b = 4.20. The test results were first assembled in order of increasing depth and then running averages of three were taken to smooth out scatter arising from random experimental errors. (This smoothing process was generally used: all data shown is of this type unless otherwise stated.) This figure shows the factor by which the sum of the calculated zonal flows has to be multiplied to agree with the total discharge measured in the supply pipes (DISADF), plotted against relative depth. The flow passes through three distinct regions of behaviour:

- *Region 1* is at relatively shallow depths where the interference effects progressively increase with depth up to relative depth 0.2, when the "loss" of conveyance is over 10 percent.

- *Region 2* covers depth ratios to 0.4 for this particular geometry, with the interference effect diminishing towards a discharge loss of about 4 percent.

- *Region 3* occurs with further increase in depth, which again increases the interference effect, presumably because of some change in secondary currents.

- Also shown on Figure 2 is COH, and it will be seen that DISADF always lies between COH and unity, ie always exceeds the "single channel" computation but is less than the sum of the zonal computations. It seems possible that, had experiments been continued to greater depths, they would have followed the COH function, ie a single channel computation becomes appropriate at considerable depths of flood berm inundation. This forms *Region 4*.

3.4.5 The depth limitations between the regions shown in the sample plot of Figure 3.2 are not general; they depend on various parameters, and differ considerably with rougher flood plains: nor can it be assumed at this stage that if $(H-h)/h > 0.5$, the interference effects are negligible. What is clear, however, is that different flow regions exist, and different design formulae are required for each zone, as well as the means for establishing which region a particular design case will lie within.

Influence of flow depth and flood plain width

3.4.6 The discharge adjustment factor, DISADF, has the merit of illustrating directly the magnitude of the interference effect, and its variation with flow depth and flood plain/main channel width ratio. DISADF is shown plotted against the relative depth, $(H-h)/H$, in Figure 3.3. The four cases tested show related variations of DISADF with depth ratio, but the trends are discontinuous due to the different regions of flow. Taking test 2, $B/b_C = 4.2$, from $(H-h)/H = 0$ to 0.20, (region 1), DISADF reduces from unity when the flow first reaches the flood plain to a minimum value of

0.895: in other words, at this minimum condition the actual flow is some 11% less than calculated by adding the separate zonal figures. As (H-h)/H rises from 0.20 to 0.40, (region 2), DISADF tends back towards unity, rising in fact to 0.965: in other words the zonal calculation becomes more accurate, but never better than within say 3%. There is a kink in the trend at (H-h)/H = 0.40, towards lower values of DISADF again, with a value of 0.94 when (H-h)/H = 0.50. (Region 3). This complex pattern is well established: the other cases show rather similar features.

3.4.7 It is of interest at this stage to see what might be learned from the channel coherence, as defined earlier. Values of COH for these cases have been plotted on Figure 3.4, to the same scales as Figure 3.3 - but note the different range of depths. A comparison with the experimental results shows that in all cases DISADF lies between COH and unity. This means that a single channel basis of calculation provides a lower boundary to the channel conveyance and the zonal calculation provides an upper boundary. What is required is a group of relationships, covering the different flow regions, to show where between these limits the true value lies.

3.4.8 Figure 3.5 illustrates the different regions of flow in terms of relative depth, (H-h)/H, with the bounding value of DISADF = COH. This is a generalised diagram so is un-scaled. The four flow regions are indicated, though in some cases 2 and 4 might almost link together as 3 diminishes. Starting at shallow flood plain depths,

Region 1 is at relatively shallow depths on the flood plain, with interference increasing broadly in proportion to flood plain flow depth. The extent of region 1 depends on the flood plain width, narrow flood plains permitting it to extend to deeper flows.

Region 2 is where the trend of DISADF is similar to but lies below the COH function. The section is behaving more like a single channel, but interference between flood plain and main channel adds to resistance.

Region 3 which is most apparent with wide flood plains, indicates a change of flow pattern (in secondary currents for example) which gives rise to diminishing interference.

Region 4 is at relative depths large enough for it to be possible to treat the cross-section as a single zone, with perimeter weighting of the friction factor, when calculating the stage/discharge function. This is so when COH > 0.95 or thereabouts.

3.4.9 DISADF has been plotted against COH for these four cases of varying flood plain width in Figure 3.6. The line DISADF = COH is the result given by a single channel calculation, with overall friction factor calculated from the perimeter weighted zonal values. The results for greatest depth approach this condition, but have not extended to sufficient depth to confirm it. It appears probable that a single channel calculation becomes acceptable at a depth ratio (H-h)/H exceeding 0.5, ie when the depth of flow over the flood plain is somewhat greater than the depth of the main channel. (It will emerge later that this very definitely does not apply when the flood plains are rougher than the main channel). The different trends in the flow regions are also identifiable in this plot. The four regions will be considered in turn, beginning with the performance relevant with fairly shallow flood plain flows.

Region 1

3.4.10 At very shallow depths on the flood plain, the Reynolds number is below the usual values considered necessary for turbulent flow: at a flood plain depth of 0.10m ($H_* = (H-h)/H = 0.0625$), $Re_F = 4500$, so results for $H_* < 0.0625$ have been disregarded.

3.4.11 Although the parameters DISADF, DISDEFBF and Q_{*1} were also considered, the Q_{*2} version of the discharge deficit was found most useful in representing Region 1. One of ite advantages is that it provides linear functions with the relative depth, $H_* = (H-h)/H$, as in fig 3.7, where parallel lines provide a good fit to the experimental results:

$$B/b = 6.667: Q_{*2} = 0.89 + 9.48 H_* \quad \ldots 3.5$$

$$B/b = 4.2: Q_{*2} = 0.14 + 9.48 H_* \quad \ldots 3.6$$

$$B/b = 2.2: Q_{*2} = - 0.58 + 9.48 H_* \quad \ldots 3.7$$

These are approximately linear with B/b:

$$Q_{*2} = - 1.240 + 0.329 \text{ B/b} + 9.48 \text{ H}_* \qquad \text{... 3.8}$$

The lower limit of application should probably ensure that Q_{*2} is not allowed to be negative at shallow depths: there would never be an addition to the calculated total discharge. The upper limit of applicability of these Region 1 functions will be given by intersection with the function for region 2, which is considered next.

Region 2

3.4.12 Region 2 is at increased depths where the interference effects diminish progressively, and extends to the depth at which the discharge adjustment factor tends to kink back towards lower values again. The discharge adjustment factor was seen to have a somewhat similar trend to the channel coherence in region 2: for the four width ratios treated here, figure 3.4 shows that the COH values interlace somewhat, and the experimental values of DISADF interlace in much the same way in flow region 2 (Fig 3.3). It is a strange finding that on the plots against H_*, the COH functions provide a convincing fit to the DISADF results, *provided* they are overlain with a vertical shift in (H-h)/H of about 0.15. There seems to be no physical explanation of this: it is a rather obscure empirical result.

3.4.13 In its functional form, the channel coherence may be written as:

$$\text{COH (H*, channel geometry) = function (H*, A*, P*, f*)} \qquad \text{... 3.9}$$

Thus the empirical finding implying a shift of 0.15 in H_* can be written as:

$$\text{DISADF}(H_*, \text{ channel geometry}) = \text{COH } ([H_* + 0.15], \text{ channel geometry}) \quad \text{... 3.10}$$

This states that a calculation of COH at $H_* + 0.15$ does duty as DISADF for H_*. The lower limit of application of the above (region 2 of the performance) is provided by its intersection with region 1: the upper limit is formed by its intersection with region 3.

Region 3

3.4.14 Although this limited region of a return to increasing interference with flow depth is not clearly defined in all test series, it appears from Figure 3.6 to be best explained as:

$$DISADF = 1.567 - 0.667\ COH \quad \ldots\ 3.11$$

This result may have been influenced by one or too extraneous results, so this point will be reconsidered later in the light of other results.

Region 4

3.4.15 Region 4 is essentially defined as being when the channel is sufficiently coherent for it to be treated hydraulically as a one unit: in other words, stage discharge computations need not be built up from separate zonal calculations. The definition effectively provides its governing equation:

$$DISADF = COH \quad \ldots\ 3.12$$

and this has been shown on figure 3.6. The FCF tests did not extend to depths sufficient to provide good confirmation but none of the data indicated that DISADF ever exceeded COH.

Influence of channel side slope

3.4.16 Three tests were carried out to examine the effect of channel side slope, test series 02, 08 and 10, with s_C respectively 1, 0 and 2. (s_F = 1 in each case). These were all with the same actual flood plain width as well as the same main channel bed width, b_F/b = 2.25/0.75 = 3. In consequence the ratio B/b varied, being respectively 4.2, 4.0 and 4.4. Considering the shallower range of flows of region 1 first, figure 3.8 shows the Q_{*2} results. The range of the data is narrow, showing that the influence of bank slope on Q_{*2} is modest. Equation 3.8 has been shown on Figure 3.8 (full lines) for the bounding values of B/b, 4.0 and 4.4 corresponding to tests 8 and 10 respectively. However, the experimental data tend to have the inverse correlation: test 8 agrees better with B/b = 4.4 and test 10 with B/b = 4.0. This suggests that an adjustment is required to allow for dependency on bank slope.

3.4.17 The direct correlation of B/b with bank slope can be inverted, however, by using a width ratio based on half top width of main channel, w_C. Equation 3.8 then becomes:

$$Q_{*2} = -1.240 + 0.395\ B/w_C + 9.48\ H_* \qquad \ldots\ 3.13$$

and this is shown by broken lines on Figure 3.8 for the bounding values of B/w_C, 4.0 and 3.14 for tests 8 and 10 respectively; but now in the desired sequence to agree with the experimental trend. This suggests that expressing the width ratio in terms of the top width of the main channel rather than its bed width is more appropriate.

3.4.18 Figure 3.9 shows DISADF against H_* for all flow regions but within region 2 (H_* broadly from 0.27 to 0.37) the plots for the three side slopes come close together. Region 1 clearly differs but that region is best covered by Q_{*2}. The upper bound of region 2 also seems to vary somewhat with s_C as do regions 3 and 4 when plotted as DISADF against H_*. Figure 3.10 shows the calculated values of COH plotted to the same scales. Series 02 and 10 show good agreement when shifted vertically by 0.15 in H_* value, but it appears that series 08, for $s_C = 0$, rectangular main channel, requires a shift in H_* of, 0.09 rather than 0.15 for good agreement. This is not surprising perhaps: the behaviour in terms of momentum transfer may indeed be changed with a square bank top from that applying with a more gentle transition between channel and flood plain.

3.4.19 Looking at Figures 3.9 and 3.3 together, there is a question about how best to represent Region 3. Although test series 01 and 02 showed a pronounced backward kink in DISADF in region 3, this is not confirmed by tests 10 and 8. Is the backward kink in tests 01 and 02 a somewhat spurious result of just a few data points being away from the real trend? The data for tests 08 and 10 indicate not a backward kink so much as a vertical transition at about DISADF = 0.94, whilst tests 03 and 05 (narrow flood plains) hardly show a region 3, going fairly directly from region 2 to 4 at similar value of DISADF. 0.955 would be an appropriate average for region 3 for tests 01 and 02.

3.4.20 It may be more appropriate therefore to take region 3 as providing

$$DISADF = 0.95 \qquad \ldots\ 3.14$$

the upper bound of the region being when COH = 0.95, and the lower bound defined by comparing with the region 2 calculation: if the region 2 calculation gives DISADF > 0.95, then region 3 (or 4) applies. The question of which formula is best for region 3, 3.14 or 3.18, will be returned to later. There is no evidence that either region 2 or 3 is sensitive to bank slope,

Influence of asymmetry

3.4.21 Figure 3.11 shows the comparable symmetric and asymmetric tests, 02 and 06, in the form of Q_{*2} against H_*. Equation 3.8 was deduced from the tests with varying flood plain width and was then tuned to agree with the tests with different side slopes, equation 3.12. Provided B is still defined as half the channel plus flood plain width at flood plain elevation, the same equation also takes care of asymmetry, the relevant values of B/w_C being 3.50 for the symmetric case (02) and 2.25 for the asymmetric case (06). Q_{*2} thus proves to be a robust parameter for region 1, being dependent linearly on H_* and B/w_C, but not sensitive to s_C or the presence of one or two flood plains.

3.4.22 Figure 3.12 shows DISADF against H_*, for comparison with the "COH shift" method. The asymmetric tests series 06 is included in Figure 3.10, and demonstrates that the calculation of COH is affected by the number of flood plains. However, the experimental data in Figure 3.12 show little difference between the two cases in region 2 and the conclusion is that the shift in H_* required is different when the channel is asymmetric: 0.10 would be the appropriate value to use in the procedure of equation 3.10.

3.4.23 With asymmetry, Figure 3.12 suggests that region 3 may be treated as a zone where DISADF = constant and as before 0.95 is an appropriate value. Region 4, (DISADF = COH, hence apply single channel procedures), was not really entered in the asymmetric tests, as in all other cases.

3.5 Separation of main channel and flood plain effects

3.5.1 The detailed information obtained on velocity distribution provided a basis for assessing the discharges over the main channel and flood plain zones separately. The sum of these "velocity traverse" discharges generally agreed to within one or two percent of the discharge measured by the orifice meters in the supply lines, but in general the velocity traverse data were then adjusted to agree with the total discharge given by the orifice meters. Because of the extensive data set obtained at each depth to cover its other uses in the research programme, detailed cross section information was obtained at relatively few depths, typically eight, the lowest of which was in any event suspect because of rather low flood plain Reynolds Numbers. Because of the fewer depths covered and their relatively wide spacing, no averaging of data was permissible.

3.5.2 Figure 3.13 shows the discharge adjustment factors required for the flood plain and main channel flows calculated separately, and typifies the data plots showing the separate influences of flow interaction on the two zones. This figure shows the three widths of smooth flood plain tested. Region 1 of the flow behaviour identified from the overall analysis extends up $H_* = 0.30$, 0.27 and 0.23 for series 01, 02 and 03 respectively. Region 2 follows up to $H_* = 0.39$ approx, with region 3 extending towards $H_* = 0.5$ or so. Unfortunately regions 2 and 3 were not well covered by the separate zonal information: there is perhaps only one data set near the boundaries of the higher flow regions, with insufficient evidence to establish trends within them.

3.5.3 Figure 3.19 clearly shows that the main channel discharge is hampered by the flood plain interference, to an increasing extent as flow depth rises through region 1. The maximum reduction in main channel flow is between 12 and 18% depending on B/b. Interference enhances the flood plain flows by a diminishing amount in region 1, reducing to some 3 to 13% (depending on B/b) at the upper limit of region 1. Thus region 1 is characterised by increasing effects on the main channel but decreasing effects on the flood plain as the flow depth increases.

3.5.4 Through regions 2 and 3, the separated flows confirm the general behaviour established from the stage-discharge data. On the flood plain, interaction effects appear to increase with increasing depth up to $H_* = 0.40$

(region 2) and decrease again to the maximum depth tested, whilst in the main channel the reverse happens. Looking at the separated zones also demonstrates that at maximum depth there is still significant interaction between the zones, even though the total discharge is by then close to that which would be predicted for the complete section using the perimeter weighted friction factor.

3.5.5 Figure 3.14 shows the non-dimensional discharge deficit, Q_{*2}, for both zones, and may be compared with the overall data in Figure 3.7. The main channel component dominates, being an order of magnitude greater than the flood plain component. Both vary linearly with H_* in region 1 (as did the composite value) and the relevant equations are:

$$Q_{*2F} = -0.64\ H_* \qquad \ldots\ 3.15$$

$$Q_{*2C} = Q_{*2} - 2\ Q_{*2F} \qquad \ldots\ 3.16$$

and so for consistency with equation 3.13:

$$Q_{*2C} = -1.240 + 0.395\ B/w_C + 10.76\ H_* \qquad \ldots\ 3.17$$

This has been added to Figure 3.14 and shows good agreement. Thus the separate discharge data confirms the overall data and shows the division of interference effect between main channel and flood plain.

3.5.6 Because of the sparse data in those regions, neither DISADF nor Q_{*2} information for the separate flow zones permits any deductions to be made for regions 2, 3 or 4, other than to confirm that the region 1 conclusions can not be extrapolated to greater depths of flow, and to indicate a somewhat stepped relation. Plots using COH as the vertical scale were also prepared for the separate data, but added nothing of value to the picture. COH was useful especially in region 2, 3 and 4, but there is insufficient separated data to confirm the equations derived from the total discharge information.

3.5.7 The results for several main channel bank slopes are shown in Figure 3.15 as DISADF against H_*. Adjustments required to both zones show an influence of bank slope. Test 08 had vertical banks which increased the proportionate effect on the main channel flow compared with tests 02 (s_C=1) and 10 (s_C=2) in region 1, becoming less clear cut at the increased depths of regions 2 and 3. Discounting the data at minimum flood plain depth, the vertical bank case diminished the influence on the flood plains at some depths, but the trend with bank slope is not obvious. One interesting feature of Figure 3.15 is the confirmation for all bank slopes of a quirk in flood plain behaviour at $H_* = 0.40$, about at the transition from region 2 to 3.

3.5.8 Figure 3.16 may be compared with figure 3.7: Q_{*2} versus H_* for these three bank slopes. Any influence of s_C on Q_{*2C} is satisfactorily eliminated by expressing the width ratio in terms of main channel top width. Equation 3.16 is shown for the two bounding values of B/w_C and represents the region 1 data well.

3.5.9 Q_{*2} is also an illuminating parameter for the asymmetric case: test 06 had one flood plain but was otherwise comparable with test 02. The results from the separate zones are shown on figure 3.17, and show that the discharge deficit on the flood plain is the same whether there is one or there are two. There is some difference in main channel influence however (despite some extra scatter in the asymmetric data): the main channel discharge deficit is reduced for the single flood plain, though not halved, but this appears fully explained by the difference in B/w_C.

3.5.10 Because there are few velocity/area data sets in regions 2 and 3, it has not been possible to establish formulae for adjusting the separate zonal flow calculations, though there had been sufficient stage/discharge measurements based on orifice meter readings in the supply pipes to establish adjustments to total flow in those higher regions of flow. There may, however, be occasions when an estimate of the flows in the separate zones is required for Regions 2, 3 and 4: this will be so if any sediment calculations are required (see Chapter 9). Figures 3.13 (various width ratios) and 3.15 (various bank slopes) suggest how this problem may be tackled, if only approximately. Despite some scatter in the plotted data, there does not seem to be much variation in $DISADF_C$, the adjustment to the main channel flow, at depths above the Region 1 limit. Hence it would be reasonable to retain the value of $DISADF_C$ at the limit of region 1 through regions 2 and 3. It should be mentioned that if the flood plains are appreciably rougher than the main channel, the problem does not arise, as flow stays in Region 1 for which $DISADF_C$ is calculable.

3.5.11 It might be thought that these tests with smooth channel and flood plains were unrealistic as most practical situations involve rough perimeters. However, they should be viewed as simulating equal roughness on flood plain as in main channel: the above tests represented equal values of Manning's n in all elements of cross-section. The methods of analysis used get round any limitation that might have arisen through using smooth, rather than rough, surfaces; and also remove any concern over scale effects.

3.6 Influence of flood plain roughness differing from main channel roughness

Form of additional roughness used

3.6.1 In certain of the tests at Wallingford the flood plains were roughened by surface piercing rods. The basic pattern used consisted of a triangular distribution of angle 60°, designed to have a density of 12 rods per m². The system of roughening is illustrated in Plate 2. All the roughened flood plain experiments were carried out with a flood plain bed width of 2.25m. A small number of tests were made with reduced roughness, by omitting every other rod from alternate rows. The rods were of 25mm diameter, made of timber but effectively smooth cylinders.

3.6.2 Preliminary tests were made to determine the actual resistance of the rod roughness. The hydraulic resistance is the sum of the drag of the rods and the friction arising from the smooth cement mortar finish of the solid channel surface, with allowance for the blockage effect of the rods. The friction arising from the channel boundary was assessed from the modified smooth turbulent equation used in the analyses already described.

The calibration analysis, and the resulting equations and calculation procedures, are given in Appendix 2. The method is general in the sense that it could be applied equally well to the alternative rod spacings used, and could take account of different numbers of rods in alternate rows.

3.6.3 The rod roughness provided much higher friction factors on the flood plain than in the unroughened main channel, a radically different case from those already described. This is illustrated in Figure 3.18, which shows the ratio of flood plain to main channel friction factor for the two conditions (tests 02 and 07: $s_C = s_F = 1$; $B/b_C = 4.2$). With smooth flood plains, f_F/f_C varies from 3 at very low depths reducing progressively to 1.2 when $H_* = 0.5$. With rough flood plains, the variation is from 4.6 increasing with depth up to almost 20 at $H_* = 0.5$. So although in the smooth case increasing depth helps bring the frictional characteristics of the zones together, it does the reverse in the rough case: they become even more disparate.

3.6.4 It follows that the variation of COH with depth also differs radically. This is illustrated in Figure 3.19, where channel coherence is plotted against relative depth for this geometry. As we saw earlier, the smooth compound channel becomes more coherent with depth, with COH increasing from 0.43 at shallow depths on the flood plain to a value of 0.94 at $H_* = 0.5$. On the other hand, in the rough case it increases from 0.36 to 0.45 in the range $H_* = 0.06$ to 0.21 and then varies around 0.41/0.42 as the depth increases to $H_* = 0.5$. The variation is a little irregular, because there are complex features at work: the balance between surface drag on the boundary and the form drag of the rods; the degree of blockage; variation of Reynolds Number, etc. However, the overall range of COH for the rough flood plains is restricted and no matter what depth of flow occurs the channel coherence remains low.

3.6.5 The roughened flood plain tests were interspersed with the series of tests into different main channel bank slopes and so cover a single flood plain width, though coupled with three values of s_C. They are listed in table 3.1 together with other relevant information. In one of these cases, $s_C = 1$, some tests were also made with reduced roughness. The measurement procedures were much the same as with all other series: in most cases there were many stage discharge measurements, but fewer velocity traverses on which to assess the separate flows in the main channel and flood plain zones.

Experimental results

3.6.6 The first question to resolve is whether the compound channel with extra roughness on the flood plains shows similar differentiation between regions of behaviour as the depth increases. To compare the smooth and rough flood plains, results for tests 07 (a and b for the two roughness densities tested) and test 02 (same geometry but smooth flood plains) are plotted in Figure 3.20 in the form discharge adjustment, DISADF, factor against relative depth, H_*. The flow regions for test 02 are indicated but, bearing in mind that region 1 is the zone of increasing interference with depth (reducing value of DISADF), there is no evidence that the tests with rod roughness on the flood plains ever entered region 2, let alone 3 or 4. In fact the results show progressively increasing interference effects up to the maximum depths covered, reaching the very severe condition approaching 40% loss of conveyance when the depth on the flood plains equals the depth of the main channel. As expected, the tests with reduced density of rods, 07b, show somewhat less loss of capacity than those with full density. If flood plains are much rougher than the main channel, this clearly has a major effect on flow.

3.6.7 Figure 3.21 shows the discharge deficit normalised by bank full flow for these comparable tests. It is noteworthy that at the maximum depth tested, the loss of capacity compared with the traditionally recommended text book procedures exceeds bank full flow!

3.6.8 Q_{*2} was found of especial value in Region 1 in terms of fitting general equations for the smooth channels tested, and this is plotted in fig 3.22, with the friction factor ratios, f_F/f_C, added. Also shown is the equation for region 1 for smooth flood plains, equ 3.13. It would be feasible to adjust the slope of this smooth function to provide a satisfactory fit to the rod roughness data. In fact the equation,

$$Q_{*2} = 14.0 \, H_* \qquad \ldots \; 3.18$$

is appropriate for run 07a. However, as in neither set of tests did the friction factor ratio remain constant, there is no obvious way to correlate the slope of this graph with flood plain roughness. Fortunately, by considering the main channel and flood plain effects separately, this problem is circumvented. Four (unaveraged) results from test 07b are also shown: these were with reduced flood plain roughness and lie between the smooth and full roughness results, as might be expected.

3.6.9 Figure 3.23 groups comparable sets of smooth and rough flood plain tests, 02 and 07a with $s_C = 1$ and 10 and 11 with $s_C = 2$, with Q_{*2} plotted against H_*. Remembering that region 1 extends to an H_* value of about 0.2 only with smooth flood plains but extends over the full depth range when they are rough, clear distinctions can be seen in this figure. Firstly, although interference effects significantly increase the flood plain discharge when they are smooth, any increase is quite negligible when they are rough. Presumably this is because the faster main channel flow is not able to penetrate so readily - or exchange some of its extra momentum so readily - when the flood plains are very resistant. Secondly, there is relatively little difference between the interference effects on the main channel flow between the smooth and rough cases when expressed in the form of Q_{*2}: the region 1 data follow similar trends in the two cases, although the greater extent of the data from the roughened flood plains would suggest some modification to the best fit equation.

3.6.10 Discounting any addition to the flood plain flow permits the main channel velocity traverse data on Figure 3.23 to be considered together with the orifice plate discharge measurement in Figure 3.22: they both define the discharge deficit in the main channel when normalised as Q_{*2}. Taking into account also the features determined earlier from the wide range of tests with smooth flood plains, the modified version of equation 3.22 for rough flood plains becomes:

$$Q_{*2} = -1.240 + 0.395B/w_C + 13.0 \, H_* \qquad \ldots \; 3.27$$

This is shown on Figure 3.23. The test 11 results show more variation and may be less reliable: flood plain flows were not measured and so the main channel flows could not be corrected in any way to agree with the orifice meter readings.

3.6.11 Tests 07a and 07b were made with main channel side slopes of 1 in 1. Two other cases were also tested: 09 with vertical sides ($s_C = 0$) and 11 with $s_C = 2$. Q_{*2} is shown against H_* for these three cases in fig 3.24. Test 09 conforms very closely to the smooth channel version of the function, equ 3.17: tests 07a and 11 results are very similar and follow the modification in equ 3.19. Although there is some variation from the equation for Q_{*2C} as a function of H_* derived from the smooth flood plain tests, the degree of agreement is quite remarkable when one considers that tests over a range of friction factor ratios from 1.5 to about 3 have been extrapolated to $f_F/f_C = 20$ without any major revision. Q_{*2} is a powerful parameter for describing region 1 flows, being firmly correlated with B/w_C and H_* but independent of all other variables covered in the Wallingford tests.

3.6.12 A feature yet to be established is the limiting condition for region 1 to apply with rough flood plains. The upper limit was previously considered to be where the predictive equation for region 2 would give a higher discharge than that for region 1. The function for region 2 that equates DISADF to COH with a shift in H_*, equ 3.10, would also succeed with the rod roughened flood plains in the sense that it would yield lower discharges than the region 1 function (COH being around 0.4) and so be discarded for flows in region 1.

3.6.13 The overall conclusion from the rod roughness experiments was that the flow lay in region 1 in all cases. It could be represented reasonably well by the Q_{*2C} function established with smooth flood plains, but differs in that Q_{*2F} is negligible (no addition to flood plain discharge). We are left with the requirement of a criterion for determining when to neglect Q_{*2F}: it has to be phased out with increasing friction factor ratio. This can be achieved by amending equation 3.15 to:

$$Q_{*2F} = -1.0\ H_* \ f_C/f_F \qquad \text{... 3.20}$$

This reverts to equation 3.15 when $f_F/f_C = 1.56$, a typical smooth flood plain value towards the limit of region 1, but becomes negligible with rod roughness. Whether the assumed linear phasing out is correct would require more - and very accurate - data, but as the term is a minor part of the required discharge adjustment, the point is of little consequence.

3.6.14 Equation 3.17 for smooth flood plain tests may be linked to equation 3.19 for rough flood plains to give a general function for Q_{*2C}, at the same time taking account of the comment in para. 3.6.11 concerning rough flood plains associated with vertical main channel banks. This is achieved by the following functions:

$$Q_{*2C} = -1.240 + 0.395B/w_C + G\ H_* \qquad \text{... 3.21}$$

where

For $s_C \geqslant 1.0$:

$$G = 10.42 + 0.17\ f_F/f_C \qquad \text{... 3.22}$$

For $s_C < 1.0$:

$$G = 10.42 + 0.17\ s_C f_F/f_C + 0.34\ (1-s_C) \qquad \text{... 3.23}$$

3.6.15 There is an obvious gap in the available results from the Wallingford test facility. The tests with roughened flood plains gave such a high disparity between the friction factors on the flood plain and in the main channel, which moreover increased with flow depth, that no region 2 or 3 data were obtained except with equal roughnesses. There must, however, be many practical cases where a modest difference in roughness exists and so transition to region 2 behaviour (diminishing interference effects) would be expected, and ultimately to regions 3 and 4 perhaps. Although the ability of the parameters including $V_C - V_F$ to accommodate the full range of conditions tested has been demonstrated in region 1, any comparable demonstration in the higher regions eludes us because the data are not available from the FCF research. Other sources of data covering modest differences in roughness will be considered later (Chapter 5).

3.7 Hydraulic design formulae

3.7.1 The purpose of the above analyses was to deduce formulae that could be used to predict the flow in compound channels, i.e. establish their stage/discharge functions. Alternatives were considered and progressively developed to cope with the range of conditions tested. The results are summarised above: they were detailed in Technical Report number 4, October, 1990 (unpublished). Because of the complexity of the flow behaviour, involving different regions of behaviour, there is obviously no single formula to cover all conditions. Moreover, the preferred form of equation and the parameters it depends on differ from one region to the next, and a logical method has to be established for determining which flow region applies in any given case. In general, the equations are simple in form, with linear variation with the governing parameters. Application in practice will probably utilise a computer program that includes the logic for determining which region of flow applies. The following summarises the equations so far deduced:

Region 1.

3.7.2 This is the region of relatively shallow depths where interference effects increase progressively with depth. Q_{*2} was shown as a simple linear function of B/b and H_* in Figure 3.7. When converted into a form imvolving the ratio of overall width at flood plain level to main channel top width, it was found to be independent of s_C and asymmetry. It needed some modification to cope with the high flood plain roughness tested, but was not very sensitive to the friction factor ratio. The velocity area measurements separated Q_{*2} into its flood plain and main channel components, and these were in turn adjusted to a general form covering both the smooth and the roughened flood plain results, equations 3.20 to 3.23. This group of equations covers all the test conditions, and so form the predictors for region 1:

REGION 1:

$$Q_{*2F} = -1.0\ H_* f_C/f_F \qquad \ldots\ 3.24$$

$$Q_{*2C} = -1.240 + 0.395\ B/w_C + G\ H_* \qquad \ldots\ 3.25$$

For $s_C \geqslant 1.0$:

$$G = 10.42 + 0.17\ f_F/f_C \qquad \ldots\ 3.26$$

For $s_C < 1.0$:

$$G = 10.42 + 0.17\ s_C f_F/f_C + 0.34\ (1-s_C) \qquad \ldots\ 3.27$$

It will emerge from studying data from other sources in Chapter 5 that these Region 1 functions require amendment before application to compound channels where the main channel width to depth ratio differs from the figure of 10 that applied to all the FCF work. A modification is put forward that effectively redefines Q_{*2}, and hence Q_{*2C} and Q_{*2F}, to allow for the effect of main channel aspect ratio where it differs from 10.

Region 2.

3.7.3 This is the zone of greater depth where the interference effect diminishes again. The upper flow regions are where the channel coherence, COH, proved promising. For Region 2, the procedure involved calculating COH with a shift in H_* and equating the discharge adjustment factor, DISADF, to it, and this was found to be applicable to all geometries tested and for both smooth and rough flood plains. The procedure was stated in functional form in equ 3.10, but this needs some adjustment to take into account a different "shift" in H_* to provide a satisfactory fit for s_C = 0 and for the asymmetric case.

DISADF (H_*, channel geometry and roughness)
= COH_3([H_*+shift], channel geometry and roughness) ... 3.28

where for $s_C \geqslant 1.0$

$$\text{shift} = 0.05 + 0.05\ N_F \qquad \ldots\ 3.29$$

for $s_C < 1.0$,

$$\text{shift} = -0.01 + 0.05\ N_F + 0.06\ s_C \qquad \ldots\ 3.30$$

In the above N_F is the number of flood plains. Function 3.28 above has not been established for region 2 with different roughnesses on flood plain and in main channel, but it is hoped that it proves of more general applicability than prescribed by the FCF tests. The test series did not cover asymmetric conditions with $s_C < 1$, so that is also a gap in confirmation of equ 3.30

Region 3.

3.7.4 This is a relatively narrow region of flow, for which equ 3.11 was derived, giving DISADF as a function of COH. The data are somewhat uncertain in establishing this as a region of increasing interference effects, and it was suggested that when taking all results together a constant value of DISADF would not be unreasonable. There were,however, these two alternatives with uncertainty over which might be the best fit:

$$\text{DISADF} = 1.567 - 0.667\ \text{COH} \qquad \ldots\ 3.31$$

or: $\text{DISADF} = 0.95$ ... 3.32

Region 4.

3.7.5 This is the region where the coherence of the cross-section is such that it may be treated as a single section, with perimeter weighting of friction factors, when calculating overall flow. This is equivalent to:

$$\text{DISADF} = \text{COH} \qquad \ldots\ 3.33$$

It should be remembered, however, that this does not mean that interaction effects are negligible: the main channel discharge may be appreciably reduced compared with the basic zonal calculation, see paragraph 3.5.10.

Choice of region.

3.7.6 The logic behind the selection of the appropriate predictive equation is dependent upon the calculation of discharge for all regions in turn, referred to as Q_{R1}, Q_{R2}, Q_{R3} and Q_{R4} respectively. The choice of the appropriate region and hence appropriate total discharge proceeds as follows:

Region 1 or 2?

If $Q_{R1} \geq Q_{R2}$ then $Q = Q_{R1}$ ... 3.34

Region 2 or 3?

If $Q_{R1} < Q_{R2}$ and $Q_{R2} \leq Q_{R3}$ then $Q = Q_{R2}$ ... 3.35

Region 3 or 4?

If $Q_{R1} < Q_{R2}$ and $Q_{R3} < Q_{R2}$ then $Q = Q_{R3}$ unless $Q_{R4} > Q_{R3}$ when $Q = Q_{R4}$ ... 3.36

3.7.7 The calculation of Q_{R1} etc begins with the basic computation of the separated main channel and flood plain flows, using an appropriate resistance formula and associated roughness values. It then utilises the equations summarised above, together with the respective definitions of the dimensionless groups used, Q_{*2F}, Q_{*2C} and DISADF, to adjust that basic calculation for the interference effects arising from compounding. It is advisable to calculate for all four regions at any given depth, unless there is firm information about which region or regions might apply. The logic route given in the previous paragraph then selects the appropriate region and corresponding evaluation of discharge. As there are two alternative equations for DISADF in region 3, both might be considered in turn. This will not only give slightly different alternative values for Q_{R3}, it will also result in the boundaries of this flow region changing in the two cases. The relative merits of these residual alternatives will be discussed again later.

3.7.8 It will be appreciated that the logic of selection between the equations for different regions does not provide any transition between them. This accords with close examination of the individual test results: there is little evidence of a curved transition between the zonal equations; the switch is quite sudden.

3.7.9 If a separate assessment of discharges and mean velocities in the main channel and flood plain are required, they may be calculated in Region 1 using equations 3.24 and 3.25 with the definitions of Q_{*2C} and Q_{*2F}. The separate assessment of zonal flows in the higher flow regions is not so well covered by the empirical methods above, but paragraph 3.5.10 indicates the way forward.

3.7.10 It remains to check the performance of this set of predictive equations by reference back to the experimental data. The formulae were added to the program used in data analysis, and the percentage discrepancies between the individual results and the predicted discharges for the observed depths, geometries etc were assessed. These discrepancies were subjected to statistical analysis, to obtain mean errors and the standard error of estimate. The former statistic indicates the overall goodness of fit, and the latter the variability. This variability can have two components: any imperfection in the trend of the predictive equations and also the inevitable experimental scatter due to random errors of measurement. Table 3.2 summarises these results, with statistics for groups of experiments as well as for the total set, including those with roughened flood plains. Table 3.2 is in two sections, the first utilising equation 3.31 for region 3 and the second equation 3.32. Within region 3, the former provides the better fit: mean error 0.13% compared with -0.28% taking all results together; standard error of that estimate 0.70% compared with 0.91%. Either would be acceptable in an engineering context.

3.7.11 The least satisfactory group of results is with rod-roughened flood plains. They all lie in region 1 and although the mean error of 0.07% indicates high accuracy on average, the standard error of 1.46% is the highest of any region or any grouping. Bearing in mind that the method essentially calculates the adjustment to a basic calculation summing the individual nominal discharges on flood plain and in the channel, the adjustment itself is much greater with the very rough flood plains used in this test series than with smooth flood plains. This probably explains the increased error of the overall adjustment: it is easier to predict accurately when the correction to be made is say 10% than when it is as high as 30 or 40%. For the smooth flood plains i.e. equal Manning's n for flood plains as for main channel, the mean errors for the various groups of tests are all under a third of a percent; and the variability (standard error of estimate) under half a percent. The former shows the excellence of the set of predictive equations in fitting the experimental trends; the latter could hardly be bettered in terms of consistency of laboratory measurement. The complete data set is fitted almost exactly on average by these predictive methods: mean error -0.001%. The variability of 0.8% is highly satisfactory, bearing in mind that perhaps 0.5% arises from the experimental observations themselves, and that the one set of equations is applied to both similar and very dissimilar roughness conditions, to asymmetric as well as symmetric cases, to a range of flood plain widths and channel bank slopes, over a range of flow depths covering four different regions of flow.

3.7.12 It will be appreciated that these checks complete the circle of dimensional analysis, experiment, empirical assessment, establishment of formulae and back-checking. Validation of these predictive equations against independent experimental data for different geometric and roughness conditions is a necessary part of establishing their generality, or indeed their limitations and this is dealt with in Chapter 5.

3.7.13 For a direct exposition of the design procedures, readers are referred to the "Summary and Design Method", and also to the example given in Appendix 6. The equations listed above are not the final, general, versions: they will be found in Chapter 10, Section 10.1.

TABLE 3.1

SUMMARY OF EXPERIMENTS UNDERTAKEN ON THE SERC-FCF: SERIES A, STRAIGHT

All dimensions are in metres: see fig 2.2 for nomenclature: for the asymmetric channel, B = half total width at flood plain elevation: the numbers of results refer to above-bank stage-discharge measurements.

TEST NUMBER	ROUGHNESS Channel	Flood pl.	b_{WC}	b_{WF}	b	B	w_C	s_C	s_F	B/b	B/w_C	No of results	NOTES
01	Smooth	Smooth	1.5	4.10	0.75	5.00	0.90	1	0	6.67	5.56	27	Symmetric Two F P's
02	Smooth	Smooth	1.5	2.25	0.75	3.15	0.90	1	1	4.20	3.50	29	"
03	Smooth	Smooth	1.5	0.75	0.75	1.65	0.90	1	1	2.20	1.83	22	"
04	Smooth	-	1.5	-	0.75	-	0.90	1	-	-	-	-	No F P's (calibration)
05	Smooth	Smooth	1.5	0.975	0.75	1.875	0.90	1	1	2.50	2.08	8	as R Main
06	Smooth	Smooth	1.5	2.25	0.75	2.025	0.90	1	1	2.70	2.25	20	Asymmetric One F P
07a	Smooth	Rough	1.5	2.25	0.75	3.15	0.90	1	1	4.20	3.50	22	
07b	Smooth	Rough	1.5	2.25	0.75	3.15	0.90	1	1	4.20	3.50	4	Reduced rod density
08	Smooth	Smooth	1.5	2.25	0.75	3.00	0.75	0	1	4.00	4.00	25	Rectangular main channel
09	Smooth	Rough	1.5	2.25	0.75	3.00	0.75	0	1	4.00	4.00	10	"
10	Smooth	Smooth	1.5	2.25	0.75	3.30	1.05	2	1	4.40	3.14	19	
11	Smooth	Rough	1.5	2.25	0.75	3.30	1.05	2	1	4.40	3.14	16	

TABLE 3.2

STATISTICAL ANALYSIS OF PERFORMANCE OF PREDICTIVE EQUATIONS IN REPRESENTING RESULTS FROM THE SERC-FCF: SERIES A, STRAIGHT

KEY: No - number of tests in series; SEE% - Standard error of estimate, percent, ie r.m.s. of variation about average discrepancy; ME% - Mean error, ie average percentage discrepancy between prediction and experiment.

I - Using equation 3.31 for region 3.

Test series	Flow region:-	1	2	3	4	All	Group
1, 2,	No	33	34	8	0	75	Varying B/b
3, 5.	SEE%	0.225	0.360	0.354	0	0.308	
	ME%	-0.412	-0.044	-0.216	0	-0.225	
8, 10.	No	17	13	5	3	38	Varying s_C
	SEE%	0.137	0.392	1.047	0.403	0.467	
	ME%	0.122	0.437	0.721	0.257	0.319	
6	No	11	3	2	1	17	Asymmetric
	SEE%	0.312	0.205	0.636	0.370	0.355	
	ME%	0.074	-0.001	0.022	0.429	0.075	
7a, 7b,	No	44	0	0	0	44	Rough flood pl.
9, 11.	SEE%	1.463	0	0	0	1.463	
	ME%	0.072	0	0	0	0.072	
All	No	105	50	15	4	174	All cases
	SEE%	0.962	0.362	0.697	0.395	0.801	
	ME%	-0.072	0.084	0.128	0.300	-0.001	

II - Using equation 3.32 for region 3.

Test series	Flow region:-	1	2	3	4	All	Group
1, 2,	No	33	29	13	0	75	Varying B/b
3, 5.	SEE%	0.225	0.274	1.126	0	0.521	
	ME%	-0.412	0.068	-0.984	0	-0.326	
8, 10.	No	17	11	8	2	38	Varying s_C
	SEE%	0.137	0.303	0.596	0.486	0.350	
	ME%	0.122	0.351	0.629	0.446	0.312	
6	No	11	3	3	0	17	Asymmetric
	SEE%	0.312	0.205	0.361	0	0.305	
	ME%	0.074	-0.001	0.0326	0	0.105	
7a, 7b,	No	44	0	0	0	44	Rough flood pl.
9, 11.	SEE%	1.463	0	0	0	1.463	
	ME%	0.072	0	0	0	0.072	
All	No	105	43	24	2	174	All cases
	SEE%	0.962	0.277	0.906	0.486	0.833	
	ME%	-0.072	0.133	-0.283	0.446	-0.044	

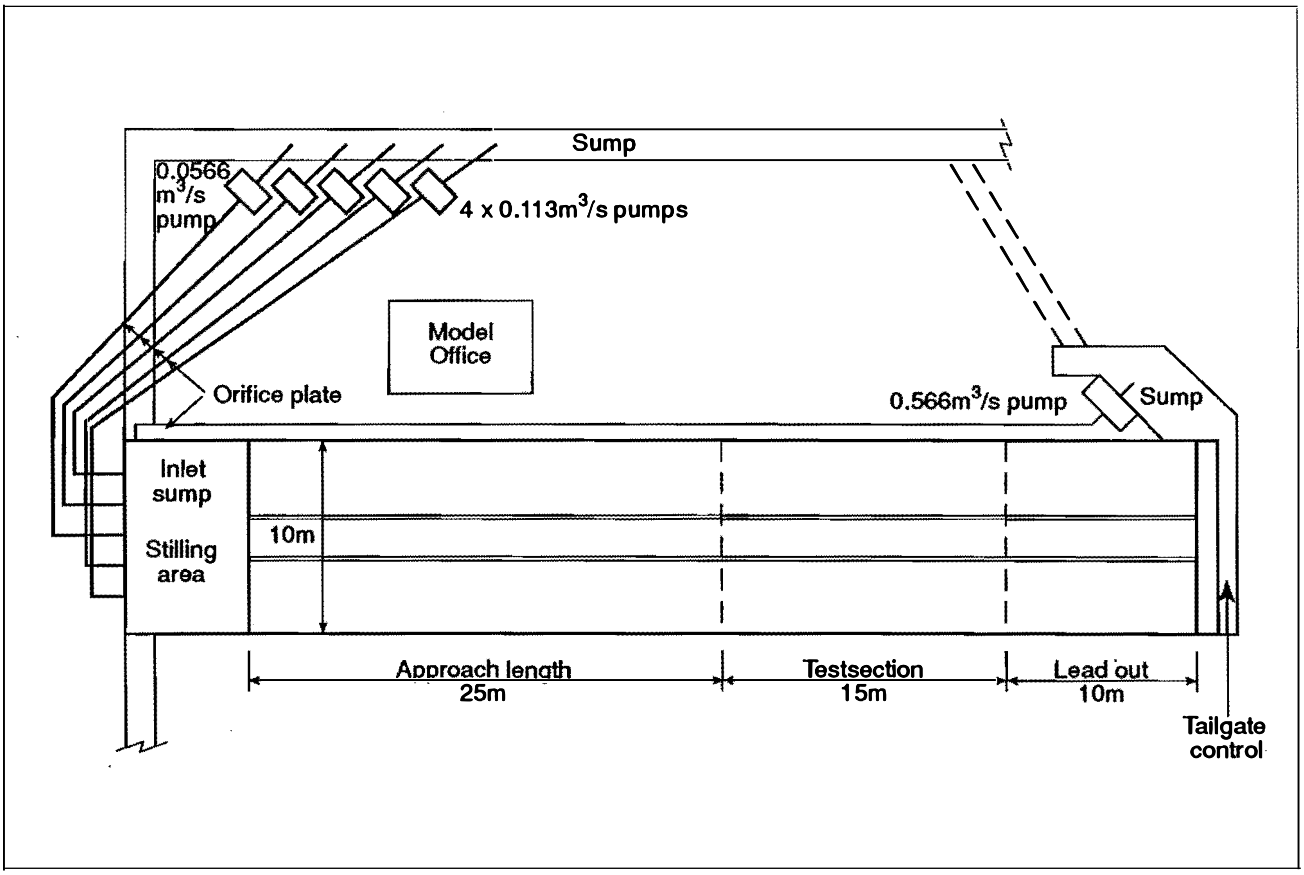

Fig 3.1 Layout of SERC facility at Wallingford

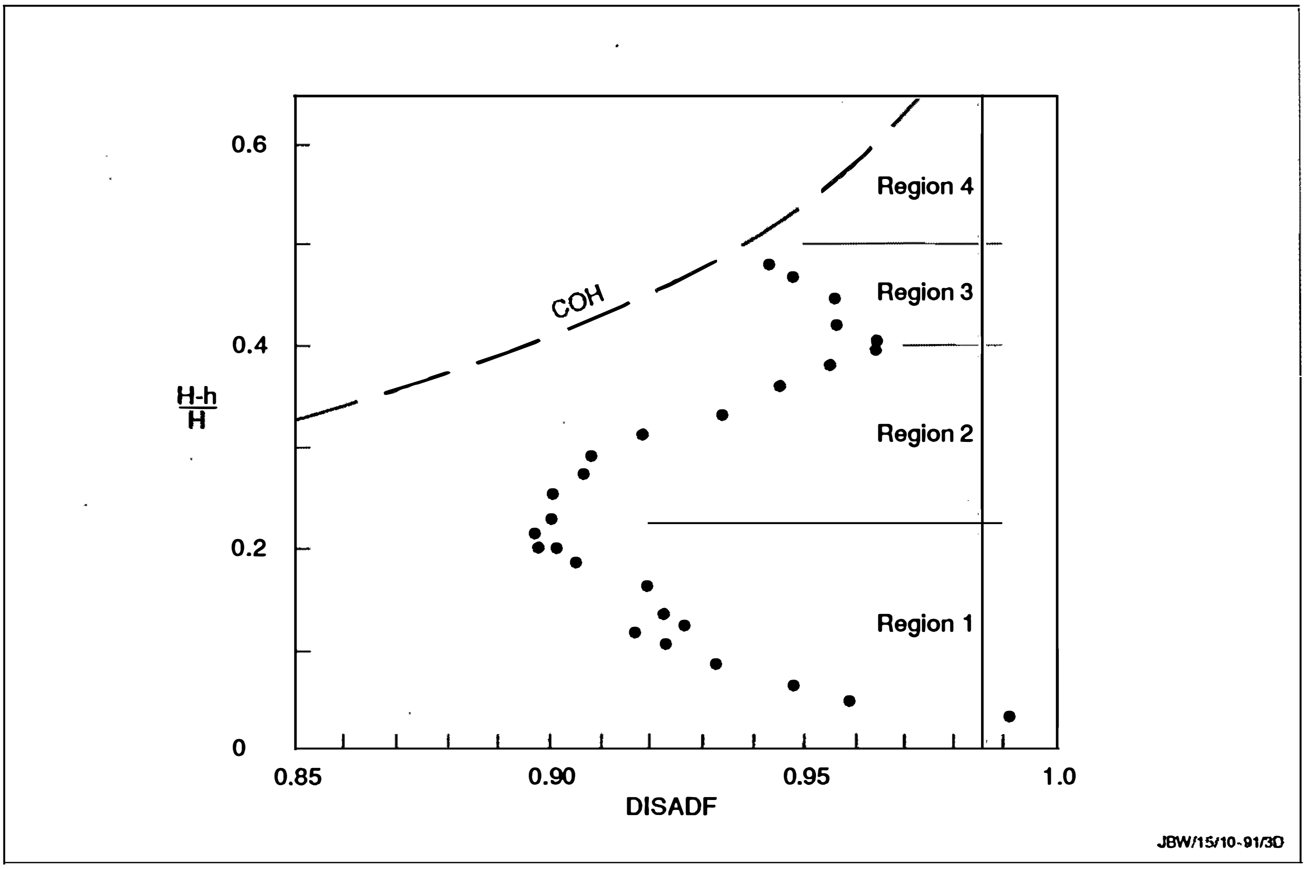

Fig 3.2 Discharge adjustment factor (ratio of measured discharge to sum of zonal calculated flows) versus relative flow depth: also COH to same scales; test series 02, averages of three.

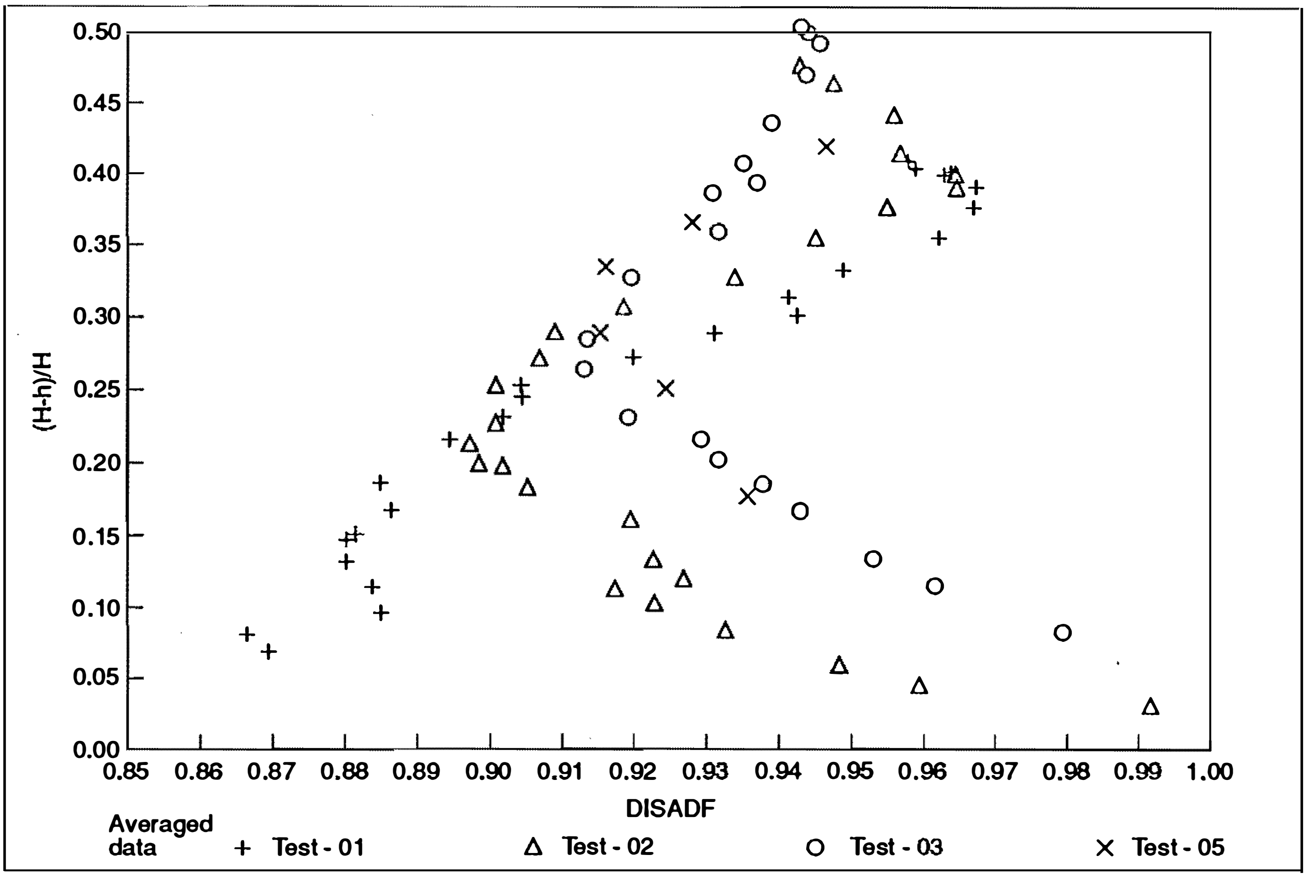

Fig 3.3 Effect of varying flood plain width on discharge adjustment factor - DISADF, as function of (H-h)/H = H*

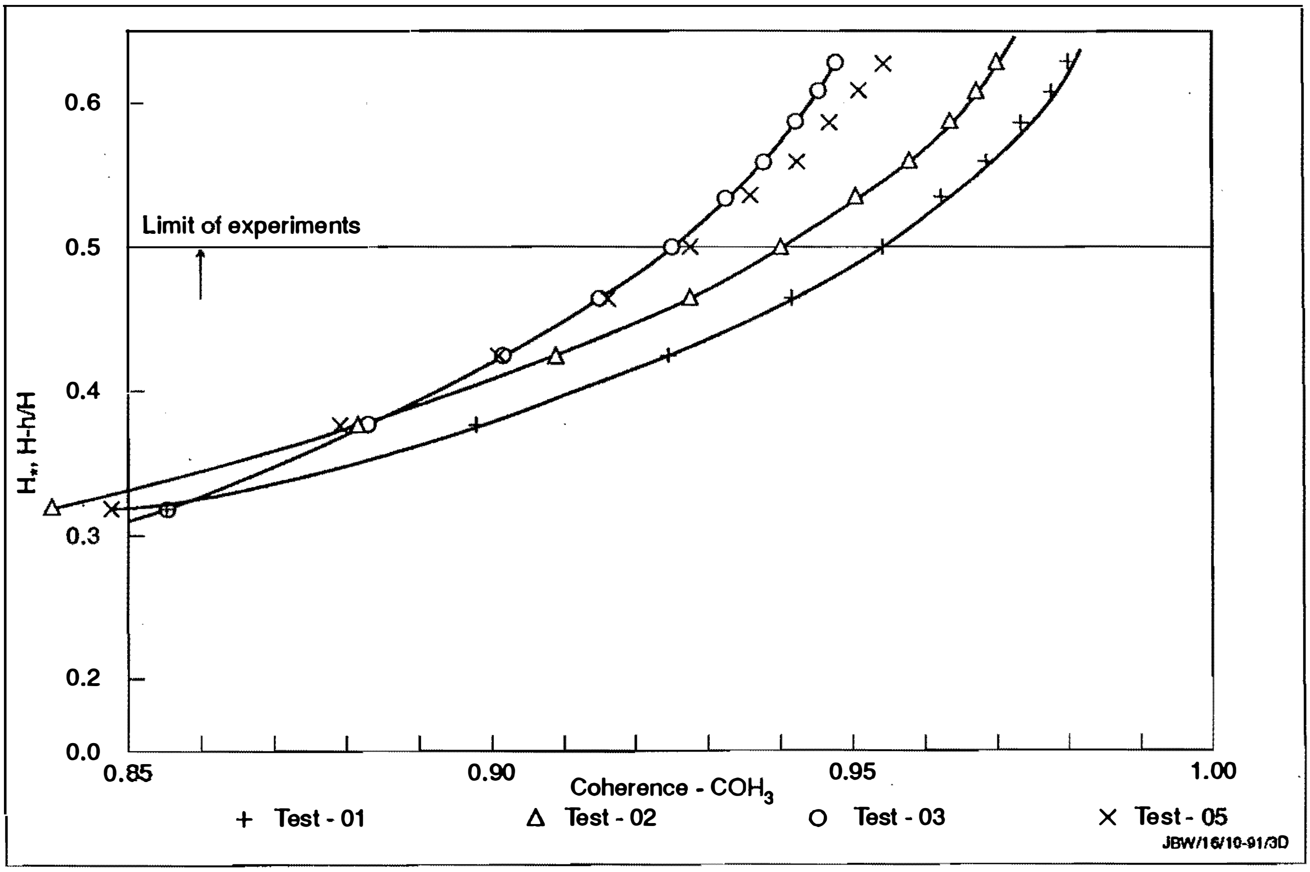

Fig 3.4 Calculated coherence - COH, Wallingford channel, various B/b ratio

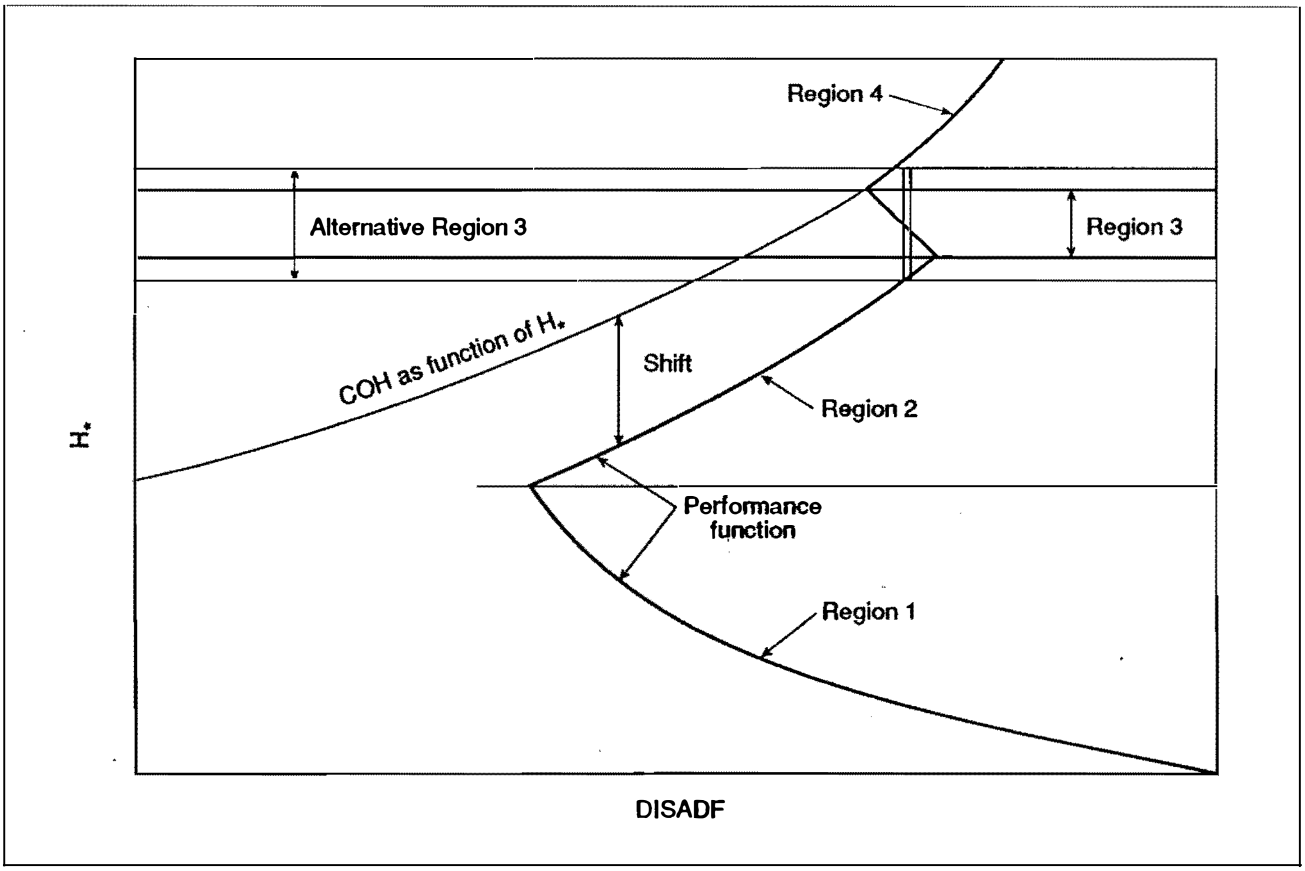

Fig 3.5 Illustration of different regions of flow

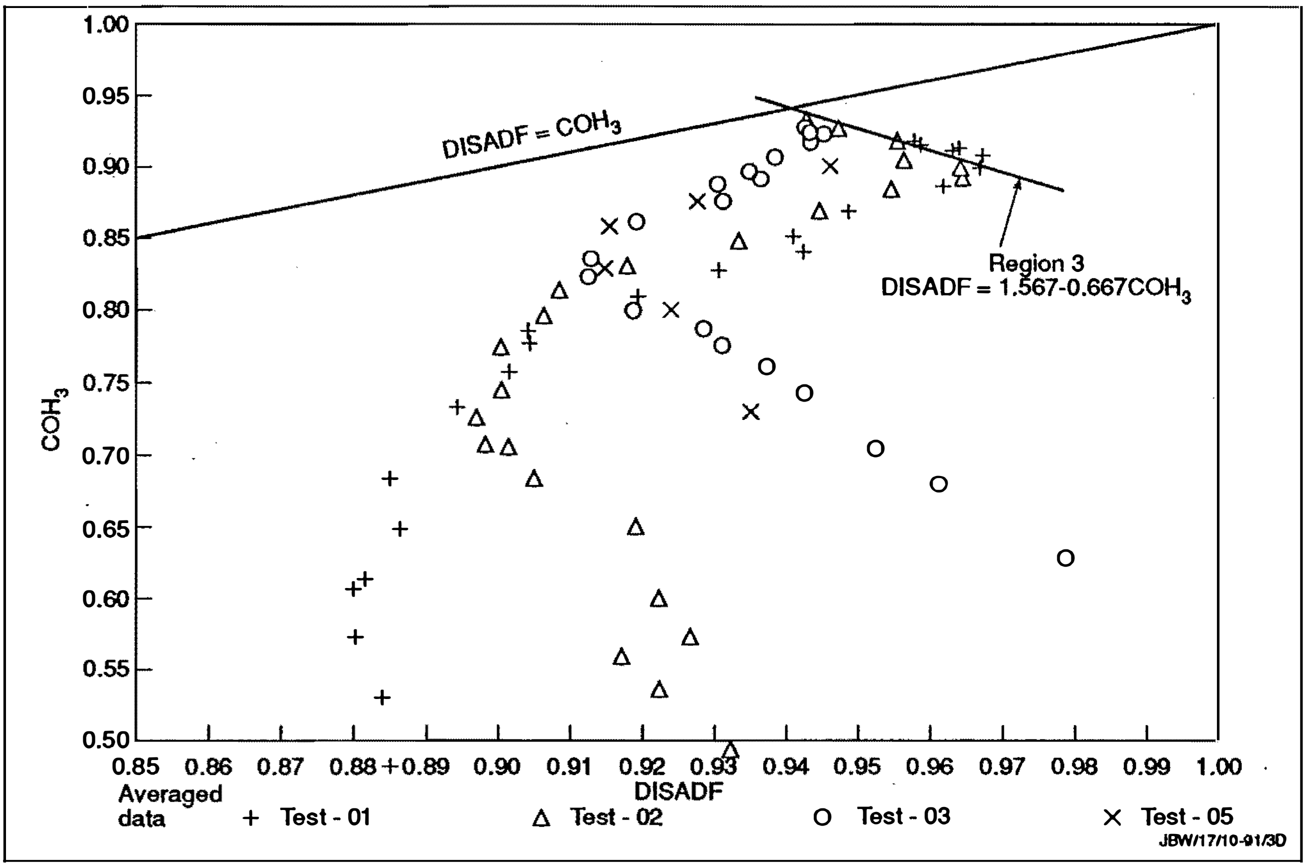

Fig 3.6 Results for four plain widths, DISADF against COH (running averages)

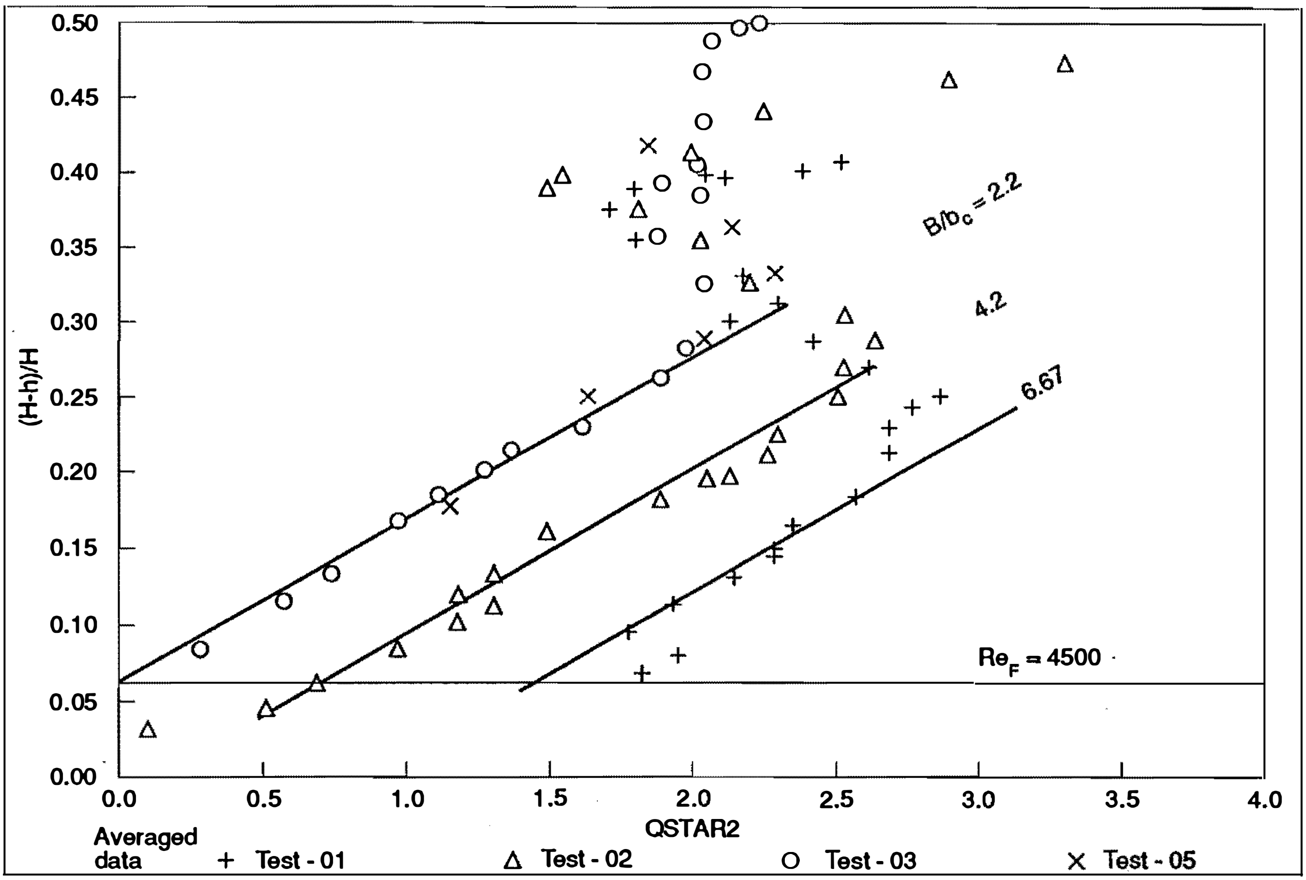

Fig 3.7 Averaged results for four flood plain widths: Q_{*2} against H_*: Q_{*2} = DISDEF/[(V_C-V_F)Hh]

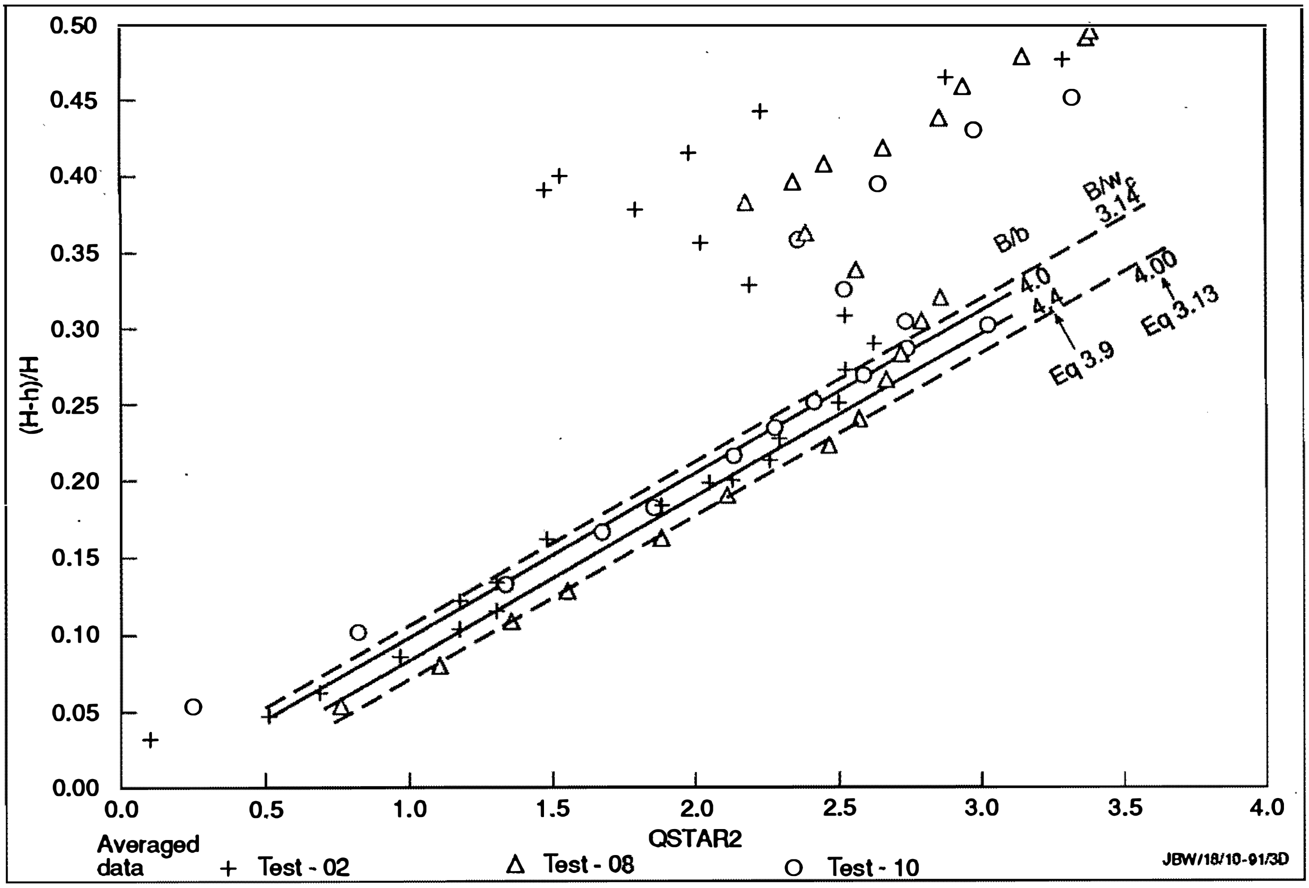

Fig 3.8 Averaged results for three side slopes: Q_{*2} against H_*

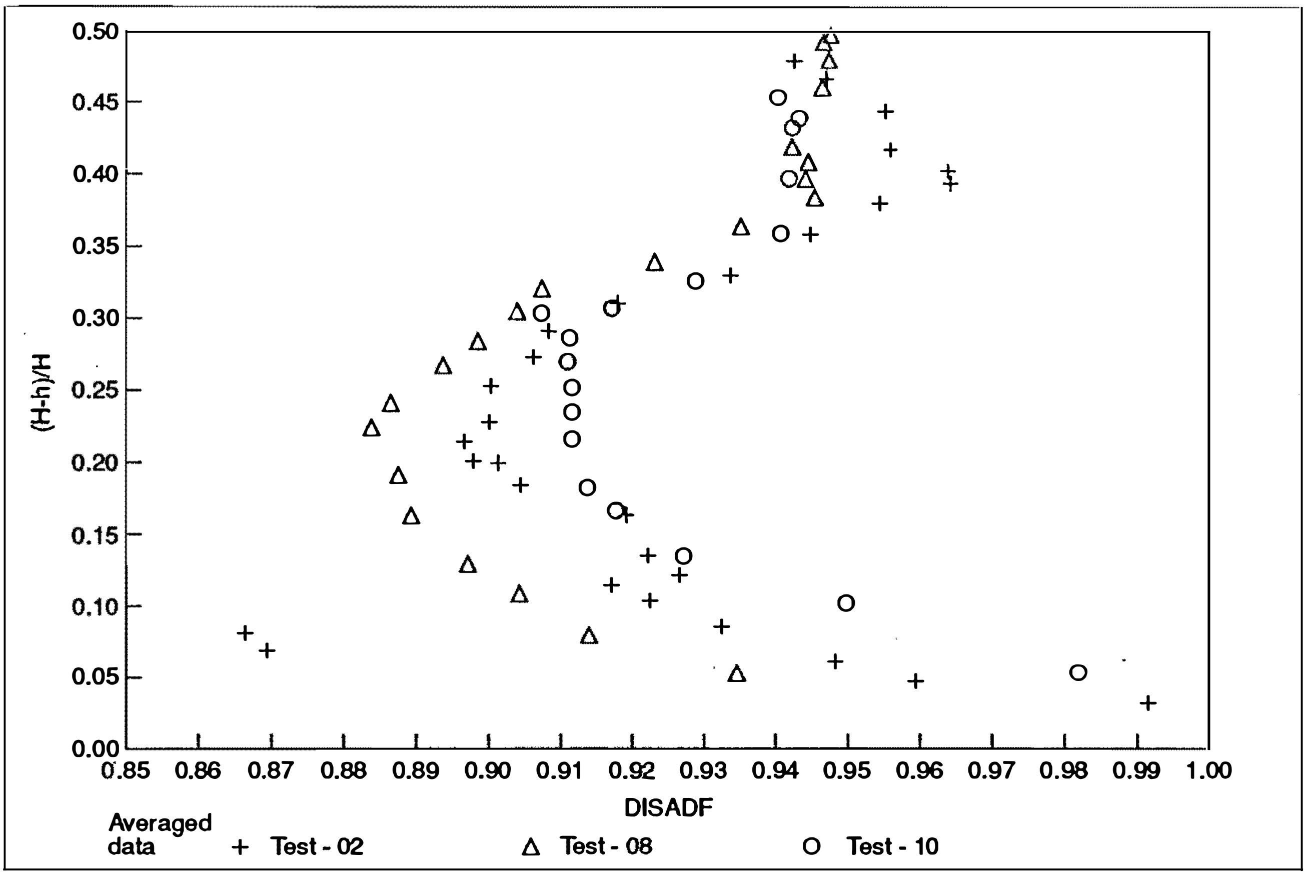

Fig 3.9 Averaged results for three side slopes: DISADF against H*

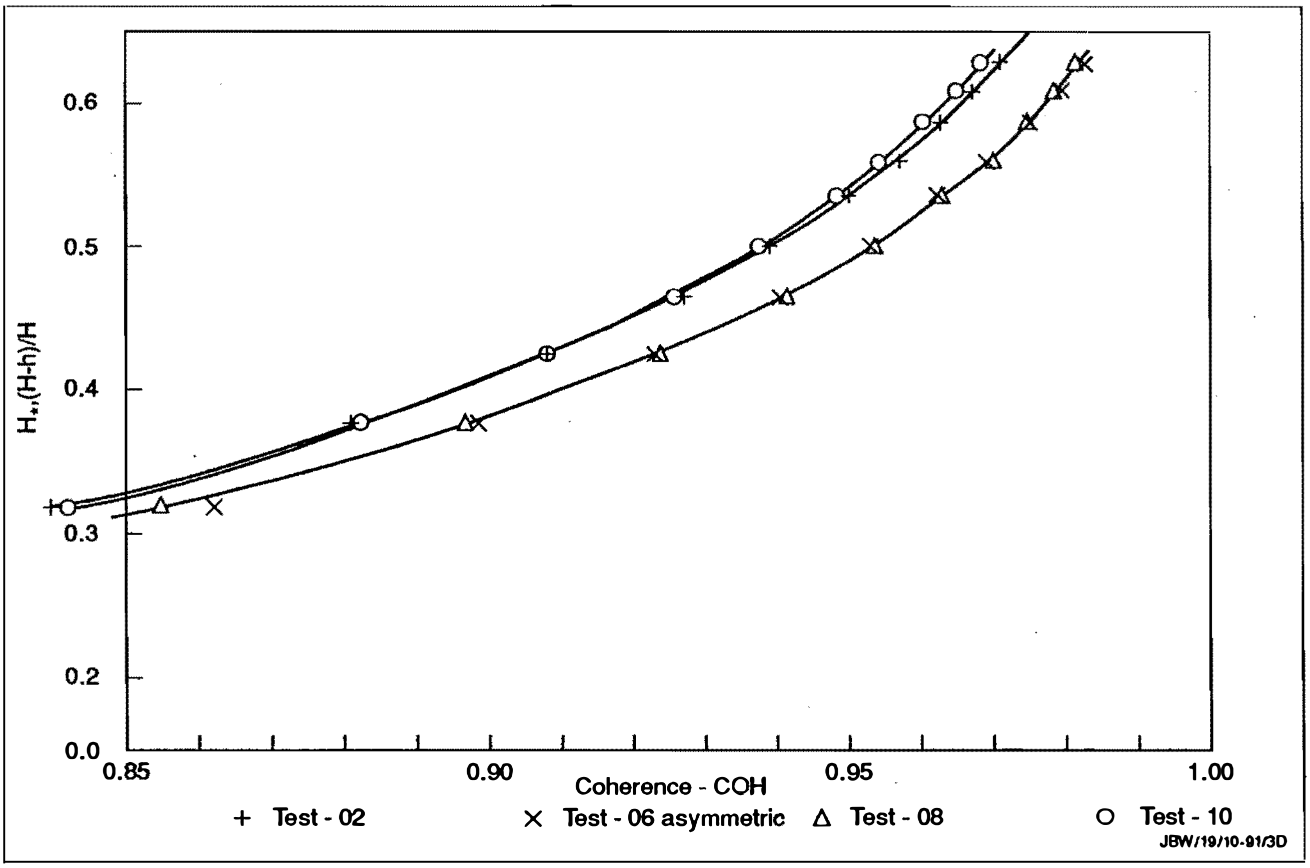

Fig 3.10 Calculated coherence - COH, for FCF, various s_c values; also asymmetric case

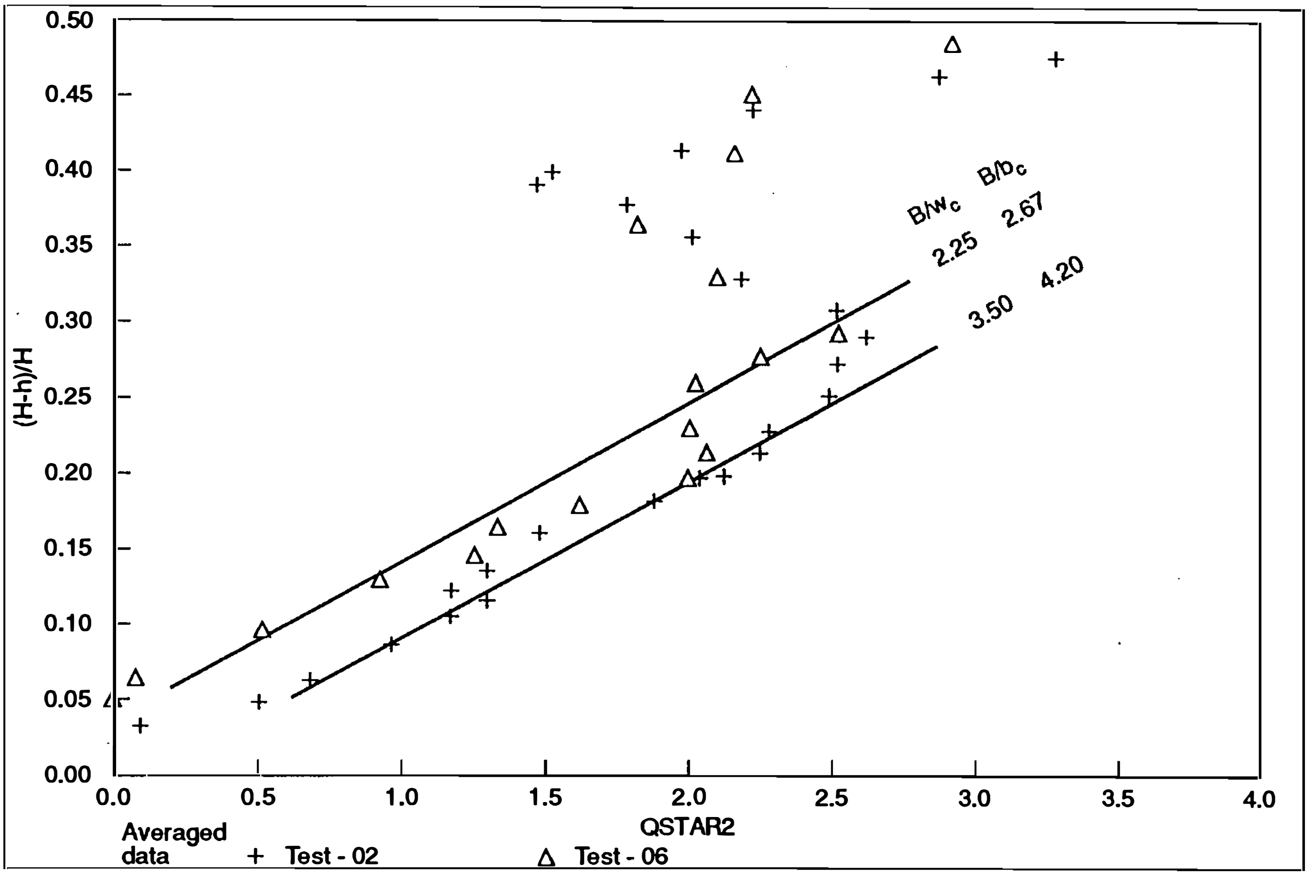

Fig 3.11 Asymmetric and symmetric cases (averaged data): Q_{*2} against H_*

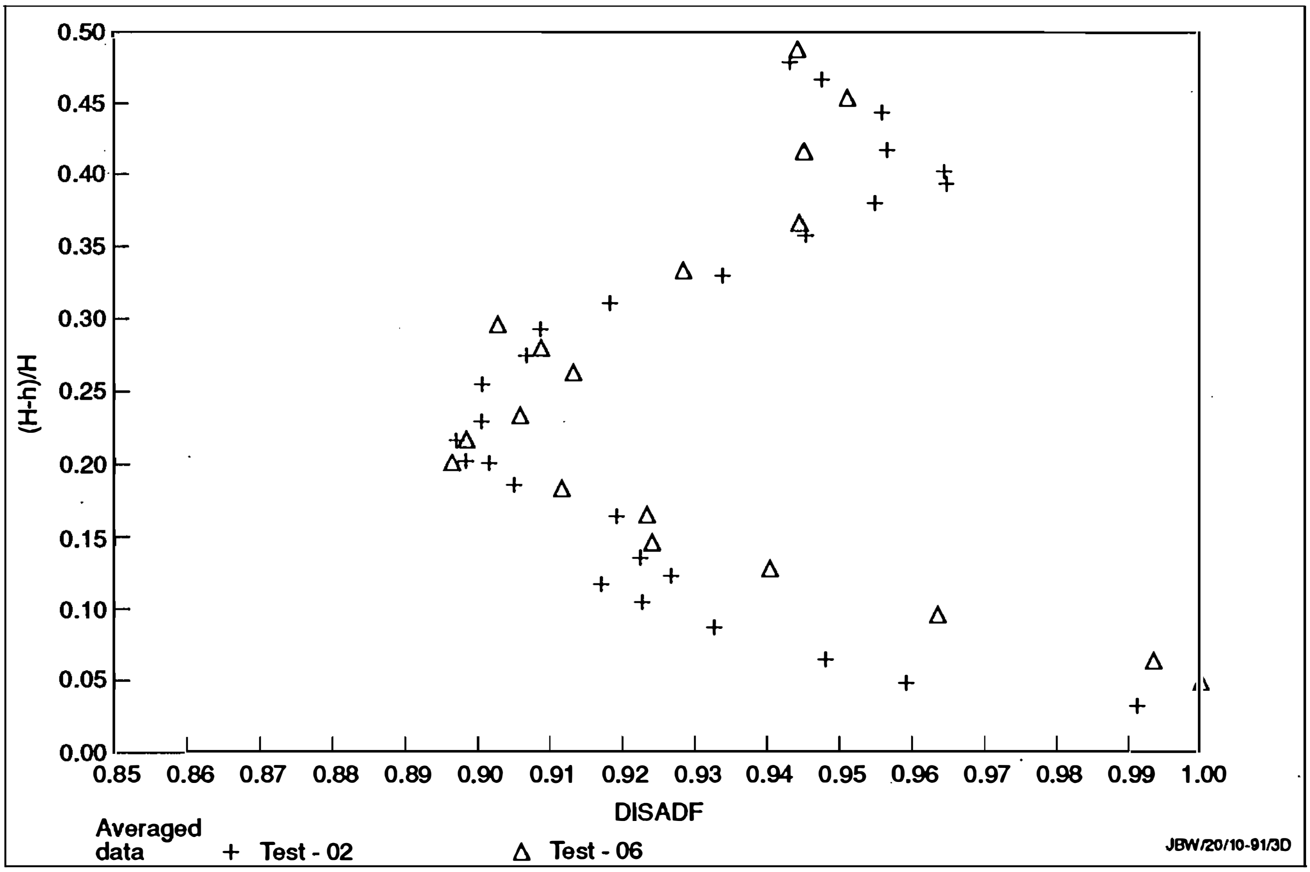

Fig 3.12 Asymmetrical and symmetrical cases (averaged data): DISADF against H_*

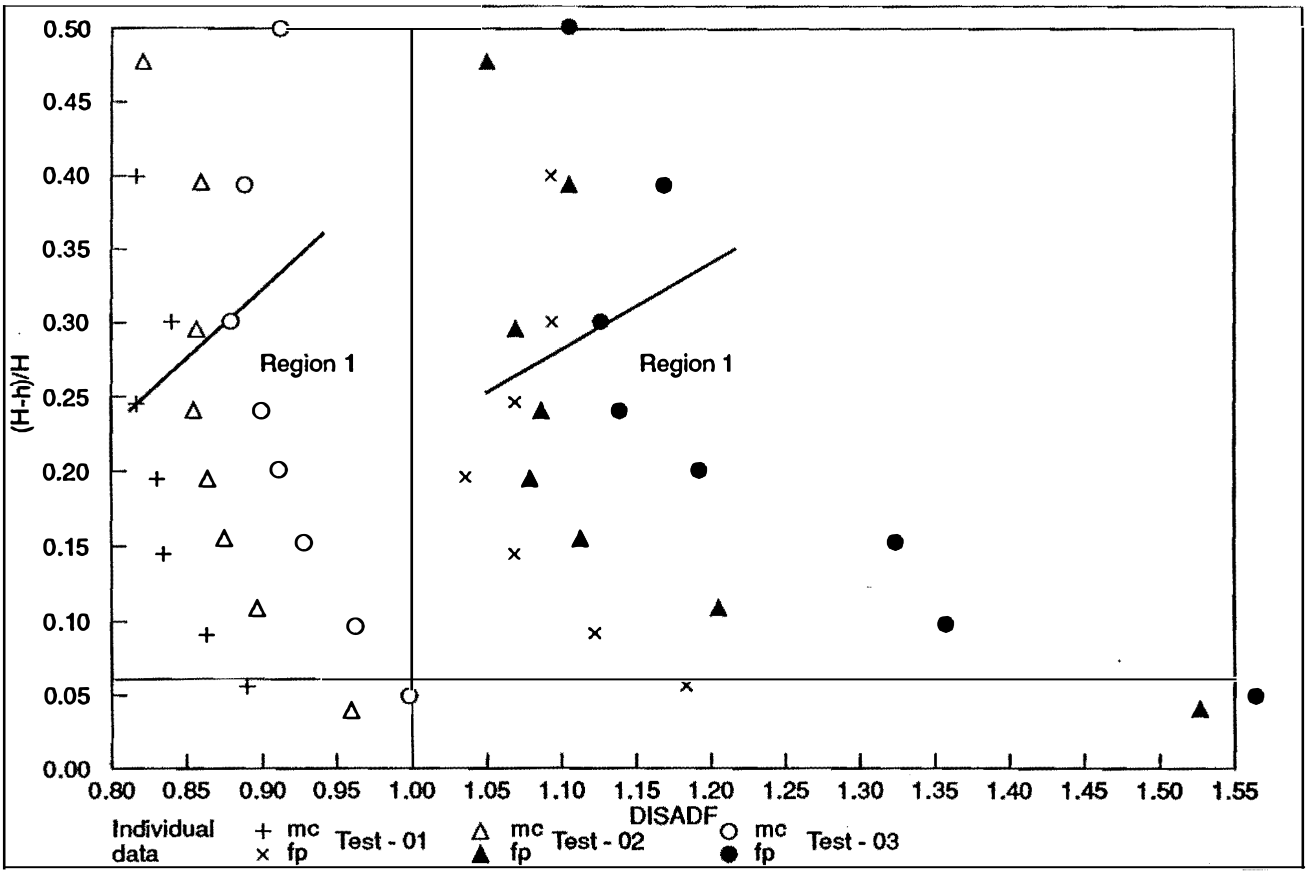

Fig 3.13 Adjustments factors for separate zones: various width ratios

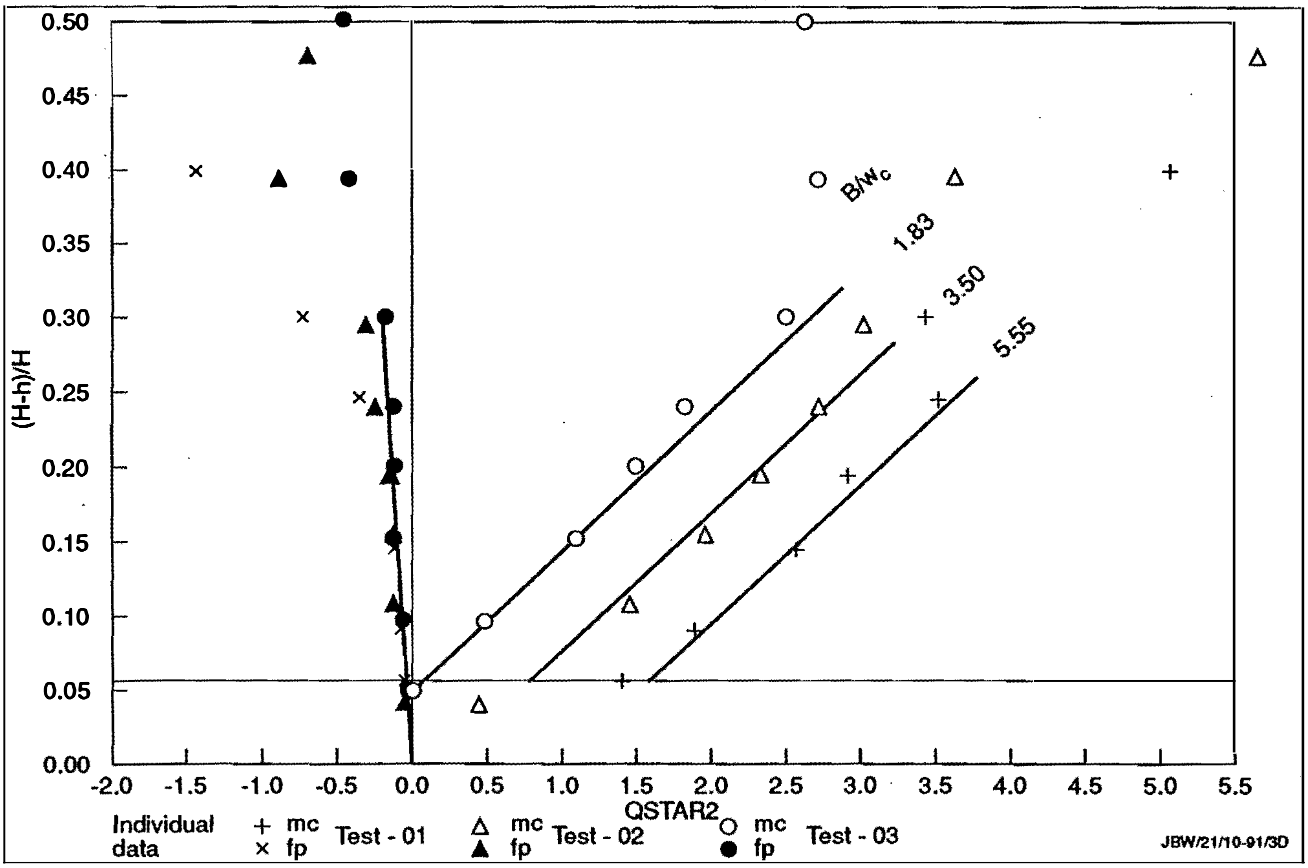

Fig 3.14 Q_{*2} against H_* for separate zones: various width ratios

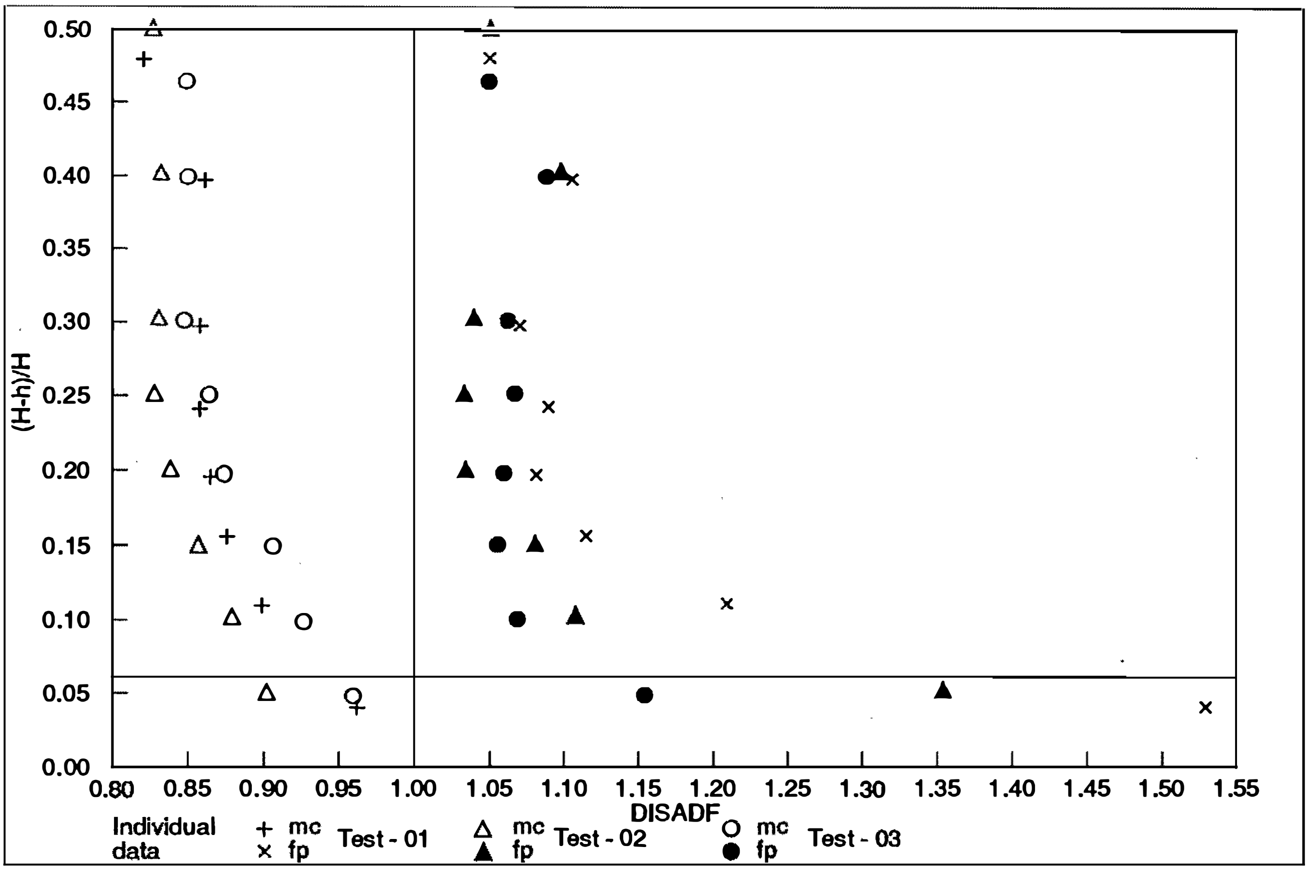

Fig 3.15 DISADF against H* for separate zones: various bank slopes - s_c

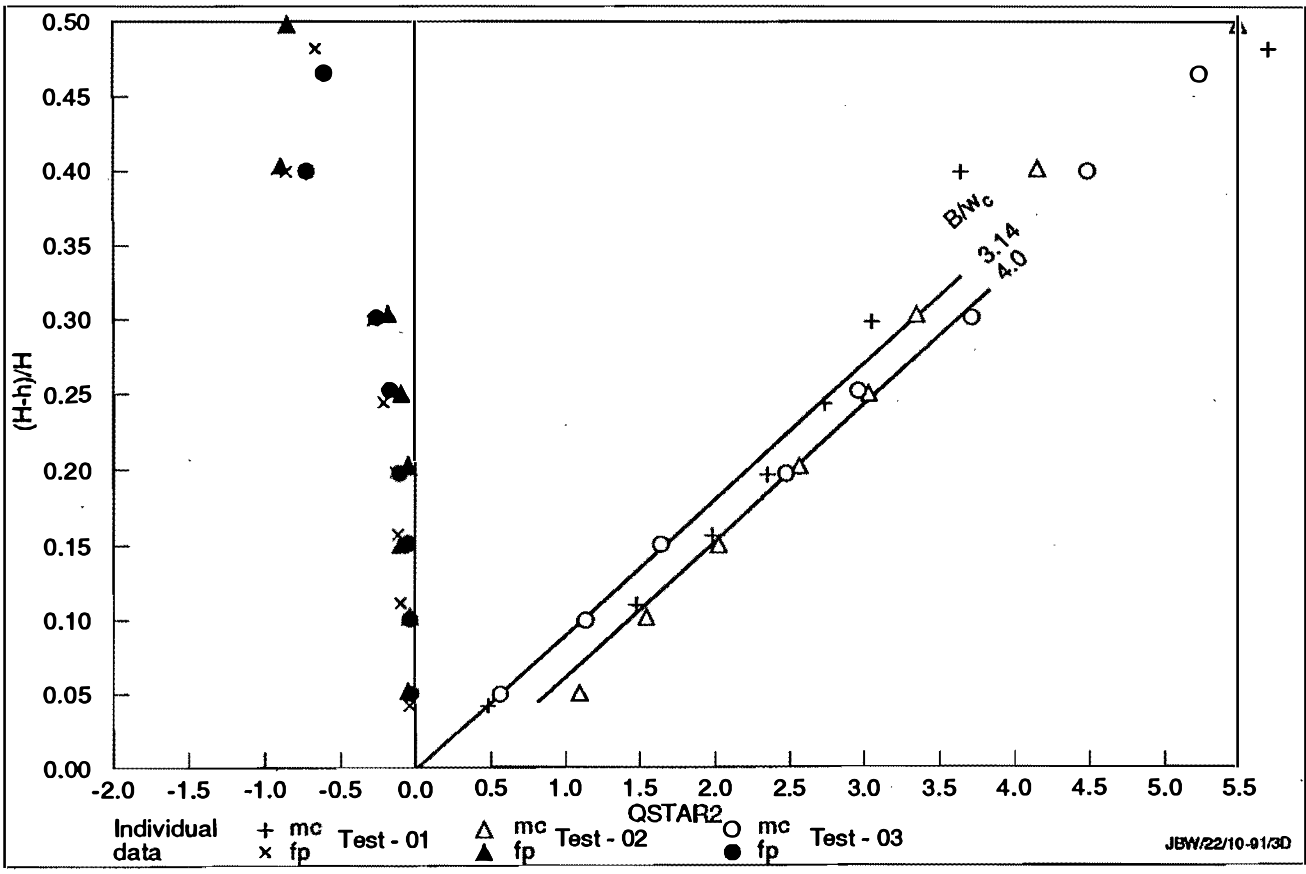

Fig 3.16 Q_{*2} against H* for separate zones: various bank slopes - s_c

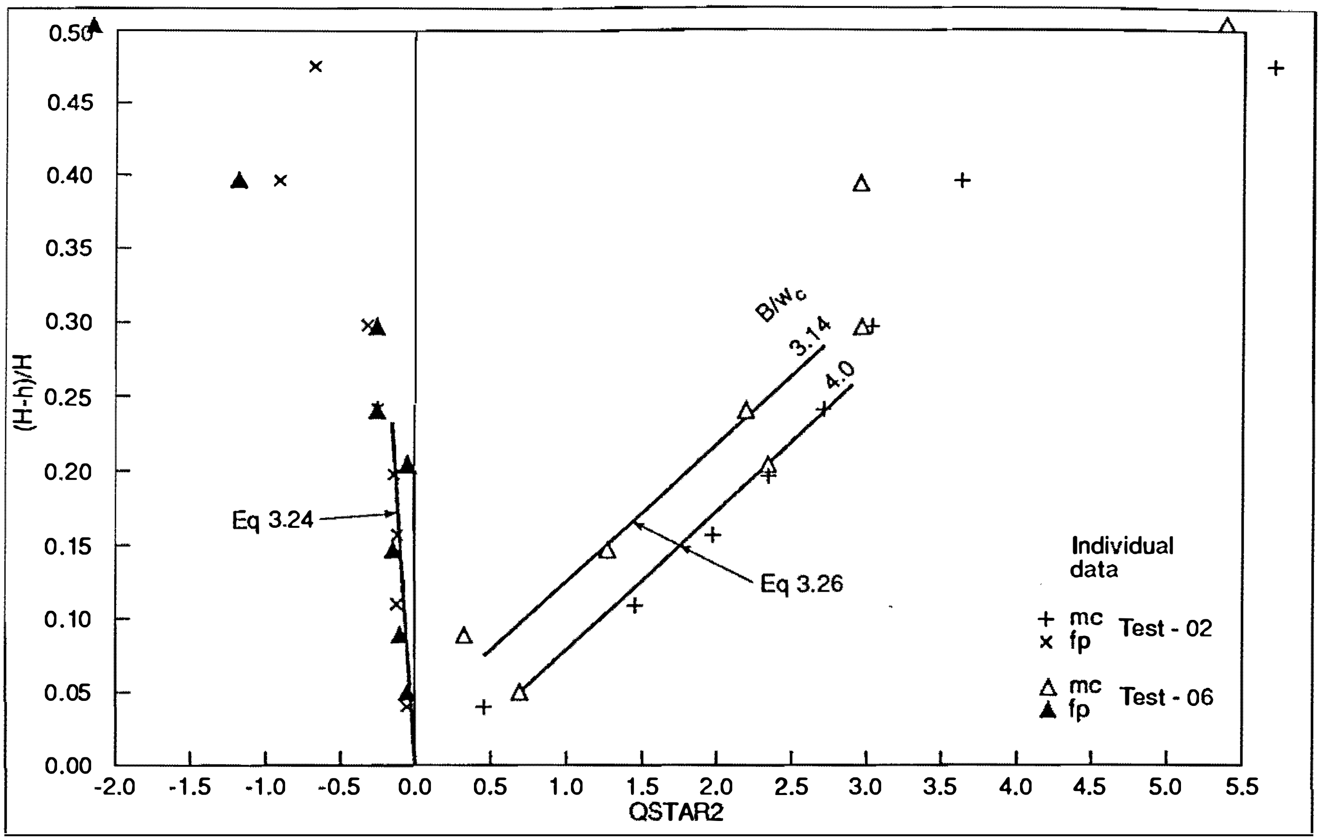

Figure 3.17 Q_{*2} against H_* for separate zone: symmetric/asymmetric comparison

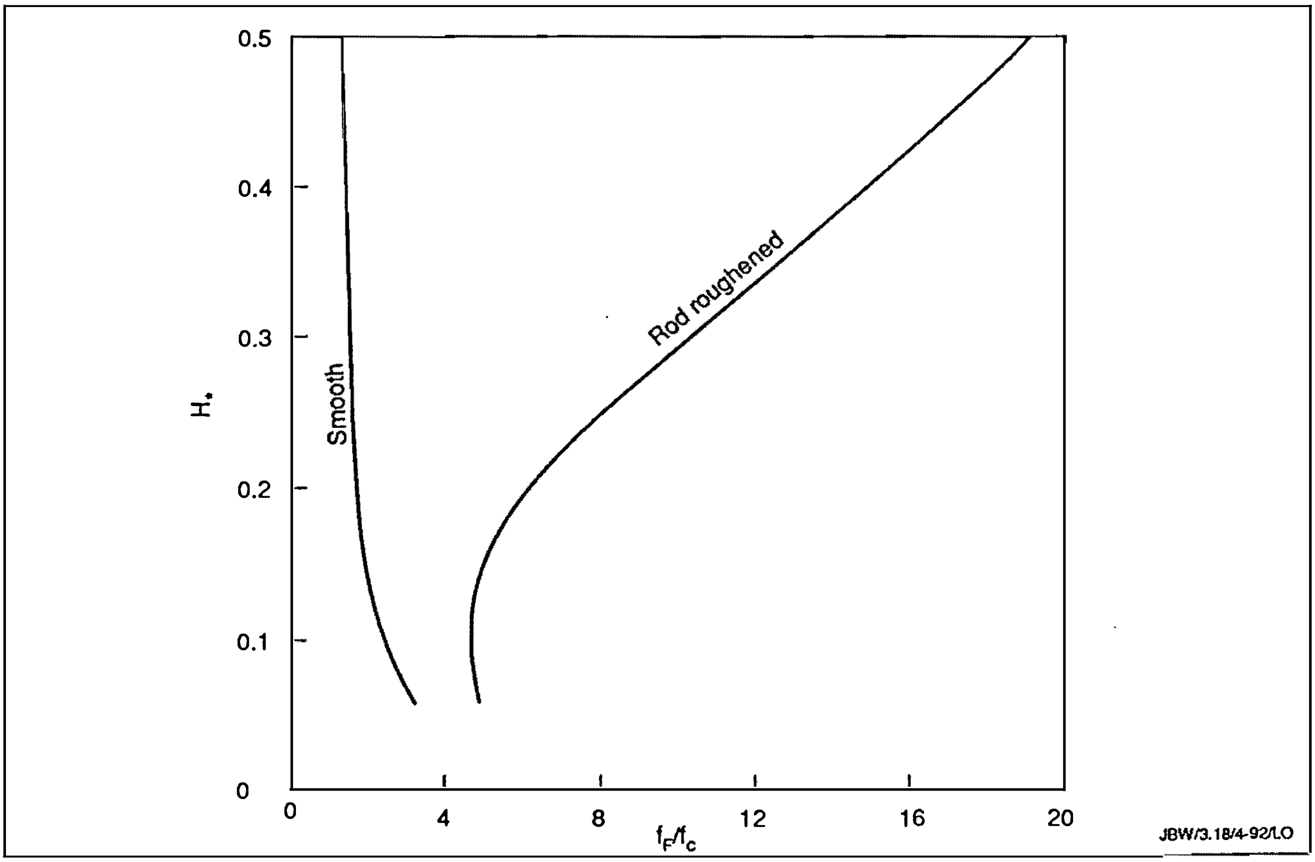

Figure 3.18 Variation of flood plain/main channel friction factor ratio for smooth and rod-roughened flood plains, B/b = 4.2, $s_C = s_F = 1$

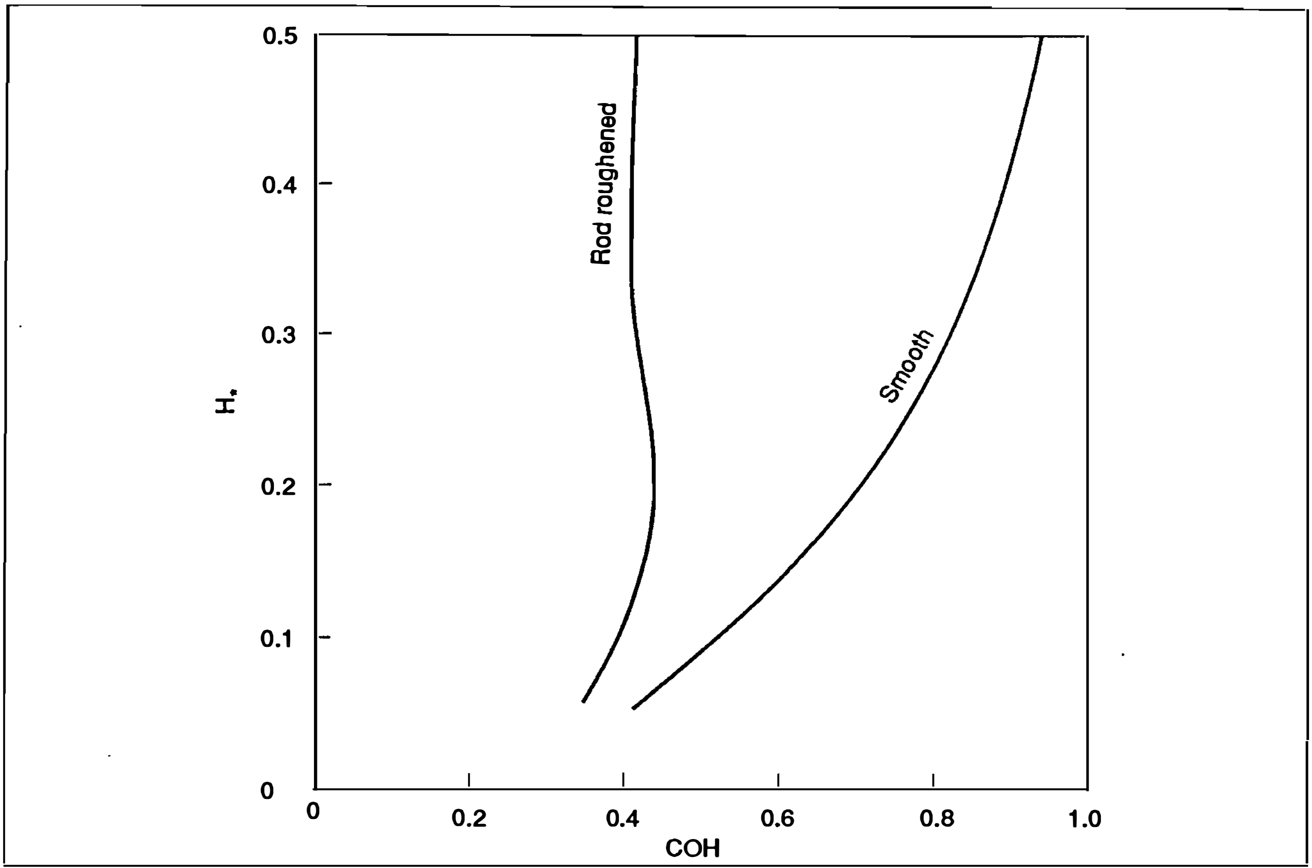

Fig 3.19 Variation of channel coherence - COH, with smooth and rough flood plains, B/b = 4.2, $s_C = s_F = 1$

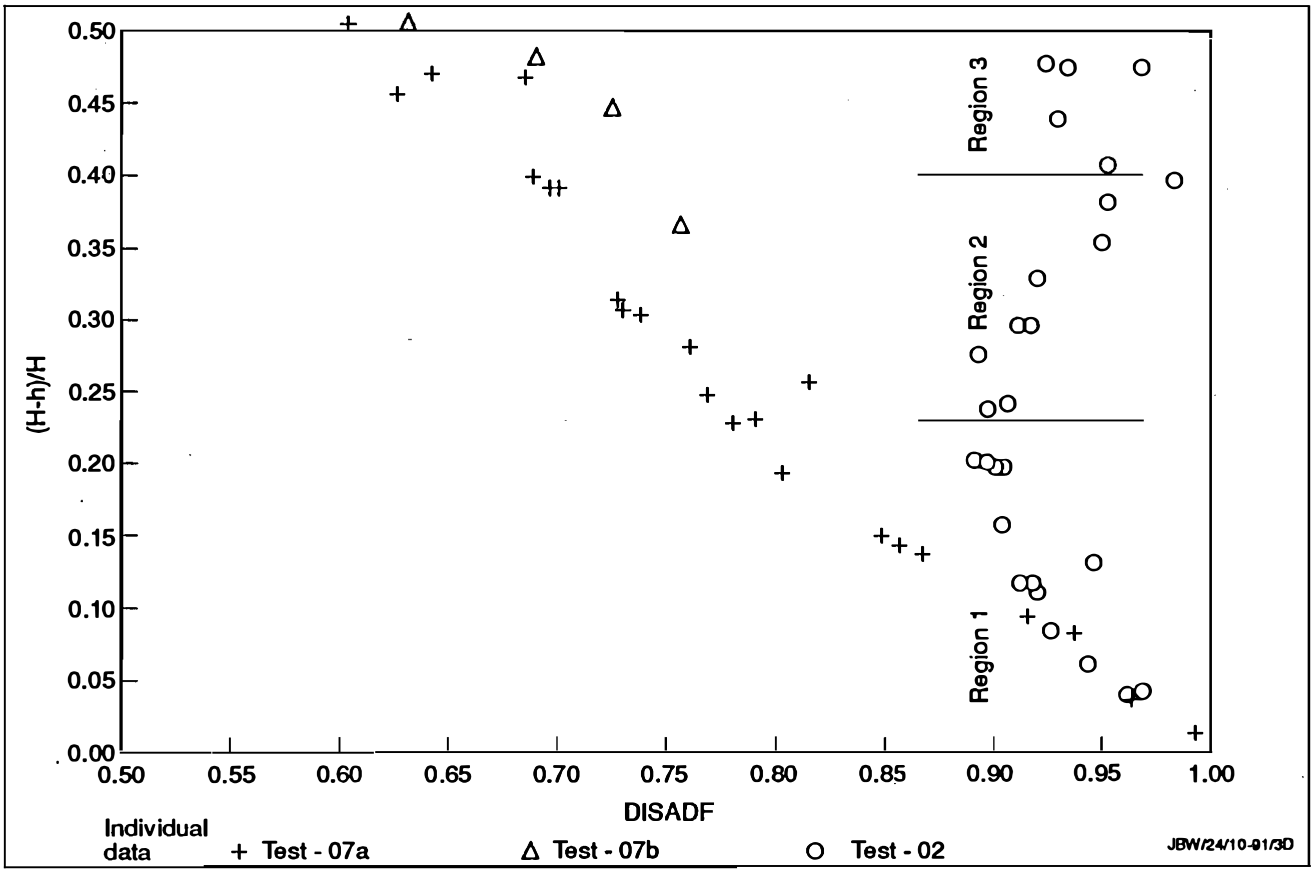

Fig 3.20 DISADF against H*: comparison between smooth and rough flood plains

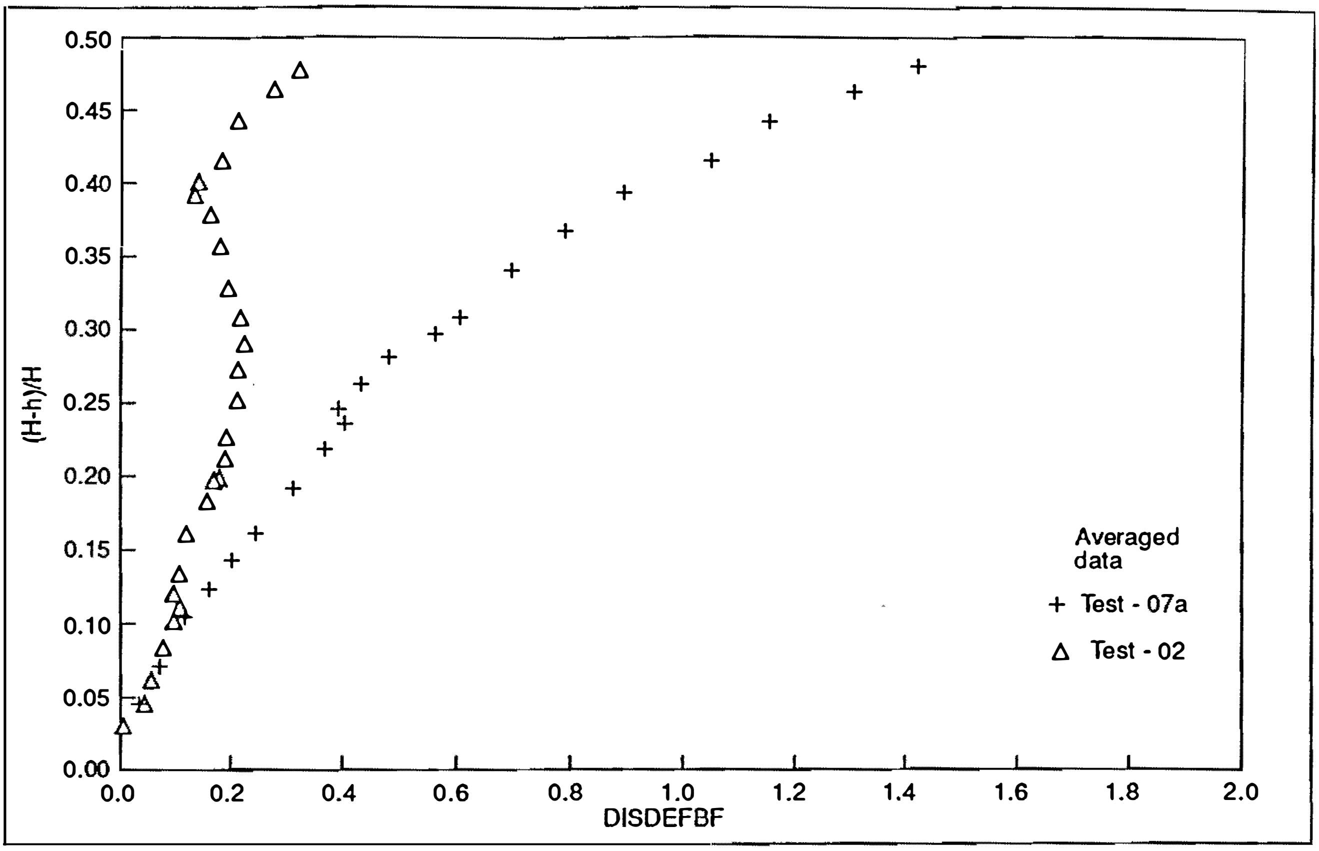

Figure 3.21 DISDEFBF against H*: comparison between smooth and rough flood plains

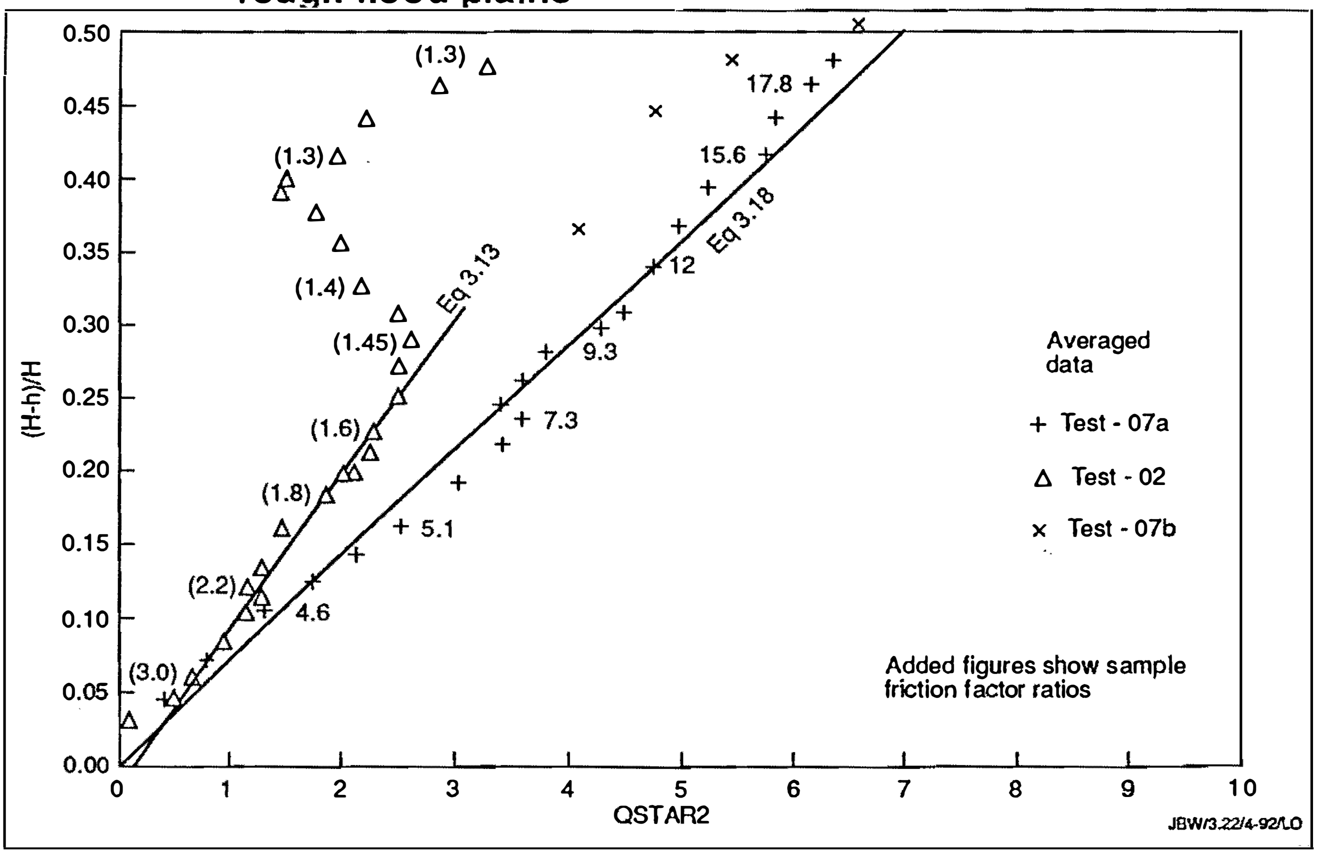

Figure 3.22 Q_{*2} against H*: comparison between smooth and rough flood plains

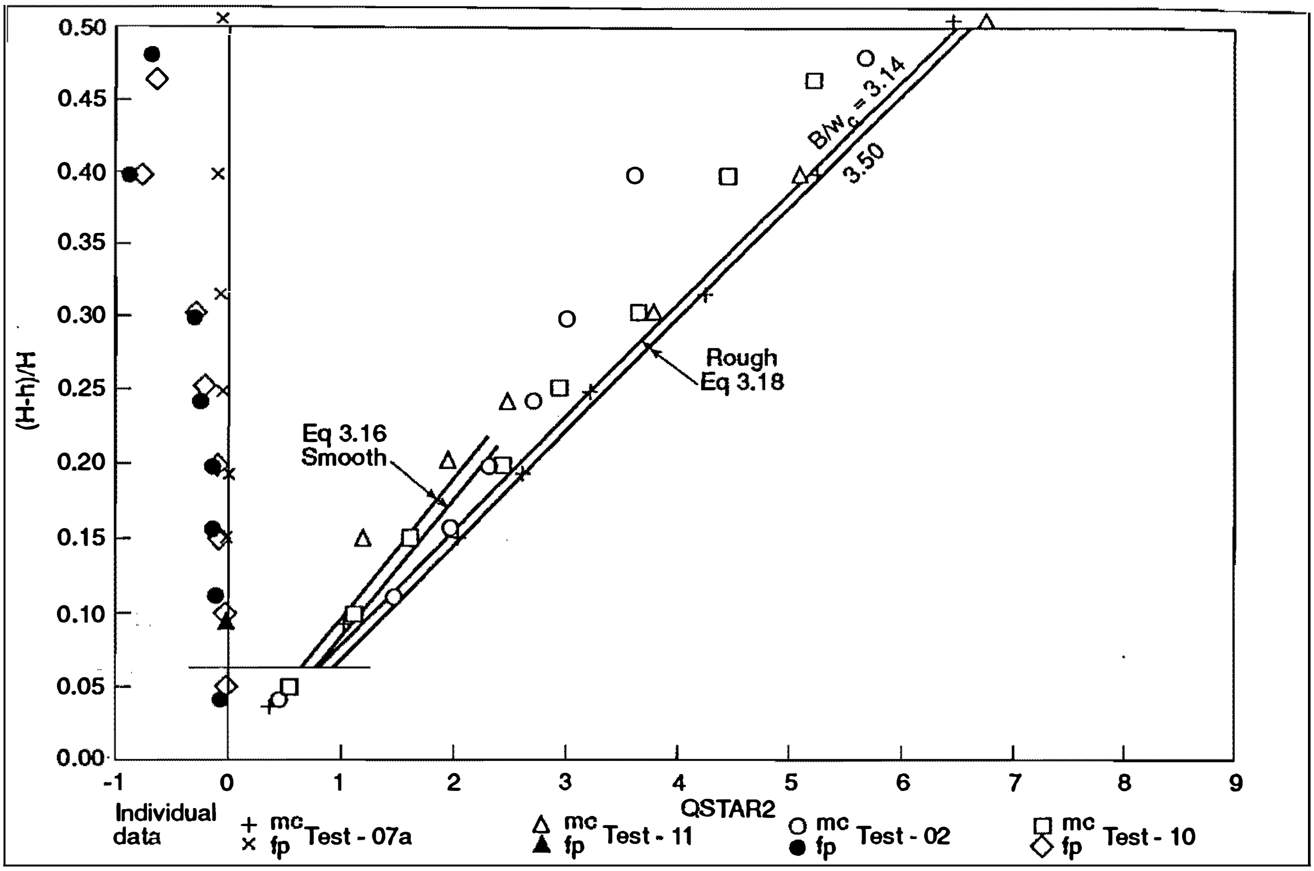

Fig 3.23 Q_{*2} against H_* for separate zones: comparison between smooth and rough flood plains, for channel side slopes, s_c of 1 and 2

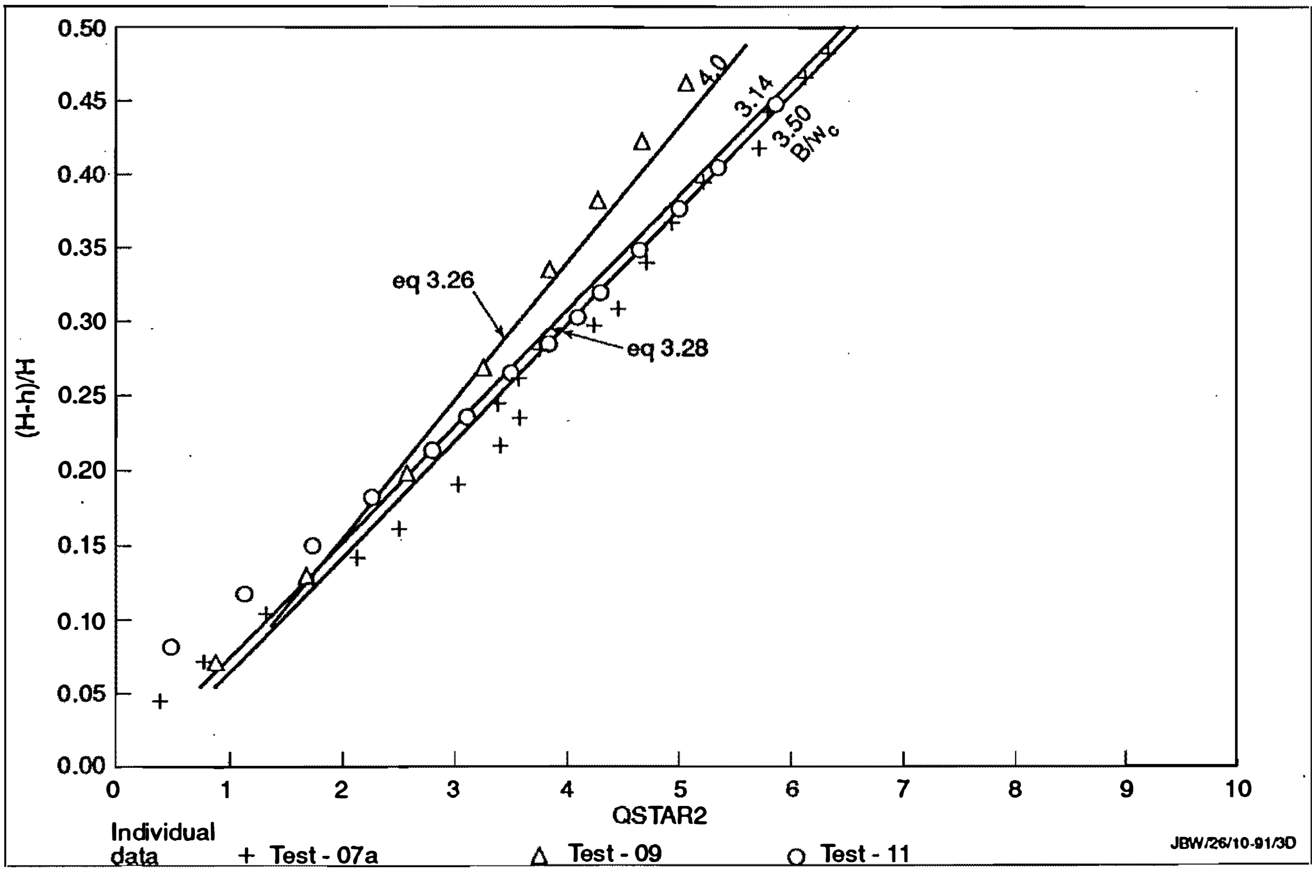

Fig 3.24 Q_{*2} against H_*: rough flood plains with various side slopes - s_c

4. SKEW CHANNELS

4.1 The importance of momentum transfer with non-aligned flow.

4.1.1 If the main channel is not aligned with the flood plains, there will be lateral transfer of discharge between the main channel and flood plains, and of course this implies transfer of momentum. At the junction between the contracting flood plain and main channel, flow with relatively low momentum will be added to the channel, rather like that occurring at a side-channel spillway. This flow requires some additional energy to accelerate towards the general velocity in the main channel. Conversely at the junction between the main channel and the expanding flood plain, flow will be leaving the channel with excess velocity and momentum compared to that generally developed on the flood plains. This excess velocity will be dissipated as it proceeds downstream on the flood plain.

4.1.2 This direct exchange of momentum is a somewhat different mechanism from the indirect exchange which occurs due to interfacial shear adjacent to the banks of aligned compound channels, and is also asymmetric. One might anticipate radically different secondary circulations therefore, even where the angle of skew is quite modest. The detailed mechanism of energy loss will also differ in the two cases. The question of prime interest here is the influence of skewness on the overall head loss as exemplified by the stage-discharge function.

4.1.3 Compound channels where the main channel is at an angle to the flood plains formimg the valley floor can not be of unlimited length: with large angles of skew the channel soon reaches the other side of the valley floor, so the main channel must deflect, perhaps curving round to the opposite direction of skew. Several such reversals would be referred to as meandering. It is only with small angles of skew that one may treat a limited reach of river or artificial drainage channel as a variant of an aligned straight compound channel, rather than as a meandering system where the influence of bends is an integral part of the overall system hydraulics. Also, only small angles of skew can be studied in the laboratory separate from the influence of intervening bends.

4.2 Research on skew compound channels

4.2.1 The only large scale programme of research on skewed channels to date is that carried out by the Bristol research group (Elliott and Sellin, 1990). Their main work on the FCF covered angles of skew up to 9.2° (see Plate 3) and included extensive investigation into velocity fields, shear stresses, Reynolds stresses and secondary currents for a range of angles, with alternative bank slopes. Most of the tests were with smooth channel and flood plains, moulded in cement mortar. One set of tests was with roughened flood plains. The roughness used was a variation of that described in Appendix 2, with a pattern of 25mm diameter rods on the flood plains, extending through the depth of flow. The basic resistance function for the smooth condition is a modified form of the smooth-turbulent equation. The resistance of the rod roughness was developed in Appendix 2, and is a combination of the form drag due to the rods and the surface drag of the wetted perimeter, as used for the aligned channels. The functions derived were sufficiently general to apply to the particular density used in the skew channel tests, where the total numbers of rods in successive transverse rows (left flood plain plus right flood plain) were 12 and 7. The overall density was 9.3 rods per m^2 of flood plain.

4.2.2 For present purposes, only the stage discharge results are considered. The main channel was of aspect ratio 10 throughout, 1.5m bed width and 0.15m deep. See fig 4.1 for cross-section and plan view of the test facility. The side slope applied to the temporary walls forming the edges of the flood plains was 1 in 1 throughout. The overall width of the valley floor was kept constant, and was set at the maximum attainable in the facility with a skew of 9.2°. The test series had to be interspersed with other work in the FCF, so although angles of 2.1, 5.1 and 9.2° were considered, and three main channel side slopes, the coverage was selective, as shown in the following table.

TABLE 4.1 SKEW CHANNEL EXPERIMENTS IN FCF

Series	No of tests	Skew angle, $\phi°$	s_C	2B m	Average FP width m	B/b	Remarks
14	14	5.1	1	5.6	1.90	3.733	Smooth F Ps
15	16	9.2	1	5.6	1.90	3.733	"
16	11	5.1	0	5.6	2.05	3.733	"
17	9	2.1	0	5.6	2.05	3.733	"
18	12	5.1	2	5.6	1.75	3.733	"
19	7	5.1	1	5.6	1.90	3.733	Rough F Ps

4.2.3 The main point of interest is the degree to which the angle of skew affects the interaction between the main channel and flood plains. The basic case with which to compare is that of an aligned compound channel, and although a B/b ratio of 3.733 was not one of those tested in the main series of runs, it is within the range tested and so full confidence can be expressed in the calculation of the aligned channel stage discharge function, for comparison with the skew channel results. These are shown in Figure 4.2 and 4.3 as discharge adjustment factors and relative discharge deficits against relative depth. DISADF is the factor by which the the basic computation of the sum of the main channel and flood plain flows (before allowing for interference effects) has to be multiplied to obtain the true predicted flow for aligned systems, or the actual measurement with skewed systems. The predictive functions used are those derived from the main series of tests described in the previous chapter, which are accurate to better than 1%.

4.2.4 Figures 4.2 and 4.3 (upper) show that in all cases with smooth flood plains the general trend of DISADF for skew channels is similar to that for aligned channels, but the interference effect is somewhat enhanced, i.e. the departure from the basic summation of calculated flows is rather greater. The indications are that the flow goes through the same regions as depth increases as were observed with aligned systems. In terms of its effect on the overall stage discharge function, the interference effect increases with depth at modest relative depths (region 1), then diminishes at greater depths (region 2) and probably goes through the transition region

3 before approaching the region 4 condition where the discharge may be calculated from the overall channel section geometry with perimeter weighting of friction factors. With rod roughened flood plains, an angle of skew of 5.1° adds a relatively modest but somwhat variable amount to the interference effect, which from the values of DISADF plotted for this case is in any case considerable. Incidentally, the high ratios of calculated friction factors for main channel and flood plain (up to 18) mean that flow stays in region 1 in this case, whereas with smooth flood plains flow had apparently progressed through the regions.

4.2.5 One way to express the extra interference effect brought on by skewness is to factor the discharge deficit that would be calculated in the absence of skew. The individual test results in each series show this to be a reasonable approximation, certainly accurate enough in the context of hydraulic design. The average factors by which the discharge deficit has to be multiplied to allow for skew to provide a good fit to the experiments, together with their standard deviations (bracketted), are listed below:

TABLE 4.2 INCREASED EFFECT OF INTERFERENCE DUE TO SKEWNESS

Channel side slope, s_C	Factor by which the calculated discharge deficits for an aligned system have to be increased: average(SD)			
	2.1°	5.1°	9.2°	Angle of skew
0	1.20 (0.21)	1.12 (0.19)		Smooth FP
1		1.54 (0.14)	1.69 (0.20)	"
2		1.41 (0.16)		"
1		1.12 (0.15)		Rough FP

4.2.6 The experimentally determined discharge adjustment factors were typically of the order 0.85 to 0.93 in these tests, while the calculated aligned channel values were correspondingly of the order of 0.90 to 0.95. Thus a 1% tolerance on the experimental values, say of discharge, would appear as a tolerance of 10% to 20% on the adjustment to discharge deficit for skewness. The figures in the above table are therefore quite sensitive, not only to any experimental tolerances but also to any imprecision in the aligned channel predictions. The conclusions are therefore somewhat approximate, but it appears that:

- the general trend of interference effect with depth for skew channels is similar to that for aligned channels, but enhanced somewhat
- the adjustment required to the discharge deficit may be treated as a multiplying factor independent of relative depth
- there is no conclusive evidence of dependence on channel side slope: the results are somewhat scattered
- for equal roughness on flood plain as in main channel, the factors are approximately 1.2, 1.4 and 1.7 for angles of skew of 2°, 5° and 9° respectively.
- when the flood plain roughness is considerably greater than the main channel roughness (friction factor ratios exceeding say 5) then the adjustment required may be somewhat reduced but the evidence is inconclusive (but see Chapter 5, section 5.4).

4.3 Extension of design method to skew channels

4.3.1 The information on which to base the design of skew channels is very limited, though there is some data from small scale tests to be referred to in Chapter 5. These other results cover a relatively narrow channel, but even so do not extend coverage to an adequate range of channel geometries or roughness combinations. Any recommendations for allowing for skew in assessing the stage/discharge function of compound channels are therefore tentative. What information is available suggests the following procedure:

- follow the procedures for a straight channel of the same overall geometry, assuming that the varying flood plain widths may be averaged and equally divided to left and right
- the aligned channel discharge deficit is the difference between the discharge calculated using the full predictive procedures and that calculated from the simple addition of main channel and flood plain discharges
- for reasonably comparable roughnesses on flood plain and in main channel, these deficits should be multiplied by the following factors

Angle, °	1	2	3	4	5	6	7	8	9	10
Factor	1.10	1.20	1.27	1.33	1.40	1.48	1.56	1.63	1.70	1.77

- in equation form, these factors may be represented as

$$DISDEF_{SKEW} = DISDEF_{ALIGNED} * (1.03 + 0.074\phi) \text{ for } 1<\phi<10° \qquad ...6.1$$

- if the roughness conditions are such that the flood plain friction factor exceeds that in the main channel by a factor of more than 5, the above skewness factors may be somewhat conservative
- no information is available for greater angles of skew and extrapolation is inadvisable

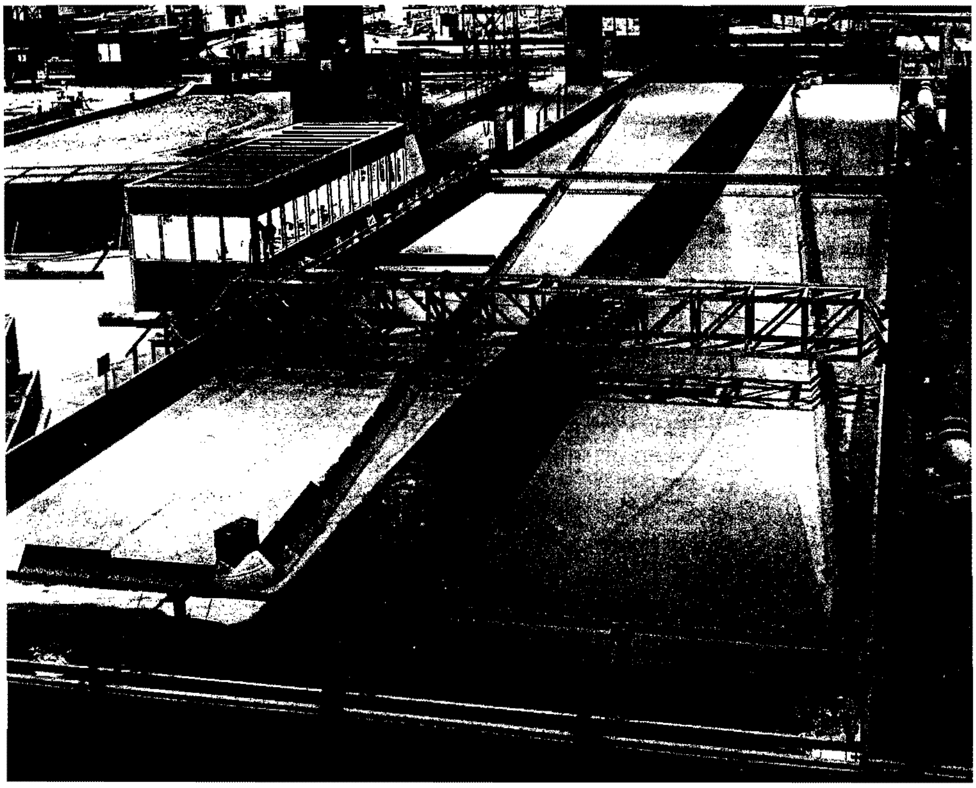

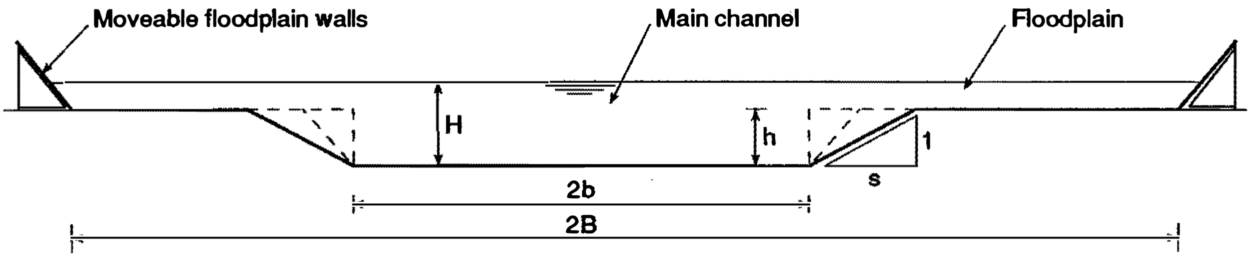

A-A Cross-section of SERC Skew Channel

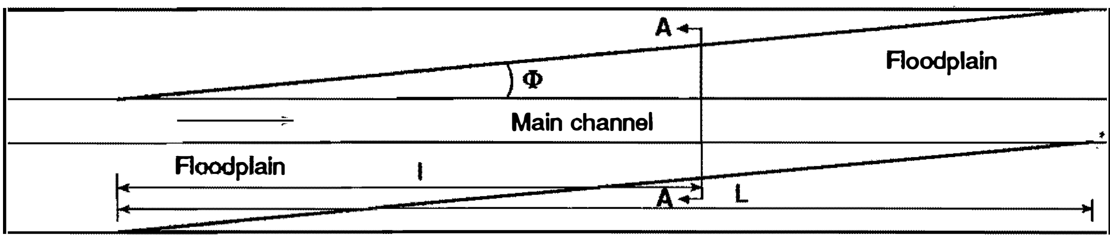

Plan of SERC Skew Channel

JBW/27/10-91/3D

Fig 4.1 SERC Flood Channel Facility, skew channel layout and geometry

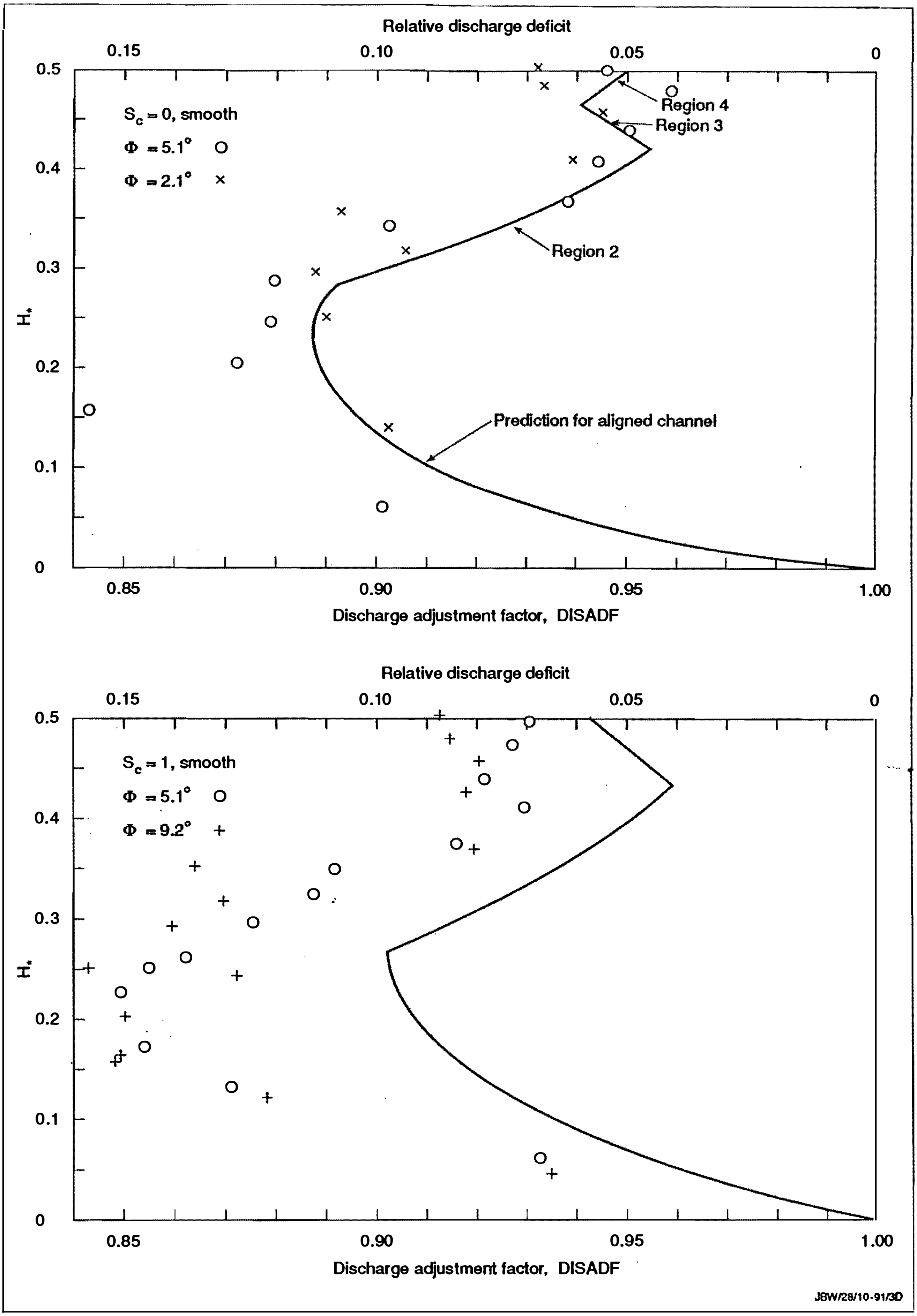

Fig 4.2 Skew channel results, DISADF and relative discharge deficit compared with predictions for aligned channels

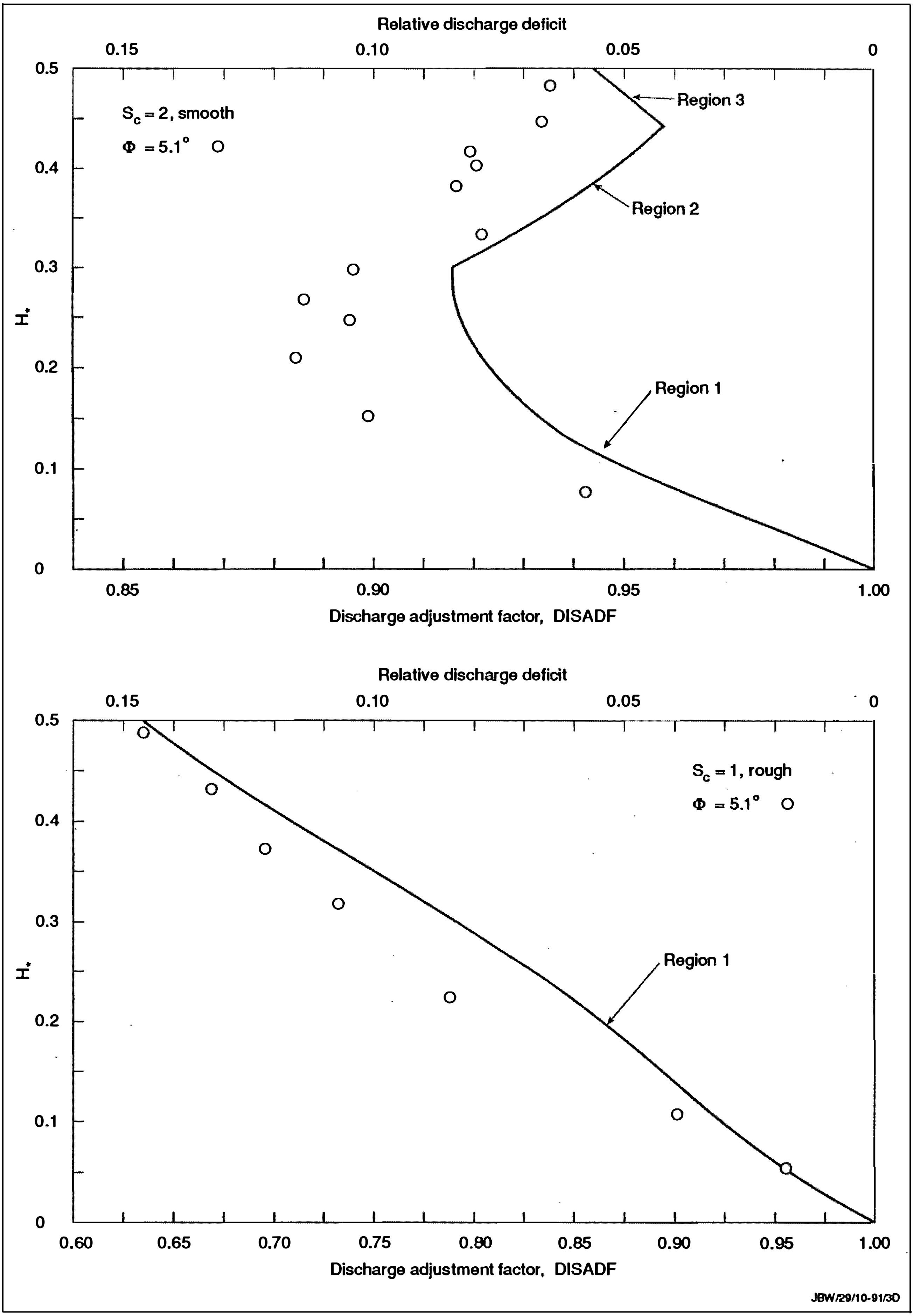

Fig 4.3 Skew channel results, DISADF and relative discharge deficit compared with predictions for aligned channels

5. OTHER SOURCES OF DATA FROM COMPOUND CHANNELS

5.1 Allowance for width/depth ratio in generalised predictive functions

5.1.1 One of the limitations of the FCF at Wallingford is its restriction to a single aspect ratio of deep channel: in other words the ratio of its bed width to depth had the fixed value of 10 for all tests. Dimensional analysis can give no guidance on the relative merits of channel width or channel depth as a normalising dimension in such a test series. The depth h was included in the definition of Q_{*2} on the basis that if the interaction with the flood plain was a localised phenomenon not extending across the full width of main channel, then it was inappropriate to use the channel width to normalise the discharge deficit arising from that interference: channel depth would be more appropriate. On the other hand, if the main channel was narrow enough to contain the full width of the interactive zone, then it would be appropriate to include bed width in the normalised form of discharge deficit, as explained in Appendix 1. In the event, analysis of the FCF research shows that the interference effect is both appreciable and extensive so far as the main channel flow is concerned, and evidence from secondary current measurements shows their potential for distributing the influence over the whole of the main channel, at least up to the aspect ratio of ten covered at Wallingford. The "wide channel" assumption behind the use of h rather than b in Q_{*2}, though legitimate in terms of dimensional analysis and providing a successful basis for the empirical analyses as in Chapter 3, is very much open to question because the FCF research could not provide any distinction between a width-based or depth-based definition of the normalised discharge deficit for Region 1.

5.1.2 In all the work reported in Chapters 3 and 4 it would have been equally valid from the dimensional point of view to replace main channel depth, h, by main channel bed width, 2b: the former had the constant value of 0.15m, the latter the constant value of 1.5m. The empirical analyses would not have been affected by so doing: the goodness of fit would have remained unchanged. Thus the predictive formula for region 1 could equally well be quoted in terms of a new variable, Q_{*0}, where:

$$Q_{*0} = (Q_{CALC} - Q_{MEAS})/(V_C - V_F)2bH \qquad \ldots\ 5.1$$

and, as

$$Q_{*0} = Q_{*2}\ h/2b = Q_{*2}/10 \qquad \ldots\ 5.2$$

then equations 3.24 and 3.25 may be re-written as:

$$Q_{*0F} = -0.1\ H_* f_C/f_F \qquad \ldots\ 5.3$$

and

$$Q_{*0C} = -0.1240 + 0.0395B/w_C + 0.1\ G\ H_* \qquad \ldots\ 5.4$$

(G remains as in equations 3.26 and 3.27).

5.1.3 At this stage it is not known whether the original depth-based definition of Q_{*2} will prove satisfactory when tested against other sources of data, or whether Q_{*0} above will be better. There is also the possibility that the influence of main channel aspect ratio might be intermediate between those limiting forms of equation, and this desirable flexibility can be accommodated by re-defining Q_{*2} as $(Q_{CALC} - Q_{MEAS})/(V_C - V_F)Hh(ARF)$ where ARF is an "aspect ratio adjustment factor". For predictive purposes, therefore:

$$Q_{R1} = Q_{TB} + hH(Q_{*2C} + N_F\ Q_{*2F})(V_C - V_F)ARF \qquad \ldots\ 5.5$$

For the aspect ratio of 10 applicable to the FCF, ARF = 1 of course: but to yield equation 5.1 above, ARF would have to be set to aspect ratio/10.

5.2 Other sources of research data

Scope and limitations

5.2.1 There have been many reports of laboratory research on two-stage channels ever since the large scale studies of the resistance to flow of meandered channels carried out in the mid 1950s at the US Waterways Experiment Station. Compound channels have enjoyed increasing popularity as a hydraulics research project in the last decade. Many of the publications on the subject contain experimental data listings, and it was hoped to validate - or further calibrate as necessary - the formulae derived from the large scale work in the FCF at Wallingford, by using additional data for different section geometries. The other sources of information which have been utilised in this way were published by the following authors (references are given in Chapter 12):

Asano, Hashimoto and Fujita, 1985
Kiely, 1991
Knight, Demetriou and Hamed, 1984; Knight and Demetriou, 1983
Myers, 1978, 1984, 1985
Prinos and Townsend, 1983, 1984
US WES, U S Waterways Experiment Station, 1956
Wormleaton, Allen and Hadjipanos, 1982
Ervine and Jasem, 1991 (skew channels)

5.2.2 These tests in hydraulics laboratories covered a wide range of conditions, as indicated in Table 5.1. The range of main channel aspect ratios was from 1.3 to 30; width ratio B/b up to 30; gradients from 0.22 to 1.8/1000; and flood plain roughnesses up to three times the main channel value, in terms of Manning's n. However, much of this research was carried out in University hydraulics laboratories, and so was of relatively small scale. In order to avoid severe Reynolds number effects e.g. possibly laminar flow, as well as measurement difficulties, depths had to be kept relatively high compared with widths in most of this published research. There is thus a dominance of work at channel aspect ratios of the order of two, somewhat removed from the usual range of practical compound channels, and very different from rivers with flood plains. The exception to this is the research by Asano and colleagues, who used a range of channel aspect ratios based on an analysis of rivers in Japan. This is the only work at aspect ratios greater than that used in the FCF at Wallingford. The main channels of Japanese rivers show a dominant width/depth ratio between 20 and 30; and a dominant B/b ratio of 3 to 5. These values may be representative of many rivers of modest size in the UK too.

5.2.3 The criterion for choosing data for analysis was largely the availability in the published papers of a set of stage-discharge results. However, information given was seldom as comprehensive as required. Although a number of researchers used artificial roughness on the flood plain for at least some of their tests, in some cases Manning's n values quoted were rounded to two significant figures, implying an uncertainty in the value approaching 5%, and it is not usual to find full details - and in many cases any details - of the basic calibration of the particular form of roughening used; nor tolerances on the coefficient values or indication of how accurately the Manning equation represented the resistance function over the range of depths tested. In several cases, as indicated in the Notes in Table 5.1, resistance calibrations were available for re-assessment, perhaps as a result of a personal request for extra information. Considerable importance was attached to this matter, because without a good knowledge of the basic resistance functions for both main channel and flood plains, the comparison of the stage discharge data under compound flow with the predictive methods is problematical. Both the Asano and Prinos data sources suffer from lack of calibration details.

5.2.4 Another typical, though less significant, gap in information is the fluid viscosity, which is temperature dependent. Much of the research was in smooth surfaced flumes, so it is perhaps surprising that the analyses in the published papers are dominated by the use of the Manning formula. This is most appropriate for rough turbulent conditions, when hydraulic resistance is independent of viscosity and Reynolds Number. The relevance of viscosity in smooth turbulent flow not always being appreciated, temperature measurements were not usually available. In some cases, however, Authors were able to respond to a request for temperatures observed at the time of the stage discharge measurements, and from these the viscosity for individual tests could be calculated. It is shown in Appendix 2 that the Manning equation can represent smooth conditions in a laboratory sized system at a given gradient and viscosity reasonably well, though Manning's n will then depend on hydraulic gradient and viscosity. In the re-analysis of the research on smooth channels, thought was given to the best equation to represent the particular form of construction: in some cases the smooth- turbulent equation was used i.e. Colebrook-White with $k_S = 0$; in other cases appropriate k_S values were obtained from the calibration data, perhaps with the wide channel conversion of the transition formula; and in some cases there was little scope for other than the assumption of Manning with the researcher's own coefficient values. On the whole, the results were not found to be sensitive to the choice of resistance function, provided it accurately represented the basic frictional resistance under simple (non-compound) open-channel conditions over the depth range of interest.

5.2.5 There have been many research projects on compound channels, and not all data from past research have been reviewed. Only if the published paper contained stage discharge tables and also provided other basic information required, or there appeared reasonable prospect of obtaining it, was a particular series of tests considered. In one or two cases, the research was at too small scale or at geometries too far removed from practical conditions to be considered worth following up. Only if more data becomes available at main channel aspect ratios of say 4 or more, including roughened flood plains, supported by full calibration information, would it be worth re-opening this study.

Methodology

5.2.6 The analysis of these other sets of data proceeded from the calculation of the basic zonal discharges, using the best friction formula and coefficient values availible from the calibration data, then adjusting the sum of those discharges for interaction using the predictive functions derived in Chapter 3 from the FCF research. The adjustments were made as if the flow could be in any of the four defined flow regions, using the equations appropriate to each region in turn. Then the logic of choice between regions as given in equations 3.34 to 3.36 was followed, so identifying also the correct predicted flow from the four alternatives. These predictions were compared with the recorded observations, test by test, and the differences determined. These differences were finally expressed as percentages of the predicted flow. For any given test series - usually a particular geometry and roughness combination from one data source - the group of results could be expressed statistically, as mean discrepancies and their standard deviations, again as percentages. The mean discrepancy of course shows the overall goodness of fit of the predictive method. The standard deviation has two components: the random scatter in the data due to experimental tolerances and also any difference in the trends of the theory compared with the data. Usually the assumption is made that a confidence band at 95% level will be twice the standard deviation. This assumes a normal distribution of errors, which is probably reasonable for the experimental tolerances but may not represent any difference in trends properly. In summarising the results of the re-analysis, the mean errors and standard deviation were assessed: both are important, the latter especially so as it includes any difference in trends between theory and experiment. Any error in the basic knowledge of resistance would appear primarily in the mean error.

Preliminary analysis

5.2.7 As an illustration of the task of achieving agreement between any method of prediction and the range of experimental results, Figure 5.1 shows data from several sources where the main channel and flood plain were of equal roughness, in the form DISADF against relative depth, H_*. The selected tests are for very similar geometries, with generally smooth main channels and flood plains, and they are shown in comparison with the large scale data from the SERC-FCF, at about the same width ratio (B/b of between 4 and 5). The small scale work shown was all at main channel width/depth ratios of about 2 to 3, compared with ten at Wallingford. The FCF results plotted are the running averages of three: because of this, and the large number of results and their accuracy, they show very little scatter and distinct trends through flow regions 1, 2 and 3. The other data are more scattered, over a band of the order of 5% in DISADF. There is broad similarity of trend of reducing interference effects as depths increase, with some evidence of a kink between $H_* = 0.36$ and 0.44 that would be consistent with a Region 3 transition zone. Most results appear to be in region 2: reducing interference with depth. There is no evidence of Region 1 (increasing interaction effects with depth at shallow depths) in the small scale work, but this may result from the exclusion of data at shallow flood plain depths from the recorded information, because of Reynolds Number limitations.

5.2.8 Not all the Myers results for different gradients were included in Figure 5.1 because they would overload the figure. As there are very many results from this source, it was decided to consolidate them for the range of gradients used into one set, to place them in depth order, and then take running averages of three. The resulting plot is in Figure 5.2, and although there remains scatter over a band of several percent, the indication is of performance proceeding through region 2 via region 3 into region 4. Results for roughened flood plains are shown in Figure 5.3. The

Prinos and Wormleaton cases are for a flood plain Manning's n of 0.17, whilst the FCF results are for surface piercing rods, which result in increasing n values with depth. The trends of the two sets of data are diametrically opposite, with the rod roughness giving progressively increasing interference effects, but the other two data sets showing diminishing interference with depth. So although the large scale data came entirely in Region 1, it appears that none of these smaller scale rough flood plain results were in that region. The Prinos and Wormleaton results shown are, however, consistent with one another.

5.2.9 Figures 5.4 and 5.5 show the predicted interference effect as DISADF using the formulae derived in Chapter 3. On Figure 5.4, alternative values for the aspect ratio factor, ARF, discussed earlier are shown: unity and, in a broken line, channel aspect ratio/10 (also unity for the FCF of course). Alternative functions for Region 3 are shown, the two originals in terms of COH and using a constant DISADF value of 0.95, with a third related to H_*. This last was intended to give a good representaion of the group of results in Figure 5.1 that are probably straddling the transition of Region 3. Comparing with the selected data in Figure 5.1 for equal main channel and flood plain roughness, clearly the predictive equations shown in Figure 5.4 work quite well in that they give results through the middle of the scatter band, but in order to avoid region 1 conditions a value of ARF above aspect ratio/10 seems desirable. In fact the original value of 1 would achieve this, but is not proven because there is no data in this region, nor indeed any evidence that Region 1 type of flow occurred in these small scale rather narrow channels. The FCF results are well forecast, not surpisingly because these data were included in the set upon which the predictive functions were based. For this particular Wallingford geometry, with $s_C = 0$, Region 3 seems to indicate a constant DISADF (the other values of s_C tended to support the alternative function depending on COH in Region 3). Note that the Region 2 predictions, where the equation is based on channel coherence, nicely follow the different trends for the two aspect ratios covered.

5.2.10. Figure 5.5 shows similar predictions for rough flood plains, using the rod roughness functions in the one case and the Manning formula in the other. Surprisingly good agreement with the very disparate trends of data in Figure 5.3 is obtained, with no adjustment to the FCF based functions. It should be remembered that f_*, f_F/f_C, for the rod roughness increases progressively with depth of flow. This is not so with boundary roughness, which is why the trends differ radically. The ability of the predictive functions to cover a quite different aspect ratio and radically different type of roughening is notable. It is not proven that ARF = 1, however, as a range of values above aspect ratio/10 would suffice in terms of this sample of data. To provide a good fit, ARF merely has to be high enough to avoid any Region 1 predictions over the range of depths for which the small scale data are available.

5.2.11 At this stage it might be thought that the predictive functions derived in Chapter 3 are fully validated; that no modification is required for aspect ratios differing from 10. The equations adapt well in this sample of results to different geometries, and even accommodate boundary roughness though originally based on flood plains roughened by surface piercing rods. Detailed analysis of the full range of data available show that not all results fall so readily into this neat pattern of agreement, however.

Difficulties

5.2.12 As illustration of the problem posed by some ot the published data, the test results from Prinos and Townsend for 305mm and 406mm channel widths are shown on Figure 5.6, for the four flood plain roughnesses they considered. The only difference between these test conditions was channel width, changing the aspect ratio from 3 to 4. At aspect ratio 3, there was considerable interference effect, with up to 30% loss of conveyance. There was strong dependence on roughness too. Yet with aspect ratio 4, the interference effect has dropped to under 4%, with a few positive effects rather than the expected reduction of discharge - and no identifiable influence from flood plain roughness. The natural conclusion was that no predictive method could reasonably be expected to reconcile such results. This problem was resolved to some extent on referring the initial analysis of these results to the originator of the data, who then advised that there was a discrepancy between his Thesis and the stage-discharge data published in 1983. The experiments had been repeated with extra care in setting uniform flow, and so a revised and radically different set of results was provided. These revised data have been used in the final analysis, of course. The Prinos and Townsend procedures and results will be referred to again later. In essence, they confirmed that ARF should not be less than aspect ratio/10, preferably rather higher than that. However, the agreement between the predictive method and these experiments became less and less satisfactory as the roughness of the flood plains was increased. The basic roughness of the meshes used is open to question, however: no calibration data were available but it is known from other work with mesh roughness that the Manning equation with constant coefficient does not accurately represent the hydraulic resistance over a range of depths.

Asano et al (1985)

5.2.13 Turning attention now to the widest aspect ratios covered in any of the published research, of about 30, as studied by Asano and colleagues: the problem with these results is that the flow was non-uniform in almost all the tests reported. There seems to have been little attempt to ensure uniformity, and the common situation was with water surface slope exceeding the channel slope, by up to 50% for the deepest cases, (in one case 70%!). To avoid including test results where a large proportion of the flow was being 'squeezed out' of the flood plain, the re-analysis excluded water surface slopes more than 20% in excess of the channel gradient, but even with this limitation the pattern of secondary circulations and shear zone effects must have been affected.

5.2.14 Several different assumptions were made in carrying out the analysis of the Asano et al data. A range of aspect ratio adjustment factors were considered, with ARF going from the basic value of unity to aspect ratio/10, i.e. 3. As well as using the Authors' Manning's n values, the wide channel resistance function was applied with the in-bank tests to assess suitable k_S values. Although the construction method was the same throughout the series, the Authors quote a range of n values from 0.0091 to 0.0114, so the actual resistance is rather questionable. However, the conclusion was that, taking the overall average, none of the alternatives tried proves any advantage over the use of the Manning formula with the Authors' quoted coefficients for each test series, coupled with ARF = 1. Some individual series tended to support ARF = 3, i.e. aspect ratio/10. Many of the test series have residual overall discrepancies between prediction and observation, but this may well arise because of uncertainty over the basic -

and strangely variable - main channel roughness coefficients recommended, which could give systematic errors. The average agreement overall is within 3% with a scatter of 2.3%, so within the tolerance that might reasonably be expected, especially bearing in mind the possible influence of non-uniform flow in many tests. Most of these results come into Region 1, so they are indeed providing a test of the definition of Q_{*2} in this zone. Being the only available results at aspect ratio > 10, they are potentially very valuable; but as flow was non-uniform and no detailed calibration data was published, this potential value has not been fully realised.

US WES (1956)

5.2.15 As shown in Table 3.1, the tests carried out at the US Waterways Experiment Station were at large scale, though rather few of them concerned straight channels: the main thrust of the research concerned meandering channels (see Chapter 8). The necessary minimum calibration data were available in the published report for both the main channel and the flood plains, both smooth and with mesh roughening, though it was found necessary to reanalyse these and establish the variation of Manning's n with depth of flow to avoid too much approximation in determining the basic resistances. A 1ft wide channel was tested with a 30 ft total width across the flood plains, but this gave no useful results, as the original researchers themselves concluded. This is because the main channel carried such a small proportion of the total discharge, the interference effect proved unmeasurable in terms of stage discharge. This led to the testing of a 2ft wide channel, with width/depth ratio of 4 and relative width, B/b, = 8. In terms of large scale, the form of roughness used (panels of wire mesh), and geometry these tests are of considerable interest, coming much closer to reality in terms of scale and geometry than much of the laboratory work.

5.2.16 Serious errors of prediction were obtained with ARF = 1 as implicit in the original set of predictive formulae. Region 1 was being properly tested, in that results in that region were included in all 9 runs (3 at each of 3 flood plain roughnesses) and so the rather firm conclusion could be drawn from these tests that ARF should equal aspect ratio/10, i.e. that the definition of Q_{*2} should be modified to include channel width rather than depth. For the 2ft channel, this gave a mean error of 5% with 5% variability using the calibration values of k_s in the wide channel transition function as the basic resistance. Some adjustment to those values reduced average error to 0.7% and variability to under 4%. It was this early but positive finding from the US WES research that led to much effort in seeking to optimise ARF as a function of B/b and 2b/h, though in the final analysis there does not appear to be any complex function involved.

Kiely (1991)

5.2.17 Information about very recent research was obtained privately from Dr Kiely, of University College, Cork, Eire. As with the US WES, his main interest was in meandered channels, but he had also researched a particular straight channel geometry, with aspect ratio 3.7 and B/b = 6, so in terms of geometry coming closer to the US WES geometry than any other. He tested with both smooth and roughened flood plains and provided good calibration data for both conditions. There were five tests of compound flow for smooth and for rough flood plains. The conclusion here was again that the allowance for the inflence of the main channel width/depth ratio on the interaction effects in Region 1 was best achieved with ARF set at aspect ratio/10, though with the smooth flood plains any higher value was equally valid as no Region 1 results remained in the data set for ARF > aspect ratio/10. The finding that ARF = aspect ratio/10 was fairly positive with rough flood plains.

Knight et al (1984)

5.2.18 The research described by Knight, Demetriou and Hamed (1984) on smooth compound channels is characterised by particular care to achieve uniform flow, and so the doubts and possible criticism of some of the other research on that score do not apply here. Also, calibration data for the flume were available from within bank tests. They tested 3 width ratios, B/b = 2, 3 and 4, but the one aspect ratio of 2: a typical narrow laboratory set-up, rather far from the geometry of two-stage channels of hydraulic engineering and alluvial rivers. 18 pairs of stage discharge data are available, with smooth flood plains and main channel. (Knight and Hamed (1984) also reported an extension of the test series to cover roughened flood plains, but the data were not published in detail and have not been analysed here). Their results for B/b = 4 are included in Figure 5.1, and comparing with Figure 5.4 they are seen to agree well with the prediction. The result at minimum depth lies exactly on the prediction of Region 1 in Figure 5.4 for ARF = aspect ratio/10 - though one point can hardly be said to provide proof. In fact values of ARF from 0 to 1 were considered, and for the B/b ratio 4 the prediction was exactly correct on average, with 2% variability about that mean, for ARF = 0.2. The best fit for B/b = 3 was when ARF = 0.4, but at B/b = 2, ARF = 0 was best - in other words, the effect of any interference was negligible in terms of stage discharge function. Results were thus somewhat variable in respect of the allowance for channel aspect ratio, though good accuracy was achievable be treating ARF as a variable to be optimised.

Myers (1984)

5.2.19 Myers' pre-85 research concerned smooth conditions in a relatively small laboratory flume. Some tests were with only one flood plain; others were symmetric with two flood plains, and although all the data were re-analysed, only the symmetric cases will be referred to here. These were with aspect ratio 2 and B/b ratios of 3.2 and 4.7 (see Table 5.1 for details of test geometries). One feature of Myers' research programme was the coverage of a range of slopes, so that in all 153 pairs of stage discharge results were obtained, over 40% of the total data set from other laboratory research. At the minimum flume slope of 0.22/1000, one might anticipate considerable difficulty in measuring the water surface gradient and therefore in achieving uniform flow. Typical tolerances on setting and measuring hydraulic gradient, and hence the equivalent tolerance on discharge, will be referred to again later. Based on the full flume length, there may in this case have been a potential tolerance of 10% when expressed as equivalent discharge at minimum gradient, dropping to perhaps 2% at maximum gradient. Of course, this source of random experimental error does not apply only to the research by Myers: it applies to most of the others as well, where the flume length or gauging length was restricted by the available facilities, and especially where gradients under 1/1000 were applied.

5.2.20 In re-analysing Myers' data, a range of possible adjustments for width/depth ratio were tested, with ARF from 0.2 to 1. As might have been anticipated from the sample of results examined earlier in Figures 5.1 and

5.2, there were no Region 1 flows within the range of depths studied, so that the only conclusion to be drawm about optimum ARF values from this research is that ARF could take any value from aspect ratio/10 to unity with little effect on the statistics of goodness of fit between prediction and experiment. With B/b = 4.7, 2b/h = 2, the mean discrepancy from the predicted flows was 1.6%, with variabiliy 2.9%; with B/b = 3.2, 2b/h = 2, mean discrepancy under 1%, variability under 6%. Thus the predictive functions may be regarded as validated to much the same order of accuracy that could apply to the data, though as Region 1 was not covered by the research results, the validation is confined to the higher Regions of behaviour.

Wormleaton (1982)

5.2.21 The research by Wormleaton and colleagues detailed in the 1982 paper was for one channel geometry but it covered a wide range of flume slopes and also 3 sets of artificial roughness in addition to the series with smooth flood plains. The artificial roughness took the form of 10mm dia hemispheres, at different densities, and this form of roughness was calibrated, i.e. its basic resistance function determined, in separate flume studies. Although not included in the original publication, this calibration data was made available for re-analysis in the present study, so that an independent check was made of the roughness coefficients for each density, and of the accuracy of fit of the Manning formula to the observations. Dr Wormleaton, in a personal communication, commented as follows on the tolerances applicable to laboratory scale reseach: "Assuming the multi-manometer scale can be read to 0.5mm accuracy, then the corresponding depth accuracy will be 0.2mm. Although the scale of the vernier point gauge can be read easily to 0.1mm, its accuracy in setting to a moving water surface is probably no better than 0.2mm. Clearly over a 2.5m test length, this can lead to an error in the water surface slope of 0.00016. However, errors of this magnitude are unlikely since six tappings are used over the 2.5m length... As a general point, it is clear that in any small- scale laboratory work, assessment of hydraulic gradient is far more prone to error than measurement of depth or discharge." If the error in head difference was, say, 0.00005, this represents a little over 10% for the majority of the tests in this research programme, which would feed back to a 5% or so error in basic discharge assessment, and this is probably typical of the tolerances to be expected in small scale laboratory tests in this field.

5.2.22 In these tests the compound channel was formed from precast concrete blocks, placed either side of the base of a Perspex flume. The roughness of the concrete was well established from the calibration data. The main channel walls were then lined with Perspex so as to have the same surface roughness as the bed.

5.2.23 Several values for the factor allowing for any influence of aspect ratio on region 1 flows were tested against the available stage discharge results. The aspect ratio of this channel was 2.4, and ARF values both sides of 0.24 were considered, and the detailed statistics of the goodness of fit were derived. The data for a flood plain Manning's n of 0.017 are included in the plot of Figure 5.1: with data for a common gradient linked together. The more comprehensive of these sets, compared with the other data in Figure 5.1, suggests that there may be a positive systematic discrepancy, but there is no evidence of region 1 flow. This is indeed what emerges from the statistics of the comparison with the predictive method: generally speaking, the Wormleaton et al results are well represented by a high enough value of ARF to ensure avoiding any Region 1 predictions over the ranges of depths studied. There is no evidence from these results of requiring any change to ARF = 1 implicit in the basic method, but again no proof that ARF = 1.

Prinos and Townsend

5.2.24 The Prinos and Townsend results have already been referred to, and because there are 80 pairs of stage discharge results over a range of different aspect ratios and relative widths, with 4 different flood plain roughnessess, they are an important source of information. Basic calibrations were obviously carried out to assess the wire-mesh roughness utilised, but the details were not included in the published paper, and could not be provided by the Authors, so their quoted n values have not been subject to any checking. Detailed stage discharge information was published, that in 1983 for the 406 and 508mm channels, and separately in 1984 for the 203 and 305mm channels, but the latter set of data was apparently unreliable and the first Author provided a set of corrected stage/discharge data. The Authors also examined procedures for assessing the stage discharge function, using the concept of interfacial shear stress to produce predictive methods.

5.2.25 Broadly speaking, the smoother of the flood plain conditions tested by Prinos and Townsend show interference effects reasonably consistent with ARF = aspect ratio/10, though a somewhat higher value would improve agreement in many of the series of tests. Less satisfactory results were obtained from the data for the two roughest flood plain conditions, however: there was greater variability as well as greater residual errors, so that no firm conclusions could be drawn.

5.3. Summary of information from other laboratory research

5.3.1 The re-analysis of data from other sources contains too much detail to include here. It was given in greater detail in Technical Report number 5 of the project, which is unpublished but was available to most of the research workers directly concerned for their comments. Some further details, in the form of summaries of the statistical analyses, will be found in Appendix 7.

Region 1: influence of width/depth ratio of main channel

5.3.2 The information relevant to any modification of the original predictive functions to accommodate a full range of main channel width/depth ratios is summarised on Figure 5.7. This provides the evidence in terms of optimum, or acceptable, ARF values in the matrix of aspect ratio, 2b/h, and relative width, B/b. Coverage of the field is rather sparse and irregular, with so much of the available data being for rather narrow laboratory scale systems.

5.3.3 The original formulation of Q_{*2} used in the predictor for Region 1 was derived on the assumption that the channel was wide in relation to the zone of interference from the flood plain, so it would not be surprising to find the obviously narrow channels used in many of the University studies departing from that assumption, and approaching a width rather than depth based discharge deficit, i.e. tending towards ARF = 2b/10h. Conclusions from the US WES and Kiely research plotted in fig 5.7 show this trend, as does one of the geometries tested by Knight. Myers results are not inconsistent with this evaluation of ARF, and this applies also to the smoother of the Prinos and Townsend flood plain conditions. It was originally hoped that Figure 5.7 would lead to a contouring of suitable ARF values but the coverage is sparse and no realistic contouring could reconcile all the results from narrow channels. These include some showing almost no interference effect, which is consistent with ARF = 0, effectively making region 1 dominate the picture but with the discharge adjustment factor set to 1; others show no evidence of Region 1 flow (increasing interaction effects with flow depth) and this would be consistent with confining Region 1 to depths below those for which data is available, by setting ARF = 1. Test series suggesting either ARF = 0 or ARF >> 2b/10h are rather negative, in that they are not really providing information on how Region 1 flows may be influenced by main channel aspect ratio; though they may at the same time be quite positive in their confirmation of the predictions for Regions 2, 3 and 4.

5.3.4 There is no reason to doubt the experimental skills and careful measurements of the researchers whose results may be out of line with others or which do not fit well the empirical functions derived from the large flood channel facility at Wallingford. It is known from turbulence modelling (as described in Chapter 6) that the momentum transfer is just as much a result of secondary circulations as it is of lateral variation of mean depth velocity giving rise to additional shear across the interfacial plane. Might some of these research projects have been conducted in facilities that were not long enough to generate a representative system of secondary circulations as would be expected in very long channels? Might these secondary circulations also be sensitive to inlet conditions, or to any non-uniformity of flow? And is Region 1 particularly sensitive to the momentum exchange via such secondary circulations?

5.3.5 It is worth stressing, however, that on the whole the predictive method has proved robust in that it transferred well to other very different geometries and roughnesses. It is only region 1 that obviously required modification to fit some series of tests to allow for the influence of main channel width/depth ratio, and this requirement had been anticipated for narrow systems. In this context, it is interesting to look again at some of the published information at shallow flood plain depths. Some research suggests that a radical step would occur in the stage discharge function as the flow went above bank. Prinos and Townsend (1984) give a figure that shows their own results for aspect ratios of 2 and 3 with comparable data from Wormleaton's and Myers' work. This is reproduced as Figure 5.8, and if one extrapolates these results towards $H_* = 0$ (assuming no Region 1 flows in effect), then at just above bank full, the discharge could drop to 70% - even as low as 40% - of its bank full value. Certainly the tests in the FCF at Wallingford did not show anything like that degree of obstruction to discharge soon after the flow went over bank; and there is no evidence from the field either that the "kink" in stage discharge function at bank full is ever of such a magnitude (see also section 5.5 following). It is for this reason that preference is given in the final interpretation to those results which suggest a relatively gentle increase of interference effects as to flow goes over-bank as given by ARF = aspect ratio/10.

5.3.6 What about wider channels than the FCF with its aspect ratio of 10? One would expect that the wide channel assumption for the definition of Q_{*2} in Region 1 would become increasingly valid as the aspect ratio increases. Unfortunately there is only the Asano et al data at aspect ratios above 10, and this does not provide the degree of reliability that one would hope for (non-uniform flow; absence of calibration details; uncertain basic resistance). The evidence from that research, however, is that its aspect ratio might be above the lower limit for being effectively wide, in that the results divide between those best represented by ARF = aspect ratio/10 = 3 and a lower value, although it seems clear that the FCF aspect ratio of ten was below the limiting value. The provisional conclusion is that we might assume a channel aspect ratio of 20 as the limit between *wide*, when ARF in the predictive functions takes the value at that limit, i.e. 2, and *narrow* when the appropriate value becomes aspect ratio/10: thus

For aspect ratios > 20, ARF = 2.0

For aspect ratios $\leqslant$ 20, ARF = 2b/10h

Region 3

5.3.7 Another question in mind as the analysis of data from other sources was carried out was the best function to describe region 3. The SERC-FCF results had shown preference for equ. 3.31, though the simpler formula 3.32 was almost as good. A third function is shown on Figure 5.4:

$$DISADF = 1.233 - 0.667\ H_* \qquad \ldots\ 5.5$$

It transpired, however, that few data sources provided a real test of Region 3. Some did not extend to sufficient depth; some were at a few wide-spread depths that missed out Region 3; in fact Region 3 proved rather elusive so that most data sets gave no basis for making any recommendation. The consolidated and averaged Myers' results in Figure 5.2 appear to support a constant DISADF of 0.95 in Region 3, though individual results plotted in 5.1 seem more consistent with equation 3.31 or 5.5. Myers was the only data set that clearly included Region 3 and contained sufficient points to make an analysis of the alternatives worth while. The statistical details of how well the three alternatives fit these data, both considering Region 3 results by themselves, and also taking all regions together, are as follows:

	Mean errors and standard deviations: %	
	All data:	Region 3 only:
Equation 3.31 (COH):	$+ 0.47 \pm 4.19$	$+ 1.72 \pm 4.43$
Equation 3.32 (constant):	$+ 0.49 \pm 4.15$	$+ 1.12 \pm 3.39$
Equation 5.5 (H_*):	$- 0.39 \pm 4.00$	$+ 1.86 \pm 3.32$

5.3.7 There is no clear cut conclusion to be drawn regarding Region 3. There is no firm evidence to suggest changing from the formula that best representing the SERC-FCF results, namely equ 3.31 in terms of channel coherence, COH.

5.4. Skew channels

5.4.1 Ervine and Jasem, (1991) tested two-stage channels with skewed flow. These are the only independent results featuring skew channels, but they also take on extra significance in the definition of the aspect ratio adjustment factor, ARF. The test flume at Glasgow was small compared with the FCF at Wallingford, and might be regarded as providing a vertically exaggerated model, about 1/10 scale on plan and 1/2.5 scale vertically, so providing 4 times vertical exaggeration, with width/depth ratio about 2.5 rather than 10 as in the FCF. Having surface piercing rods as its artificial flood plain roughness in some tests, it also provides results with high ratios of flood plain to main channel friction factor.

5.4.2 The Glasgow flume in which these tests were conducted is 8.5m in length, 0.764m wide, and the skew channel was 150mm wide by 61mm deep. The angle of skew was 5.84°, and it differred from the FCF in that the flood plain was aligned with the gradient axis rather than the main channel being so aligned. However, at such low angles of skew this is unlikely to matter. The slope was 1/1000, which implies 0.9948/1000 along the channel axis, which would influence discharge by about 1/4%. This effect has been neglected in the analysis which follows. The 10mm dia. rods used for flood plain roughening were in staggered rows, the rows being at 100mm centres longitudinally and the transverse spacing also 100mm.

5.4.3 Comprehensive calibration tests were made to establish the basic resistance of the main channel, and of the flood plains when both smooth and rough. Modified versions of the smooth turbulent equation were derived as basic resistance formulae for main channel and smooth flood plain. The calibration of the rod roughness was analysed in the same way as the similar roughening in the FCF at Wallingford, as described in Appendix 2. The range of ratios of flow depth to rod diameter differed from the FCF range, and a somewhat modified form of drag coefficient function was derived, with C_D being proportional to the -0.4 power of the ratio z/d. The availability of good calibration data with very modest experimental tolerances gives more than average confidence in the analysis of the results from this research.

5.4.4 The way in which the factor ARF works is very similar to the operation of the allowance for skew deduced in Chapter 4: they are both multipliers of a calculated discharge deficit. Dealing first with the roughened flood plain case, several combinations of assumed values for ARF and of the allowance for skew were considered. All these results lie in Region 1, except with the highest value of ARF tested when a small proportion passed into Region 2. The dominance of Region 1 is to be expected with high friction factor ratios, f_F/f_C ranging from 5.4 to 14.4 in these tests. The relative depth, H_*, rose to 0.7, a higher coverage of H_* than in any other test series examined. These results are therefore important in providing a good test of the ARF concept, though if comparable aligned channel tests had been carried out the results would have been of double value. The allowance for skew deduced for smooth flood plains as given in Chapter 4 is in the form:

$$DISDEF_{SKEW} = DISDEF_{ALIGNED} * (1.03 + 0.074\phi) \qquad \ldots 5.6$$

and this yields a factor of 1.46 for $\phi = 5.84°$. However, the conclusion was also drawn from the FCF tests with rough flood plains that if the friction factor ratio exceeded 5 (as in this case) then the allowance should be less. An intermediate value of 1.17 was tested, based on the FCF rough flood plain value, as well as 1.00 i.e. no allowance for skewness. These three skewness allowances were combined with several values of ARF, from 0.15 to 0.30 but the agreement between prediction and observation proved quite sensitive to the product skewness factor x ARF. This is shown by the following table of results:

TABLE 5.2. ANALYSIS OF ERVINE AND JASEM SKEW CHANNEL RESULTS: rod roughened flood plains.

The upper figure is the mean discrepancy between experimental and predicted discharges,%; the lower figure is the variability (S.D.), ±%.

Skewness factor used	Aspect ratio factor, ARF					
	0.15	0.18	0.20	0.22	0.246 @	0.30
1.00		-7.93	-4.75	-1.32	+3.54	
		3.83	3.43	3.10	2.95	
1.17		-2.96	+1.23	+5.83	+12.53	+24.15ϕ
		3.25	2.97	3.05	3.96	3.45
1.46	-1.50	+6.96			32.51	
	3.12	3.13			9.66	

Notes: @ this is aspect ratio/10

ϕ includes region 2 flows for $H_* > 0.52$

5.4.5 It is clear from the above that ARF does not exceed aspect ratio/10; and nor can it be much less than this value. Bearing in mind that the observed discharge varies from 85% of the basic zonal calculation at the shallowest depth tested down to only 65% at the maximum depth tested, the accuracy achievable of 2% with variability not much above that arising from the experiments themselves is heartening. In fact, with ARF x skew allowance = 0.227, the average discrepancy reduces to zero and the standard deviation is 3.0%. There is evidence of slight curvature in the detailed results. The 3% deviation is thus partly from the use of a linear functions when allowing for relative depth and the effect of the relative roughnesses of main channel and flood plain.

5.4.6 The overall conclusion from these rough flood plain tests is to confirm once again that the appropriate value of ARF is close to aspect ratio/10, perhaps rather less than aspect ratio/10 when the main channel width/depth ratio is as low as 2.5. Also confirmed is the indication from the FCF results that the allowance for skewness when the friction factor ratio exceeds 5 is relatively small. The combination of ARF = aspect ratio/10 and the "smooth" skewness factor would be unduly conservative. A small amount of skewness appears to have very little additional interaction effect when the flood plains are very rough.

5.4.7 Various assumptions were also tested against the results with smooth flood plains. The combination of ARF = 0.246 and the skewness factor of 1.46 based on the FCF formulation gave a mean discrepancy of -3.8% with standard deviation 2.7%, a reasonable accuracy of prediction, though the analysis does not in fact test the ARF value as none of the data turn out to be in Region 1. The results progress through Regions 2 and 3 to 4, with a large proportion being in region 4, half the results being for H_* values above 0.35. The overall conclusion from these smooth flood plain skew channel tests is that the predictive method based on the FCF data with ARF = aspect ratio/10 is about 4% optimistic when compared with the conditions in the Glasgow research. This is within the combined tolerances to be expected in this extension of the proposed design procedures and those that might have arisen in the experiments themselves.

5.5. Field information

5.5.1 Ramsbottom (1989) considered alternative methods of assessing flood discharges, making considerable use of field data from British rivers, supplied from the water data records of ten Water Authorites. Several of the rivers he studied are two-stage channels of reasonably classical cross-section: there is a main river channel flanked on one or both sides by flood plains. There is obviously much more stage/discharge information available for within bank flows, but the reason for choosing the rivers to study was the availability of a proportion of above-bank data. The within-bank data provides the basic calibration of main channel roughness that any method of assessing flood conditions requires, but in general there is much less prospect of obtaining corresponding calibration information about flood plain resistance. Several of the river sections considered by Ramsbottom were also suitable for analysis in the context of the predictive methods now proposed, though not all were sufficiently akin to a conventional compound channel section, and some had too few stage discharge data for above bank conditions to provide a worth-while test of the method.

5.5.2 Another source of information is the field research carried out by Myers (1990) on the River Main in Northern Ireland. He has coupled together laboratory research on a model of an improved reach of the river with extensive field measurements, determining the discharge by many measurements across the width using a current meter reading at 0.6 depth as the depth-average velocity. There are two study sections in this reach of the River Main, which are of classic two-stage channel shape though with appreciably sloping flood plains. Again there are measurements at discharges below bank full to provide a basic resistance function for the main channel.

5.5.3 In the study by Ramsbottom, the within-bank data were analysed to provide basic values of Manning's n, which were compared with those that might be deduced from published values for similar rivers (see Section 7.4 and Appendix 5). Also, from inspection of the particular river reaches, as well as from the flow measurements on the flood plain in one or two cases, suitable flood plain values for Manning's n were assessed. The same discharge data, plus those obtained by courtesy of Myers for the River Main, were also used by Wark under a Case Studentship with H R, Wallingford to test the latest version of the lateral distribution turbulence method under field conditions. As he had analysed the within-bank flows to determine suitable Manning's n values - including their variation with depth - there was scope for cross-checking with the analyses for this project, though on the whole the near-bank-full values of n used in what follows are the same as those derived by Wark. Five river sections and associated stage/ discharge data were selected for analysis, and brief descriptions now follow:

5.5.4 *River Main, Northern Ireland:* This reconstrusted 800m long reach is described by Myers (1990) and by Higginson, Johnston and Myers (1990). Its purpose was to provide adequate freeboard for agricultural land in the upper reaches of the catchment, whilst improving the channel conveyance past industrial premises in the lower reaches. Strong fisheries interests led to the adoption of a compound cross section through the reach adjacent to the factory development. The main channel is 12m wide, with depth between 0.9 and 1m, and each berm slopes towards the channel at 1/25. The gradient of the study reach is 1/520, and the water surface slope was shown to match this well over a wide range of flows. The river bed is coarse gravel, with

D_{50} between 100 and 200mm. The side slopes of the main channel consist of quarried stone up to 0.5 tonne weight, and the berms are usually covered with heavy weed growth. Two of the surveyed sections, nos 6 and 14, are used in the analyses, with the flow data having been collected from a bridge at the upstream end of the experimental reach.

5.5.4 *River Severn, Montford Bridge.* This is a much studied reach of river already mentioned in Chapter 2. This is a natural river section with a cableway extending over the full width including the flood plains, and a large body of accurate current metering data provides perhaps the best available information about a natural channel with flood plains. These are grass covered, and the gauged section is on a straight part of the river. The width is about 40m, with a bank full depth of 6.3m. Cross-section parameters for this site are shown on figure 2.2.

5.5.5 *River Torridge, Torrington, Devon.* This is a natural river section with one flood plain on the left. Flow measurement is from a cable way which spans the river channel itself and also the inner flood plain up to a flood bank. In fact all the data available refer to conditions with flow confined within the span of the cableway: higher floods can overtop the bank and gain access to the remaining width of flood plain, but such conditions are not included in the available data. The channel bed is of small stones up to 0.3m boulders. The flood plain is pasture, with trees at the river bank and on the flood bank. The river itself is 29m wide and nearly 3m deep and is fairly straight, with gradient 1.39/1000.

5.5.6 *River Trent at North Muskham.* This is really a three-stage channel, in that it has a narrow berm at an elevation of some 5m above river bed, with an extensive flood plain at a slightly higher elevation. The flow gauging is confined to the main channel and narrow berm by the limits of the cableway, but visual assessments of flood plain flows are made at higher depths to add to the gauged discharge. There is extensive data at this site for the two lower stages, rather less for the third stage when the ungauged wide flood plain might contribute up to 25% of the total discharge (result of model study at HR, Wallingford, as well as from computation). The channel bed here is of fine gravel and alluvial silts, so would be expected to become mobile at high stages. The main channel itself is 72m wide, and the gradient is 0.35/1000. The flood plain vegetation is mostly grass with some small trees and bushes. Although this site is really three stage, the lower two stages are well within the scope of the procedures developed in the manual. Extension to the third stage is rather problematical, both because of the geometric approximations that then have to be made and also because the stage/discharge data include an unmeasured proportion of flood plain flow.

5.5.7 Further details of all these sites will be found in Table 5.3, and their cross sections are included in figures 5.9 to 5.13. The actual cross-sections had to be somewhat simplified, as will be explained in Chapter 7, section 7.1, to provide the various parameters that enter into the predictive functions: bed width, 2b; top width of channel, 2 w_C; mean channel depth, h; width across flood plains, 2B, including the reduction to this when flow only partially inundates sloping flood plains; and average bank slope, s_C. These simplified shapes are also shown on the cross-section drawings: it should be noted that the method is intrinsically suited to using the actual cross-sections in the basic flow calculations, though computer program limitations for this study meant that the simplified sections were used throughout.

5.5.8 It having been established at this stage that the allowance for width to depth for Region 1 flow should assume ARF = 2b/10h, the appropriate ARF value was fixed for each geometry. Also, with one exception to be mentioned later, the Manning's n value established from stage discharge approaching but not exceeding bank-full depth was applied to the range of increased depths in flood conditions. There was some flexibility in the choice of Manning's n for the berms, however, as there is no calibration value available in the usual field situation. The predicted flows were compared with the observed above bank data for each river, and mean discrepancies and standard deviations were calculated. The values with the range of assumptions tested are listed in Table 5.3. The predicted stage discharge functions using the preferred combination of roughness coefficients etc. are shown together with the full range of observations in figures 5.9 to 5.13.

5.5.9 Figure 5.9 shows the River Main at section 6 and the comparison of prediction with measurement. The full line is for n_C = 0.028 and n_F =

0.040. The extrapolation to above bank conditions is quite good, though on average the predictions are 3.5% high with a standard deviation of 8.6%. It seems quite possible that the variability comes as much from the field data as from any imperfection in the prediction method. The observations appear to follow two trends, one set lying above the theoretical curve and another set below, as might occur due to seasonal effects in terms of bank vegetation or a change in actual channel roughness. This possibility is examined by taking n_C = 0.030 and n_F = 0.050, shown as a broken line. This agrees rather better with the bulk of the field data, but leaves some distinctly off-line, and hence the mean discharge discrepancy is +6.0%, with standard deviation 9.1%.

5.5.10 Figure 5.10 shows similar results for the River Main at section 14, with n_C = 0.0247, the best-fit within-bank value at high stage, and n_F = 0.025. It should be mentioned here that the predictive procedure required an assumption to be made to extend the formulae based on a horizontal flood plain to cope with a sloping one. Clearly the flow is unaware of the full width of berm when it is only partly submerged, and so the effective width, 2B, is taken to be the water surface width (see also Figure 7.1 of Chapter 7). Also, with sloping berms it is far more likely that the normal Region 1 formula will change sign at very shallow depths. This point was covered in paragraph 3.4.11 but in analysing these results it seemed desirable to allow for some residual minimum interference under this shallow partial inundation conditions. Hence, a minimum value of Q_{*2C} of 0.5 was applied. This becomes relevant at shallow flood plain depths with low B/b ratios, such as occur on sloping berms. Several of the data sets brought this limit into play over the lower range of flood plain depths. Agreement overall is quite good, and to the same order as the field tolerances implicit in using single measurements in each vertical: an average discrepancy of +3.5% with standard deviation 6.5%.

5.5.11 The particular feature about the River Severn stage discharge data shown in figure 5.11 is that it is very extensive, with 39 values above bank level. The theoretical curves shown are for n_C = 0.0307 and n_F 0.0338, this n_C value being just 1% lower than the best fit value for within-bank flows and the n_F value being an average figure for the two flood plains. With so many field measurements available, it was considered justifiable to take running averages of three to minimise the effect of random errors, a practice that was adopted for most of the data from the FCF. The average discrepancy between theory and measurement is +0.3%, with standard deviation of 2.7%. This is perhaps the best set of field data, and agreement with it could hardly be bettered, using the now standard value of ARF = aspect ratio/10, and a well documented n_C value. It is worth mentioning that over much of the range of flood flows, the discharge adjustment factor is betwen 0.95 and 0.90, and all flows are in Region 1.

5.5.12 The data for the River Torridge shown on Figure 5.12 include only 5 results clearly above bank, with one marginally above bank-full. The predicted curve (full line) is for n_C = 0.026, the best fit value for the higher within bank condition, and n_F = 0.030. Agreement is less satisfactory, with a mean difference of 8.7% and standard deviation 6.5%. The main discrepancy can be eliminated by setting n_c= 0.024 and n_f= 0.026. It is possible that there are seasonal differences here that increase the conveyance at times of flood. This river has an alluvial bed, so it is conceivable that the roughness changes at high stages when some of the sediment will become mobile, there could be a delivery of different size material into the reach from upstream, or there might be local scour that has not been taken into account.

5.5.13 The final example is the River Trent at North Muskham, shown in Figure 5.13. Here again there is quite a lot of data, but the section is complicated by having a berm and then a wider flood plain at higher elevation, giving rise to a dual "bankfull" elevation shown on the figure. The detailed information on this site refers to the possibility of this reach of the river being affected by its confluence with a tidal reach downstream, so some of the data may relate to a hydraulic gradient differing from the constant figure assumed. The influence of flow over the first berm can be assessed without much problem, as the section up to main flood plain level close to a conventional asymmetric compound channel. For this case, n_C = 0.032 based on the analysis of within bank flows (mean error 0.3%; standard deviation 2.9% average taking running averages of threes). The same value has been taken for n_F to give the theoretical stage/discharge function between BF_1 and BF_2. This agrees reasonably well with the data: average error 1.0%, standard deviation 3.3%. (The observations have been averaged in running threes).

5.5.14 In effect the third level of this River Trent site provides another test case, though to apply the normal theory the section has to be approximated somewhat as shown on Figure 5.13. Also the upper range of flow incorporates an unmeasured flood plain component, so the data is not ideal. In order to achieve reasonable agreement it has been necessary to adjust the main channel Manning's n value with stage, and the theoretical line shown uses n_C varying linearly from 0.033 at flood plain stage to 0.0266 at 0.5m greater depth. Other treatments of these data have also been obliged to bring in a reduction of main channel roughness at very high stages, which could well be justifiable and realistic in view of the alluvial nature of the river bed, and the possibility of a change in effective gradient in large floods.

5.5.15 The use of field data to validate a predictive method is less rigorous that using good laboratory data because there is usually no calibration data to provide the basic flood plain resistance, and also the roughness coefficient of the main channel is known to be variable in many cases - and suspected of varying in other cases too at high stages when an alluvial bed may be in motion. However, from the engineering point of view, validation by comparison with large scale information from natural and improved rivers is particularly significant. Such validation has been accomplished, without need for any further consideration of the necessary adjustment for width/depth ratio, to the expected level of accuracy. In fact, with some of the better data sets, agreement has been to within the tolerance band of the measurements themselves.

5.5.16 It is interesting to note that these practical cases are for the most part dominated by Region 1 flows: only the River Main progresses to Region 2 over the depths considered. Yet Region 1 behaviour was virtually absent from nearly all the small scale laboratory work considered earlier in this Chapter. This is ample justification for the programme of research in the FCF at Wallingford, undertaken by several groups of dedicated investigators from Universities, supported by funding from SERC.

5.6. Conclusions from other data sources

5.6.1 The predictive functions based on the results from the large SERC-supported FCF at Wallingford proved robust in that they transferred well to most other sources of stage discharge data, both from laboratory and field, covering a discharge range from 5 l/s to over 500 m^3/s. Regions 2, 3 and 4 were well validated by independent laboratory scale information to within the likely tolerances of the data, though not all sources of data with rough flood plains could be satisfactorily reconciled. Region 1 was also well validated by independent data involving some skew, and also by the field data.

5.6.2 Regions 2, 3 and 4 are predicted by functions depending on channel coherence, COH, and so the satisfactory transfer to radically different geometries and roughness types demonstrates that the channel coherence is a useful measure of the way in which interference between main channel and flood plain flows affects the stage discharge function.

5.6.3 Region 3 is not well covered by the independent test series, but the one series which covered that region adequately did not provide a strong differentiation between three alternative functions for that region. Thus the function derived as the best representation of large scale tests, in terms of COH, should be retained.

5.6.4 Region 1 presents a significant problem in small channels of narrow main channel aspect ratio. Data from different sources can present somewhat different pictures, either implying the absence of region 1 and interference effects causing major reduction in conveyance at shallow depths over the flood plain, or the virtual absence of interference effects on the stage discharge curve at any depth. No such doubts arise with large scale or field data: Region 1 clearly exists and there is a gentle increase in interaction effects as the flood plain becomes inundated, as observed in the FCF.

5.6.5 There may be some doubt as to whether all the laboratory testing used sufficiently long approach sections to achieve secondary circulation patterns that were representative of uniform flow in very long channels, though clearly the larger scale tests were adequate in that regard. The interpretation of some of the laboratory research has to remain somewhat open. In any event, its relevance to large systems with greater width/depth ratios is dubious.

5.6.6 Some flexibility was introduced into the Region 1 formulation to allow for an anticipated effect from main channel aspect ratio. This takes the form of an additional aspect ratio factor, ARF, and with this flexibility built in the great majority of test results from other sources could be predicted within the order of accuracy implicit in the laboratory procedures and field observations.

5.6.7 The conclusions drawn from the re-analysis of laboratory scale research on the best value of ARF to use for Region 1 were not very robust, in that many test series did not - and could not because of low flood plain Reynolds Numbers - include flows shallow enough to provide a reasonable test for region 1. However, other test data included this region and it was suggested that for main channel aspect ratios exceeding 20, a constant value of ARF = 2 should be taken (a wide channel condition), whereas for narrower conditions ARF = aspect ratio/10, making the discharge deficit proportional to channel width rather than depth. This last point was then fully confirmed by field data, though no very wide rivers were included.

5.6.8 Much research effort went into laboratory studies of compound channels with small main channel aspect ratios, but it now appears that their performance may not have a very close relationship with the more practical range of geometries and channel sizes. Of course this practice stemmed from the limited size of typical university facilities, and the inapplicability of much of the small scale research to engineering design shows also the wisdom of those who fought strongly for the provision of large scale facilities.

5.6.9 Particular importance is attached to the satisfactory prediction of flood discharges in the real rivers for which data were available, with agreement being achieved to within the probable tolerances of the data and well within the objective in mind at the start of the project in terms of accuracy of computation method.

TABLE 5.1

OTHER SOURCES OF STAGE DISCHARGE DATA (Laboratory research)

NAME	Date	Max 2B mm	Max h mm	Range of B/b	Range of 2b/h	Range of flume sl. /1000	s_C hor/vert	Total no of results	Flood plain roughnesses, Manning's n values	NOTES
ASANO	1985	3000	121	1.25 - 3.33	10 - 30	0.94 - 1.07	0	44	0.0098	No detailed calibration. Very non-un. flow
ERVINE	1992	764	61	5.10	2.5	1.00	0	14	Varies with depth	5.84° skew Rod roughness 10mm dia in 100mm grid
KIELY	1991	1200	54	6	3.7	1.0	0	10	0.010, 0.0157 (with bed shift)	Plotted calibrations
KNIGHT	1983 1984	610	76	1.00 - 4.01	2	0.97	0	18	0.010	Special care re uniformity Calibration available
MYERS	1978 1983 1984	760	121	3.21 - 4.74	1.32 - 1.99	0.22 - 2.28	0	153	0.0098	5 calibration runs, 1977 Some asymm. data
PRINOS	1983 1984	1270	102	2.70 - 5.26	2.0 - 5.0	0.297	0.5	80	0.011, 0.014, 0.018, 0.022	No calibration data available Anomoly between narrow & wide
US WES	1956	9100	152	8.0 - 30.0	2.0 - 4.0	1.0	0.5	9	0.012, 0.025, 0.035 approx.	Calibration available. Large scale.
WORMLEATON	1982	1210	120	4.17	2.42	0.43 - 1.8	0	39	0.0107, 0.0135, 0.017, 0.021	Many calibration runs for all roughnesses

TABLE 5.3.

ANALYSIS OF FIELD DATA FROM RIVERS FOR WHICH STAGE/DISCHARGE DATA ARE AVAILABLE.

River	Location	Number of obs.	Width/ depth ratio	Disch. range m^3/s	Gradient /1000	n_C	n_F	Mean disc. %	S.D %
Main, section 6	N. Ireland	14	12.3	14.8 - 57.8	1.906	0.032	0.040	+8.0	10.5
						0.030	0.040	-8.7	9.2
						0.028	0.040	-3.5	8.6
						0.030	0.050	+6.0	9.1
Main, section 14	N. Ireland	11	11.0	18.5 - 57.8	1.906	0.0247	0.040	+10.6	11.5
						0.0247	0.030	+6.7	7.9
						0.0247	0.025	+3.5	6.5
						0.0247	0.020	0	5.8
Severn	Montford Bridge, England	36 @	3.0	170 - 313	0.195	0.031	0.035	+1.2	2.8
						0.032	0.035	+4.1	2.8
						0.030	0.035	-1.7	2.9
						0.030	0.033	-2.4	2.7
						0.031	0.037	+1.8	3.1
						0.0307	0.0338	0	2.7
Torridge	Torrington Devon, England	6	8.3	208 - 314	1.45	0.026	0.060	+11.5	6.9
						0.026	0.030	+ 8.7	6.5
						0.024	0.026	+ 0.1	6.0
Trent	N Muskham, England	25 @	7.4	395 - 530	0.320	0.032	0.032	+1.0	3.3
		9	3.3	595 - 857		0.030 -	0.040	+10.0	2.3
						0.025			
						0.027			
						0.023		-1.0	2.0

@ denotes running averages of three were taken.

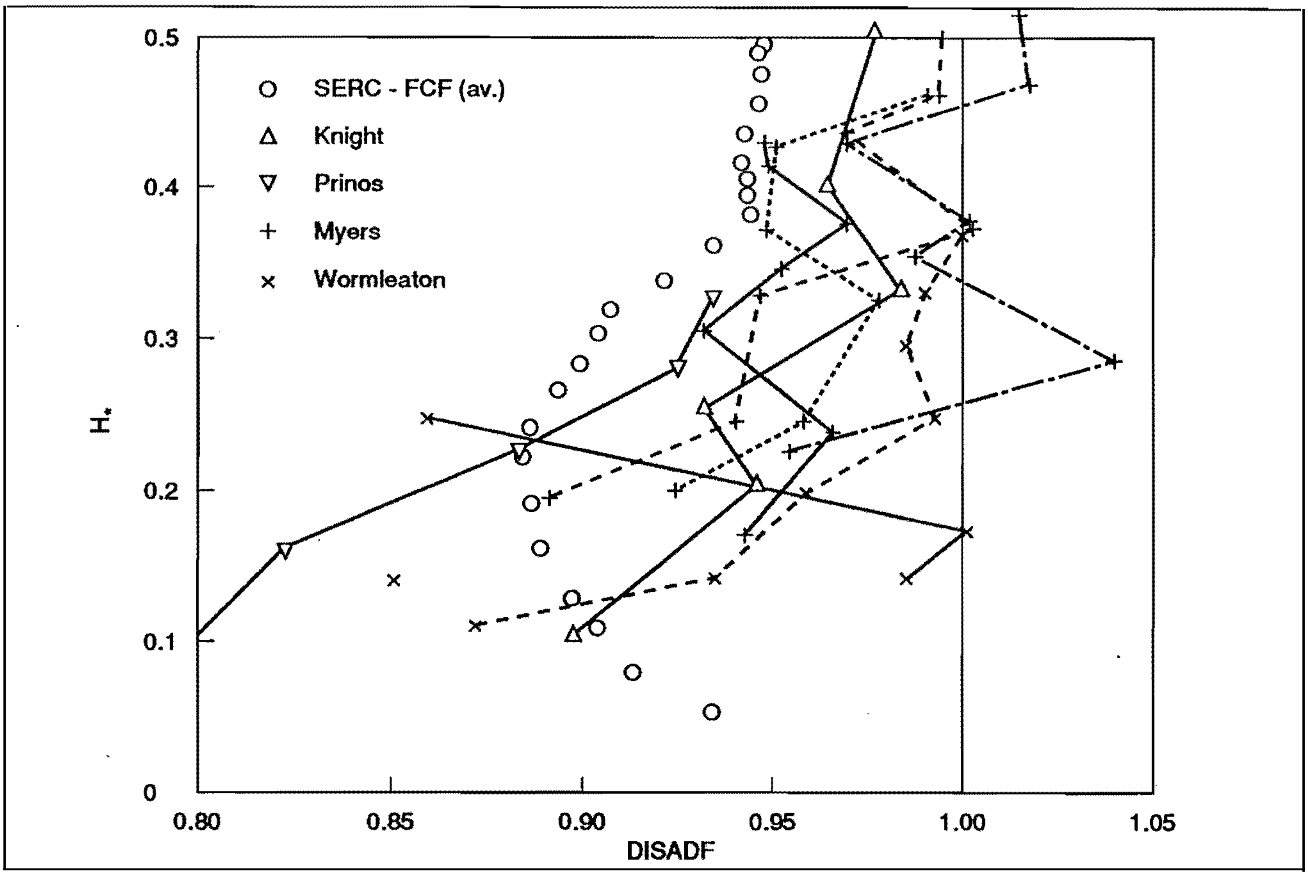

Fig 5.1 Selected data channels with equal main channel and flood plain roughness: discharge adjustment factor - DISADF, versus relative depth - $H_* = (H-h)/H$

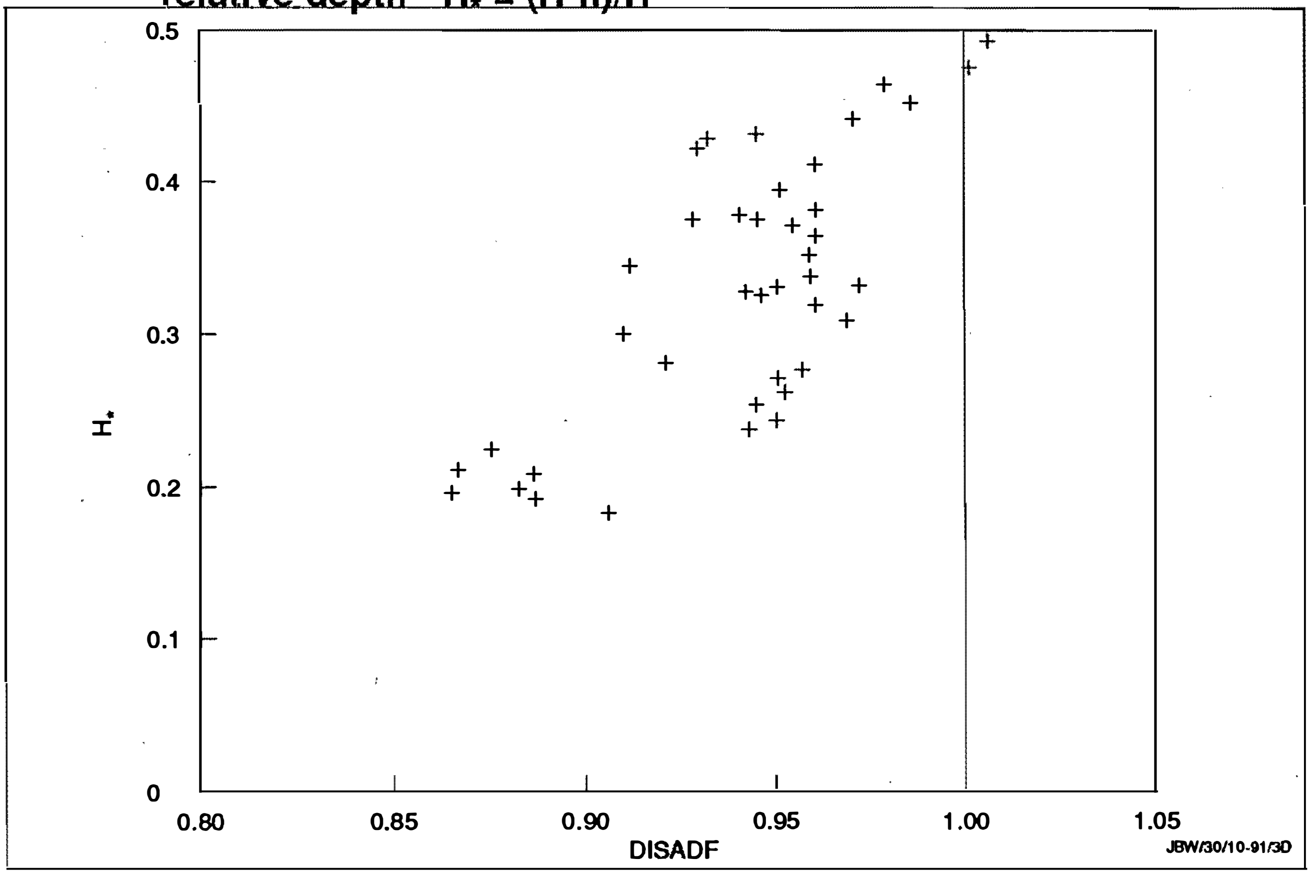

Fig 5.2 Myers' results consolidated with running averages of three

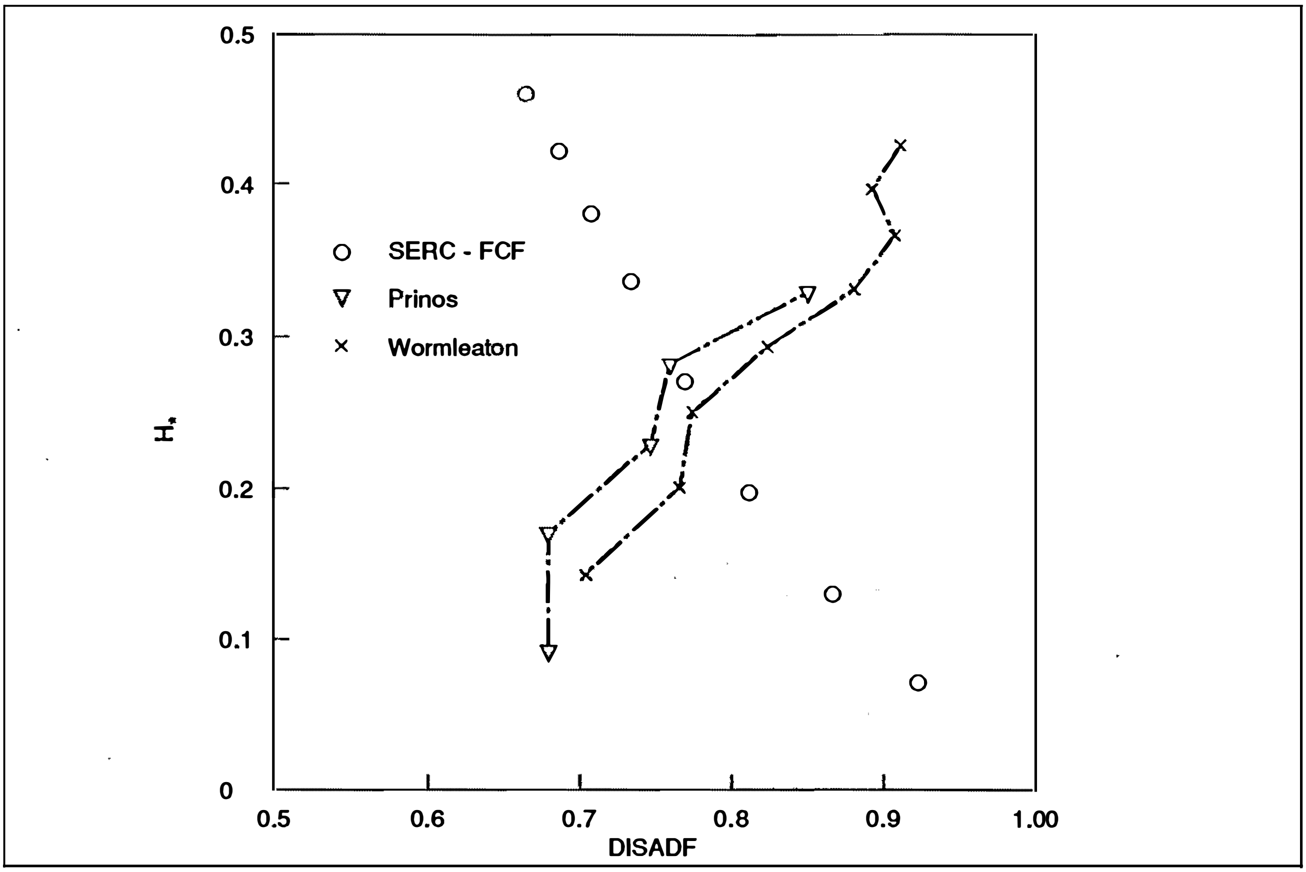

Fig 5.3 Selected data from channels with flood plain Manning's n approx. 50% above main channel value: discharge adjustment factor - DISADF, versus relative depth - $H_* = (H-h)/H$

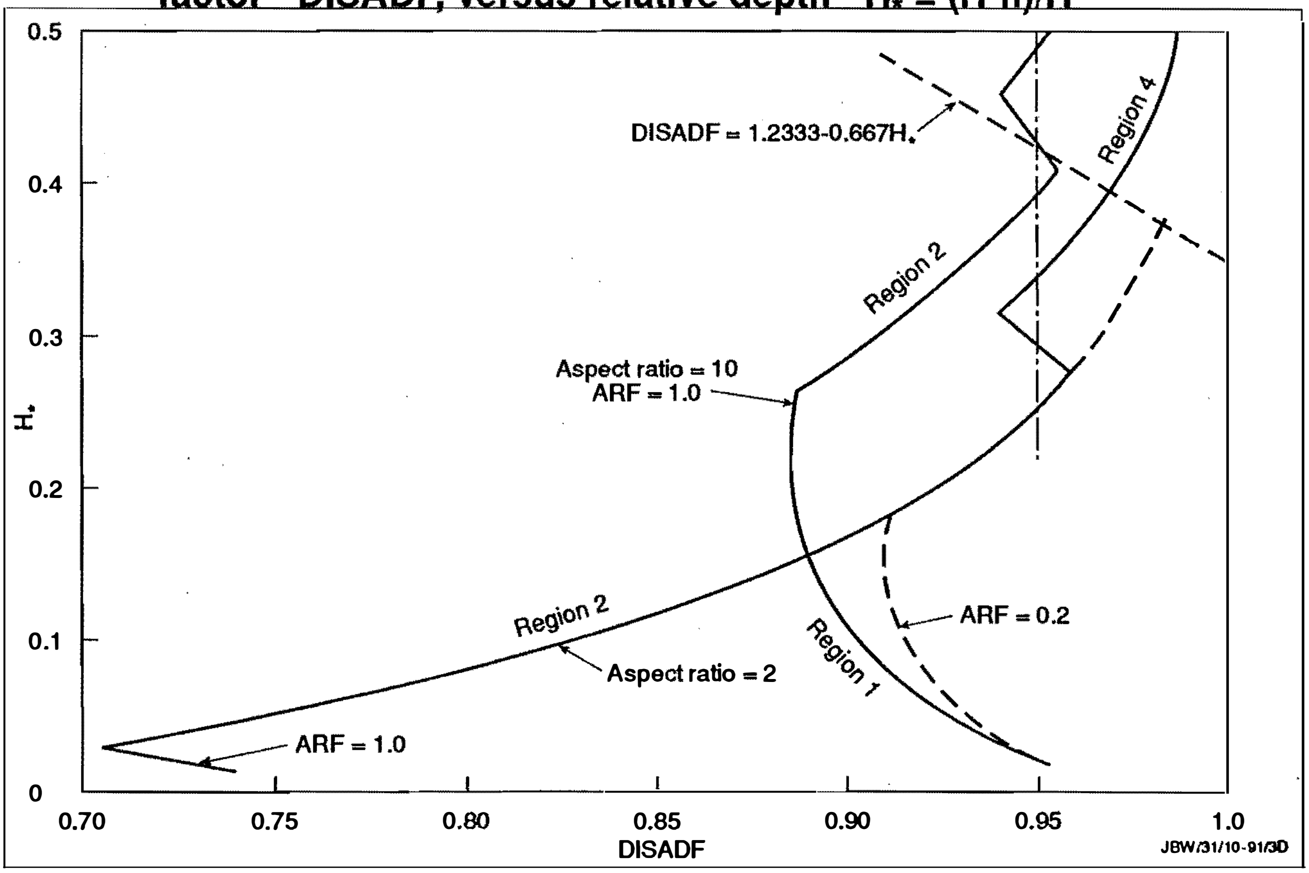

Fig 5.4 Predictive functions for two geometries: SERC-FCF, aspect ratio 10, B/b = 4, s_c = 0; Knight, aspect ratio 2, B/b = 4, s_c = 0; equal main channel and flood plain roughness

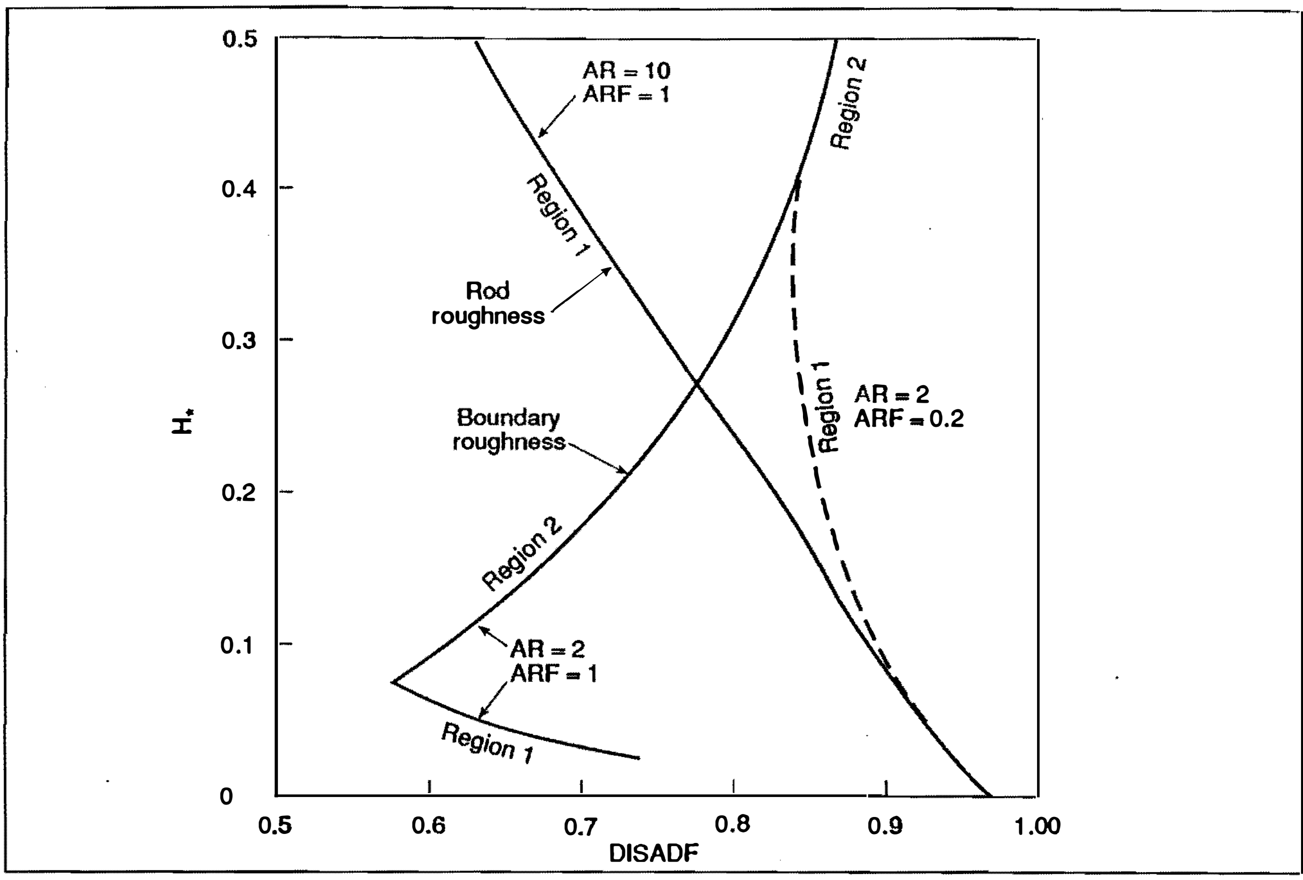

Fig 5.5 Predictive functions for two geometries and roughness types: aspect ratio 10, rod roughness on flood plain; aspect ratio 2, boundary roughness with flood plain Manning's n approx. 50% above main channel n

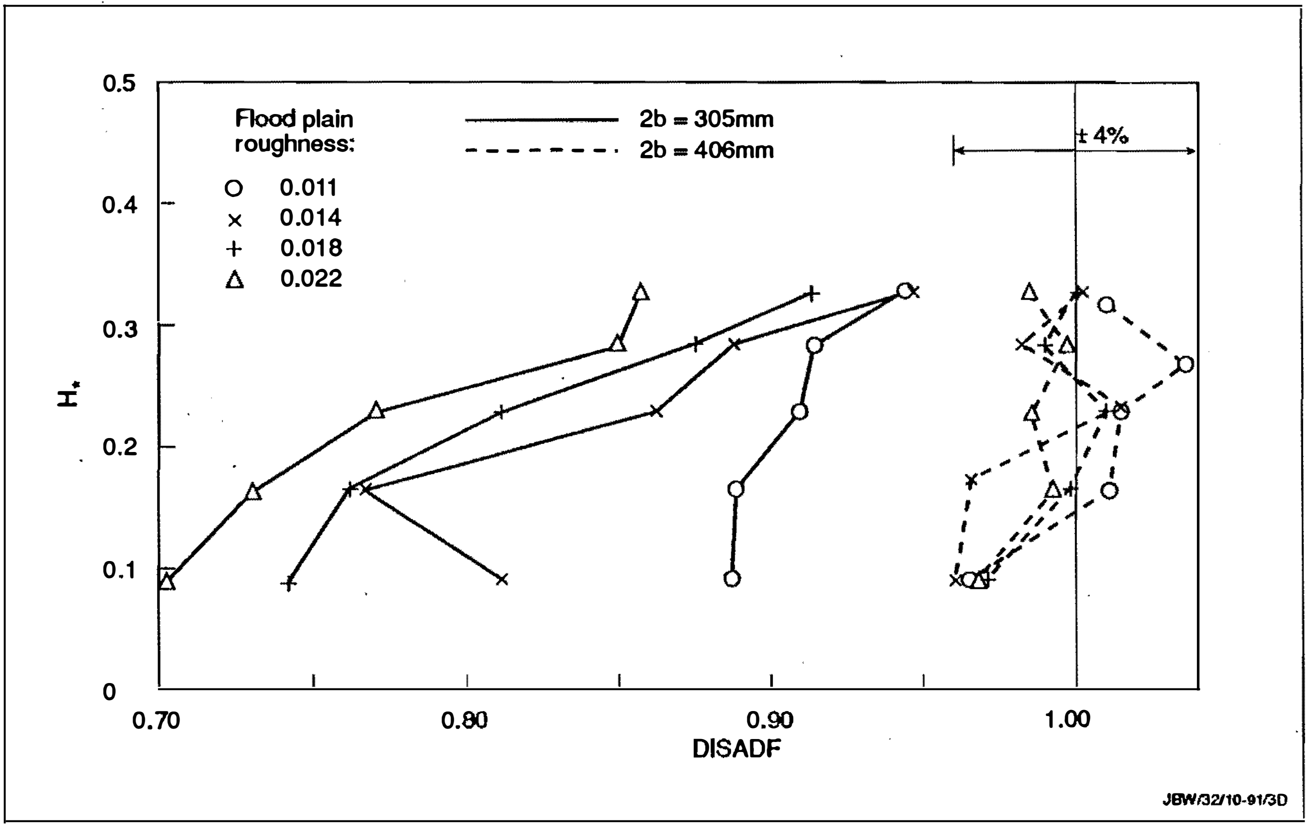

Fig 5.6 Prinos and Townsend's results for channel aspect ratios of 3 and 4: DISADF versus relative depth, four different flood plain roughnesses

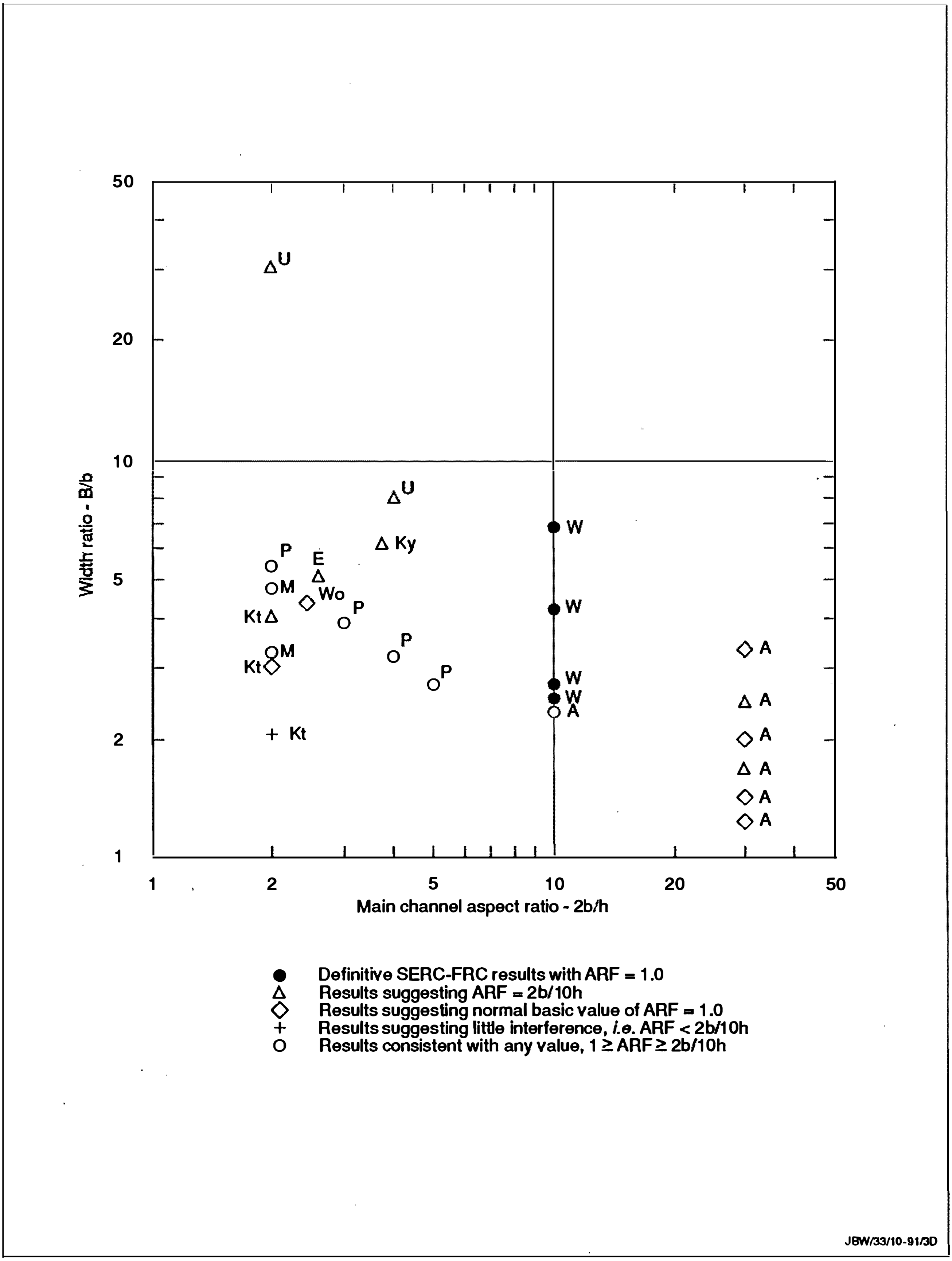

Fig 5.7 **Scope of geometries covered by review of stage discharge information, in terms of width ratio - B/b, and main channel aspect ratio - 2b/h: also showing influence of aspect ratio on predictive function.**
Sources: A - Asano et al, Kt - Knight et al, Ky - Kiely, M - Myers, P - Prinos and Townsend, U - US WES, W - SERC FCF, Wo - Wormleaton, E - Ervine and Jasem (skew)

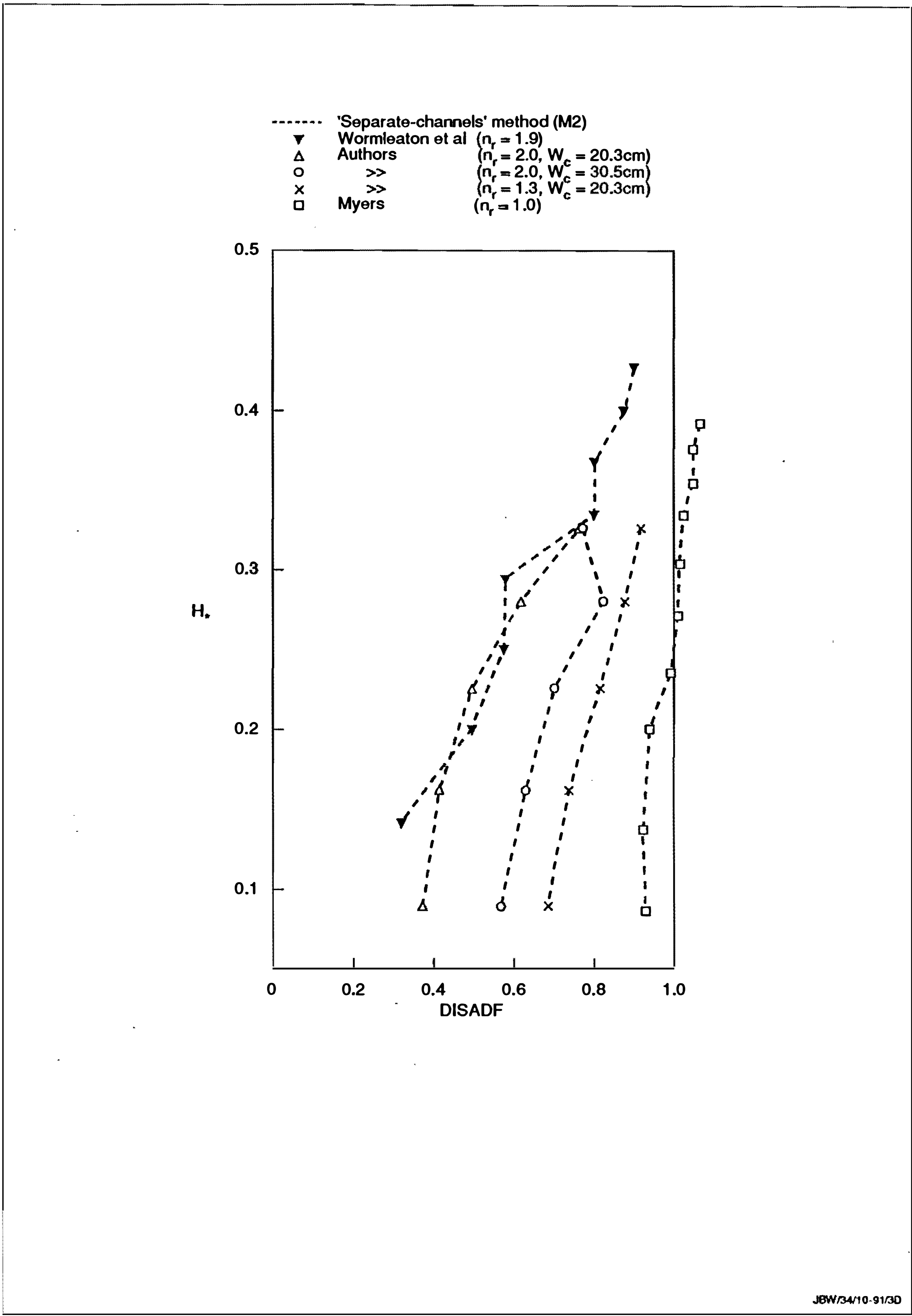

Fig 5.8 Prinos and Townsend plot of DISADF against relative depth for their own narrow channels and other data sources: n_r is ratio of flood plain to main channel Manning's n

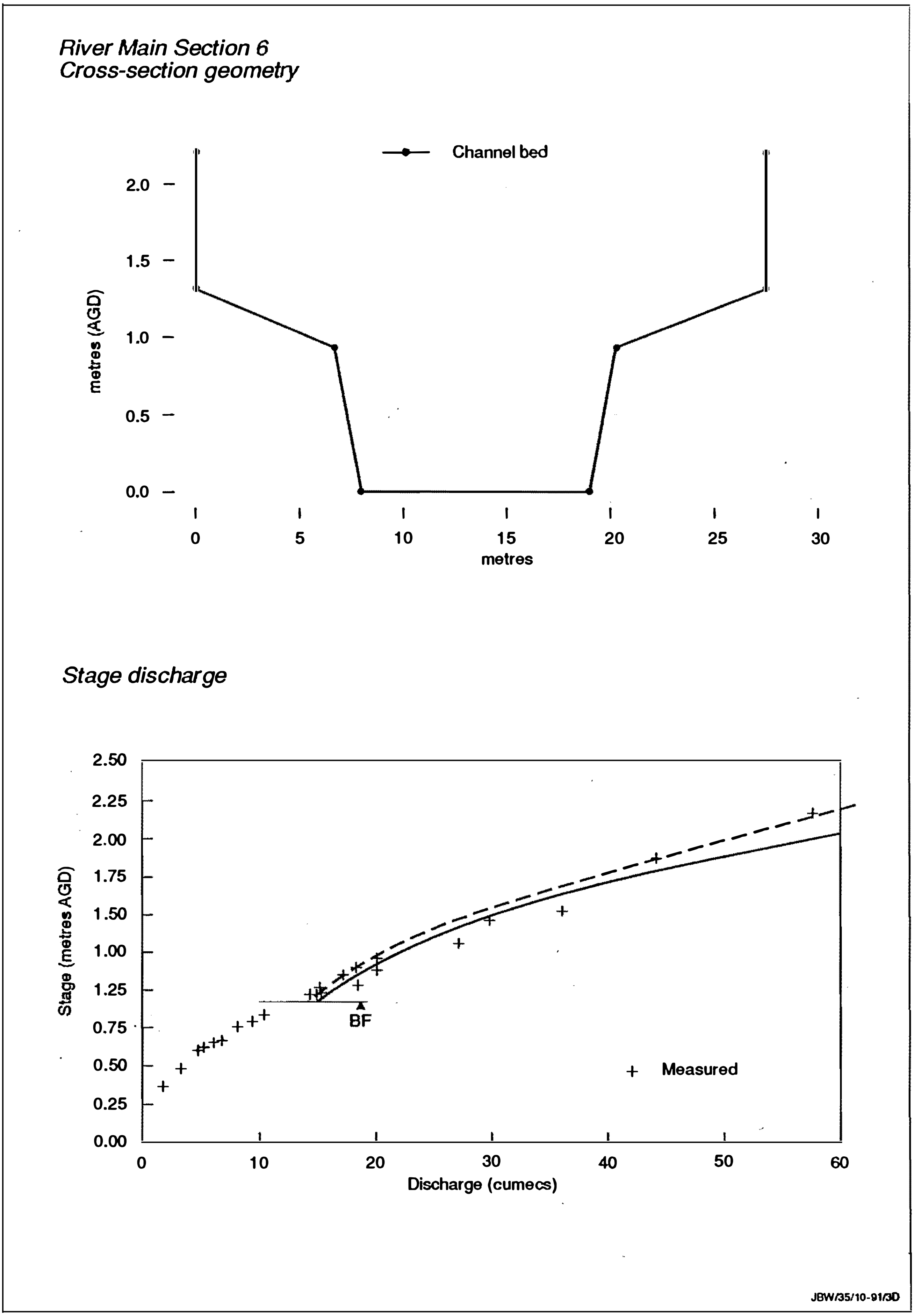

Fig 5.9 Field information: River Main, N.I., section 6. Predicted stage discharge curve for $n_C = 0.028$, $n_F = 0.040$, full line; $n_C = 0.030$, $n_F = 0.050$, broken line

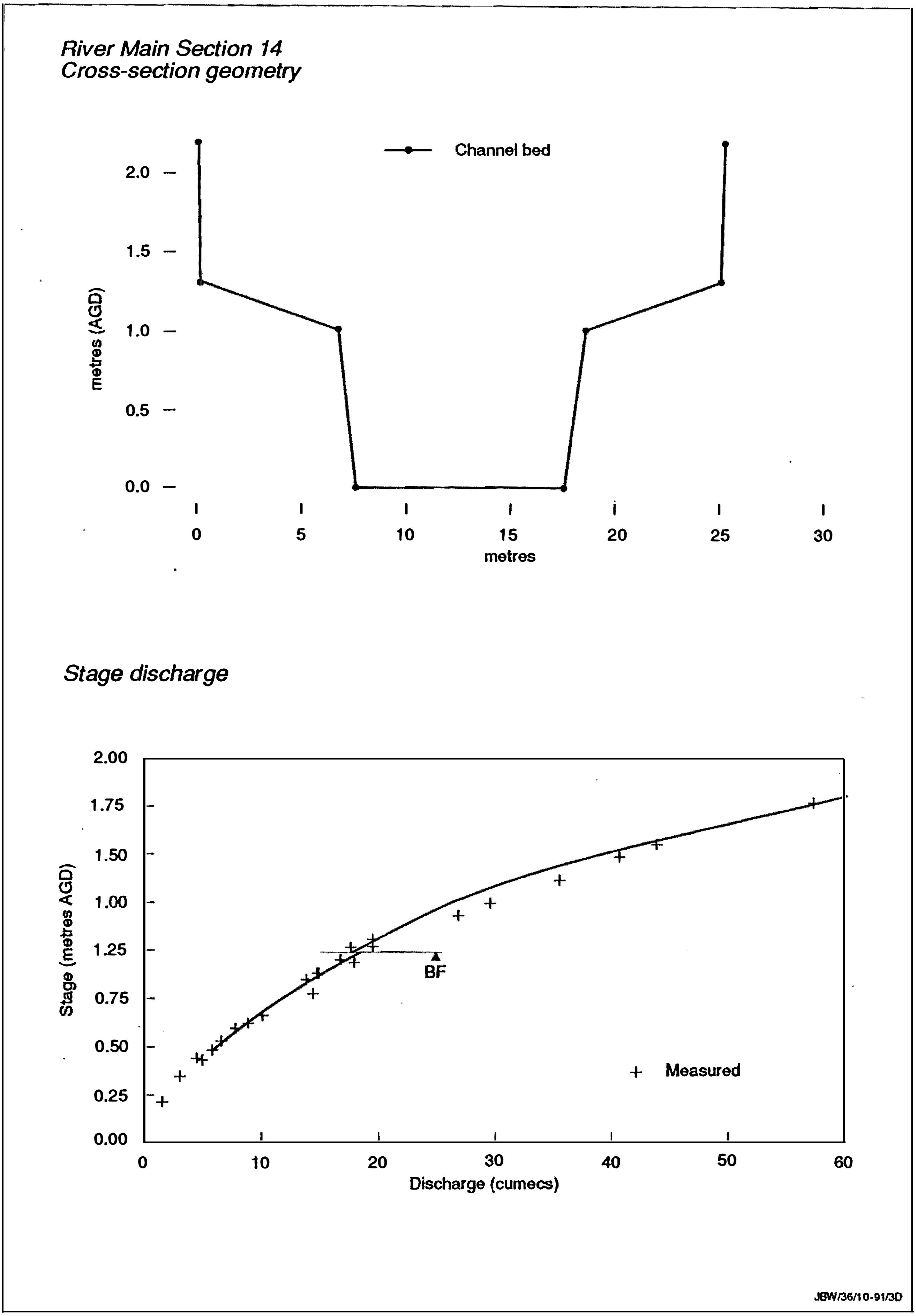

Fig 5.10 Field information: River Main, N.I., section 14. Predicted stage discharge curve for $n_C = 0.0247$, $n_F = 0.025$

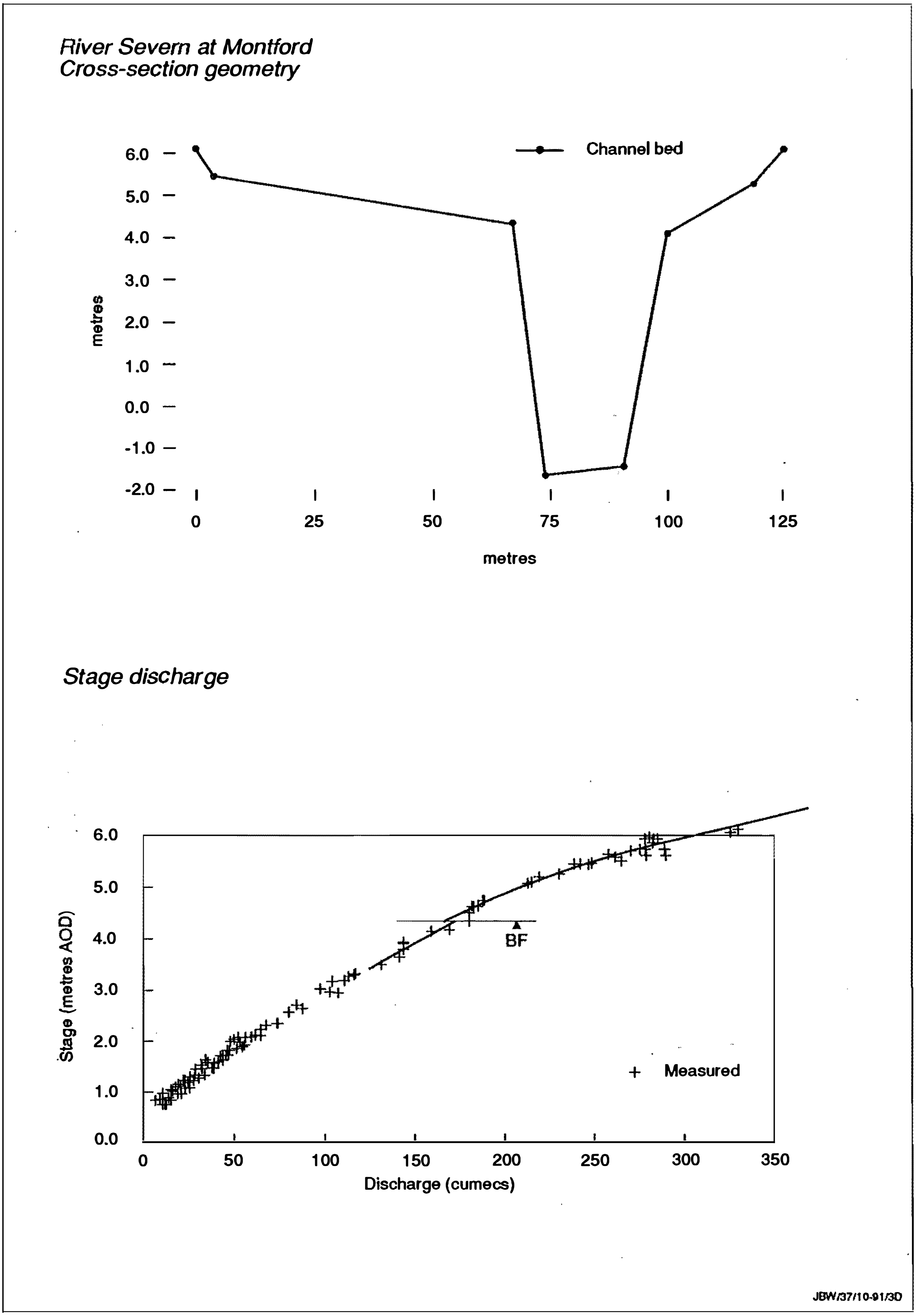

Fig 5.11 Field information: River Severn at Montford Bridge. Predicted stage discharge curve for $n_C = 0.0307$, $n_F = 0.0338$

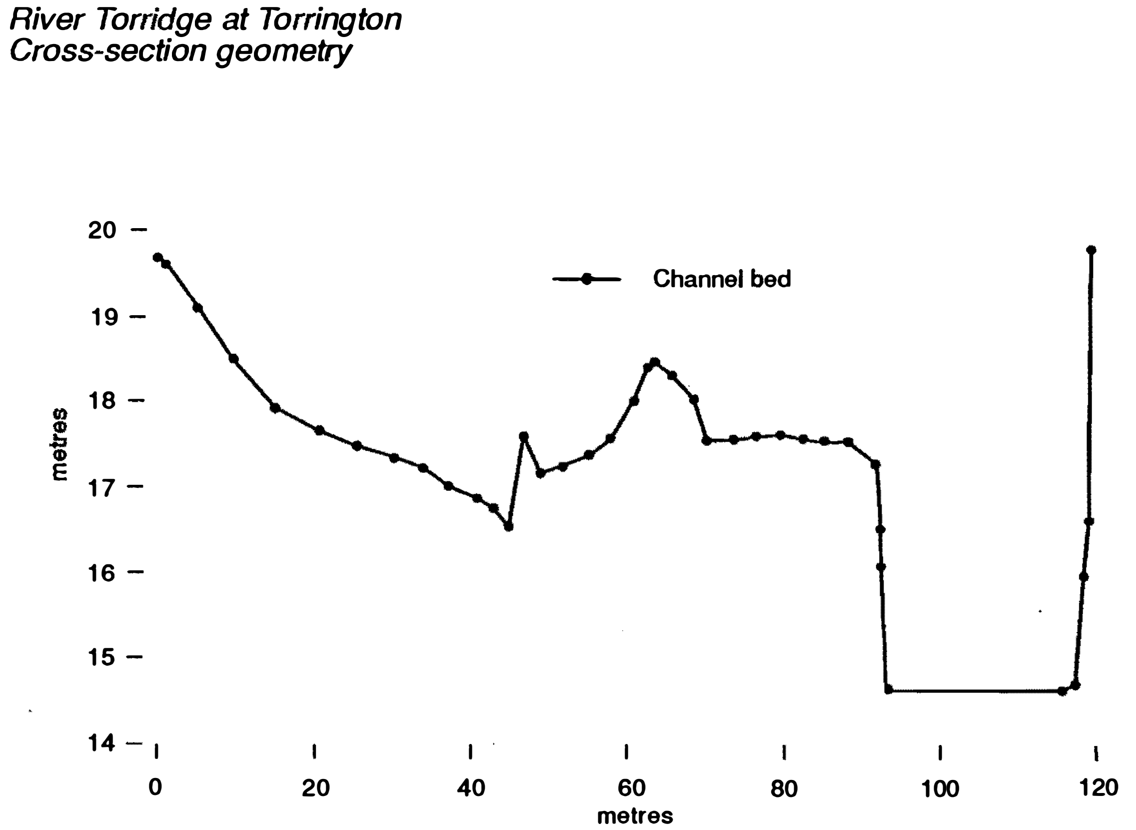

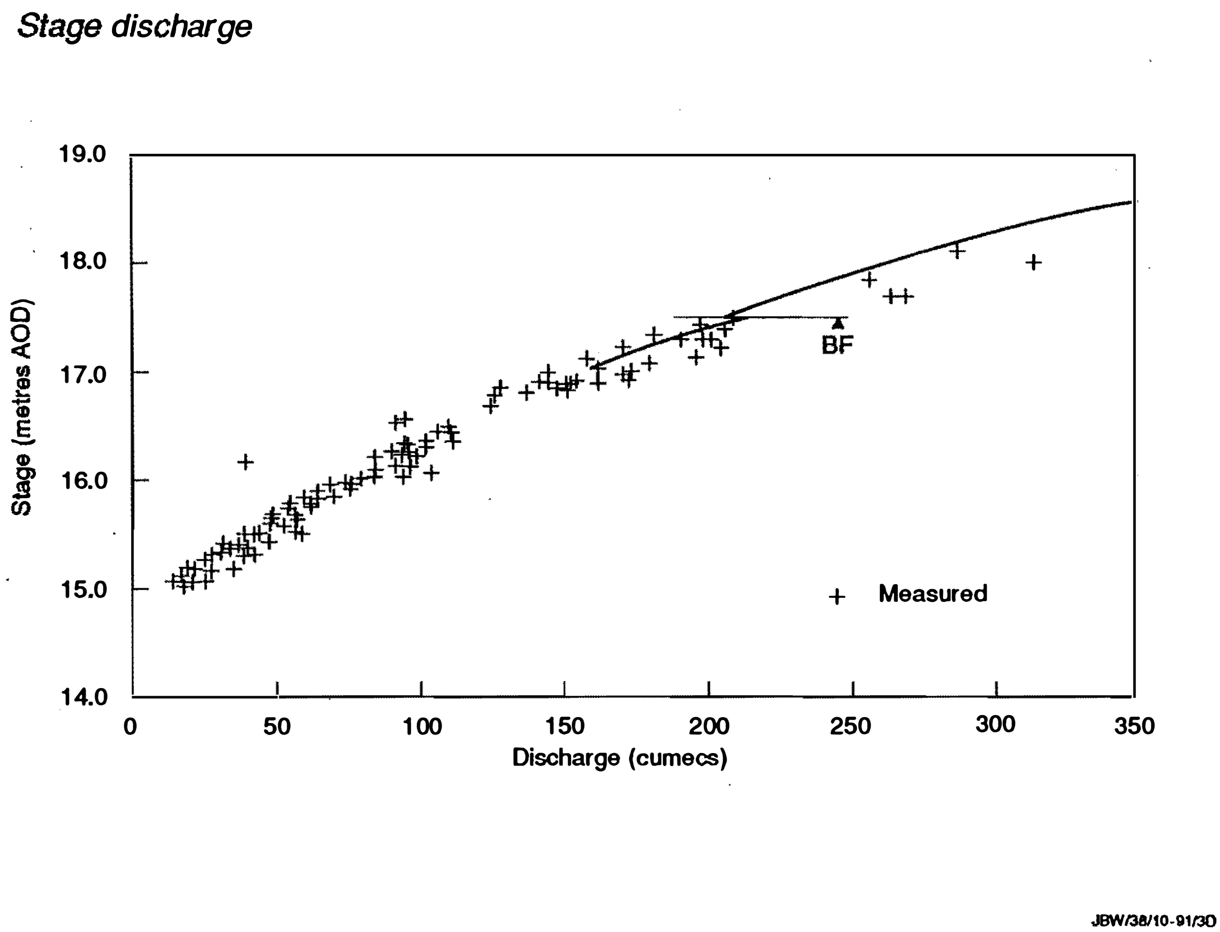

Fig 5.12 Field information: River Torridge, Devon. Predicted stage discharge curve for $n_C = 0.026$, $n_F = 0.030$

River Trent at North Muskham
Cross-section geometry

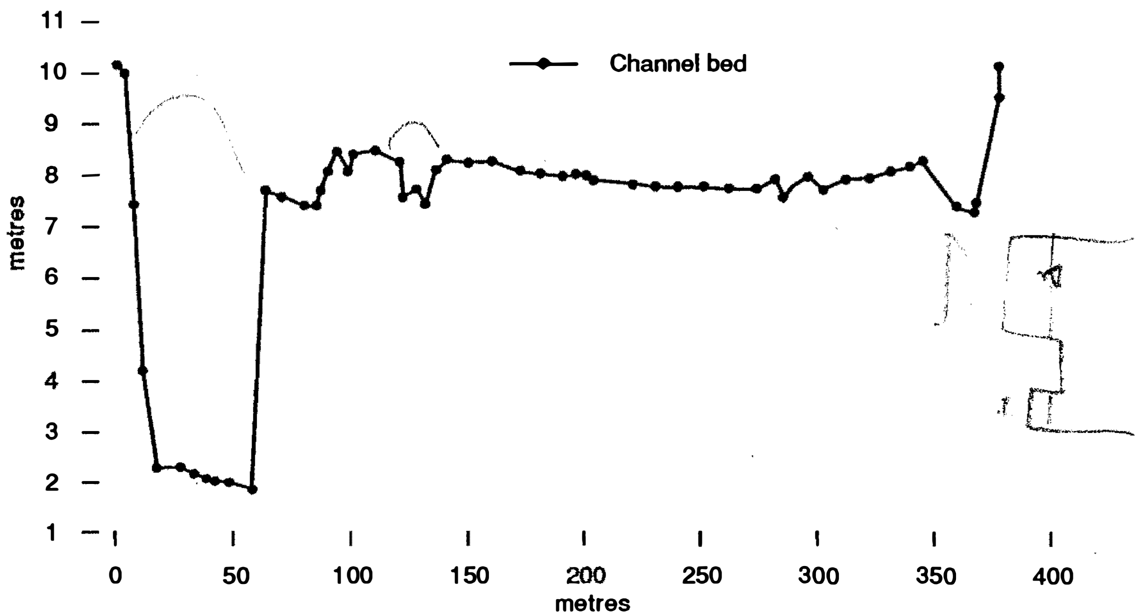

Stage discharge

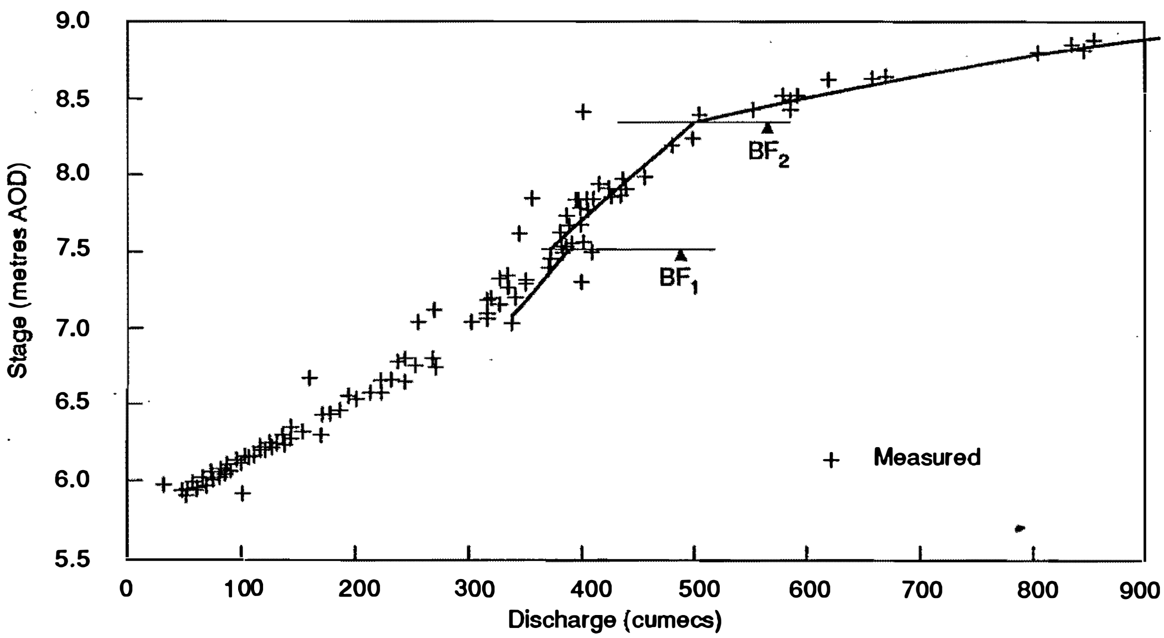

JBW/39/10-91/3D

Fig 5.13 Field information: River Trent at North Muskham. Predicted stage discharge curve for n_C = 0.032, n_F = 0.032 at first flood berm (BF_1 to BF_2); n_C variable above flood plain (BF_2), n_F = 0.036

6. TURBULENCE METHODS

6.1 Resume of turbulence theory as currently applied to compound cross-sections

6.1.1 The method of predicting the stage-discharge function derived by empirical analysis of the FCF results has its limitations. Although based on dimensional analysis and well supported by independent sources of information, there remains a question about its generality. One problem is its transfer to compound channels that do not have such a simple geometric shape as the ones typically tested, with their symmetry and horizontal flood plains. A method is described in Chapter 7, section 7.1, for extending the empirical equations to more natural sections, which does not stretch the procedures too far beyond the scope of the supporting research, but it would have been more satisfying to have a method which does not depend so much on the geometry's conformity to some near-ideal norm. Turbulence methods have that degree of generality and so deserve serious consideration. It will be demonstrated, however, that at their present stage of development there remain uncertainties over their application in the general design of compound channels.

6.1.2 Turbulence theory was briefly reviewed in Chapter 2, 2.3.13 to 2.3.16. It is based on the most fundamental equations of fluid motion, which include terms describing the mechanism whereby turbulence generates energy dissipation within the body of fluid. It differs from the hydraulic equations familiar to engineers, such as Manning, Chezy and even the more complex formulae for non-uniform flow (the Bernoulli equation) and for non-steady flow (the St Venant equations) in that it is based on the internal mechanics of the fluid, rather than on a knowledge of the external forces on the whole cross-section. Turbulence equations bring in the local internal system of stresses (the Reynolds stresses) which arise from the gradients across the section in the three dimensional velocity structure. Full solution of the resulting three-dimensional equations is possible for steady uniform flow in open channels of almost any cross-section, but is expensive in computer time even with present-day facilities and is by no means straightforward: it remains very much a research area. It is more usual therefore to simplify the turbulence equations to give a quasi two-dimensional approach which considers any cross-section geometry but takes the lateral distribution of vertically averaged velocity (or discharge intensity) as a sufficient measure of the flow structure arising from the irregular cross-sectional shape.

6.2. Turbulence methods and comparison with FCF data

6.2.1 Shiono and Knight (1990 a,b) have reviewed the more practical methods in the literature, drawing attention to the importance of momentum exchange arising from secondary currents as well as from the Reynolds stresses. They develop the depth averaged momentum equation in the longitudinal direction for uniform flow at depth H for any point in the cross section and clearly distinguish between the Reynolds stress term, which depends on the mean value of the product of local instantaneous forward and transverse velocities, and the secondary current terms, which depends on the product of average forward currents and average secondary currents. (See Appendix 4 for detailed theory). With certain assumptions, these simplify to the following partial differential equation:

$$\rho g d S + \frac{\partial}{\partial y} [d(\epsilon_s + \epsilon_t) \frac{dU}{dy}] - \tau_b = 0 \qquad \ldots 6.1$$

where d is the local flow depth, S the channel gradient, ρ the fluid density, g is the gravitational acceleration, y is a position across the flow section, U_d is the depth average velocity at position y, τ_b is the local bed shear stress, and ϵ_s and ϵ_t are the equivalent eddy viscosities arising from secondary currents and turbulence respectively.

6.2.2 As Shiono and Knight (1990 a,b) point out, whenever such lateral distribution turbulence models come to be used, they immediately pose the problem of what values to use for the eddy viscosity terms. Some researchers have adopted a single constant value for non-dimensional eddy viscosity, NEV = ϵ/U_*H, across the whole section, say 0.16 which is a typical value for non-compound open channels, equivalent to setting:

$$\epsilon_s + \epsilon_t = 0.16\ U_* H_1 \qquad \ldots 6.2$$

where U_* is the local value of the shear velocity at the boundary and H_e is local depth.

Other have varied the NEV value across the section according to some relationship based on laboratory results or field data (Shiono and Knight, 1990 a,b; Knight, Shiono and Pirt, 1989; Knight, Samuels and Shiono, 1990). Wormleaton (1988) used a two-component eddy viscosity, the second component being based on the length scale and velocity scale of the shear layer, to account for the turbulence that is clearly generated by the shear zone at the interface. NEV is commonly treated as a catch-all parameter covering the various turbulence effects, including both the shear layer and the influence of secondary currents. However, although there is now some understanding of the balance between these turbulence sources, there is as yet no general method for determining the appropriate value of turbulence coefficient for various geometries and roughness conditions. It is this lack that makes even the simplified turbulence models difficult to justify in a hydrailic design context unless local calibration data is available over a good range of conditions.

6.2.3 The equation used by Wark, Samuels and Ervine (1990) is the discharge intensity form of lateral distribution equation, rather than the depth averaged velocity version used by Shiono and Knight (1990 a,b), the two forms giving significantly different results where the depth varies strongly, i.e. at the bank line.

$$\rho g d S - \frac{\beta\ f\ q^2}{8\ d^2} + \frac{\partial}{\partial y}\left[\epsilon_t \frac{\partial q}{\partial y}\right] = 0 \qquad \ldots 6.3$$

where β is a factor relating stress on an inclined surface to that in the horizontal plane. In the above, f is the local friction factor arising from boundary shear, as determined from the appropriate resistance equation for the local values of depth, d, and discharge intensity, q. The terms in this equation express the balance between gravity,and bed shear plus lateral shear. Of course if ϵ_t is used as a catch-all term, the third term also includes the shears generated by secondary currents. These Authors found that the most appropriate form of finite difference solution to equ. 6.3 is one that computes the lateral shear term at mid-node positions. The equation is non-linear and Newton's method of iteration is applied, with an initial 'seed' solution obtained by setting the term to zero, in other words using the basic zonal calculation of main channel and flood plain discharge intensities. Convergence usually occurs within five or six iterations, though the final result may be 15-20% different from the intial seed value. The question is, how well does it perform?

6.2.4 This had been examined in broad terms in the 1990 paper by Wark, Samuels and Ervine for a selection of data from the FCF at Wallingford and elsewhere. Their figures reproduced as Figures 6.1 and 6.2 illustrate that reasonable agreement is possible, though it has to be remembered that what is being sought is a correction to a basic calculation that is already approximately correct. Close inspection of Figures 6.1 and 6.2 is required to judge how accurate the simulation might be in reproducing the observed stage discharge curve. The plotted observations tend to traverse the sequence of theoretical curves for different values of NEV, requiring an increasing value as depth increases for some distance, then reversing the trend to cross the sequence back to lower values.

6.2.5 Research funding for a more detailed comparison between this turbulence method and the full set of FCF data became available through the Ministry of Agriculture, Fisheries and Food research programme at HR, Wallingford. The first approach was to test the method with a range of values of NEV from 0.16 to 0.29, to examine how well each value represent the observed data for all geometries, with both smooth and rough flood plains. The goodness of fit was represented by the mean discrepancy and the standard deviation about that average. This was done with both the individual stage discharge readings and also with running averages of threes to eliminate some of the experimental tolerances. (These procedures had previously been followed in the empirical analysis of the results described in Chapter 3). Only the averaged data results are summarised here in Table 6.1 appended. Taking all the smooth flood plain cases together, it will be seen that NEV = 0.27 gave the best fit of the values tested, with mean error about 0.4% and variability under 4%. This was not the optimum NEV value for all the geometries however: some required higher and some lower values of NEV for best prediction. (Geometrical information for the numbered test series is given in Table 3.1). With roughened flood plains, taken all together, NEV = 0.22 gave best results, though this was not true of the rough series taken individually.

6.2.6 Just three examples of the results in graphical form are shown, as Figures 6.3, 6.4 and 6.5. The first two are for NEV = 0.27, the best overall value with smooth flood plains, and the third is for NEV =0.22, the best for rough flood plains. They show the residual discrepancy ratio between the turbulence prediction and the observations, plotted against the ratio of flood plain flow depth to main channel depth, (H-h)/h. (Relative depth, H_* = (H-h)/H, is shown as an additional non-linear scale). This is a much more sensitive way of plotting than that of Figures 6.1 and 6.2 and illustrates how the error varies systematically as depth increases. Figures 6.3 concerns the sequence of tests with varying width ratios, B/b. The variability expressed as standard deviation about the mean error of under 4% typifies all the smooth flood plain series, but here the plotted observations cover an actual error band from -5% to +10% though of course the many points with discrepancies below 4% dominate the picture. (Statistically about 2/3rds of the data should lie within the band defined by SD.) What is interesting about this plot is the clear indication that a fixed value of NEV, even when chosen as best fit to a set of data, does not provide a prediction method of high accuracy: its performance varies with relative depth. Also, there are indications that the turbulence procedures somehow fail to account for the different regions of flow that are observed as depth increases. Figure 6.4 provides corresponding results where the channel side slope is varied from series to series, with much the same overall spread of discrepancies but with a rather different pattern with depth. Figure 6.5 is for the rod roughened flood plain tests, which also varied series to series in their main channel side slope. There is a somewhat wider spread of residual discrepancy, 10%: the statistical finding was that the standard deviation for the whole of the rough flood plain data was under 6% with this value of NEV.

6.2.7 The next form of analysis was to assess the optimum value of NEV for each individual stage/discharge result in all the FCF test series. This involved multi-stage iteration: the solution of the lateral shear turbulence equation is itself an iterative finite difference solution, but it had to be applied repetitively to converge on the value of non-dimensional eddy viscosity, NEV, that gave agreement with the measured discharge. Tolerances and also maximum numbers of iterations were specified. This approach was also applied to the in- bank calibration data for the main channel, and the mean value of NEV obtained for the non-compound trapezoidal section was 0.125 ± 0.10, appreciably below the average values found appropriate for compound cross-sections.

The figure for all the smooth results was 0.290 ± 0.13, and for all the rough results 0.217 ± 0.08. The average best fit values of NEV and their variability are given in the following table:

Test series	Av. NEV	S D	
1	0.314	0.120	
2	0.259	0.103	
3	0.195	0.052	
5	0.240	0.057	
6	0.207	0.077	
7	0.201	0.045	rough flood plains
7a	0.152	0.029	rough flood plains
8	0.356	0.150	
9	0.137	0.030	rough flood plains
10	0.429	0.109	
11	0.300	0.071	rough flood plains

6.2.8 It is thus apparent from the variation of the average values of NEV from series to series that the geometry and roughness condition affects the value that best fits the data. The standard deviation expresses the variability from depth to depth in any one series using the optimum value of NEV; the variability is clearly appreciable. In the main, this variation is not a random scatter: there is sytematic variation with depth as shown vividly by Figures 6.6 to 6.8. In these, individual values of NEV are plotted against flood plain depth ratio, (H-h)/h, with H_* as an additional scale. (Note that the test data are averages of three, to reduce experimental scatter). Figure 6.6 refers to the test series at varying width ratios (see Table 3.1 for geometric details), and clearly as the flood plains first become inundated NEV is close to the single channel value of 0.125, increasing through Region 1 to between about 0.27 and 0.45 depending on width ratio, B/b. Then through Region 2 as depth increases the value of NEV reduces again, with some hint of a different trend through Region 3 and beyond. At greater depths, where the channel coherence is above about 0.95, the optimum value of NEV seems to be returning towards a basic value of the order of 0.15 again, (which is typical of the values usually quoted for smooth laboratory flumes), for the narrowest flood plains, test 03.

6.2.9 Figure 6.6 referred to tests with channel side slopes of 1:1. In Figure 6.7 this bank slope is represented by test 02, whilst 08 is for s_C = 0 and 10 is for s_C = 2. Series 08, with rectangular main channel, appears to have a sudden switch from the basic low value of NEV to a much higher value at relative depth, H_*, about 0.23, $(H-h)/h = 0.3$. Does this indicate a reluctance for secondary currents to cross the bank line when banks are vertical, until some triggering depth is reached? The three series do not form a coherent sequence of results, however: s_C = 1 does not lie between the results for 0 and 2, although all show a characteristic S-shape as depth increases. There is no evidence of a return to a basic low value of NEV at greater depths in this plot.

6.2.10 Figure 6.8 gives the results for the test series with rod-roughened flood plains. Again at first inundation of the flood plains the optimum NEV value is close to the basic simple channel value. It increases with depth, with quite strong dependence on the bank slope, s_C. Here the sequence is logical, with the vertical bank condition (series 09) requiring lower NEV values than the other series with sloping banks. The vertical bank condition requires little increase over the basic value of NEV, which suggests a limited influence of secondary current exchange between main channel and flood plain.

6.2.11 It is apparent that to achieve accurate predictions from a simplified lateral distribution turbulence model with an all-embracing non-dimensional eddy viscosity or turbulence coefficient, a considerable degree of empiricism would still be required to accommodate the apparent dependence on relative depth, width ratio, channel side-slope and flood plain roughness. It appears that the different regions of flow identified from the original empirical analysis of the FCF results are confirmed by the variation of NEV, and would therefore have to be represented separately in any empirical functions for NEV.

6.3. Application, generality and confirmation of turbulence methods

6.3.1 The application of this type of relatively simple turbulence model holds great promise and will probably form the basis of a next-generation design procedure although it requires a significant computation effort to solve the governing partial differential equation. The engineer does not normally have those procedures at his finger tips, though clearly the software could be made available so that he would just have to supply the geometric and roughness information, plus the value of NEV to use. It is this last which provides the problem, because at present the method of determining reliable values of the turbulence coefficient is not established. Also the evidence from the analysis of the FCF results does not support the concept of using field observations within bank - nor even with shallow flood plain flows - to provide a site-specific turbulence coefficient. The evidence is that it will not be constant for a given geometry and roughness condition, but will vary appreciably with depth. So although the basic equations are general, there is insufficient knowledge at present about the NEV function. In this function is hidden the complexity of compound channel performance.

6.3.2 This review of the current application of the turbulence equation to compound channels has been limited to a consideration of how well a particular version of the method fits the large scale laboratory data from the FCF at Wallingford. This leaves considerable uncertainty over the NEV function even in those ideal geometries, and it was felt that further research effort was needed, beyond the scope of the present exercise, into the best method of assessing the turbulence coefficient before looking to other sources of information. It should be realised, however, that the search for a single value of NEV to apply to the whole cross-section is not the only approach that might be followed. Knight, Shiono and Pirt (1989) allowed it to vary across the section when analysing results from a natural river, the Severn at Montford Bridge. They developed analytical solutions for constant depth and for linear depth variation, and were then able to use gauged data at four depths to solve for the required NEV values in the seven zones forming the cross-section (deep part of main channel, sloping sides of main channel, two flood plains, two sloping edges to flood plains). They deduced values of 0.07 for the deep part of the main channel, 3.0 for the flood plains, and 0.2 for each of the four sloping boundaries. The degree of agreement achieved with some observed stages and discharges was as follows, for the Knight, Shiono and Pirt (1989) method with varying NEV: also shown are the results for an overall section value of 0.16:

		Variable NEV		Constant NEV of 0.16	
Stage	Observed discharge	Calculated discharge	Error,%	Calculated discharge	Error, %
m	m^3/s	m^3/s		m^3/s	
6.09	330.8	334.1	1.0	346.0	4.5
5.20	220.6	229.8	4.2	235.2	6.6
4.73	188.8	195.6	3.6	197.3	4.6

So reasonable accuracy of prediction is feasible provided there is sufficient accurate field data to calibrate the particular reach of river - though with more field information it might emerge that the zonal values of NEV derived for the Montford Bridge section are of more general validity.

6.3.3 One of the benefits of turbulence modelling is that it also provides an estimate of the distribution of shear stress and also of the lateral variation of discharge intensity. Its potential is illustrated in Figure 6.9 from Knight, Shiono and Pirt for these same data sets. The observed lateral variation of depth mean velocity is shown in comparison with the calculated variation. There are problems adjacent to the bank line where discrepancies are quite significant, but agreement within the main channel and on the flood plain away from the bank is good. Other approaches to turbulence modelling also suffer from problems in the river bank zone, so there remains some deficiency in all the simpler two-dimensional approaches. The potential benefit of knowing the distribution of shear stress around the perimeter of the channel and flood plain will be recognised by those involved with sediment transport and river morphology.

6.4 <u>Comparison of turbulence method with empirical method of prediction.</u>

6.4.1 Turbulence methods even with the restriction of vertical averaging provide more detailed information on flow distribution than can be obtained from the empirical procedures of stage/discharge prediction. However, where they would be of particular interest near the main channel bank, the turbulence methods suffer from some inaccuracy.

6.4.2 In terms of providing the stage discharge function for the FCF tests, the turbulence method which uses a single valued cross-sectional figure for NEV proved somewhat less accurate than the empirical method based on the same data. Table 6.1 indicates a best performance for all the smooth flood plain cases of -0.38% average error (which could obviously be reduced by using a value of NEV intermediate between those actually tested) with variability of 3.7%. The corresponding rough flood plain figures are -0.35% with variability 5.4%. These standard deviations are not primarily experimental errors, but represent mostly the imperfection in the trend of the theory compared with the trend of the data, and so indicate a need for further consideration and refinement. The empirical method achieved almost exact agreement with the data used in its calibration on average, smooth and rough together without any differentiation in treatment, with a residual variability of 0.8%, part of which is the tolerance in experimental measurement. The empirical method transfers satisfactorily to other geometries and roughnesses, in most cases with very satisfactory agreement as shown in Chapter 5.

6.4.3 The recommended empirical method seems justified as the first choice at the present time for engineers to apply, but it is clear that the full potential of the two-dimensional lateral distribution turbulence models has not yet been realised. It appears that either the value of non-dimensional eddy viscosity for use in the method has to be obtained from a set of empirical functions bringing in width ratio, roughness ratio, relative depth and bank slope, or else some different approach to its evaluation has to be developed from the research data. It is hoped that such development will proceed to a satisfactory outcome, given the excellent and detailed data base now available.

TABLE 6.1: LATERAL DISTRIBUTION TURBULENCE METHOD: ANALYSIS OF FCF DATA

Test series	Number of tests	Values of NEV used:	0.16	0.22	0.24	0.27	0.29
SMOOTH FLOOD PLAINS:							
01	24	Mean	+4.54		+2.16	+1.37	+0.89
		S D	6.21		3.82	3.22	2.86
02	27	Mean	+2.95		+0.04	-0.93	-1.52
		S D	4.53		3.63	3.98	4.29
03	20	Mean	+1.27		-1.81	-2.82	-3.45
		S D	2.58		3.50	4.34	4.94
05	6	Mean	+2.82		-0.20	-1.10	-1.67
		S D	3.46		1.95	2.30	2.78
06	18	Mean	+2.30		-1.65	-2.91	-3.70
		S D	4.58		4.34	5.18	5.79
08	23	Mean	+4.34		+1.15	+0.12	-0.53
		S D	5.96		5.41	5.75	6.08
10	17	Mean	+5.94		+3.87	+3.17	+2.70
		S D	6.73		4.72	4.11	3.75
All smooth:		Mean	+3.49		+0.58	-0.38	-0.98
	135	S D	3.14		3.53	3.70	3.82
ROUGH FLOOD PLAINS:							
07a	16	Mean	+4.25	-0.70	-1.95		
		S D	5.97	3.30	3.56		
07b	4*	Mean	-0.87	-6.59	-8.80		
		S D	3.18	8.16	10.20		
09	8	Mean	-2.05	-7.50	-9.45		
		S D	3.67	9.24	10.90		
11	14	Mean	+8.26	+5.03	+3.93		
		S D	10.36	2.29	5.94		

TABLE 6.1 (cont)

All rough:				
40*	Mean	+5.54	-0.35	-1.70
	S D	5.07	5.44	5.62

Notes: Mean discrepancies and standard deviations (S D) are percentages.
* denotes too few data points for averages of three to be meaningful though the 'All rough' results did incorporate averaging for series 07a.

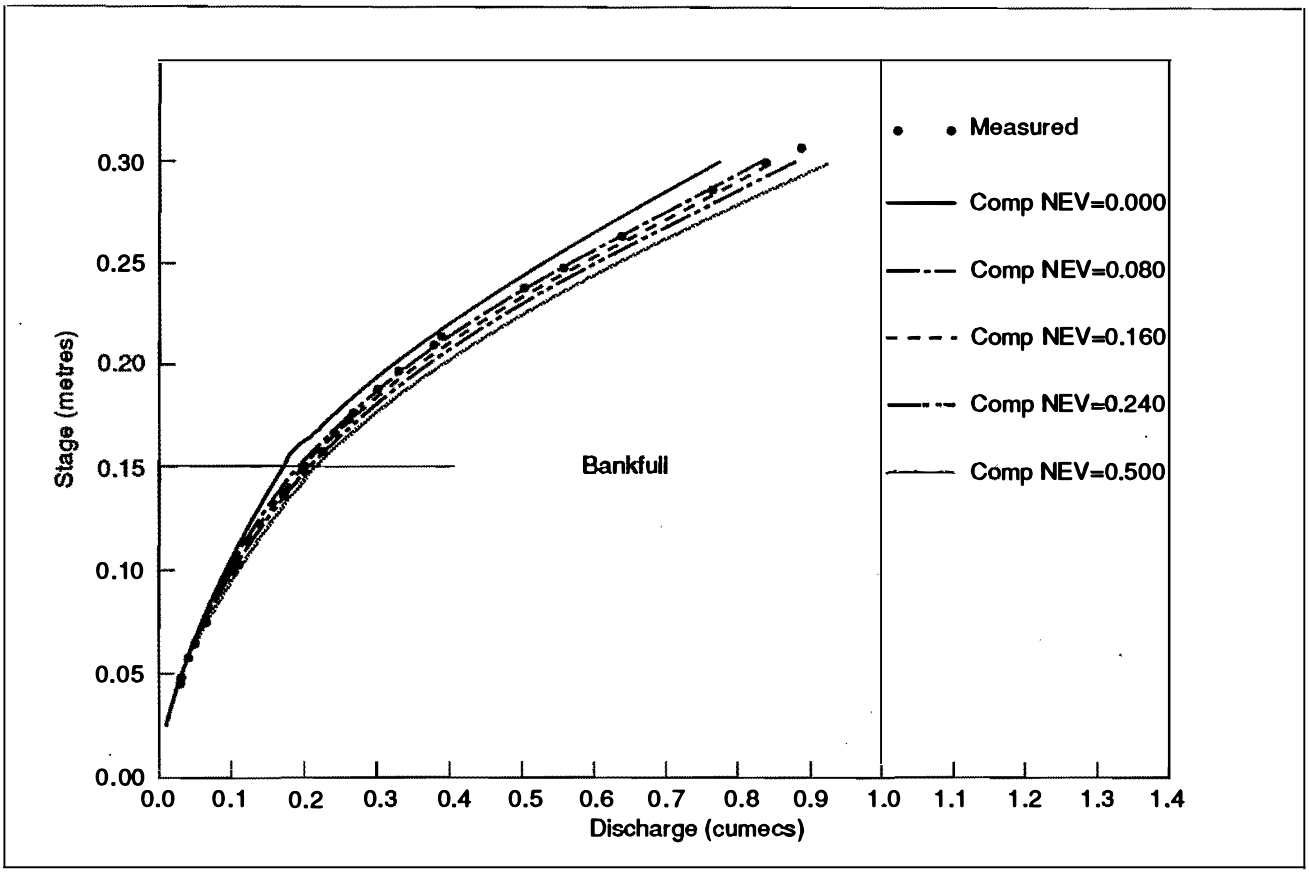

Fig 6.1 **Stage-discharge relationship for FCF at Wallingford; narrow flood plains, B/b = 2.2; series 03 observations compared with predictions from lateral distribution turbulence method**

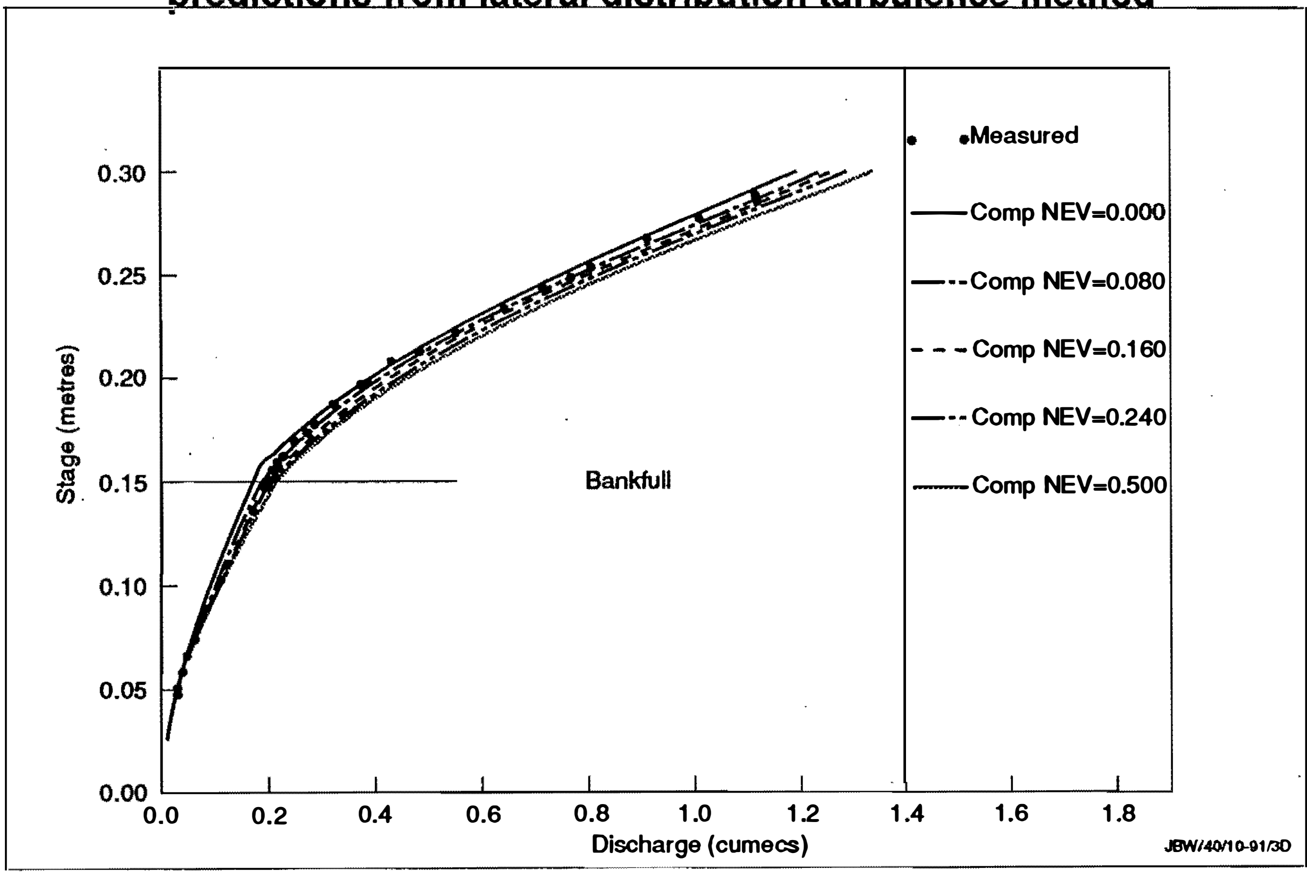

Fig 6.2 **Stage-discharge relationship for FCF at Wallingford; medium flood plains, B/b = 4.2; series 02 observations compared with predictions from lateral distribution turbulence method**

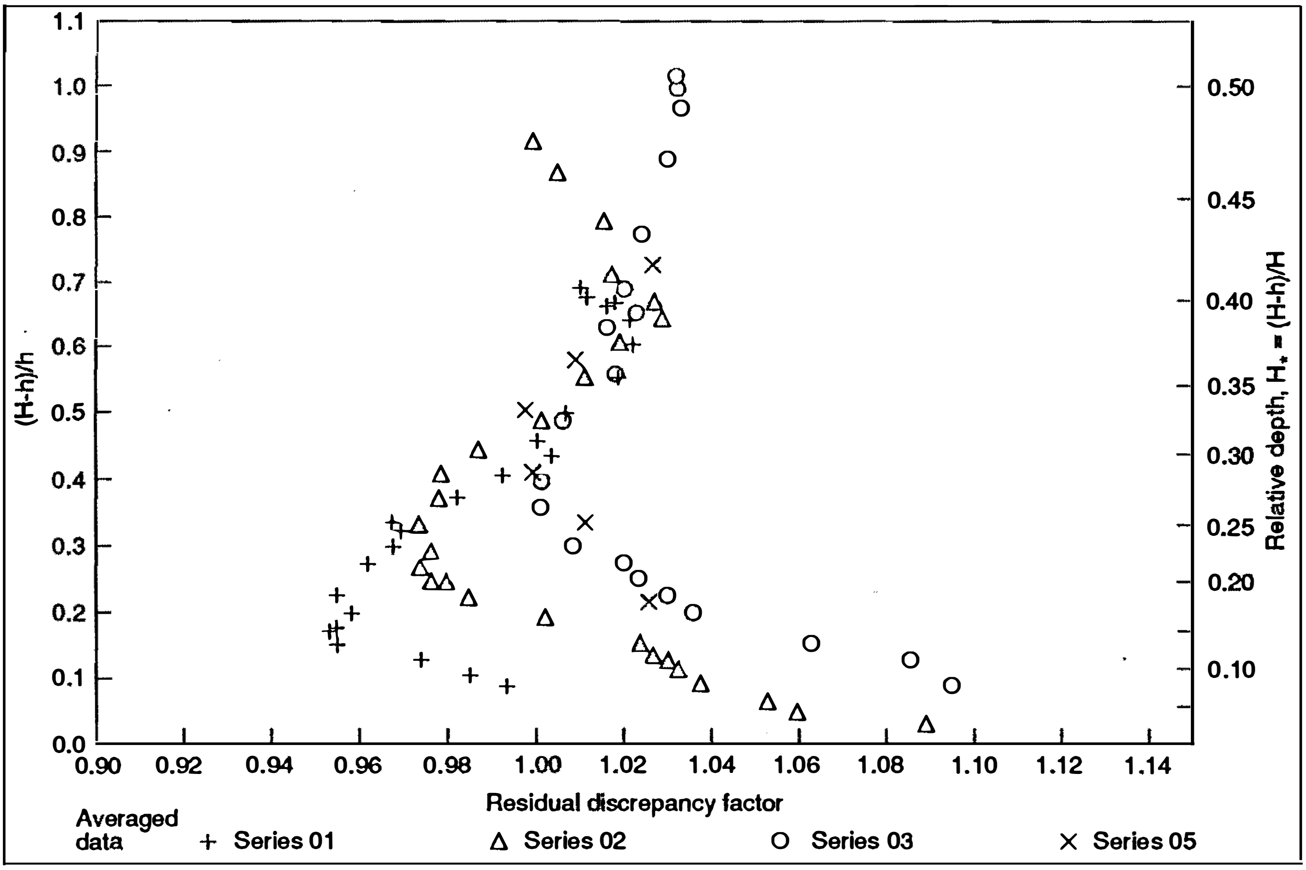

Fig 6.3 Residual discrepancy factor between observation and prediction using lateral distribution turbulence method; various relative widths; averaged data; NEV = 0.27; smooth flood plains

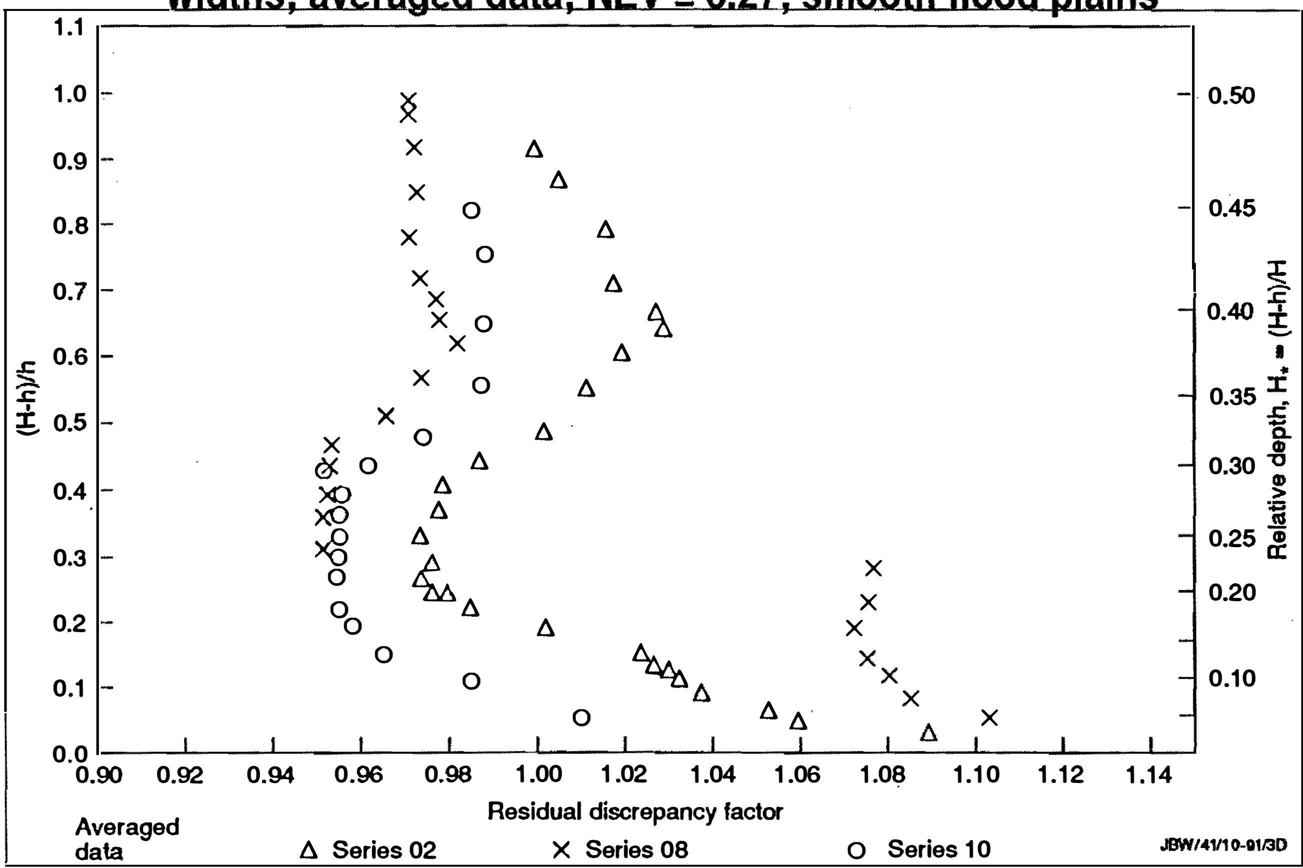

Fig 6.4 Residual discrepancy factor between observation and prediction using lateral distribution turbulence method; various main channel side slopes; averaged data; NEV = 0.27; smooth flood plains

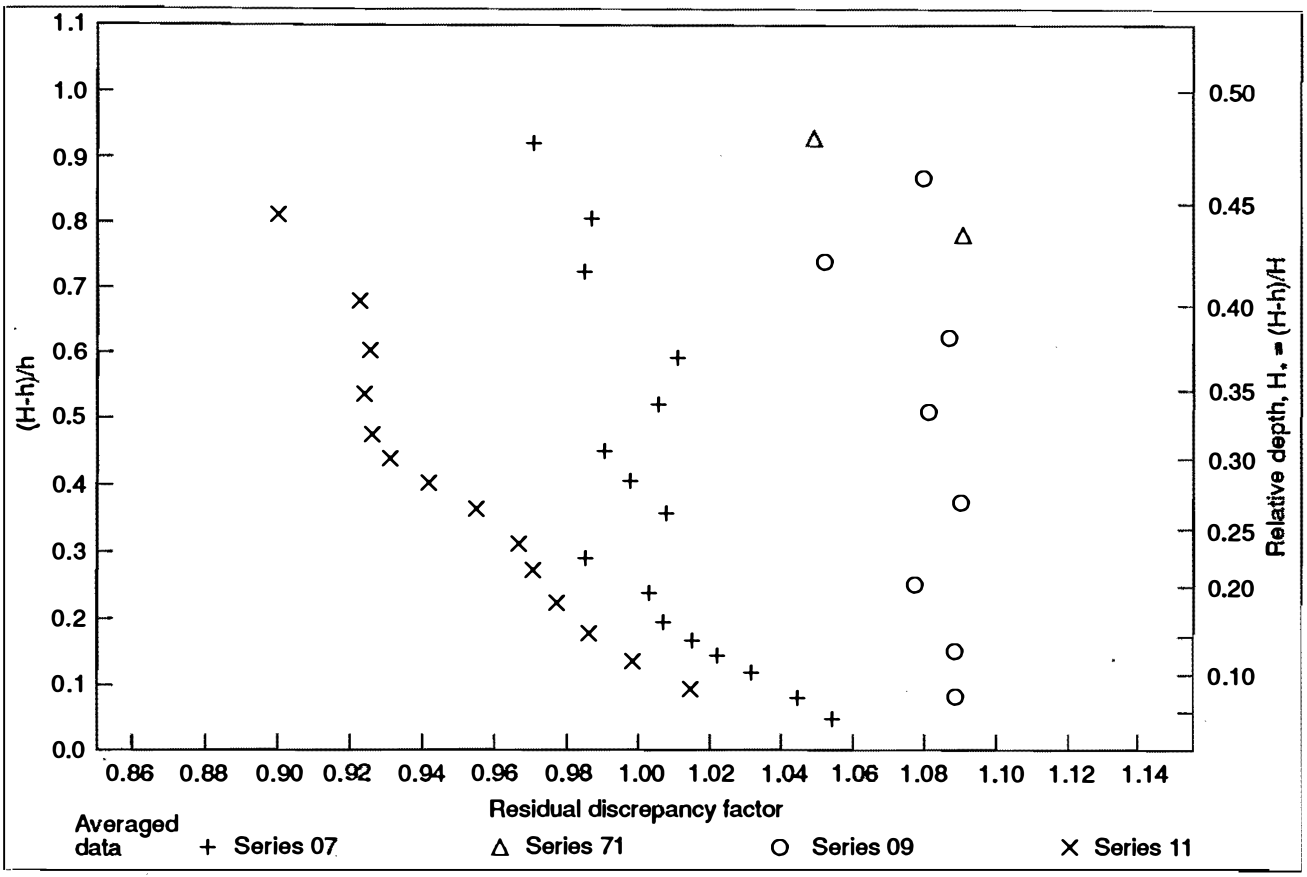

Fig 6.5 Residual discrepancy factor between observation and prediction using lateral distribution turbulence method; various main channel side slopes; averaged data; NEV = 0.22; rod-roughened flood plains

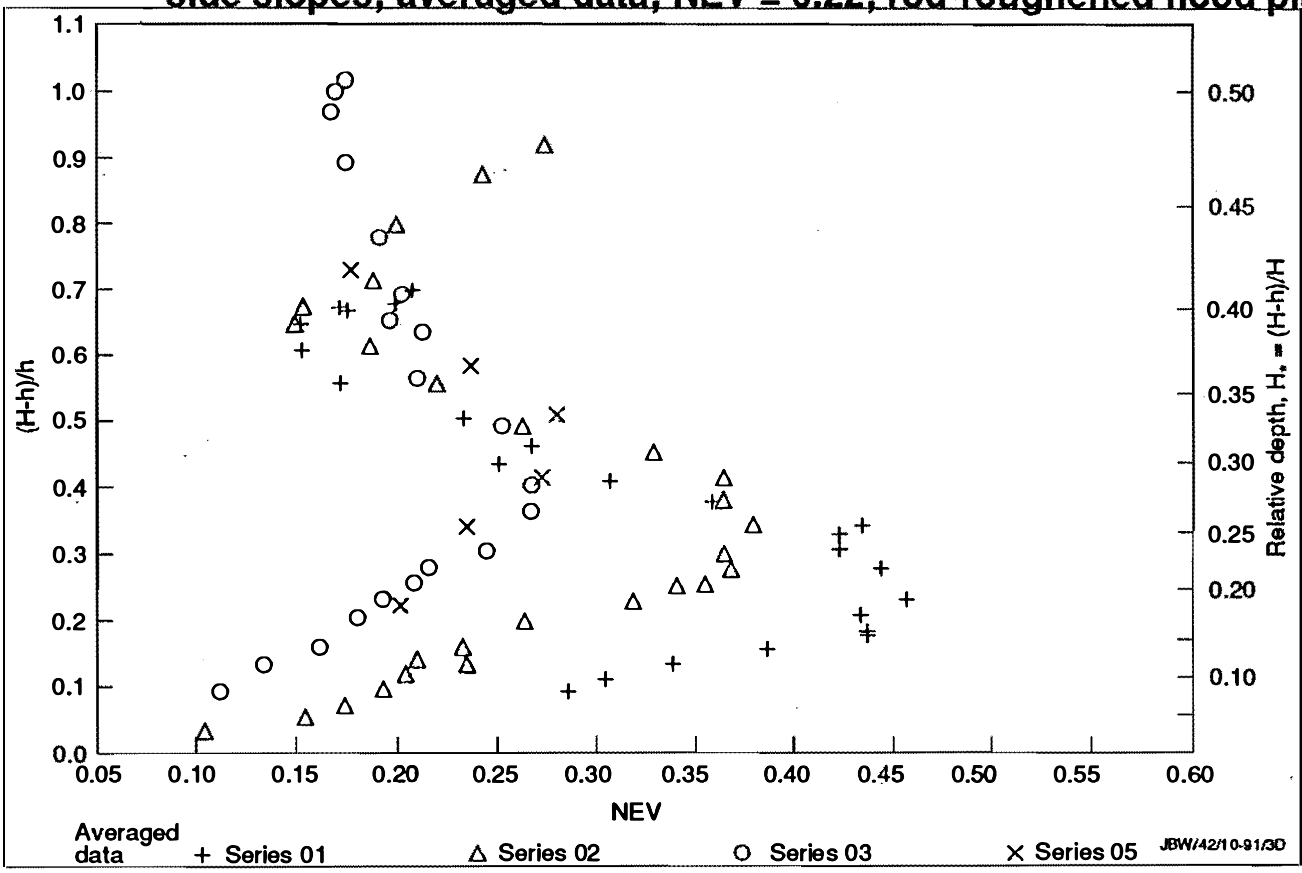

Fig 6.6 Optimum values of NEV for individual stage-discharge observations as function of depth: various relative widths; smooth flood plains

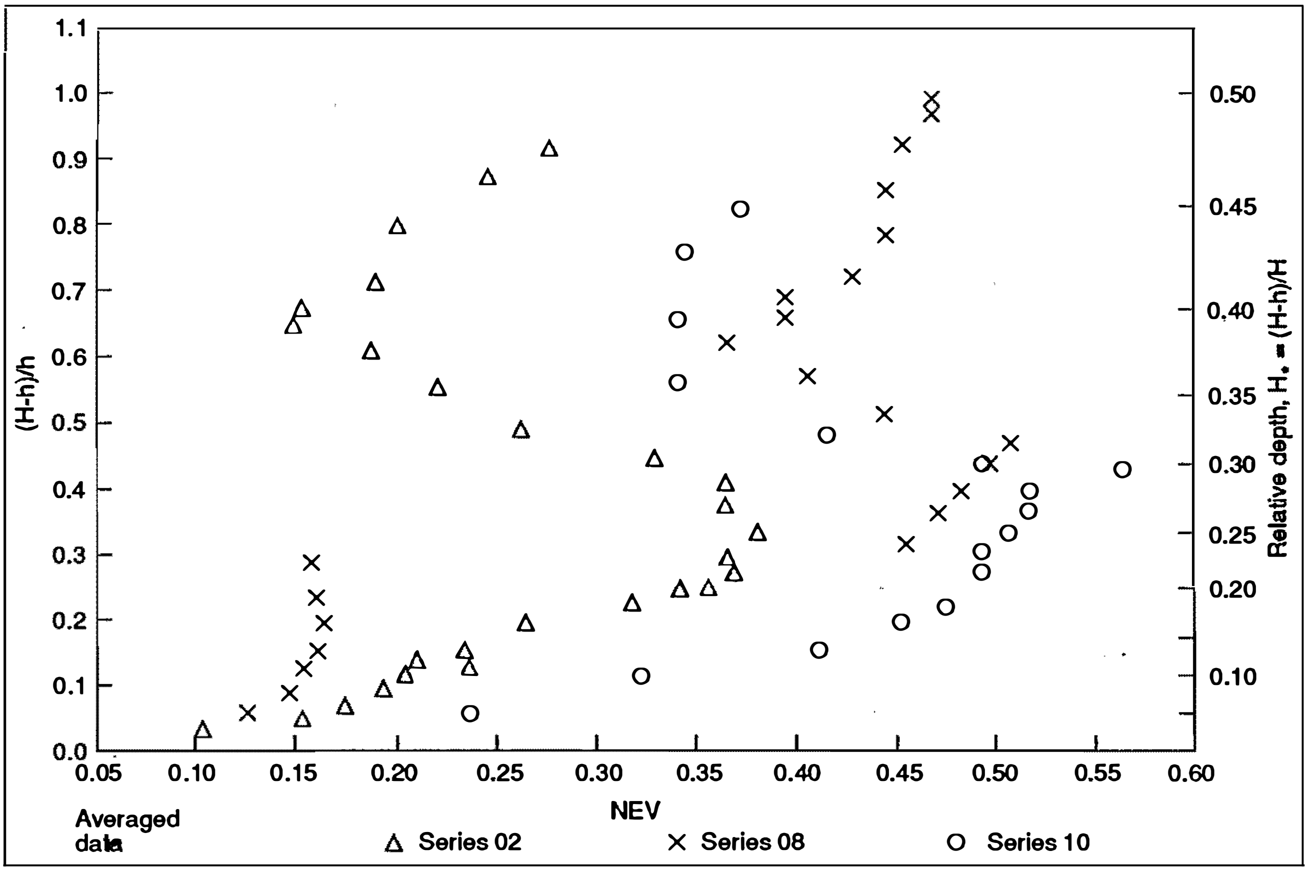

Fig 6.7 Optimum values of NEV for individual stage-discharge observations as function of depth: various main channel side slopes; smooth flood plains

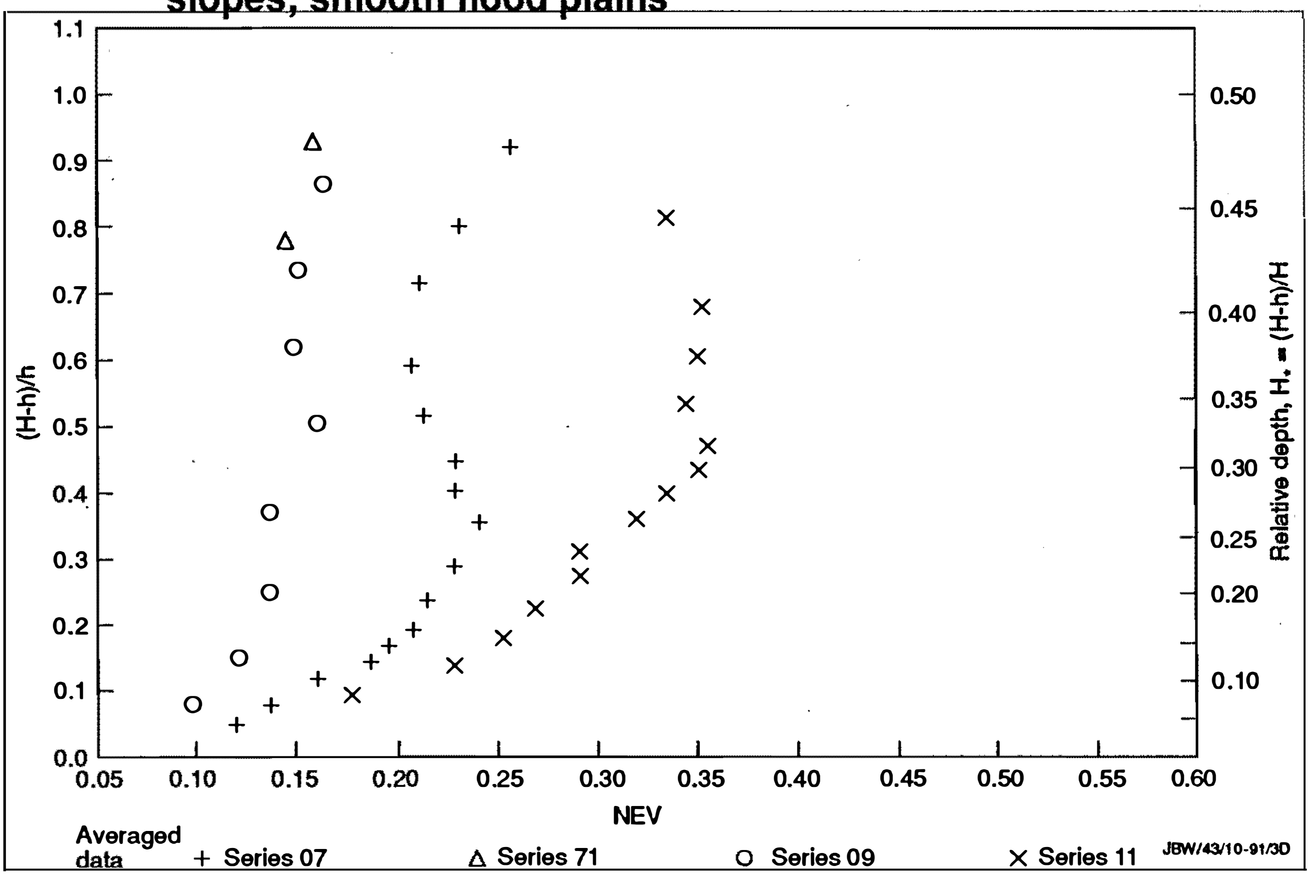

Fig 6.8 Optimum values of NEV for individual stage-discharge observations as function of depth: various side slopes; rough flood plains

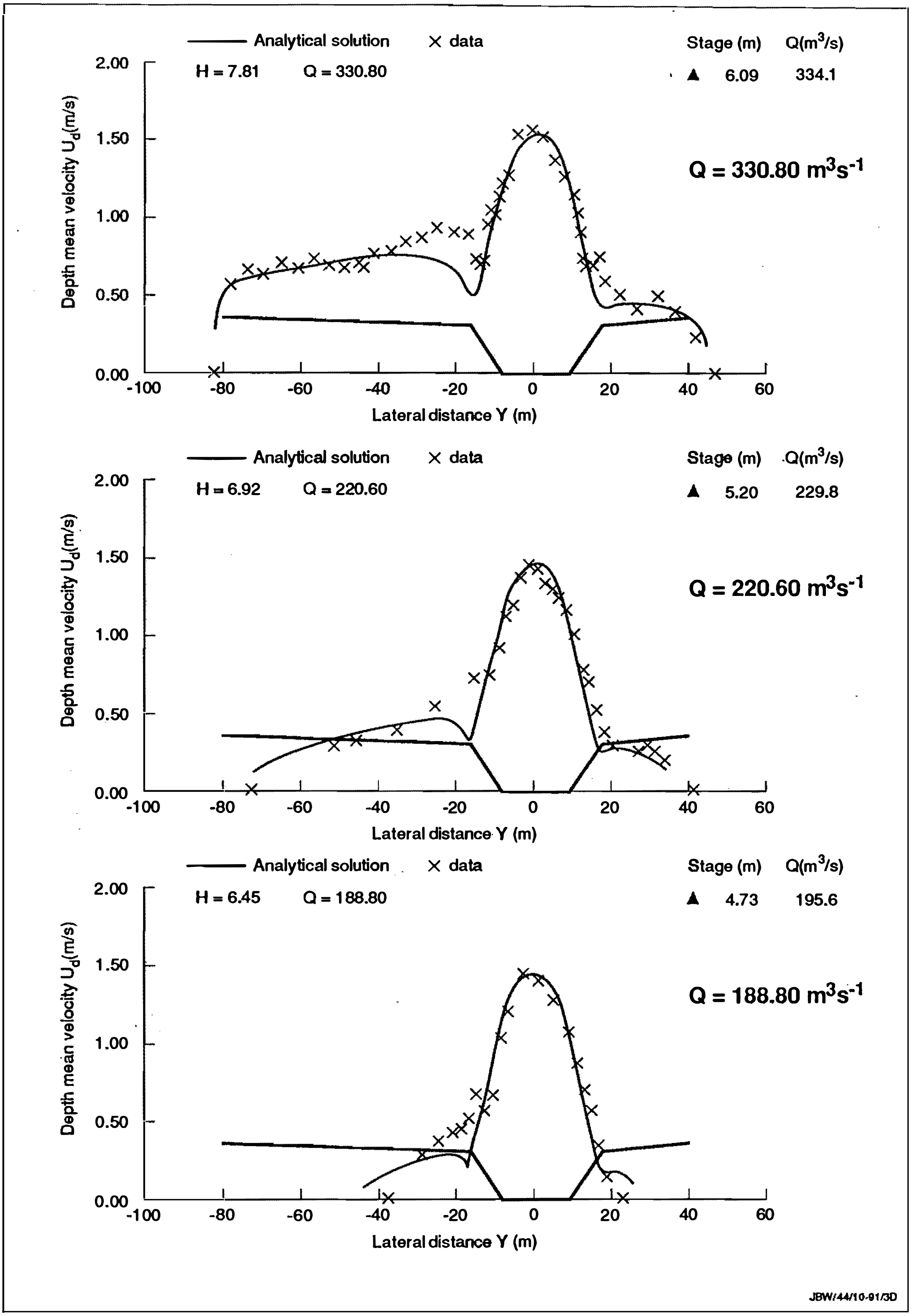

Fig 6.9 Lateral distribution of depth mean velocity: comparison between field observation and calibrated model of Knight, Shiono and Pirt, 1989, River Severn at Montford Bridge (from Knight, Shiono and Pirt, 1989)

HR Wallingford

HYDRAULIC DESIGN OF
STRAIGHT COMPOUND CHANNELS

VOLUME 2

by

P Ackers, Hydraulics Consultant

Contents of Volume 2

Detailed development of design method,
- Part 2
Appendices.

Report SR 281
OCTOBER 1991

Address: **Hydraulics Research Ltd,** Wallingford, Oxfordshire OX10 8BA, United Kingdom.
Telephone: 0491 35381 International + 44 491 35381 Telex: 848552 HRSWAL G.
Facsimile: 0491 32233 International + 44 491 32233 Registered in England No. 1622174

This report describes the development of new and improved design procedures for two-stage (compound) flood channels. This work was carried out by Peter Ackers as consultant to HR Wallingford, with funding made available by the Regional Water Authorites in 1988, prior to their demise when their responsibilities in this context passed to the National Rivers Authority. These funds were provided for the better dissemination of research results on this subject into engineering practice.

The report is in two volumes. The first begins with a Summary and Design Method which effectively provides a Manual for the hydraulic design of two-stage channels. The detailed review supporting these new procedures follows, continuing into volume 2, which also contains several Appendices.

The hydraulic engineer will find the essential information in the first section, Summary and Design Method, but will probably wish to refer to some of the details given in the main body of the report and in the Appendices to extend his understanding of the complex behaviour of two-stage flood channels.

Appendix 7 provides a design example of the computation procedures, including tables indicating how observed stage-discharge data might be used to extend the stage-discharge function. These tables will also provide a cross-check for any computer programme developed to solve the recommended hydraulic equations and logic procedures.

It is stressed that the equations given in this Manual are for the hydraulic design of straight parallel two-stage conveyances, although information will be found extending the application to small angles of skew (not exceeding 10°). Information given on meandering channels in Chapter 8 of the main text (see volume 2) shows that they behave quite differently. Improvements in the hydraulic calculations for meandered and irregular channels must await further work.

DETAILED DEVELOPMENT OF DESIGN METHOD

CONTENTS

PART 1 (See VOLUME 1)

CONTENTS (CONT'd)

CONTENTS (CONT'd)

CONTENTS (CONT'd)

7. ANCILLARY TOPICS

7.1 Application to more complex sections.

7.1.1 Natural river cross-sections and also many artificial or "engineered" two-stage channels differ in shape from the classic compound trapezoid for which most of the research evidence is available. Their berms, or flood plains, are likely to have a cross fall and the main channels of natural rivers are seldom of simple trapezoidal shape. Their beds may irregular, deeper on one side than the other; and their banks may not be trimmed to an even gradient. Despite these complexities of form, the hydraulic engineer has traditionally handled real cross-sections using the basic parameters of cross-sectional area and wetted periemter, which jointly provide a measure of hydraulic mean depth, $R = A/P$. What is required is an extension of the basic methods of handling complex cross-sections so that the methods derived from research on "classic" sections can be applied in practice.

7.1.2 As the recommended method starts from the basic computation of flows in the lower-stage main channel and the upper-stage flood plain separated by vertical divisions, using conventinal friction formulae, there is no problem in terms of the basic computation: the "real" cross section can be used, with appropriate areas, wetted perimeters and hydraulic mean depths of the zones of flow. The problem arises solely from the need to simplify the section geometry to deduce the values of several of the independent variables contained in the adjustment equations, particularly for Region 1 flow, the shallower range of depths of flood plain inundation. The relevant geometric variables to be defined are:

h - main channel mean depth
H - depth of flow relative to mean bed level, hence $H_* = (H-h)/h$
w_C - half top width of channel
B - effective half width of valley floor at flood plain level
s_C - bank slope
N_F - number of flood plains

7.1.3 Reasoning that the interaction effect is mainly dependent on condition adjacent to the bank line of river, H_* has to be defined so that

(H-h) is the flow depth on the flood plain at the river edge, not an average depth assuming the flood plain to have a cross fall. w_C is probably the most obvious of these geometric variables: the tops of the river banks define the vertical divisions between main channel and berm flows, and the distance between is obviously $2w_C$. The bank slope is less readily defined as the bank itself may be formed of a compound slope or curve. From the engineering point of view, what is required is a representative value and it is suggested that the way to achieve this is to plot the actual cross-section and "eye-in" an average bank slope at each side matching the upper two thirds, say, of the actual bank profile. This is illustrated on Figure 7.1. s_C is then the average value of the left and right bank figures. Having identified w_C and s_C, the mean bed level is also fixed, by the requirement that the area of the trapezoid so defined is the same as the true channel cross-section.

7.1.4 The number of flood plains or berms will usually be self-evident, and so this leaves only B to be defined. For horizontal flood plains, for the analysis of the experimental data, B was half the total width between the outer limits of the berms. Where they are sloped, this is clearly the most appropriate definition when the flood plains are inundated over their full width. However, with partial inundation of the flood plains, the flow "knows nothing" of the dry part of the cross-section, so that for partial inundation the value of B is half the effective width of the above berm flow, i.e. half the actual water surface width. This can be defined from the "real" geometry at any flow stage. These procedures for defining the geometric parameters are illustrated in Figure 7.1. (The use of b as the semi-channel bed width and B as the semi above-berm width stems from the terminology adopted as standard by the teams of researchers using the FCF at Wallingford. It was considered preferable to retain these definitions in the present publication, whilst stressing their special nature in the engineering context. w_C is also a semi-dimension.)

7.1.5 The discharge adjustments in flow Regions 2, 3 and 4 are based on the channel coherence, COH, which is explained and defined in Chapter 3, paras 3.3.4 to 3.3.6. These definitions and the formulations of equations 3.1, 3.2 and 3.3 are general and can be applied to the real section, however complex, or to a simplified section following the derivation of the previous paragraphs. The value of coherence derived will not be very sensitive to the method used, which can therefore be chosen for convenience of calculation.

7.2 Shear Stress

7.2.1 The variation of shear stress around the boundary of a compound channel was illustrated in a qualitative way in Figure 2.9. Shiono and Knight,(1990b), provided a valuable picture of the various processes at work, including the boundary shear stress distribution, reproduced as Figure 7.2. In the absence of lateral shear and secondary flows, the distribution of horizontal shear in the vertical is linear, varying from zero at the water surface to ρgyS at the bed. However, Figure 7.2 shows that momentum transfer at the interface and also secondary circulations may modify the basic depth-related distribution of stress on the solid boundary by bringing to it some higher - or indeed lower - velocities. Hence the shear stress distribution is complicated by several processes arising from the interaction between main channel and flood plain zones.

7.2.2 Knight, Samuels and Shiono (1990) analysed some early results from the research on the FCF showing the vertical distributions of shear stress at positions across the channel, for a particular flow depth, see Figure 7.3. There is reasonable approximation to the "normal" linear variation with depth at the centre line (Y = 0, where Y is the distance from the centre line), and towards the edge of the flood plain (Y = 1.5), but there are major departures over much of the width, especially in the region of the sloping banks. Clearly the conventional formula for the shear stress on any horizontal surface, $\tau_H = \rho g(y - z)S$ does not apply (y = flow depth, z = vertical distance from bed of point of interest). Shiono and Knight (1990b) continuing analysis of the same source of data plotted the boundary shear stress, τ_B, in the form of the difference from what might be considered a standard value, $\tau_o = \rho gyS$:

Relative change in shear stress, $\delta\tau_* = (\tau_o - \tau_B\sigma)/\tau_o$ ... 7.1

where $\sigma = \sqrt{(1 + 1/s^2)}$ ... 7.2

s being the local cross-slope of the bed. σ is thus an allowance for the fact that where the boundary has a cross slope its horizontal component of length defines the shear action on the column of water above. Shiono and Knight's results are illustrated in Figure 7.4, for three flood plain widths and a range of relative depths, H_*.

7.2.3 Although these plots are at too small a scale to be used directly in design, the information therein is very significant. Within the main channel, $\delta\tau_*$ is positive indicating a reduction of shear stress from its "normal" value, and with $\delta\tau_*$ = approx 0.15 to 0.35, the reduction is important, for example in the context of sediment movement. Over the flood plains, $\delta\tau_*$ is negative and so indicates an increase in shear stress over the normal value, ρgyS, again by a significant proportion even remote from the channel bank line with relative wide flood plains.

7.2.4 For the particular geometry upon which Figure 7.4 is based, the channel bed extends to Y = 0.75m, and the bank top is at Y = 0.9m. The bank top shows a considerable increase of stress over the normal value, with $\delta\tau_*$ ranging up to and even beyond 4. This signifies that the shear stress locally at the edge of the channel bank with shallow flood plain depths, H_* = 0.1 approx, is five times its normal depth-based value. This arises because the high velocity within the main channel spills on to the berm, and this spillage effect extends some distance across the flood plain, perhaps to Y = 1.3m, i.e. up to 3 times the channel depth of 0.15m beyond the bank line. At the base of the sloping channel bank, Y = 0.75m, the positive value of $\delta\tau_*$ is rather above that at the centre line, indicating a rather lower actual shear stress. This is characteristic of shear stress distribution in trapezoidal channels, it diminishes towards the re-entrant corner, and in theory would drop to zero if the corner was truly sharp and there were no secondary currents. So over the depth of the sloping main channel bank, the shear stress distribution passes from a "below normal" value to an "above normal" value, very much above normal at shallow overbank flows.

7.2.5 In broad engineering terms, the reason for the significant reduction in bed shear stress in the main channel below the value given by ρgyS is that the component of weight down the stream gradient is only partly balanced by the boundary shear stress. With a two-stage channel, the interaction between the flow zones gives additional stress on the interface between main channel and flood plain, and also the secondary circulations and the turbulence arising from momentum exchange change the flow structure from that in a simple channel. As a first attempt to quantify the magnitude of the effect, it might be reasoned that the mean bed shear stress will approximate to that which would occur with the same mean velocity. The discharge, as we have already seen, is reduced below the basic calculated figure for the main channel considered separately by a factor, $DISADF_C$, that depends on the flow geometry and roughnesses of the zones, but which is calculable. The mean velocity reduces by the same factor, of course, and with a square law of boundary drag, as in the Manning and rough-turbulent equations, the resultant mean boundary shear stress is proportional to V^2. Hence, to a first order of approximation, one might expect that the mean shear stress on the main channel bed would be given to a sufficient approximation for engineering purposes by:

$$\tau_{BAV} = \rho \ gHS \ (DISADF_C)^2 \qquad \ldots \ 7.3$$

or by:

$$\tau_{BAV} = \rho \ gR_CS \ (DISADF_C)^2 \qquad \ldots \ 7.4$$

depending upon whether the channel may be considered wide or not.

7.2.6 From the detailed measurements of shear stress (using a Preston tube) in the FCF program of research, the average bed shear stresses were established for the range of test conditions, though here only the results for varying flood plain width are considered, with channel bank slope, s_C = 1, and smooth channel and flood plains. For these smooth conditions, the square law of rough turbulence does not strictly apply, but in Appendix 2, eq.3.6, it was shown that a power law of 1.8 would be appropriate. The two equations above can therefore be modified by providing $DISADF_C$ with the exponent 1.8 as an alternative. Thus, using the procedures for calculating the discharge adjustment factor, with the logic of selecting regions and the approach to the separation of the zonal adjustments for Regions other than 1 as explained in Chapter 3, para 3.5.10, theoretical values of τ_{BAV} can be calculated for comparison with experiment. Figure 7.5 shows this, with the upper diagram for test series 02 (see Table 3.1 for the geometry). Both methods of calculation, using the hydraulic mean depth of the main channel, R_C, and the water depth, H, were used, coupled both with the square law exponent of 2 and the smooth law value of 1.8. One would expect the data to lie between the two theoretical graphs for exponent 1.8 (shown as full lines) and indeed they do. The observed data τ_{BAV} lie fairly close to but above the plot based on h.m.d., R_C, and as the plotted function is really an indication of mean shear stress around the whole solid perimeter, it is to be expected that the mean value on the bed will exceed this. Test series 01 and 03 at different B/b ratios are shown in the lower part of Figures 7.5, and the picture remains much the same, the observed mean bed shear stress lies between the values calculated on the basis of flow depth and on the basis of h.m.d., lying nearer to the latter. It appears that the simple procedure incorporated in equations 7.3 and 7.4 above straddle the true value of mean bed shear stress, whilst explaining the bulk of the departure from the "normal" value, ρgyS. This calculated adjustment, $DISADF_C^{1.8}$, accounts for a reduction of up to 30% in this particular test series.

7.3 Critical flow, energy and water levels

7.3.1 Critical flow is usually defined in standard hydraulics textbooks as the flow condition in an open channel when the specific energy for a given discharge is at a minimum, and for which maximum discharge occurs for a given energy level. It also indicates a change in flow state, in that small surface disturbances will travel upstream with sub-critical conditions but cannot do so with super-critical conditions. It is this latter criterion that makes the concept of critical flow of particular significance in numerical calculations of non-uniform or non-steady flows. The theory of critical flow is dealt with at some length by Jaeger (1956) including the proof that whether energy or momentum is considered the same conventional definition of critical flow in an open channel of general cross-sectional shape applies *provided* it may be assumed that the velocity distribution is uniform. This leads to the conventional definition of Froude number, $Fr = V/(gA/W)$, where V is the mean velocity of flow, A the cross-section area, W the water surface width and g the gravitational acceleration. Critical flow is when $Fr = 1$.

7.3.2 The assumption of uniform velocity distribution may not be an unreasonable approximation for simple cross-sections but it is clearly inadmissable with compound channels. The velocity variation across the section can be described by α or β, depending on whether one is concerned with energy or momentum, and the incorporation of these factors into the energy and momentum equations then gives differing formulations for the Froude Number, Fr:

Energy basis:

$$Fr = \sqrt{\left[\left(\frac{\alpha W}{A} - \frac{d\alpha}{dd}\right)\frac{Q^2}{2gA^2}\right]} \qquad \ldots\ 7.5$$

Momentum basis:

$$Fr = \sqrt{\left[\left(\frac{\beta W}{A} - \frac{d\beta}{dd}\right)\frac{Q^2}{2gA^2}\right]} \qquad \ldots\ 7.6$$

which revert of course to the conventional definition for $\alpha = \beta = 1$. The appearance of the water surface width, W, in the above functions indicates that in a channel with horizontal berms, there will be a discontinuity in the calculated Froude number/stage function for a given channel gradient, and there could be duality in the critical condition in more general cases.

7.3.3 Knight and Yuen (1990) carried out experiments to examine and compare aspects of critical depth in a compound channel with b = h = 75mm, B = 225mm and $s_C = s_F = 1$, with variable slope, and for a range of relative depths, $0.05 < H_* < 0.5$. They were concerned not only with the concept of an overall value for the Froude Number but also with its local variation across the channel. With depths and velocities being measured at many verticals across the width, they were able to assess the local values of Froude number, $U/\sqrt{(gy)}$, and specific energy, $E = y + U^2/2g$ where U is the depth mean velocity at any vertical. It is worth mentioning at this stage that the water level is the same at each point across the section, no doubt because with an aligned system of flow there is hydrostatic pressure throughout. The lateral variation of Froude number when the overall flow is critical is illustrated in Figure 7.6. This confirms that there can be local zones of super-critical velocity on the berms near the channel bank line, induced by the increase of discharge intensity due to lateral shear, although on the berms away from the bank line the flow is sub-critical, as it is within the central deep section.

7.3.4 Petryk and Grant (1978) examined methods of calculating the Froude number in compound channels, referring to field observations of surface disturbances that clearly indicated a variation of Froude number across the section. They were seeking explanation for the observation of a pattern of surface waves in the main channels of flooded rivers, when overall the flow might be expected to be sub-critical. With cross-sections more typical of natural rivers than those tested by Knight and Yuen, there can obviously be conditions where the high velocity in the main channel can yield locally high Froude numbers when the shallow depth and roughness of the flood plain render the flow there sub-critical. There is also the condition already mentioned when the penetration of fast main channel flow on to the edge of the flood plain can generate a pattern of surface waves on the berm itself because there the depth is shallow, so increasing the Froude number above the main channel value. Viewed in the context of surface wave patterns, there are clearly different possible combinations according to the local values of Froude number across the channel width.

7.3.5 Samuels (1989) includes a review of the influence of Froude number on numerical modelling, and how it might properly be calculated incorporating values of the momentum coefficient, β. The subject is a complex one and further research is required for a full understanding. For hydraulic engineering purposes, the important point is perhaps that the simple "text book" definition of Froude number no longer applies to compound channels, and that with a knowledge of the separate flows as calculated by the method given earlier in the Manual, approximate values for the main channel and for the flood plain zones could be calculated. They will not be the same as the overall section value but are probably more relevant for engineering purposes.

7.4 Sources of basic information on roughness

General

7.4.1 The main resistance functions used in open channel design are the Manning equation and the Colebrook-White equation. The former is for rough turbulent flow and so should not be used for relatively smooth construction materials, such as good quality concrete lining; the latter is for turbulent conditions embracing all surface conditions from smooth to rough, so is more general. However, the choice of equation can not be separated from the data base available on the roughness coefficient. The Manning equation has been so widely used in engineering practice that extensive listings of the coefficient value, Manning's n, are available in the literature, based on the body of experience in the use of that equation in hydraulic design. Ven Te Chow (1959) gives such information for a whole range of construction materials, through metal, wood, brick, masonry and concrete, to channels excavated in earth, gravel and even rock; natural streams in the mountains or plains, weedy reaches and also variously described flood plains. These values are listed in Appendix 5, Table A5.1.

7.4.2 The roughness coefficient in the Colebrook-White function is less empirical in that it has a physical basis, namely the textural roughness of the surface referred to as an "equivalent sand roughness, k_S", the diameter of grains forming a plane granular surface that would provide the same resistance. This fundamental concept has been extended over the years to incorporate empirical information from a wide range of surfaces and construction materials, including typical values for rivers and gravel bed streams etc. Table A5.2 in Appendix 5 gives values for concrete and some other materials.

7.4.3 The Manning equation will normally be used for natural channels, and for rivers in an "engineered" condition. The methods given above apply only to straight, or very gently skewed or curved channels (limiting deflections say 10°), and wherever possible the roughness coefficient used should be based on actual measurement of the river under study. It is usually found that the Manning's n value varies in a systematic way with stage and Figure 7.7 illustrates the results of field measurements in five Scottish rivers, by Sargent (1979). The coefficient value reduces with increase of stage, possibly because there are typically features in the bed, such as bars, shoals and scour holes, that have a greater influence at shallow depths than at stages approaching bank full. The value of main channel n to use for above-bank flows would be the value obtained when flow is just below bank-full. However a coefficient variation of the form shown in Figure 7.7. can also arise where the relative roughness is somewhat over-severe for the Manning equation to apply, when the Colebrook-White equation might prove more robust.

7.4.4 A conversion between the Manning coefficient and the value of k_S (in metres) is available through the formula:

$$n = k_S^{1/6}/26 \qquad \dots 7.7$$

but the Manning equation is only theoretically correct where $7 < R/k_s < 130$, so Manning might not be expected to provide a good fit to measured data when:

$$n \gg 0.03\ R^{1/6} \qquad \ldots\ 7.8$$

This suggests restrictions at shallow flow depths in typical rivers.

Gravel bed rivers

7.4.5 The dominant size of sediment found in the beds of alluvial rivers is related to their gradient, so that steep rivers in mountainous terrain have beds of boulders and coarse gravel, those in the sub-montane region will have gravel beds with some sand, and in the plains beyond will have sand and silt beds. A particular feature of coarse bed streams is the wide range of sediment sizes found in them - and being transported through them. Considerable sorting is observed between different parts of the stream bed as well as in depth. Armouring frequently occurs, where a one or two grain thick layer of coarse material overlies the bulk of the bed with its mix of a wide range of sizes. This armour layer is left by decreasing flows after a flood event, by the winnowing out of finer material when the flow is no longer competent to move the coarsest fraction. This layer then protects the underlying material with smaller D_{50} size, until a flow large enough to initiate motion in the armour layer occurs, so triggering rapid transport of the sediment forming the bulk of the bed.

7.4.6 The resistance of boulder and gravel bed rivers is associated with the texture of the bed arising from the coarser fractions of material there, and so current methods use various modifications of the rough turbulent equation, (which is one of the limiting regions of the Colebrook-White function), relating the linear roughness of that equation, k_s, to the bed material size. A variant of that is to use the Strickler form of the Manning equation, with its linear measure of roughness determined from bed grading (Strickler, (1924)). The Limerinos (1970) equation was based on Californian data, and effectively incorporates the conversion into Manning's n of the k_s value that would be used in the rough turbulent function:

$$n_m = 0.113\ R^{1/6}/[1.16 + 2\log(R/D_{84})] \qquad \ldots\ 7.9$$

D_{84} is the grain size for which 84 percent of the bed material is finer.

7.4.7 Bray (1982) reviewed the resistance of gravel bed rivers, generally confirming the Limerinos function. Hey (1979) effectively used a modified form of this rough turbulent equation which included a cross-section shape parameter. There have been two international conferences dealing specifically with gravel bed rivers, from the morphological, sedimentological and hydraulic points of view, and the proceedings of these conferences provide an excellent state-of-the-art summary: Hey, Bathurst and Thorne (eds) (1982); Thorne, Bathurst and Hey (eds) (1987).

Sand bed channels

7.4.8 In laboratory experiments starting with a plain sand bed, once the flow conditions are able to generate sediment movement, ripples or dunes will form. The normal condition in nature is also for similar features to form on the bed: a plane bed is an unusual condition and is more likely to occur at high transport rates when the stream velocity is high enough to wash out the pre-existing features. The presence of bed features means that the overall resistance of the bed will comprise both the drag due to the obstruction of ripples or dunes (form drag) and the resistance of the granular texture itself (grain resistance).

$$\tau_o = \tau_{form} + \tau_{grain} \qquad \ldots 7.10$$

where

$$\tau_o = \rho\, gyS \qquad \ldots 7.11$$

y = flow depth

S = hydraulic gradient

7.4.9 The grain resistance for coarse material can be estimated from the rough-turbulent equation, as was noted for gravel bed rivers, but for sand bed rivers the subject is considerably complicated by the existence of bed features. Ripples and dunes and combinations of them are known as "lower regime" and the high transport plane-bed region of rapid flow, together with the anti-dune condition that can arise in steep channels at high Froude numbers, forms the "upper regime". The distinction between lower and upper regime is not clear cut: there is a transition between them as velocities increase and it is possible for different parts of the bed to be in one regime or the other, or to be somewhere between, when flow conditions are not clearly one side or the other of the dividing criterion. Features are dependent also on sediment size: gravel bed rivers do not have ripples and have shoals rather than dunes.

7.4.10 White, Paris and Bettess (1980) used the same parameters as appear in the Ackers and White (1973) sediment transport calculation method, for assessing the resistance of rippled and duned sand bed rivers, and it is possible to combine these functions in given circumstances to assess suitable values of Manning's n, as illustrated by Ackers (1980) for irrigation canals. Although the method has been shown to be reliable and forms the basis of modern design procedures for sand bed irrigation canals, it is too complex to cover in detail here. Bettess and Wang Shiqiang (1987) also used the same sediment parameters to study upper regime bed form resistance, and the transition between upper and lower bed forms, but again it would be inappropriate to detail their procedures here. Suffice it to say that typical Manning's n values for straight sand bed channels are in the range 0.022 to 0.040 depending on size of channel and size of sediment, but major sand bed rivers can show considerable variation in times of severe flood if the bed of main channel goes through the transition from ripples and dunes to plane bed. This was illustrated from the river Indus by Hogg, Gugenasherajah, Gunn and Ackers (1988)), using flood data for 1976 and 1986, showing a reduction in n_m to about 0.011 as the dunes are washed out and the bed becomes plane, later reverting to a duned bed with n about 0.03. The different bed forms possible in sand bed rivers are thus of significance to hydraulicians, though within UK few rivers would come into this category, many having effectively rigid beds.

Vegetation

7.4.11 River vegetation falls into three categories: mid-channel aquatic weed; channel edge growth (grass, reeds, willows etc); and bankside/flood berm vegetation (pasture, growing crops, orchards, trees, shrubs, hedges etc). This rich variety is environmentally desirable but it inevitably has an influence on the hydraulic performance of the system. Moreover it varies seasonally, and so assessment of the roughness coefficient can not be considered an accurate science. Clearly, past experience based on measurements at the site of interest will provide the best guide, though of course any seasonal changes must be borne in mind. Research has also provided important sources of information, though again caution is required in transferring results from one geographic zone to another, which may support different flora.

7.4.12 The most extensive work on grass comes from America, and is described by Kouwen, Li and Simons (1981). The method is to identify a retardance class based on a US Dept of Agriculture classification, as shown in Table 7.1, and then to use a simple formula involving the product of mean velocity and hydraulic mean depth to assess the Manning's n value. There are dual functions depending on VR: at very low values long grasses will remain erect and increasing depth and velocity will increase the n value due to greater depth of immersion. Above a limiting value, they will deflect so that Manning's n reduces with increasing depth and velocity. For shorter stands of grass, n diminishes progressively with increasing VR, though not very strongly. The governing equations are given in Table 7.2.

TABLE 7.1. GRASS COVER RETARDANCE CLASSIFICATION.

Average length	Stand: GOOD Class	FAIR Class
Longer than 0.76m	A	B
0.28 - 0.60m	B	C
0.15 - 0.28m	C	D
0.05 - 0.15m	D	D
Less than 0.05m	E	E

TABLE 7.2. MANNING'S N VALUES FOR GRASS SURFACES.

The coefficients p and q apply to the equation

$$n = p + q/(VR) \qquad \ldots 7.12$$

Retardance class:	Coefficients in equation p	q	Limits of VR m^2/s
A	0.440	-1.617	< 0.154
	0.046	+0.022	> 0.154
B	0.403	-3.336	< 0.053
	0.046	+0.010	0.053 - 0.179
	0.035	+0.012	> 0.179
C	0.034	+0.046	< 0.083
	0.028	+0.005	> 0.083
D	0.038	+0.002	< 0.100
	0.030	+0.003	> 0.100
E	0.029	+0.001	< 0.123
	0.0225	+0.002	> 0.123

7.4.13 Regarding channels with aquatic weeds, research by HR Wallingford led to the following formula, depending on the extent of weed coverage:

$$n_C = n_{basic} + 0.02\ K_W/Fr \qquad \ldots\ 7.13$$

where n_{basic} is the Manning's n value for the channel without weeds
K_W is the fractional surface area coverage of weed growth
Fr is the channel Froude number, $V/\surd(gA/W_C)$

Larsen, Frier and Vestergaard (1990) describe both field work in a weed affected reach of river and flume tests, and develop a similar type of function as those given for grasses in Table 7.2 above. They relate Manning's n to VR, with the dry weight of growth in g/m^2 forming a further parameter. They suggest that there is a basic winter function for n in terms of VR, and that the summer function will depart from this for VR < 0.4 m^2/s, the presumption being that above this value the weeds will lay flat or be scoured away. One field measurement may then characterise the trend of the summer roughness function. The influence of weed growth on an East Anglian river was investigated by Powell (1978) clearly demonstrating the strong seasonality of the roughness coefficient, also indicating large tolerances on its assessment.

7.4.14 Regarding flood plain roughness, Klaasen and Van der Zwaard (1973) carried out laboratory research on modelled vegetation, including such features as orchards and hedges, which may be a helpful source of information. So far as orchards and forests and forests are concerned, provided there is no undergrowth and the water surface is below the top growth, the method of analysis used for the rod roughness in the FCF can also be applied, utilising a knowledge of the typical diameter and spacing of tree trunks. There is also the information in Appendix 5. However, in the absence of actual measurements under above bank conditions, there will probably be greater tolerances on estimating the conveyance due to uncertainty in the roughness coefficient than will arise from the computation of the recommended adjustment to these basic values to allow for the flood plain/channel interaction.

7.5 Need for and utilisation of field data

7.5.1 If river engineers are to make best use of existing knowledge of the behaviour of compound channels when assessing the flood conveyance of their river system, it is important that they not only acquire the best quality field data over as wide a range of depths as feasible, but also that they interpret them correctly in the framework of what is now known about the complexity of two-stage channels. Understanding of the processes at work has been deficient in the past, and so conventional methods of treating field data under over-bank conditions has probably led to serious errors. It has been demonstrated quite positively that the main result of interaction between main channel and flood plain flows is the reduction of the main channel flow, yet the conventional treatment of above-bank stage discharge data has, in effect, been to allow for any interaction by adjusting the flood plain roughness coefficient, the basic resistance function for the main channel being assumed to correctly represent its component discharge at above-bank flow. This has perhaps been inevitable, given the previous state of knowledge, but the net result may have been the use of inflated values of flood plain roughness. The combination of this with inaccurate methods of treating the compound section must have led to many errors - and in some cases large errors - in assessing the flood conveyance of rivers. Thus it is firmly recommended that all future analyses of stage- discharge data under above-bank conditions should make full use of the new methodology.

7.5.2 The problem is illustrated by some sample calculations for a small river, bed width 15m, channel depth 1.5m, side slopes 1/1, Manning's n = 0.03, two flood plains of width 20m, Manning's n = 0.06, channel gradient 0.3/1000, (this is the same cross-section as later used to typify a small sand bed river in Chapter 9). The stage discharge function for depths up to 3m is shown in Figure 7.8a on a log- log basis for a range of assmptions. The basic calculation before making allowance for interaction is shown in the upper part of Figure 7.8 as a broken line, and shows the full depth flow as 80.34 m^3/s. With allowance for interaction, this reduces to 61.81 m^3/s as at the terminal point of the full line. The chain dotted line illustrates the assumption that would have to be made about the flood plain roughness in order to achieve close agreement at the highest stages if no allowance is made in the analysis for interaction effects: this is with n = 0.60, TEN times the true value assumed in this example. This unrealistic value comes about because what is being attempted is to get the correct discharge by adjusting the flood plain roughness coefficient when in reality the "loss" of conveyance under above-bank conditions occurs in the main channel, and not on the flood plains.

7.5.3 It may be noted that the predicted stage discharge curve shown by the full line in the upper Figure 7.8 has a change in gradient at bank full, with a humped character over the lower range of flood plain depths. This is very similar to many field observations of real rivers (see for example Chapter 5, section 5.5.). Even with a false increase in flood plain roughness there is no way that this characteristic hump can be produced without taking account of interaction. The line drawn for $n_F = 0.60$ forecasts significantly higher discharges in this range, even though it can give approximately correct discharges at high stages. Note also that the stage-discharge function with allowance for interaction does not give a straight line on this log-log plot and so methods of interpreting and extrapolating from observed stage/discharge data that presume the existence of a power law i.e. a straight line on a log-log plot, for above-bank flows are likely to be inaccurate and could be somewhat misleading.

7.5.4 The false picture of the division of flow that emerges if one tries to compensate for interaction effects in this way is shown in the lower Figure 7.8. There are two sets of curves corresponding to the assumptions explained above, for both Q_C/Q_T and Q_F/Q_C. The full predictive method shows Q_C/Q_T reducing from unity at bank full to 0.624 at depth 3m ($H_* = 0.5$). The figure with no allowance for interference would be 0.719, but using the increase of n_F to achieve the correct maximum flow suggests that the main channel component of the total is 0.962. Turning to Q_F/Q_C, with Q_F being for both flood plains, the correct prediction at maximum depth is 0.602, the basic calculation with the true n values gives 0.390, whilst the falsely assessed n_F value would yield 0.040. This is a gross distortion of the reality of the flow division and the consequent potential for serious error using the traditional methods of analysis must cause considerable concern.

7.5.5 It is not the purpose here to explain in detail the field procedures for the measurement of stage and discharge. There are British and

International Standards on the subject as well as codes of practice. The subject is well described in the book Hydrometry, edited by Herschy (1978).

7.6 Incorporation into numerical models.

7.6.1 One of the mathematical procedures used for assessing flood wave propagation down a river system is channel routing of the Muskingum-Cunge type, see for example Cunge (1969). This takes account of the speed of movement of the flood wave and also its dissipation, utilizing the flow parameters section by section along the river valley. Garbrecht and Brunner (1991) have recently published a development of the method which specifically aims to take account of two-stage channel effects. They do this by separately computing for main channel and flood plains in a given reach, and then joining the outflows from these zones together before progressing to the next reach. However, they neglect the interaction effect between the zones so that the velocities used are the basic values which we have seen may be 15% or so different from the true values under over-bank conditions. Clearly the methods of allowing for interaction developed in this Manual could be incorporated into such a routing model, thereby improving its ability to simulate real rivers. In their recent paper, Garbrech and Brunner compare their hydrologic routing method with the U S National Weather Services fully dynamic DAMBRK model (Fread, 1984), using the latter as a bench mark. However, the bench mark method itself also has the shortcoming of not making allowance for the interaction effects of compound cross-sections.

7.6.2 One dimensional dynamic computational models typically solve the St Venant equations of energy (or more strictly momentum) and continuity in a time and space framework, utilising geometric information at many cross-sections defining the fluvial system. Some models may use the cross-section data to define a unitary channel: this is no longer to be recommended because by so doing the roughness coefficient is also required to take account of spurious changes due to the geometric anomalies introduced by flow over the flood plains, as well as real changes in roughness with stage as the flood plains are inundated, and the extra resistance due to interference effects. However, if the model requires the sections to be treated as units, not divided into main channel and flood plain zones, the predictive methods given above could be used as a roughness/cross-section pre-processor, to deduce overall equivalent conveyance functions in terms of flow depth, which could be incorporated into the model data store as "look up" tables.

7.6.3 Other models will use cross-section information in its more rational form, with separate data for flood plain and main channel. In this case also it would seem appropriate to use the predictive methods given here in the form of a pre-processor to provide the conveyance/depth function at each section in the model. Conveyance, K, is usually defined by:

$$K = Q/\sqrt{S} \qquad \ldots\ 7.14$$

where S is the hydraulic gradient, so can readily be assessed from the predictive equations over the required range of depths. From a knowledge of the distribution of flow between the main channel and flood plain zones, it is also possible to assess the momentum coefficient, to be associated with the conveyance as a function of stage. Both are required for use in one-dimensional models.

7.6.4 The question of Froude Number, Fr, was dealt with in Section 7.3. and it was explained that in a two-stage channel the Froude Numbers in the main channel and on the berms will be different, and also different from a whole cross- section value. These differences are real, of course, and as the Froude Number is a measure of the speed of propagation of a small surface disturbance, it is significant in assessing the stability of numerical schemes and their associated time steps. It is therefore conceivable that the flood plain component could be computationally stable whilst the main channel component would be unstable - and that the stability status could not be obtained from the whole-channel parameters. Clearly care has to be exercised, with recent improvements in the understanding of compound channel flow providing scope for a significant step forward, both in the reliability of simulating real rivers in 1-D models and in assessing the stability of computational schemes.

7.6.5 This report deals essentially with straight rivers in their flood plains, and so, in a modelling context, it provides a one-dimensional treatment of a one-dimensional system. It will be clear from Chapter 8 that the methods developed here are not applicable to systems with irregular plan form, where the processes at work are significantly different. The methods of allowing for interaction effects with straight aligned systems are not adequate, therefore, for 1-D models of highly irregular rivers, nor are they appropriate for models incorporating two dimensions on plan. It will be apparent from Chapter 8 that there is much to be learned about how to incorporate the exchanges of flow and momentum into numerical models of meandering or very irregular rivers. Such models, even if two-dimensional, are currently over-simplified. Improvements corresponding to those that are now possible in dealing with 1-D systems will have to await the outcome of detailed analysis and review of the findings from later phases of research in the FCF at Wallingford.

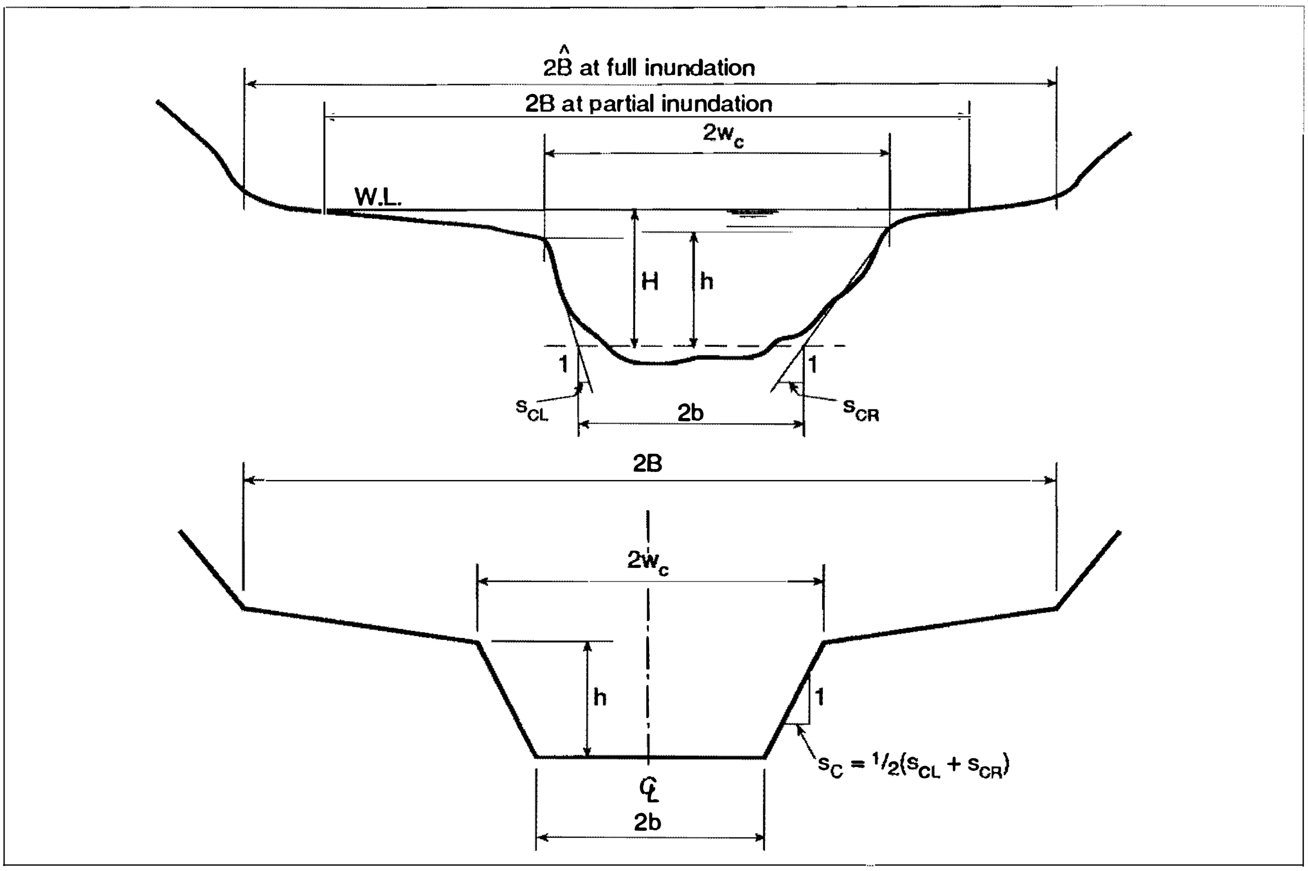

Fig 7.1 Illustration of method of assessing the sectional goemetry parameters for a natural river cross-section

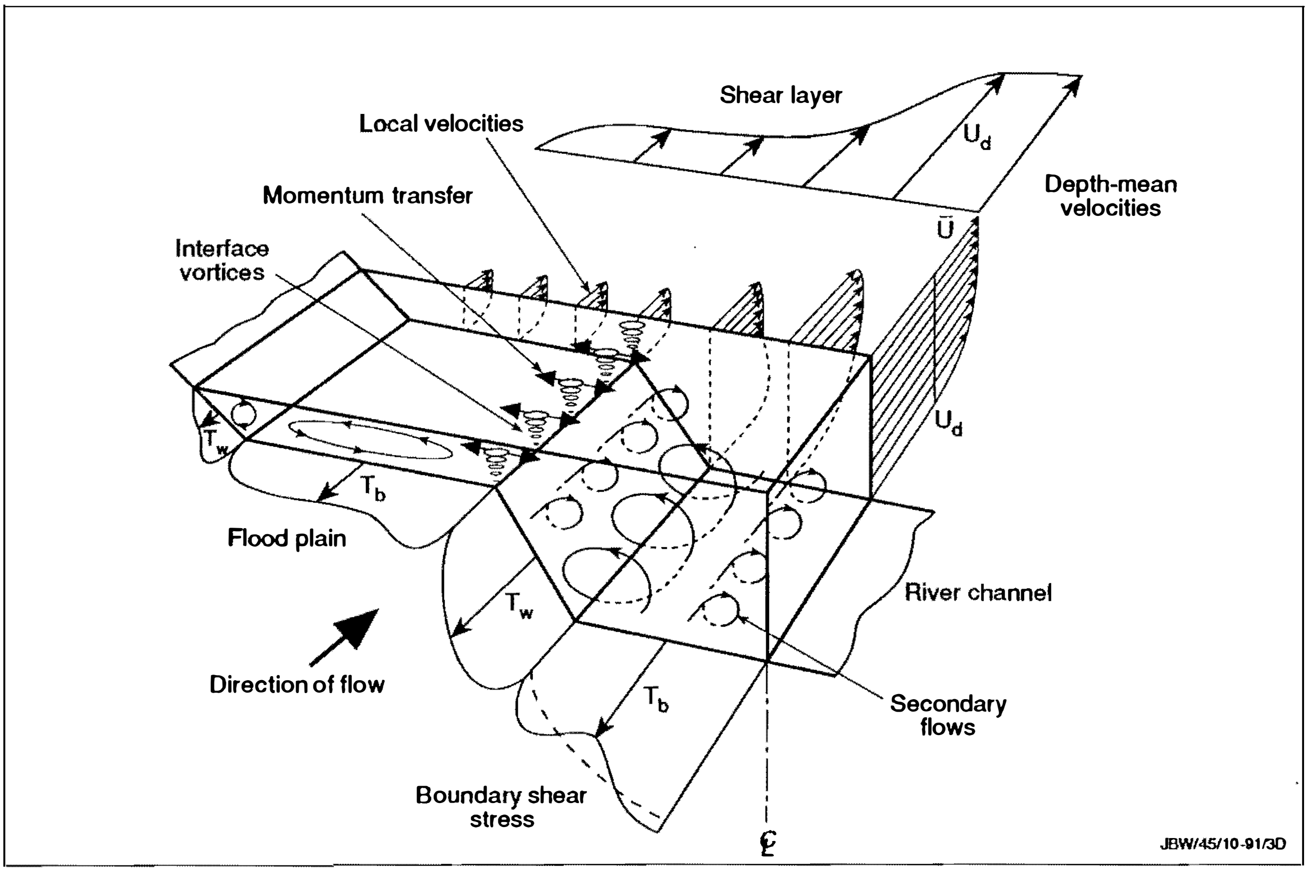

Fig 7.2 Some of the flow processes in two-stage channels, with their influence on boundary shear stress (Shiono and Knight, 1991)

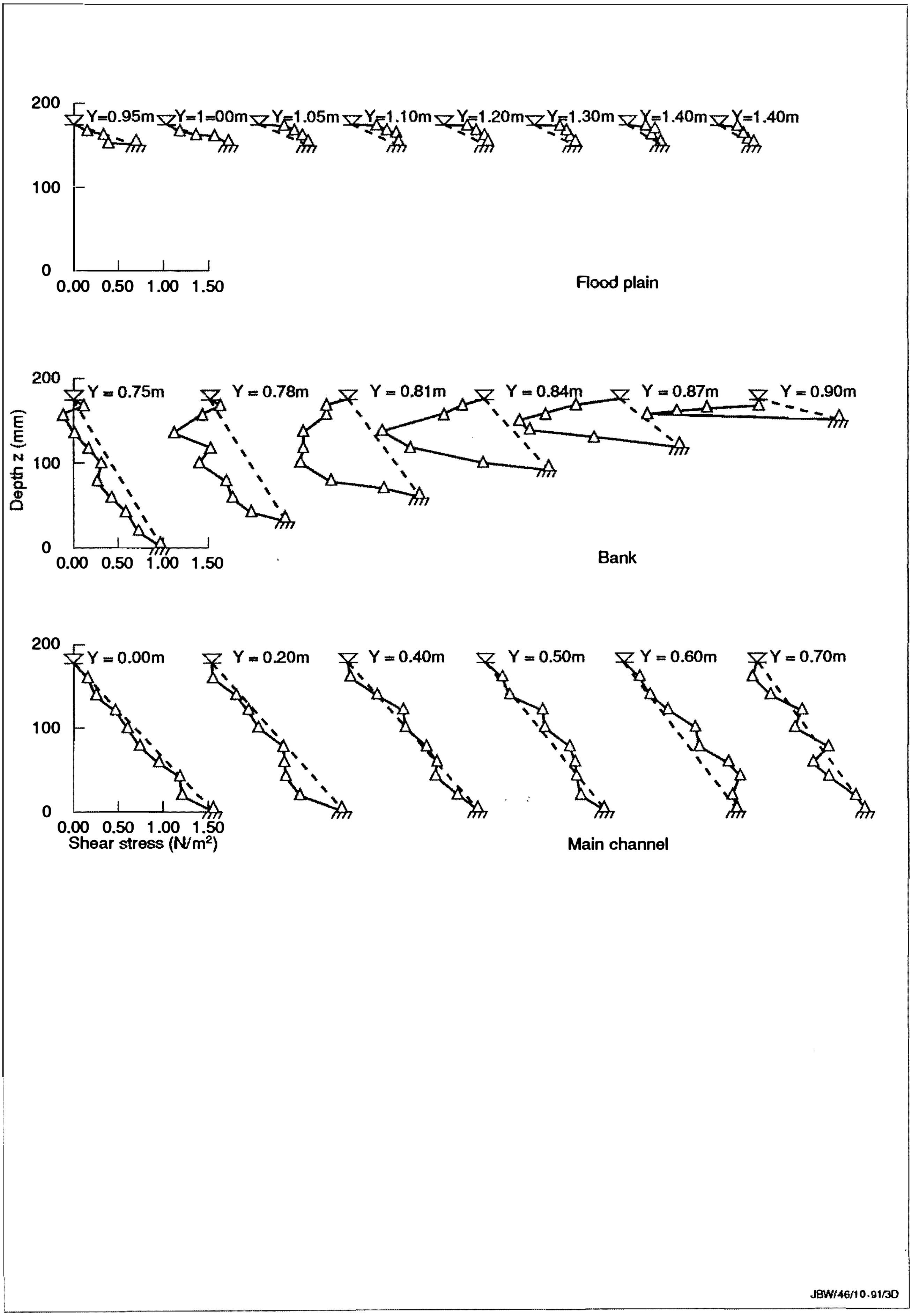

Fig 7.3 Vertical distributions of shear stress, τ_H: bed values based on Preston tube measurements, others using laser doppler anemometry. Y denote lateral distance from centre-line. $H_* = 0.152$. (Knight, Samuels and Shiono, 1990)

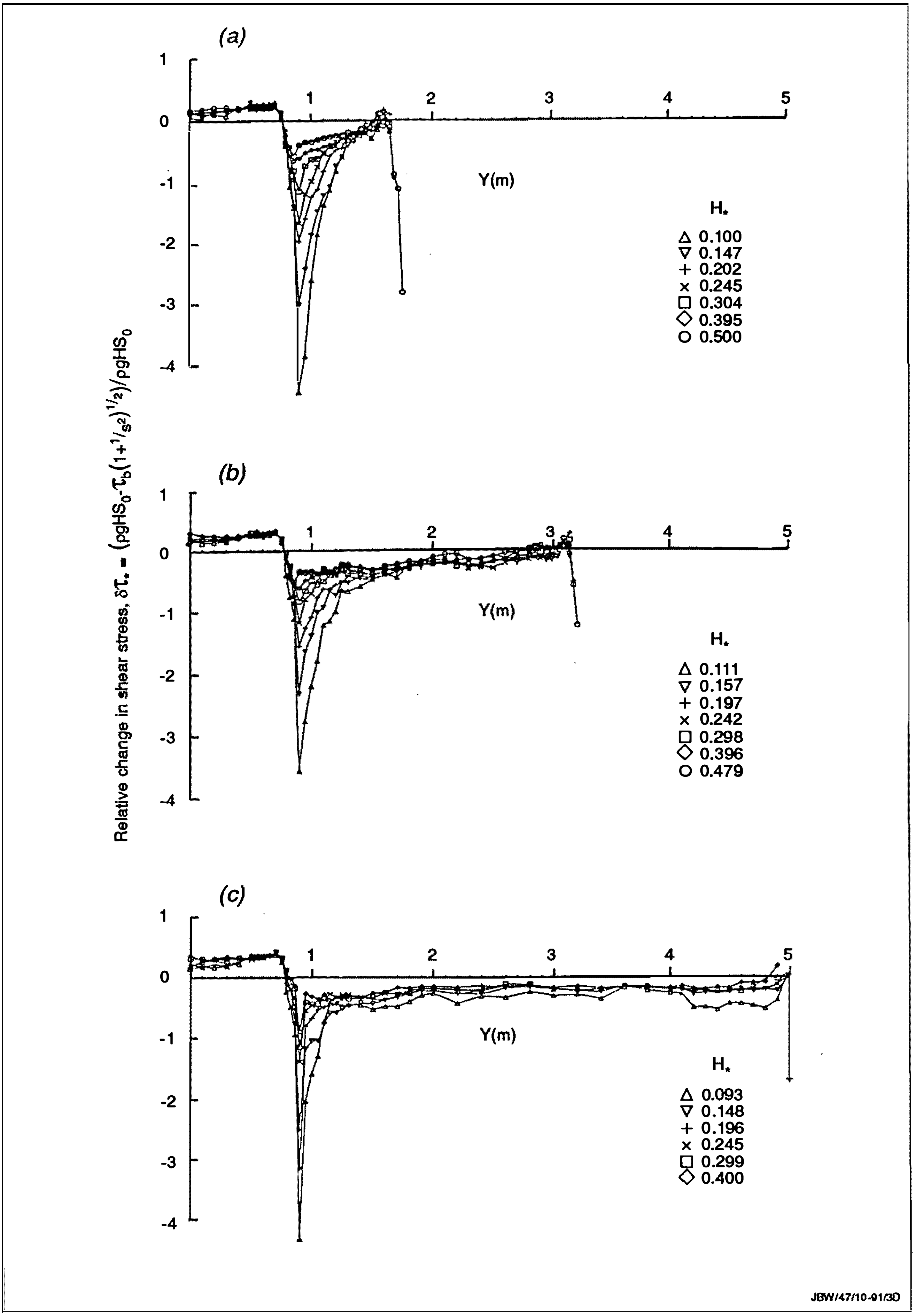

Fig 7.4 Lateral variation of boundary shear stress for different relative depths, H*, for B/b = 2.2, 4.2 and 6.67, (series 01, 02, 03) (Shiono and Knight, 1991)

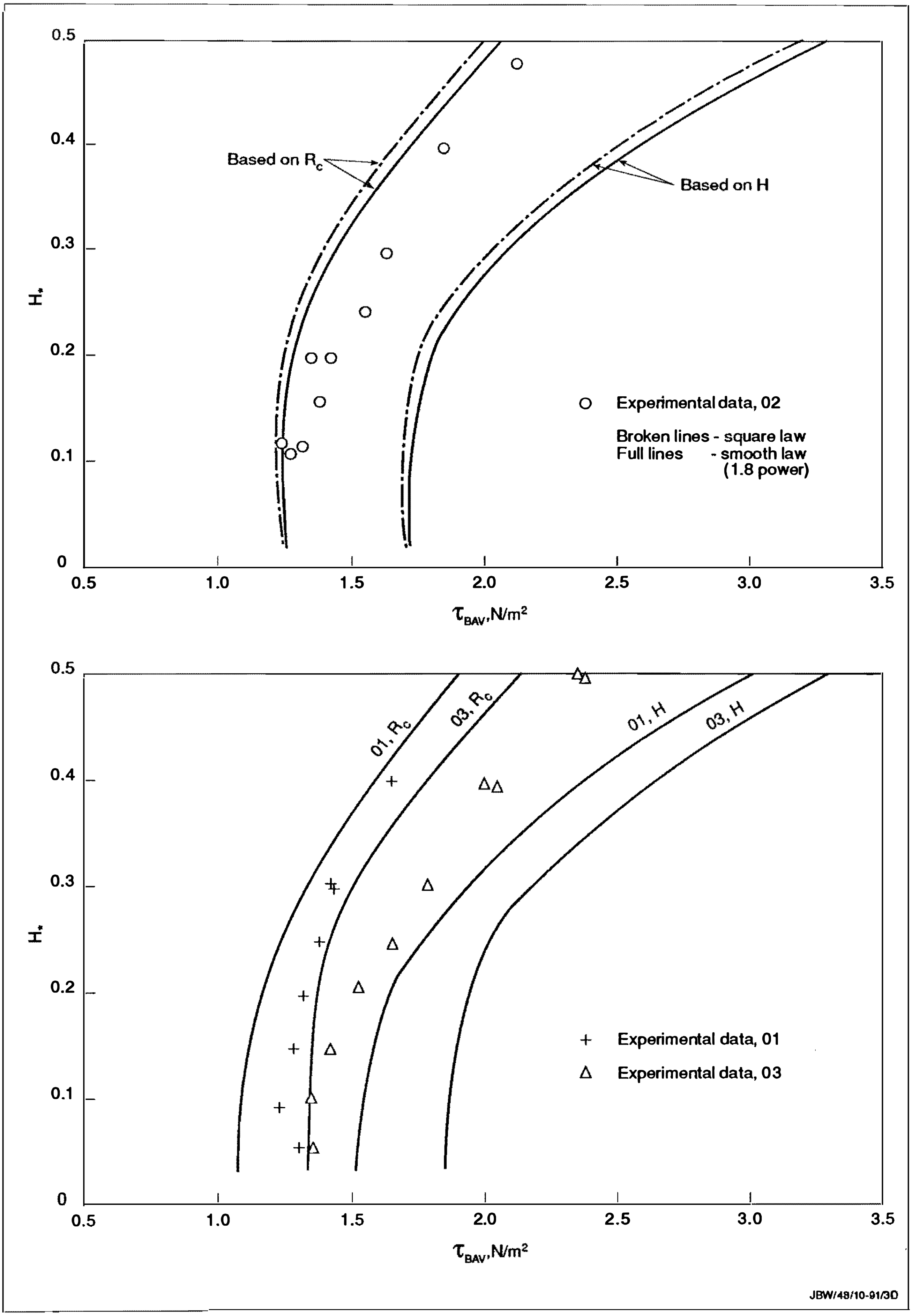

Fig 7.5 Comparison of observed average shear stress on bed of main channel with calculated values based on flow depth, H, and hydraulic mean depth, Rc, series 01, 02 and 03 (see table 3.1 for details of geometry).

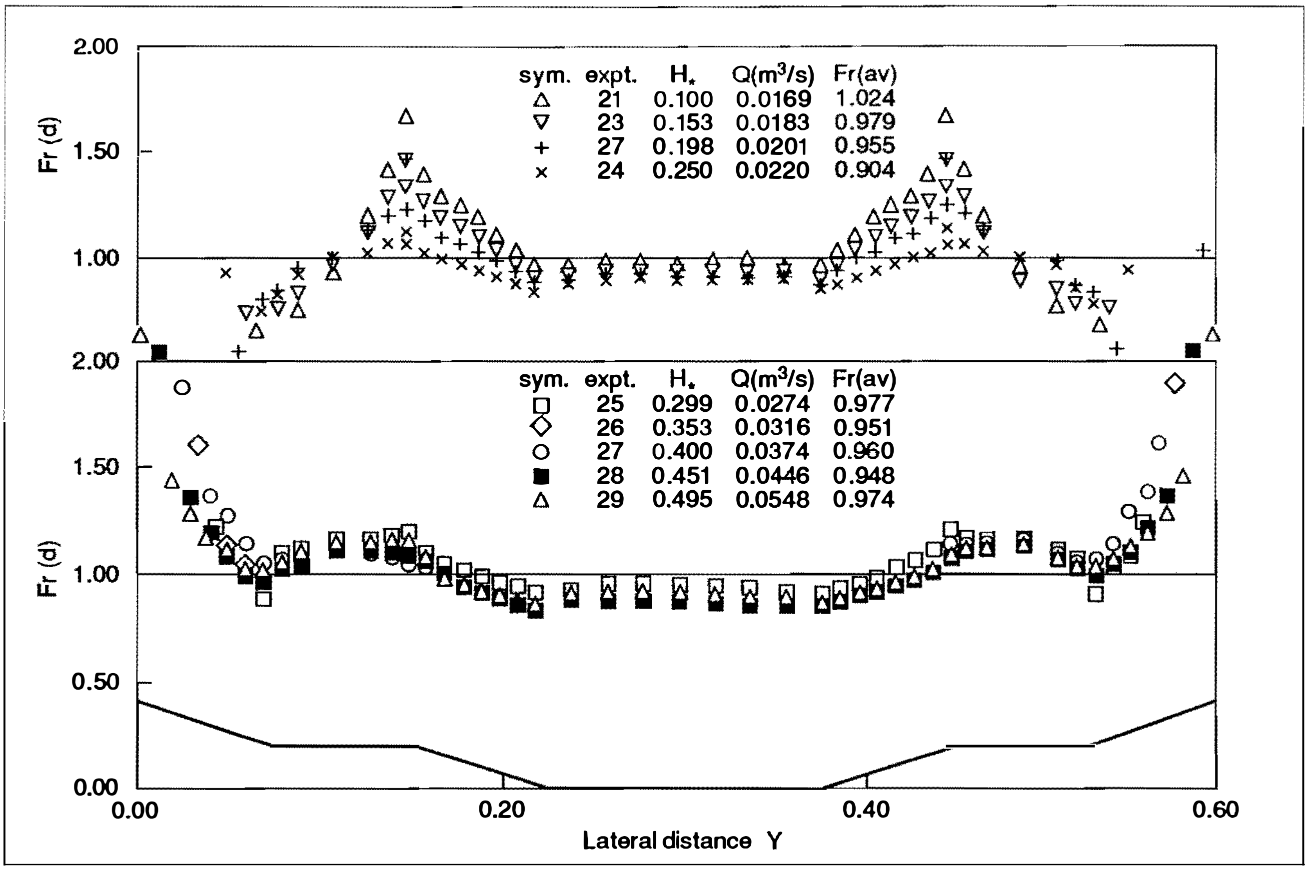

Fig 7.6 Lateral distribution of local Froude number when overall flow condition is critical (Knight and Yuen, 1990)

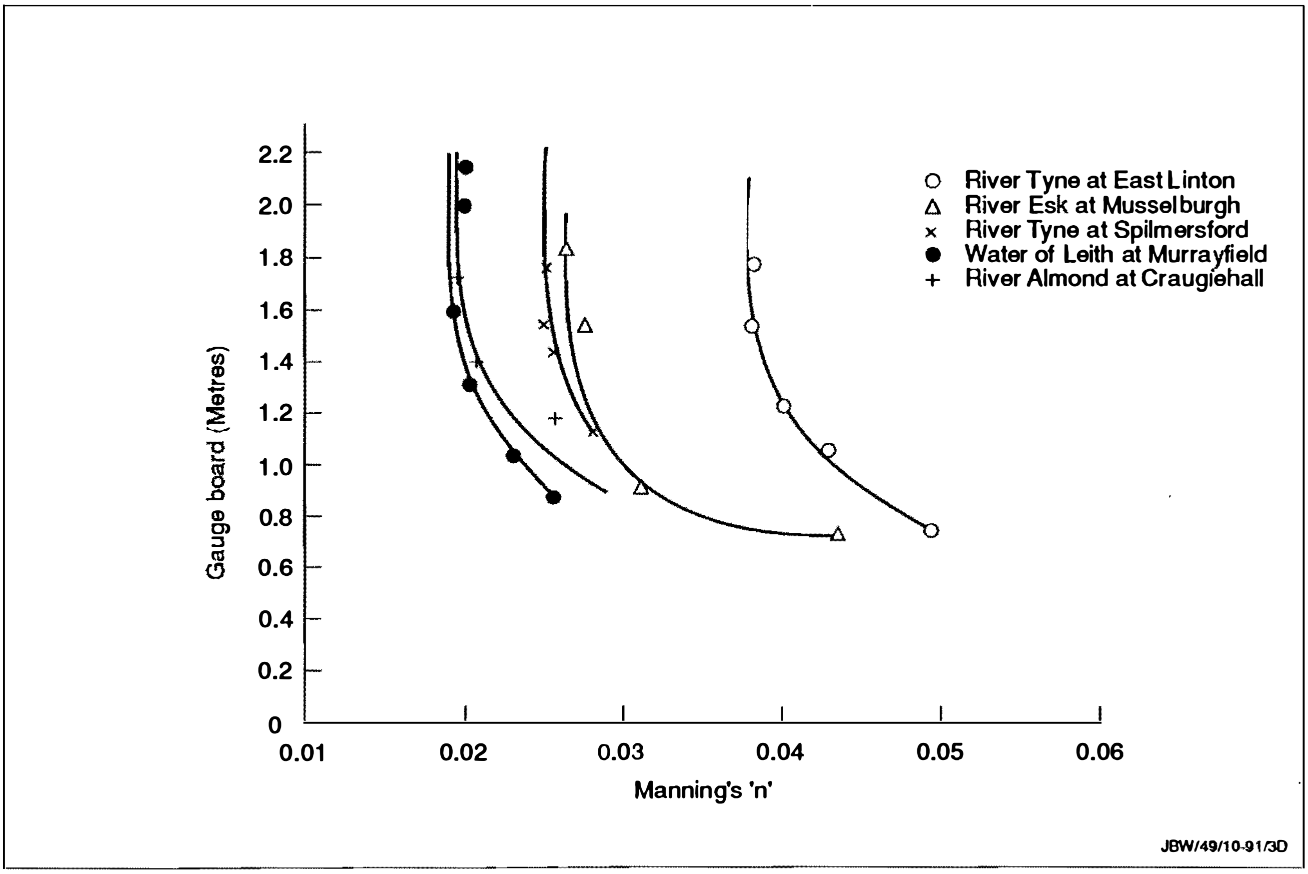

Fig 7.7 Manning's n values for within bank flows in five Scottish rivers, (Sargent, 1979)

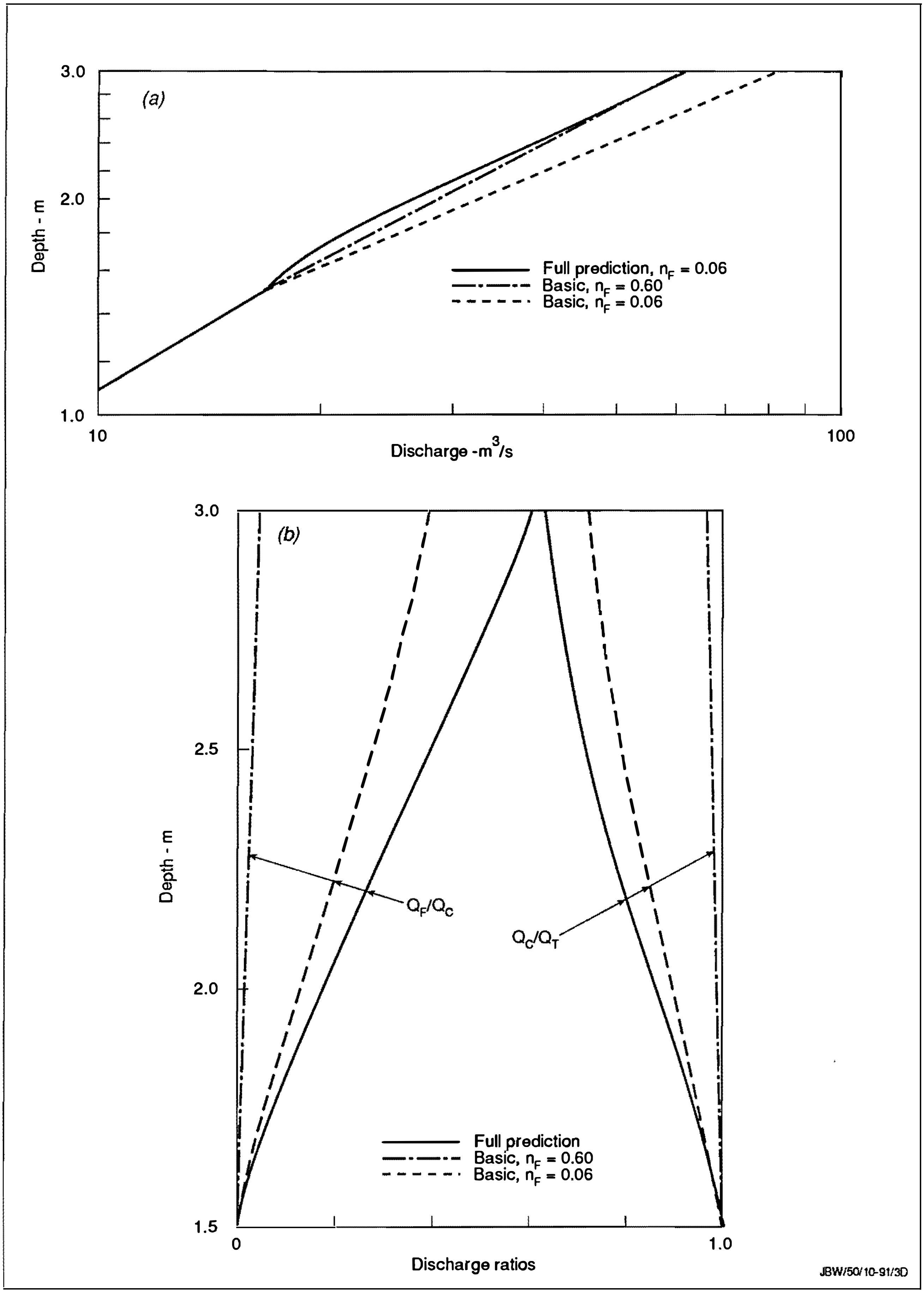

Fig 7.8 **(a) Stage discharge function for a hypothetical small river, comparing full prediction allowing for interaction with traditional calculations.**
(b) Ratios of discharges; channel/total, and flood plain/channel, with and without allowance for interaction effects

8. IRREGULAR PLAN FORM

8.1 Features of meandering flows in-bank

8.1.1 Even when flowing below bank-full, a curved or meandered channel shows distinctive flow features that make its hydraulic performance significantly different from straight channels. When a fluid flows round an open channel bend, secondary currents are generated because the radial pressure arising from the horizontal curvature is not in balance at all points in the depth with the centripetal acceleration imposed by the mean curvature in plan. The faster moving upper layers tend to move outwards; the slow near bed layers move towards the inner bank. This sets up a secondary circulation which develops as flow proceeds round the bend. In a meandering system, the secondary current cell set up in one bend decays as flow passes through the cross-over and is replaced by one of opposite hand as flow passes through the subsequent bend.

8.1.2 In a meandering system, the length of stream is greater than the straight line distance along the valley, of course, and thus the available hydraulic gradient along the stream is less than the valley slope. The bank full capacity is therefore reduced by two effects, this loss of available gradient as a result of channel sinuosity and also the additional head losses arising from the succession of bends. This "bend loss" occurs in the secondary circulations, their development, decay and reversal in quick succession, from redistributions of flow across the channel width and from flow separation from the convex bank.

8.1.3 The system of secondary currents, and the special form of those currents in meandered channels, also affects the morphology of those channels. There is a familiar deepening of mobile bed channels on the outsides of bends, accompanied by shoaling on the insides of bends. The hydraulic engineer often makes good use of these secondary currents in siting intakes to avoid blockage by bed material and to minimise the intake of suspended sediments. In the context of hydraulic capacity, however, these natural channel forms with almost triangular cross sections, switching regularly from deep on the left to deep on the right and vice versa in a meandered system, would be expected to perform somewhat differently from an artificial meandered channel with trapezoidal cross-section. The hydraulics of channels with irregular plan form is clearly very complex, even without the interactions with flood plain flow when above bank.

8.1.4 There have been many research studies into the flow round open channel bends, and several into meandering channels, see for example the recent text by Chang (1988). It is not the purpose here to provide a comprehensive review of previous work but rather to point out some salient features. Ervine and Ellis (1987) included in-bank meandering in their review of flow in rivers with flood plains, and they provided the following summary of some of the typical geometric features, with the terminology defined also in figure 8.1.

TABLE 8.1 **Typical geometric details for meandered rivers.**

$$\text{Sinuosity (Sy)} = \frac{\text{channel length along curved "thalweg"}}{\text{straight line "valley" length}}$$

Description:	Straight, Sy = 1.00 to 1.05
	Sinuous, Sy = 1.05 to 1.5
	Meandered, Sy > 1.5

Meander wavelength (between bends of same hand),		$L_M = 10\ tw_C$ approx.
Average radius of curvature in bends,		$R_M = 2.7\ tw_C$ "
Double amplitude of meanders,	for Sy = 1.5,	$a_M = 0.5\ L_M$ "
	for Sy = 2,	$a_M = 0.8\ L_M$ "
	for Sy = 3,	$a_M = 1.4\ L_M$ "
	for Sy = 4,	$a_M = 2.0\ L_M$ "

Meander belt width, $W_M = a_M + tw_C$ by definition

The reader is referred to Leopold and Wolman (1957) and Jansen et al (1979) for a more comprehensive treatment of fluvial morphology. However, according to the above classification, many of the research projects on meandered channels have actually concerned sinuous channels, as the sinuosity was below 1.5. A meandering channel with the cross-over sections at 60° to the valley axis would typically have a sinuosity of 1.4 or so. Such a channel is illustrated in plate 4 (Volume 1, following summary report).

8.1.5 The balance between the various components of overall channel resistance when within bank can be broadly assessed from the large scale research at the US WES Station reported in 1956. The main series of tests on meandering channels was with overbank flow, with a channel of bed width 0.6m. They were, however, preceded by within bank calibration runs, with a straight channel of the same cross-section and also with bank full conditions at each of three sinuosities. Knowing the sinuosity in each case, the loss of bank full capacity because the gradient has been reduced by the factor 1/Sy is readily computed. In fact, the observed bank full flows are lower again, and this is because a proportion of the gradient along the thalweg is taken up by the form drag of the succession of bends on plan, with the balance overcoming the basic boundary friction. In the straight channel, of course, the boundary friction accounts for the whole of the energy dissipation. The following table summarises those results:

TABLE 8.2 Allocation of energy dissipation in US WES experiments.

Sinuosity, Sy	Bankfull discharge allowing for the reducted gradient along thyalweg	Observed bankfull discharge	Reduction factor for planform losses	Proportion of thalwed slope used in planform form losses
	l/s	l/s		
1.00	62.89	62.89	1.00	0
1.20	57.41	43.91	0.765	0.415
1.40	53.15	39.09	0.736	0.459
1.57	50.19	34.56	0.6886	0.526

8.1.6 The above tests were made with a trapezoidal channel cross-section rather than a naturally shaped channel, and although artificial it does provide a basic comparison. With the greatest sinuosity of 1.57 tested, the main channel bankfull capacity was reduced by an overall factor of 0.55. 0.80 of this ($1/\sqrt{Sy}$) comes from the greater path length of the channel, and a further 0.69 ($\sqrt{(1-0.526)}$) from planform losses, giving 0.80 x 0.69 = 0.55. Thus depending on the sinuosity, up to half the total energy dissipation can be ascribed to planform losses in these particular tests.

8.1.7 Similar information is available from a preliminary analysis of information from the early within bank tests in the FCF at Wallingford with a meandered channel of 60° cross-over angle and sinuosity 1.37 (see Plate 4). The section geometry differed from any of the straight channels tested (as described in Chapter 3) but from the initial calibration of those straight channels the basic resistance function for the cement mortar construction was known (see Appendix 2). Hence the equivalent straight channel capacity could be calculated with confidence. There was no attempt to obtain a discharge measurement at precisely bankfull but a whole series of stage discharge tests were carried out over a range of depths up to about 96% of bank full. There were 18 such groups of data, and the running averages of threes were taken, as explained in connection with the straight channel tests, to minimise experimental scatter. It was then possible to assess the reduction factor for planform losses for these within-bank flows, the loss of gradient due to sinuosity being fixed by the plan geometry of course. The planform reduction factor varied from 0.95 at shallow flows (when the boundary drag would be more significant) to 0.86 at 88% of bank full. Extrapolating to bankfull, the form drag reduction factor would become about 0.82, implying that about one-third of the thalweg gradient was used up in planform losses and two-thirds in boundary drag. The bankfull capacity of the corresponding straight channel would have been 0.120 m^3/s, reduced to 0.101 m^3/s by the greater channel length, and further to 0.082 m^3/s by the planform losses. In these FCF tests, the planform losses were rather less than in the nearest comparable US WES tests, though the reason for this is not yet established. Perhaps the width to depth ratio of the channel has a significant effect, as might the details of plan geometry.

8.1.8 If a resistance formula with an empirical coefficient e.g. the Manning equation, is used to determine conditions in an irregular, sinuous or meandering channel, the use of stage discharge observations to establish the coefficient value will automatically take account of the form losses due to plan irregularity as well as the boundary drag arising from the composition of its bed and banks. It is to be anticipated that the coefficient values in such cases will be much in excess of those for straight channels with otherwise similar boundary compositions and roughness texture. Sources of information on channel roughness are mentioned in Chapter 7, section 7.4, and some details are given in Appendix 5. Cowan (1956) proposed a system of building up Manning's n for a channel from various elements of resistance and then applying a factor to allow for meandering. For sinuosities below 1.2 he suggested no specific addition to the n value; for Sy = 1.2 to 1.5, factor n by 1.15; for Sy above 1.5 factor n by 1.30. These last two n factors are equivalent to allowing 25% and 40% of the thalweg gradient to be used up by planform losses.

8.1.9 The above refers to within bank flows, and demonstrates the compexity of the flow in channels of irregular or meandering planform compared with straight channels. What effect the combination of a meandered main channel with a reasonably straight flood plain will have on the channel processes is considered next.

8.2 Above-bank flows in meandering channels

8.2.1 Ervine and Ellis (1987) reviewed conditions where a deep channel meanders through a relatively straight flood plain, commenting that there had been little attention paid to the mechanics of overbank flow under such conditions. It will be obvious that with the main channel flow no longer confined within its banks, there will be exchanges of flow (with its accompanying momentum) between the main channel and the flood plains. With fairly gentle meanders of modest sinuosity, the expectation is that flow would leave the tapering flood plain to enter the main channel, at the same time squeezing flow out from the opposite bank of the channel on to the opposite flood plain. In more tortuous systems, one might anticipate that major flood flows along the valley floor would almost ignore the main river channel, except for its obstructing influence as the dominant flood flood plain flows crossed and recrossed it as a transverse trough in the valley floor.

8.2.2 There has been much recent detailed work, both in the FCF and elsewhere, in which the details of this three-dimensional flow structure have been examined. Willetts (1991) provides early pointers to the results of that research, with figure 8.2. Showing how the secondary current that occurs with within-bank flows reverses with overbank flow. This also changes the direction of bed movement, and there have been many cases of field observations following major floods that confirm this picture, bed sediments having been lifted out of the deep channel on to the flood plain beyond. So far as the water flow is concerned, with a reasonable depth of flow over the flood plains, the continuity of flow within the main channel is broken: no longer is it basically the same body of water proceeding down the river channel; it is being exchanged continuously with the flood plain waters, at least within the meander belt width. This exchange involves additional head loss, because of differences in the momentum vectors between these continually mixing flows. Figure 8.3 (Ervine and Ellis, 1987) illustrates these flow complexities.

8.2.3 There are very many geometric and roughness conditions involved in any comprehensive study of even the simplest aspect of meandering river flood flows, i.e. their stage discharge function. The research in the FCF at Wallingford is not yet complete (Summer, 1991) and it would be premature to attempt an appraisal in sufficient detail to provide a full design method for irregular channels. However, some preliminary indications of the order of magnitude of the influence of channel irregularities on the hydraulics compound channels will not be amiss.

8.2.4 The early work at the US WES published in 1956 has been referred to already in the context of straight compound channels. The main thrust of that research was into meandered channels, concentrating on the influence of a meandering main channel on the flood capacity. The tests were at large scale and covered three sinuosities, as well as three roughness conditions on the flood plains, created by laying down sheets of expanded metal. In terms of the detail in the published results and the accuracy with which the basic roughnessses were determined, the test series was not ideal. For example only three flow depths were tested the shallowest of which was of the same order of depth as the expanded mesh roughening, which photographs in the original publication show to have been somewhat irregular (expanded metal is difficult to keep flat and uncurled at the edges). However, the scale of the tests and their scope make them a useful reference source.

8.2.5 Perhaps the most useful of the presentations of information in the original publication is that reproduced as figure 8.4. It is in non-dimensional form, showing the reduction in main channel discharge compared with a straight aligned channel system. (The main channel section is defined by vertical divisions at the banks.) This reduction is based on the premise that the flood plain flows themselves may be assumed unchanged, compared with their "straight channel" values, so that any deficit is ascribed solely to the main channel component. When flow first submerges the flood plain, there is already a 30 - 45% reduction in main channel conveyance, depending on the sinuosity. This was explained earlier in this Chapter as being due to the extra stream length due to sinuosity plus the component of energy dissipation arising from planform losses. When overbank depth reaches 0.6 x channel depth ($H_* = 0.375$) this reduction in apparent main channel conveyance has increased to between 45 and 77% when the flood plains have the same roughness as the main channel, yet with very rough flood plains ($n_F/n_C = 3$ approx) the increase with depth is more modest.

8.2.6 The assumption that the loss of conveyance should all be allocated to the main channel whilst the theoretical flood plain flows are unchanged is hardly a realistic model in terms of flow details, although with straight channels it was found in the FCF work that the main channel discharge deficits were much greater than any compensating addition to flood plain flow. However, it is quite likely bearing in mind what is now known about the detail of the flow exchanges that the main channel component of discharge must suffer considerably from the periodic influxes of flood plain flows and compensating effluxes of main channel flows, so the concept of loss of main channel conveyance was a far-sighted contribution.

8.2.7 Table 8.3 shows the US WES results in two different ways: F1 is the factor by which the measured straight channel discharge at the given depth would have to be multiplied to yield the measured discharge under meandering conditions; F2 is the factor by which the discharge estimated by adding together the main channel flow extrapolated from the observed meandering bank full condition and the estimated flood plain flow, neglecting interference effects, would have to be multiplied. This provides a matrix, albeit sparse, of results for a range of sinuosities, range of relative depths and range of roughness ratios.

TABLE 8.3: Discharge and conveyance reduction factors for meandering channels flowing above bank-full.

F1: Factor by which the experimentally observed aligned channel discharge would have to be modified to account for meandering of main channel.
F2: Ratio of observed total discharge to that obtained by summing the main channel discharge, as extrapolated from the observed bank-full meandered flow, and the experimental flood plain discharge, proportioned down to the actual flood plain width.

Ratio of Manning's n on F P to main channel value	Relative flow depth, H_m	Sy = 1.20 F1	Sy = 1.20 F2	Sy = 1.40 F1	Sy = 1.40 F2	Sy = 1.57 F1	Sy = 1.57 F1
1.0	0.167	0.804	0.960	0.729	0.937	0.617	0.854
	0.286	0.819	0.974	0.713	0.891	0.651	0.854
	0.375	0.783	0.944	0.686	0.860	0.630	0.821
2.0	0.167	0.698	0.741	0.616	0.718	0.541	0.696
	0.286	0.867	0.816	0.784	0.790	0.696	0.751
	0.375	0.830	0.854	0.775	0.843	0.714	0.820
3.0	0.167	0.624	0.691	0.576	0.693	0.511	0.695
	0.286	0.713	0.735	0.687	0.747	0.605	0.731
	0.375	0.802	0.802	0.767	0.819	0.717	0.817

8.2.8 The above refer to a particular flood plain width, corresponding to B/b = 4, which in these tests was a varying amount in excess of the meander belt width. It would be reasonable to assume, perhaps, that if the flood plains were wider those reduction factors might still apply to the zone within 2B = 4 x 2b whilst the sections outside might be relatively unaffected. This question also illustrates how difficult it is to generalise from a limited range of experiments when so many geometric parameters can be involved - and why a sound co-ordinating theory is required to generalise any design procedures for irregular channels. It can not be assumed that the above empirical adjustment factors apply to geometries differing from those tested by US WES.

8.2.9 Turning next to recently acquired data, only the FCF work with a 60° cross-over angle and sinuosity 1.37 has been analysed for the treatment that follows. Other cases studied in the FCF and elsewhere include a "naturalised" main channel cross-section with outer bank deep zones and inner bank shoals, and also various distributions of flood plain roughening. Work with a 110° cross-over has also been carried out at Wallingford, and in this geometry the direction of the deep channel partially reverses to simulate high sinuosity. The simple case of equal roughnesses on flood plain and in main channel with a trapezoidal main channel cross-section forms the first progression from the aligned and skewed channels considered in earlier Chapters, so provides a first tentative picture of broad effects.

8.2.10 The geometry selected for this meandering system was not a direct development of one of the cross-sections used in the main series of straight channel tests: the constraints of the flume width and typical meander geometries dictated otherwise. Whereas all the straight channels had a bed width of 1.5m, the meandering channel had a bed width of 0.9m, so that its aspect ratio (width to depth ratio) was 0.9/0.15 = 6, rather than 10. It had 1:1 side slopes and was installed in a total flood plain width, 2B, of 10m, so that B/b = 5.556. Thus there were no actual measured discharges either within bank or over bank for an exact straight channel equivalent. Instead, any comparisons with the corresponding aligned system had to rely on computations for the latter, using the well established basic resistance function for this method of construction. These calculations could either be the basic flows obtained as the sum of the calculated zonal flows, or could include the allowance for interference effects deduced from the comprehensive data analysis of aligned systems reported in Chapters 3 and 5.

8.2.11 Figure 8.5 shows four plots:

I. The predicted flows for an equivalent aligned system, with the main channel calculated basic discharge allowing for both the sinuosity and the allocation of 1/3rd of the available gradient along the thalweg to planform losses, and also for main channel/flood plain interaction effects using the straight channel procedures developed in Chapters 3 and 5; ARF = 0.6. These results are shown as the ratio of the predicted flows to the basic zonal calculation, (i.e. DISADF).

II. The predicted flows for an equivalent straight system, no allowances being made for sinuosity, but including the interaction effects worked out using the methods of Chapter 3 and 5 (ARF = 0.6 = width/depth ratio/10), shown as DISADF.

III. The observed stage discharge data for the meandered channel, in comparison with the basic zonal calculation, with the main channel component allowing for both the sinuosity and planform losses assessed on the basis of in-bank performance, but not for interaction effects.

IV. The ratio of observed discharge to that predicted under I above.

8.2.12 Some features of figure 8.5. require explanation. In computing graph I, the main channel is effectively much rougher than the flood plain, because of sinuosity and planform losses. In consequence the interference effects calculated from the methods deduced from the analysis of straight aligned channels are somewhat reduced, and at the upper limit the velocity difference calculated from the basic resistance of main channel and flood plain has been reversed: the main channel flow is theoretically moving slower than the flood plain flow. This is not a condition ever covered with aligned channels: there the presumption is always that the flood plain offers greater resistance than the main channel. This diminution of velocity difference as depth increases, until they become equal and even reverse, causes the "standard" aligned channel interference equations to show quite small effects, reaching zero (DISADF = 1) when H_* = 0.43 approx. Thus any attempt to allow for meandering as an extension of the computation procedures for straight channels must fail, as the extra resistance of the main channel diminishes rather then enhances the calculated interference effect. The exchanges of flow between flood plain and main channel, with radically different flow structures and discontuity of fluid fluxes in both the deep and shallow sections, rule out any extension of the methods for straight aligned or mildly skewed systems to fully meandered or irregular channels.

8.2.13 With the type of flow structure illustrated in figure 8.3, it is to be expected that the observations of stage discharge plotted as DISADF against H_* on figure 8.5 (points shown by circles, III) will show much more interference than either of the above computations. The gross exchanges of flow and momentum between the flood plain flow and main channel flow over the meander belt width induce much more powerful mechanisms for energy dissipation than the dispersion across the shear zone at the bank line in straight aligned systems: there are large secondary circulation cells with secondary velocities perhaps an order of magnitude greater than in straight channels, and something akin to expansion and contraction losses as flows move from flood plain to main channel and vice versa. The crosses of plot IV on figure 8.4 show this excess in effect. The values of DISADF for plot IV are the ratios of observed discharge to predicted discharge using scheme I above.

8.2.14 At shallow overbank depths, the conveyance of this system with sinuosity 1.37 is about 70% of the sum of the zonal flows, calculated as if there was no interference or added energy loss due to flow and momentum exchange. This drop in conveyance is additional to that which comes from the extra resistance of the main channel itself. We saw in paragraph 8.1.8 that the bank full capacity reduces from 0.120 m^3/s to 0.082m^3/s due to sinuosity; a factor of 0.68. As depth increases, the ratio to the basic sum of meandered main channel flow plus flood plain flow increases and steadies at about 0.80. Thus the exchange of momentum for this particular geometry reduces the conveyance compared with a basic calculation, such as might be extrapolated from a knowledge of the meandered channel's resistance coefficient plus a calculation for the flood plain, by 20%, for H_* from 0.25 to 0.50, but can be as much as 30% at lower depths. This is a somewhat greater influence than shown by the comparable F2 factors in Table 8.3, for Sy = 1.4 and Manning's n ratio 1, obtained from the US WES tests.

8.2.15 These few examples of the influence of meandering on the stage discharge function for overbank flow clearly demonstrate that the effect is important in an engineering context and should be allowed for in hydraulic computations. The best method for doing this must await the completion of the current research programmes, especially the large scale work in the FCF at Wallingford, including the complex analyses that will no doubt be required in order to quantify the results in a general form to provide a reliable design method. Although systems with a small angle of skew were shown in Chapter 4 to be amenable to a simple extension of straight aligned channel methodology, the evidence for meandered channels is that the interference effects with overbank flow are of a radically different character, rendering any extension of straight channel procedures inappropriate: a quite different co-ordinating theory is required.

8.2.16 Table 8.3 above provides a matrix of plausible adjustment factors for discharge and conveyance in comparison with equivalent straight aligned systems: the F1 values. However, for engineering purposes the concept of an equivalent aligned system is less useful than an extrapolation from observed or estimated conditions at bank full flow in the actual meandered river: F2 is then the appropriate adjustment for interference effects. These were based on limited data from 1956. Figure 8.5 provides a first example using more recent and more detailed research results of the influence of flow and momentum exchange under overbank conditions on the extrapolation of stage discharge functions beyond bank full. However, neither Table 8.3 nor figure 8.5 is put forward as an established design procedure for irregular channels. Some indications of the way forward to such a method are suggested in the following section.

8.3 Flow models for sinuous, meandering and irregular channels

8.3.1 Flow in meandering channels with over-bank flow is a complex three-dimensional system, with reversals of secondary currents and major exchanges of discharge and momentum between the main channel and flood plain. These interactions between the different flow regions differ radically in their mechanisms of energy loss from those found in straight channels aligned with their flood plains. There have, however, been several attempts at developing theoretical models of the complex flow structure.

8.3.2 Ervine and Ellis (1987) offered a hydromechanics approach to the problem, considering the flow over the meander belt width (see figure 8.1 for illustration) as if it repeatedly expanded and contracted as it passed from the flood plain to angle across the main channel and then on to the opposite flood plain. They considered four main sources of energy loss in the main channel and three in the flood plain.

Main channel

1. Frictional resistance of the wetted perimeter of the channel itself, which could be assessed from a knowledge of bed material size or other information on its surface condition, using the Colebrook- White equation (or Manning with n related to the surface texture).

2. Meander bends with their secondary currents akin to large scale turbulent eddies occupying most of the cross-section. Energy loss would arise from internal shear and also transverse shear at the boundaries.

3. Turbulent shear stress on the horizontal surface at bank top level due to the overflowing flood plain flow. The velocities of the two streams will differ in magnitude and direction, with the effect that an apparent shear stress will be generated on the interfacial plane, with an influence on the main channel that might be positive or negative depending on the direction of momentum exchange.

4. There may also be pool-riffle sequences in the meandered channel, and indeed the characteristic deepening on the outside of the bend and shoaling on the inside with cross-overs between bends induces the flow along the thalweg to follow a sequence of deeps and shallows as with a pool-riffle sequence. This source of energy loss is likely to be more significant at shallow flows than with over-bank flows.

Flood plain

1. Friction losses over the wetted perimeter, as determined from a conventional resistance equation.

2. The expansion loss where the flood plain flow encounters the deep main channel.

3. Contraction losses where the flow leaves the main channel to re-enter the flood plain from the opposite bank.

8.3.3. These assumptions simplified the flow situation to permit conventional hydraulic assessments to be made of the various sources of energy dissipation. Ervine and Ellis proceeded on these lines, treating the flood plain flow within the meander belt width separately from that outside the belt width, as the latter would not suffer the expansion and contraction losses mentioned above. The values for expansion and contraction losses came from work by Yen and Yen (1983): the losses due to secondary currents were assessed using a method published by Chang (1983): the Colebrook-White or Manning equation would provide the boundary friction loss: but losses due to the interface shear were omitted. Assembling the various head loss terms and taking account of continuity, an equation was developed that could be used to obtain the stage-discharge function for a given geometry.

8.3.4 This method was tested against the same US WES data used earlier (US WES, 1956) with promising results. These are illustrated in figure 8.6 (taken from Ervine and Ellis, 1987). This shows for two of the sinuosities and two of the flood plain roughnesses tested at Vicksburg how the theoretical prediction compared with observation. Ervine and Ellis commented as follows: "The most obvious conclusion is that the predicted discharge is generally underestimated at higher flood plain depths and overestimated at lower flood plain depths. .... The reason for overestimating discharge at low flood plain depth may be related to the omission of the co-flowing turbulent shear stress term .... In this region, the predicted discharges are of the order of 0 - 20% greater than the experimental data. For larger flood plain depths the predicted discharges are of the order of 10% too low. It should be noted that the assumption for energy loss due to secondary cells in the main channel was derived for in-bank flow and may be greatly repressed at higher flood plain depths. This is combined with the fact that the assumption of three sub-sections of cross-sectional area acting independently of each other, with no interaction between each section, represents a crude attempt to rationalise a complex three-dimensional situation."

8.3.5. Ervine and Ellis also compared their theory with smaller scale research by Toebes and Sooky (1967), which had the advantage of separate measurements of discharge distribution across the floodway. They concluded

"...predicted discharge is low compared with the experimental data in the area of the main channel and inner flood plain, with the opposite occurring in the outer flood plain. This would imply an overestimation of head loss in the inner regions either in the secondary cells or expansion and contraction losses". The graphical comparison between the Ervine and Ellis theory and Toebes and Sooky data is shown in figure 8.7.

8.3.6 Preliminary analysis of the very detailed data on flow pattern, velocity vectors and secondary currents obtained from the FCF at Wallingford indicates that the above hydromechanics model would require appreciable modification to conform closely to the reality of flow in meandered channels, but the general approach via component head losses remains a valid avenue of development.

8.3.7 A somewhat more fundamental hydromechanics model might be developed through the momentum equations, though their full solution depends on a knowledge of all boundary shears and pressures. It would be easy to assume hydrostatic pressures, but this begs the question: the water surface is not a simple sloping plane, and the flow separations where the flood plain discharges enter the deeper main channel will create non-hydrostatic conditions at the channel margins. However, it is possible that a model could be developed with the simplifying assumptions that could then be calibrated against the available data.

8.3.8 A stage beyond the above would be to use refined grid numerical modelling in two dimensions on plan, solving the 2-D St Venant momentum and continuity equations for the geometries for which data is available. No doubt there would be some need for empirical adjustments to obtain good agreement, but once achieved the model could be used to generate stage discharge functions, or conveyance functions, for any other geometry of sinuous, meandering or irregular compound channel with over-bank flow. However, it may be necessary to add a third dimension, effectively using a layered model, to obtain satisfactory simulation. These are questions for future study but are essential if hydraulic design information on complex channels is to achieve the standard of accuracy and reliability that is now becoming available for straight compound channels. In the meantime, the methods available are somewhat crude and inadequately confirmed by wide ranging data at large scale.

8.3.9 Design methods for irregular compound channels are outside the scope of this report. The treatment of the subject here is intended to illustrate the need for and importance of further analysis before a comparable design method for irregular channels can be prepared, whilst providing the reader with some indication of the order of magnitude of the interference effects in such systems.

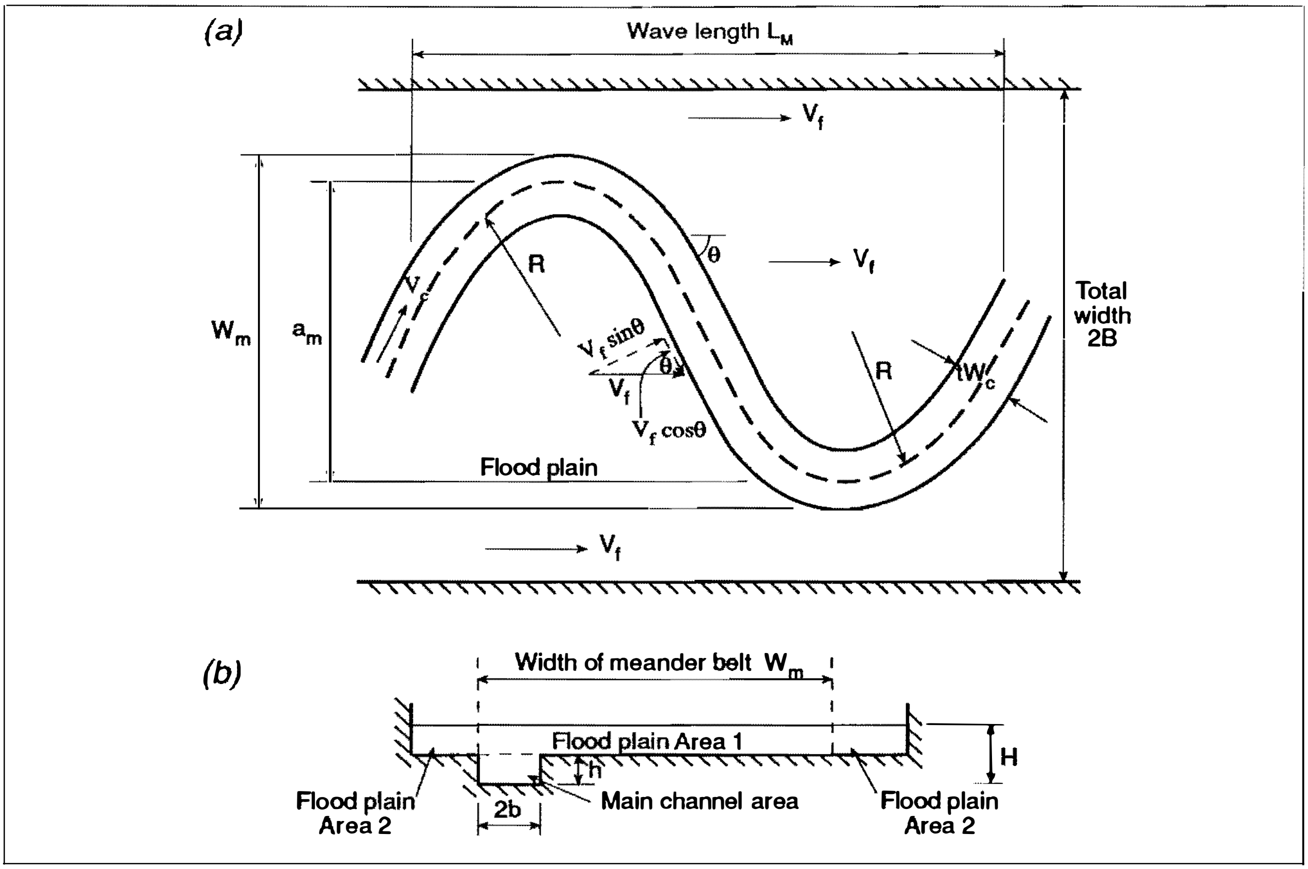

Fig 8.1 Plan and cross-section of meandered channel, with definition of main symbols used. Cross-section shows subdivisions of area used in Ervine and Ellis (1987) theory

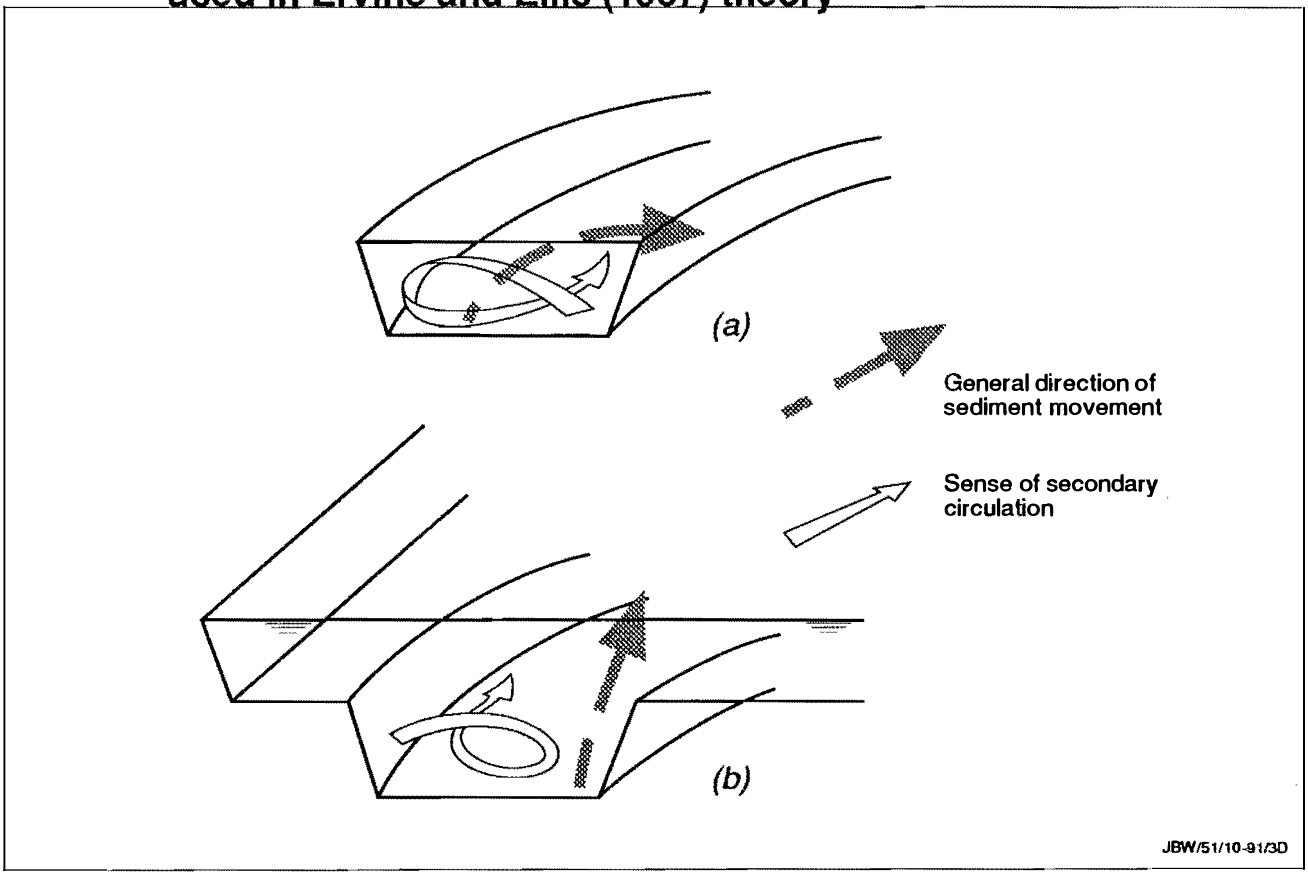

Fig 8.2 Established secondary currents in bend and main direction of bed movement in meandered channels: (a) within bank flow; (b) over-bank flow

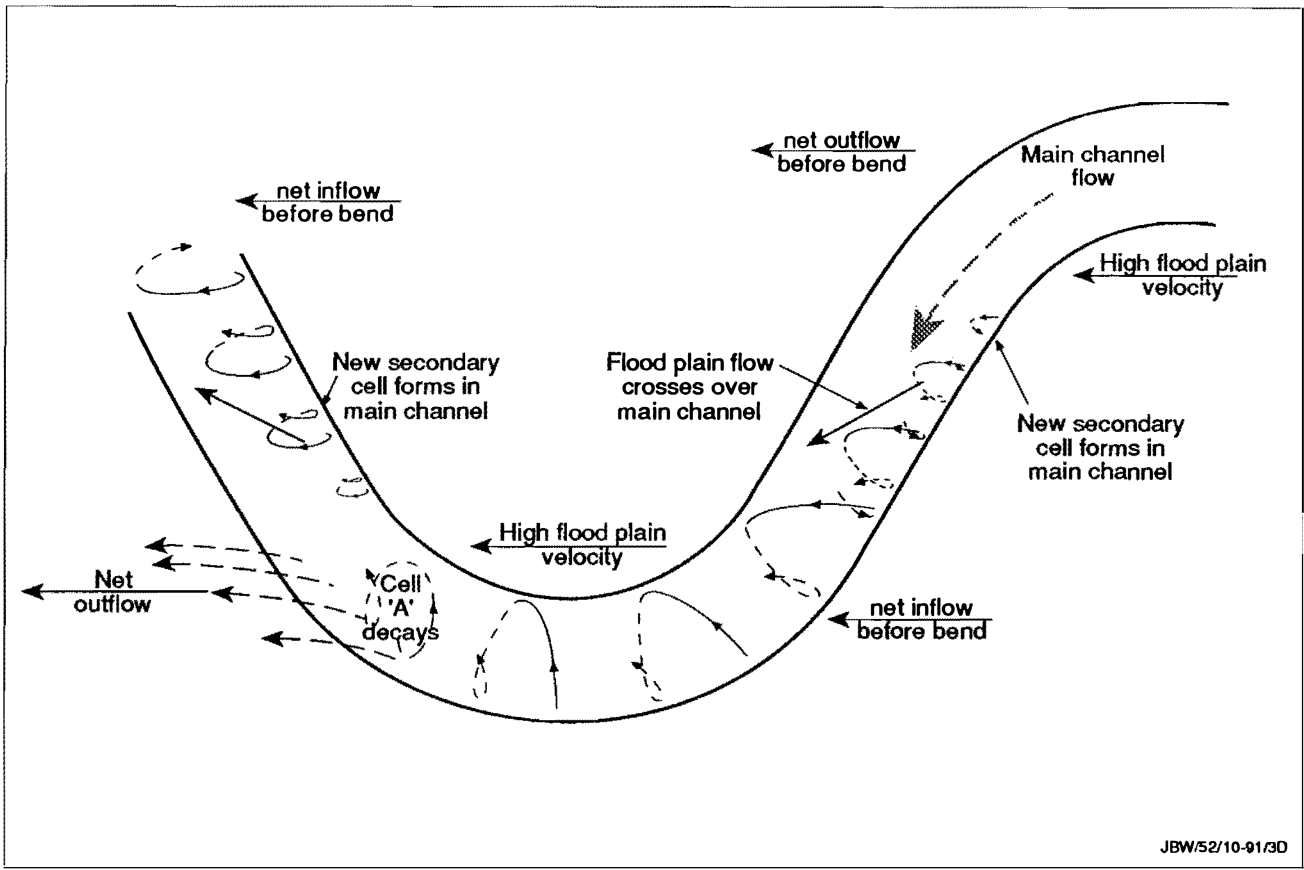

Fig 8.3 Illustration of flow exchanges and secondary cell development in successive meander bends, Ervine and Jasem (1991).

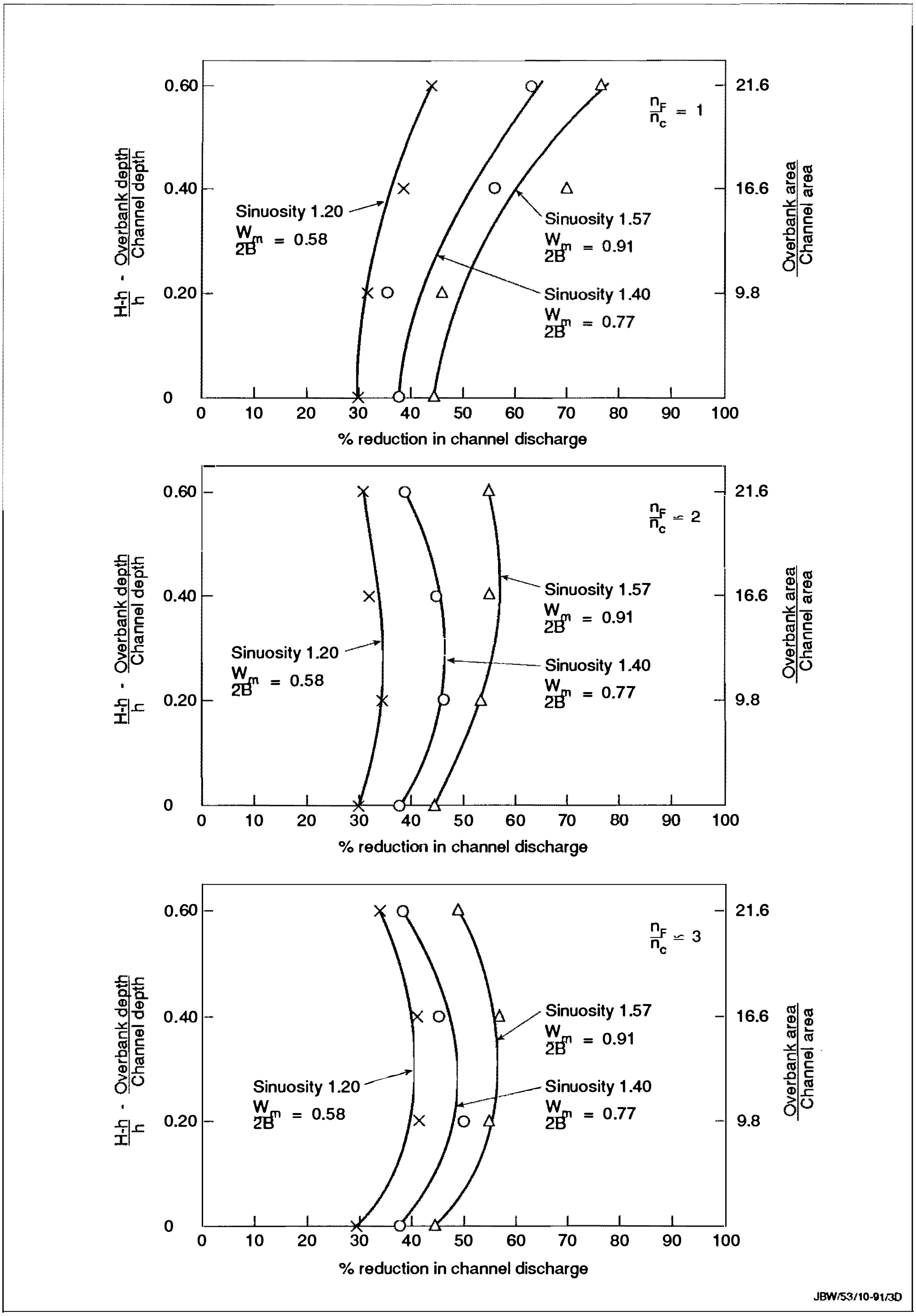

Fig 8.4 Reduction in channel discharge (assuming flood plain flow is unaffected) for three channel sinuosities and three ratios of flood plain roughness to main channel roughness: US WES (1956)

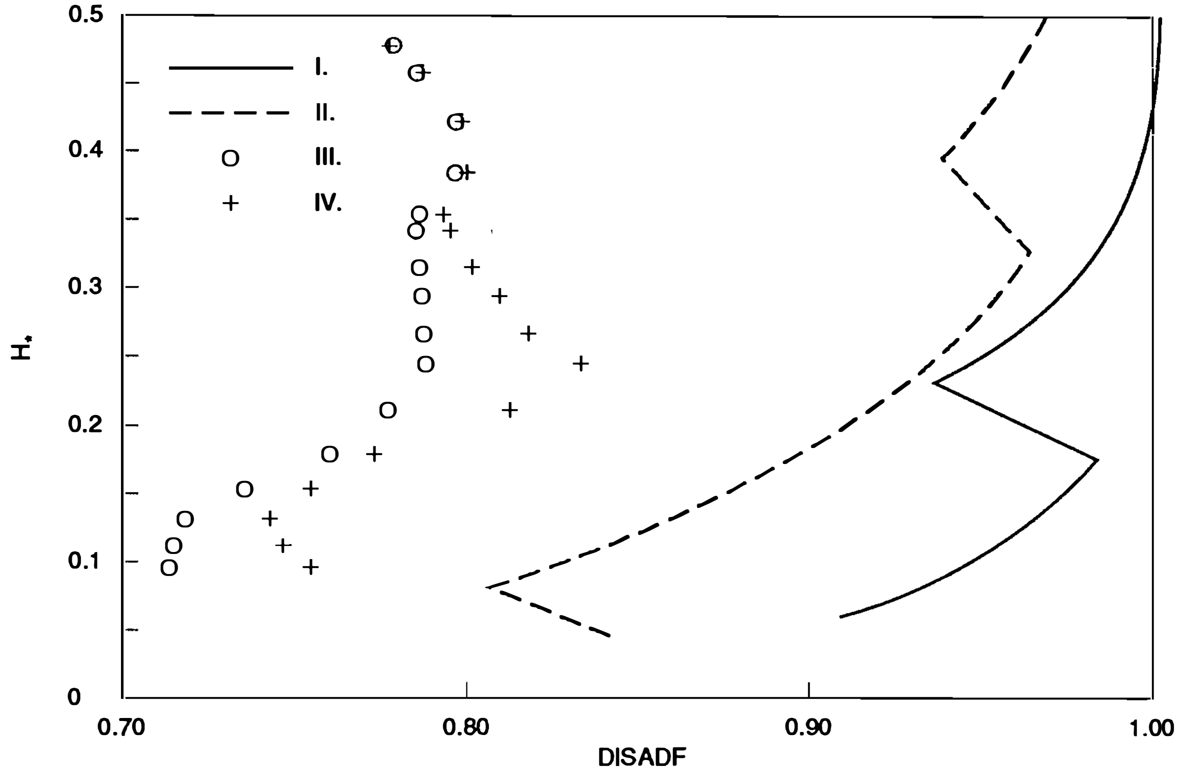

Key

I. Predicted function for equivalent straight system, but with main channel flow computation based on thalweg slope and allowing for planform losses.

II. Predicted function for straight system of same basic cross-section.

III. Observed data in comparison with basic zonal computations, with main channel calculation using thalweg slope and allowing for planform losses.

IV. The ratio of observed discharges to the computations under I, i.e. the interference effect with meandering additional to the allowance for thalweg slope and planform losses in main channel.

JBW/54/10-91/3D

Fig 8.5 Discharge adjustment factors for straight and meandered channels, FCF experimental results for meandered case for B/b = 5.56, 2b/h = 6, 60° cross-over, L_M/W_C = 10, Sy = 1.37, with prediction for equivalent straight system.

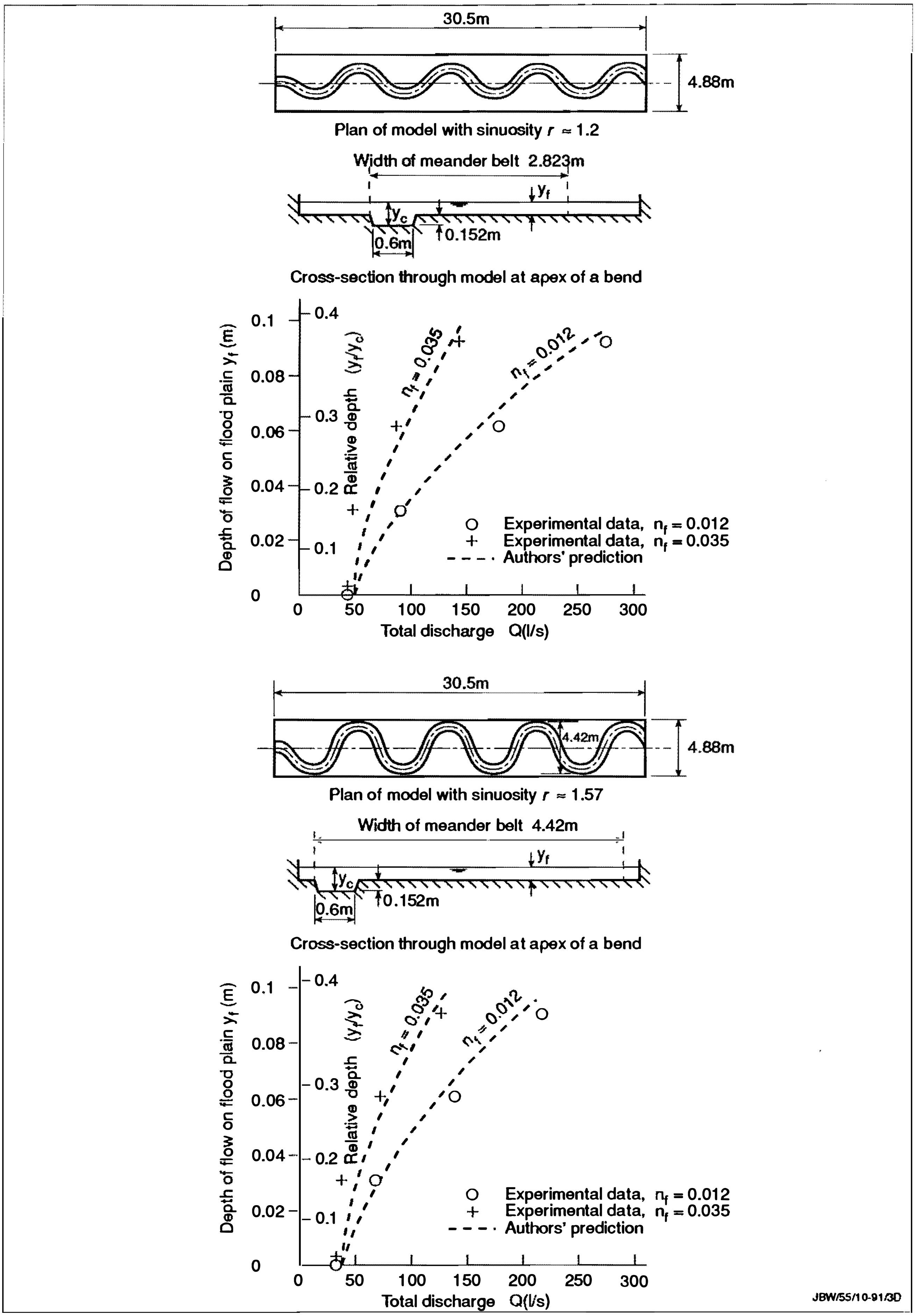

Fig 8.6 Comparison by Ervine and Ellis (1967) of their theory with selected cases from the US WES (1956) report: ratios of flood plain roughness to main channel roughness of 1 and approx. 3 (Manning coefficients); for two sinuosities. Geometries shown above.

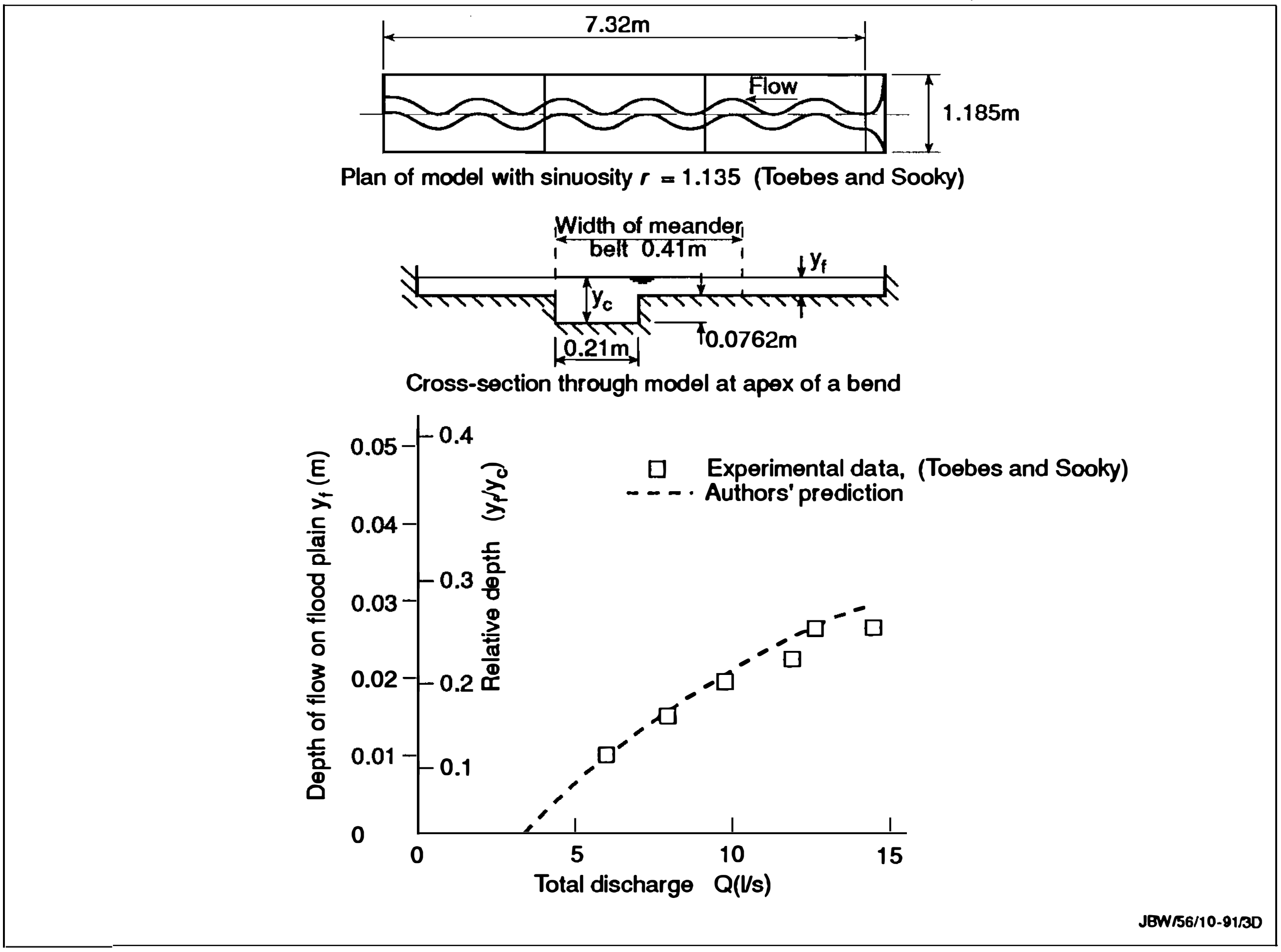

Fig 8.7 Comparison by Ervine and Ellis (1967) of their theory with Toebes and Sooky (1967) report: equal flood plain and main channel roughness; Sy = 1.135. Geometry shown above.

9. SEDIMENT TRANSPORT

9.1 General aspects of sediment transport

9.1.1 The development and utilisation of water resources for irrigation, hydro-power and public supply can be severely affected by sediment in many parts of the world. Where there is a mature and well vegetated landscape, sediment problems may be relatively minor; but where slopes are steep and vegetation sparse, the yield of sediment from the catchment gives high concentrations in the rivers. In utilising these water resources, and also in managing rivers in terms of flood protection, an understanding of the hydraulics of alluvial channels is vital. So far only the water conveyance aspects have been considered, but it is also important to review the impact of the research on flow and resistance in channels with flood berms in the context of its implications for sediment movement. Only through better understanding of fluvial morphology can the rivers be controlled and managed sympathetically in respect of the environmental requirements, and the long term success of engineering projects in rivers carrying sediment be secured.

9.1.2 Sediment may be transported either in suspension (fine material in turbulent flow) or as bed load (by the creep and saltation of particles close to the bed). These modes of transport are governed by somewhat different laws. In practice a range of sediment sizes may exist in a river - or an intermediate size even if of narrow grading - so that design methods for handling sediment problems have also to deal with all conditions between the extremes of fully suspended wash loads and coarse gravel and boulders moving in contact with the bed. Over the years, many formulae have been derived relating the transport of bed material, whatever its size, to the hydraulic properties of flow, but in the last decade or so it has been shown that few are of acceptable accuracy and even the best are far from precise as predictive equations. Nevertheless, recent theories are sufficiently comprehensive to represent not only fine and coarse material but the intermediate sand sizes which dominate many alluvial systems.

9.1.3 Because of the range of sediment sizes of interest and differing transport mechanisms involved, a few definitions are in order:

Bed load: The material that moves in close contact with the bed.
Suspended bed material load: That part of the suspended load consisting of particle sizes found in samples taken from the bed.
Total bed material load: The sum of the above, i.e. the total transport of those particle sizes present in bed samples.
Wash load: That part of the total sediment discharge consisting of particle sizes smaller than are present in the bed; frequently taken to be sizes below 0.06 mm.

9.2. Transport process and theory

9.2.1 The transport of sediment by even a steady uniform flow is a complex process as yet incompletely understood. Many theories have been put forward to provide frameworks for the analysis of data on sediment transport, and very many experiments have been carried out over a period of some 50 years under controlled conditions in laboratory flumes. Some theories begin from the analysis of the mechanics of motion of individual particles, others use similarity principles or dimensional analysis as the starting point. All, however, include a measure of empiricism in providing coefficient values based on laboratory experiments or field measurements. Dimensional analysis provides a set of governing variables as follows:

9.2.2 The minimum set of basic quantities which influence the process of sediment transport in two-dimensional, free-surface flow are the unit mass of fluid, ρ, the unit mass of solids, ρ_s, the viscosity of the fluid, ν, particle diameter,D, water depth, d, shear velocity at the bed $\sqrt{(gdS)}$, denoted v_*, and acceleration due to gravity, g. Dimensional analysis yields four groups:

$$Re_* = v_* D/\nu \qquad \text{... 9.1}$$

$$Y = v_*^2/(s - 1)gD \qquad \text{... 9.2}$$

$$Z = d/D \qquad \text{... 9.3}$$

$$s = \rho_s/\rho \qquad \text{... 9.4}$$

9.2.3 One of the most significant contributions to the science of sediment motion was made by Shields (1936), who analysed experimental data on the initiation of movement of granular material using the first two of the above four non-dimensional groups. For established motion, an additional parameter is needed to represent the transport rate, for example Einstein's (1950) non-dimensional expression:

$$\Phi = qs/\rho[(s - 1)gD]^{3/2} \qquad \ldots 9.5$$

where qs is the sediment transport rate as submerged weight per unit time per unit width. It follows that:

$$\Phi = \text{function } [\ Re_*;\ Y;\ Z;\ s\ ] \qquad \ldots 9.6$$

Most transport theories use the above parameters or their equivalent. For example, Ackers and White (1973) replaced the above particle Reynolds number, Re_*, by:

$$D_{gr} = D[g(s - 1)/\nu^2]^{1/3}. \qquad \ldots 9.7$$

9.2.4 One of the more significant studies of the total load of non-cohesive sediments was by Engelund and Hansen (1967). They used a sub-set of the functions indicated by equation 9.6, to provide a simple relationship between transport and channel hydraulics:

$$\Phi\ f/4 = 0.1\ Y^{5/2} \qquad \ldots 9.8$$

9.2.5 The Ackers and White (1973) theory considered coarse sediment and fine sediment separately, and then sought a transitional function between them. These transitional sizes include the sands and silts that are of great practical interest in alluvial systems. Their analysis is typical of several in the last fifteen years which have used the power of modern computation to make the fullest use of the mass of data available from laboratory and field. Their results are also typical in that the optimisation procedures used to "calibrate" the theory provided a set of equations from which the total transport of bed material could be calculated within a factor of two on about two occasions out of three. The transport rate was based on the stream power concept introduced by Bagnold (1966), and the different mechanisms applicable to coarse and fine sediments led to two sets of parameters derived from Y,Z and D_{gr} which were linked by a transition parameter n_{gr} which was expected to be - and confirmed as - a function of Dgr.

$$G_{gr} = C_{gr}[(F_{gr} - A_{gr})/ A_{gr}]^{mgr} \qquad \ldots 9.9$$

where:

Transport rate -

$$G_{gr} = \frac{Xd}{SD} \frac{v_*}{V}^{ngr} \qquad \ldots 9.10$$

Sediment mobility -

$$F_{gr} = \frac{v_*^{ngr}}{\surd(gD(s-1))} \frac{V}{\surd 32 \log(10d/D)}^{(1-ngr)} \qquad \ldots 9.11$$

and

$$A_{gr}, C_{gr}, m_{gr}, n_{gr} = \text{functions} (D_{gr}) \qquad \ldots 9.12$$

X is the transport rate expressed as the ratio of sediment flux to fluid flux, by mass or weight, akin to a concentration which will be referred to as the "sediment charge". Data correlations provided simple algebraic formulae for all the functions 9.12, so forming a direct method of prediction. The original data analysis of Ackers and White (1973) has recently been updated, providing improved formulae for the functions 9.12, HR, Wallingford (1990c).

9.2.6 White, Milli and Crabbe (1975) reviewed the then available methods and found that few could approach the level of prediction of the Ackers and White method, the nearest comparable formulation being by Engelund and Hansen (1967). Since then, there have been other contenders, for example van Rijn (1984), (rather complex to detail here) as well as the contemporary multi-dimensional empirical correlation of Yang (1972).

$$\log X' = 5.435 - 0.286 \log (wD/\nu) - 0.457 \log (v_*/w) + [1.799 - 0.409 \log (wD/\nu) - 0.314 \log (v_*/w)] \times \log [(V - V_{cr})(S/w)] \qquad \ldots 9.13$$

In the above, X' is in parts per million, V_{cr} is the mean channel velocity at initial motion, w is the fall velocity of the particles. The above formula requires evaluation of V_{cr} and Yang gave a group of expressions depending on the value v_*D/ν.

9.2.7 These formulae for the total load of bed material are of similar reliability, but are not precise predictors. In fact it is by now clear that sediment transport is so sensitive to the hydraulics of the stream and the grading and condition of the stream bed that it is unlikely that it will ever be possible to predict transport rates from the overall hydraulic parameters to much greater accuracy than at present. It is this sensitivity to hydraulic conditions, especially the mean flow velocity and the consequent stress on the bed, that makes a consideration of the interference effects of flood plain flows on main channel flows particularly significant. In what follows in this Chapter, the 1990 up-date of the Ackers-White transport functions is used to examine the effect of compound flow on bed material transport, though very similar conclusions would emerge whichever of the relatively reliable calculation procedures mentioned above was used.

9.2.8 The suspension of finer material by the stream turbulence is broadly described by the theory developed by Rouse (1937). In this the gravitational effect through the fall velocity of particles is countered by the upward turbulent movement that arises from the vertical distribution of sediment. The concentration, C, at elevation, z, above the bed is related to that at some reference elevation, C_o at z_o, through the equation:

$$\frac{C}{C_o} = \left[\frac{(y - z)\, z_o}{z\, (y - z_o)}\right]^{\Omega} \qquad \ldots 9.14$$

where

y = flow depth

Ω = a turbulence parameter given by w/v_*K

v_* = shear velocity, $\sqrt{(gRS)}$
K = von Karman turbulence constant

9.2.9 The period of developing understanding has brought a number of text books on the subject of sediment transport, for example Yalin (1977), Graf (1971), Garde and Ranga Raju (1977), Allen (1985) and Thorne, Bathurst and Hey (eds) (1987). Papers by the originators of the more reliable transport functions should be read for full details of their methods.

9.3. The influence of compound flow on bed material transport

9.3.1 It is clear that there is considerable interference of the flood plain flow with the main channel flow through lateral shear effects and exchange of momentum via secondary circulations, and that this interference increases the apparent hydraulic resistance of the main channel, reducing the mean velocity therein significantly. It is this change in hydraulic conditions in the main river that will give rise to changes in the rate of transport of bed sediment. This sediment charge is a function of velocity (and other factors to a lesser degree), and velocity dependence is to a power above one: hence the sensitivity to the hydraulic conditions. Using sediment transport theory, it is therefore possible to assess the effect of compound flow, taking account of the interference effect by using the calculation procedures developed earlier. This is the basis of what follows: in effect they are computed examples using the best of the available knowledge, though it is hoped in due course that research on transport in compound channels will be carried out to confirm, or up-date as necessary, these forecasts.

9.3.2 The Ackers-White functions are straight forward to apply: no iterations are required and the equations for the various parameters are readily programmable for computation. They have the advantage of covering a very wide range of sediment sizes, and also by working in terms of the total transport of bed material they automatically take account of the balance between suspended load and bed load. The transition parameter n_{gr} allows for the fact that the transport of fine material is a suspension process, depending on the overall turbulence level in the stream, whilst the transport of coarse material is a bed process depending more on the bottom shear stress developed by the average velocity. In applying the equations, some assumptions were necessary:

- the turbulence level relevant to sediment processes in the main channel of a compound section is determined by the stream gradient, through the shear velocity, $v_* = \sqrt{(gRS)}$.

- the bed stress relevant to sediment transport is dependant on the mean channel velocity in the same way in a compound section as in a simple section.

- the effect of the flood plains on the main channel velocity is given by the methods described in Chapters 3 and 5. This is directly calculable in flow Region 1, but in the higher Regions of flow, the assumption is made that the main channel discharge adjustment factor remains the same as at the limit of Region 1. See Chapter 3, para 3.5.10.

- there is no transport of channel bed sediment over the flood plain. This is consistent with non-availability of such material on the flood plains, which would typically be vegetated, and so no material comparable to the main channel bed sediment would be exposed.

9.3.3 For purposes of illustration, a cross-section was chosen typical of small rivers: bed width 15m, channel depth 1.5m, flood plain width, 2 x 20m, channel and flood plain side slopes 1 in 1, thus 2b/h = 10, and B/b = 3.87. Two gradients were examined: 0.3/1000 which might represent a river with an active sand bed, and 3/1000 to represent a gravel bed stream. The Manning equation was used for the basic hydraulic calculations, with n_C = 0.03 and two values of flood plain coefficient, n_F = 0.03 and 0.06. The smoother of the flood plain conditions gave equal roughnesses over the perimeter, so was akin to most of the tests in the FCF, with flow progressing with depth through Regions 1 to 4. With the rougher flood plain condition, the flow stayed in region 1, as expected from the work with roughened flood plains. The range of depths considered covered within-bank flows and relative flow depths, H_*, up to 0.5, i.e. a depth of flow on the flood plain equal to the actual main channel depth, 1.5m. The channel of lower gradient was assumed to have a bed of 0.25mm sand, while the steeper channel bed was taken as gravel of 30mm dia. These were chosen with some trial and error to provide interesting illustrations: obviously the sediment size chosen should provide transport at bank full flow if it was to provide any simulation of a real alluvial channel.

9.3.4 Figure 9.2 shows the calculated stage-discharge functions for all four cases. These show the by now characteristic change of slope and curvature when flow first goes over-bank. Figure 9.2 shows the calculated sediment charge in the main channel for the four cases considered. Taking the sand bed case first (shown by full lines) sand movement occurs from quite shallow depths in the main channel increasing to over 100×10^{-6} (100 mgm/l) at bank full. With the rougher flood plain, this is effectively the maximum sediment charge at any discharge. Above bank full the charge diminishes because of interference effects from the flood plain, before rising again at depths above about 2m. With the smoother flood plain, interference effects are less, and so after some hesitation in the rate of increase in charge with depth above bank full, at higher depths the charge rises above 200×10^{-6}.

9.3.5 The gravel bed case in figure 9.2 shows initial sediment movement in the main channel at a flow depth of 1.0m, 2/3rds channel depth. The charge increases to about 60×10^{-6} at bank full, with a steep rate of increase up to that depth. Beyond bank full, with the rougher flood plain the diminution of transport above bank full due to interference effects is also sharp, with the charge, X, dropping to perhaps a third of its bank full value at depth 2.0m, i.e. 0.5m depth over the flood plain. There is a sharp drop in X just above bank full flow with the smoother flood plains too, though the drop is short lived giving a return to rapid increase with depth again at depths over 2m.

9.3.6 These estimates of how compounding may affect sediment transport in natural rivers are of considerable interest, and although different examples would show somewhat different results, the broad picture would be expected to remain: a significant change in the sediment transport function when flow goes above bank, with the main channel becoming less effective than it would be in the absence of flood plains or channel berms.

9.3.7 Figure 9.3 shows the information in several different ways. Here sediment charge, X, is plotted against water discharge, Q. The upper diagram is for the sand bed river, with the rougher of the two flood plain conditions. Graph I is the same data as shown in figure 9.2, the charge obtained by calculating conditions in the main channel. Graph II also refers to the main channel, but here the interference effect from the flood plains has been ignored to demonstrate what the trend in the transport function would have been like if there was no information on interference and the sediment transport calculation had been based on the main channel in isolation. The latter becomes seriously in error as depth increases, by a factor exceeding 2. Graph III converts the estimated charge shown in graph I to the average over the whole stream, on the basis that there will be no additional transport of this material generated by the flow over the flood plain, but the flow over the flood plain is an additional diluent. Graph IV will be referred to later.

9.3.8 The lower diagram of figure 9.3 is similar information for the gravel bed river. Graph I and III show a very pronounced peak at bank full, indicating that in terms of transport capacity the system becomes much less efficient above bank full, with the interference effect generated by rough flood plains so severe in the example given that transport almost stops again. In fact parallel computations were also made for gravel sizes of 40mm and 50mm: 50mm material is just mobile at bank full but not at lesser or greater depths, 40 mm material is mobile over a range of depth but virtually ceases moving again at about 0.5m depth on the flood plain.

9.3.9 The results for flood plains with equal roughness to the main channel show similar but rather less dramatic effects. They form graphs V (charge based on main channel discharge) and VI (charge based on total discharge).

9.3.10 There is often discussion as to whether a compound channel is more efficient at transporting sediment than a single section without berms. To examine this question, some assumption has to be made about the hydraulic equivalence, and a simple trapezoidal section has been assumed, with side slopes 1/1, giving the same conveyance at depth of 3m as the compound section with flood plains having double the Manning's n value of the main channel. The equivalent simple section has bed width 17.15m compared with

15m in the compound section: their stage discharge curves intersect at 3m. The sediment calculations for this equivalent section form graphs IV on figure 9.3. Below bank full this wider section is less efficient in terms of sediment transport that the compound one: graph IV lies below graph I (graphs I, II and III are identical below bank full, of course). The drop in efficiency within bank is small with sand, but rather more significant in the gravel bed case where initial motion is delayed to a higher discharge. However, for above bank flow the interference effect diminishes the compound channel transport efficiency so much that the single channel has a much better performance: this is shown by comparing graph IV with graph III.

9.3.11 This comparison of graph IV with graph III may also be regarded as representing the situation where a small river confined in a narrow valley without flood plains disgorges into a wider valley or on to an alluvial plain. Under the confined valley condition, major floods will carry sediment according to graph IV, but where the valley opens out to provide flood plains then graph III will apply. The morphological inference is that in high floods the reach with flood plains can not carry forward an excess of sediment delivered from the confined valley. The river channel itself will accrete, partially block, force more flow on to the flood berms and in due course deposit the load of sand or gravel on those berms. These theoretical sediment forecasts for typical systems are consistent with geomorphological information on the development of alluvial plains and with experience of river behaviour in major floods.

9.3.12 The purpose here is to draw attention to the influence of a compound cross section with flood berms on the transport of bed material. The improved knowledge of the conveyance of such sections, allowing for the interference between flood plain and main channel, can feed forward into improved computations for river morphology. Even these preliminary sample calculations are of significance in respect of fluvial morphology, but they are theoretical and involve assumptions, and so should not be regarded as factual until there has been some experimental confirmation. There is ample scope for research on transport in compound channel systems, with much of interest in straight systems as well as in meandered systems. Until the results of such research are available, the method used here provides evidence of the importance of compounding on sediment transport capacity and a provisional calculation procedure.

9.4. Suspended solids in compound channels

9.4.1 The turbulent structure in compound channels is undoubtedly different from that in simple channels without flood berms, and so the basic turbulent suspension theory summarised in equation 9.14 will not be applicable without some modification. In terms of broad effects, however, the most significant feature that arises with compounding is the strong lateral shear generated around the bank line which will diffuse the sediment in the upper layers of the main channel across on to the flood plains, where the flow's capacity for keeping the sediment in suspension will be less. Hence there will be deposition on the flood plains of suspended load originating in the main channel.

9.4.2 Allen (1948) has described this process in some detail, as well as reminding us of the ample evidence from the field through levee building etc. that this is indeed a well authenticated process. Using the general concept that the capacity to maintain material of a given size in suspension is a function of the velocity, and that the velocity will be less on the berms than in the deep channel, Allen shows that the concentration sustainable on the flood plains would be less than that in the main channel by the factor (h/H). The lateral dispersion from main channel to flood plain thus increases the concentration above the sustainable value, so a balance can only be achieved through deposition.

9.4.3 Much detailed information on turbulence under the conditions of compound flow has been obtained from the programme of research on the FCF, including dispersion tests using dyes. This new information should provide a basis for better understanding of sediment dispersion, but it is hoped that a subsequent research programme will examine this topic directly, by using suspended solids.

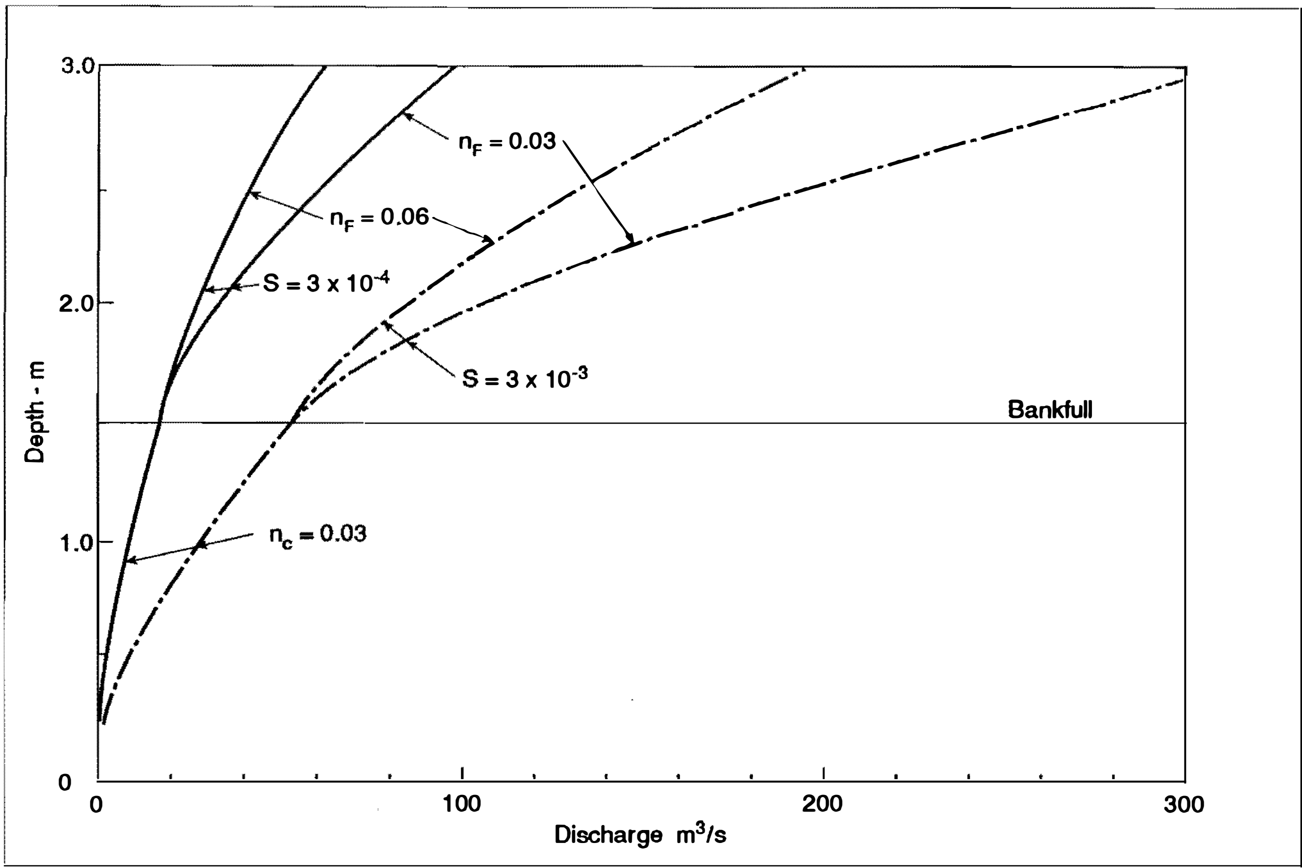

Fig 9.1 **Stage discharge curves for example rivers: main channel 15m bed width, 1.5m deep, 1/1 side slopes; flood plains 20m wide, 1/1 side slopes, main channel Manning's n = 0.03**

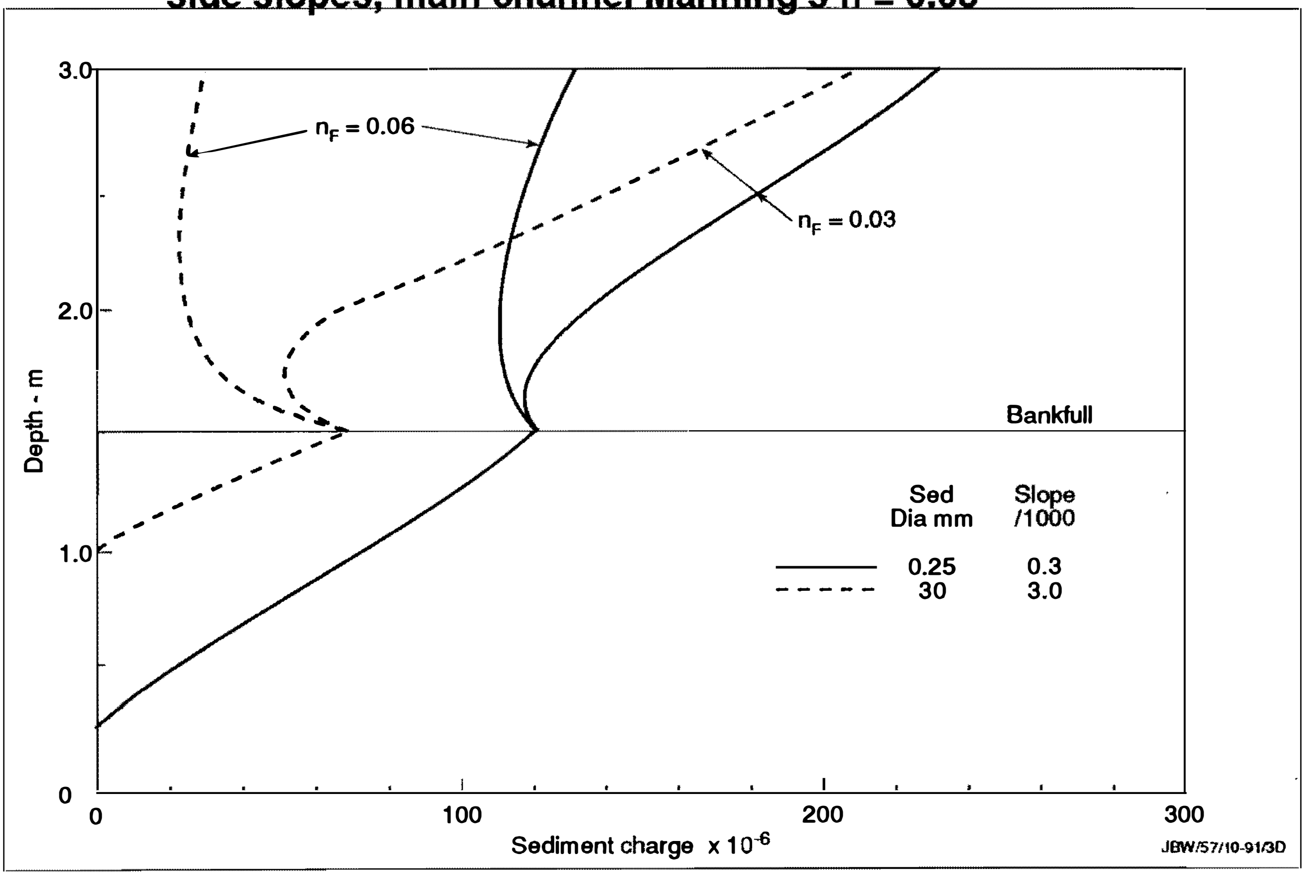

Fig 9.2 **Sediment charge - X, versus stage, for sand river at S = 0.3/1000 and for gravel bed river at S = 3/1000**

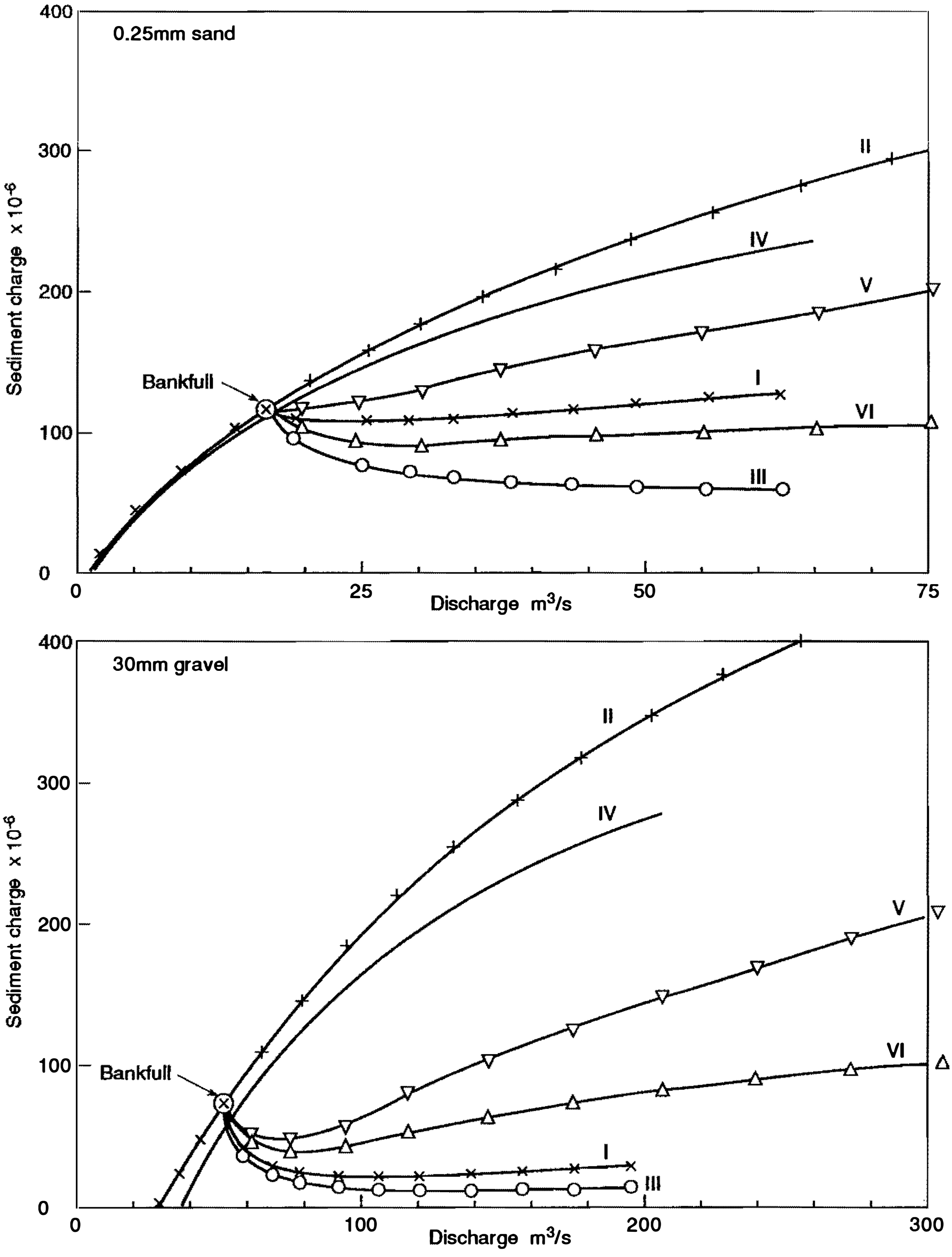

Key:

Graph I, X calculated for main channel allowing for interference from flood plain with n_F double that in main channel
Graph II, values of main channel X if interference is ignored
Graph III, sediment transport as calculated in I but expressed as ratio to total fluid flux
Graph IV, X calculated for an equivalent trapezoidal section (equal conveyance at depth 3m)
Graph V, as I but with flood plain roughness same as main channel
Graph VI, sediment transport as calculated in V but expressed as ratio to total fluid flux

JBW/58/10-91/3D

Fig 9.3 Sediment charge - X, versus total discharge: upper diagram for 0.25mm sand, lower diagram for 30mm gravel

10. CONCLUDING REMARKS

10.1 Summary of hydraulic design formulae for the conveyance of straight compound channels.

10.1.1 As a result of the analysis of the new information from the large scale flood channel facility at Wallingford, as described in Chapter 3, a set of equations was derived for assessing the stage/discharge relationship for compound channels, or in other words the conveyance of their cross-section. The basic method is a development of the common approach dividing the cross-section into zones by vertical interfaces at the channel bank line. The basic discharges in the main channel and on the flood plains are first calculated separately from an appropriate conventional friction formula and roughness coefficients consistent with the character of the boundaries, excluding the vertical division planes from the wetted perimeters. The sum of these basic discharges have then to be adjusted to allow for the effects of the interaction between the zones, which has a significant effect on the channel conveyance. Several alternative methods of adjustment were considered within the broad framework provided by dimensional analysis, and they were progressively developed to be able to cope with the full range of conditions tested. Because of the complexity of the flow structure involving different regions of behaviour, no single formula could cover all conditions. Moreover, the form of equation and the parameters it depends on were found to differ from one region to the next, and so a logical method was established for determining which flow region applies at any particular flow depth. The equations derived are basically simple in form, with linear variation with the governing parameters, but it is expected that application in practice will utilise a computer program that incorporates the logic for determining which region of flow applies.

10.1.2 Being empirical functions based on data from channels with a main channel bed width/depth ratio of ten, it was necessary to confirm the general application of these equations by reference to data from other sources. Although the predictive equations turned out to be robust in the sense of being transferable in the main to most cross-sections and types and combinations of roughness, as explained in Chapter 5, the equations for Region 1 flow - that covering the lower range of depths - required revision for general application. This possibility had been envisaged in the dimensional analysis of Appendix 1: the question hinged on whether or not the main channel was wide in relation to the zone of interaction from the flood plains. The wide channel assumption proved not to be valid for width/depth ratios below, say, twenty but a relatively simple modification was found adequate to cover the range of width/depth ratios for which research data was available, and those of practical interest. This involved introducing an aspect ratio factor, ARF, proportional to the main channel width/depth ratio. The resulting set of design equations for straight compound channels is as follows:

10.1.3 **REGION 1**: This is the region of relatively shallow depths where interference effects increase progressively with depth. The formula for this region is based on Q_{*2}, the discharge deficit normalised by the product $(V_C-V_F)Hh$ (see Appendix 1 for nomenclature), with adjustment for aspect ratio. The discharge deficit is the deduction required from the basic calculation, i.e. the sum of the basic flows in the flood plains and main channel, to obtain the 'true' discharge. This is calculated as the sum of the separate deficits for flood plains and main channel. The flood plain deficit proved to be the minor part and is negative, i.e. an addition to flood plain flow. It depends linearly on the depth ratio, H_*, but to cover the case with roughened flood plains is progressively reduced by the factor f_C/f_F as the flood plain friction increased. The major part, the main channel deficit, depends linearly on both the width ratio (width over flood plains divided by top width of main channel) and relative depth, the relative depth multiplier also depending (though not very strongly) on friction factor ratio and channel side slope. Thus for region 1:

$$Q_{*2F} = -1.0\ H_*\ f_C/f_F \qquad \text{... 10.1}$$

$$Q_{*2C} = -1.240 + 0.395\ B/w_C + G\ H_* \qquad \text{... 10.2}$$

(Q_{*2C} is never permitted to be negative, and perhaps should not be less than 0.5, to provide some minimum interaction effect: if this limit applies then also $Q_{*2F} = 0$: see para 5.5.10)

For $s_C \geq 1.0$:

$$G = 10.42 + 0.17\ f_F/f_C \qquad \text{... 10.3}$$

For $s_C < 1.0$:

$$G = 10.42 + 0.17\ s_C f_F / f_C + 0.34\ (1 - s_C) \qquad \ldots\ 10.4$$

10.1.4 **REGION 2.** This is the zone of greater depth where the interference effect reduces again. The most appropriate form of design function for this region relates the requisite discharge adjustment factor to the channel coherence, which is an expression for the degree of similarity of hydraulic conditions within the main channel and on the flood plains. Channel coherence itself is dependent on the section geometry and roughnesses involved and is defined and explained in paras 3.3.4 to 3.3.6, and by equations 3.1, 3.2 and 3.3. It was found that the correction factor to allow for interference effects is rather more than the calculated value of coherence at that depth: it is nearer to the coherence value at a somewhat greater depth, in other words requiring a shift in relative depth. The basic discharge calculation has thus to be factored as follows in region 2:

$$\begin{aligned} &\text{DISADF } (H_*,\ \text{channel geometry and roughness}) \\ &\qquad = \text{COH}((H_* + \text{shift}),\ \text{channel geometry and roughness}) \end{aligned} \qquad \ldots\ 10.5$$

where for $s_C \geq 1.0$,

$$\text{shift} = 0.05 + 0.05\ N_F \qquad \ldots\ 10.6$$

for $s_C < 1.0$,

$$\text{shift} = -0.01 + 0.05\ N_F + 0.06\ s_C \qquad \ldots\ 10.7$$

In the above N_F is the number of flood plains. The test conditions in the FCF did not provide any Region 2 results with different roughnesses on flood plain and in main channel - the FCF rough flood plain results remained in Region 1 at all depths - but data from other sources has provided reasonable confirmation of this approach for more modest differences of roughnesses.

10.1.5 **REGION 3.** This is a relatively narrow transitional region of flow, for which alternative approaches were considered, a simple constant discharge adustment factor for the zone or an equation giving DISADF as a function of COH_3. Further data analysis showed that the latter was a somewhat more accurate representataion of the FCF data and so for Region 3 the following function is recommended:

DISADF = 1.567 - 0.667 COH ... 10.8

However, the alternative form:

DISADF = 0.95 ... 10.9

is almost as accurate overall.

10.1.6 **REGION 4.** This is the region where the coherence of the cross-section is such that it may be treated as a single section when calculating overall flow, with perimeter weighting of friction factors. This does not, however, mean that the separate zonal flows calculated provide accurate assessments of the flows in those zones: significant interaction effects remain, and the method for adjusting the main channel flow separately is given later. For total flow computation however, in region 4:

DISADF = COH ... 10.10

10.1.7 **ASPECT RATIO FACTOR.** The aspect ratio factor, ARF, is generally given by the main channel width/depth ratio/10, i.e. 2b/10h. However, if the aspect ratio exceeds 20, the channel should be assumed to be "wide", when ARF = 2.

10.1.8 **COMPUTATION PROCEDURE.** The actual computation of discharge depends on the choice of basic friction formula and associated coefficient for the conditions under review, as well as on the cross-section geometry and hydraulic gradient. Nothing in the derivation of the set of predictive equations limits that choice of friction formula: the engineer is free to choose Manning, Colebrook-White or whatever is most appropriate for the particular situation. The cross-section geometry provides the values of area, wetted perimeter (excluding the vertical division plane) and hence hydraulic mean depths for the main channel and flood plain zones. The friction formula then provides "basic" values of Q_{FB}, Q_{CB} and hence Q_{TB}.

The calculation of the various parameters to permit the use of equations based on a classical compound channel form was explained in section 7.1. The best estimate for flow if in region 1 is then obtained from:

$$Q_{R1} = Q_{TB} - (Q_{*2C}+N_F Q_{*2F})(V_C-V_F)Hh^*ARF \qquad \ldots\ 10.11$$

If flow is in regions 2, 3 or 4, then the best estimate is obtained from:

$$Q_{R2,\ 3\ or\ 4} = DISADF_{R2,\ 3\ or\ 4}\ Q_{TB} \qquad \ldots\ 10.12$$

10.1.9 **CHOICE OF REGION.** The logic behind the selection of the appropriate predictive equation is dependent upon the calculation of discharge for all regions in turn, referred to as Q_{R1}, Q_{R2}, Q_{R3} and Q_{R4} respectively. The choice of the appropriate region and hence appropriate total discharge proceeds as follows:

Region 1 or 2?

If $Q_{R1} \geq Q_{R2}$ then $Q = Q_{R1}$ ... 10.13

Region 2 or 3?

If $Q_{R1} < Q_{R2}$ and $Q_{R2} \leq Q_{R3}$ then $Q = Q_{R2}$ ... 10.14

Region 3 or 4?

If $Q_{R1} < Q_{R2}$ and $Q_{R3} < Q_{R2}$ then $Q = Q_{R3}$ unless $Q_{R4} > Q_{R3}$ when $Q = Q_{R4}$ ... 10.15

10.1.10 The calculation of Q_{R1} etc utilises the equations summarised above, equs 1.1 to 1.12, together with the respective definitions of the dimensionless groups used, namely Q_{*2F}, Q_{*2C} and DISADF. The logic route given in the previous paragraph then selects the appropriate value. There is no transition between them, in accordance with the individual test results: there was little if any evidence of a curved transition between the regional equations.

10.1.11 TOLERANCES. The performance of this set of predictive equations was checked by reference back to the original Wallingford experimental data, and the percentage discrepancies between the individual results and the predicted discharges for the observed depths, geometries etc were assessed. These discrepancies were subjected to statistical analysis, to obtain mean errors and the standard error of estimate. The former statistic indicates the overall goodness of fit, and the latter the variability. This variability can have two components: any imperfection in the trend of the predictive equations and also the inevitable experimental scatter due to random errors of measurement. With main channel and flood plains of equal roughness, the mean errors for the various groups of tests were all found to be under a third of a percent; and variability under half a percent (standard error of estimate: some two-thirds will lie within this with normal distribution of errors). The former shows the excellence of the set of predictive equations in fitting the experimental trends; the latter could hardly be bettered in terms of consistency of laboratory measurement. The tests with roughened flood plains were not represented quite so well: although the mean error of 0.07% indicates good agreement on average, the standard error of 1.5% indicated greater variability in the predictions. The complete data set was fitted almost exactly on average by these predictive methods: mean error -0.001%. The variability of 0.8% was very satisfactory, bearing in mind that perhaps 0.5% arose from the experimental observations themselves, and that the one set of equations was applied to smooth and rough conditions, to asymmetric as well as symmetric cases, to a range of flood plain widths and channel bank slopes, over a range of flow depths covering four different regions of flow.

10.1.12 The purpose of the analyses of data from other sources covered in Chapter 5 was to validate - and to adjust and calibrate further as necessary - the method based on the FCF results by comparing its predictions with a wider range of experimental data, covering many more geometries and roughness combinations. The only adjustment found necessary was the inclusion of the parameter ARF in the formula for Region 1: otherwise the formulae transferred well and were able to explain several unsuspected differences in trends of behaviour. However, many of these other results were obtained at small scale, when measurement problems, especially the setting of uniform flow and measurement of gradient, give higher tolerances than were obtainable in the large FCF at Wallingford.

Consequently the degree of agreement between prediction and observation was variable and in nearly all cases not as good as for the main data base. Some of this increased discrepancy was undoubtedly due to wider experimental tolerances, but some may have arisen because of inaccuracy in transferring the set of empirical equations to geometries and roughnesses well outside the range covered by the original derivation. It is therefore difficult to specify tolerances on the formulae themselves. The probable error in predicting discharge at 95% confidence level due to deficiency in the prediction method could be as low as 2%, but for most circumstances is almost certainly below 5%. To this must be added the tolerances in the basic friction formula and the knowledge of the roughness of the channel boundaries.

10.1.13 **CALCULATION OF MAIN CHANNEL CONDITIONS.** For some purposes it is not sufficient to calculate the stage/discharge curve: separate assessments of discharge in the main channel and flood plain are required, duly corrected for interaction effects. One such example is in the calculation of bed material load in the river itself. The method of obtaining the adjusted value of the main channel and flood plain flows in Region 1 will be evident from the definitions of Q_{*C} and Q_{*F}. Equations 10.1 to 10.4 yield those values, and then:

$$Q_{CR1} = Q_{CB} - Q_{*2C}*(V_C-V_F)Hh*ARF \qquad \ldots\ 10.16$$

$$Q_{FR1} = Q_{FB} - Q_{*2F}*(V_C-V_F)Hh*ARF \qquad \ldots\ 10.17$$

Other parameters such as the mean velocities in those zones can then be calculated.

10.1.14 Extending this separate zone adjustment to the higher regions of flow has not been so well established, because of lack of data. However, this may be achieved to engineering accuracy by the method indicated in paragraph 3.5.10. As the calculations proceed from shallow depths through Region 1, the value of $DISADF_C$ may be calculated from Q_{CR1}/Q_{CB}, depth by depth. The logic for choosing the regions (based on total flow) will in due course indicate a change to Region 2, but the value of the main channel discharge adjustment factor for region 1 is then taken to apply at all higher flows. This is simply achieved by retaining the value of $DISADF_C$

calculated at the limit of region 1 at all higher stages, so that in Regions 2, 3 and 4:

$$Q_{CR2,3,4} = Q_{CB} * DISADF_{C \text{ at R1 limit}} \quad \ldots \ 10.18$$

10.2 <u>The advantages of compound channels.</u>

10.2.1 The environmental and ecological advantages of two-stage channels stem partly from their more natural appearance, but also because berms or flood plains provide useful amenities. Their use has, of course, to be compatable with inundation from time to time. The most general use of flood plains is for agriculture, especially where they are a natural feature of the landscape, but they may also form parks or playing fields, and even relatively narrow berms alongside urban drainage channels can be developed as linear parks. There are, however, precautions to be followed, such as making good forecasts of frequency and duration of inundation, and the elevation of the normal water table which will have an important bearing on the vegetation growth, and hence the cost of maintenance and the consequent hydraulic resistance.

10.2.2 A case is described by Sellin, Giles and van Beeston (1990) of a small river improvement project which was designed with the ecology very much in mind. This proved less efficient than expected hydraulically and also in terms of the need for and access arrangements for maintenance. This is the River Roding in Essex, draining a catchment of 250 km to the project location. The scheme in reality forms a three stage system. There is a curvilinear main channel with some straighter but skewed reaches, with berms out to a fairly regular retired bank line, all set below the general level of an extensive flood plain. Because the berms are not much higher than normal water level, they provide a wet habitat, which may be the delight of ecologists but because of the luxuriant growth of water-loving reeds and other plants, offers a very high resistance except just after cutting. The object of the scheme had been to provide a 70 year standard of protection to a neighbouring town through the provision of flood berms, but in practice this is not normally achievable, even with considerable maintenance effort. Cutting the growth on the berm increases the flood capacity at 1.35m depth on the berm by 50%. The actual capacity can be as low as 15 m^3/s with uncut vegetation, trees, tussock development and debris, but is typically 25 m^3/s after a full season's growth, rising to to 40 m^3/s after cutting, compared with a design standard of 50 m^3/s. This example shows that the use of two-stage channels is not without its problems. What is ecologically highly beneficial in a river corridor has to be reconciled with the social requirement of limited flood frequency. This depends on hydraulic performance, which in turn depends on the normal use of the berms or flood plains and on the vegetation thereon.

10.2.3 The environmental implications of river engineering are covered in a report by Hey (1990). He also draws particular attention to the problems of a high water table relative to the berm elevation and to the impact of vegetation on flow capacity, whilst pointing the way through river corridor surveys and post-construction audit surveys to achieving the desired balance between what is environmentally desirable and what may be essential in meeting hydraulic objectives. This involves not only vegetation, of course, but also within channel features such as shoals and embayments which may attract fish and provide attractive habitats for much wild life and plant species. Brookes (1988) treats the environmental management of channelized rivers in detail, with many examples of good and bad practice. This contains a wealth of experience and expertise on all aspects of environmental assessment: habitat evaluation procedures, biotic indices, aesthetic evaluation, stream morphology, fish and fisheries, aquatic plants. Figure 10.1 illustrates improvements to river cross-sections to increase their conveyance whilst retaining desirable ecological features within a two-stage channel, though of course the river engineer has still to assess the likely roughness coefficients and meet the hydraulic objectives of the project.

10.2.4 The hydraulic advantage of a compound channel when drainage improvements are required is the increased flood capacity for a given increase in stage, arising from the flow over the berms or flood plains. This advantage may not always be as great as might have appeared from the traditional methods of calculation, because the interaction between the zones of different flow depth increases energy dissipation, as clearly demonstrated by research and now calculable with the methods recommended herein. Nevertheless, the advantage is very real in practice where the available flow depth is limited. Irrespective of any hydraulic advantage, a knowledge of two-stage channel behaviour is necessary because they occur naturally: the cross-section of typical river channels is determined by the discharge which occurs for a combined period of the order of 2 days per year, so it is obvious that major floods will inundate their associated flood plains, so that the design condition is when they are indeed two-stage systems.

10.2.5 The provision of berms alongside artificial channels has also advantages in terms of access for maintenance. There is no need for such access to be above water level even during floods, as maintenance work is almost invariably carried out when the system is not near capacity. It therefore makes good sense to provide two-stage channels, even in circumstances where they may have little or no amenity value: they combine good access with increased hydraulic conveyance.

10.3 State of knowledge and need for further reseach

10.3.1 The detailed and extensive research programme carried out on the SERC-FCF at Wallingford has reaped the benefit of being the first major programme to combine large scale, a high standard of accuracy of measurement, attention to detail and collaboration between different groups with complementary interests. The large scale has permitted the use of a width/depth ratio more in line with the practical range of main channel aspect ratios, and in several respects has provided results quite different from those reported from small scale narrow faciliies that typified much of the earlier research. This research investment has been rewarded with a detailed knowledge of the flow in two-stage channels that was not previously available from any source, and this new data base confirms that a radically different approach is required to the hydraulic design and assessment of such systems. Previous methods were seriously in error.

10.3.2 The analysis of the research results and the application of those findings to related topics such as the extrapolation of stage/discharge functions and the transport of bed material shows that the consequences of the new knowledge are not confined to improved estimates of channel conveyance. They cut across established practice by providing new insights into channel morphology, the computational modelling of river systems, the hydraulic consequences of following environmentally desirable river management practices, etc. This report deals only with the results relevant to straight channels aligned with, or only mildly skew to, their berms or flood plains, but subsequent aspects of the research programme have concerned meandering channels and will undoubtedly give rise to equally significant changes in the approach to the hydraulics of irregular channels when the analysis and interpretaion is completed.

10.3.3 Even with straight aligned channels, the research programme in the FCF has left some question marks; some gaps in the coverage and confirmation of ideas and concepts. The following items deserve further study at large scale when opportunity and funding levels permit:

- Stage discharge data is required of comparable detail and accuracy for channels with differing aspoect ratios. The limitation of the FCF to a main channel width/depth ratio of 10 has made confirmation of the influence of this feature somewhat elusive.

- Stage discharge data is also required with boundary roughness of various degrees on the flood plains. Any artificial roughness would require accurate and detailed calibration, of course, but without such research there remains a possibility that the influence of flood plain roughening in the form of surface piercing rods may not be the same as that of boundary-type roughening: the design equations using the ratio of the flood plain to main channel friction factors may leave scope for refinement for application to the more usual roughness condition.

- The different regions of flow apparently include Region 3 as a transition between Regions 2 and 4, and this may be associated with an unstable re-organisation of secondary circulations. There is scope for using the existing detailed information on flow structure to seek a cause for this transition in the stage discharge function.

- Turbulence methods will undoubtedly oust the empirical procedure recommended here in course of time, but their adoption requires better understanding of the role of different interactions between the main channel and flood plain, and any dependence of their relative importance on flow depth and cross-section geometry. A careful study of the formulation of the turbulence coefficent in the lateral distribution method is required, making full use of the data set now available, with particular attention paid to accuracy of simulation of total flow and also the division of flow, and any variation with flow depth.

- The implications for sediment transport of the reduction in main channel discharge and velocity consequent upon interaction from the flood plains requires experimental study. Without experimental verification, the methods used to indicate the order of magnitude of the likely effect used in Chapter 9 are open to question, and in any event are unlikely to have taken adequately into account all the complexities of the flow structure.

10.3.4 Regarding the later phases of research on meandering channels, it is important that the results are reviewed within the context of simulating the fluid and momentum exchanges in computational models with two-dimensions on plan. Only thus can the work on meandering channels be extrapolated to irregular plan geometries in general: they clearly can not be handled as a simple extension of the methods developed here for straight channels. The new insights already gained on the flow structures in such systems with overbank flow, as illustrated in Chapter 8, provide a vital starting point for incorporating appropriate mechanisms into any model.

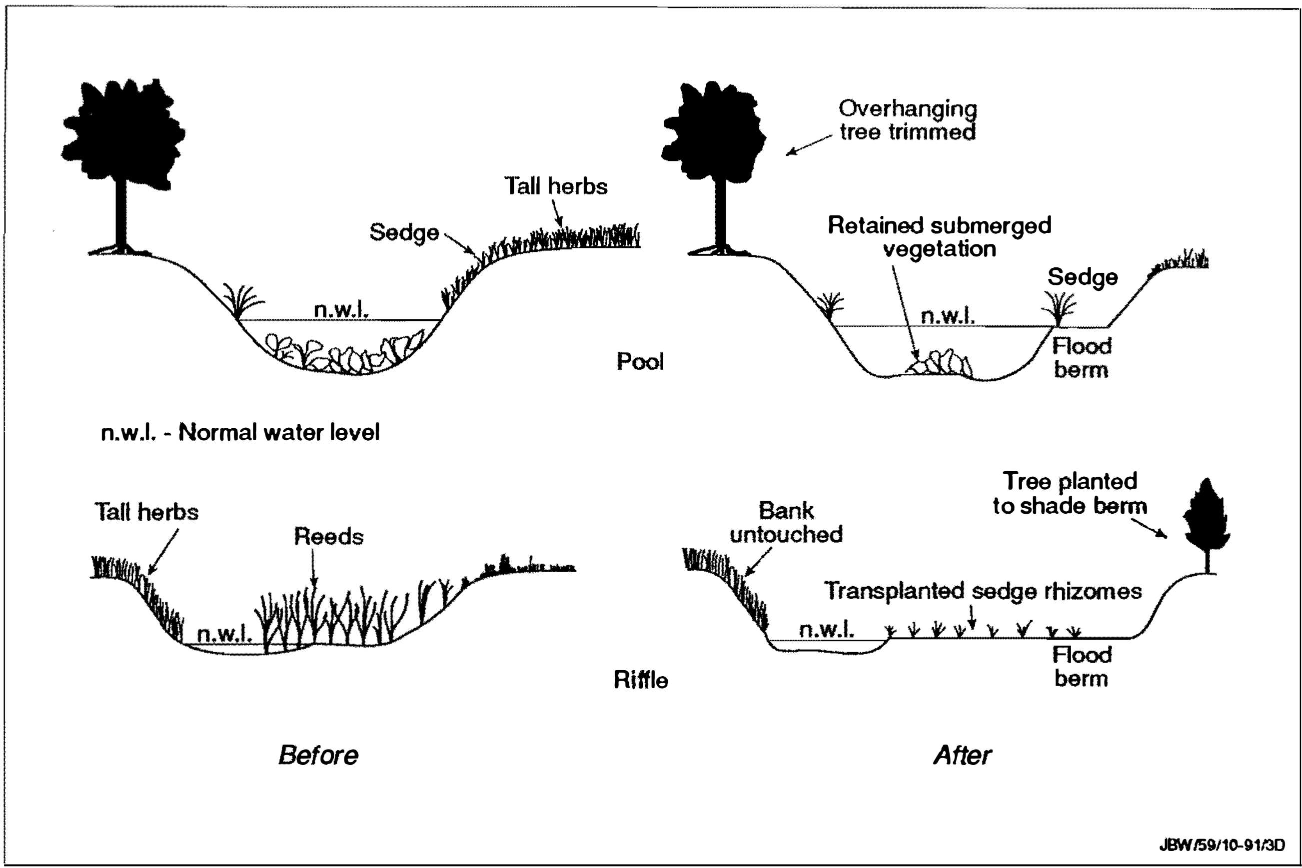

Fig 10.1 Ecologically attractive two-stage channel design proposed for River Ray in Oxfordshire (Brookes, 1988, after Hinge and Hollis)

11. ACKNOWLEDGEMENTS

This analysis of compound channels would not have been possible without the support of funding from several Water Authorities, whose river duties have now been taken over by the National Rivers Authority. It has depended on support from staff of HR, Wallingford, as well as liaison with the SERC Project Co-ordinator, Dr D W Knight, of the University of Birmingham. The careful and detailed work of the UK research groups involved deserves special mention. Without their research and the availability of their high calibre results, the work described here could not have proceeded to a successful conclusion. The co-operation of many other research groups and individuals is also acknowledged: they have readily supplied additional details of their research, as will be clear from Chapter 5, and have also provided valued comments on the Technical Reports which in essence provided drafts of sections of the manual. Dr James Wark, now at HR, Wallingford, carried out the detailed work on turbulence methods reported in Chapter 6, as part of the research programme for the Ministry of Agriculuture, Fisheries and Food; Mark Morris of HR performed the analysis that formed the basis of Chapter 3; their help was invaluable. I am also indebted to the many authors and publishers of figures and other information re-used here: the references to them provide their sources.

12. REFERENCES

Ackers P, (1958), Resistance of fluids flowing in channels and pipes, Hydraulics Research Paper no 1, HMSO, London, 1958.

Ackers P, (1980) Use of sediment transport concepts in stable channel design, Int. Workshop on Alluvial River Problems, Roorkee, India, 1980.

Ackers P and White W R, (1973), Sediment transport: new approach and analysis, Proc American SCE, Nov 1973, vol 99, HY11, pp 2041 - 2060.

Allen J R L, (1985), Principles of physical sedimentatology, George Allen and Unwin, London, (1985), ISB 0-04-551096-2.

Asano, T, Hashimoto, H and Fujita, K, (1985), Characteristics of variation of Manning's roughness coefficient in a compound cross section. International Association for Hydraulic Research, Proc 21st Congress, Melbourne, Vol 6, August 1985, pp 30-34.

Baird J I and Ervine D A, (1984), Resistance to flow in channels with overbank flood plain flow, Proc 1st Int Conf on Channels and Channel Control Structures, Southampton, UK, p 4-137-150.

Bagnold R A, (1966), An approach to the sediment transport problem from general physics, US Geological Survey, Prof. paper 422-1, US Gov. Printing Office, Washington, 1966.

Blasius H, (1913), Das ahnlichkeitsgesetz bei reibungsvorgangen in flussigkeiten, V D I Forschungshaft, no 131.

Bray D I, (1982), Flow resistance in gravel bed rivers, In: R D Hey et al. (1982)

Bridge J S and Jarvis J, (1982), The dynamics of a river bend: a study in flow and sedimentary processes, Sedimentology, vol 29, 1982, 499-541.

Brookes A, (1988), Channelized rivers: perspectives for environmental management, John Wiley and Sons, Chichester, UK.

Chadwick A and Morfett J, (1986), Hydraulics in civil engineering, Allen and Unwin, London.

Chang H H, (1983), Energy expenditure in curved open channels, Proc ASCE, vol 109, J Hydraulic Engineering, no 7, July 1983, 1012-1022.

Chang H H, (1988), Fluvial processes in river engineering, John Wiley and Sons, 1988.

Clauser F H, (1954), Turbulent boundary layers in adverse pressure gradients, J Aeronuatical Sciences, Feb 1954.

Colebrook C F, (1939), Turbulent flow in pipes, with particular reference to the transition region between the smooth and rough pipe laws, Journal Instn. Civil Engineers, London, vol 11, p 133.

Cowan W L, (1956), Estimating hydraulic roughness coefficients, Agricultural Engineering, vol 37, no 7, July 1956, 473-475.

Cunge J A, (1969), On the subject of a flood propagation computation method (Muskingum method), J. Hydraulics Res., vol 7, no 2, 1969, 205-230

Einstein H A, (1950), The bed load for sediment transportation in open channel flow, Ser. Tech. Bull. US Dept Agriculture and Soil Conservation, 1026, 1950

Elsawy E M, McKee P M and McKeogh E J, (1983), Application of LDA techniques to velocity and turbulence measurements in open channels of compound section, Proc 20th Int Congress IAHR, vol 3, Moscow, p255-263.

Elliott S C A and Sellin R H J, (1990), SERC flood channel facility: skewed flow experiments, Journal of Hydraulics Research, Vol 28, 1990, no 2, p197-214

Engelund F and Hansen E, (1967), A monograph on sediment transport in alluvial streams, Teknisk Vorlag, Copenhagen, Sweden, 1967.

Ervine D A and Ellis J, (1987), Experimental and computational aspects of overbank flood plain flow, Trans. Royal Society of Edinburgh: Earth Sciences, vol 78, 1987, 315-325.

Ervine A and Jasem H K, (1991), unpublished PhD thesis and private communication.

Fread D L (1984), DAMBRK: the NWS dam-break flood forecasting model, Office of Hydrology, National Wether Service, National Oceanic and Atmospheric Admin., U S Dept. Commerce, Silver Spring, Md, USA.

Garbrecht J and Brunner G, (1991), Hydrologic channel-flow routing for compound sections, J Hydraulic Eng., American Soc. Civil Engrs, vol 117, 5, May 1991, 629-642.

Garde R J and Ranga Raju K G, (1977), Mechanics of sediment transportation and alluvial stream problems, Wiley Eastern Ltd, 1977.

Graf W H, (1971), Hydraulics of sediment transport, McGraw-Hill, 1971.

Herschy R W, ed. (1978), Hydrometry, John Wiley and Sons, Chichester, UK, 1978.

Henderson F M, (1966), Open channel flow, Macmillan Company, New York, 1966.

Hey R D, (1979), Flow resistance in gravel-bed rivers, ASCE, J Hyd. Div, vol 105, HY4, April 1979, 365-379.

Hey R D, (1990), Environmental river engineering, J. Inst. Water an Environmental Management, vol 4, no 4, Aug 1990, 335-340.

Hey R D, Bathurst J C and Thorne C R, (editors) (1982), Gravel bed rivers, fluvial processes, engineering and management, Wiley, New York, 1982.

Higginson N N J, Johnston H T and Myers W R C, (1990), Effect of scale distortion in a compound river channel model study, Proc. Int. Conf. on River Flood Hydraulics, Wallingford, Sept 1990, ed. W R White, John Wiley and Sons, 391-403.

Hogg I G G, Guganesharajah K, Gunn P D S and Ackers p (1988), The influence of river regime on the flood management of the Sukkur Barrage, Pakistan, Int Conf. on River Regime, ed White W R, Hydraulics Research, Wallingford, UK, May 1988.

Hollinrake P G, (1987, 1988, 1989), The structure of flow in open channels - a literature search, vols 1, 2 and 3, Reports SR 96, SR153 and SR209, Hydraulics Research, Wallingford, UK.

Hydraulics Research, (1988), Hydraulic performance of environmentally acceptable river engineering schemes, Report EX 1799, Hydraulics Research, Wallingford, UK.

Hydraulics Research, (1990a), Charts for the hydraulic design of pipes and channels, 6th edition, Hydraulics Research, Wallingford, UK, pub. Thomas Telford, London.

Hydraulics Research, (1990b), Tables for the hydraulic design of pipes, 5th edition, Hydraulics Research, Wallingford, UK, pub. Thomas Telford, London.

Hydraulics Research, Wallingford (1990c), Sediment transport: The Ackers and White theory revised, Report SR 237, HR Wallingford, Oxon, UK

Jaeger C (1956), Engineering fluid mechanics, Blackie and sons, London, 1956.

Jansen P Ph, van Bendegom L, van den Berg J, de Vries M and Zanen A, (1979), Principles of river engineering, Pitman, London, 1979.

Kiely G, (1991), unpublished thesis plus personal communication.

Keller R J and Rodi W, (1984), Prediction of two-dimensional flow characteristics in complex channel cross-section, Proc Hydrosoft 84 conf., Portorez, Yugoslavia, Elsevier, p 3-3-14.

Keller R J and Rodi W, (1988), Prediction of main channel/flood plain flows, J Hydraulic Research, vol 26, no 4, p 425-441.

Keulegan G H, (1938), Laws of turbulent flow in open channels, Journal of Research, Nat. Bureau of Standards, Washington D C, Res. Paper 1151, vol 21, no 6, pp 707-741.

Klaassen G J and Van der Zwaard J J, (1974), Roughness coefficients of vegetated flood plains, J Hydraulics Research, vol 12, 1974.

Knight D W and Demetriou J D, (1983), Flood plain and main channel interaction, Proc ASCE, J Hydraulic Eng, vol 109, no 8, Aug 1983, 1073-1092.

Knight D W, Demetriou J D and Hamed M E, (1983), Hydraulic analysis of channels with flood plains, Proc Int Conf on Hydrol Aspects of Floods, BHRA, Bedford, UK, p 129-144.

Knight D W, Demetriou J D and Hamed M E, (1984), Stage discharge relations for compound channels, Proc 1st Int Conf, Channels and Channel Control Structures, April 1984, ed Smith K V H, Springer Verlag, 1984, 4.21-4.36.

Knight D W and Hamed M E (1984), Boundary shear in symmetrical compound channels, Proc ASCE, J Hydreaulic Eng., vol 110, HY10, Oct. 1984, 1412-1430.

Knight D W and Sellin R H J, (1987), The SERC Flood Channel Facility, J Inst Water and Env. Management, London, vol 1, no 2, 1987, 198-204.

Knight D W and Shiono K, (1990), Turbulence measurements in a shear layer region of a compound channel, J Hydraulic Research, vol 28, no 2, 1990, IAHR, Delft, 175-196

Knight D W, Shiono K and Pirt J, (1989), Prediction of depth mean velocity and discharge in natural rivers with overbank flow, Conf. on Hydraulic and Environmental Modelling of Coastal, Estuarine and River Waters, ed. Falconer, Goodwin and Matthew, Gower Tecnical Press, 1989, 419-428.

Knight D W, Samuels P G and Shiono K, (1990), River flow simulation: research and developments, J. Inst. Water and Environmental Management, vol 4, no 2, April, 1990, 163-175

Knight D W and Yuen K W H (1990), Critical flow in a two stage channel, Int. Conf. on River Flood Hydraulics, Sept 1990. Hydraulics Research, Wallingford, Wiley and Sons, 1990.

Kouwen N, Li R N and Simons D B, (1981), Flow resitance in vegetated waterways, Trans Amer. Soc Agric. Engrs, vol 24,(3), 684-690, 698.
Larsen T, Frier J-O and Vestergaard K (1990), Discharge/stage relations in vegetated Danish streams, Int. Conf. on River Flood Hydraulics, Wallingford, Sept 1990, John Wiley and Sons, 187-196.

Leopold L B and Wolman M G, (1957), River channel patterns: braided meandering and straight, USGS Prof. Paper 282-B, 1957.

Limerinos J T, (1970), Determination of the Manning coefficient from measured bed roughness in natural channels, U S Geological Survey Water Supply Paper 1898-B, 1970.

Manning R, (1891), On the flow of water in open channels and pipes, Proc Inst Civil Engrs, Ireland, 1891 vol 20, p161, 1895 vol 24, p 179.

Morris H M, (1959), Design methods for flow in rough conduits, Proc American Soc. Civil Engineers, vol 85, HY7, July 1959, p 43.

Myers W R C, (1978), Physical modelling of a compound river channel, Proc. Int. Conf. on River Flood Hydraulics, Wallingford, Sept 1990, ed. W R White, John Wiley and Sons, 381-390.

Myers W R C, (1978), Momentum transfer in a compound channel, J Hydraulic Research, vol 16, IAHR Delft

Myers W R C, (1984), Frictional Resistance in channels with flood plains; Channels and channel control structures, 1st Int Conf, Southampton, England, 1984, ed K V H Smith, pub Springer-Verlag, 1984, p 4.73-4.87.

Myers W R C, (1985), Flow resistance in smooth compound channels, experimental data, University of Ulster, March 1985.

Myers W R C and Brennan E K, (1990), Flow resistance in compound channels, J Hydraulic Research, vol 28, no 2, 1990, IAHR, Delft, 141-156.

Nalluri C and Judy N D, (1985), Interaction between main channel and flood plain flows, Proc 21st Congress IAHR, Melbourne, Australia, p 377-382.

Nikuradse J, (1933), Stronungsgesetze in rauhen rohren, VDI Forschungsheft, 1933, p 361.

Nikuradse J, (1932), Gesetzmabigkeit der turbulenten stromung in glatten rohhren, VDI Forschungsheft, 1932, p 356.

Patel V C, (1965), Calibration of the Preston tube and limitations on its use in pressure gradients, J Fluid Mechanics, vol 23, Part 1, 1965, 185-195

Petryk S and Grant E U, (1978), Critical flow in compound channels, ASCE, J Hyd Div, vol 104, HY5, 1978, 583-594

Powell K E C, (1978), Weed growth - a factor in channel roughness, Hydrometry, ed Herschy R W, John Wiley and Sons, 1978, 327-352.

Prandtl 1, (1933), Neuere Ergebnisse der Turbulenzforschung, ZVDI vol 77, p 105.

Prinos P and Townsend R D, (1983), Estimating discharge in compound open chanels, Canadian Soc for Civil Engineering, 6th Canadian Hydrotechnical Conference, Ottawa, Ontario, June 1983, p129-146.

Prinos P and Townsend R D, (1984), Comparison of methods for predicting discharge in compound open channels, Advances in Water Resources, 1984, vol 7, Dec, CML Publications, 180-187.

Radojkovic M, (1976), Mathematical modelling of rivers with flood plains, 3rd annual symp. Waterways, Harbours and Coastal div, ASCE, vol 1, rivers.

Radojkovic M and Djordjevic S, (1985), Proc 21st Congress IAHR, Melbourne, Australia, vol 3, p 368-371.

Rajaratnam N and Ahmadi R M, (1981), Hydraulics of channels with flood plains, J Hyd Research, vol 19, 1, 1981.

Ramsbottom D M, (1989), Flood discharge assessment - interim report, Hydraulics Research, Wallingford, SR 195, March 1989.

van Rijn L C, (1984) Sediment transport: part I: bed load transport; part II: suspended load transport; part III: bed forms and alluvial roughness, Proc ASCE, vol 110, HY 10, Oct 84, p 1431; HY11, Nov 84, 1613-1641; HY12, Dec 84, 1733-1754.

Rouse H, (1937), Modern conceptions of mechanics of fluid turbulence, Trans Amer. Soc. Civ. Engrs, vol 102, 1937.

Rouse H, ed (1950), Engineering Hydraulics, John Wiley and Sons, New York, 1950, reprinted 1961 etc.

Samuels P, (1989), The hydraulics of two-stage channels - review of current knowledge, Inst Water and Environmental Management, River Eng's Conf., University of Loughborough, July, 1989.

Samuels P, (1988), Lateral shear layers in compound channels, Fluvial Hydraulics 88 conf, VITUKI, Budapest, Hungary.

Sargent R J, Variation of Manning's n roughness coefficient with flow in open river channels, J. Inst Water Engineers, vol 33, no 3, 1979, 290-294

Sellin R H J, Giles A and van Beeston D P, (1990), Post-implementation appraisal of a two-stage channel in the River Roding, Essex, J. Inst Water and Environmental Mnagement, vol 4, no 2, April 1990, 119-130

Shields A,(1936), Anwendung der Ahnlichkeitsmechanik und Turbulenzforschung auf die Geschiebebewegung, Mittiel., PVWES, Berlin, no 26, 1936.

Shiono K and Knight D W, (1988), Two dimensional analytical solution for a compound channel, Proc 3rd Int. Symp. on Refined Flow Modelling and Turbulence Measurement, Tokyo, Japan, July 1988, 503-510.

Shiono K and Knight D W, (1990a), Mathematical models of flow in two or multi-stage straight channels, Int. Conf. on River Flood Hydraulics, Sept. 1990, Wallingford, ed White W R, John Wiley and Sons, Chichester, 1990, 229-238.

Shiono K and Knight D W, (1991), Turbulent open channel flows with variable depth across the channel - a general model and new data, J Fluid Mechanics, vol 222, September 1991, 617-646.

Strickler A, (1924), Beitrage zur frage der geschwindig-keitsformal und der rauhigkeitsahlen fur strome, kanale und geschlossene leitungen, Eidg. Wasserwirtshaftsamt Bern, Milleilung, 1923; Schweitz. Bauztg, 1924, vol 83, 23.

Thorne C R, Bathurst J C and Hey R D, (eds), (1987), Sediment transport in gravel bed rivers, John Wiley and Sons, 1987.

Toebes G H and Sooky A A, (1967), Hydraulics of meandering rivers with flood plains, Proc ASCE, vol 93, J Waterways and Harbours, no 2, May 1967, 213-236.

US WES, (1956), Hydraulic capacity of meandering channels in straight floodways, Tech. Memo. 2.249, Waterways Experiment Station, Vicksburg, Mississippi, March 1956.

Ven te Chow, (1959), Open channel hydraulics, McGraw-Hill, New York.

Wark J B, Samuels P G and Ervine D A, (1990), A practical method of estimating velocity and discharge in compound channels, Int Conf on River Flood Hydraulics, September 1990, HR, Wallingford, Pub J Wiley and Sons, 163-172.

Willetts B B, (1991), The hydraulics of meandering channels, Seminar on River and Flood Plain Management, 22 March, 1991, Scottish Hydraulics Study Group, Glasgow.

White W R, Paris E and Bettess R (1980), The frictional characteristics of alluvial streams: a new approach, Proc. Inst. Civil Engrs, vol 69, (2), 737-750.

White W R, Bettess R and Wang Shiqiang, (1987), Frictional characteristics of alluvial streams in the lower and upper regimes, Proc. Inst. Civil Engrs, vol 83, (2), 685-700.

White W R, Milli H and Crabbe A D, (1975), Sediment transport theories: a review, Proc Inst Civ Engrs, Part 2, June 1975, vol 59, 265-292.

Wormleaton P R, (1988), Determination of discharge in in compound channels using the dynamic equation for for lateral velocity distribution, Proc IAHR Conf. on Fluvial Hydraulics, Vituki, Budapest.

Wormleaton P R, Allen J and Hadjipanos P, (1982), Discharge assessment in compound channel flow, Proc ASCE, vol 108, J Hy Div, p 975-994

Wormleaton P R and Merrett, (1990), An improved method of calculation for steady uniform flow in prismatic main channel/flood plain sections, J Hydraulic Research, vol 28, no 2, 1990, IAHR, Delft, 157-174.

Yalin M S, (1977), Mechanics of sediment transport, 2nd ed., Pergamon Press, 1977.

Yang C T, (1972) Unit stream power and sediment transport, Proc ASCE, vol 98, HY10, Oct 1972, 1805-1826.

Yen B C and Yen C L, (1983), Flood flow over meandering channels, Rivers Meandering Conf, 1983, 554-561.

Zheleznyakov G V, (1985), Problem of the interaction of the main channel and flood plain flows, Proc 21st Congress IAHR, Melbourne, Australia, vol 3, p373 - 376.

The following form a limited circulation unpublished series "SERC flood channel research, Water Authority funded project for the development of a design manual, Technical Report Series, Consultant P Ackers".

1, Resistance functions for the Wallingford facility, August 1989.

2, Resistance functions for the Wallingford facility, rod roughness, Nov 1989.

3, The hydraulic resistance of compound channels, review and proposed method of approach, Nov 1989.

4, Review and analysis of research at Wallingford, in the context of empirical design methods, October 1990.

5, Review and analysis of other sources of data in the context of empirical design equations based on WFCF data, March 1991.

6, Skew channels, February 1991.

7, Turbulence methods, April 1991.

8, Irregular plan form, April 1991.

9, Sediment transport in compound channels, April 1991.

13. NOMENCLATURE

NOTE: The nomenclature is not unique. To follow established convention and to avoid an excess of subscripts and Greek symbols, some characters are used in more than one sense. The context in which they appear will make clear which is intended.

A	Cross sectional area
A, B	Parameters in the logarithmic smooth-turbulent velocity distribution
A, B	Empirical coefficients
A_{gr}, C_{gr}, F_{gr}, G_{gr}, m_{gr}, n_{gr}	Parameters in sediment transport function
ARF	An adjustment factor in the Region 1 functions to allow for the effect of main channel width/deth ratio (aspect ratio)
B	Half total width of channel plus berm or berms (flood plains), at the elevation of the berms (flood plains). If the berms slope and are partially inudated, B is taken as half the water surface width
b'	Mean width, defined as area/flow depth (normally with subscript for main channel or flood plain)
bw	Bed width (normally with subscript for channel, flood plain)
b_C	Half bed width of main channel
b_F	Bed width of one of a pair of berms or flood plains
B, b	Parameters in a generalised form of the exponential smooth-turbulent Blasius equation
C, D	Parameters in a generalised form of the logarithmic smooth-turbulent law
C, C_o	Concentration of suspended solids, reference value at prescribed elevation, z_o
C_D	Drag coefficient of rods
COH	Channel coherence; subscript indicates method of calculation
D	Pipe diameter; sediment diameter
D_{gr}	A dimensionless indicator of grain size
d	Flow depth; diameter of rods forming roughness
DISADF	Factor by which zonal calculation has to be multipied to allow for interference
DISDEF	Difference between zonal calculation of discharge and actual flow
DISDEFBF	Ratio of DISDEF to bank full discharge
e	Base of Naperian logarithms, denoted by ln
F_T ,C,F	Adjustment factors

F_{ROD}	form drag of rods per unit channel length
f	Friction factor, $8gRS/V^2$
f_S	Friction factor arising from smooth channel boundaries
f_{TOT}	Total of rod roughness and smooth perimeter resistance, expressed as friction factor
G	A parameter in predictive equation for region 1
g	Gravitational acceleration
H	Total flow depth; depth of flow in main channel
H_F	Flow depth on flood plain, H - h
h	Depth of main channel below berm level
H_*	Ratio of flow depths on flood plain and in main channel
K	Von Karman turbulence constant
K_V	Conveyance as conventionally defined, e.g. in Ven Te Chow
K_D	Conveyance, $Q/\sqrt{(8gS)} = A/\sqrt{(A/fP)}$
k_S	Linear measure of roughness, after Nikuradse and Colebrook White
ln	Logarithm to base e
log	Logarithm to base 10
N	Number of roughening rods per unit channel length
n	Manning's roughness coefficient, from $1/n = V/(R^{2/3}\sqrt{S})$
n	Number of rods in a transverse row
N_F	Number of flood plains
Q	Discharge
Q_{*1}	Discharge deficit (DISDEF) normalised by $(V_C-V_F)(H-h)h$
Q_{*2}	Discharge deficit (DISDEF) normalised by $(V_C-V_F)Hh$
q	Discharge intensity, i.e. discharge per unit width
q_S	Sediment transport rate as submerged weight per unit time per unit width
R	Hydraulic radius (or h.m.d.), cross section area/wetted perimeter
Re	Reynolds number, $4VR/\nu$
Re_*	Grain Reynolds number in sediment transport, v_*D/ν
Re_*	Roughness Reynolds number, $u_*\ kS/\nu$
s	Channel/flood plain side slope, horizontal/vertical
s	Relative specific weight/mass of sediment to fluid
s_{BF}	Slope of flood plain towards main channel
S	Hydraulic gradient of channel
SF_I	Shear force at interface
tw_c	Top width of channel

U	Mean velocity over the flow depth
u	Local mean stream velocity
u_*, v_*	Friction velocity, $\sqrt{(gRS)}$
V	Average flow velocity through cross-section, or with suscript through one zone of cross-section
W	Water surface width
w	Fall velocity of particles of sediment
w_C	Half width of main channel at elevation of bank top
Y	A non-dimensional form for bed shear stress in sediment transport
y	Local flow depth at point in cross-section
Z	Ratio of flow depth to sediment diameter
Z_*	Ratio of local flow depth to rod diameter, z/d
z	Distance from solid boundary; local flow depth
α	Velocity distribution coefficient
β	Blockage coefficient arising from rod roughness
δ	A correction term
Φ	Radojkovic interaction index; a function of ....
ρ	Density of fluid
τ	Shear stress
μ	Fluid viscosity
ν	Kinematic viscosity of fluid, μ/ρ
Ω	turbulence parameter for solids suspension

Subscripts:

AV	Average
BF	Bank full
B,basic	Basic values before allowing for interaction
C	Main channel
CALC	Calculated value
F	Flood plain
i	Interval: one of a series of values
I	Interface
MEAS	Measured value
R1, R2, R3, R4	Regions of flow behaviour
T	Total i.e. main channel plus flood plains
*	Ratio between flood plain and main channel values (except where otherwise defined)

Appendices

APPENDIX 1

DIMENSIONAL ANALYSIS APPLIED TO COMPOUND CHANNELS

1. The *independent variables* that determine steady uniform friction-controlled flow in a prismatic compound trapezoidal channel are the fluid properties, the roughness of the surfaces, gravity, channel slope and cross-section geometry:

ρ - mass density of fluid
μ - fluid viscosity
k_{SC} - roughness of main channel perimeter
k_{SF} - roughness of flood plain
g - acceleration due to gravity
S - slope of channel
b_C - half bed width of deep channel
b_F - bed width of each flood plain
s_C - side slopes of deep channel, 1 vertical to sc horizontal
s_F - side slopes of flood plain edges
h - depth of main channel
H - total flow depth, measured over deep channel

The dependent variables include:

Q_T - total discharge in the compound section
Q_C - component discharge in deep channel
Q_F - component discharge in the flood plains
V - average velocity over whole cross section
V_C;V_F - component average velocities etc.

Any *dependent variable* is a function of the independent variables listed:

$$DVAR = \Phi\ [\ \rho,\ \mu,\ k_{SC},\ k_{SC},\ g,\ S,\ b_C,\ b_F,\ s_C,\ s_F,\ h,\ H\ ] \qquad \text{...A1.1}$$

2. These 12 independent variables will yield 9 dimensionless groups, which could be derived in many different ways. To proceed, it is desirable to introduce similarity concepts, such as those familiar when dealing with friction controlled flow in simple cross-sections. Taking total discharge

as the dependent of immediate practical concern, and also linking S with g because it is the weight component down the slope that has physical significance, and considering the system as one channel:

3. *Single channel method*

$$\frac{Q^2P}{8gS^3} = \Phi \left\{ \frac{Q/P}{\mu/\rho}; \frac{H}{H-h}; \frac{Q}{\sqrt{(gA/W)}}; \frac{k_{SC}}{H}; \frac{k_{SF}}{H-h}; \frac{b_C}{H}; \frac{b_F}{H-h}; s_C; s_F \right\} \qquad \ldots A1.2$$

where

A = total cross-section area = $\Phi_A[\, b_C;\ b_F;\ s_C;\ s_F;\ h;\ H \,]$
P = total wetted perimeter = $\Phi_P[$ ditto $]$
W = total water surface width = $\Phi_W[$ ditto $]$
ν = kinematic viscosity, μ/ρ

These dimensionless groups are recognisable as:

$\frac{Q^2P}{8gSA^3}$	= 1/f where f is the friction factor treating the whole section as one
$\frac{Q/P}{\nu}$	= Reynolds number of whole section
$\frac{Q}{\sqrt{(gA/W)}}$	= Froude number for whole section
$H/(H-h)$	= ratio of channel flow depth to that on flood plain
k_{SC}/H	= relative roughness of channel
$k_{SF}/(H-h)$	= relative roughness of flood plain
b_C/H	= width/depth (aspect) ratio of main channel
$b_F/(H-h)$	= width/depth (aspect) ratio of flood plain
s_C	= side slope of main channel
s_F	= side slope of flood plain

4. If we are to proceed on these lines, treating the whole section, then some simplification is possible if we confine attention to:

(i) Rough-turbulent conditions on flood plain as well as in the deep channel (when viscous effects are no longer significant)

(ii) Velocities low enough to avoid energy lossses due to surface waves (when the Froude number becomes irrelevant).

Also the side slopes of the main channel may become less significant if the aspect ratios are based on mean channel widths, b_C' and b_F', so that we may then reduce the problem to one with 7 independent variables, with two (bracketted) of lower significance perhaps:

$$\frac{Q}{(8gSA^3/P)} = \frac{1}{\sqrt{f}} = \Phi \left\{ \frac{H}{H-h}; \frac{k_{SC}}{H}; \frac{k_{SF}}{H-h}; \frac{b_C}{H}; \frac{b_F}{H-h}; \frac{b_F}{H-h}; (s_C); (s_F); \right\} \qquad \ldots A1.3$$

If there is equal roughness on flood plain and in channel, this further simplifies to:

$$f = \Phi \left[H/(H-h); k_S/H; b_C'/H; b_F'/(H-h) \right] \qquad \ldots A1.4$$

5. In general, single channel approaches use a restricted sub-set of the above:

$$f = \phi_1 \left[k_S/R \right] \times \phi \left[H/(H-h); b_F'/b_C' \right] \qquad \ldots A1.5$$

...A1.5

where R is the hydraulic mean depth of the whole section (replacing H in the preceding form) and the aspect ratios of the separate zones are replaced by the ratio between their widths.

6. Splitting dimensionless statements in this way is strictly not permissible, however. Consider the general relationship:

$$c = \phi \left[a; b \right] \qquad \ldots A1.6$$

Replacing this by:

$$c = \Phi_1[\ a\ ] \times \Phi_2[\ b\ ] \qquad \text{...A1.7}$$

limits the relationship to one that would plot as a set of parallel curves on a log-log plot, clearly much less general than the function it seeks to replace.

Replacing it by:

$$c = \Phi_1[\ a\ ] + \Phi_2[\ b\ ] \qquad \text{...A1.8}$$

means restricting it to a set of parallel curves when plotted to linear axes. So although split dimensionless statements are convenient, especially in terms of data analysis, whether or not they are acceptable is a matter requiring justification. It is common in design practice to split complex relations by assuming that the various factors influencing a process can be allowed for separately, i.e. assuming the various factors do not interact, but the legitimacy of this procedure requires testing in the particular case under review.

7. *Divided channel method*

Continuing the assumption that viscous and surface wave influences are negligible, the divided channel approach in its basic form separates the cross-section into deep channel and flood plain zones. Various assumptions about the planes of division between the zones have been considered in the past, but here they are vertical plains at the bank line, and the interface so created is not included in the wetted perimeter of either zone. With the further assumption that the effect of the aspect ratio is solely on friction loss so that it may be accounted for by using the hydraulic mean depth, the method is basically as follows:

$$Q = Q_C + Q_F \qquad \text{...A1.9}$$

where

$$Q_C = \sqrt{(8gSA_C^3/P_Cf_C)} \qquad \text{...A1.10}$$

and

$$Q_F = \sqrt{(8gSA_F^3/P_Ff_F)} \qquad \text{...A1.11}$$

$$f_C = \Phi_C \, [\ k_{SC}P_C/A_C\ ] \qquad \text{...A1.12}$$

$$f_F = \Phi_F \, [\ k_{SC}P_F/A_F\ ] \qquad \text{...A1.13}$$

8. The above is defective as it ignores any interaction effect between the separate zones. Hence we must introduce correction factors, F_C and F_F to adjust the calculated channel and flood plain flows for the effect of their interaction, or an overall correction factor for the total flow, F_T;

$$Q_T = F_T \times (Q_C + Q_F) \qquad \text{...A1.14}$$

9. In the above, Q_C and Q_F are the basic values calculated from the friction formulae appropriate to their particular features, e.g. smooth, rough or transitional. The correction factors will be functions of other flow or geometric parameters. The minimum requirement from purely dimensional considerations is:

$$F_C = \Phi_1[\ H/(H-h);\ k_{SC}/H;\ k_{SF}/(H-h);\ b_C'/H;\ b_F'/(H-h);\ s_C;\ s_F\ ] \qquad \text{...A1.15}$$

$$F_F = \Phi_2[\ \text{ditto}\ ] \qquad \text{...A1.16}$$

and

$$F_T = \Phi_3[\ \text{ditto}\ ] \qquad \text{...A1.17}$$

10. Different authors have used different restricted forms of the above, perhaps related to the scope of experiments they have made, for example:

$$F_{C,F,T} = \Phi_{(1,2,3)}\ [\ H/(H-h);\ f_F/f_C;\ b_F/b_C\ ] \qquad \text{...A1.18}$$

For equal roughness on flood plain and in main channel, this would reduce to sets of curves giving correction factors plotted against relative depth, $H/(H-h)$, with the width ratio as the third variable for each set. Different sets would be required for different values of the friction factor ratio - but a further four possibly relevant parameters have also to be accounted for, or shown to be insignificant. (Four because the seven parameters of equs A1.15 to 17 have been reduced to three)

11. Let us consider the features to be expected where both the flood plains and main channel are very wide relative to their flow depths: in the limit this is the junction at a bank line of two semi-infinite sheet flows. The expectation in that case is for the flow to be affected for a limited zone either side of the bank line, and is is worth considering therefore using an *additive/subtractive* correction to the flows either side of the bank rather than using *multiplying* correction factors. In the wide channel case, then:

$$Q = Q_C + Q_F \qquad \text{...A1.19}$$

where

$$Q_C = Q_{Cb} + \delta Q_C \qquad \text{...A1.20}$$

$$Q_F = Q_{Fb} + \delta Q_F \qquad \text{...A1.21}$$

Q_{Cb} and Q_{Fb} are the channel and flood plain flows calculated by the appropriate resistance equation for the main channel and flood plains respectively, ignoring any interaction effects: the additive/subtractive corrections take account of the actual interaction. The question then arises as to how best to "normalise", i.e. convert to non-dimensional form, these discharge corrections. An argument can be developed that they should be normalised by the local flow parameters characterising the junction between the assumed semi-infinite sheet flows, e.g. $(H-h)^2(V_C-V_F)$.

12. The implication behind this is that the cross-section of the zone of influence has dimensions related solely to the depth on the flood plain,

and any velocity defect/increment is basically proportional to the difference between main channel and flood plain velocities. However, Rajaratman and Ahmadi (1981) considered this very point on the basis of experiments in a vertical sided compound channel and demonstrated that the width of the zone of influence was proportional to bank full depth, h, so that normalisatiom by $h^2(V_C-V_F)$ or $hH(V_C-V_F)$ might prove preferable.

13. Zheleznyakov (1985) had earlier suggested the concept of additive or subtractive corrections to the flood plain and main channel flows and demonstrated that it was the loss of main channel flow rather than any increase in flood plain flow that dominated the situation. He went on to suggest that changes could be expressed in terms of bank full flow. This would not be appropriate for very wide systems approaching the semi-infinite situation hypothecated above, however.

14. Thus there are several alternative concepts for normalising the suggested discharge correction. From the pragmatic point of view, bank full discharge is a straight forward quantity to use, but so also are the alternatives. Only by comparing the possible normalising procedures when analysing experiments can we decide on the most relevent non-dimensional groupings. For very wide systems, the semi-infinite concept would lead to:

$$\delta Q_T/(H-h)^2(V_C-V_F) = \Phi_{\delta T}\ [\ H/(H-h);\ f_F/f_C;\ s_C] \qquad \text{...A1.22}$$

though from the dimensional analysis viewpoint the term (H-h) in the left parameter could equally well be any combination of H and h with the dimensions of an area, e.g. (H-h)h or Hh.

15. To cover compound channels in general, the function would have to allow for the restriction of the flow interaction by the channel width and edge of the flood plain. The relevant aspect ratios have therefore to be re-introduced. Also, because of viscous influences, especially in smooth laboratory channels, it is conceivable that the Reynolds number may be significant, although it is hoped that the friction factors would be a sufficient flow description for both smooth and rough situations. The generalised statement thus becomes:

$$\delta Q/(\text{Area})(V_C - V_F) = \Phi_{\delta T}[\ H/(H-h);\ f_F/f_C;\ s_C;\ b'_C/H;\ b'_F/(H-h);(s_F)] \quad \ldots A1.23$$

where (Area) is intended to cover any product of two independent variables of length dimensions to give a plausible area of influence. Combinations of interest might be Hh, (H-h)h, 2bH etc. As the FCF at Wallingford has a fixed value of main channel aspect ratio, 2b/h = 10, in terms of data analysis the use of Hh or 2bH would not be distinguishable: the latter is always 10 times the former, and the issue could only be resolved by resorting to other data sources with different main channel aspect ratio.

16. This concept, equivalent to additive/subtractive correction to the overall flow (or more basically in the separate zones of flow) can be tested alongside other methods, for example the use of discharge adjustment factors either for the separate zonal calculations or for the sum of those basic discharges. There is no reason from the dimensional analysis viewpoint to prefer any particular method of expressing the required correction to the basic calculated flows. The criteria for choice might include:

- goodness of fit
- insensitivity to some variables
- simplicity of function e.g. linearity
- convenience of application in hydraulic design

APPENDIX 2

RESISTANCE FUNCTIONS FOR THE SERC-FCC AT WALLINGFORD

1. *Background*

1.1 The Flood Channel Facility at Hydraulics Research, Wallingford, consists of a compound channel moulded in cement mortar. It is of fixed gradient, although a number of alternative cross-section geometries has been tested. Tests were conducted by several independent research groups concentrating on different aspects, but in all cases important flow parameters were the discharges at which the experiments have been conducted and the corresponding mean depths of flow relative to the bed of the main channel. From discharge and depth, with the known fixed gradient of about 1 in 1000, all other conventional measures of channel performance can be calculated, e.g. mean velocity, Froude number, friction factor, Reynolds number etc.

1.2 In the context of analysing the experimental results for the preparation of a design manual, the resistance of the channel is of prime importance, and this required the establishment of the most appropriate resistance formula for the Wallingford channel, based on the analysis of experiments conducted on channels without flood plains. If the function were not a good fit for simple channels, there would be much less prospect of identifying and formulating the additional resistance arising under compound flow conditions: and indeed misleading conclusions could emerge. Hence a priority task was a review of the basic resistance function. It must be stressed that the conclusions in this Appendix relate specifically to the Wallingford channel: they do not apply to the rougher channels in engineering practice.

1.3 It might be thought that the choice of the Colebrook-White transition function would have been automatic and uncontentious bearing in mind that it has been in general use, at least for the smoother range of manufactured and constructed surfaces, for both pipes and channels. If that had been the case, all that would have been necessary was to assess a suitable value of k_S. Analyses of the data by the various research teams, however, left the matter in some doubt, because the different groups had used different basic functions, including forms of smooth turbulent equation, the turbulent transition function of Colebrook-White and Manning's equation, as well as friction factor/Reynolds Number plots.

1.4 A perhaps surprising feature of the previous analyses was that several alternative resistance laws were, at face value, equally valid, even equations such as Manning's, which is normally regarded as restricted to rough channels, providing a good fit with constant n for the simple channels. To avoid continuing confusion, as well as to provide a sound basis for further analysis of stage/discharge data, reconsideration of the basic resistance function was therefore considered essential.

2. *Brief review of resistance functions*

2.1 Most text books on hydraulics contain a review of hydraulic resistance, and include a friction factor/Reynolds number diagram (often ascribed to Moody, see for example Chadwick and Morfett, 1986) based on the Colebrook-White transition function. Almost without exception, this diagram will relate to pipe flow but a method of conversion to open channels or non-circular cross-sections may be given, using the equivalence for circular sections, namely :

$$R = D/4 \qquad \ldots 2.1$$

2.2 This is an oversimplification, because the Colebrook-White formula derives from the smooth turbulent and rough turbulent functions obtained by integrating the logarithmic velocity distribution law over the flow cross-section. There are constants of integration that depend on the shape of section, and so an additional adjustment is required over and above the R = D/4 conversion. In normal engineering the distinction is not very important (because of uncertainties elsewhere in the design process), but in the accurate analysis of research results it could be significant. The two versions of the rough turbulent equation in the literature, for circular and wide open-channels respectively, are:

Circular sections:

$$1/\sqrt{f} = 2 \log (k_S/3.7D) = 2 \log (k_S/14.8R) \qquad \ldots 2.2$$

Wide open-channels:

$$1/\sqrt{f} = 2 \log (k_S/12.3R) \qquad \ldots 2.3$$

This last form was obtained by Keulegan (1938) who also showed that a similar correction for channel shape is required for smooth turbulent flow. The corollary to this is that if the Colebrook-White transition function is to be adjusted for shape, botwb elements require the same adjustment factor (Ackers, 1958) so that the two versions of the function are:

Circular sections:

$$1/\sqrt{f} = -2 \log [(k_S/14.8R) + (1.255\nu/R\sqrt{(32gRS)})] \qquad \ldots 2.4$$

Wide open-channels:

$$1/\sqrt{f} = -2 \log [(k_S/12.3R) + (1.510\nu/R\sqrt{(32gRS)})] \qquad \ldots 2.5$$

Unfortunately the need for adjustment to the smooth term is not so generally recognised so that sometimes the wide channel adjustment is made only to the roughness term in the transition function. In what follows, the wide-channel transition function will be taken as equ. 2.5.

2.3 A major distinction between smooth and rough turbulent flows is the influence of fluid viscosity on the resistance function: in the former case, the friction factor, f, depends on Reynolds number, decreasing with increasing size and velocity; in the latter case, the friction factor is independent of Reynolds number. This distinction also results in only rough turbulent flow following a square law of resistance, i.e. velocity being proportional to the square root of hydraulic gradient (other parameters of flow being unchanged). The very popular "square law" Manning equation may be thought of as an approximation to equation 2.2 or 2.3, with Manning's n given by $k_S^{1/6}/26$ (k_S in mm) It can be shown that the approximation is close for relative roughnesses R/k_S between about 10 and 100, which confirms application to many of the rougher engineering constructions and to natural channels. It follows from the form of the Manning equation that it should only be applied to rough turbulent flow, when the flow is not being influenced by viscosity and so is independent of Reynolds number.

2.4 The transition between rough and smooth turbulent flows embodied in the Colebrook-White function allows for the progressive change from viscosity dominated flow to roughness dominated flow as the Reynolds number increases. The form this transition takes in a friction factor/ Reynolds number plot is not fixed, but depends on the character of the roughness: for example, the Nikuradse diagram for a uniform coverage of glued-on sand grains has different transitions from the Moody/Colebrook White chart which is for isolated protuberances. The latter has a much more gradual and extended curve into the smooth law and this is thought to arise because the isolated roughness elements continue to exercise a local disruption on the laminar sub-layer: they are not so readily submerged as is the uniform coverage of grains with equal k_s value.

2.5 An important distinction between experiments conducted on pipes and those on open channels is that the former will be at a constant relative roughness, because in any test series both surface texture and flow cross section remain constant: it is the hydraulic gradient (slope) which varies as the discharge is varied. Open channels, on the other hand, have the flexibility of cross-section change: whether they are at constant slope or variable slope will depend on the experimental arrangement, but the Wallingford flood channel facility imposes constant slope, so that relative roughness is not constant. Thus any sequence of test results for a fixed gradient open channel runs across the constant relative roughness lines on a Moody- type diagram rather than following one of them.

2.6 Myers and Brennan (1989) when analysing the Wallingford data generalised the smooth turbulent function to the following:

$$1/\sqrt{f} = C \log (Re\sqrt{f}) - D \qquad \text{...2.6}$$

The smooth component of the Colebrook-White formula for pipes sets C = 2.00 and D = 0.80, values deduced from Nikuradse's tests on pipes many years ago. They were empirical adjustments to values deduced theoretically from the velocity distribution: 2.03 was considered a more fundamental value of C, corresponding to the generally accepted value for the turbulence constant, K, of 0.40. For wide open channels, Keulegan had suggested D = 1.08. Using a slight variant of equ. 2.4 (Henderson, 1966), a k_S value of 0.06mm was deduced for the Wallingford channel. Myers and Brennan reasoned that as $Re_* = u_* k_S/\nu$ had a maximum value about the same as the value of 4 suggested by Henderson as an upper limit for smooth turbulent flow, the flow should indeed be considered as smooth turbulent throughout. However, the limit of 4 is more appropriate to a uniform sand textured surface, being based on Nikuradse's rough pipe experiments: the Colebrook-White transition extends from $Re_* = 0.3$ to 50, so the question about whether the flow should be considered as smooth rather than transitional was unresolved.

2.7 The form of equation 2.6 indicates that the main influence of any variation in the term D is to provide a vertical shift to a plot of $1\sqrt{}/f$ against Re. The effect of channel shape obtained by integrating the velocity distribution accounts for a change in D of 0.17: $(0.5 - \ln 2)/K\sqrt{}/8 \simeq 2(\log 14.8 - \log 12.3)$. However, since the time when Keulegan studied the question, a great deal of additional experimental evidence on turbulent flows has become available which has providing updated equations for the turbulent velocity distribution in smooth channels, which in turn lead to up-dated open channel friction functions.

2.8 The logarithmic velocity distribution law for smooth boundaries takes the form:

$$v/v_* = A \ln(v_* z/v) + B \qquad \ldots 2.7$$

where v is the local velocity at distance z from the wall, and v_* is the shear velocity at the wall $(=\sqrt{}(\tau/\rho))$. There is still some contention over the best values of A and B, which are essentially empirical as they depend on experimental measurement of velocity distribution. The generally accepted values in a historic context have been those due to work by Nikuradse (1932), Clauser (1954), Patel (1965) and the consensus from the Stanford conference of 1968.

2.9 Integrating the velocity distribution over the depth for a wide open channel gives equation 2.6, where:

$C = 2.3026\ A/\sqrt{8}$ ...2.8

$D = -\ (1 + \ln 4\sqrt{8})A + B$ ...2.9

and on this basis it is possible the smooth channel resistance functions that may derived from the 'historic' velocity distributions may be compared:

Source	Date	A	B	C	D
Nikuradse	1932	2.50	5.50	2.035	1.083
Clauser	1954	2.49	4.90	2.027	1.283
Patel	1965	2.39	5.45	1.946	0.968
Stanford	1968	2.44	5.00	1.986	1.188

2.10 From the appearance and feel of the moulded surface at Wallingford, it is apparent that the surface is not far from smooth: it certainly can not be characterised as rough. In those circumstances the Manning equation would not be expected to provide a good fit to resistance data without using the coefficient, n, in an artificial way to illustrate the departure from rough turbulent "square law" resistance: yet as previously mentioned it provides a surprisingly good fit without varying n. The reason for this will be discussed in detail later, but one factor is that open channel tests at constant gradient are not well conditioned to distinguish between smooth turbulent, rough turbulent and transitional conditions, given that all contain at least one parameter which is based on the particular set of experiments. A shift from the classical smooth turbulent line on an f, Re plot, whilst remaining approximately parallel to it, can be obtained by altering D in the logarithmic smooth-turbulent formula, by a non-zero value of k_S in the transition formula for a wide channel (or indeed in the corresponding pipe equation) or by varying depth and hence relative roughness in a rough turbulent formula.

2.11 These three equations are shown in fig A2.1: the Myers and Brennan (1990) modified smooth turbulent equation, the wide channel transition function with kS = 0.07 mm and the Manning equation with n = 0.010. The upper diagram shows the conditions for the Wallingford main channel cross-section at a gradient of 1:1000: only at the shallowest flows is there much difference between the three functions.

2.12 On the basis of this review, from purely theoretical considerations the Manning equation should be ruled out on the grounds that applying a rough turbulent equation to a rather smooth channel at slack gradient would be misleading. Any agreement with the Manning equation is the fortuitous result of having a fixed gradient. Had the gradient varied, a fixed Manning's n could not have provided an acceptable fit to the data. In fact, the flow is not rough turbulent and some viscous influence is expected. The appropriate resistance function from theoretical considerations alone is expected to be the transition law or a modification of the smooth turbulent law.

3.*Analysis of resistance calibration data*

3.1 Depth discharge data were obtained in the various phases of the investigation for 'simple', i.e. non-compound flow conditions, with bank side-slopes of 2:1 (hor:vert), 1:1 and vertical. In all cases the bed width was 1.5 m and the channel hydraulic gradient very close to the mean channel gradient of 1.027/1000. The average stage was obtained by taking the mean of the measured depths over the experimental length of well established uniform flow, the discharge was measured by orifice meters in the supply lines, the hydraulic gradient was assessed from the slope of the total energy line. Velocity was derived from continuity, knowing the mean cross sectional area. Viscosity was obtained from the water temperature. On the whole, the water temperature remained close to 15°C. Unfortunately at the time this analysis was carried out not all the measured temperatures had been added to the data set, and where they were missing a figure of 15°C was assumed, but in view of the small variation from this standard value any error introduced would be insignificant. (This assumption did not apply to the analysis of compound channels: measured temperatures were then available.)

3.2 There were four sets of information referred to as channels 1 to 4:

Channel number	Side slope, s	Date of experiments	Number of tests	Depth range mm
1	2	Jan-Feb 89	14	45 - 150
2	1	Nov 86-Sept 87	28	25 - 149
3	1	Sept 87	13	150 - 296
4	0	Oct-Nov 88	11	40 - 148

(These dates refer to the bulk of tests at the stated side-slope: a few tests at other dates are included)

Channel 3 relates to tests carried out as an extension to those on channel 2, having extended the banks upwards with temporary side slopes to cover the range of depths of interest with over-bank flow. One of the tests on channel 2 seemed to be away from the general trend, so some analyses were made omitting it, though with very little effect on the overall picture. As channels 2 and 3 were in essence one channel tested over different depth ranges, some analyses were made combining these data: and also combining all four data sets.

3.3 There has been an observable change in the surface texture of some sections of the main channel with time. There are some hard, possibly calcareous deposits over sections where the bed level was marginally below the perfect line. These have perhaps occurred because of slower draining and subsequent drying out in these zones in the periods between tests, so giving a deposit from the hard laboratory water. The texture of these zones seemed even smoother to the touch than the original surface (they were somewhat slippy) but they may have introduced minor irregularities that could have increased roughness rather than reducing it. A secondary objective of the data analysis was to show whether any change was significant.

3.4 The equations considered were:

- Colebrook-White transition in original form, equ 2.4
- The same but modified for wide channels, equ 2.5

- Manning equation
- Generalised smooth turbulent, equ 2.6

The aim of the analysis was to find the best fit coefficient values for the data set, and then to assess the variation about that function by calculating the root mean square error, both as a percentage and as an absolute error in predicted velocity. The first two equations have k_s as the empirical coefficient; Manning's n applies to the third. The generalised smooth turbulent function has two parameters, C and D, which give greater flexibilty in the fitting procedure - effectively a shift from the smooth turbulent law and a tilt if need be. The results are given in Table A2.1.

3.5 The broad conclusion from the results in Table A2.1 is that there is not much to choose between the four equations tested. The Colebrook-White transitional equation is in most cases marginally the worst whether in terms of percentage discrepancy or absolute discrepancy, but it is also apparent that most of the discrepancy from any of the equations is due to inevitable experimental tolerances rather than basic inadequacy of the theoretical functions. Apart from channel 1 (2:1 side slopes), the wide-channel modification of the C-W equation is a slightly better fit. Perhaps surprisingly, the Manning equation is better than either form of transition, whether taking data sets separately or in combination. Despite its extra degree of freedom, only in one case (channel 4, vertical sides) does the generalised smooth turbulent function turn out to be significantly better than the others. In this particular case, values of A and D have emerged from the best-fit routine that differ considerably from those for the other data sets: they have provided a tilt that better accommodates these particular results.

3.6 The k_s values for the C-W and wide-channel equations provide a sensitive measure of any roughness changes with time. For the wide-channel formula, the mean value of k_s for the first set of experiments carried out from November 1986, to January 1987 on the channel with 1:1 side slopes (channel 2) was 0.071 mm: a low value indicating how nearly smooth the steel floated finish to the channel was. This increased in tests made in September, 1987 on channel 2 to about 0.090 mm, showing marginal roughening but within the range of experimental error. Further tests in with the same side-slope of 1:1 but at depths above 0.15 m, also in September 1987, gave k_s = 0.046 mm, seemingly smoother. Later tests in October and November 1988 with vertical sides (channel 4) gave a value of 0.111 mm, but then tests made in January and February 1989 with side slopes of 1:2 (channel 1) yielded a mean roughness of 0.010 mm, implying virtual smoothness, and suggesting that the deposition has smoothed rather than roughened the channel. However, the deposits were already present in the 1988 tests.

3.8 The Manning roughness values provide a somewhat less sensitive measure of any change in resistance of the basic channel. The first tests results may be regarded as setting a standard and then the average values from subsequent groups of tests can be used to indicate a percentage increase or reduction in calculated velocity or discharge, as in the following table:

Channel number	Side slope H:V	Test date	Mean n	Percentage change in V Increase Smoother	Percentage change in V Reduction Rougher
2	1:1	Nov 86 - Jan 87	0.01000	-	-
2	1:1	Sept 87	0.01014		1.4
3	1:1	Sept 87	0.01002		0.2
4	Vert	Oct - Nov 88	0.01001		0.1
1	2:1	Jan - Feb 89	0.00965	3.5	

3.9 Factors apart from change of surface texture with age may influence calculated values of k_s and Manning's n, for example any effect of change in cross sectional shape not fully accounted for by the hydraulic radius R. The conclusion, however, is that any changes of roughness were minor and with no apparent direct association with age. Thus all test data may be regarded as a single set for a channel of constant roughness. Bearing in mind experimental tolerances, real change can not be identified with any confidence. Thus all test data were regarded as a single set for a channel of constant roughness.

3.10 Returning to the choice of a preferred resistance function, tests over a wide range of depths are best suited to this purpose. The 40 tests on channels 2 and 3 covered depths from 25-300mm, and a Reynolds number range from 20 000 to 900 000. Table A2.1 shows the order of performance to be:

1- Manning;

2- modified smooth-turbulent equation (S-T);

3- wide channel;

4- Colebrook-White equation (C-W).

The distinction is small, and does not by itself provide a rational basis of selection. All have a percentage discrepancy of between 1.7 and 2.0 percent. However, careful inspection of the detailed plots showed that the modified S-T equation had best followed the trend of data at shallow depths. Figs A2.2 and A2.3 show the discrepancy between computed velocity and measured velocity for channels 2 and 3 (1:2 side slopes) and for all results respectively. (Actual velocities were of the order of 0.5 m/s at minimum depth, 0.8 m/s at a depth of 0.15m, bank full when operating as a compound channel, and 1.2 m/s at maximum depth of 0.3 m.) Although shallow depths in the main channel are not important, they are significant in the analysis of compound channels: some of the most illuminating results were expected to be those with shallow flows over the flood plain. Thus the preferred equation was the generalised smooth- turbulent function with C = 2.02 and D = 1.38, i.e.

$$1/\sqrt{f} = 2.02 \log (Re\sqrt{f}) - 1.38 \qquad \text{...3.1}$$

3.11 This is is remarkably close to the resistance law deduced from the velocity distribution by integration for the wide channel case with Clauser's (1954) parameter values (C = 2.027, D = 1.283). It is a little further removed from the classic smooth turbulent law of Nikuradse, in effect shifting several percent towards increased resistance. As already mentioned the classic Keulegan value for the second parameter for wide channels is 1.08, so equation 3.1 is a further shift of 0.3 in the $1/\sqrt{f}$ value. Reference to the more recent work by Clauser suggests that this might largely be explained without recourse to any significant increase in resistance over a smooth surface, although the Stanford consensus would still leave a change of 0.20 in the value of D to be explained as increased resistance.

3.12 Morris (1959) put forward some novel concepts on resistance functions, distinguishing between three types of flow:

- semi-smooth turbulent generated by isolated roughness elements
- hyper-turbulent, where there is interference between the wakes from roughness elements
- quasi-smooth, where there were additional localised sources of energy loss, such as flow skimming over grooves

The last of these provided a shift in the friction factor / Reynolds number plot whilst remaining parallel to the smooth- turbulent line. Possibly the Wallingford facility is following this quasi-smooth function because of such localised additional energy losses, even if they cannot be identified. Whether the resistance law of equ 3.1 represents quasi-smooth or fully smooth flow with full allowance for channel shape is immaterial in terms of data analysis. Because many readers will be unfamiliar with the term quasi-smooth, the latter explanation has been adopted in the main report.

3.13 There remains the question of why the Manning equation provides a good fit to data from a smooth channel. The Manning equation is exponential rather than logarithmic, and a well-known exponential smooth-turbulent formula is that proposed by Blasius (1913):

$$f = 0.08\ Re^{1/4} \qquad \ldots 3.2$$

This was derived as a good fit to experimental data over a particular range of Reynolds number, but let us examine a more general form of the Blasius type of formula:

$$f = B\ Re^{-b} \qquad \ldots 3.3$$

which can be expressed in detail as:

$$8\ gRS/V = B\ (4VR/\nu)^{-b} \qquad \ldots 3.4$$

This in turn yields:

$$V = R^{(1+b)/(2-b)}\ S^{1/(2-b)}\ [8g\ 4^{b}/B\nu^{b}]^{1/(2-b)} \qquad \ldots 3.5$$

3.14 For R to appear to the 2/3 power as in the Manning equation, b must equal 0.2, not very different from the Blasius value of 0.25. Inserting this value then gives a Manning "look alike":

$$V = R^{2/3}\ S^{1/2}\ (8g/B)^{5/9}\ (4/\nu)^{1/9}\ S^{1/18} \qquad \ldots 3.6$$

Thus one could consider the application of Manning in the present context to be for quasi-smooth conditions with the coefficient n depending on viscosity, gravity and hydraulic gradient as opposed to its usual role as a descriptor of surface texture:

$$n = [(8g/B)^{5/9}\ (4/\nu)^{1/9}\ S^{1/18}]_{-1} \qquad \ldots 3.7$$

Because slope remained constant and water temperature approximately so in the Wallingford tests, the Manning equation provided a good fit: n as defined by equation 3.7 remained constant. If the Blasius value of b had been retained, namely 0.25, then the hydraulic mean depth would be raised to power 0.714 rather than 0.667, but conceivably would have also given a good fit.

3.15 For the best fit value of n = 0.010 to apply, with S = 1.027x10-3 and ν = 1.14x10-6m/s, then it can be shown that B = 0.20, and hence the Blasius/ Manning smooth equation becomes:

$$f = 0.20\ Re^{-0.20} \qquad \ldots 3.8$$

This would be a more appropriate expression of the Manning-like resistance of the Wallingford channel. It would plot on fig A2.1 virtually identical with the Manning line shown, passing through f = 0.02, Re = $0.1\text{x}10^6$.

4.*Rod roughness*

4.1 Some of the experiments on the Flood Channel Facility at Wallingford have been carried out with the flood plains roughened by vertical rods extending through the full depth of water. In order to establish the basic resistance function for this type of roughening, data is available from a set of seven tests carried out with the main channel roughened with the same pattern of rods used under compound channel conditions. These basic single channel tests covered depths of flow from 44mm to 119mm, a large part of the range of flood plain depths observed in the roughened flood plain tests.

4.2 The pattern of rods used consisted of a triangular distribution, of angle 60°. This was designed to have a density of 12 rods per m², and so the sides of the equilateral triangles forming the grid was 0.310m. This was the spacing between the rods transverse to the flow, and the longitudinal spacing of rows was therefore 268.5mm. See fig A2.4.

4.3 Under these conditions the resistance to flow is made up of the drag of the rods and the shear force at the channel boundaries. It is assumed that these may be treated separately as if the presence of the rods does not influence the boundary drag of the channel surface, except through the increase of velocity imposed by the blockage effect. Also it is assumed that any influence of the vertical velocity distribution on the drag on each rod can be accommodated by incorporating a suitable distribution coefficient into an equation that utilises the mean channel velocity calculated allowing for the blockage effect of the rods, by using the net cross sectional area in the plane of the row of rods.

4.4 The equation for the drag at the solid surface was derived earlier and is given by equ 3.1, applied in this case with subscript s denoting that part of the total friction factor arising from shear at the solid surface:

$$1/\sqrt{f_S} = 2.02 \log (Re\sqrt{f_S}) - 1.38 \qquad \ldots 4.1$$

where:

f_S = the friction factor arising from the drag on the channel perimeter
Re = the Reynolds number of the flow as a whole

4.5 The drag of the rods arises from three sources: internal vortex sheet drag due to flow separation behind the rods; free surface drag arising from induced waves; and skin friction on the rods themselves. These effects might be affected by wake interference, i.e. each rod may provide some sheltering of the rod next downstream. The first of these components is the dominent one: the so-called form drag.

$$F_{ROD} = C_D N\ d\ z\ \rho\ \alpha U^2/2 \qquad \ldots 4.2$$

where

F_{ROD} = the form drag of the rods per unit length of channel

C_D = the drag coefficient
N = number of rods per unit channel length
d = dia of rods
z = flow depth
ρ = specific mass of fluid
α = velocity distribution coefficient
U = the mean velocity over the flow depth

The velocity distribution coefficient allows for the variation of velocity over the length of the rod, i.e. the depth of flow. The depth mean velocity U is calculated allowing for the blockage of the transverse rows of rods:

$$U = Q/(A - n\ z\ d) \qquad \ldots 4.3$$

where

Q = discharge
A = channel cross-section
n = number of rods in each row

On this basis, a blockage coefficient, β, may be defined:

$$\beta = (U/V)^2 = (1 - n\ z\ d/A)^{-2} \qquad \ldots 4.4$$

4.6 The total drag per unit length of channel is then given by:

$$F_{TOT} = \beta\rho\ V^2(\alpha N\ d\ z\ C_D/2 + f_S\ P/8) \qquad \ldots 4.5$$

where

P = wetted perimeter of channel

4.7 The drag equation can be converted into a conventional form of resistance equation using the force balance equation:

$$F_{TOT} = \rho g\ A\ S = \rho gRSP \qquad \ldots 4.6$$

where

g = acceleration due to gravity
A = cross sectional area of flow
S = channel gradient
R = hydraulic mean depth, A/P

$$f_{TOT} = 8gRS/V = \beta[4(N\ d\ z/P)\ \alpha C_D + f_S] \qquad \ldots 4.7$$

where

f_{TOT} = overall friction factor

4.8 Equation 4.7 with the value of f_S obtained from equ. 4.1 formed the basis of analysing the test data. Note that the Reynolds Number, Re, for calculating the surface resistance incorporates U rather than V. For the main channel calibration tests, N was given by 10/0.2685 = 18.62 per unit length. Taking C_D as the unknown, all other parameters in equ. 4.7 were known, so that C_D could be calculated. (When using equation 4.7 in the reverse direction with f_{TOT} or V as unknown, iteration is required because f_S depends on the overall Reynolds Number, which in turn depends on the unknown mean channel velocity.)

4.9 The fact that resistance is generated over the full depth of flow by the rod roughness, with a minor part generated by the surface drag at the solid boundaries gives a more-than-usually uniform velocity distribution in the vertical. Thus the role of α is probably small compared with the blockage coefficient, in this case approximately [310/(310-25)] = 1.18, though varying with flow depth because the cross section is trapezoidal.

4.10 The basic assumption that the surface drag can be assessed by ignoring the presence of the rods (except, of course, in respect of the blockage and the reduction in channel Reynolds Number because the extra drag reduces mean velocity) was open to question. It might be argued that the surface drag would be reduced because in the wake of the rods the velocity close to the boundary would be less than average, and could even be reversed over some area behind each rod. On the other hand, the effect of the rods will produce irregularity of the transverse distribution of velocity and this would increase the average surface drag. Furthermore, the disruption to the boundary layer might modify the basic smooth law. There was no way of knowing which direction any change would be, let alone quantifying it from previous knowledge. The major effect is almost certainly due to blockage, which was taken into account through β. Some preliminary analyses with this calculated surface drag modified by factors either above or below unity did not provide any improvement in the correlations.

4.11 Figure A2.5 shows the variation of C_D calculated as above with the channel Reynolds Number. Figure A2.6 shows essentially the same information, but plotted against the ratio of flow depth to rod diameter: Figure A2.6 also shows the calculated values of the blockage coefficient. The experimental results display smooth trends with very little scatter. C_D varies from a minimum of about 0.97 at the shallowest flow tested (minimum Re) through a maximum approaching 1.22 at intermediate depths, dropping again at the deepest flow (maximum Re) to 1.16. These values may be compared with values for the drag coefficient of isolated cylinders in the literature: see for example Rouse 1950. The Reynolds number of the rods themselves varies over a very narrow range, 4100 to 4600, because the mean channel velocity varies only from 0.19 to 0.22 m/s. This is a range where the drag coefficient is not expected to show any rapid change with the rod Reynolds Number, so it is most unlikely that the variation of drag coefficient is a Reynolds number effect.

4.12 The drag coefficient to be expected will depend on whether the rods are effectively smooth or rough. The former would give about 0.95 according to previously available information: the latter would be expected to be higher though data at this range of Reynolds Number are lacking. A further possible influence is the effect of the wake from the rods on those downstream from them. However, the actual longitudinal spacing between rods in this case was over 20 diameters, so although undoubtedly there would be some residual effect, it was probably very small. It would, moreover, remain the same in all tests so would not cause variation in the drag coefficient.

4.13 The above analysis takes no account of wave drag that could arise because the rods are "surface piercing" elements. It might be anticipated that if wave drag were significant, following the work of Froude on ship resistance, it would be expected to depend on channel Froude Number, $V/\sqrt{(gz)}$. This would also affect any surface interference between the rods as the pattern of waves would be angled to the channel axis as a function of Froude number. Although the channel Froude Number varies over quite a narrow range, from 0.3 at the shallowest flow to 0.2 at the deepest, it is conceivable that the surface wave pattern could pass through some sensitive zone within the range of these tests. Indeed Froude found that the wave drag showed a peak value at modest Froude numbers, falling before increasing again at high Froude numbers. The variation of overall drag coefficient may therefore arise from the free surface effects. The conclusion was that the drag coefficient is best expressed as a function of relative depth, i.e. flow depth/rod diameter.

4.14 A curve fitting exercise gave the following formula for the drag coefficient:

For $1.75 < Z_* < 6.6$......

$$\alpha C_D = 1.184 - 0.277\, Z_* + \sqrt{(0.529\, Z_* - 0.843)} \qquad \text{...4.8}$$

where

Z_* = flow depth/rod diameter

This is shown also on Figure A2.6 and provides a good fit over the range of data for the Wallingford tests.

4.15 There remains the problem of extrapolation outside the range of test results. From the evidence of past research on the drag of cylinders, it seemed inappropriate to allow the value of C_D to drop below 0.95 at shallow depths, which was the value obtained at the shallowest flow considered. It might be argued that allowing for interaction between the rods (the influence of the wake from one on the rod in line downstream) might reduce the expected drag coefficient, there is no direct evidence of this. At higher depths in the Wallingford flume, up to the maximum Z_* value of 6, the empirical equation predicts a drop in C_D towards 1.05. It is not necessary to extrapolate beyond this for this series of tests, but work at Glasgow by Ervine and Jasim (private communication) suggests that higher values of Z_* would give a continuing downward trend towards a value of perhaps 0.8 or 0.85 as a limiting value for $Z_* > 10$.

4.16 When applying the functions to the tests on compound channels, there was a minor complication, because the number of rods in alternate rows differed. Thus the basic equations for the combination of drag on the rods and the surface drag were reformulated, as with different rod numbers in alternate rows, the blockage coefficients differed in alternate rows.

5 *Conclusions*

5.1 The SERC Flood Channel Facility at Wallingford is effectively smooth.

5.2 From the empirical and pragmatic point of view, there was little to choose between four resistance functions that were compared with the data from tests on simple channels. These were the Colebrook-White equation for transitional turbulent flow in pipes, the conversion of this to a wide-channel form, the Manning equation and a generalised logarithmic smooth turbulent function.

5.3 Most variation between the test data and any of these established equations for flow resistance was due to experimental scatter: tests in an open channel at fixed slope are not well conditioned to differentiate between resistance functions.

5.4 On theoretical grounds, the Manning equation should not be used for analysing flow in smooth channels. It is most appropriate for rough-turbulent flow, which is not the situation in any of the tests in the Wallingford flood channel facility.

5.5 However, the Manning equation provided a good fit to the experimental results. This was so because an exponential formula with the hydraulic mean depth raised to the power 2/3 can also be derived from a power-law smooth-turbulent function, with the coefficient n dependent on viscosity and gradient, rather than surface texture.

5.6 In the context of the Wallingford flood channel facility, a preferable exponential formula is a modification of the Blasius smooth turbulent equation to suit wide open-channel conditions:

$$f = 0.20\ Re^{-0.20}$$

5.7 The wide range of depths covered in tests on the channel with 1:1 side slopes made these data the most suitable for selecting a preferred equation. Paying due weight to shallow depths of flow, which are of significance in the analysis of the tests on compound channels with flood plains, a special form of the smooth-turbulent equation was derived and recommended for all subsequent analyses of Wallingford test data:

$$1/\sqrt{f} = 2.02 \log (Re\sqrt{f}) - 1.38$$

5.8 Although there was an observable change in the surface character of some sections of the test facility due to a hard deposit, this appears to have had very little influence on the flow resistance, although experimental tolerances make any influence difficult to detect or quantify.

5.9 The use of other equations in earlier analyses of the Wallingford results, including some published papers, did not introduce significant errors, but was potentially confusing.

5.10 It is preferable to distinguish between roughness coefficients and resistance coefficients. The former will not change because of the flow cross section becoming compound as they define the physical roughness of the channel which will be unchanged. The extra resistance arising from the interference effects with flood plain flow is best expressed as an adjustment to the shear streses, friction factor, velocity or discharge, leaving the basic roughness coefficients unchanged.

5.11 The basic resistance of the Wallingford channel when roughened with full depth rods can be described by combining the specific form of smooth law for the channel surface with the additional drag due to the rods.

5.12 A form of drag coefficient is used which also incorporates a velocity distribution factor. The values obtained are within the range of expectation, bearing in mind the values of drag coefficients for cylinders given in the literature and the actual blockage ratio. The drag coefficient has been expressed as a function of the relative depth of flow.

5.13 Basic resistance calculations for rod roughness as in the Wallingford tests may be based upon the following set of formulae, which allow for different numbers of rods in alternate rows:

$$\beta_1 = (1-n_1 z\ d/A)^{-2}$$

$$\beta_2 = (1-n_2 z\ d/A)^{-2}$$

For $1.75 < Z_* < 6.6$:

$$\alpha C_D = 1.184 - 0.277\ Z_* + \sqrt{(0.529\ Z_* - 0.843)}$$

else $\alpha C_D = 0.95$

$$1/\sqrt{f_S} = 2.02 \log(Re\sqrt{f_S}) - 1.38$$

$$f_{TOT} = 8gRS/V^2 = 4\alpha C_D(\beta_1 N_1 + \beta_2 N_2)\ d\ z/P + (\beta_1 + \beta_2)f_S/2$$

where

- Re = Reynolds number of blocked channel = $2\ V\ R\ (\sqrt{\beta_1}+\sqrt{\beta_2})/\nu$
- $\beta_{1,2}$ = blockage effect, i.e. square of area ratios for alterate rows
- $n_{1,2}$ = number of rods of dia d across channel/flood plain, rows 1 and 2
- $N_{1,2}$ = number of rods per unit length of main channel/flood plain, in ditto
- z = depth of flow in main channel/on flood plain
- A = gross cross sectional area of zone under consideration
- f_S = friction factor due to smooth boundary
- f_{TOT} = overall friction factor
- V = nominal velocity given by component discharge/A
- αC_D = effective drag coefficient of rods
- Z_* = z/d
- R = hydraulic mean depth A/P, for zone under consideration
- S = hydraulic gradient (water surface slope)

TABLE A2.1. ANALYSIS OF RESISTANCE DATA

Channel	Side slope hor/vert	Range of depths mm	No. of tests	Colebrook-White ks mm	Colebrook-White RMS error % of V (V,cm/s)	Wide channel trans ks mm	Wide channel trans RMS error % of V (V,cm/s)	Manning equation n	Manning equation RMS error % of V (V,cm/s)	Mod. smooth turb't A, D	Mod. smooth turb't RMS error % of V (V,cm/s)
1	2	45-150	14	0.028	1.66 (1.20)	0.014	1.84 (1.33)	0.0096	1.61 (1.19)	2.00, 0.96	1.64 (1.18)
2	1	25-149	28	0.085	4.77 (2.86)	0.050	4.64 (2.85)	0.0096	4.36 (2.58)	2.20, 2.12	4.27 (2.84)
2	1	25-149	27	0.096	3.96 (2.15)	0.059	3.82 (2.13)	0.0100	3.66 (1.96)	2.08, 1.67	3.49 (2.12)
3	1	150-296	13	0.065	1.17 (1.12)	0.041	1.11 (1.08)	0.0100	1.10 (1.05)	1.91, 0.88	1.06 (1.03)
4	0	40-150	11	0.075	3.86 (1.81)	0.041	3.62 (1.72)	0.0991	3.46 (1.65)	2.53, 3.56	2.22 (1.26)
2 & 3	1	25-296	40	0.081	3.51 (1.94)	0.050	3.31 (1.89)	0.0100	3.06 (1.72)	2.02, 1.38	2.97 (1.84)
1,2,3,4	0,1,2	25-296	65	0.072	3.57 (1.99)	0.041	3.44 (1.97)	0.0994	3.30 (1.90)	1.91, 0.84	3.38 (1.99)

The bracketted error figures are the root mean square errors in velocity for the series of experiments, comparing measurement with best-fit formula prediction. The unbracketted figures are the RMS percentage differences.

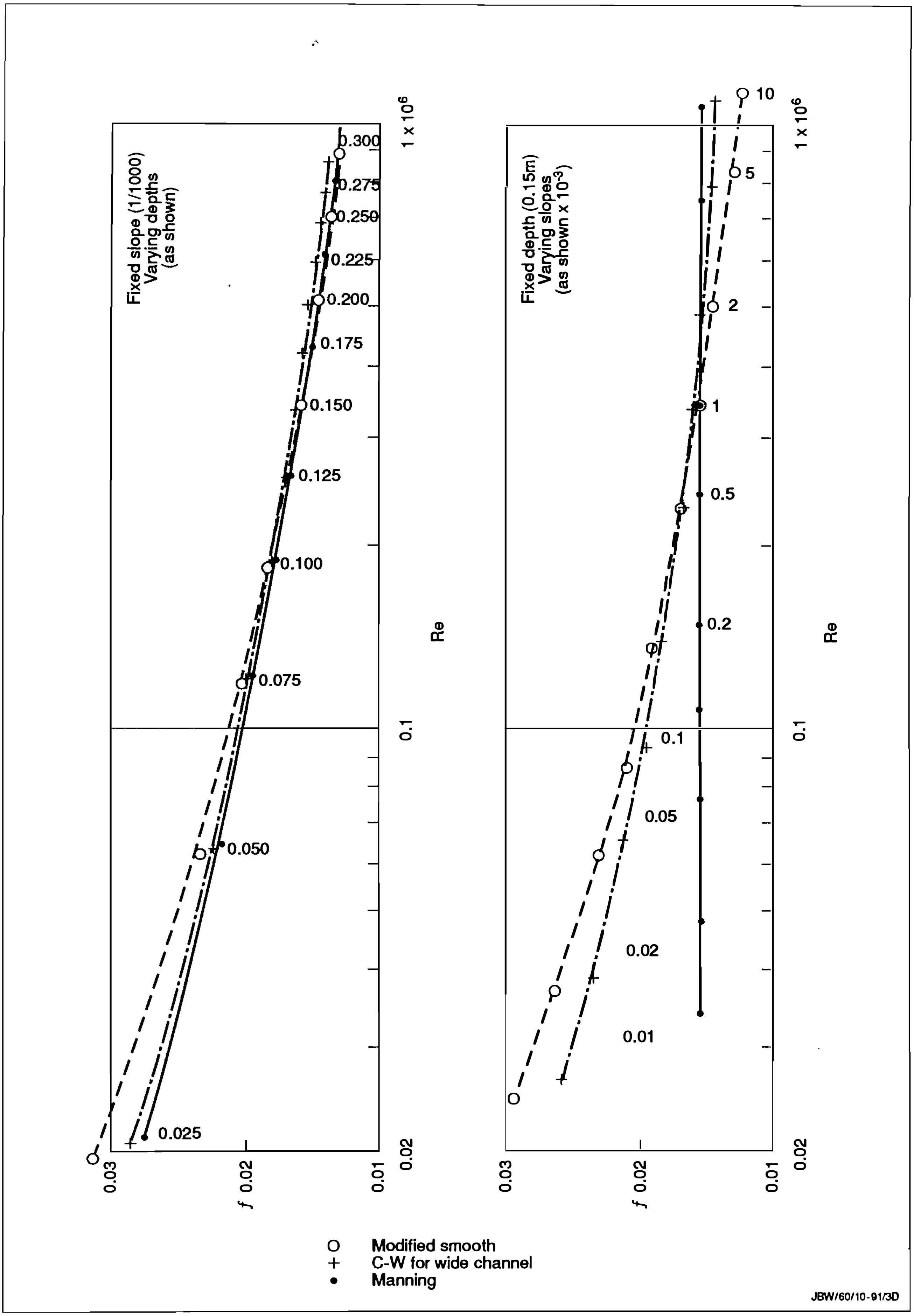

Fig A2.1 Comparison of friction formulae: (a) for fixed slope; (b) for fixed depth

Fig A2.2 Smooth channel calibration: 1/2 side slope

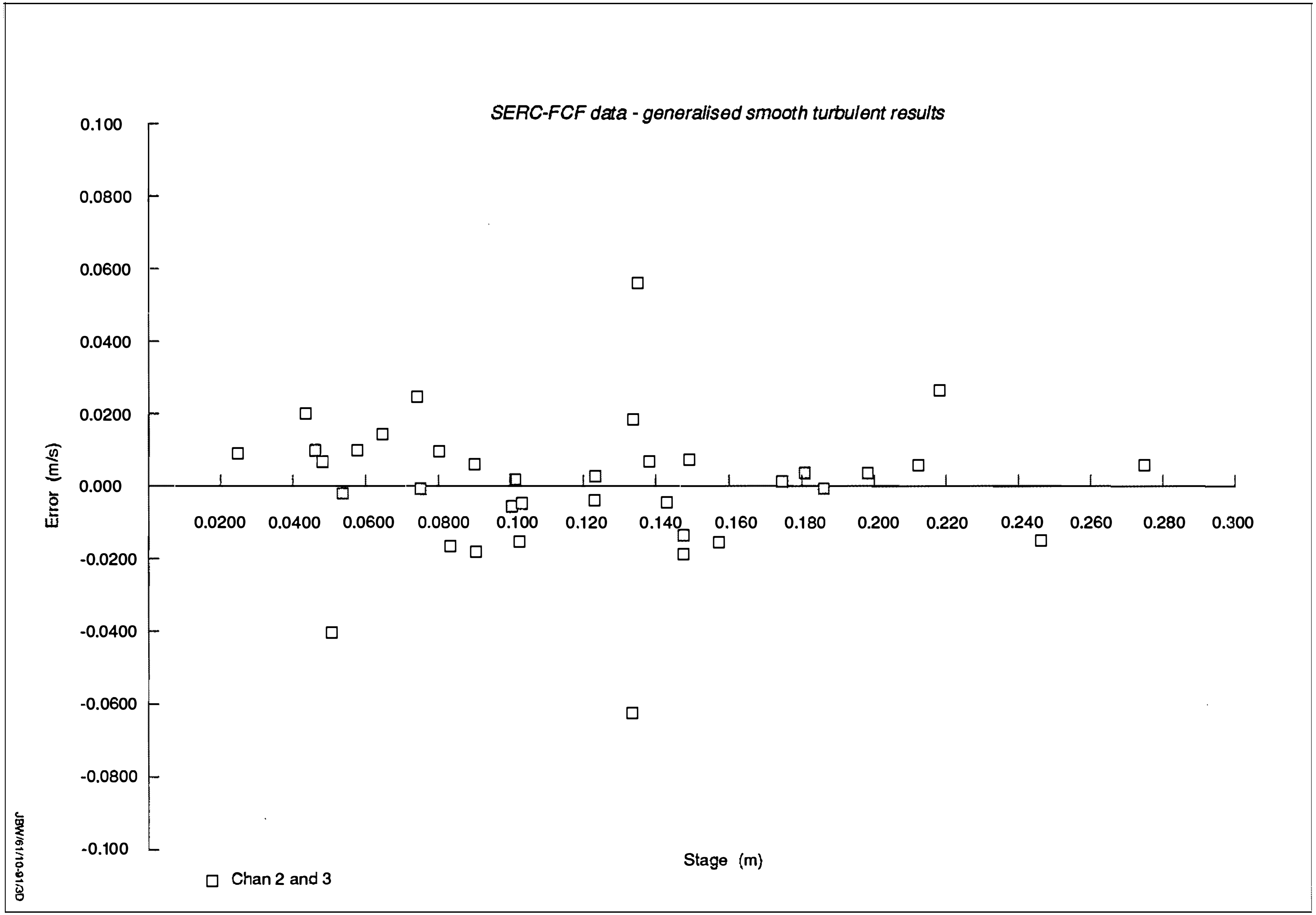

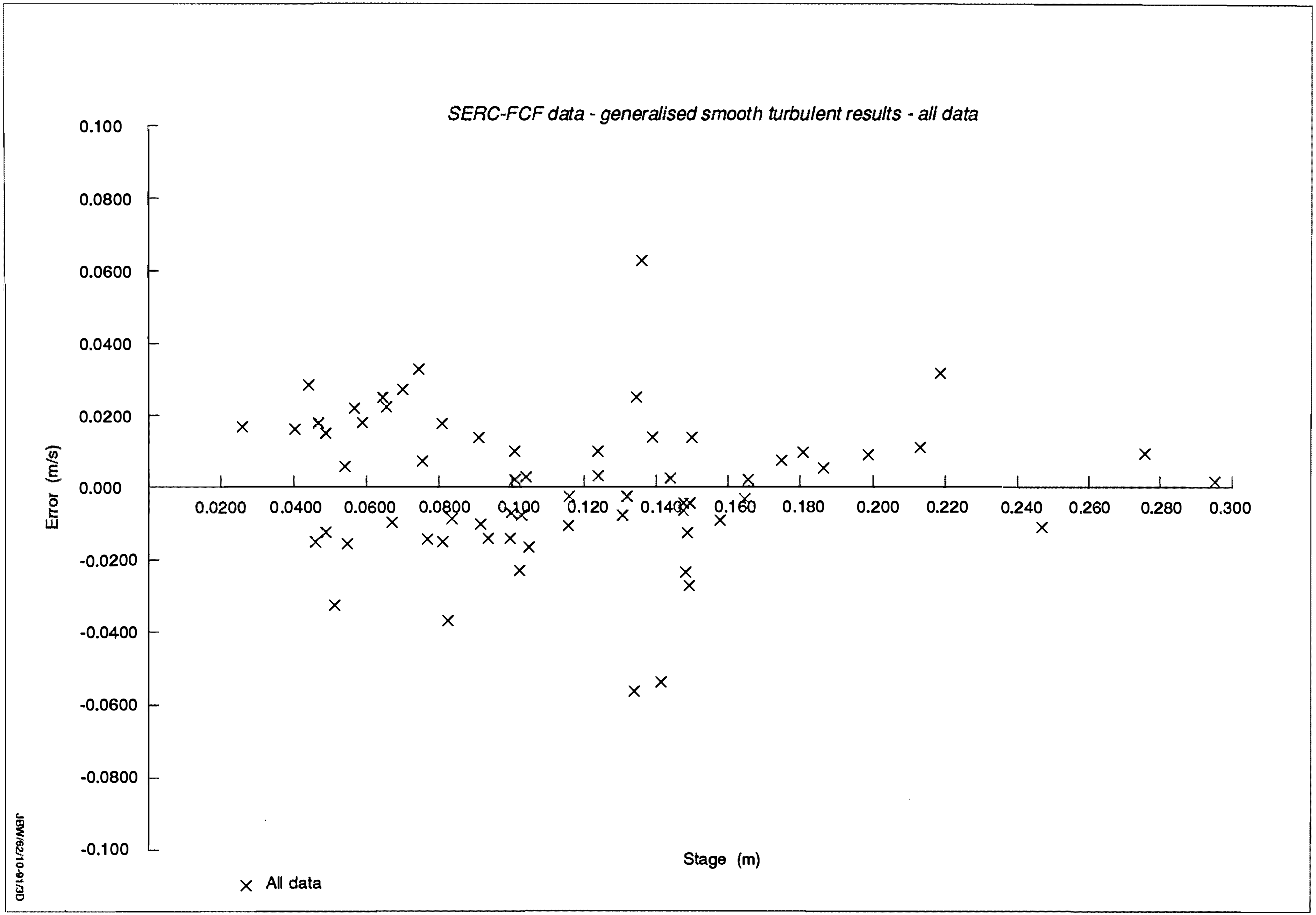

Fig A2.3 Smooth channel calibration: all results

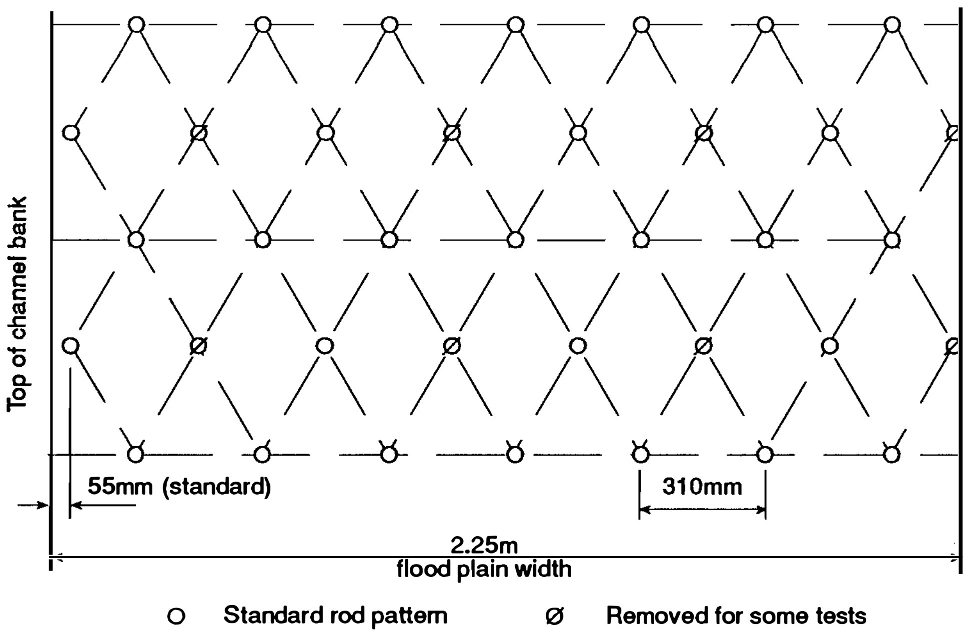

Fig A2.4 Pattern of roughness used on flood plains

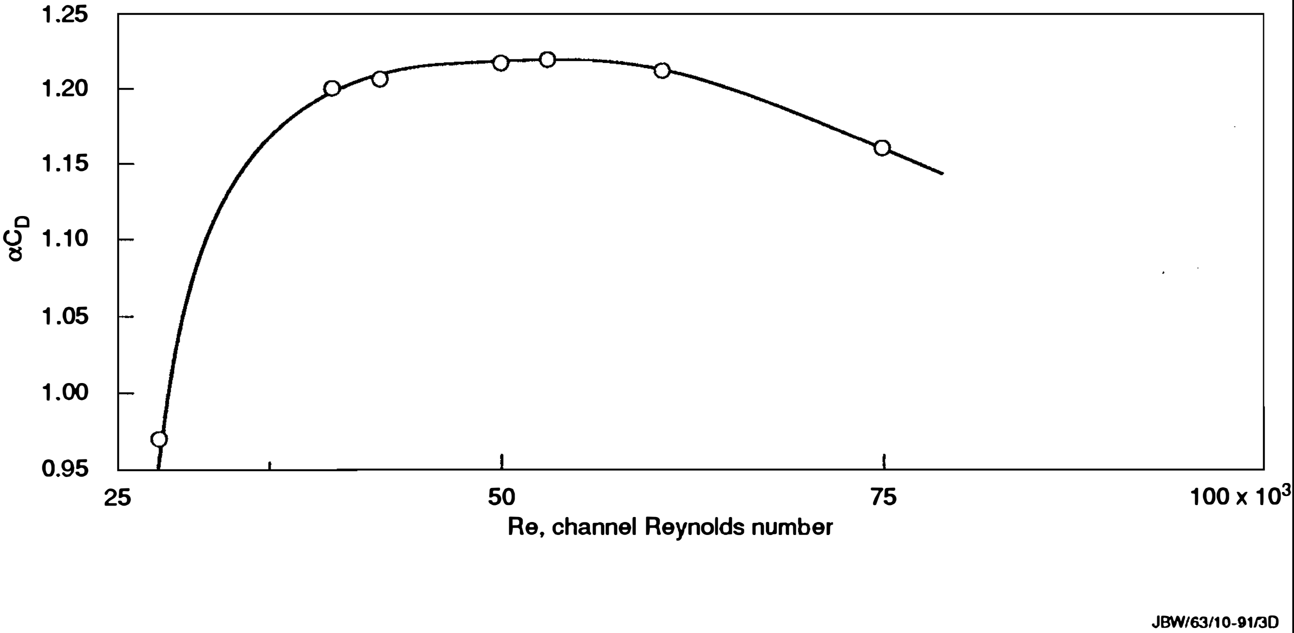

Fig A2.5 Drag coefficient as function of channel Reynolds Number

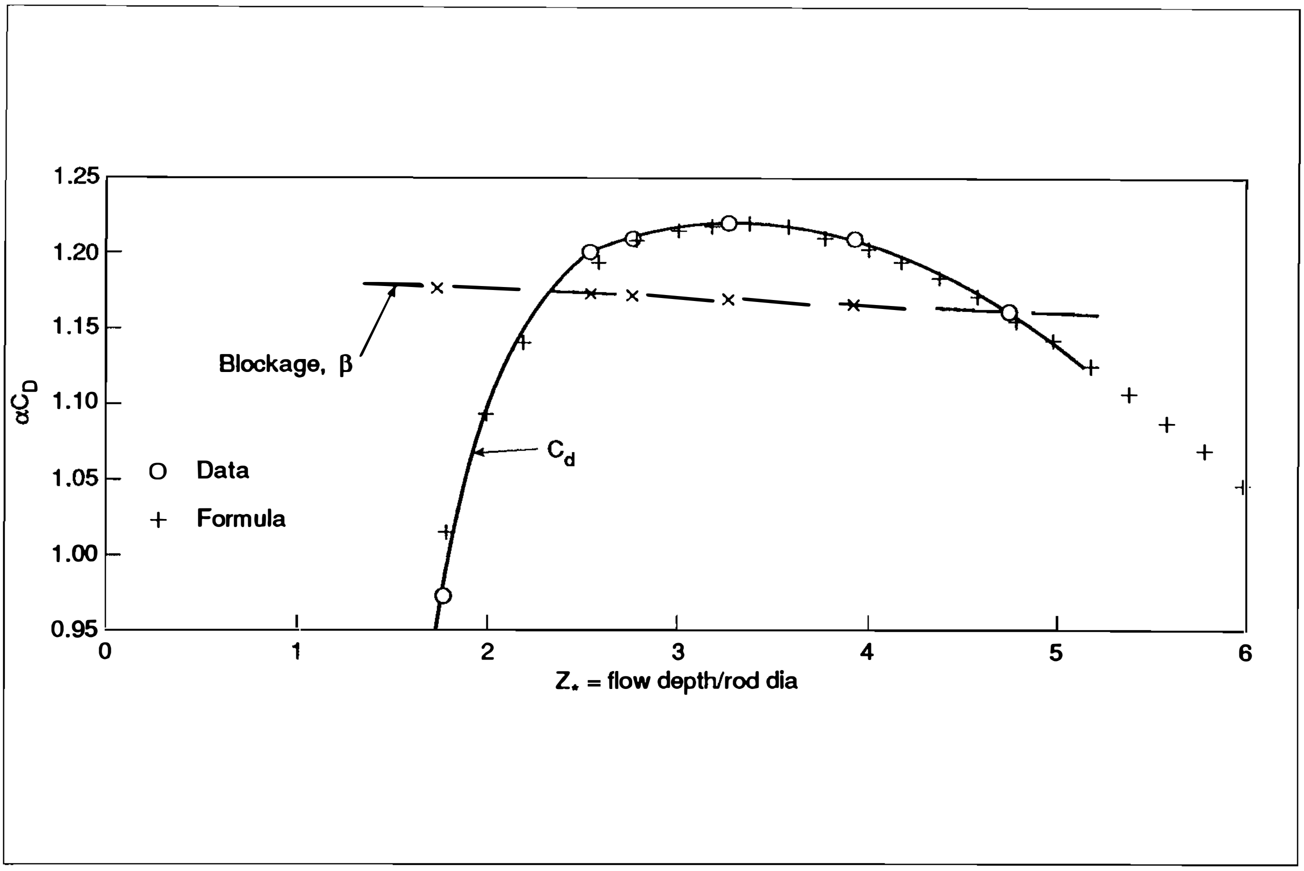

Fig A2.6 Drag coefficient and blockage coefficient as functions of ratio of flow depth to rod diameter, Z*

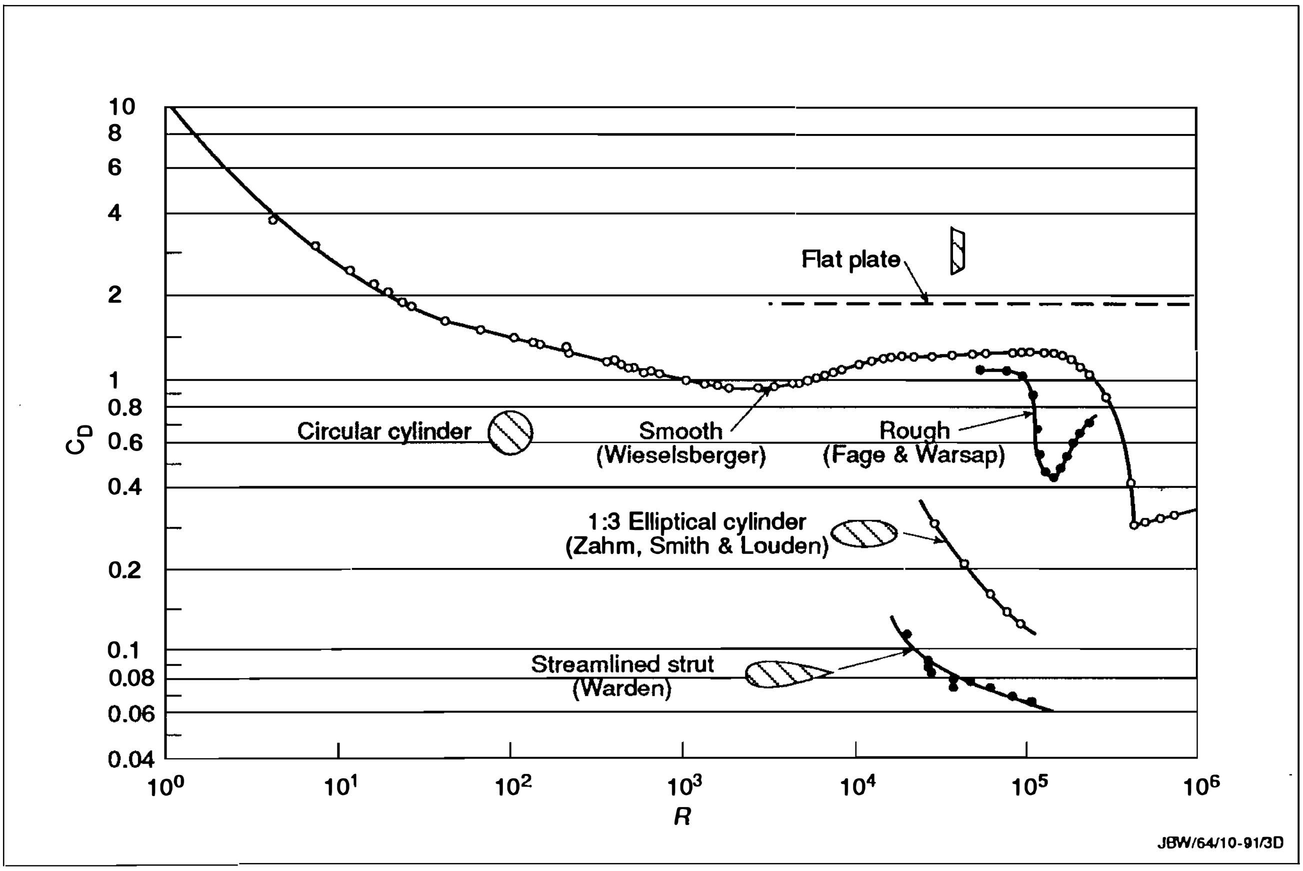

Fig A2.7 Coefficients of drag for two dimensional forms (Rouse, ed., 1950)

APPENDIX 3

CHANNEL COHERENCE

1. The influence on the discharge of the interaction between main channel and flood plain flows depends on how comparable the hydraulic conditions in these zones are: if velocities and depths are very similar, then we can expect interaction effects to be small; if they are very dissimilar, then major effects are to be expected. The degree to which the different zones exhibit flow similarity will be referred to as their "coherence": the greater their coherence the more likely is the hydraulics of the section to approach simple channel (negligible interaction) conditions.

2. Channel conveyance is a useful parameter in developing the concept of coherence. Conveyance, K}V|, was defined by Ven Te Chow (1959) as:

$$K_V = Q/\sqrt{S} \qquad \ldots A3.1$$

but it is preferable to redefine it to be consistent with dimensional analysis, as

$$K_D = Q/\sqrt{(8gS)} = A\sqrt{(A/fP)} \qquad \ldots A3.2$$

Thus the conveyance of a simple channel can be represented by the cross-section area, wetted perimeter and friction factor. For a compound section, the theoretical conveyance before allowing for any interaction effects is given by the sum of the conveyances of the main channel and flood plains:

$$K_D = A_C\sqrt{(A_C/f_CP_C)} + 2\ A_F\sqrt{(A_F/f_FP_F)} \qquad \ldots A3.3$$

for the situation of two symmetrical flood plains. If the Manning equation is appropriate, then this becomes

$$K_D = A_C(A_C/P_C)^{2/3}/n_C\sqrt{(8g)} + 2\ A_F(A_F/P_F)^{2/3}/n_F\sqrt{(8g)} \qquad \ldots A3.4$$

3. This leads to a parameter for the coherence of the channel section, namely the ratio of the theoretical conveyance calculated by treating it as a single unit to that calculated by summing the conveyances of the separate zones. Ideally, the section coherence would be defined as:

$$COH_1 = \frac{\sum_{i=1}^{i=n} Ai\sqrt{[} \sum_{i=1}^{i=n} Ai/ \sum_{i=1}^{i=n} Ai/\ fo \sum_{i=1}^{i=n} Pi\ ]}{\sum_{i=1}^{i=n} [\ A_i\sqrt{(}A_i/f_i\ P_i)\ )} \qquad \ldots A3.5$$

Note that f_i represents the friction factors for the separate zones, calculated from the appropriate zonal values of Manning's n, Re or relative roughness according to the resistance function being used. f_0, on the other hand, is a global value calculated on the basis of the summed section parameters.

4. There is a problem with the above definition: in general f_0 is not known, because in engineering practice it would depend on some whole-section compendium value of Manning's n. It is calculable if the flood plain and main channel follow identical resistance functions e.g. both smooth, or having the same Manning's n value. So equation 3.5 could be used as the definition of COH for the smooth laboratory case - but could not cover the rough flood plain condition or the general case when different roughnesses or resistance functions apply to different zones. A more useful definition for design purposes is obtained by replacing f_0 by the perimeter weighted equivalent deduced from the separate (and calculable) values for the main channel and flood plains.

$$COH_3 = \frac{\sum_{i=1}^{i=n} A_i\sqrt{[} \sum_{i=1}^{i=n} A_i/ \sum_{i=1}^{i=n}(f_iP_i)]}{\sum_{i=1}^{i=n} [A_i\sqrt{(}A_i/f_iP_i)} \qquad \ldots A3.6$$

5. This parameter, COH_3, varies with flow depth in a given channel, of course, and three cases are illustrated in fig A3.1: the Wallingford channel illustrated in Figure 2.3; the same but with flood plains reduced to 0.25m wide; and the Montford Bridge natural river section shown in Figure 2.2. For the smooth Wallingford channel, the appropriate friction factors were

using (varying with depth because Re varies with depth) and for the Montford Bridge section a constant value of Manning's n was applied for this illustration, with depths related to the lower edge of the flood plains. The artificial channel with horizontal flood plain and flood plain/main channel bed width ratio 1.5 (defined here as the ratio of width of each flood plain to bed width of main channel) has a very low COH value, below 0.3, when the flood plains are first inundated, increasing to 0.94 when the flood plain flow depth equals the depth of main channel. With narrow flood plains, width ratio 0.167, COH is less sensitive to depth and closer to unity, lying between about 0.5 and 0.94. The natural river section has wide flood plains with some cross fall (note that Figure 2.2 has considerable vertical exaggeration) with minimum COH value (0.52), not just above bank full but when the full width of flood plain is inundated. Above this the trend is very similar to the wide laboratory channel, whilst below the trend is towards unity because its sloping flood plains avoid the discontinuity in COH at bank full. (For these calculations the main channel zones 3,4 and 5 of Figure 2.2 were taken together, as were the remaining flood plain areas)

6. For a conventional compound cross-section geometry, the coherence of the section may be expressed in terms of the geometric ratios: let $A_* = N_F A_F/A_C$; $P_* = N_F P_F/P_C$; $H_* = (H-h)/H$; and $f_* = f_F/f_C$, where N_F is the number of flood plains. Then

$$COH_3 = \frac{(1 + A_*)\sqrt{[(1 + A_*)/(1 + f_* P_*)]}}{1 + A_*(A_*/f_* P_*)} \qquad \ldots A3.7$$

In this form it is obvious that as A_* becomes large (deep flow on flood plain) then COH_3 approaches unity, for equal roughness of main channel and flood plain (when f_* approaches unity as the depth increases). Also when A_* is very small (flood plains just inundated) COH_3 approaches $1/\sqrt{(1 + f_* P_*)}$. As A_* and P_* depend on H_*, then for a given geometry COH_3 also depends on H_*.

7. If the Manning equation applies, and perimeter weighting of the friction factor is applied, then the coherence equation becomes:

$$COH_2 = \frac{(1 + A_*)^{3/2} / \sqrt{(1 + P_*^{4/3}\ n_*^2\ /A_*^{1/3})}}{1 + A_*^{5/3}\ /n_*\ P_*^{2/3}} \qquad \ldots A3.8$$

8. Whether the most general form of these definitions of channel coherence (equation A3.7) provides a useful co-ordinating parameter in the analysis of the experimental results remains to be seen. Its potential benefit is that it brings together in one parameter most of the factors expected to influence the hydraulics of compound channels, and so might take the place of relative depth as an indicator of how like a single channel the performance might prove. An expected corollary is that the closer to unity COH approaches, the more likely it is that the channel can be treated as a single unit, using the overall geometry. As f_* is included in the general definition of COH_3 (see equ A3.7), there is some prospect too that dissimilar roughnesses will automatically be covered.

APPENDIX 4: TURBULENCE METHOD, SOLUTION FOR GENERAL CROSS-SECTION SHAPES

The following theory is given by Shiono and Knight (1991), whose assistance is gratefully acknowledged. Some small corrections to equations 11 in the published version have been provided by the Authors. The method uses the depth averaged momentum equations and is general in the sense that it can be applied to any cross-section which can be described by a series of zones with linear cross-fall. The following text is a direct quotation from the 1991 paper:

This paper describes an improved analytical solution, developed from the earlier work of **Shiono & Knight (1988)**, which now includes the effects of secondary flow. Data from the Science and Engineering Research Council Flood Channel Facility (SERC-FCF) are used to quantify the apparent shear stresses across a two stage channel arising from turbulence and secondary flow effects. These apparent shear stresses are then depth averaged to give dimensionless depth averaged eddy viscosity values. The analytical solution is thus capable of reproducing the lateral distributions of depth mean velocity and boundary shear stress in compound or two stage channels. It has been applied to several natural river channels in the Severn-Trent catchment in order to extend the stage discharge relationship for overbank flow. See **Knight, Shiono & Pirt (1989)** and **Knight, Samuels & Shiono (1990)**. A typical symmetric two stage channel in which there is no crossfall in regions 1 & 3 is shown in Fig.2. For a sufficiently wide river channel (region 1) and flood plain (region 3), the depth averaged velocity, U_d, and boundary shear stress, τ_b, will attain constant but different values in the two regions, thus creating a shear layer in the vicinity of region 2. Due to the re-entrant and channel corners in this region the flow is also strongly affected by secondary flows.

2. ANALYTICAL SOLUTION

In order to predict the lateral variation of depth mean velocity and boundary shear stress in open channel flow, the depth mean momentum equation has to be solved for steady uniform turbulent flow in the streamwise direction. The equation for the longitudinal streamwise component of momentum on a fluid element may be combined with the continuity equation to give

$$\rho \left[\frac{\partial \bar{U}\bar{V}}{\partial y} + \frac{\partial \bar{U}\bar{W}}{\partial z} \right] = \rho g S_o + \frac{\partial}{\partial y}(-\rho\overline{uv}) + \frac{\partial}{\partial z}(-\rho\overline{uw}) \qquad \ldots (1)$$

where
- x, y, z are streamwise, lateral and normal directions respectively
- $\bar{U},\bar{V},\bar{W}$ are temporal mean velocity components corresponding to x,y,z
- u,v,w are turbulent perturbations of velocity with respect to the mean
- ρ is the density of water
- g is the gravitational acceleration
- S_o is the bed slope gradient ($S_o = \sin\theta$)

The depth mean averaged momentum equation can be obtained by integrating **equation (1)** over the water depth, H. Provided $\bar{W}(H) = \bar{W}(O) = 0$, then **Shiono and Knight (1988)** show that equation (1) becomes

$$\frac{\partial H(\rho\bar{U}\bar{V})_d}{\partial y} = \rho g H S_o + \frac{\partial H\bar{\tau}_{yx}}{\partial y} - \tau_b\sqrt{1 + \frac{1}{s^2}} \qquad \ldots (2)$$

where τ_b is the bed shear stress

s is the side slope (1 :s, vertical:horizontal)

$$(\rho\bar{U}\bar{V})_d = \frac{1}{H}\int_0^H \rho\bar{U}\bar{V}dz \quad \text{and} \quad \bar{\tau}_{yx} = \frac{1}{H}\int_0^H (-\rho\overline{uv})dz$$

Analytical solutions have been obtained to **equation (2)** based on the eddy viscosity approach and by neglecting the secondary flow contribution i.e. $(\partial(H\rho\bar{U}\bar{V})_d/\partial y = 0)$. The eddy viscosity approach has been adopted because of its common usage by numerical modellers. In this model the depth averaged transverse shear stress, $\bar{\tau}_{yx}$, is expressed in terms of the lateral gradient of depth mean velocity

$$\bar{\tau}_{yx} = \rho\bar{\varepsilon}_{yx}\frac{\partial U_d}{\partial y} \quad \text{.... (3)}$$

Since the eddy viscosity has dimensions of m^2s^{-1}, it is often related to the local shear velocity, U_* and depth, H, by the dimensionless eddy viscosity coefficient, λ, defined by

$$\bar{\varepsilon}_{yx} = \lambda U_* H \quad \text{... (4)}$$

However as **equation (2)** shows, the local shear velocity, U_* $(= \sqrt{(\tau_b/\rho)})$ is affected by the free shear layer turbulence and the secondary flows. In regions of high lateral shear it might be argued that the U_* in **equation (4)** should be replaced by the primary or shear velocity difference between the two regions. However in the interests of simplicity and because of its common usage by hydraulic modellers the form of **equation (4)** is retained with λ being regarded as a 'catch all' parameter to describe various 3-D effects. In order to express **equation (2)** in terms of one variable only (U_d or τ_b), the Darcy-Weisbach friction, f $(=8\tau_b/(\rho U_d 2))$ is used to link U_* and U_d, giving

$$U_* = \left(\frac{f}{8}\right)^{\frac{1}{2}} U_d \quad \text{.... (5)}$$

The depth averaged eddy viscosity in **equation (4)** may then be expressed in the form

$$\bar{\varepsilon}_{yx} = \lambda H \left(\frac{f}{8}\right)^{\frac{1}{2}} U_d \quad \text{... (6)}$$

Substituting **equations (3) & (6)** into **equation (2)** gives

$$\rho g H S_o - \rho\frac{f}{8}U_d^2\sqrt{1+\frac{1}{s^2}} + \frac{\partial}{\partial y}\left\{\rho\lambda H^2\left(\frac{f}{8}\right)^{\frac{1}{2}} U_d \frac{\partial U_d}{\partial y}\right\} = \frac{\partial}{\partial y}\left\{H(\rho\bar{U}\bar{V})_d\right\} \quad \text{.... (7)}$$

In an earlier paper, **Shiono & Knight (1988)** assumed that $\partial(H\rho\bar{U}\bar{V})_d/\partial y = 0$ and obtained analytical solutions to **equation (7)** for channels of various shape. The experimental results which are described in a later section of this paper suggest that for the particular cases considered the shear stress due to secondary flow, $(\rho\bar{U}\bar{V})_d$, decreases approximately linearly either side of a maximum value which occurs at the edge of the flood plain and the main channel. Although this is a first order approximation to the data, as **Fig.7** will later show, it does have the merit that it then allows **equation (7)** to be solved analytically. Further data from a wider range of channel geometries are clearly needed before this assumption may be generally accepted. However, if this is so, then the lateral gradient of the secondary flow force per unit length of the channel may be written as

$$\frac{\partial (H \rho \bar{U}\bar{V})_d}{\partial y} = \Gamma_{mc} \text{ or } \Gamma_{fp} \qquad \dots (8)$$

where the subscripts mc and fp refer to the main channel and flood plain respectively. The analytical solution to **equation (7)** may then be expressed for a constant depth H domain as

$$U_d = \left\{ A_1 e^{\gamma y} + A_2 e^{-\gamma y} + \frac{8gS_oH}{f}(1-\beta) \right\}^{\frac{1}{2}} \qquad \dots (9)$$

and for a linear side slope domain as

$$U_d = \left\{ A_3 \xi^{\alpha_1} + A_4 \xi^{-\alpha_1 - 1} + \omega\xi + \eta \right\}^{\frac{1}{2}} \qquad \dots (10)$$

where $\gamma = \left(\frac{2}{\lambda}\right)^{1/2}\left(\frac{f}{8}\right)^{1/4}\frac{1}{H}$, $\beta = \frac{f\Gamma}{8gS_oH}$

$$\alpha_1 = -\frac{1}{2} + \frac{1}{2}\left\{1 + \frac{s\sqrt{1+s^2}}{\lambda}\sqrt{8f}\right\}^{\frac{1}{2}}$$

$$\omega = \frac{gS_o}{\frac{\sqrt{1+s^2}}{s}\frac{f}{8} - \frac{\lambda}{s^2}\sqrt{\frac{f}{8}}}$$

$$\eta = -\frac{\Gamma}{s\sqrt{1+s^2}\,\frac{2}{\lambda}\sqrt{\frac{f}{8}}} \qquad \dots (11)$$

and ξ = depth function on the side slope domain (e.g. ξ = H - ((y-b)/s) for the main channel side slope).

Equations (9)-(11) give the lateral variation of depth mean velocity and boundary shear stress (via **equation (5)**) in a channel of any shape provided its geometry can be described by a number of linear boundary elements. For a constant depth domain, **equation (9)** shows that as $y \rightarrow \infty$ with $\gamma > 0$, since the flow must become two dimensional ($U_d = \{8gS_oH/f\}^{1/2}$) in the far field where no secondary flow exists ($\beta = 0$), therefore $A_1 = 0$. For a sloping side slope domain, **equation (10)** shows as $s \rightarrow \infty$, A_3 must be zero in order that a solution might exist. **Equations (9)** and **(10)** also require boundary conditions of continuity of HU_d and $\partial(HU_d)dy$ across joints of domains, together with the no slip condition, $U_d = 0$, at the remote boundaries. The sub division of the channel cross section into various sub areas with either constant depth domains or sloping side slope domains will therefore require sufficient computer capacity for the matrix inversion of the coefficients $A_1 \dots A_n$. Examples of complex natural geometries modelled in this way are given in **Knight, Shiono & Pirt (1989)** and **Knight, Samuels & Shiono (1990)**.

APPENDIX 5: DATA ON CHANNEL ROUGHNESS

The following information is extracted from Ven Te Chow (1959) and retains his classification, with the omission of closed conduit data (class A). Refer to Chapter 7 for additional information on channel roughness. The following table is intended to provide some guidance where no other information may be available, but wherever practicable the roughness coefficients should be based on observations from the system under review, or from similar systems for proposed channels. The information in Table A5.1 here is in terms of Manning's n, but this is not to be taken as a general recommendation for the best resistance function. In many circumstances, and especially in lined channels, the Colebrook-White function might be more appropriate. Some information on k_s values for use in the Colebrook-White equation is given in a supplementary table, A5.2, at the end of the Appendix.

TABLE A5.1. RECOMMENDED ROUGHNESS COEFFICIENTS FOR USE IN MANNING EQUATION AS GIVEN BY VEN TE CHOW. ("Normal" values are typically used).

Type of channel and description	Min	Normal	Max
B Lined or built-up channels			
B-1 Metal			
(a) Smooth steel surface			
1. Unpainted	0.011	0.012	0.014
2. Painted	0.012	0.013	0.017
(b) Corrugated	0.021	0.025	0.030
B-2 Non-metal			
(a) Cement			
1. Neat, surface	0.010	0.011	0.013
2. Mortar	0.011	0.013	0.015
(b) Wood			
1. Planted, untreated	0.010	0.012	0.014
2. Planed, creosoted	0.011	0.012	0.015
3. Unplained	0.011	0.013	0.015
4. Plank with battens	0.012	0.015	0.018
5. Lined with roofing paper	0.010	0.014	0.017
(c) Concrete			
1. Trowel finish	0.011	0.013	0.015
2. Float finish	0.013	0.015	0.016
3. Finished, with gravel on bottom	0.015	0.017	0.020
4. Unfinished	0.014	0.017	0.020
5. Gunite, good section	0.016	0.019	0.023
6. Gunite, wavy section	0.018	0.022	0.025
7. On good excavated rock	0.017	0.020	
8. On irregular excavated rock	0.022	0.027	
(d) Concrete bottom float finished with sides of:			
1. Dressed stone in mortar	0.015	0.017	0.020
2. Random stone in mortar	0.017	0.020	0.024
3. Cement rubble masonry, plastered	0.016	0.020	0.024
4. Cement rubble masonry	0.020	0.025	0.030
5. Dry rubble or rip-rap	0.020	0.030	0.035
(e) Gravel bottom with sides of:			
1. Formed concrete	0.017	0.020	0.025
2. Random stone in mortar	0.020	0.023	0.026
3. Dry rubble or rip-rap	0.023	0.033	0.036
(f) Brick			
1. Glazed	0.011	0.013	0.015
2. In cement mortar	0.012	0.015	0.018
(g) Masonry			
1. Cemented rubble	0.017	0.025	0.030
2. Dry rubble	0.023	0.032	0.035
(h) Dressed Ashlar	0.013	0.015	0.017
(i) Asphalt			
1. Smooth	0.013	0.013	
2. Rough	0.016	0.016	
(j) Vegetal lining	0.030	-	0.500

DATA ON CHANNEL ROUGHNESS (cont'd)

Type of channel and description	Min	Normal	Max
C. Excavated or dredged			
(a) Earth, straight and uniform			
1. Clean, recently completed	0.016	0.018	0.020
2. Clean, after weathering	0.018	0.022	0.025
3. Gravel, uniform section, clean	0.022	0.025	0.030
4. With short grass, few weeds	0.022	0.027	0.033
(b) Earth, winding and sluggish			
1. No vegetation	0.023	0.025	0.030
2. Grass, some weeds	0.025	0.030	0.033
3. Dense weeks or aquatic plants in deep channels	0.030	0.035	0.040
4. Earth bottom and rubble sides	0.028	0.030	0.035
5. Stony bottom and weedy banks	0.025	0.035	0.040
6. Cobble bottom and clean sides	0.030	0.040	0.050
(c) Dragline-excavated or dredged			
1. No vegetation	0.025	0.028	0.033
2. Light brush on banks	0.035	0.050	0.060
(d) Rock cuts			
1. Smooth and uniform	0.025	0.035	0.040
2. Jagged and irregular	0.035	0.040	0.050
(e) Channels not maintained, weeds and brush uncut			
1. Dense weeds, high as flow depth	0.050	0.080	0.120
2. Clean bottom, brush on sides	0.040	0.050	0.080
3. Same, highest stage of flow	0.045	0.070	0.110
4. Dense brush, high stage	0.080	0.100	0.140
D. Natural streams			
D-1 Minor streams (top width at flood stage <100 ft)			
(a) Streams on plain			
1. Clean, straight, full stage no rifts or deep pools	0.025	0.030	0.033
2. Same as above, but more stones and weeds	0.030	0.035	0.040
3. Clean, winding, some pools and shoals	0.033	0.040	0.045
4. Same as above, but some weeds and stones	0.035	0.045	0.050
5. Same as above, lower stages more ineffective slopes and sections	0.040	0.048	0.055
6. Same as 4, but more stones	0.045	0.050	0.060
7. Slugish reaches, weedy, deep pools	0.050	0.070	0.080

		8. Very weedy reaches, deep pools, or floodways with heavy stand of timber and underbrush	0.075	0.100	0.150
	(b)	Mountain streams, no vegetation in channel, banks usually steep, trees and brush along banks submerged at high stages			
		1. Bottom: gravels, cobbles, and few boulders	0.030	0.040	0.050
		2. Bottom: cobbles with large boulders	0.040	0.050	0.070
D-2	Flood plains				
	(a)	Pasture, no brush			
		1. Short grass	0.025	0.030	0.035
		2. High glass	0.030	0.035	0.050
	(b)	Cultivated areas			
		1. No crop	0.020	0.030	0.040
		2. Mature row crops	0.025	0.035	0.045
		3. Mature field crops	0.030	0.040	0.050
	(c)	Brush			
		1. Scattered brush, heavy weeds	0.035	0.050	0.070
		2. Light brush and trees, in winter	0.035	0.050	0.060
		3. Light brush and trees, in summer	0.040	0.060	0.080
		4. Medium to dense brush, in winter	0.045	0.070	0.110
		5. Medium to dense brush, in summer	0.070	0.100	0.160
	(d)	Trees			
		1. Dense willows, summer, straight	0.110	0.150	0.200
		2. Cleared land with tree stumps, no spouts	0.030	0.040	0.050
		3. Same as above, but with heavy growth of sprouts	0.050	0.060	0.080
		4. Heavy stand of timber, a few down trees, little undergrowth, flood stage below branches	0.080	0.100	0.120
		5. Same as above, but with flood stage reaching branches	0.100	0.120	0.160
D-3	Major streams (top width at flood stage > 100 ft). The n value is less than that for minor streams of similar description, because banks offer less effective resistance.				
	(a)	Regular section with no boulders or brush	0.025	–	0.060
	(b)	Irregular and rough section	0.035	–	0.100

TABLE A5.2. RECOMMENDED ROUGHNESS VALUES, k_s IN MM, FOR LINED CHANNELS, FOR USE IN COLEBROKE-WHITE EQUATION

	CONDITION		
CONCRETE:	Good	Normal	Poor
Class 4: Monolithic construction against oiled steel forms, with no surface irregularities.	0.06	0.15	-
Class 3: Monolithic construction against steel forms, but less perfect surface.	-	0.15	0.3
Class 2: Monolithic construction against rough forms; cement gun surface (for very coarse texture take k_s = aggregate size in evidence)	0.6	1.5	-
Class 1: Smooth trowelled surfaces	0.3	0.6	1.5
BRICKWORK:			
Well pointed brickwork	1.5	3	6
Old brickwork in need of pointing	-	15	30

APPENDIX 6: EXAMPLE OF CHANNEL GEOMETRY CONVERSION AND STAGE DISCHARGE COMPUTATION.

Channel geometry conversion

1. As natural channels, and also many man-made compound channels, do not have the "classical" shape of a symmetric two-stage trapezoidal cross-section, some method of working out an equivalent section is required, in order to define the various parameters that appear in the various formulae for predicting the discharge as a function of flow depth. The method was explained in Chapter 7, section 7.1, and examples from real rivers were illustrated in Figures 5.12 and 5.13. It should be appreciated, however, that the calculation of many of the basic geometric elements and discharges does not require any conversion or approximation: the full detail of the surveyed cross sections may be - and ideally should be - used for calculating the areas, wetted perimeters and hydraulic mean depths of the main channel and flood plain, once the vertical divisions at the top edge of the channel banks have been determined. An idealised section is, however, required to determine bank slopes, mean bed level, mean level of the bank tops (hence channel depth), channel top width, channel bed width and flood plain width. These geometric parameters of a somewhat idealised cross-section are required to solve the equations for Region 1 in particular.

2. The channel considered here is based on a real river which has been improved as part of a flood relief project. Thus realistic simulated flow data can be associated with it based on measured data, but the river section and flow data have been scaled and modified so that it becomes an anonymous case. The upper part of Figure A6.1 shows the section as it might have been surveyed, and crosses have been added to mark the eight points defining the idealised section in the lower part of the figure. The x-y co-ordinates of the idealised section are shown below. The vertical divisions between main channel and flood plains are now identified, as are bank slopes, mean bed level, bed width etc. In what follows, two depths of flow are considered in detail, corresponding to stages of 3.0m and 4.5m, to illustrate the detailed computation procedure. However, normally a computer program would be used for this, and so these two sample depths are set in the context of tabular summaries of the results of applying a program written in Basic. This

program was developed for analysing laboratory data so has some extra simplifications: it converts the idealised section of figure A6.1 into a completely symmetrical section before working out the geometry.

Using within bank data to assess main channel resistance coefficient

3. It is unnecessary to explain in detail how to work out Manning's n for within bank flows for a given set of stage discharge data: this is very conventional hydraulic computation. Similarly, if another friction equation such as the Colebrook-White formula was preferred, the calculations, though a shade more complex, are straight forward. Table A6.1 is computed output, showing:

- the geometric details
- the set of stage-discharge data available (z = stage relative to channel bed)
- the analysis of these data both in terms of Manning and Colebrook-White (wide channel version)
- check calculations for n_C = 0.025 to examine how good a fit to the data it is.

4. The stage-discharge data here assumes that the hydraulic gradient matched the channel slope in all cases. This is not necessarily so, and if reliable measurements of hydraulic gradient are available, they should be used, of course. The temperature is required in order to assess viscosity, though in practice in real rivers the viscous term in the Colebrook-white equation is small, and in some cases negligible. The analysis of the data shows n_C (Man in the table) to vary in the range 0.022 to 0.026, with perhaps a marginal trend to increase with depth. The results approaching bank full (z = 2.0m) suggest using n_C = 0.025, hence the final part of table A6.1. Here Qex/Qt shows the ratio of observed discharge to calculated discharge, with average 1.026 and standard deviation 5.56 %. Much of the positive discrepancy comes from one result at depth 1.58m, so the conclusion is that a Manning's n value for the main channel of 0.025 is appropriate for the computations under compound flow. The variability of around 5%, or 10% at 95% confidence, is fairly typical of field observations. As there are ten results, the accuracy of determination of the roughness coefficient is

about 3% (2 x s.d./√no. of observations, at 95%). It would have been equally valid to proceed using the Colebrook-White function, with k_S having an average value of 64mm.

Detailed calculations: sample for two flow depths

5. *Geometry*: Refer to figure A6.1 for co-ordinates, hence dimensions. Areas 1 to 7 proceed from left to right.

Side slopes: s_{FL} = 0.30/1.47 = 0.204, s_{CL} = 1.66/1.86 = 0.892
s_{FR} = 2.10/1.68 = 1.25, s_{CR} = 2.20/2.14 = 1.028
s_{Fav} = 0.727 s_{Cav} = 0.960

Areas:

	Stage 3.0m:		Stage 4.5m:	
1.	0.42 x 0.204/2	0.018	1.92 x 0.204/2	0.376 m
2.	(0.42 + 1.07) 13.26/2	9.879	(1.92 + 2.57) 13.26/2	29.769
3.	(1.07 + 2.93) 1.66/2	3.320	(2.57 + 4.43) 1.66/2	5.810
4.	(2.93 + 3.07) 22.03/2	66.090	(4.43 + 4.57) 22.03/2	99.135
5.	(3.07 + 0.93) 2.20/2	4.400	(4.57 + 2.43) 2.20/2	7.700
6.	(0.93 + 0.36) 13.05/2	8.417	(2.43 + 1.86) 13.05/2	27.992
7.	0.36 x 1.25/2	0.081	1.86 x 1.25/2	2.162
	A_C	73.810		112.645 m²
	2 x A_F	18.395		60.299 m²
	A_T	92.205		172.944 m²

Wetted perimeters: $\sqrt{(1 + s_{FL})}$ = 1.021; $\sqrt{(1 + s_{CL})}$ = 1.340
$\sqrt{(1 + s_{FR})}$ = 1.601; $\sqrt{(1 + s_{CR})}$ = 1.434

Stage 3.0m: Stage 4.5m:

1.	1.021 x 0.42	0.429	1.021 x 1.92	1.960 m
2.	(13.26 + 0.65)	13.276		13.276 m
3.	1.340 x 1.860	2.492		2.492 m
4.	(22.03 + 0.14)	22.030		22.030 m
5.	1.434 x 2.14	3.067		3.067 m
6.	(13.05 + 0.57)	13.062		13.062 m
7.	1.601 x 0.36	0.576	1.601 x 1.86	2.978 m
	P_C	27.592		27.592 m
	$2 \times P_F$	27.343		31.276 m
	P_T	54.935		58.868 m

Hydraulic mean depths:

Stage 3.0m		Stage 4.5m	
R_C = 73.810/27.592	2.675	112.645/27.592	4.083 m
R_F = 18.395/27.343	0.672	60.299/31.276	1.928 m

Ratios:

A_* = 18.395/73.810	0.249	60.299/112.645	0.535
P_* = 27.343/27.592	0.991	31.277/27.592	1.134
R_* = 0.672/2.675	0.251	1.928/4.083	0.472

6. *Basic resistance calculation*: The best value of the Manning coefficient for the main channel was established at 0.025 by utilising stage-discharge observations at high within-bank flows. There is no direct way of establishing the appropriate flood plain value, so there is an element of trial and error involved. Of course through experience and other sources of information, a reasonable first guess may be made. The flood plains here are grass berms, usually well maintained. Table A5.1 of Appendix 5 suggests that the flood plain roughness might be in the range 0.025 to 0.035 (Pasture, no brush, short grass) so the first assumption is that n_F = 0.030.

$S = 0.470/1000$ so $s = 0.02168$.

Stage 3.0m		Stage 4.5m	
$V_C = 2.675^{2/3} \times 0.02168/0.025$	1.671	$4.083^{2/3} \times 0.02168/0.025$	2.215 m/s
$Q_C = 1.671 \times 73.810$	123.34	2.275×112.645	249.55m³/s
$V_F = 0.672^{2/3} \times 0.02168/0.030$	0.554	$1.928^{2/3} \times 0.02168/0.030$	1.119 m/s
$2\ Q_F$ (sum of flood plain flows) =			
0.0554×18.395	10.20	1.119×60.299	67.50 m³/s
Q_{Tbasic}	133.54		317.05 m³/s

Friction factors: $f = 8gRS/V^2$; $8gS = 8 \times 9.81 \times 0.470/1000 = 0.03689$

Stage 3.0m		Stage 4.5m	
$f_C = 0.03689 \times 2.675/1.671$	0.03535	$0.03689 \times 4.083/2.215$	0.03068
$f_F = 0.03689 \times 0.672/0.554$	0.08050	$0.03689 \times 1.928/1.119$	0.05682
$f_* = f_F/f_C$	2.277		1.852

Coherence: all necessary parameters are now available to calculate coherence, COH, using eq 13 of the Summary and Design Method.

Stage 3.0m

COH =

$$\frac{(1+0.249)\sqrt{[(1+0.249)/(1+2.277\mathrm{x}0.991)]}}{1 + 0.249\sqrt{(0.249/2.777\mathrm{x}0.991)}} = 0.7144$$

Stage 4.5m

$$\frac{(1+ 0.535)\sqrt{[(1+0.535)/(1+1.852\mathrm{x}1.134}}{1 + 0.0535\sqrt{(0.535/1.852\mathrm{x}1.134}} = 0.8506$$

7. In effect, the calculations for stages of 3.0m and 4.5m are examples of what would normally be a sequential set of calculations for a full range of stages, progressing in sufficiently small depth steps to provide all the geometric information required to establish a close coverage of the stage-discharge function. It is assumed that the actual range of depths for this case goes up to 5m, to cover a rare flood, but when calculating for Region 2 flows some geometric information is required for greater depths, as values of coherence, COH, are needed as will be explained later. In consequence, the computer version of the geometric calculation has been taken up to 8m depth, in steps of 0.25m, as given in table A6.2. A

cross-check with the detailed calculation at depths, $z = H$ of 3.0m and 4.5m shows close agreement, though as mentioned earlier the particular program used approximates the idealised section by a fully symmetric one, which marginally changes wetted perimeters. This feeds through the remaining computations to yield small differences to the values of COH. Note that these coherence values are specific to the assumed roughness coefficients for main channel and flood plain: any change in those would require a recomputation of friction factors etc. With this body of basic information, we may proceed to calculate discharges for our sample stages, for the four Regions of flow in turn.

8. Region 1: Some further parameter values are required: For both sample depths, the full flood plain width is inundated, which therefore provides the value of 2B. At shallower depths, 2B would be defined by the variable water surface width, as shown in Table A6.2.

$2B = 52.50 - 0.30 = 52.20$m

$2b = 37.25 - 15.22 = 22.03$m; $b = 11.015$m

$2w_C = 39.45 - 13.56 = 25.89$m

$h_{av} = (1.93 + 2.07)/2 - (0.07 + (-0.07))/2 = 2.00$m

Aspect ratio = 22.03/2.00 = 11.015

As this is below 20 (see para 10.1.7), ARF = aspect ratio/10 = 1.10. Region 1 flows are calculated from the equations 2 to 9 of the Summary and Design Method. As $s_C < 1$, equ. 7 applies:

Stage 3.0m: $H_* = 0.3333$	Stage 4.5m: $H_* = 0.5556$
Eq 7; $G = 10.42 +$	$10.42 +$
$0.17 \times 0.960 \times 1.852 + 0.34(1-0.960)$	$0.17 \times 0.960 \times 2.277 + 0.34(1-0.960)$
$= 10.42 + 0.3716 + 0.0136 = 10.805$	$= 10.42 + 0.3022 + 0.0136 = 10.736$
Eq 2;	
$Q_{*2F} = -1.0 \times 0.3333/2.277 = -0.146$	$-1.00 \times 0.5556/1.852 = -0.300$
Eq 3;	
$Q_{*2C} = -1.240 + 0.395 \times 52.20/25.89$	$-1.240 + 0.395 \times 52.20/25.89$
$+ 10.805 \times 0.3333$	$+ 10.736 \times 0.5556$
$= -1.240 + 0.7964 + 3.6017 = 3.158$	$= -1.240 + 0.7964 + 5.9649 = 5.521$

Eq 8; DISDEF =

(3.158-2x0.146)(1.671-0.554)x 3.00 x 2.00 x1.10 =	21.13 m^3/s	(5.521-2x0.300)(2.215-1.119) x 4.50 x 2.00 x 1.10 =	53.39 m^3/s
Eq 9; Q_{R1} = 133.54 - 21.13	<u>112.41 m^3/s</u>	317.05 - 53.39 =	<u>263.66 m^3/s</u>

9. <u>Region 2</u>: This depends on coherence calculated with a shift in H_*. As $s_C < 1$, eq 12 applies:

shift = -0.01 + 0.05 x 2 + 0.06 s_C = 0.09 + 0.06 x 0.960 = 0.1476

<u>Stage 3.0m</u>; H_* = 0.3333		<u>Stage 4.5m</u>; H_* = 0.5556	
H_* + shift =	0.4809		0.7032

From the definition of H_*, $H_* = (H-h)/H$ and so $H = h/(1 - H_*)$

Shifted value of H = 2.00/(1 - 0.4809) =	3.853	2.00/(1-0.7032) =	6.739

(Extending the depth beyond the real section raises some conceptual problems but as it results from empirical analysis these need not cause concern. In practice, the flood plain back slopes should be extended upwards as necessary).

The detail for calculating COH at these values of H_* in essence repeats the calculations in paragraphs 1 to 6 above, but with the "shifted" hypothetical depths of flow. In practice a computer program would be used, as mentioned earlier leading to Table A6.2. The easy option of interpolating between the values in this table will be taken: and this also explains why that table was continued beyond the flow depth of 5m which the stage/discharge function is to cover.

<u>Stage 3.0m</u>		<u>Stage 4.5m</u>	
Eq 10: DISADF = COH for shifted H_* = 0.819			0.894
Hence Q_{R2} = 0.819 x 133.54	<u>109.37 m^3/s</u>	0.894 x 317.05	<u>283.44 m^3/s</u>

10. Region 3: This depends on the value of COH (without H_* shift)

	Stage 3.0m		Stage 4.5m	
Eq 16: DISADF				
= 1.567 - 0.667 x 0.7144	1.090		1.567 - 0.667 x 0.8506	0.9996
Q_{R3} = 1.090 x 133.54 =	145.62 m³/s		0.9996 x 317.05 =	316.94 m³/s

11. Region 4:

	Stage 3.0m	Stage 4.5m	
Eq 18: DISADF = COH			
Q_{R4} = 0.7144 x 133.54	95.40 m³/s	0.8506 x 317.05	269.68 m³/s

12. Logic for selection of region of flow: Equations 20, and if necessary in turn 21 and 22, are applied to determine which region the flow is in:

Stage 3.0m

From eq 20,

$Q_{R1} = 112.41$, $Q_{R2} = 109.37$,

$Q_{R1} > Q_{R2}$, hence:

REGION 1: $Q_{PRED} = 112.41$ m³/s

Stage 4.5m

$Q_{R1} = 263.66$, $Q_{R2} = 283.44$,

$Q_{R1} < Q_{R2}$, so region 1 is eliminated

From eq 21: $Q_{R3} = 316.94$, hence

$Q_{R1} < Q_{R2}$ AND $Q_{R2} < Q_{R3}$ so

REGION 2: $Q_{PRED} = 316.94$ m³/s

(Eq 22 only becomes relevant if the test of eq 21 fails).

Continuation of stage/discharge assessment

13. The above assumed that a Manning's n value of 0.030 was appropriate for the flood plains. However, the hydraulic engineer should have access to some above- bank data when carrying out this project, so should compare the results obtained with this value of n_F with the available observations. If no computer program were available, he/she would have to go through the above procedure for each of the observed flow depths, and then compare the

predicted discharges with the measured values. This is illustrated in Table A6.3, the nine assumed observations being listed at the top of the table. These go up to a depth of about 1.5m on the flood plains, though the stage/discharge function requires extending to some 3m depth on the flood plains.

14. With the benefit of a computer program, it is only a matter of a few minutes work at the PC to test a range of assumptions about flood plain roughness. Table A6.3 looks at n_F = 0.030, 0.025 and 0.0275 in turn, the column headed Qex/Qpr being the ratio of observed discharge to predicted flow. The comparison is summarised in terms of the average and standard deviation of these ratios, so indicating the goodness of fit. The first assumption of n_F = 0.030 under-predicts by about 3.3 percent on average, with a variability of about 5%. This led to trying n_F = 0.025, which over-predicts by about half a percent, but reduces the variability. So the third attempt was with n_F = 0.0275, giving agreement to within 1.6% on average, with some 3.6% variability. This may well be the preferred assumption with this data set: at high stages n_F = 0.0275 tends to be a conservative assumption. Note that a Q_{*zc} limit of 0.5 was applied and affected stages below 2.2m only.

15. Having decided upon the best roughness coefficients in this way, the stage/ discharge function over the full range required may be calculated. Obviously this would be considered tedious if all calculations were manual, but with the benefit of suitable PC software, is quickly accomplished. Table A6.4 provides the extended stage/discharge functions for the three alternative flood plain roughnesses considered, the final one being the preferred prediction. Note the transition from Region 1 to Region 2 at a depth of 3.25m, and the trend of the discharge adjustment factor, DISADF. This drops to about 0.85 at the limit of region 1, but rises through Region 2 to 0.93. It is also interesting to note that with equal roughness on flood plain as in main channel, the second case, the flow reaches Region 3, with DISADF approx. 0.95 at maximum depth. This illustrates how the progress through the regions depends on the ratio of the roughnesses: high flood plain roughness will delay that progression, and perhaps result in only Region 1 applying.

Table A6.1 **Use of within-bank field observations to assess roughness of main channel: channel geometry; stage/discharge observations; analysis of individual observations to determine Manning's n and k_s in Colebrook-White equation (wide channel version); tabular assessment of goodness of fit of Manning equation with selected n_c value**

geono	g	bed w	FP w	No FP	chdepth	sc,H/V	hfp	sf,H/V	sfp,V/H	S/1000	Aspect
99.000	9.810	22.030	13.155	2.000	2.000	0.965	2.610	0.727	0.046	0.470	11.015

Experimental data: sampwb.obs Test numbered 1

z exp	Q exp	S/1000	Temp
1.060	21.780	0.470	15.000
1.200	25.560	0.470	15.000
1.280	29.690	0.470	15.000
1.360	33.180	0.470	15.000
1.580	47.050	0.470	15.000
1.720	45.470	0.470	15.000
1.770	48.900	0.470	15.000
1.780	48.170	0.470	15.000
1.900	58.610	0.470	15.000
1.920	54.290	0.470	15.000

Analysis of experiments as single channel

z	z/h	Q	A	P	R	V	ReE6	FF	V*	V/V*	Man	Kse
1.060	0.530	21.780	24.436	24.976	0.978	0.891	3.060	0.045	0.067	13.271	0.024	54.205
1.200	0.600	25.560	27.826	25.365	1.097	0.919	3.536	0.048	0.071	12.916	0.025	70.231
1.280	0.640	29.690	29.779	25.588	1.164	0.997	4.071	0.043	0.073	13.610	0.024	56.159
1.360	0.680	33.180	31.746	25.810	1.230	1.045	4.511	0.042	0.075	13.879	0.024	53.199
1.580	0.790	47.050	37.216	26.421	1.409	1.264	6.248	0.033	0.081	15.687	0.022	29.162
1.720	0.860	45.470	40.746	26.811	1.520	1.116	5.951	0.045	0.084	13.331	0.026	82.198
1.770	0.885	48.900	42.016	26.949	1.559	1.164	6.367	0.042	0.085	13.727	0.025	71.764
1.780	0.890	48.170	42.271	26.977	1.567	1.140	6.265	0.045	0.085	13.407	0.026	82.164
1.900	0.950	58.610	45.341	27.311	1.660	1.293	7.530	0.037	0.087	14.775	0.024	49.869
1.920	0.960	54.290	45.855	27.366	1.676	1.184	6.961	0.044	0.088	13.470	0.026	85.642

MAIN CHANNEL EQUATION
Manning calculation
Main channel Man = 0.025
Bank full discharge at 15 degC 60.0457605
FLOOD PLAIN EQUATION
Manning calculation
Flood plain Mannings n = 0.03

z	Qex	Vm	Qm	Vfp	Qfp	Qt	FmE2	FfpE2	FtE2	Qex/Qt
1.060	21.780	0.855	20.884	0.000	0.000	20.884	4.941	0.000	4.941	1.043
1.200	25.560	0.922	25.666	0.000	0.000	25.666	4.756	0.000	4.756	0.996
1.280	29.690	0.959	28.573	0.000	0.000	28.573	4.663	0.000	4.663	1.039
1.360	33.180	0.995	31.603	0.000	0.000	31.603	4.578	0.000	4.578	1.050
1.580	47.050	1.090	40.554	0.000	0.000	40.554	4.376	0.000	4.376	1.160
1.720	45.470	1.146	46.708	0.000	0.000	46.708	4.266	0.000	4.266	0.974
1.770	48.900	1.166	48.990	0.000	0.000	48.990	4.230	0.000	4.230	0.998
1.780	48.170	1.170	49.451	0.000	0.000	49.451	4.223	0.000	4.223	0.974
1.900	58.610	1.216	55.127	0.000	0.000	55.127	4.142	0.000	4.142	1.063
1.920	54.290	1.223	56.097	0.000	0.000	56.097	4.130	0.000	4.130	0.968

Average Qratio = 1.02647054 Standard deviation = 5.56235E-02

Table A6.2 Geometric calculations: x-y coordinates; summary of idealised geometry (assumed symmetric); geometric parameters and channel coherence

COMPOUND TRAPEZOIDAL CHANNELS: FIELD DATA, version TRAPEZ21, june 91

X coord	Y coord
0.000	4.050
0.300	2.580
13.560	1.930
15.220	0.070
37.250	-0.070
39.450	2.070
52.500	2.640
54.600	4.320

geono	g	bed w	FP w	No FP	chdepth	sc,H/V	hfp	sf,H/V	sfp,V/H	S/1000	Aspect
99.000	9.810	22.030	13.155	2.000	2.000	0.965	2.610	0.727	0.046	0.470	11.015

MAIN CHANNEL EQUATION
Manning calculation
Main channel Man = 0.025
Bank full discharge at 15 degC 60.0457605
FLOOD PLAIN EQUATION
Manning calculation
Flood plain Mannings n = 0.03
Geometry of compound channel

z	H*	Am	Pm	Rm	Afp	Pfp	Rfp	At	Pt	Rt	P*	A*	f*	2 Beff	COH3
0.250	-7.000	5.568	22.725	0.245	0.000	0.000	0.000	5.568	22.725	0.245	0.000	0.000	0.000	25.890	
0.500	-3.000	11.256	23.420	0.481	0.000	0.000	0.000	11.256	23.420	0.481	0.000	0.000	0.000	25.890	
0.750	-1.667	17.065	24.115	0.708	0.000	0.000	0.000	17.065	24.115	0.708	0.000	0.000	0.000	25.890	
1.000	-1.000	22.995	24.809	0.927	0.000	0.000	0.000	22.995	24.809	0.927	0.000	0.000	0.000	25.890	
1.250	-0.600	29.045	25.504	1.139	0.000	0.000	0.000	29.045	25.504	1.139	0.000	0.000	0.000	25.890	
1.500	-0.333	35.216	26.199	1.344	0.000	0.000	0.000	35.216	26.199	1.344	0.000	0.000	0.000	25.890	
1.750	-0.143	41.508	26.894	1.543	0.000	0.000	0.000	41.508	26.894	1.543	0.000	0.000	0.000	25.890	
2.000	0.000	47.920	27.589	1.737	0.000	0.000	0.000	47.920	27.589	1.737	0.000	0.000	0.000	25.890	
2.250	0.111	54.393	27.589	1.972	0.674	5.397	0.125	55.740	38.383	1.452	0.391	0.025	3.613	36.673	0.666
2.500	0.200	60.865	27.589	2.206	2.696	10.794	0.250	66.256	49.177	1.347	0.783	0.089	2.977	47.456	0.612
2.750	0.273	67.338	27.589	2.441	5.861	13.342	0.439	79.060	54.273	1.457	0.967	0.174	2.550	52.200	0.653
3.000	0.333	73.810	27.589	2.675	9.198	13.651	0.674	92.206	54.891	1.680	0.990	0.249	2.280	52.200	0.715
3.250	0.385	80.283	27.589	2.910	12.580	13.960	0.901	105.443	55.510	1.900	1.012	0.313	2.128	52.200	0.757
3.500	0.429	86.755	27.589	3.145	16.008	14.269	1.122	118.771	56.128	2.116	1.034	0.369	2.030	52.200	0.788
3.750	0.467	93.228	27.589	3.379	19.481	14.579	1.336	132.190	56.746	2.330	1.057	0.418	1.962	52.200	0.811
4.000	0.500	99.700	27.589	3.614	23.000	14.888	1.545	145.700	57.364	2.540	1.079	0.461	1.912	52.200	0.829
4.250	0.529	106.173	27.589	3.848	26.564	15.197	1.748	159.301	57.982	2.747	1.102	0.500	1.873	52.200	0.842
4.500	0.556	112.645	27.589	4.083	30.174	15.506	1.946	172.993	58.600	2.952	1.124	0.536	1.844	52.200	0.853
4.750	0.579	119.118	27.589	4.318	33.829	15.815	2.139	186.775	59.219	3.154	1.146	0.568	1.820	52.200	0.862
5.000	0.600	125.590	27.589	4.552	37.529	16.124	2.328	200.648	59.837	3.353	1.169	0.598	1.801	52.200	0.869
5.250	0.619	132.063	27.589	4.787	41.275	16.433	2.512	214.613	60.455	3.550	1.191	0.625	1.785	52.200	0.875
5.500	0.636	138.535	27.589	5.021	45.066	16.742	2.692	228.668	61.073	3.744	1.214	0.651	1.773	52.200	0.880
5.750	0.652	145.008	27.589	5.256	48.903	17.051	2.868	242.814	61.691	3.936	1.236	0.674	1.762	52.200	0.884
6.000	0.667	151.480	27.589	5.491	52.785	17.360	3.041	257.051	62.310	4.125	1.259	0.697	1.754	52.200	0.887
6.250	0.680	157.953	27.589	5.725	56.713	17.669	3.210	271.378	62.928	4.313	1.281	0.718	1.746	52.200	0.890
6.500	0.692	164.425	27.589	5.960	60.686	17.979	3.375	285.797	63.546	4.497	1.303	0.738	1.740	52.200	0.892
6.750	0.704	170.898	27.589	6.194	64.705	18.288	3.538	300.307	64.164	4.680	1.326	0.757	1.736	52.200	0.894
7.000	0.714	177.370	27.589	6.429	68.769	18.597	3.698	314.907	64.782	4.861	1.348	0.775	1.732	52.200	0.895
7.250	0.724	183.843	27.589	6.664	72.878	18.906	3.855	329.598	65.400	5.040	1.371	0.793	1.728	52.200	0.897
7.500	0.733	190.315	27.589	6.898	77.033	19.215	4.009	344.381	66.019	5.216	1.393	0.810	1.726	52.200	0.898
7.750	0.742	196.788	27.589	7.133	81.233	19.524	4.161	359.254	66.637	5.391	1.415	0.826	1.723	52.200	0.899
8.000	0.750	203.260	27.589	7.367	85.479	19.833	4.310	374.218	67.255	5.564	1.438	0.841	1.722	52.200	0.899

Table A6.3 Comparison of observations of stage/discharge with predicted flows: list of observations; calculations for three assumed values of n_F. (subscript m = main channel; fp = flood plain; Qpred is the predicted discharge)

Experimental data: sampab.obs Test numbered 2

z exp	Q exp	S/1000	Temp
2.050	60.750	0.470	15.000
2.080	63.470	0.470	15.000
2.140	63.820	0.470	15.000
2.400	79.490	0.470	15.000
2.540	84.960	0.470	15.000
2.770	91.460	0.470	15.000
3.000	117.900	0.470	15.000
3.160	140.910	0.470	15.000
3.570	183.670	0.470	15.000

MAIN CHANNEL EQUATION
Manning calculation
Main channel Man = 0.025
Bank full discharge at 15 degC 60.0457605
FLOOD PLAIN EQUATION
Manning calculation
Flood plain Mannings n = 0.03
Following uses full predictive functions. Region 1 incorporates an aspect ratio factor for both Q*2F and Q*2C:
aspect ratio of this geometry is 11.015
Aspect ratio used in following = 1.1

z	H*	Qex	Vm	Qm	Vfp	Qfp	F*	Qpred	Qex/Qpr	Region	QtR1	QtR2	QtR3	QtR4
2.050	0.024	60.750	1.276	62.773	0.062	0.002	5.975	60.040	1.012	1.000	60.040	39.079	63.752	51.903
2.080	0.038	63.470	1.289	64.433	0.084	0.006	5.135	61.689	1.029	1.000	61.689	39.733	67.317	50.477
2.140	0.065	63.820	1.315	67.805	0.123	0.026	4.305	65.049	0.981	1.000	65.049	41.279	73.488	49.240
2.400	0.167	79.490	1.428	83.196	0.247	0.426	3.161	76.955	1.033	1.000	76.955	58.578	96.653	52.550
2.540	0.213	84.960	1.486	91.998	0.302	0.949	2.918	82.747	1.027	1.000	82.747	69.295	109.025	57.135
2.770	0.278	91.460	1.580	107.216	0.430	2.632	2.521	95.999	0.953	1.000	95.999	88.423	126.818	74.119
3.000	0.333	117.900	1.671	123.352	0.555	5.109	2.280	112.463	1.048	1.000	112.463	109.386	145.645	95.440
3.160	0.367	140.910	1.733	135.105	0.633	7.191	2.175	125.173	1.126	1.000	125.173	124.948	160.126	111.123
3.570	0.440	183.670	1.887	167.139	0.808	13.718	2.009	168.336	1.091	2.000	161.937	168.336	201.724	154.686

Average Qratio = 1.03326263 Standard deviation = 4.92698E-02

Main channel Man = 0.025
Flood plain Mannings n = 0.025
Following uses full predictive functions. Region 1 incorporates an aspect ratio factor for both Q*2F and Q*2C:
aspect ratio of this geometry is 11.015
Aspect ratio used in following = 1.1

z	H*	Qex	Vm	Qm	Vfp	Qfp	F*	Qpred	Qex/Qpr	Region	QtR1	QtR2	QtR3	QtR4
2.050	0.024	60.750	1.276	62.773	0.074	0.002	4.149	60.068	1.011	1.000	60.068	43.730	61.934	54.630
2.080	0.038	63.470	1.289	64.433	0.101	0.007	3.566	61.730	1.028	1.000	61.730	44.569	65.107	53.796
2.140	0.065	63.820	1.315	67.805	0.147	0.031	2.990	65.117	0.980	1.000	65.117	46.485	70.759	53.355
2.400	0.167	79.490	1.428	83.196	0.296	0.511	2.195	77.857	1.021	1.000	77.857	65.311	92.710	58.862
2.540	0.213	84.960	1.486	91.998	0.362	1.138	2.026	84.292	1.008	1.000	84.292	76.857	104.650	64.585
2.770	0.278	91.460	1.580	107.216	0.515	3.158	1.751	99.140	0.923	1.000	99.140	97.646	122.042	83.753
3.000	0.333	117.900	1.671	123.352	0.666	6.130	1.584	120.598	0.978	2.000	117.713	120.598	140.805	107.496
3.160	0.367	140.910	1.733	135.105	0.760	8.629	1.510	137.707	1.023	2.000	132.125	137.707	155.384	124.989
3.570	0.440	183.670	1.887	167.139	0.970	16.462	1.395	185.651	0.989	2.000	174.020	185.651	197.659	173.672

Average Qratio = 0.995695525 Standard deviation = 3.12895E-02

Main channel Man = 0.025
Flood plain Mannings n = 0.0275
Following uses full predictive functions. Region 1 incorporates an aspect ratio factor for both Q*2F and Q*2C:
aspect ratio of this geometry is 11.015
Aspect ratio used in following = 1.1

z	H*	Qex	Vm	Qm	Vfp	Qfp	F*	Qpred	Qex/Qpr	Region	QtR1	QtR2	QtR3	QtR4
2.050	0.024	60.750	1.276	62.773	0.067	0.002	5.021	60.053	1.012	1.000	60.053	41.315	62.836	53.276
2.080	0.038	63.470	1.289	64.433	0.092	0.006	4.315	61.708	1.029	1.000	61.708	42.054	66.214	52.133
2.140	0.065	63.820	1.315	67.805	0.134	0.028	3.617	65.080	0.981	1.000	65.080	43.770	72.143	51.267
2.400	0.167	79.490	1.428	83.196	0.269	0.465	2.656	77.375	1.027	1.000	77.375	61.829	94.752	55.581
2.540	0.213	84.960	1.486	91.998	0.329	1.035	2.452	83.462	1.018	1.000	83.462	72.965	106.926	60.687
2.770	0.278	91.460	1.580	107.216	0.469	2.871	2.118	97.445	0.939	1.000	97.445	92.917	124.503	78.714
3.000	0.333	117.900	1.671	123.352	0.606	5.573	1.916	114.877	1.026	1.000	114.877	114.855	143.255	101.205
3.160	0.367	140.910	1.733	135.105	0.691	7.845	1.828	131.172	1.074	2.000	128.370	131.172	157.748	117.760
3.570	0.440	183.670	1.887	167.139	0.882	14.965	1.688	176.770	1.039	2.000	167.494	176.770	199.562	163.787

Average Qratio = 1.01602969 Standard deviation = 3.58727E-02

Table A6.4 Calculated stage discharge functions up to stage of 5.0m: three assumed values of n_F in turn

Main channel Man = 0.025
Flood plain Mannings n = 0.03
Following uses full predictive functions. Region 1 incorporates an aspect ratio factor for both Q*2F and Q*2C: aspect ratio of geometry is 11.015
Aspect ratio factor used in following, ARF = 1.1

z	H*	Vm	Qm	Vfp	Qfp	F*	Qt	Qpred	Region	QtR1	QtR2	QtR3	QtR4	DISADF
2.000	0.000	1.253	60.046	0.000	0.000	0.000	60.046	60.046	0.000	60.046	38.188	94.092	0.000	1.000
2.250	0.111	1.363	74.163	0.181	0.122	3.613	74.406	71.578	1.000	71.578	47.396	83.562	49.524	0.962
2.500	0.200	1.470	89.447	0.287	0.773	2.977	90.992	81.013	1.000	81.013	66.187	105.449	55.677	0.890
2.750	0.273	1.572	105.856	0.418	2.448	2.550	110.751	94.676	1.000	94.676	86.680	125.306	72.326	0.855
3.000	0.333	1.671	123.352	0.555	5.109	2.280	133.569	112.463	1.000	112.463	109.386	145.645	95.440	0.842
3.250	0.385	1.768	141.902	0.674	8.482	2.128	158.866	134.047	2.000	132.744	134.047	168.724	120.268	0.844
3.500	0.429	1.861	161.477	0.780	12.490	2.030	186.457	160.582	2.000	155.259	160.582	194.193	146.905	0.861
3.750	0.467	1.953	182.052	0.877	17.080	1.962	216.211	188.906	2.000	179.822	188.906	221.854	175.335	0.874
4.000	0.500	2.042	203.601	0.966	22.212	1.912	248.025	218.935	2.000	206.291	218.935	251.575	205.518	0.883
4.250	0.529	2.130	226.104	1.049	27.856	1.873	281.816	250.589	2.000	234.550	250.589	283.256	237.405	0.889
4.500	0.556	2.215	249.540	1.126	33.987	1.844	317.514	283.793	2.000	264.506	283.793	316.822	270.949	0.894
4.750	0.579	2.299	273.893	1.200	40.584	1.820	355.061	318.476	2.000	296.082	318.476	352.211	306.103	0.897
5.000	0.600	2.382	299.143	1.269	47.631	1.801	394.406	354.572	2.000	329.211	354.572	389.370	342.825	0.899

Main channel Man = 0.025
Flood plain Mannings n = 0.025
Following uses full predictive functions. Region 1 incorporates an aspect ratio factor for both Q*2F and Q*2C: aspect ratio of geometry is 11.015
Aspect ratio factor used in following, ARF = 1.1

z	H*	Vm	Qm	Vfp	Qfp	F*	Qt	Qpred	Region	QtR1	QtR2	QtR3	QtR4	DISADF
2.000	0.000	1.253	60.046	0.000	0.000	1.067	60.046	60.046	0.000	60.046	42.524	94.092	0.000	1.000
2.250	0.111	1.363	74.163	0.217	0.146	2.509	74.455	71.981	1.000	71.981	53.270	80.216	54.655	0.967
2.500	0.200	1.470	89.447	0.344	0.927	2.067	91.301	82.356	1.000	82.356	73.506	101.187	62.792	0.902
2.750	0.273	1.572	105.856	0.501	2.937	1.771	111.730	97.653	1.000	97.653	95.743	120.549	81.758	0.874
3.000	0.333	1.671	123.352	0.666	6.130	1.584	135.613	120.598	2.000	117.713	120.598	140.805	107.496	0.889
3.250	0.385	1.768	141.902	0.809	10.178	1.478	162.258	147.733	2.000	140.729	147.733	164.081	135.199	0.910
3.500	0.429	1.861	161.477	0.936	14.988	1.410	191.453	177.059	2.000	166.392	177.059	189.973	164.968	0.925
3.750	0.467	1.953	182.052	1.052	20.496	1.362	223.043	208.487	2.000	194.481	208.487	218.252	196.787	0.935
4.000	0.500	2.042	203.601	1.159	26.655	1.327	256.910	241.931	2.000	224.826	241.931	248.759	230.614	0.942
4.250	0.529	2.130	226.104	1.258	33.427	1.301	292.959	277.309	2.000	257.294	277.309	281.378	266.399	0.947
4.500	0.556	2.215	249.540	1.352	40.784	1.280	331.109	314.547	2.000	291.774	314.547	316.019	304.091	0.950
4.750	0.579	2.299	273.893	1.440	48.701	1.264	371.295	352.609	3.000	328.175	353.571	352.609	343.644	0.950
5.000	0.600	2.382	299.143	1.523	57.158	1.251	413.459	391.086	3.000	366.418	394.315	391.086	385.013	0.946

Main channel Man = 0.025
Flood plain Mannings n = 0.0275
Following uses full predictive functions. Region 1 incorporates an aspect ratio factor for both Q*2F and Q*2C: aspect ratio of geometry is 11.015
Aspect ratio factor used in following, ARF = 1.1

z	H*	Vm	Qm	Vfp	Qfp	F*	Qt	Qpred	Region	QtR1	QtR2	QtR3	QtR4	DISADF
2.000	0.000	1.253	60.046	0.000	0.000	0.741	60.046	60.046	0.000	60.046	40.281	94.092	0.000	1.000
2.250	0.111	1.363	74.163	0.197	0.133	3.036	74.428	71.768	1.000	71.768	50.212	81.934	52.016	0.964
2.500	0.200	1.470	89.447	0.313	0.843	2.501	91.133	81.635	1.000	81.635	69.735	103.402	59.075	0.896
2.750	0.273	1.572	105.856	0.456	2.670	2.143	111.196	96.047	1.000	96.047	91.095	123.004	76.823	0.864
3.000	0.333	1.671	123.352	0.606	5.573	1.916	134.498	114.877	1.000	114.877	114.855	143.255	101.205	0.854
3.250	0.385	1.768	141.902	0.735	9.253	1.788	160.408	140.721	2.000	136.415	140.721	166.371	127.419	0.877
3.500	0.429	1.861	161.477	0.851	13.625	1.706	188.728	168.610	2.000	160.378	168.610	191.977	155.562	0.893
3.750	0.467	1.953	182.052	0.956	18.633	1.648	219.317	198.434	2.000	186.564	198.434	219.860	185.621	0.905
4.000	0.500	2.042	203.601	1.054	24.232	1.606	252.064	230.107	2.000	214.816	230.107	249.876	217.553	0.913
4.250	0.529	2.130	226.104	1.144	30.389	1.574	286.881	263.548	2.000	245.012	263.548	281.919	251.309	0.919
4.500	0.556	2.215	249.540	1.229	37.077	1.549	323.694	298.683	2.000	277.051	298.683	315.906	286.840	0.923
4.750	0.579	2.299	273.893	1.309	44.274	1.529	362.440	335.439	2.000	310.848	335.439	351.770	324.099	0.926
5.000	0.600	2.382	299.143	1.385	51.962	1.513	403.067	373.748	2.000	346.332	373.748	389.455	363.043	0.927

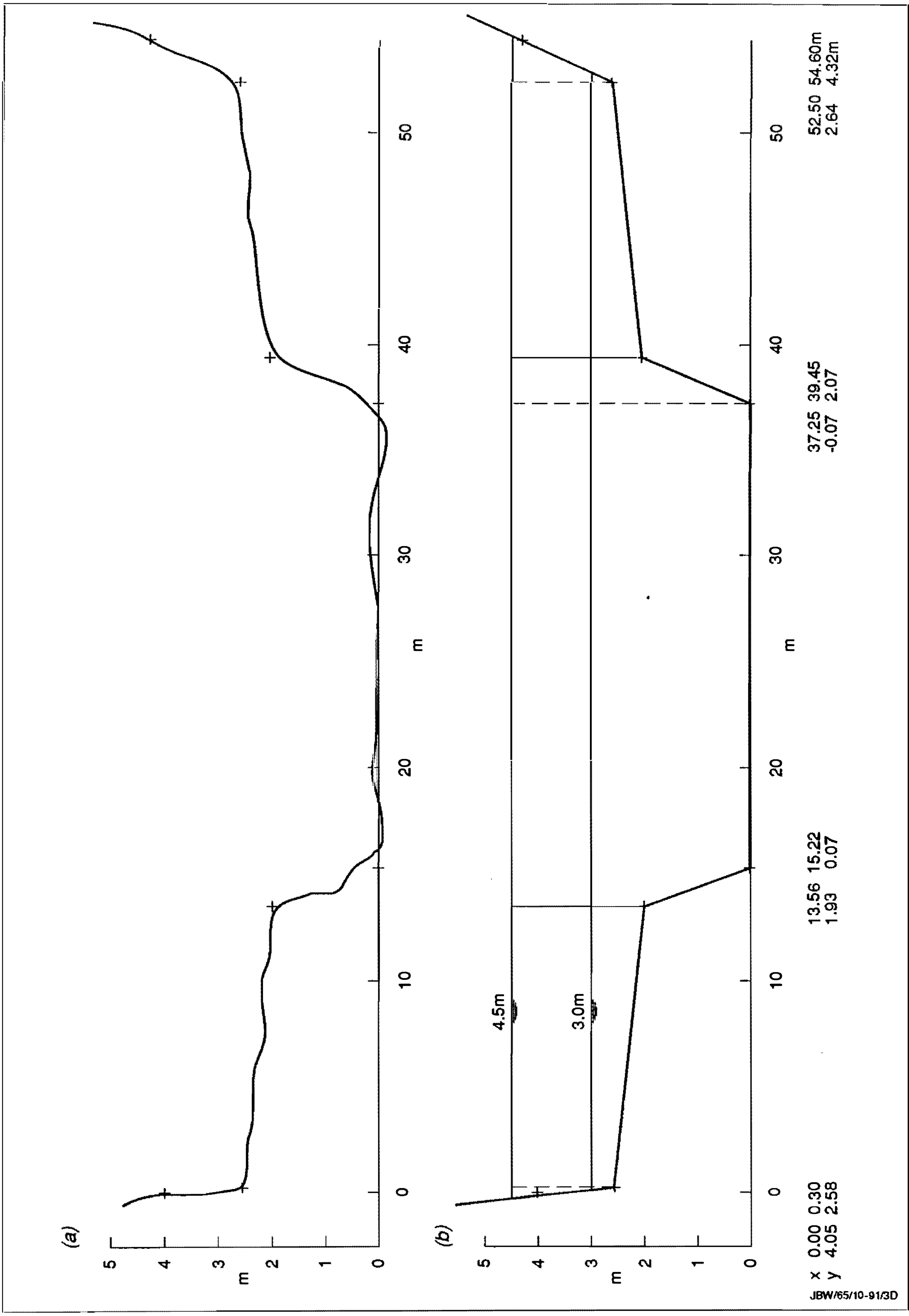

Fig A6.1 **(a): river channel as surveyed.**
(b): idealised form of cross-section, with co-ordinates defining its shape

APPENDIX 7 : ANALYSIS OF OTHER SOURCES OF LABORATORY DATA

1. Asano T, Hashimoto H and Fujita K. Characteristics of variation of Manning's roughness coefficient in a compound cross section. International association for Hydraulic Research, Proc. 21st Congress, Melbourne, Vol 6, August 1985, pp 30-34.

TABLE A7.1 : STATISTICAL ANALYSIS OF GOODNESS OF FIT BETWEEN VARIOUS PREDICTION ASSUMPTIONS AND ASANO et al RESULTS

Upper — Average ratio of experimental discharge to prediction.
Lower — Standard deviation expressed as percentage variation.

Series	B/h	B/b	Case 1	Case 2	Case 2a	Case 3	Case 4	Case 5	Case 6	Case 6a	Case 7	Case 8
5	10	2.50	0.998			0.913	0.955	0.997			0.913	0.913
			1.77			1.46	1.73	1.77			1.46	1.46
Values of ARF:			1	3	2	3	3	3	1	2	2	1
3	30	2.50	1.072	1.137	1.108	1.004	1.051	1.032	0.942	0.975	0.975	0.942
			5.27	4.80	4.54	3.06	4.39	2.81	4.02	3.25	3.25	4.02
9	30	3.33	1.031	1.082	1.058	1.011	1.029	1.030	0.968	0.991	0.991	0.968
			3.37	4.59	3.74	3.79	4.80	4.61	3.43	3.42	3.42	3.43
10	30	2.00	0.917	0.962	0.942	1.021	1.068	1.005	0.987	1.006	1.006	0.987
			1.48	3.81	2.81	2.51	4.20	3.39	0.79	1.49	1.49	0.79
11	30	1.67	1.029	1.074	1.056	1.032	1.060	1.039	1.000	1.019	1.019	1.000
			2.31	1.72	0.77	2.73	3.14	3.17	2.35	1.87	1.87	2.35
12	30	1.42	1.012	1.044	1.031	1.008	1.004	1.022	0.980	0.997	0.997	0.980
			1.55	3.44	2.15	3.05	3.46	3.52	1.54	1.89	1.89	1.54
13	30	1.25	0.945	0.980	0.983	0.992	1.032	0.994	0.967	0.984	0.982	0.967
			1.36	1.97	5.46	1.55	2.24	2.03	1.24	1.52	1.57	1.24
AVER	30		1.001	1.046	1.030	1.011	1.047	1.020	0.974	0.995	0.995	0.974
	ONLY		2.55	3.39	3.25	2.78	3.71	3.25	2.23	2.24	2.25	2.23

CASE 1. Chap 3 predictors with k_s = 0.15mm on both flood plains and in main channel, using wide channel transition function for the basic resistance

CASE 2. Q_{*2} for region 1 redefined to depend on main channel bed width rather rather than depth, ie aspect ratio factor, ARF = aspect ration/10, k_s = 0.15mm

CASE 2a Q_{*2} for region 1 redefined to depend on channel aspect ration, but using an intermediate value of ARF = 2 for aspect ratio 30, k_s = 0.15mm

CASE 3. Redefined Q_{*2}, ARF = aspect ratio/10, using Manning equation with the Authors' values for individual test series for main channel, flood plain constant at 0.0098

CASE 4. Redefined Q_{*2}, ARF = aspect ratio/10, but with wide-channel transition, k_s values for individual test series calculated from within bank tests in that series, and applied also to flood plain

CASE 5. As above but some massaging of channel values, coupled with k_s = 0.15mm on flood plain

CASE 6. Reverting to Authors' Mannings n values, original definition of Q_{*2} ie ARF = 1

CASE 6a Authors' Mannings n, redefined Q_{*2} but ARF at intermediate value of 2 for main channel aspect ratio of 30

CASE 7. As 6a but with the alternative Region 3 formula, DISADF = 0.95

CASE 8. Authors' Mannings n, ARF set at 1, Region 3 - DISADF = 0.95

---

2. US WES, Hydraulic capacity of meandering channels in straight floodways, Tech. Memo. 2.249, Waterways Experiment station, Vicksburg, Mississippi, March 1956.

TABLE A7.2 : CALIBRATION DATA FOR THE WES EXPERIMENTAL FACILITY

Condition	WES value of Manning's n quoted; 10^{-3}			Calculated value of Manning's n; 10^{-3}			Calculated value of k_s ; mm		
Roughness case:	0	1	2	0	1	2	0	1	2
1ft bankfull	12			11.8			0.64		
2ft bankfull	12			12.0			0.72		
0.1ft on FP	12	25	35	11.3	28.1	43.4	0.39	27.9	69.4
0.2ft on FP	12	25	35	11.7	22.9	33.0	0.56	21.1	62.2
0.3ft on FP	12	25	35	12.3	21.9	30.9	0.83	20.5	65.2

TABLE A7.3 : US WATERWAYS EXPERIMENT STATION RESEARCH: COMPARISION OF PREDICTION WITH MEASUREMENT FOR VARIOUS ASSUMPTIONS

Case	Channel width	Roughness coefficients Channel	Flood plain for roughness 0, 1, 2	Av. error %	S E E (1) %
1. Manning, ARF = 1,					
original defn	1ft	0.012	as Table 7.2	6.3	9.4
of Q_{*2}	2ft	0.012	as Table 7.2	25.5	31.7
2. Manning,	1ft	0.012	as Table 7.2	6.3	9.4
Q_{*2} mod	2ft	0.012	as Table 7.1	2.4	5.2
3. Manning, ARF = aspect ratio/10					
Q_{*2c} & Q_{*2F}	1ft	0.012	as Table 7.2	6.3	9.4
modified	2ft	0.012	as Table 7.2	2.9	5.0
4. Wide-transition, ARF = 1,					
orig defn	1ft	0.68mm	0.60, 23.2, 65.6mm	3.6	5.1
of Q_{*2}	2ft	0.68mm	ditto	18.8	19.6
5. Wide-transition,	1ft	0.68mm	ditto	3.6	5.0
Q_{*2c} mod	2ft	0.68mm	ditto	4.6	5.1
6. Wide transition, ARF = aspect ratio/10					
Q_{*2c} & Q_{*2F}	1ft	0.68mm	ditto	3.6	5.0
modified	2ft	0.68mm	ditto	5.2	5.0
7. Wide transition,					
ARF = 0.8	2ft	0.68mm	ditto	16.9	15.0
0.6	2ft	0.68mm	ditto	11.9	7.9
8. Wide transition,					
ARF = 0.4	2ft	0.50mm	0.30, 30.0, 50.0mm	0.6	3.8
9. Wide transition,					
ARF = 0.4	2ft	0.50mm	0.30, 30.0, 50.0mm	0.7	3.7

Note (1). S E E, standard error of the estimate is the r.m.s of the variation about the mean error value, expressed here as percentage.

3. Myers W R C. Momentum transfer in a compound channel, Journal of Hydraulic Research, Col 16, 1978, No 2, 139-150
Myers W R C. Frictional Resistance in channels with flood plains; Channels and channel control structures, 1st Int. Conf. Southampton, England, 1984, ed. K V H Smith, pub Springer-Verlag, 1984, p 4.73-4.87
Myers W R C. Flow resistance in smooth compound channels, experimental data, University of Ulster, March 1985.

TABLE A7.4 : STATISTICAL ANALYSIS OF GOODNESS OF FIT BETWEEN VARIOUS PREDICTION ASSUMPTIONS AND MYERS RESULTS

Note: The following utilises the Region 3 function based on COH.

Geometry	B/b 2b/h	Using Colebrook-White, mean errors and SD's,% ARF = 0.13	0.20	0.40	0.60	1.00	Myer's equ. 0.60
1	4.68 1.99		+1.6 * 2.9	+1.6 * 2.9	+1.6 * 2.9	+1.6 * 2.9	+5.7 * 3.1
2	3.21 1.98		-1.0 5.7	-0.6 * 5.2	-0.6 * 5.2	-0.6 * 5.2	+5.5 * 5.3
3	4.74 1.32	+1.7 4.5	+1.8 * 4.5	+1.8 * 4.5	+1.8 * 4.5	+1.8 * 4.5	*7.3 * 4.0

Note: * denotes no depths shallow enough to yield Region a.

TABLE A7.5 : COMPARISON OF ALTERNATIVE FORMULA FOR REGION 3

Note: Based on Colebrook-White function with $k_s = 0$

Formula number	Geometry number	Overall fit: Number of tests	Mean error	SD %	Region 3 only: Number in region	Mean error	SD %
1	1	42	+0.16	2.90	5	+2.28	3.84
	2	49	-0.58	5.20	5	-0.06	3.98
	3	34	+1.84	4.19	4	+2.93	5.48
	Average:		+0.47	4.19		+1.72	4.43
2	1	42	+0.19	2.89	9	+1.34	3.14
	2	49	-0.64	5.17	10	-0.07	3.16
	3	34	+1.91	4.38	15	+2.08	3.86
	Average:		+0.49	4.15		+1.12	3.39
3	1	42	-0.70	2.67	7	+0.54	2.16
	2	49	-1.04	5.00	6	+3.18	4.47
	3	34	+0.56	4.32	1 *	-2.73	
	Average:		-0.39	4.00		+1.86	3.32

* omitted from average

FORMULA 1 : DISADF = 1.567 - 0.667 COH_3
FORMULA 2 : DISADF = 0.95
FORMULA 3 : DISADF = 1.06 - 0.24 H*

4. Prinos P and Townsend R D. Estimating discharge in compound open channels, Canadian Soc. for Civil Engineering, 6th Canadian Hydrotechnical Conference, Ottawa, Ontario, June 1983, 120-146.
Prinos P and Townsend R D. Comparison of methods for predicting discharge in compound open channels. Advances in Water Resources, 1984, Vol 7, Dec, CML Publications, 180-187..

TABLE A7.6 : STATISTICAL ANALYSIS OF FIT BETWEEN VARIOUS PREDICTION ASSUMPTIONS AND PRINOS AND TOWNSEND RESULTS

CHANNEL WIDTH,mm		203		305		406		508	
Manning's n used for FP	ARF	Mean	SD,%	Mean	SD,%	Mean	SD,%	Mean	SD,%
0.011	0	0.903	6.19	0.910	2.07	0.899	5.95	0.894	4.07
	0.2	0.960	6.49	0.954	* 2.78	0.933	6.88	0.921	4.51
	0.4	0.985	* 4.19	0.990	* 2.55	0.969	7.71	0.949	Φ 5.10
	0.6	0.997	* 2.58	1.008	* 1.76	0.990	6.95	0.974	Φ 5.21
	0.8	1.002	* 2.30	1.017	* 1.29	1.002	Φ 5.88	0.991	* 4.44
	1.0	1.002	* 2.30	1.024	* 1.82	1.010	* 5.04	1.003	* 3.56
0.014	0	0.841	5.76	0.857	6.17	0.869	6.09	0.865	5.09
	0.2	0.919	7.13	0.913	7.66	0.912	7.61	0.899	5.62
	0.4	0.983	6.54	0.978	9.59	0.961	9.43	0.963	6.45
	0.6	1.009	* 3.82	1.021	8.71	1.012	11.06	0.976	7.62
	0.8	1.024	* 1.63	1.042	6.42	1.043	10.46	1.013	8.20
	1.0	1.037	* 2.66	1.057	Φ 4.69	1.068	9.35	1.039	7.64
0.018	0	0.772	6.94	0.822	6.53	0.844	6.40	0.874	7.33
	0.2	0.865	9.49	0.890	8.89	0.896	8.47	0.874	7.33
	0.4	0.975	11.87	0.971	12.02	0.957	11.03	0.918	8.74
	0.6	1.027	8.72	1.059	14.82	1.027	14.24	0.968	10.65
	0.8	1.054	Φ 5.67	1.109	13.46	1.097	16.72	1.024	13.12
	1.0	1.074	3.39	1.137	11.24	1.139	16.17	1.076	14.71
0.022	0	0.721	8.03	0.783	6.25	0.808	7.88	0.798	6.56
	0.2	0.822	11.48	0.858	9.04	0.867	10.38	0.841	7.95
	0.4	0.961	16.88	0.950	12.91	0.934	13.57	0.890	9.86
	0.6	1.051	15.95	1.067	18.43	1.016	17.70	0.946	12.37
	0.8	1.097	11.81	1.149	18.89	1.116	23.19	1.010	15.64
	1.0	1.117	8.027	1.197	16.87	1.187	24.27	1.086	19.91

* These results are within 5% mean error and also 5% variability
Φ These come close to those limits

5. Knight D W, Demetriou J D and Hamed M E. Stage discharge relations for compound channels, Proc 1st Int. conf. Channels and Channel Control Structures. April 1984, ed Smith K V H, Springer Verlag, 1984, 4.21-4.36
Knight D W and Demetriou J D. Flood plain and main channel interaction, ASCE, J Hudraulic Eng. Vol 109, No 8, Aug 1983, 1073-1092.

TABLE A7.7 : STATISTICAL ANALYSIS OF GOODNESS OF FIT BETWEEN VARIOUS PREDICTION ASSUMPTIONS AND KNIGHT AND DEMETRIOU RESULTS

Aspect ratio	B/b	ARF = 1.0 Mean	SD%	ARF = 0.6 Mean	SD%	ARF = 0.4 Mean	SD%	ARF = 0.2 Mean	SD%	ARF = 0.1 Mean	SD%	ARF = 0 Mean	SD%
2	2	1.105	3.85	1.100	2.92	1.092	1.82	1.077	1.84	1.047	1.97	1.003	1.33
2	3	1.043	3.81 ±	1.043	3.81 ±	1.043	3.81 ±	1.031	5.31	1.012	6.76	0.975	6.60
2	4	1.014	3.02 ±	1.014	3.02 ±	1.014	3.02 ±	1.000	2.07	0.986	2.96	0.951	2.95

* denotes no region 1 flows predicted with this value of ARF
The underlined values are those showing least variability

---

6. Kiely: unpublished thesis plus personal communication

TABLE A7.8 : STATISTICAL ANALYSIS OF GOODNESS OF FIT BETWEEN VARIOUS PREDICTION ASSUMPTIONS AND KIELY'S RESULTS

SMOOTH FLOOD PLAINS:

Roughness used: Main ch	Flood pl	ARF values:	0.20	0.34	0.37	0.5
0.011	0.010	Av disc%	-6.0		-5.1 *	-5.1 *
		S D %	3.0		2.5	2.5

ROUGH FLOOD PLAINS:

0.011	0.0157		-3.0	+1.8		+5.2
			2.5	1.0		4.7

Note: * denotes no Region 1 results remained

---

7. Wormleaton P R, Allen J and Hadjipanos P, Proceedings ASCE, J Hy Div, Vol 108, No HY9, Sept 1982, pp 975-994

TABLE A7.9 : STATISTICAL ANALYSIS OF GOODNESS OF FIT BETWEEN VARIOUS PREDICTION ASSUMPTIONS AND WORMLEATON et al RESULTS

Upper figure: mean discrepancy %
Lower figure: variability %

Nominal n value	Assumed value of ARF:						
	1.0	0.8	0.6	0.4	0.24	0.20	0
0.011	+3.5 *	+3.5 *	+3.5 *	+2.6	+0.9	-2.0	-9.5
	6.0	6.0	6.0	6.1	5.7	5.9	6.0
0.014	+0.3 *	+0.3 *	+0.3 *	+0.3 *	-2.5	-3.8	-13.6
	2.1	2.1	2.1	2.1	4.5	5.2	5.2
0.017	+5.3 *	+5.3 *	+4.5	+1.7	-4.4	-7.3	-19.8
	2.2	2.2	2.6	6.6	9.9	9.5	7.3
0.021	+2.0 *	+2.0 *	-1.5	-7.2	-18.2	-21.3	-34.0
	6.7	6.7	11.8	16.8	16.4	15.3	11.5

Note: * indicates Region 1 is eliminated under these conditions at minimum depth tested

PGS

Our Ref : R/S/0203

add ~

Dear name ~

HR REPORT SR 281

I enclose details of corrections to the above document which came to light after the document had been printed.

The enclosed material should include :

1. A complete contents list for Volume 1.

2. A Corrigenda page for Volume 1.

3. Corrected Figures 3.18 and 3.21 for Volume 1.

4. A Corrigenda page for Volume 2.

5. Figure A3.1, which had been omitted from Volume 2.

6. A Corrigenda page supplied by Dr D W Knight for Appendix 4 in Volume 2.

Please include these amendments in the Volumes that you have.

I apologise for any inconvenience this may cause.

Yours sincerely

JAMES B WARK
Research Department

Encs

DETAILED DEVELOPMENT OF DESIGN METHOD

CONTENTS

PART 1

CONTENTS (CONT'd)

CONTENTS (CONT'd)

CONTENTS (CONT'd)

HYDRAULIC DESIGN OF TWO-STAGE CHANNELS : HR REPORT SR 281, DEC 1991

CORRIGENDA : to 22 Feb 1991, Volume 1

p9, line 2; should refer to plate 2

p20, last line levels should read levees

p47, para 2.4.8,	13;	0.43	should read	0.3
	16;	0.85		0.5
		0.94		0.9
	18;	0.61		0.52

p53; the two sentences at the foot of this page should be at the head of p55.

p64, para 3.4.20, 16;	3.18	should read	3.11
p64, para 3.4.21, 14;	3.12		3.13

p110, para 5.5.4; The information in the last sentence is based on a misunderstanding of earlier information, since amended by a personal communication from Dr Myers.

p112, 113, paras 5.5.9 to 5.5.10; The actual geometry of the R Main cross-section 14 differs from that used here, which was based on published information corrected since the report was written. The reach is now known to be of irregular gradient with non-uniform flow, so the hydraulic gradients used in the analysis are not valid. The information on the R Maine in the text, figs 5, 9 and 5.10 and in table 5.3 should be disregarded. This reach of river is no longer considered suitable for this type of analysis.

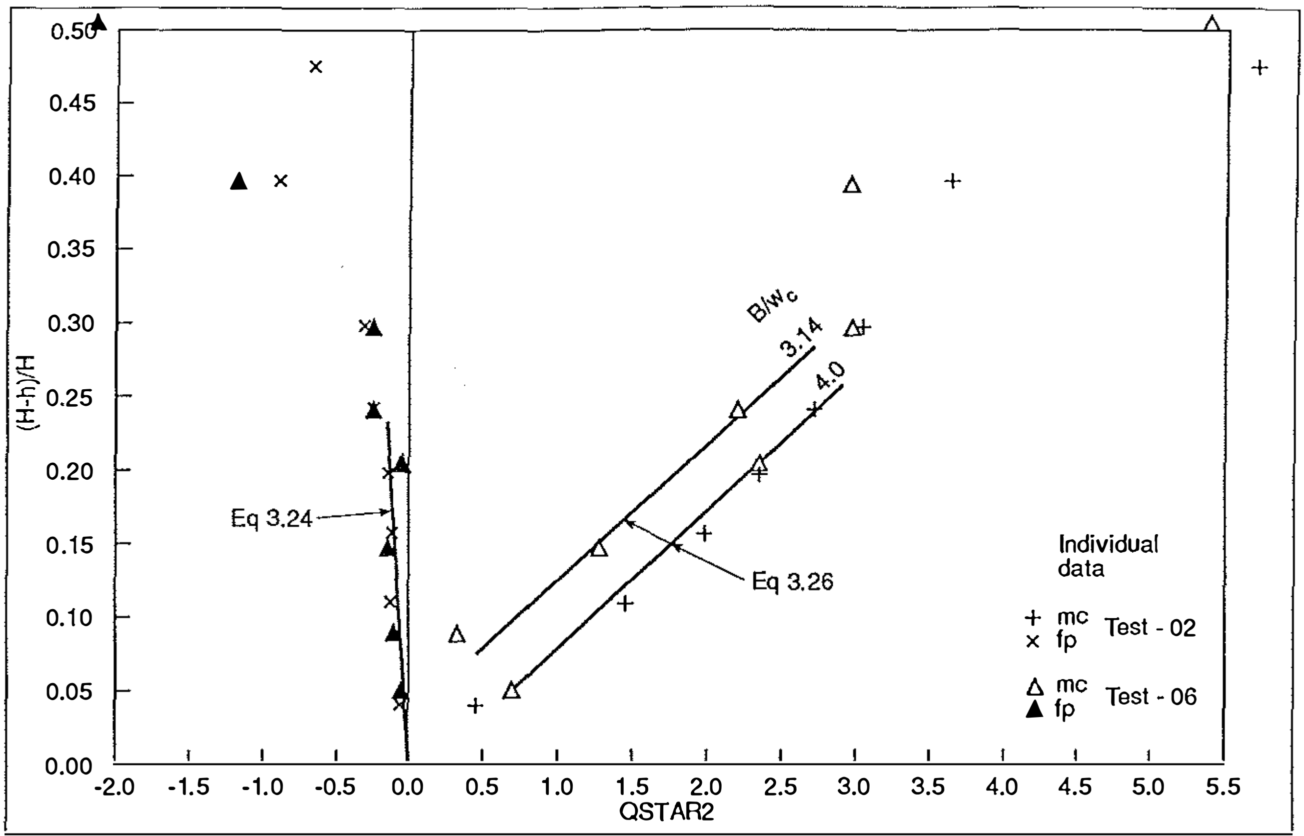

Figure 3.17 Q_{*2} against H_* for separate zone: symmetric/asymmetric comparison

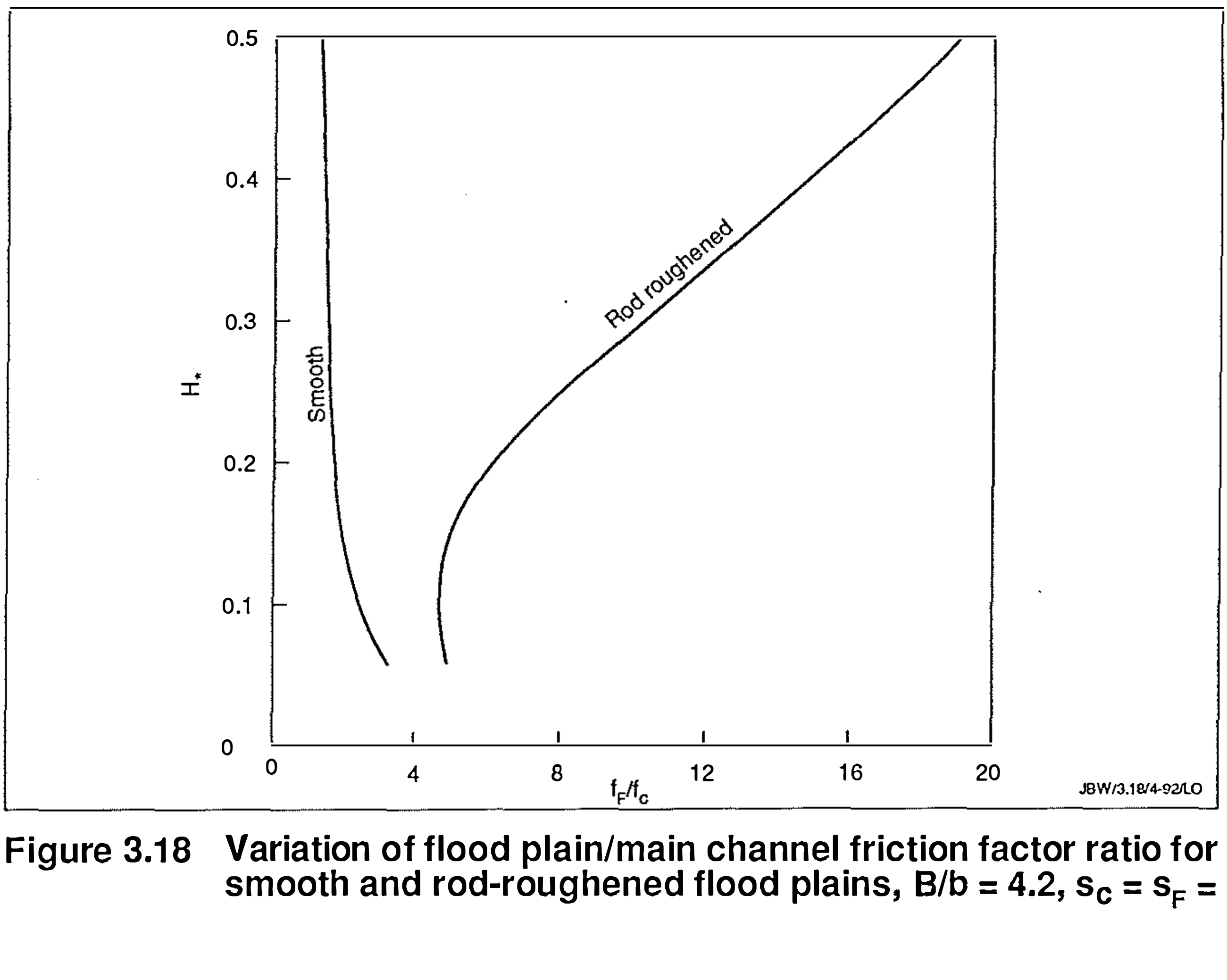

Figure 3.18 Variation of flood plain/main channel friction factor ratio for smooth and rod-roughened flood plains, $B/b = 4.2$, $s_C = s_F = 1$

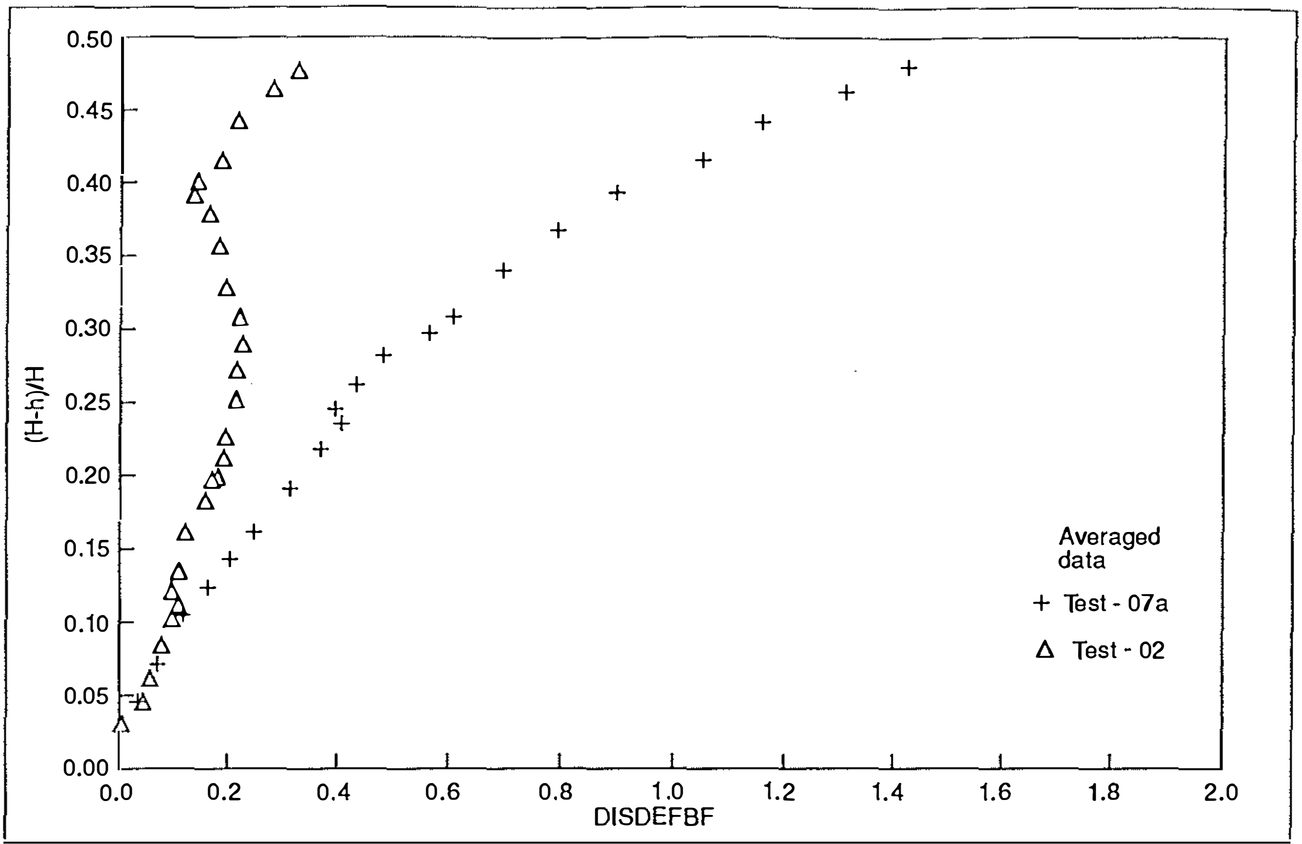

Figure 3.21 DISDEFBF against H*: comparison between smooth and rough flood plains

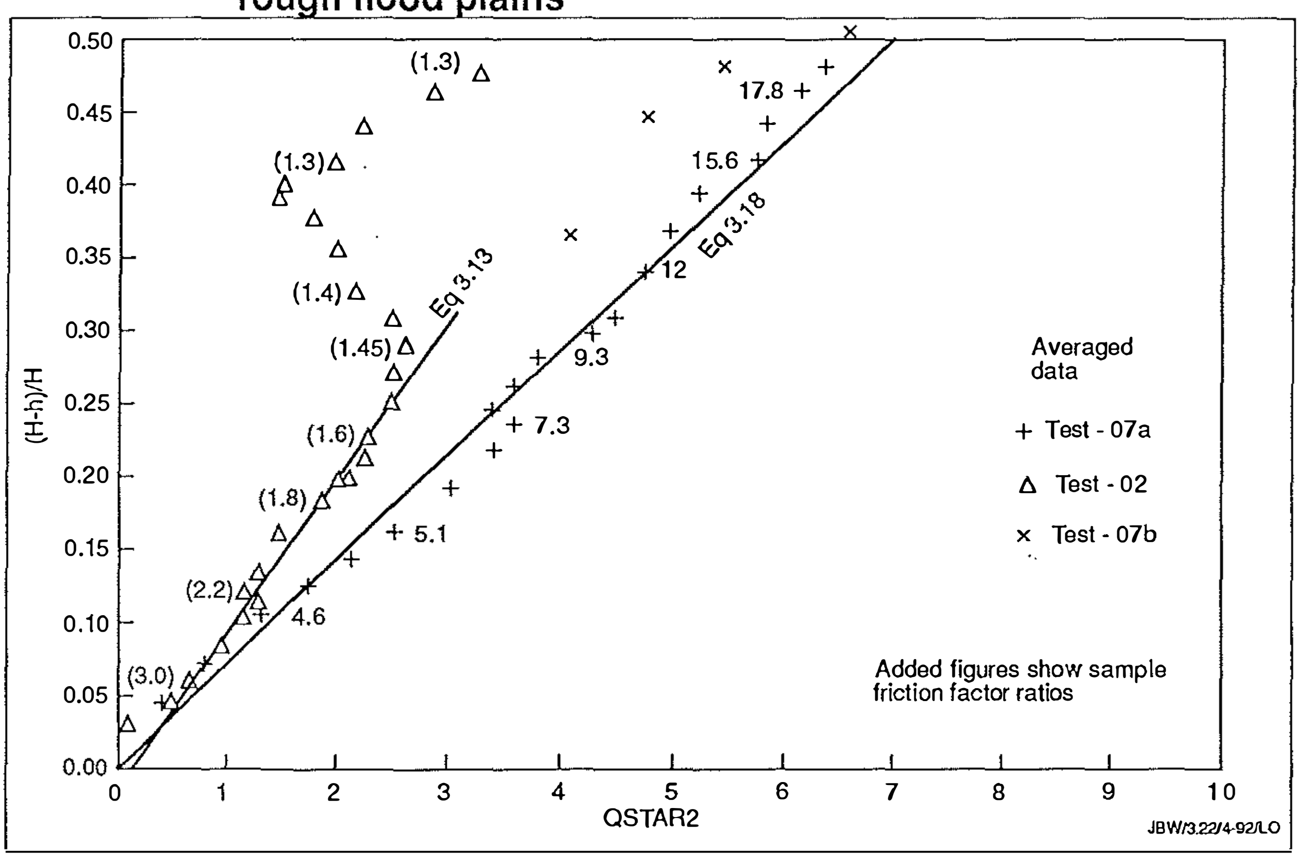

Figure 3.22 Q_{*2} against H*: comparison between smooth and rough flood plains

HYDRAULIC DESIGN OF TWO-STAGE CHANNELS : HR REPORT SR 281, DEC 1991

CORRIGENDA : to 22 Feb 1991, Volume 2

p28, table 8.3, line 13; last F1 should be F2

p41, eq 9.14; There should be double height brackets around the main part of the function on the right

p52, para 10.1.10, 12; reference to equations should be 10.1 to 10.12.

Appendix 1

Eq A1.3 should read $Q/\sqrt{(8gSA^3/P)} = 1/\sqrt{f}$

Appendix 3

Eq A3.5 should be :

$$COH_1 = \frac{\sum_{i=1}^{i=n} A_i \sqrt{[\sum_{i=1}^{i=n} A_i/fo \sum_{i=1}^{i=n} P_i]}}{\sum_{i=1}^{i=n} [A_i \sqrt{(A_i/f_i/P_i)}}$$

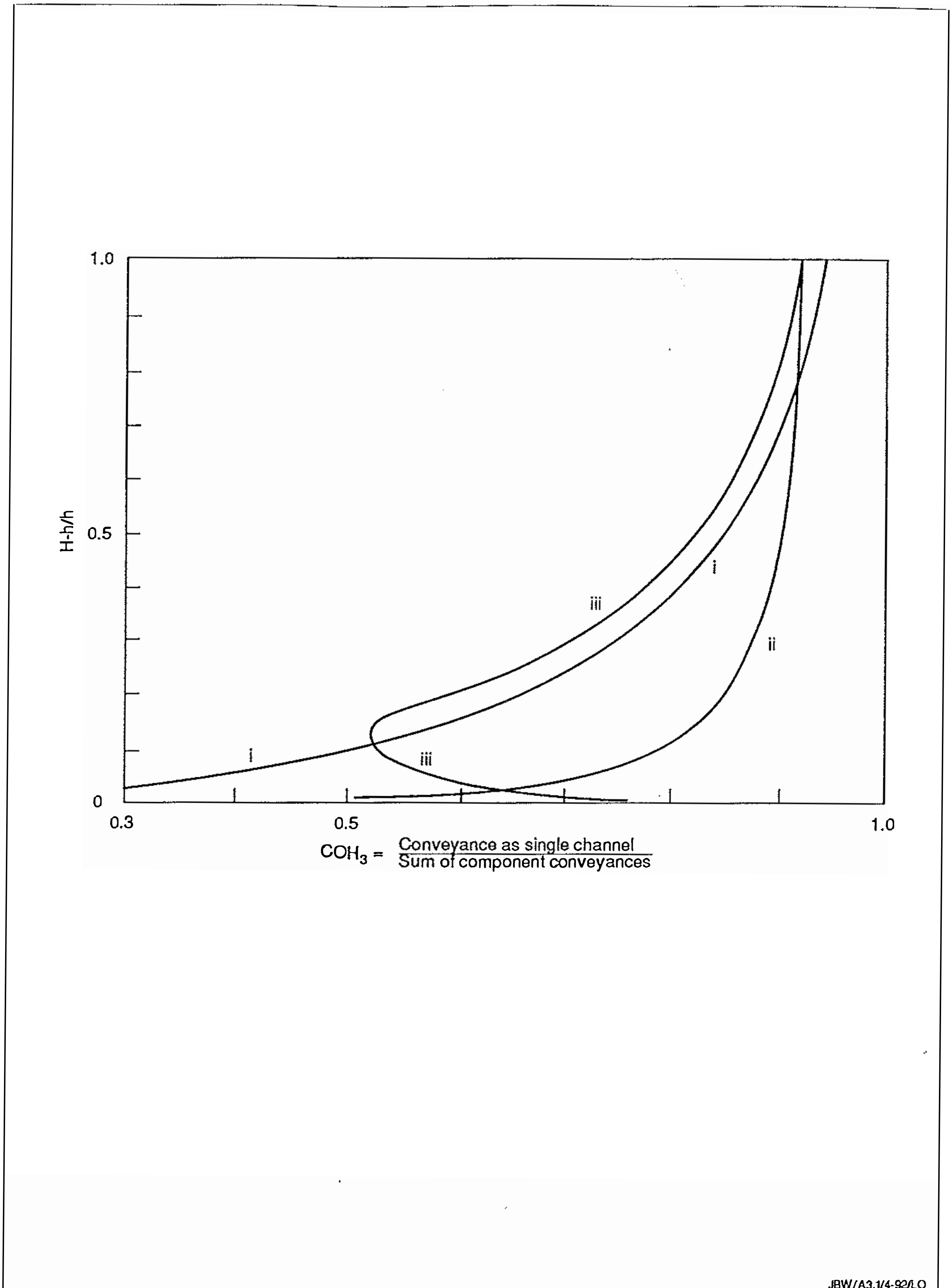

Figure A3.1 Channel coherence – COH_3, as function of ratio of flood plain flow depth to main channel depth: (i) wide horizontal flood plains; (ii) narrow horizontal flood plains; (iii) natural river channel with sloping flood plains

Our Ref: DWK/MJB

Professor J.C.R. Hunt
Editor, Journal of Fluid Mechanics
Department of Applied Mathematics & Theoretical Physics
The University of Cambridge
CAMBRIDGE

7th June 1991

Dear Professor Hunt,

CORRIGENDUM - TURBULENT OPEN-CHANNEL FLOWS WITH VARIABLE DEPTH ACROSS THE CHANNEL, SHIONO & KNIGHT, J.Fluid Mechanics (1991), Vol.222, pp.617-646.

Regrettably there is an error in **equation (11)** on **page 621** of the above paper. I transcribed the equations from an earlier draft leaving in another 'constant'. The two terms β and η should read:

$$\beta = \frac{\Gamma}{\rho g S_o H}$$

$$\eta = - \frac{\Gamma}{\frac{(1+s^2)^{1/2}}{s} \rho \left(\frac{f}{8}\right)}$$

I apologise for this oversight and would be grateful if a corrigendum could be published in a future edition.

Yours sincerely,

Dr. D.W. Knight
Reader in Hydraulics & Fluid Mechanics

c.c. Dr. K. Shiono, University of Bradford